frontiers | Research Topics

Physiological growth responses to light in controlled environment agriculture

Edited by
Xiuming Hao, Leo Marcelis and Viktorija Vaštakaitė-Kairienė

Coordinated by
Jason Lanoue

Published in
Frontiers in Plant Science

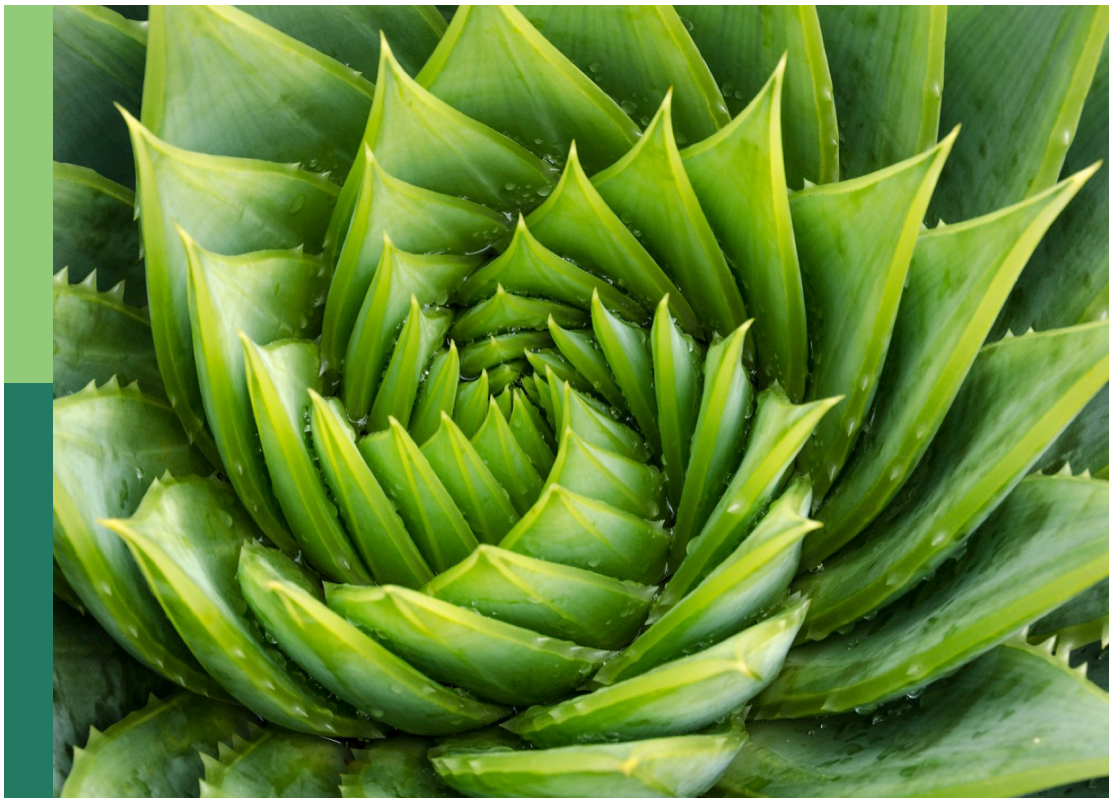

ISSN 1664-8714
ISBN 978-2-8325-5807-2
DOI 10.3389/978-2-8325-5807-2

About Frontiers

Frontiers is more than just an open access publisher of scholarly articles: it is a pioneering approach to the world of academia, radically improving the way scholarly research is managed. The grand vision of Frontiers is a world where all people have an equal opportunity to seek, share and generate knowledge. Frontiers provides immediate and permanent online open access to all its publications, but this alone is not enough to realize our grand goals.

Frontiers journal series

The Frontiers journal series is a multi-tier and interdisciplinary set of open-access, online journals, promising a paradigm shift from the current review, selection and dissemination processes in academic publishing. All Frontiers journals are driven by researchers for researchers; therefore, they constitute a service to the scholarly community. At the same time, the *Frontiers journal series* operates on a revolutionary invention, the tiered publishing system, initially addressing specific communities of scholars, and gradually climbing up to broader public understanding, thus serving the interests of the lay society, too.

Dedication to quality

Each Frontiers article is a landmark of the highest quality, thanks to genuinely collaborative interactions between authors and review editors, who include some of the world's best academicians. Research must be certified by peers before entering a stream of knowledge that may eventually reach the public - and shape society; therefore, Frontiers only applies the most rigorous and unbiased reviews. Frontiers revolutionizes research publishing by freely delivering the most outstanding research, evaluated with no bias from both the academic and social point of view. By applying the most advanced information technologies, Frontiers is catapulting scholarly publishing into a new generation.

What are Frontiers Research Topics?

Frontiers Research Topics are very popular trademarks of the *Frontiers journals series*: they are collections of at least ten articles, all centered on a particular subject. With their unique mix of varied contributions from Original Research to Review Articles, Frontiers Research Topics unify the most influential researchers, the latest key findings and historical advances in a hot research area.

Find out more on how to host your own Frontiers Research Topic or contribute to one as an author by contacting the Frontiers editorial office: frontiersin.org/about/contact

Physiological growth responses to light in controlled environment agriculture

Topic editors

Xiuming Hao — Harrow Research and Development Centre, Agriculture and Agri-Food Canada (AAFC), Canada

Leo Marcelis — Wageningen University and Research, Netherlands

Viktorija Vaštakaitė-Kairienė — Vytautas Magnus University Academy of Agriculture, Lithuania

Topic coordinator

Jason Lanoue — Harrow Research and Development Centre, Agriculture and Agri-Food Canada (AAFC), Canada

Citation

Hao, X., Marcelis, L., Vaštakaitė-Kairienė, V., Lanoue, J., eds. (2024). *Physiological growth responses to light in controlled environment agriculture*.

Lausanne: Frontiers Media SA. doi: 10.3389/978-2-8325-5807-2

Table of contents

frontiers | Frontiers in Plant Science

TYPE Editorial
PUBLISHED 06 December 2024
DOI 10.3389/fpls.2024.1529062

OPEN ACCESS

EDITED AND REVIEWED BY
Giuseppe Mannino,
University of Turin, Italy

*CORRESPONDENCE
Viktorija Vaštakaitė-Kairienė
viktorija.vastakaite-kairiene@vdu.lt

RECEIVED 15 November 2024
ACCEPTED 22 November 2024
PUBLISHED 06 December 2024

CITATION
Lanoue J, Hao X, Vaštakaitė-Kairienė V and Marcelis LFM (2024) Editorial: Physiological growth responses to light in controlled environment agriculture.
Front. Plant Sci. 15:1529062.
doi: 10.3389/fpls.2024.1529062

Editorial: Physiological growth responses to light in controlled environment agriculture

Jason Lanoue[1], Xiuming Hao[1], Viktorija Vaštakaitė-Kairienė[2]* and Leo F.M. Marcelis[3]

[1]Harrow Research and Development Centre, Agriculture and Agri-Food Canada (AAFC), Essex, ON, Canada, [2]Department of Plant Biology and Food Science, Vytautas Magnus University Agriculture Academy, Akademija, Lithuania, [3]Horticulture and Product Physiology,Wageningen University and Research, Wageningen, Netherlands

KEYWORDS

light, greenhouse, indoor vertical farming, controlled environment agriculture (CEA), food production

Editorial on the Research Topic
Physiological growth responses to light in controlled environment agriculture

Light is crucial for photosynthesis, carbon assimilation, biomass production, and plant yield. It also influences physiological and biochemical processes. The lighting environment is vital in controlled environment agriculture (CEA) to enhance growth and quality. Advancements in lighting technologies and the CEA industry have accelerated lighting research in plant science (Pattison et al., 2018). The Research Topic was oriented towards compiling research related to the impact of the light environment in CEA with respect to physiological, biochemical, and genetic responses of plants. The Research Topic garnered 10 original research papers authored by 38 researchers from around the globe, including experts from Australia, Canada, China, Croatia, Hungary, South Korea, the Netherlands, and the United States of America.

In high latitude countries, supplemental light is required during winter months to achieve the optimum daily light integral. We have reached point where fundamental plant science research can be translated to elicit specific morphological and physiological responses during production all while maximizing energy-use-efficiency and minimizing greenhouse gas emissions. This will help the CEA industry ensure sustainable year-round production of fresh fruits and vegetables to meet consumer demand.

A study by Lanoue et al. demonstrated that pepper plants can be grown under continuous lighting without the leaf injury associated with a 24-h photoperiod. In addition, it turned out that a dynamic lighting strategy was necessary for injury-free production under 24-h lighting. Applying blue and/or far-red light at night decreased phytochrome photostationary state, which increased internode length and caused a shade avoidance response; applying far-red at night elicited a significantly stronger response than applying it during the day. In this study, a treatment that provided white light during the day followed by both blue and far red during the night, is potentially the best continuous lighting for pepper production. This study shows the using a low intensity, long photoperiod ultimately culminates in reduced capital fixture and electricity costs.

In another study, Lanoue et al. found that increased carbohydrate content and ROS-scavenging capability, as well as decreased photosynthetic pigment content, may be an adverse response to continuous lighting treatment. However, pepper plants did not show any impact on yield, nor did they show a stress response using the current gold standard stress metric, dark-adapted chlorophyll fluorescence measuring quantum yield of photosystem II (F_v/F_m). Interestingly, light-adapted chlorophyll fluorescence measurements assessing quantum efficiency of photosystem II (ΦPSII) and electron transport rate (ETR) decreased under increasing nighttime light intensity. Due to the discrepancy between dark-adapted and light-adapted measurements, the researchers suggest that light-adapted measurements may be more suitable for identifying stress response in continuous light tolerant crops.

The 16-h and 24-h constant (no change in light intensity and spectrum) and two 24-h dynamic (involving changes in spectra and intensity at different timings of the day) lighting strategies were presented by Marie et al. In the study, the morphological response of tomato, photoperiodic injury–sensitive species, and mini-cucumber, a photoperiodic injury-tolerant species was investigated. Moreover, the hypothesis of photorespiration's involvement in photoperiodic injury was tested. Different dynamic strategies induced different canopy responses, opening the potential to adjust canopy architecture through counterbalances in the peak spectrum (blue) and night spectrum (far-red). Both tomato and cucumber responded well to the dynamic 16-h "day", 3-h "peak", 8-h "night" spectra by avoiding the typical compact morphology induced by extended photoperiods. A central discovery was that this strategy had a significantly higher level of photorespiration than control. Unexpectedly, photorespiration was comparable between tomato and cucumber under the same treatments, except under constant 24-h treatment. According to preliminary data, a fully tolerant tomato genotype grown under constant treatment upregulated photorespiration like mini cucumber. These results suggest that photoperiodic injury tolerance involves a sustained higher level of photorespiration under extended photoperiods.

Darko et al. investigated how the two light intensities (300 and 500 µmol m^{-2} s^{-1}) were applied in different spectral compositions - broad white LED spectrum with and without FR application and with blue LED supplement was compared to blue and red LED lightings in different (80/20 and 95/5) blue/red ratios - affect the growth, flowering, and yield of chili and the production of secondary metabolites. High light intensity increased harvest index (fruit yield vs. vegetative biomass production) and reduced flowering time. Phenolic content and radical scavenging activity was stimulated by blue light, while capsaicin accumulation was suppressed. The red color of the fruit, which is determined by content of carotenoids, was inversely related to the absolute amount of blue, green, and far-red light. These findings demonstrated that the accumulation of secondary metabolites may be altered by adjusting light fluence and spectral composition, but different spectral combinations are necessary to trigger the accumulation of various phytochemicals. It was concluded that a single spectral combination is insufficient for the optimal growth of chili and the accumulation of all metabolites, and an adjustable light environment can ensure such conditions in CEA.

The study by Naveed et al. aimed to evaluate and comprehend the impacts of diminished light intensity and quality on plant morphology and root growth. In addition, they strived to identify resistant sources from the population generated from two-drought tolerant commercial chickpea lines (Sonali as a female and PBA Slasher as a male parent). Low light conditions, created by covering one of the two benches inside two growth chambers with a mosquito net, reduced natural light availability by approximately 70%. The chickpea genotypes exhibited significant responses to these conditions, mostly altering their morphology by allocating more photosynthates to shoot growth at the expense of root growth. Shading resulted in taller plants with longer and more internodes, but with lower root, shoot, and total plant biomass, presumably as an adaptation strategy, akin to the shade avoidance syndrome concept. The findings help better understand the biomass partitioning patterns in crops exposed to low light conditions.

Another study on low-light-stress in plants was done by Cao et al. when the growth characteristics of cucumber seedlings under various LED (light emitting diode) light treatments were evaluated. Low-light-stress tolerant and sensitive cucumber lines were used as plant materials for gene expression analysis. Light intensity below 40 µmol m^{-2} s^{-1} can quickly induce low-light-stress response. A total of 11 photoreceptor genes were identified and evaluated. Among them, cryptochrome 1 had the highest expression level and was only induced in the low-light sensitive cucumber. Therefore, it was proposed that cryptochrome 1 plays a pivotal role in regulation low-light response in plants

Medical cannabis cultivation has expanded under controlled environments. Increasing inflorescence weight and specialized metabolite concentrations is crucial for product consistency. The interaction between spectrum and intensity on inflorescence weight and secondary metabolites is attracting attention. The findings by Holweg et al. showed that white light with dual red peaks at 640 and 660 nm increased inflorescence yield and light-use-efficiency (LUE) in medical cannabis plants, regardless of intensities. This was primarily due to increased total plant dry matter production and a more open plant architecture. No light spectrum or intensity effects on cannabinoid concentrations were observed. However, at higher intensity, white light with dual red peaks increased terpenoid concentrations. At low intensity, photosynthetic parameters like maximum photosynthetic rate and quantum yield increased, while spectrum had no effect at higher intensity. The addition of 640 nm and 660 nm shows potential for improving LUE and plant dry matter production.

Enhancing supplemental lighting increased photosynthesis and had a significant impact on the water usage dynamics in cannabis leaves and crops. The findings of Collado et al. highlight the potential of lighting management to enhance water-use-efficiency (WUE), with significant implications for both research and

practical applications in agriculture. Light supplementation strongly enhanced photosynthesis and plant growth while increasing WUE. It was found that a linear growth response within the range of ~18 to 52 mol m^{-2} d^{-1}. Additionally, it was found that 52 mol m^{-2} d^{-1} did not saturate the crop response to light, leaving further research to be done to identify the maximum daily light integral for cannabis cutting production.

In controlled environment agriculture, tailored light treatments using LEDs are crucial for enhancing crop quality and yield. In the study by Van Brenk et al., lettuce was grown under three different blue and red light ratios with and without far-red light. As the control treatments, white light with and without far-red light was used. Decreasing the red:blue ratio decreased fresh weight and carbohydrate concentration, whereas contents of pigments, phenolic compounds, and various minerals increased. In contrast, adding far-red light to different R:B ratios, and increase in plant fresh weight, dry weight, total soluble sugars, and starch was observed. Additionally, far-red light decreased concentrations of anthocyanins, phenolic compounds, and various minerals. Consequently, the distinct advantages of enhanced blue light proportion and additional far-red radiation can be integrated and utilized synergistically to cultivate crops of desired quality.

High planting densities result in increased light interception and harvestable yield per area, but at the sacrifice of product quality. The study of Karpe et al. aimed to maintain high light interception without negative impacts on tomato fruit quality. Dwarf tomato was grown at four densities: two constant densities (high and low) and two dynamic spacing treatments (maintaining 90% and 75% ground coverage by decreasing planting density in 3–4 steps). The study found that high ground coverage and light interception are crucial for maximizing yield per area and LUE. Plants grown at the constant high planting density utilized light most efficiently for fruit yield formation, but reduced fruit quality. Conversely, low planting density resulted in the lowest light interception and yield per cultivation area. Dynamic spacing, which involves growing plants at high planting density but spacing them apart to maintain constant ground coverages, resulted in the same fruit quality but doubled yield, thus mitigating density-induced trade-offs.

Controlled environment agriculture is a fast growing technology revolutionizing plant production. With its potential to enhance food security in harsh climates and provide consumers with fresh produce year-round, CEA offers significant promise. To unlock this potential, understanding the role of light is paramount. Lighting technologies are continuing to advance, expanding the possibilities for growers and researchers, enabling more diverse applications. However, in order to fully optimize growth, it is important to have continued research related to the interactions of light with other environmental parameters. Additionally, multi-disciplinary science studying the impact of light on pest and disease will allow for a comprehensive approach for producers. The manuscripts contained within the Research Topic serve as a foundation for these integrative advancements.

Author contributions

JL: Conceptualization, Writing – review & editing. XH: Conceptualization, Writing – review & editing. VV-K: Conceptualization, Writing – original draft, Writing – review & editing. LM: Conceptualization, Writing – review & editing.

Conflict of interest

The authors declare that the research was conducted in the absence of any commercial or financial relationships that could be construed as a potential conflict of interest.

The author(s) declared that they were an editorial board member of Frontiers, at the time of submission. This had no impact on the peer review process and the final decision.

Publisher's note

Reference

Pattison, P. M., Tsao, J. Y., and Brainard, G. C. (2018). LEDs for photons, physiology and food. *Nature* 563, 493–500. doi: 10.1038/s41586-018-0706-x

frontiers in Plant Science

ORIGINAL RESEARCH
published: 22 March 2022
doi: 10.3389/fpls.2022.801656

Modulated Light Dependence of Growth, Flowering, and the Accumulation of Secondary Metabolites in Chilli

Eva Darko[1], Kamirán A. Hamow[1], Tihana Marček[2], Mihály Dernovics[1], Mohamed Ahres[1] and Gábor Galiba[1,3]*

[1] Agricultural Institute, Centre for Agricultural Research, Martonvásár, Hungary, [2] Faculty of Food Technology, Josip Juraj Strossmayer University of Osijek, Osijek, Croatia, [3] Georgicon Faculty, Hungarian University of Agriculture and Life Sciences, Keszthely, Hungary

Chili is widely used as a food additive and a flavouring and colouring agent and also has great importance in health preservation and therapy due to the abundant presence of many bioactive compounds, such as polyphenols, flavonoids, carotenoids, and capsaicinoids. Most of these secondary metabolites are strong antioxidants. In the present study, the effect of light intensity and spectral composition was studied on the growth, flowering, and yield of chilli together with the accumulation of secondary metabolites in the fruit. Two light intensities (300 and 500 μmol m^{-2} s^{-1}) were applied in different spectral compositions. A broad white LED spectrum with and without FR application and with blue LED supplement was compared to blue and red LED lightings in different (80/20 and 95/5%) blue/red ratios. High light intensity increased the harvest index (fruit yield vs. biomass production) and reduced the flowering time of the plants. The amount of secondary metabolites in the fruit varied both by light intensity and spectral compositions; phenolic content and the radical scavenging activity were stimulated, whereas capsaicin accumulation was suppressed by blue light. The red colour of the fruit (provided by carotenoids) was inversely correlated with the absolute amount of blue, green, and far-red light. Based on the results, a schematic model was created, representing light-dependent metabolic changes in chilli. The results indicated that the accumulation of secondary metabolites could be modified by the adjustment of light intensity and spectral composition; however, different types of metabolites required different light environments.

Keywords: capsaicine, flavonoids, LED lighting, secondary metabolites, chilli

OPEN ACCESS

Edited by:
María Serrano, Miguel Hernández University of Elche, Spain

Reviewed by:
Umakanta Sarker, Bangabandhu Sheikh Mujibur Rahman Agricultural University, Bangladesh
Mark Lefsrud, McGill University, Canada

****Correspondence:***
Eva Darko
darko.eva@atk.hu

Specialty section:
This article was submitted to Crop and Product Physiology, a section of the journal Frontiers in Plant Science

Received: *25 October 2021*
Accepted: *01 February 2022*
Published: *22 March 2022*

Citation:
Darko E, Hamow KA, Marček T, Dernovics M, Ahres M and Galiba G (2022) Modulated Light Dependence of Growth, Flowering, and the Accumulation of Secondary Metabolites in Chilli. Front. Plant Sci. 13:801656. doi: 10.3389/fpls.2022.801656

INTRODUCTION

Chilli is widely used as a food additive, a flavouring and colouring agent, and as a part of traditional medicine; it is used to treat, for instance, coughs, sore throat, rheumatism, and gastrointestinal ailments. It has great importance in preventing chronic diseases, such as diabetes and high cholesterol levels, cardiovascular or neurodegenerative diseases, and it provides protection against different types of cancer (Wahyuni et al., 2013). The beneficial therapeutic effects of

the chilli fruit are mainly associated with the abundant presence of phytochemicals, such as carotenoids, flavonoids, polyphenols, and capsaicinoids. Most of these are strong antioxidants with anti-inflammatory, anticancer, and antimicrobial effects (Sarker et al., 2018c). They can act as immunomodulators (Jimenez-Garcia et al., 2013). While they can directly scavenge various free radicals, carotenoids give the attractive colours of the fruit, and flavonoids (such as quercetin and kaempferols) protect the low-density lipoprotein cholesterols from oxidation. They stimulate the enzymes involved in the detoxification of cancerogenic substrates and inhibit inflammations (Jimenez-Garcia et al., 2013).

Capsaicinoids, including trans-capsaicin (t-C), dihydrocapsaicin (DHC), nordihydrocapsaicin (n-DHC), homocapsaicin (h-C), and homodihydrocapsaicin (h-DHC) are responsible for the hotness (the pungency level) of the chilli and affect the cardiovascular and respiratory systems (Wahyuni et al., 2013). The pungency of capsaicinoidsis is usually expressed in Scoville heat units (SHU), indicating the highest dilution of a chilli fruit extract at which heat can be detected (Scoville, 1912). Nowadays, SHU is mainly determined by chromatographic methods, which are considered to be more reliable and accurate (Nwokem et al., 2010).

In chilli fruit, the amount of the main secondary metabolites shows enormous variations between the different cultivars, and it strongly depends on the maturity stage of the plants and the environmental conditions where the plants grow (Wahyuni et al., 2011; Hernández-Pérez et al., 2020). As summarised by Antonio et al. (2018), the capsaicinoid content of chilli varies from 28 to 200,000 μg of g dry fruit, providing 100–2,000,000 SHU, which enables chilli to be used for various purposes. For instance, moderate or low capsaicin content found in a cherry bomb type chilli is preferable for medical purposes due to low alkaloid toxicity (Acunha et al., 2017). The carotenoid, flavonoid, and polyphenol contents of the chilli fruit also show great variability (Wahyuni et al., 2011; Lemos et al., 2019). However, the high diversity in the metabolic profile made it a difficult task to understand the biochemical behaviour of plants grown under different environmental conditions.

Light is one of the most important environmental factors that determine the growth and development of plants. Through photosynthesis and different kinds of photoreceptors, light intensity and spectral composition affect biomass and yield formation through the modification of the primary and secondary metabolic pathways. The application of LED (light-emitting diode) technology in plant cultivation has accelerated the research on the effect of light fluence and wavelength on plant metabolism.

The influence of LEDs on growth and yield production has been widely investigated in many vegetable crops as summarised in several papers (Olle and Viršile, 2013; Darko et al., 2014; Loi et al., 2021). These studies have revealed that different light environments (including light intensity and spectral composition) are optimal for different kinds of crops, and that the use of a continuous wide spectrum composed of white, red, and blue LEDs is more suitable for plant cultivation than red and blue LEDs only (i.e., the lack of the green region) (Song et al., 2017; Liu et al., 2019; Naznin et al., 2019).

However, comparing the ample amount of data obtained from different species grown under different environmental conditions is difficult. The main light factors determining a given morphological or physiological parameter have not been identified in many species. Is it the absolute amount or the relative ratio of different light wavelengths that counts? Even less information is available about how the different kinds of LEDs affect the individual metabolic pathways—this is especially true for the production of secondary metabolites—in spite of the fact that LEDs provide unique possibilities for the targeted manipulation of plant metabolism (Darko et al., 2014). Only a few papers discuss the metabolic changes in chilli grown under LEDs. An early research studied the leaf and stem anatomy of Hungarian wax chilli (Schuerger et al., 1997). Later, changes in the primary (sugar, starch, and proteins) and secondary (fruit colour and the pungency level of capsaicinoids) metabolites were compared in chilli grown under monochromatic red or blue LEDs and under a 1:1 mixture of red and blue LEDs (Gangadhar et al., 2012). The highest biomass and yield were found under combined blue and red LEDs, and were accompanied by intense fruit colour. However, pure blue LEDs stimulated the accumulation of capsaicinoids. Recently, detailed metabolomic analysis focusing on capsaicinoids has been carried out on the fruit of a super-hot chilli grown in a greenhouse (under sunlight) supplemented with monochromatic red, blue, and red + blue (1:1) lightings for 5 h (Yap et al., 2021). Although the yield was the highest under sunlight (control), the additional blue LEDs significantly increased the accumulation of capsaicinoids, including C, DHC, n-DHC, h-C, and h-DHC (Yap et al., 2021). These results indicate that applying LED technology in the growth of chilli plants can be utilised for modifying the quality of the product, especially the secondary metabolite contents.

The aim of this research was to study the growth, yield, and the accumulation of several secondary metabolites (carotenoids, capsaicinoids, and phenolic compounds) and the antioxidant capacity of the fruit of chilli grown under pure artificial (LED) lighting conditions. The effects of blue and red LEDs were compared to different broad white spectrums with and without far-red application and with an increased blue region. Correlation analyses were performed to reveal the light factors affecting the production of these secondary metabolites.

MATERIALS AND METHODS

Plant Materials and Growth Conditions

A cherry bomb type Hungarian chilli (*Capsicum annuum* cv. Kalocsai) was used in the experiments. The treatments were arranged following a completely randomised block design and repeated 3 times. Before reaching the eight-leaf stage, the plants were grown in 10-cm- × –10-cm- × –6.5-cm jiffy pots (Jiffy Group, Oslo, Norway) placed in streamline half-strength Hoagland solution under the same conditions; the temperature was between 22 and 25°C, and the light intensity was 250 ± 12 μmol m^{-2} s^{-1}, provided by fluorescent lamps

for 12 h per day. Afterward, the plants were transplanted into 5-L plastic pots (1 plant/pot) filled with a 2:1:1 (v/v/v/) mixture of garden soil, humus, and sand. About 72 pots were randomised into 6 groups, and the plants were grown under 6 different light regimens (designated regimen A-F) for 87 days (till maturity) at 16/8 h photoperiod, 22/25°C day/night temperature, and 70% humidity in growth chambers (PGV-36, ConvironEnv LTD, Winnipeg, MB, Canada). The light was provided by LED modules. Each LED module is composed of wide-spectrum LEDs and 4 types of narrow-bandwidth LEDs with dominant wavelengths of 420 and 448 nm ("blue LED"), 665 nm ("red LED"), and 750 nm ("far-red LED"), respectively. All of them could be controlled independently. In the present study, different LED-based light combinations (regimens) were tested; as basic spectrums, only the red and blue LEDs were used at moderate (300 μmol m^{-2} s^{-1}) light intensity in two different red/blue proportions: 95/5% (regimen A) and 80/20% (regimen B). Since sunlight has a wide spectrum, another spectrum was designed, containing white, red, and blue LEDs in a proportion of 65:20:15 of blue:green:red regions, giving a total light intensity of 300 μmol m^{-2} s^{-1} (regimen C). Furthermore, to simulate sunrise and sunset (Kotilainen et al., 2020), the latter spectrum was also supplemented with 5% far-red light in the first and last hours of the light periods (Regimen D). To study whether the absolute or the relative amount of different spectral regions is important, this latter spectral combination was also used at a higher (500 μmol m^{-2} s^{-1}) light intensity (Regimen E). Finally, the light regimen E was modified by increasing the proportion of the blue region by 5% in the middle of the light cycle for 4 h (Regimen F). The light spectrums and the programmes are presented in **Supplementary Figure 1**. In addition, the light intensities and the spectral characteristics of the light were integrated daily (DLI), as summarised in **Table 1**. This type of calculation was used for correlation analysis. During the growth period, the plants were rearranged regularly within the light regimens and watered every day. A nutrient solution containing 41 mg/L N; 7 mg/L P_2O_5; 21 mg/L K_2O; 4 mg/L Mg; 5 mg/L Ca; and 1 mg/L B, Cu, Mn, Fe, and Zn was applied two times a week to ensure adequate water and nutrient supply.

Morphological Parameters

At harvest (87 days after the start of the light treatments), several morphological parameters were determined, such as the aboveground plant height and mass (with and without yield) and the amount and weight of the fruit. In the present study, the aboveground plant mass without yield is designated as green mass, which includes the weight of the shoot and leaves. The number of flowers was counted during the flowering period (16–46 days after the light treatments). Harvest index (HI) was calculated as the ratio of the fruit yield and total aboveground biomass production of each plant. The morphological parameters were determined from 10 plants per light treatment.

Metabolomics Analysis

For the metabolomics analyses, the ripe fruit was collected from each plant. The fruit was frozen in liquid nitrogen and kept at −80°C until preparation. Five samples were prepared per light regimen. Each sample consisted of 10 pieces of fruit collected from two plants (5 pieces of fruit per plant). During the extraction, the samples were homogenised using a blender as required for the analytical methods.

The total carotenoid content was determined from fruit pericarps according to the protocol described by Acunha et al. (2017). For each sample, 0.5-g fruit extract was homogenised with 10-ml solvent composed of hexane/methanol/acetone/toluene at 10:6:7:7 for 1 h in the dark. Next, carotenoids were transferred to the hexane (10 ml) phase, and their amount was measured spectrophotometrically, using a UV-visible spectrophotometer (160A, Shimadzu Corp., Kyoto, Japan).

Total phenolic content was determined according to Gomes et al. (2021). The samples (0.5-g fruit pericarps for each) were extracted in methanol (1:10), and the phenolic content was

TABLE 1 | Spectral characteristics of light used in the experiments according to daily light integral (DLI), a red/blue ratio, and a proportion of different regions.

Light regimens	DLI (mol/day)					Red/Blue ratio	Red%	Green%	Blue%	Far-red%
	SUM	Blue region (400–500 nm)	Green region (500–600 nm)	Red region (600–700 nm)	Far-Red region (> 700 nm)					
A	17.28	0.86	0	16.42	0	19	95	0	5	0
B	17.28	3.46	0	13.82	0	4.0	80	0	20	0
C	17.28	2.59	3.46	11.23	0	4.3	65	20	15	0
D	17.28	2.59	3.46	11.12	0.11	4.3	65	20	15	0.6
E	28.8	4.32	5.76	18.53	0.18	4.3	65	20	15	0.6
F	28.8	4.72	5.76	18.53	0.18	3.9	64	20	16	0.6

Light regimens used: Regimen A, red and blue LEDs were used with a 95:5 ratio at moderate (300 μmol m^{-2} s^{-1}) light intensity; Regimen B, utilisation of red and blue LEDs with an 80:20 ratio at moderate (300 μmol m^{-2} s^{-1}) light intensity; Regimen C, a wide spectrum (containing white, red, and blue LEDs) in an average proportion of 65:20:15 of red:green:blue at moderate (300 μmol m^{-2} s^{-1}) light intensity: Regimen D, a wide spectrum supplemented with far-red application in an average proportion of 65:20:15:0.6 of red:green:blue:far-red at moderate (300 μmol m^{-2} s^{-1}) light intensity; Regimen E, a wide spectrum supplemented with far-red application in an average proportion of 65:20:15:0.6 of red:green:blue:far-red at high (500 μmol m^{-2} s^{-1}) light intensity; Regimen F, a wide spectrum supplemented with far-red and blue light application in an average proportion of 64:20:16:0.6 of red:green:blue:far-red at high (500 μmol m^{-2} s^{-1}) light intensity. The total photosynthetic photon flux density (PPFD) integrated between 400 and 750 nm and the spectral distribution were determined by PG200N Spectral PAR Meter (Uprtek Europe DI Technology GmbH, Aachen, Germany), where the blue region was integrated between 400 and 500 nm, the green region between 500 and 600 nm, the red region between 600 and 700 nm, and the far-red region between 700 and 750 nm.

measured spectrophotometrically based on its reaction with Folin-Ciocalteu reagent. Gallic acid standard was used for the calibration curve, and the results were expressed in gallic acid (Merck-Sigma group, Darmstadt, Germany) equivalents (mg/g fresh mass).

The antioxidant activity of the fruit was determined by a DPPH (2,2-diphenyl-1-picrylhydrazyl) free radical assay according to Oney-Montalvo et al. (2020), and the radical scavenging activity was calculated in DPPH% reduction determined after 30-min reaction time.

The amount of capsaicinoids and phenolic composition were determined by the use of a Waters Acquity I-class Ultra performance liquid chromatography (UPLC) system equipped with a PDA detectors, which was coupled to either a Xevo TQ-XS Triple Quadrupole Mass Spectrometer (Waters Corp.; Milford, MA, United States) or a Vion IMS-QTOF-MS (Waters). The full protocols, including the preparation of samples, separation, identification, and the quantification of compounds, are detailed in **Supplementary Material** (Worksheets a–c); here, only the main parameters are given.

The extraction of capsaicinoids was carried out according to the Hungarian Standard Method "MSZ9681-4:2002." Briefly, homogenised fruit samples (0.5-g dry mass) were extracted with 50-ml methanol in two steps by ultrasonication. The extracts were combined, centrifuged (4,000 × g for 15 min), and the supernatants were filtered through 0.22-μm PTFE syringe filters and were diluted 20-fold prior to analysis. The separation of capsaicinoids was achieved on a Supelco Core Phenyl-Hexyl analytical column (2.7 μm; 4.6 mm × 150 mm; Merck-Sigma group) under water: acetonitrile gradient elution. A Xevo TQ-XS MS detector equipped with a Unispray source was used in multiple reaction monitoring (MRM) and a positive ion mode. Quantification of the compounds was based on the characteristic fragment of m/z 137 of the $[M + H]^+$ parent masses of capsaicinoids. A detailed description is found in **Supplementary Material** (Worksheet a).

The extraction and chromatographic analyses of phenolic compounds were carried out according to Vrhovsek et al. (2012) and Pál et al. (2019) with slight modifications. Homogenised fruit pericarps (0.5-g FW) were spiked with 50 ng $[^2H_6](+)$- *cis-, trans*-abscisic acid (OlChemIms.r.o. Olomouc, Czech Republic), serving as an internal standard before the extraction with 2-ml- × –2.5-ml methanol: water (2:1 v/v%). After centrifugation (at 14,000 × *g;* 4°C; for 10 min), 2.5 ml of n-hexane was added to the supernatants to remove carotenoids. Then, the phases were separated by centrifugation and the methanol: water phase was filtered through 0.22-μm PTFE syringe filters prior to analysis. Separation of phenolic compounds was achieved on an HSS T3 column (1.8 μm; 100 mm × 2.1 mm; Waters) under water: acetonitrile gradient elution (details to be found in **Supplementary Material**, Worksheet b). Xevo TQ-XS MS was utilised in MRM mode, and the respective MRM transitions used for quantification are listed in **Supplementary Material** (Worksheet b). Furthermore, identification of major phenolic analytes detected by PDA at λ = 330 nm, which were uncovered by the MRM methods, was achieved with the UPLC-Vion IMS-QTOF-MS setup according to Jeong et al. (2011), Morales-Soto et al. (2013), Kelebek et al. (2020), Mara de Menezes Epifanio et al. (2020), and Guclu et al. (2021) (for instrumental details, see **Supplementary Materials**, Worksheet c). Quantification of these analytes was carried out at λ = 330 nm against quercetin 3-rutinoside (rutin) reference material (Merck-Sigma group). Furthermore, several compounds possessed considerably higher abundance in the function of experimental setups on the basis of UV detection at λ = 330 nm, but they could not be unambiguously identified (referred to as NI1-20). However, additional data could be provided on the basis of their UPLC-MS characteristics (retention time, tentative elemental composition, MS/MS acquisitions, etc.) in **Supplementary Material** (Worksheet c), and HR-MS figures (presented in the Supplementary PDF File).

Statistics

For each light regimen, the data presented in the tables and the figures derived from triplicate experiments involve at least 10 or 5 biological replicates of the morphological and analytical investigations, respectively. The SPSS 22 statistical programme and Tukey's *post-hoc* test were used to determine differences between the light treatments. Different letters indicate significant differences at the $p < 0.05$ level. Spearman's rank order correlation coefficients (at the significance level $p < 0.05$) were calculated with the Statistica 13.5 software (TIBCO Software Inc., Palo Alto, CA, United States) in order to determine the main light factors affecting the physiological and metabolic parameters measured. The value -1 represents negative (inverse) correlation, 1 indicates positive (direct) correlation, whereas the values close to zero indicate no correlation.

RESULTS

Plant Growth, Flowering, and Yield Production

Plant height and green mass were measured to characterise the growth of chilli under different light intensities and spectral compositions (**Table 2**). The greatest plant height was measured when the plants were grown under blue and red light with 95/5 red/blue proportion at 300 μmol m^{-2} s^{-1} light intensity (light Regimen A), whereas the lowest values were detected in those plants which were grown at high light intensities with complete spectral composition (light Regimens E and F). Surprisingly, high light intensity (light Regimens E and F) resulted in the lowest green mass (biomass without the fruit); meanwhile, the yield was the highest, which was reflected in the high harvest index (**Table 2**). In contrast, the red and blue LEDs with a 95:5 ratio (light Regimen A) provided the highest green mass, which was accompanied with the lowest fruit yield, resulting in the lowest harvest index (**Table 2**).

Considering the data of yield, the fruit mass per plant and the average fruit mass together (**Table 2**), it appeared that high light intensity with complete spectral composition (light Regimens E and F) provided large amount of fruit with medium-average fruit mass. The similar spectral composition at moderate light intensity (light Regimens C and D) provided less fruit combined

TABLE 2 | Plant morphology and biomass production of chilli grown under different light regimens (A–F).

Light regimens	Plant height (cm)	Greenmass (g)	No. of fruit per plant	Yield (g) of fruit per plant	Average fruit mass (g/pc.)	HI (yield/biomass)
A	61.5 ± 3.0a	114.7 ± 12.0a	8.9 ± 1.3a	54.4 ± 4.4b	6.11 ± 1.14*c*	0.32 ± 0.04b
B	59.4 ± 3.2a	112.3 ± 12.8a	8.6 ± 1.3ab	63.4 ± 5.3ab	7.37 ± 1.19*bc*	0.35 ± 0.05ab
C	58.8 ± 2.2a	111.6 ± 11.2a	8.4 ± 1.3ab	67.0 ± 5.6a	8.00 ± 1.24a	0.38 ± 0.05ab
D	58.0 ± 2.6ab	102.3 ± 12.4ab	7.4 ± 1.1*b*	59.2 ± 5.7ab	7.96 ± 1.25a	0.37 ± 0.05ab
E	54.4 ± 2.1*bc*	92.9 ± 10.5b	9.1 ± 1.2a	67.4 ± 5.1a	7.43 ± 1.12ab	0.42 ± 0.04a
F	51.1 ± 2.7*c*	87.8 ± 10.8b	9.0 ± 1.2a	66.1 ± 5.3a	7.34 ± 1.11ab	0.43 ± 0.04a

Green mass represents the plant mass without yield mass. HI: harvest index calculated as the ratio of fruit yield and total above-ground biomass. Light conditions used: A, application of red and blue LEDs with a 95:5 ratio at moderate (300 μmol m^{-2} s^{-1}) light intensity; B, utilisation of red and blue LEDs with an 80:20 ratio at (300 μmol m^{-2} s^{-1}) light intensity; C, a wide spectrum with an average proportion of 65:20:15 of red:green:blue at moderate (300 μmol m^{-2} s^{-1}) light intensity: D, A wide spectrum supplemented with far-red application in an average proportion of 65:20:15:0.6 of red:green:blue:far-red at moderate (300 μmol m^{-2} s^{-1}) light intensity; E, a wide spectrum supplemented with far-red application in an average proportion of 65:20:15:0.6 of red:green:blue:far-red at high (500 μmol m^{-2} s^{-1}) light intensity; F, a wide spectrum supplemented with far-red and blue light application in an average proportion of 64:20:16:0.6 of red:green:blue:far-red at high (500 μmol m^{-2} s^{-1}) light intensity. Values indicated with different letters are significantly different at $p < 0.05$.

with the highest average fruit mass. When only blue and red LEDs with high proportion of blue light (light Regimen B) were applied, the plants developed large amount of fruit with low-average fruit mass (**Table 2**). The average fruit weight was the lowest when the plants were grown under blue and red light with 95/5 red/blue proportion at moderate light intensity (light Regimen A).

However, the pairwise comparison of growth parameters (i.e., plant height and green mass) showed significant differences between light Regimens A and B, C and D, and E and F, indicating that plant height and green mass were mainly affected by light intensity. The adverse effect of a high-red proportion applied in light Regimen A was detected in the lowest harvest index and in the average fruit mass. On the other hand, the application of far-red light at the beginning and at end of the light period, as well as the addition of blue light in the middle of the light period, all appeared ineffective.

The light conditions modified the flowering period (**Figure 1**). The average number of flowers was similar under all light regimens, but high light intensity (light Regimens E and F) accelerated flowering, followed by the far-red application at moderate light intensity (light Regimen D). When only blue and red LEDs were used, the high proportion (20%) of blue light (light Regimen B) prolonged the flowering period, while the high proportion (95%) of red light (light Regimen A) delayed it.

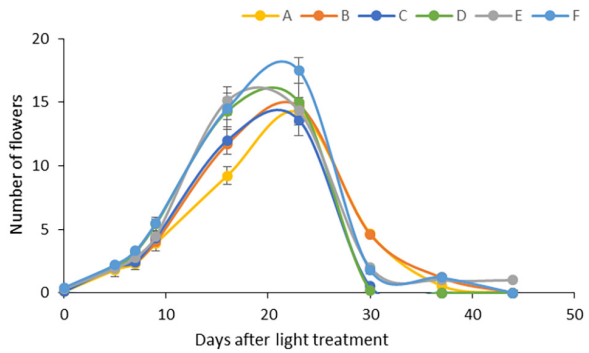

FIGURE 1 | Flowering under different light regimens: **(A)** Application of red and blue LEDs with a 95:5 ratio at moderate (300 μmol m^{-2} s^{-1}) light intensity; **(B)** utilisation of red and blue LEDs with a 80:20 ratio at (300 μmol m^{-2} s^{-1}) light intensity; **(C)** a wide spectrum with an average proportion of 65:20:15 of red:green:blue at moderate (300 μmol m^{-2} s^{-1}) light intensity: **(D)** a wide spectrum supplemented with far-red application in an average proportion of 65:20:15:0.6 of red:green:blue:far-red at moderate (300 μmol m^{-2} s^{-1}) light intensity; **(E)** a wide spectrum supplemented with far-red application in an average proportion of 65:20:15:0.6 of red:green:blue:far-red at high (500 μmol m^{-2} s^{-1}) light intensity; **(F)** a wide spectrum supplemented with far-red and blue light application in an average proportion of 64:20:16:0.6 of red:green:blue:far-red at high (500 μmol m^{-2} s^{-1}) light intensity.

Light-Induced Metabolomic Changes in the Fruit

Capsaicinoids are one of the most important components of chilli. Capsaicinoid content, including the amount of trans-capsaicin (t-C), dihydrocapsaicin (DHC), nordihydrocapsaicin (n-DHC), homocapsaicin (h-C), and homodihydrocapsaicin (h-DHC), varied significantly under different light environments (**Table 3**). Surprisingly, the total amount of capsaicinoids was reduced in the fruit of the plants grown under high light intensity (light Regimens E and F), as well as under moderate light intensity with a high proportion of blue light (light Regimen B) as compared to other spectral combinations, where the amount of blue light was lower (**Table 1**). The application of FR light did not modify significantly the amount of capsaicinoids either at moderate or at high light intensity, according to the pairwise comparisons of light Regimens C and D, and E and F, respectively. These light-induced differences were observed in most of the capsaicinoid components, providing 40–83% maximal deviations, depending on the components.

The t-C and DHC were the dominant capsaicinoids, reaching 85–90% within the total amount. The n-DHC and h-DHC represented about 5% of the total capsaicinoid content, whereas h-C was about 1–2%. When the relative proportions of each component were compared, the relative amount of t-C and DHC changed inversely with light treatment. Namely, in those cases where the total capsaicinoid content was high (under light Regimens A, C, and D), the relative amount of t-C (t-C/DHC ratio) was lower (ranged between 1.1 and 1.17) than in those cases where the total amount of capsaicinoids was low (under light Regimens B, E, and F) (**Table 3**). The h-DHC changed similarly

TABLE 3 | The amount of capsaicinoids (mg/kg DW) and the pungency level Scoville Heat Unit (SHU) value of chilli fruits: trans-capsaicin (t-C), dihydrocapsaicin (DHC), nordihydrocapsaicin (n-DHC), homocapsaicin (h-C); homodihydrocapsaicin (h-DHC), and the values of SHU.

Light regimens	Total capsaicinoids	t-C	DHC	n-DHC	h-DHC	h-C	SHU value
A	1, 216 ± 79a	624 ± 51*ab*	440 ± 26a	72 ± 5.1a	52 ± 4.8a	22 ± 2.5a	18, 303 ± 1, 174a
B	887 ± 73b	462 ± 39c	316 ± 33b	52 ± 5.8b	38 ± 3.8b	15 ± 1.6b	13, 373 ± 1, 094b
C	1, 249 ± 70a	672 ± 35a	428 ± 27a	74 ± 4.7a	50 ± 4.4a	20 ± 1.3a	18, 868 ± 1, 043a
D	1, 183 ± 82a	598 ± 42b	435 ± 38a	75 ± 6.8a	51 ± 2.5a	19 ± 1.2a	17, 799 ± 1, 240a
E	928 ± 151b	518 ± 66bc	301 ± 60b	55 ± 10.2bc	36 ± 9.7b	15 ± 3.2b	14, 030 ± 1, 992b
F	859 ± 65b	487 ± 37c	282 ± 25b	41 ± 3.7c	31 ± 2.9b	16 ± 1.8b	13, 072 ± 984b

Light conditions used: A, application of red and blue LEDs with a 95:5 ratio at moderate (300 μmol m^{-2} s^{-1}) light intensity; B, utilisation of red and blue LEDs with a 80:20 ratio at (300 μmol m^{-2} s^{-1}) light intensity; C, a wide spectrum with an average proportion of 65:20:15 of red:green:blue at moderate (300 μmol m^{-2} s^{-1}) light intensity: D, a wide spectrum supplemented with far-red application in an average proportion of 65:20:15:0.6 of red:green:blue:far-red at moderate (300 μmol m^{-2} s^{-1}) light intensity; E, a wide spectrum supplemented with far-red application in an average proportion of 65:20:15:0.6 of red:green:blue:far-red at high (500 μmol m^{-2} s^{-1}) light intensity; F, a wide spectrum supplemented with far-red and blue light application in an average proportion of 64:20:16:0.6 of red:green:blue:far-red at high (500 μmol m^{-2} s^{-1}) light intensity. Values indicated with different letters are significantly different at $p < 0.05$.

to DHC, whereas the relative proportion of other components (n-DHC and h-C) did not show significant changes. Accordingly, the SHU indices (which indicate the most characteristic feature of chilli fruit, the hotness, and the spicy flavour) ranged between 13,000 and 19,000 (**Table 3**). Higher values were observed under light Regimens A, C, and D, while lower values were detected under light Regimens B, E, and F like in the case of t-C and DHC values. The former group (light Regimens A, C, and D) contained low absolute amount of blue light, while the light Regimens B, E, and F emitted higher absolute amount of blue light (**Table 1**). The SHU values imply a moderate pungency level; however, they are significantly higher than that of a typical cherrybomb fruit, whose SHU index generally ranges between 2,500 and 5,000.

The total amounts of carotenoids and phenolics and the antioxidant scavenging activity of the fruit were determined (**Figure 2**). The carotenoid content, responsible for fruit colours, was higher when the plants were grown in moderate light intensity (under light Regimens A, B, C, and D) compared to those fruits that were grown under high light intensity (light Regimens E and F) (**Figure 2A**), indicating that amongst the light conditions used, light intensity was the most dominant light factor that influenced carotenoids. Inversely, the highest amount of phenolic content was detected under high light intensity (light Regimens E and F), followed first by moderate light intensity with a high proportion of blue light (light Regimen B), and then by Regimens A and C. The lowest value was measured when a wide spectrum was used with far-red application under moderate light intensity (light Regimen D) (**Figure 2B**). The antioxidant capacity was also high at high light intensity (light Regimens E and F), especially when additional blue light was applied (Regimen F), followed by light Regimens D, B, and C (**Figure 2C**). The lowest antioxidant capacity was found when blue and red LEDs with a high proportion of red light were used (light Regimen A). The pairwise comparison of the radical scavenging activity and phenolics showed that both the light intensity and the spectral composition influenced the production of these metabolites.

Light dependence of phenolic compounds was determined by UPLC-MS analyses. Mainly, phenolic acids, coumarins, phenylpropanoids, and flavonoids, including flavones, flavonones, and flavonols, were identified in the fruit extracts. In addition, some other non-identified compounds (NI1-20) were also detected. Since they also showed light-dependence variation, the non-identified compounds (quantified in rutin equivalent) were also included in the figures. The amounts of the metabolites were indicated in **Supplementary Table 1**, and their light-induced changes were presented in **Figure 3**. Chilli fruit contains large amounts of flavones, capsianosides, precursors of phenylpropanoids and also, many non-identified compounds (NI1, 2, 3, 9, and 10) together with smaller amounts of flavonones, flavonols, and coumarins. Several metabolites showed light-dependent variations. Significant light-induced differences (more than 200% of the lowest value) were found for chlorogenic acid, ferulic acid, most flavones, flavonones, and flavonols, as well as for capsianoside III and non-identified compounds (NI) 5, 9, 10, and 19. These compounds make up 44% of all compounds and 65% of the total amounts (in μg/g FW). The light regimen induced moderate changes (ranging between 150 and 200%) for sinapic acid and its hexoside, dihydro-phaseic acid, capsianoside IV diglucoside 2, capsianoside V, and some minor luteolin and apigenin sugar derivatives, together with many non-identified compounds, including NI3, 7, 11–13, 15, 17, 18, and 20. These make up 30% of the total compounds and 27% of the total amount. About 26% of all compounds showed slight (but statistically significant) variation under different light environments, and they make up only 8% of the total amount. These compounds are feruloylhexoside, aesculetin, abscisic acid derived from carotenoids, phaseic acid, capsianoside IV diglucoside 1 casianoside derivative and several non-identified compounds, such as NI1, 2, 4, 7, 8, 14, and 16. These results indicate that the presence of phenolic compounds strongly depends on the light conditions. According to pairwise comparisons between light regimens A and B, C and D, and E and F), the blue light and far-red light caused significant changes in the amount of main phenolic compounds.

Light Factors Affecting the Growth and Production of Various Metabolites

According to the data, it seemed that, instead of specific light conditions used in the present experiments, the overall daily light, indeed, evoked the changes in the growth and metabolic

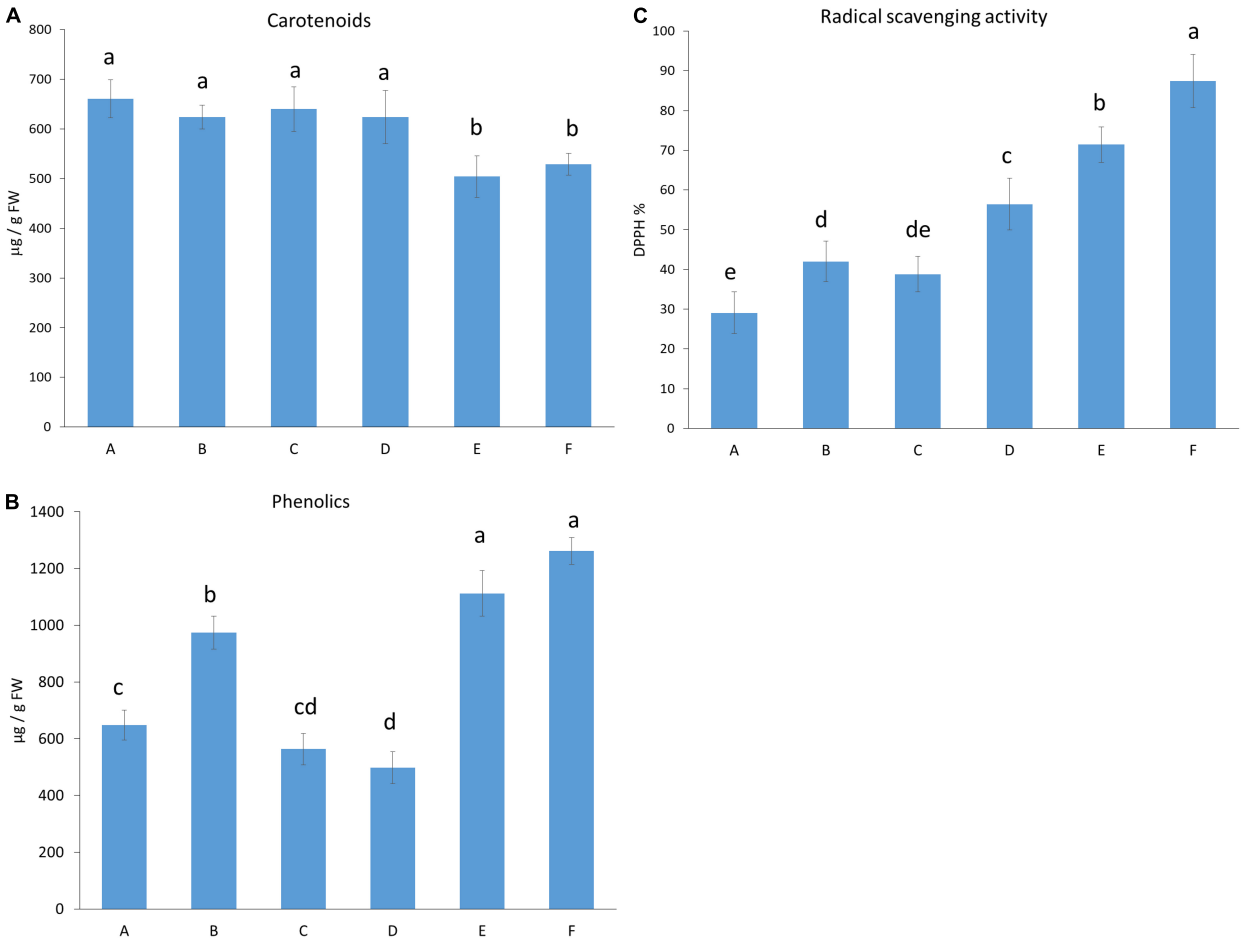

FIGURE 2 | Carotenoid **(A)** and total phenolic content **(B)**, and an antioxidant capacity of the fruit **(C)**. Light conditions used: **(A)** Application of red and blue LEDs with a 95:5 ratio at moderate (300 µmol m^{-2} s^{-1}) light intensity; **(B)**, utilisation of red and blue LEDs with an 80:20 ratio at (300 µmol m^{-2} s^{-1}) light intensity; **(C)** a wide spectrum with an average proportion of 65:20:15 of red:green:blue at moderate (300 µmol m^{-2} s^{-1}) light intensity: **(D)** a wide spectrum supplemented with far-red application in an average proportion of 65:20:15:0.6 of red:green:blue:far-red at moderate (300 µmol m^{-2} s^{-1}) light intensity; **(E)**, a wide spectrum supplemented with far-red application in an average proportion of 65:20:15:0.6 of red:green:blue:far-red at high (500 µmol m^{-2} s^{-1}) light intensity; **(F)** a wide spectrum supplemented with far-red and blue light application in an average proportion of 64:20:16:0.6 of red:green:blue:far-red at high (500 µmol m^{-2} s^{-1}) light intensity.

changes in the fruits. Therefore, a correlation analysis was performed between the light conditions used (**Table 1**) and the morphological and metabolomics values in order to reveal whether the absolute amount or the relative ratios of specific spectral regions affect the given parameters (**Figure 4**).

Plant height and green mass were related to the absolute amount of blue and green spectral regions. In addition, the percentage of green (G%) and red light (R%) moderately affected these parameters. The blue and green regions correlated negatively with growth parameters (e.g., as blue and green regions increase, the plant height and green mass decrease). The percentage of red light (R%) affected these parameters in positive direction. Yield (fruit mass per plant) was mainly affected by the amount of blue light, but the red/blue ratio appeared as important as the absolute amount of blue light. Yield was affected positively by blue light and negatively by the R/B ratio. Interestingly, the average fruit weight was affected by the G% and moderately by the R/B ratio. The harvest index strongly depended on the absolute amounts of blue, green, and far-red regions together with G%. Similar results were found for flowering time in an inverse tendency, indicating that the higher amount of blue, green, and far-red light induces early flowering of plants. These results demonstrated that, besides blue and red regions– in which the absolute amount of blue light and the R% or the R/B ratio may be effective—the green region also played an important role in plant growth, flowering, and yield production.

The accumulation of metabolites in the fruit also showed light-dependent variations. The absolute amount of blue light was the main factor affecting the accumulation of capsaicinoids, including all compounds, such as t-C, DHC, n-DHC, h-DHC, and h-C, and the SHU in this chilli. The carotenoid content was affected by the absolute amount of blue, green, and far-red regions. Both groups of metabolites showed inverse correlation with the light factors, i.e., a higher amount of light yielded a

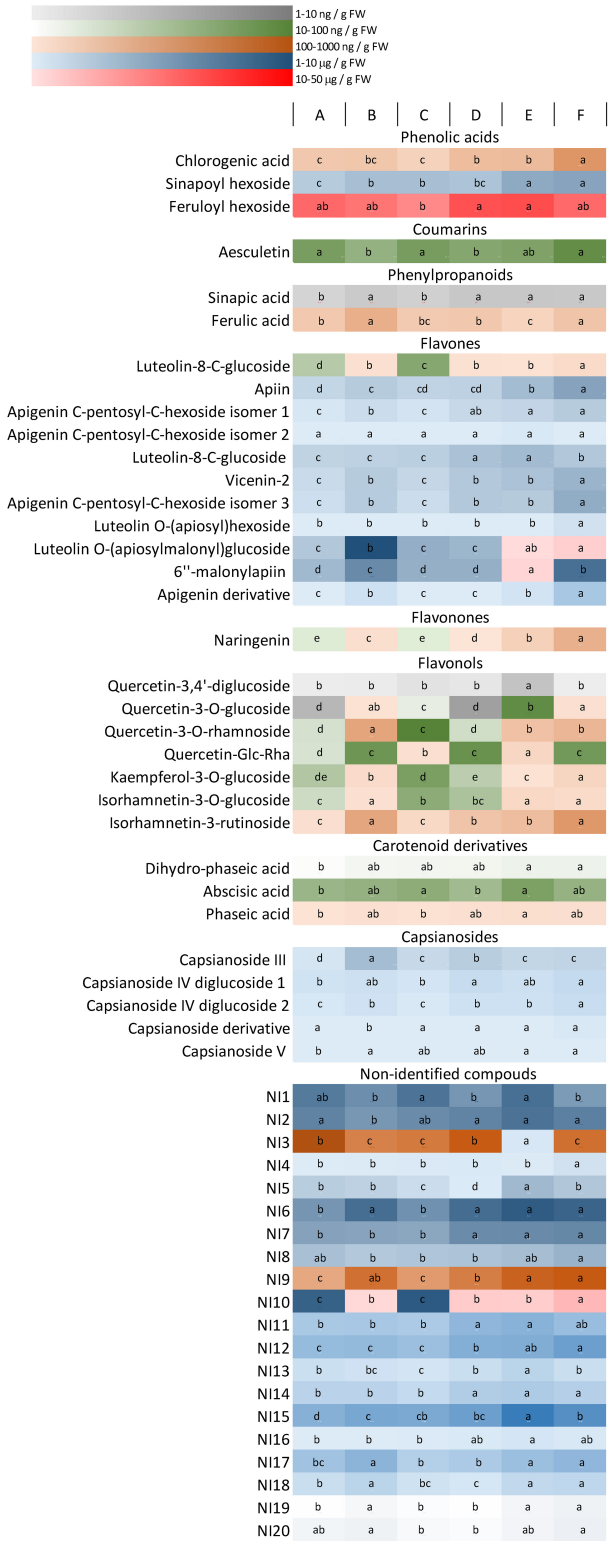

FIGURE 3 | A heat map representing the accumulation of phenolic compounds in the fruit. Different colours represent different concentration ranges. Differences between the values (within the rows) are indicated by different letters. The significance was determined at the $p < 0.05$ level, using

(Continued)

FIGURE 3 | Tukey' s *post-hoc* test. Light conditions used: **(A)** application of red and blue LEDs with a 95:5 ratio at moderate (300 μmol m^{-2} s^{-1}) light intensity; **(B)** utilisation of red and blue LEDs with an 80:20 ratio at (300 μmol m^{-2} s^{-1}) light intensity; **(C)** a wide spectrum with an average proportion of 65:20:15 of red:green:blue at moderate (300 μmol m^{-2} s^{-1}) light intensity: **(D)** a wide spectrum supplemented with far-red application in an average proportion of 65:20:15:0.6 of red:green:blue:far-red at moderate (300 μmol m^{-2} s^{-1}) light intensity; **(E)** a wide spectrum supplemented with far-red application in an average proportion of 65:20:15:0.6 of red:green:blue:far-red at high (500 μmol m^{-2} s^{-1}) light intensity; **(F)** a wide spectrum supplemented with far-red and blue light application in an average proportion of 64:20:16:0.6 of red:green:blue:far-red at high (500 μmol m^{-2} s^{-1}) light intensity.

lower amount of metabolites. In contrast, total phenolics showed direct (positive) correlation with the absolute amount of the blue and far-red regions. The antioxidant capacity of the fruit was correlated mainly with the amount of blue, green, and far-red regions and with FR%.

Detailed analysis of phenolic compounds also revealed strong light-dependent variations. Flavonoid (flavones, flavonones, and flavonols) content was mainly affected by absolute amount of the blue light but especially, in case of flavones (e.g., apigenin-sugar derivatives), far-red light also seemed to be important. A moderate effect of the green region could also be detected. Light did not significantly modify the amount of chlorogenic acid, ferulic acid, feruloylhexoside, and coumarin-type aesculetin. Similarly, the amount of abscisic acid did not change significantly, but its derivatives, phaseic, and dihydrophaseic acids were positively affected by blue, green, and far-red light and inversely by R% and the R/B proportion. The light dependency of many, approximately half of the non-identified metabolites (NI6, 7, 9–12 and 14–16), resembles that of flavones and differs from NI5, 8, 13, 17, 18, and 20. These results indicate that metabolic processes can be modified by the spectral composition of the light.

DISCUSSION

Plant cultivation under artificial light in indoor cultivation systems requires optimisation of light conditions. However, little to decide information has been available on specific light factors involved whether the absolute or the relative proportions of different spectral regions influence the growth and development of plants and their metabolic processes. Harmonisation of red and blue lighting to natural light environment can be a strategy for optimisation of artificial light environment. In the present study, the basic concept was to complete the commonly used red and blue spectra with white light, and then with FR treatment applied in the morning and evening periods (simulating the sunrise and sunset periods) at moderate and high light intensities. In addition, the energy level of light was increased in noon periods by adding supplemental blue lighting.

According to the results, the pairwise comparison of different light regimens, namely the different blue and red ratios (light Regimens A and B), and the application of white LED with or without far-red treatments (light Regimens C and D), together with the changes of light intensities (light Regimens E and F), showed that the pairwise changes were less important; indeed,

Variable	Amount of B	Amount of G	Amount of R	Amount of FR	B%	G%	R%	FR%	R/B
Plant height	**-0.883**	**-0.876**	-0.577	-0.494	-0.405	**-0.665**	**0.682**	-0.482	0.567
plant weight	**-0.813**	**-0.890**	-0.596	-0.478	-0.299	**-0.683**	**0.658**	-0.495	0.491
Fruit No.	0.472	0.118	**0.770**	0.164	0.113	-0.226	0.152	-0.116	0.011
Fruit weight	**0.822**	0.678	0.153	0.421	0.707	0.602	-0.766	0.279	**-0.809**
average fruit weight	0.333	0.559	-0.457	0.250	0.541	**0.811**	-0.483	0.371	**-0.770**
HI	**0.887**	**0.952**	0.434	**0.852**	0.677	**0.805**	-0.483	0.745	-0.689
flowering time max	**-0.886**	**-0.934**	-0.533	**-0.875**	-0.431	**-0.744**	0.766	-0.749	0.630
total caps	**-0.838**	-0.309	-0.633	-0.539	**-0.758**	0.009	0.209	-0.387	0.460
t-C	-0.728	-0.136	-0.542	-0.445	**-0.781**	0.159	0.085	-0.339	0.394
DHC	**-0.892**	-0.438	-0.680	-0.591	-0.577	-0.114	0.304	-0.406	0.496
n-DHC	**-0.821**	-0.358	-0.701	-0.534	-0.492	-0.027	0.194	-0.348	0.386
h-DHC	**-0.900**	-0.476	-0.685	-0.625	-0.560	-0.157	0.329	-0.446	0.495
h-C	**-0.925**	-0.441	-0.407	-0.580	**-0.797**	-0.214	0.479	-0.477	0.724
SHU	**-0.832**	-0.298	-0.629	-0.533	-0.592	0.020	0.201	-0.384	0.456
Total carotenoids	**-0.873**	**-0.822**	-0.491	**-0.904**	-0.359	-0.548	0.576	-0.761	0.493
DPPH %	**0.854**	**0.870**	0.553	**0.952**	0.386	0.671	-0.681	**0.881**	-0.555
Total Phenols	**0.817**	0.440	0.717	**0.808**	0.385	0.078	-0.195	0.396	-0.320
Phenolic acids									
Chlorogenic acid	0.672	0.604	0.615	**0.790**	0.207	0.371	-0.357	0.718	-0.281
Sinapoyl hexoside	**0.921**	**0.826**	0.666	**0.826**	0.437	0.566	-0.616	0.655	-0.557
Feruloyl hexoside	0.222	0.373	0.392	0.702	-0.101	0.242	-0.160	0.775	-0.015
Coumarins									
Aesculetin	0.190	0.554	0.459	0.421	-0.325	0.449	-0.216	0.306	0.118
Phenylpropanoids									
Sinapic acid	**0.800**	0.621	0.150	0.771	0.701	0.536	-0.709	**0.818**	-0.777
Ferulic acid	0.049	-0.608	-0.225	-0.456	0.476	-0.623	0.327	-0.443	-0.138
Flavones									
Luteolin-8-C-glucoside	**0.873**	0.530	0.279	0.684	**0.737**	0.377	-0.581	0.663	**-0.728**
Apiin	**0.841**	0.691	0.712	**0.784**	0.347	0.408	-0.445	0.628	-0.412
genin C-pentosyl-C-hexoside isomer 1	**0.881**	**0.750**	0.511	**0.896**	0.502	0.544	-0.622	**0.840**	-0.599
genin C-pentosyl-C-hexoside isomer 2	0.606	0.704	0.357	**0.825**	0.294	0.580	-0.593	**0.826**	-0.473
Luteolin-8-C-glucoside	0.571	**0.784**	0.274	**0.876**	0.250	**0.711**	-0.681	**0.918**	-0.485
Vicenin-2	**0.893**	**0.715**	0.526	**0.871**	0.526	0.495	-0.591	**0.805**	-0.599
genin C-pentosyl-C-hexoside isomer 3	**0.802**	**0.750**	0.448	**0.872**	0.492	0.412	-0.506	**0.729**	-0.534
Luteolin O-(apiosyl)hexoside	**0.860**	0.515	0.684	0.646	0.474	0.212	-0.335	0.476	-0.440
Luteolin O-(apiosylmalonyl)glucoside	**0.925**	0.517	0.664	0.641	0.591	0.208	-0.384	0.463	-0.541
6"-malonylapiin	**0.796**	0.638	0.701	**0.738**	0.366	0.346	-0.422	0.573	-0.429
Apigenin derivative	**0.781**	0.476	0.577	0.568	0.439	0.223	-0.327	0.421	-0.412
Flavonones									
Naringenin	**0.855**	0.641	0.700	0.783	0.397	0.352	-0.419	0.641	-0.431
Flavonols									
Quercetin-3,4'-diglucoside	0.370	0.540	0.309	0.477	0.101	0.442	-0.414	0.400	-0.272
Quercetin-3-O-glucoside	**0.852**	0.303	0.571	0.437	**0.749**	0.006	-0.244	0.258	**-0.712**
Quercetin-3-O-rhamnoside	**0.770**	0.130	0.455	0.273	**0.698**	-0.139	-0.149	0.109	**-0.750**
Quercetin-Glc-Rha	0.600	0.665	0.124	0.475	0.460	0.624	-0.701	0.398	-0.633
Kaempferol-3-O-glucoside	**0.809**	0.312	0.530	0.391	0.597	0.043	-0.248	0.211	-0.477
Isorhamnetin-3-O-glucoside	**0.931**	0.599	0.657	0.677	0.578	0.302	-0.462	0.493	-0.575
Isorhamnetin-3-rutinoside	**0.832**	0.334	0.399	0.530	0.699	0.112	-0.347	0.452	-0.590
Carotenoid derivatives									
Dihydro-phaseic acid	**0.905**	**0.858**	0.214	**0.776**	0.696	**0.773**	**-0.900**	**0.726**	**-0.867**
Abscisic acid	0.465	0.434	0.448	0.290	0.188	0.256	-0.289	0.092	-0.262
Phaseic acid	**0.901**	**0.789**	0.314	**0.815**	0.706	0.538	-0.711	**0.795**	-0.680
Capsianosides									
Capsianoside III	0.454	-0.138	-0.305	-0.020	**0.872**	-0.117	-0.251	0.047	-0.670
Capsianoside IV diglucoside 1	0.570	0.477	0.258	**0.735**	0.355	0.371	-0.425	**0.803**	-0.413
Capsianoside IV diglucoside 2	**0.769**	0.498	0.485	**0.783**	0.483	0.278	-0.398	**0.763**	-0.480
Capsianoside derivative	0.286	0.710	0.512	**0.731**	-0.295	0.592	-0.346	0.691	0.034
Capsianoside V	**0.900**	0.516	0.457	0.586	0.711	0.283	-0.507	0.449	-0.687
Non-identified compounds									
NI1	-0.296	-0.036	0.090	-0.253	-0.395	-0.037	0.168	-0.364	0.315
NI2	0.268	0.699	0.628	0.779	-0.343	0.528	-0.292	0.719	0.078
NI3	-0.007	0.330	0.502	0.495	-0.443	0.185	0.015	0.470	0.279
NI4	0.670	**0.637**	0.325	0.627	0.360	0.523	-0.542	0.569	-0.466
NI5	0.476	0.321	**0.929**	0.448	-0.068	-0.054	0.082	0.195	0.090
NI6	**0.853**	**0.685**	0.416	**0.810**	0.626	0.385	-0.553	**0.786**	-0.653
NI7	0.614	**0.783**	0.453	**0.967**	0.171	0.641	-0.578	**0.991**	-0.375
NI8	0.476	0.632	0.764	0.742	-0.159	0.378	-0.220	0.615	0.014
NI9	**0.948**	0.631	0.499	**0.800**	0.670	0.397	-0.572	0.721	-0.684
NI10	**0.798**	0.700	0.426	**0.875**	0.460	0.532	-0.595	**0.864**	-0.560
NI11	0.537	0.693	0.334	**0.880**	0.207	0.588	-0.561	**0.931**	-0.399
NI12	0.713	0.718	0.582	**0.916**	0.239	0.507	-0.486	**0.877**	-0.367
NI13	0.424	0.523	0.653	**0.726**	-0.046	0.285	-0.217	0.651	-0.077
NI14	0.460	0.491	0.504	**0.827**	0.088	0.302	-0.277	**0.859**	-0.186
NI15	**0.805**	**0.831**	0.621	**0.908**	0.329	0.600	-0.613	**0.802**	-0.496
NI16	0.730	**0.924**	0.438	**0.919**	0.294	**0.789**	**-0.757**	**0.867**	-0.545
NI17	0.541	-0.055	0.645	0.272	0.347	-0.389	0.199	0.125	-0.109
NI18	0.557	-0.041	0.662	0.159	0.364	-0.383	0.182	-0.057	-0.131
NI19	**0.883**	0.539	**0.737**	0.630	0.473	0.214	-0.340	0.423	-0.445
NI20	0.428	-0.043	**0.757**	0.173	0.112	-0.397	0.302	-0.046	0.091

FIGURE 4 | Correlation analysis between the light conditions and all studied parameters of chilli. The absolute and relative amounts of different light regions were integrated daily (DLI) and used as indicated in **Table 1**. The blue colour indicates negative (inverse), whereas red colour represents positive (direct) correlations, and more intense colour shows higher correlation. The "r" values are also presented. The bold values show the significance level at the $p < 0.05$ level.

the overall daily effect turned out to be influencing. For instance, in comparison with the light Regimens E and F, the extra energy applied during the middle of the growth period (light Regimen F) did not cause significant changes; as a whole, this modification triggered small changes in the daily light integral. In contrast, light regimens containing a high amount or a high proportion of blue light (light Regimens E, F, and B) induced similar changes in growth (e.g., decrease in plant height) and metabolism (e.g., inducing the accumulation of phenolics) in spite of the fact that they differed both in light intensities and spectral composition. Therefore, in the future, more attention should be given to the importance of the absolute amount and the relative proportion of different spectral regions.

In the present investigation, the morphological parameters mainly affected by light intensity and spectral combination were plant height, flowering time, and yield production. The absolute amount of blue light had a negative effect on plant height and green mass production and a positive effect on fruit mass and harvest indices. Apparently, this is a contradiction. However, as demonstrated by several authors previously, an increase in light intensity resulted in an increase of biomass and yield only up to a critical threshold, whereas it decreased plant height in many crops, including tomato seedlings (Huber et al., 2021), wheat (Monostori et al., 2018), and chilli (Masabni et al., 2016). The details also showed that the utilised photosynthetic energy was distributed unequally between green mass and yield production. For instance, doubling the light intensity from 250 to 500 μmol m^{-2} s^{-1} resulted in a 1.25-fold increase of green mass and a 1.5-fold increase of yield in wheat (Monostori et al., 2018). In chilli plants, growth at high light intensity did not result in elevated shoot mass as compared to moderate light intensity, whereas yield increased (Masabni et al., 2016). These results are in accordance with the present observations, indicating that when more energy is absorbed by the photosynthetic pigments, the energy can be more efficiently converted into yield production. In addition, the present results also demonstrate that spectral composition also affected green mass and yield production, resulting in the highest green mass and the lowest yield at low light dominated by the red spectral region. Similar results were found in tomato plants grown at different red/blue ratios, where the biomass production was the highest at a high proportion of red light, whereas the highest fruit production was obtained at a high proportion of blue light (Deram et al., 2014). It appeared that a low amount of blue light (at low light intensity with red dominant spectra) stimulates green mass production, whereas a sufficient amount of blue light can improve yield.

Stem elongation is controlled by many photoreceptors, including PhyA responsible for far-red light signalling, PhyB regulating red light signalling, and phototropins and cryptochroms responding to blue light regions (Wang and Deng, 2004; Zhiyu et al., 2007; Hu and Zhao, 2016; Legris et al., 2019; Pierik and Ballaré, 2021). The light-induced regulation mechanisms depend both on the fluence and the spectral composition of light (Wang, 2005). Under the light conditions used in the present experiments, plant height was mainly determined by absolute amounts of blue and green light. Since leaf numbers did not change significantly (data not shown), the blue and green lights mainly affected the stem elongation. The blue light-induced inhibition of stem elongation was also demonstrated in bell pepper (Claypool and Lieth, 2020), tomato seedlings (Deram et al., 2014), and in chrysanthemum (Kim et al., 2004). The inhibitory effect of blue light on stem elongation was also presented inversely by Runkle and Heins (2001), who reported that environments deficient in blue light promoted internode elongation in several long-day plants as compared to unfiltered sunlight with a similar daily light integral. However, in the present experiments, green light also contributed to the inhibition of stem elongation as much as the blue light (**Figure 4**), emphasising the importance of green light in the growth regulation in chilli. The participation of green light in stem elongation was also observed in lettuce (Kim et al., 2004) and wheat (Monostori et al., 2018). However, the role of green light in the regulation is not known. It is possible that the effect of green light is mediated by a special green photoreceptor as supposed by Folta (2004), or it may be due to the absorption of cryptochromes, phototropins, or phytochromes in the green region (Sellaro et al., 2010). It is likely that the light-induced morphological responses are the consequence of regulated cooperation of many photoreceptors.

Flowering is also controlled by many photoreceptors; however, the regulation mechanism can vary according to long-, short-day or day neutral plants (Lin, 2000; Kim, 2020). The present experiments showed that flowering time in chilli was accelerated at high light intensity with the high amount of blue and green regions, and far-red light was also applied. Studies of flowering responses to light in the most studied *Arabidopsis* model plant showed that flowering was accelerated by far-red and blue light, whereas red light caused repression (Lin, 2000; Kim, 2020). These processes were mediated by the far-red sensitive phytochrome A and by the blue light-sensitive cryptrochrome 1 and 2 photoreceptors, respectively, and flowering repression appeared to be mediated by the red-sensitive phytochrome B (Lin, 2000; Kim, 2020). Although, to elucidate the role of photoreceptors was not the subject of this study, our results also confirmed the role of blue and far-red light in the acceleration of flowering. In addition, the present research also highlights the possible importance of the green region in the regulation of flowering.

In greenhouses and under natural light environments, chilli is often shaded for protection against stressful sunlight. Plants 25–80% shaded provided similar or higher yields than non-shaded plants, whereas their fruit produced more capsaicinoids and carotenoids and less phenolics than those of the uncovered plants (Ombódi et al., 2016; Jeeatid et al., 2017). Likewise, higher capsaicinoid content was detected in the fruit when moderate fluorescent light was used instead of applying high light intensity in a greenhouse during the summer season (Murakami et al., 2006). These results are in accordance with the present findings, where the capsaicin and carotenoid contents were lower, whereas the phenolic content was higher under high light intensity than under moderate light. In contrast, we could not confirm the previous observations (Gangadhar et al., 2012; Yap et al., 2021), indicating that blue light stimulated capsaicin accumulation, since a negative correlation was found between the amount of

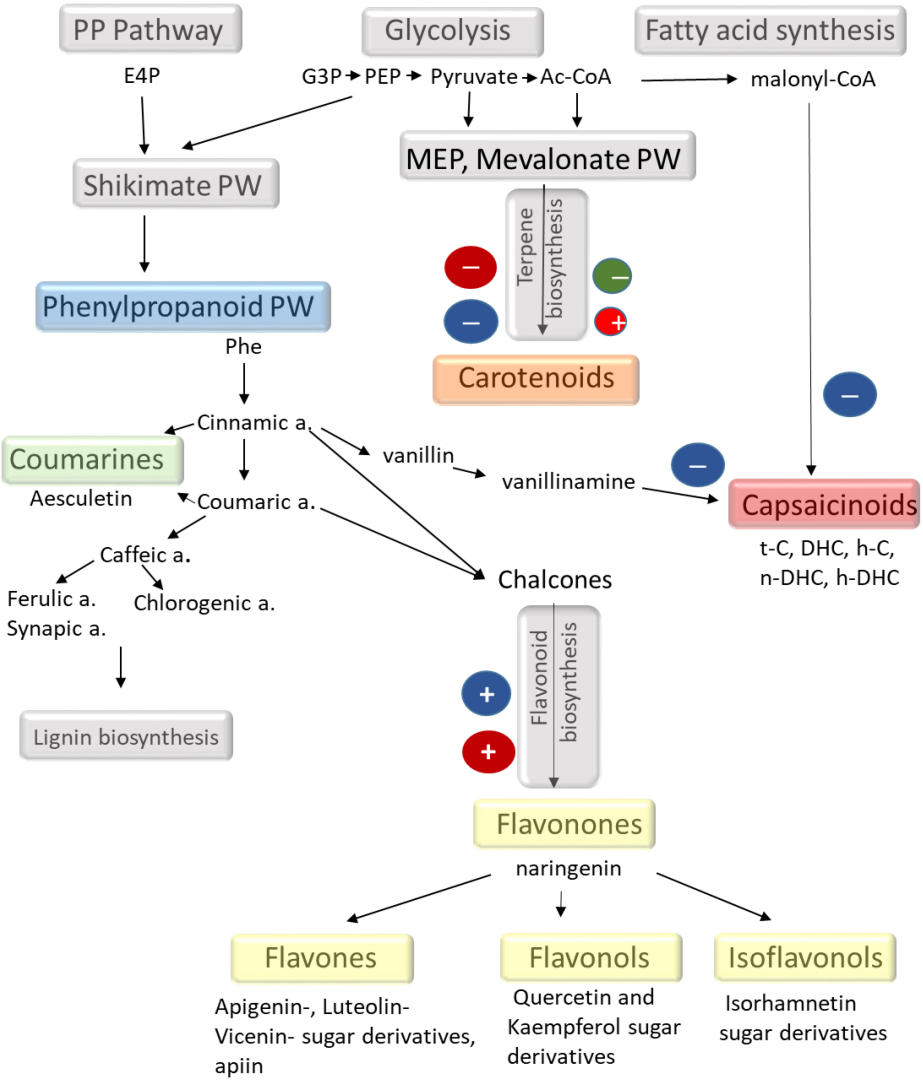

FIGURE 5 | Schematic representation of different secondary metabolic pathways focusing on the metabolites found in the chilli fruit. The effects of light observed in the present experiments are also indicated. The scheme is based on the KEGG database (maps 00998, 00941, 00940, and 01060).

blue light and the accumulation of capsaicinoids and carotenoids. However, it must be mentioned that in the before-mentioned experiments, a high amount of capsaicinoids was detected when pure blue light was used either as sole (Gangadhar et al., 2012) or supplemental lighting (Yap et al., 2021). These light conditions completely differed from the mixtures used in the present experiments in terms of both light intensity and spectral composition. The present experiments showed that, among the light factors, the absolute amount of blue light was the main factor that affected the accumulation of capsaicinoids.

As summarised in **Figure 5**, capsaicinoids are synthetised from vanillin and phenylalanine *via* phenylpropanoid pathways together with the saturated (in DHC) or unsaturated (in C) alkyl chain (Antonio et al., 2018). Phenylpropanoid pathways are also linked with the synthesis of phenolics, including flavonoids, coumarins, and antocyanins (**Figure 5**). In spite of the fact that the metabolomic composition of chilli fruit grown under different environmental conditions (Antonio et al., 2018; Lemos et al., 2019; Kim et al., 2020) and the influence of light intensity and spectral composition on the accumulation of metabolites in several plants have already been investigated (Landi et al., 2020; Loi et al., 2021), the light regulation of secondary metabolism is still not understood in detail. The present results showed that the different light conditions induced approximately 40% change in capsaicinoids, 30% in carotenoids, and approximately 250% in phenolics. According to the results presented here, the blue light may induce a shift in the phenylpropanoid pathways. Namely, the synthesis of capsaicinoids was suppressed, whereas the synthesis of phenolics (mainly flavonoids) was stimulated by the amount of blue light. In addition, the inverse light-dependent behaviour of DHC and C suggests that light may also affect the saturation

of the fatty acid chain during the synthesis of capsaicinoids. However, these metabolomic changes should be supported by further investigations.

Carotenoids, like β-carotene, α-carotene, different xanthophylls (zeaxanthin, neoxanthin, violaxanthin, lutein, etc.), are available in coloured vegetables and fruits and have strong radical quenching ability (Sarker et al., 2018b; Sarker and Oba, 2021). The red colour of chilli fruit mainly originates from capsanthin and capsorubin derived from violaxanthin and antheraxanthin. These highly apolar carotenoids are synthesised through the mevalonic acid pathways (**Figure 5**). According to the results presented here, it appeared that high light intensity did not force the accumulation of these metabolites (**Figures 2**, **4**). In fact, it was the moderate light intensity and the higher proportion of red light that could stimulate their accumulation. However, the light-induced differences did not exceed 30%, which indicates that light is not a major factor in controlling carotenoid biosynthesis during fruit ripening. Abscisic acid and its derivatives and phaseic and dihydrophaseic acids are also part of the carotenoid pathways and are derived from same precursors as the red fruit colour. The low light-induced changes of these metabolites also suggested that light conditions were not detrimental for carotenoid biosynthesis in ripe fruits.

Phenolics and flavonoids, including hydroxybenzoicacids (Sarker and Oba, 2019a), hydroxycinnamic acids (Sarker and Oba, 2018d), flavanols (Sarker and Oba, 2020a), flavonols (Sarker et al., 2020), flavones (Sarker and Oba, 2020b), and flavanones (Sarker and Oba, 2020c) are strong antioxidants, having various health benefits (Sarker and Oba, 2018e). These compounds are also associated with some physiological activities in plants, such as reducing reactive oxygen species and oxidative damage (ROS) (Sarker and Oba, 2018b), alleviating osmotic stress (Sarker and Oba, 2018c), decreasing photosynthetic activities (Sarker and Oba, 2018e), improving nutrient imbalance (Sarker et al., 2018a) in plant cells, protecting plants from drastic reduction in growth and productivity (Sarker and Oba, 2019c), and ultimately enhancing the concentration of antioxidants (Sarker and Oba, 2018a) for human diet. The strong antioxidant properties of phenolics are also confirmed in the present experiments, as the radical scavenging activity of the fruit (calculated as DPPH%) mainly correlated ($r = 0.716$; $p = 0.0136$) with the total amount of phenolics. Furthermore, both of these showed a positive correlation with the amount of blue light, which also supports that phenolic compounds contribute significantly to antioxidant capacity. Likewise, positive and significant strong associations were observed between total phenolics and antioxidant capacity (DPPH) in several *Amaranthus* species (Sarker et al., 2018a, Sarker and Oba, 2018c; Sarker and Oba, 2019b,c) that corroborate the present findings.

As indicated by Marín et al. (2004), most flavonoids are present in the form of conjugated O-glycosides and C-glycosides in chilli. Many glycosylated derivatives of luteolin, quercetin, kaempferol, and apigenin were also identified in the present study (**Figure 3** and **Supplementary Table 1**), similarly as found by Morales-Soto et al. (2013) and Kelebek et al. (2020). To our knowledge, this is the first report describing the light dependence of separated flavonoid compounds in chilli. Comparison of the light dependence of different phenolic compounds showed that most flavonoids, including luteolin, apigenin, naringenin, quercetin, kaempferol, and isorhamnetin derivatives, showed positive correlation with the amount of blue light, similarly as found for total phenolics and antioxidant-scavenging activity in fruits. This suggested that flavonoids belonging to flavone, flavonone, and flavonol groups were responsible for the accumulation of phenolics and also contributed to the antioxidant capacity of the fruit. Other phenolics belonging to the hydroxycinnamic acid family, such as chlorogenic, ferulic, and sinapic acids, and their derivatives were also found in the fruit pericarp; however, these metabolites showed less light dependence than flavonoids, except for sinapic acid and its derivatives.

Although the molecular mechanisms of flavonoid biosynthesis have been extensively studied (Tohge et al., 2014; Tang et al., 2019; Thoma et al., 2020; Al Murad et al., 2021), their light regulation has not yet been elucidated (Landi et al., 2020; Loi et al., 2021). The light regulatory units of the genes for the key enzymes, such as phenylalanine ammonia lyase (PAL), 4-coumaroyl CoA-ligase (4CL), and chalcone synthase (CHS) involved in flavonoid biosynthetic pathways, have already been identified in *Arabidopsis* and in some fruit species like grapes and apple (Hartmann et al., 2005; Zoratti et al., 2014; Liu et al., 2018). Based on these investigations, flavonoid biosynthesis may be mediated by the UVB and blue photoreceptors, such as phototropins and cryptochromes (Landi et al., 2020; Loi et al., 2021). Although the photoreceptors were not identified here, the present results also supported that phenolics, especially flavonoids, were strongly regulated by blue light in this chilli. In addition, both phenolic content and antioxidant capacity of the chilli fruit can be improved by the addition of a high amount of blue light. The light-induced metabolomic changes in chilli are summarised in a schematic figure (**Figure 5**). From these results, we can conclude that the application of LED lighting can be an alternative way to improve fruit quality in terms of bioactive compound.

CONCLUSION

In the present study, the light factors affecting the growth and development of chilli and the production of secondary metabolites were investigated. The results demonstrated that light fluence and spectral composition together affected the growth, flowering time, and fruit production of chilli, in which the absolute amount of different spectral regions paid an important role; however, the proportion of green light and the R/B ratio also had an influence. Among the light-induced changes, the increase of light fluence and the proportion of blue light stimulated flowering and yield in chilli, whereas low amounts of blue light enhanced green mass accumulation. Secondary metabolite production in the fruit was also affected by spectral composition and light fluence. Blue light (its absolute amount) stimulated the accumulation of phenolic compounds, but it inversely affected the production of capsaicinoids and carotenoids. These results proved that the accumulation of secondary metabolites can be

modified by appropriate modification of light fluence and spectral composition, but different spectral combinations are required to induce the accumulation of different types of secondary metabolites. A single spectral combination is not sufficient to ensure the optimal growth of chilli and the accumulation of all metabolites; only an adjustable light environment can ensure such conditions in indoor cultivation systems.

DATA AVAILABILITY STATEMENT

The original contributions presented in the study are included in the article/**Supplementary Material**, further inquiries can be directed to the corresponding author/s.

AUTHOR CONTRIBUTIONS

ED and GG conceived the research plan. ED and MA performed most of the experiments. KH and MD carried out the metabolomic analysis on capsaicinoids and phenolics. TM analysed the data. ED wrote the article. All authors contributed to the article and approved the submitted version.

FUNDING

This project was funded by GINOP-2.1.7-15-2016-02152 for Ledium Ltd. and by the National Research, Development and Innovation Office (Grant No. 131907).

SUPPLEMENTARY MATERIAL

The Supplementary Material for this article can be found online at: https://www.frontiersin.org/articles/10.3389/fpls.2022.801656/full#supplementary-material

REFERENCES

Acunha, T., dos, S., Crizel, R. L., Tavares, I. B., Barbieri, R. L., de Pereira, C. M. P., et al. (2017). Bioactive compound variability in a Brazilian *Capsicum* pepper collection. *Crop Sci.* 57, 1611–1623. doi: 10.2135/cropsci2016.08.0701

Al Murad, M., Razi, K., Jeong, B. R., Samy, P. M. A., and Muneer, S. (2021). Light emitting diodes (Leds) as agricultural lighting: impact and its potential on improving physiology, flowering, and secondary metabolites of crops. *Sustainability* 13, 1–25. doi: 10.3390/su13041985

Antonio, A. S., Wiedemann, L. S. M., and Veiga Junior, V. F. (2018). The genus: *Capsicum*: a phytochemical review of bioactive secondary metabolites. *RSC Adv.* 8, 25767–25784. doi: 10.1039/c8ra02067a

Claypool, N. B., and Lieth, J. H. (2020). Physiological responses of pepper seedlings to various ratios of blue, green, and red light using LED lamps. *Sci. Hortic.* 268:109371. doi: 10.1016/j.scienta.2020.109371

Darko, E., Heydarizadeh, P., Schoefs, B., and Sabzalian, M. R. (2014). Photosynthesis under artificial light: the shift in primary and secondary metabolism. *Philos. Trans. R. Soc. B Biol. Sci.* 369:20130243. doi: 10.1098/rstb.2013.0243

Deram, P., Lefsrud, M. G., and Orsat, V. (2014). Supplemental lighting orientation and Red-to-Blue ratio of light-emitting diodes for greenhouse tomato production. *HortScience* 49, 448–452. doi: 10.21273/hortsci.49.4.448

Folta, K. M. (2004). Green light stimulates early stem elongation. *Plant Physiol.* 135, 1407–1416. doi: 10.1104/pp.104.038893.1

Gangadhar, B. H., Mishra, R. K., Pandian, G., and Park, S. W. (2012). Comparative study of color, pungency, and biochemical composition in chili pepper (*Capsicum annuum*) under different light-emitting diode treatments. *HortScience* 47, 1729–1735. doi: 10.21273/hortsci.47.12.1729

Gomes, G. P., Zeffa, D. M., Constantino, L. V., Baba, V. Y., Silvar, C., Pomar, F., et al. (2021). Diallel analysis of the morphoagronomic, phytochemical, and antioxidant traits in *Capsicum baccatum* var. pendulum. *Hortic. Environ. Biotechnol.* 62, 435–446. doi: 10.1007/s13580-020-00299-7

Guclu, G., Keser, D., Kelebek, H., Keskin, M., Emre Sekerli, Y., Soysal, Y., et al. (2021). Impact of production and drying methods on the volatile and phenolic characteristics of fresh and powdered sweet red peppers. *Food Chem.* 338:128129. doi: 10.1016/j.foodchem.2020.128129

Hartmann, U., Sagasser, M., Mehrtens, F., Stracke, R., and Weisshaar, B. (2005). Differential combinatorial interactions of cis-acting elements recognized by R2R3-MYB, BZIP, and BHLH factors control light-responsive and tissue-specific activation of phenylpropanoid biosynthesis genes. *Plant Mol. Biol.* 57, 155–171. doi: 10.1007/s11103-004-6910-0

Hernández-Pérez, T., Gómez-García, M. R., Valverde, M. E., and Paredes-López, O. (2020). *Capsicum annuum* (hot pepper): an ancient Latin-American crop with outstanding bioactive compounds and nutraceutical potential. A review. *Compr. Rev. Food Sci. Food Saf.* 19, 2972–2993. doi: 10.1111/1541-4337.12634

Hu, Y., and Zhao, Y. (2016). Molecular basis for differential light responses in *Arabidopsis* stems and leaves. *Proc. Natl. Acad. Sci. U.S.A.* 113, 5774–5776. doi: 10.1073/pnas.1605750113

Huber, B. M., Louws, F. J., and Hernández, R. (2021). Impact of different daily light integrals and carbon dioxide concentrations on the growth, morphology, and production efficiency of tomato seedlings. *Front. Plant Sci.* 12:6158513. doi: 10.3389/fpls.2021.615853

Jeeatid, N., Techawongstien, S., Suriharn, B., Bosland, P. W., and Techawongstien, S. (2017). Light intensity affects capsaicinoid accumulation in hot pepper (*Capsicum chinense* Jacq.) cultivars. *Hortic. Environ. Biotechnol.* 58, 103–110. doi: 10.1007/s13580-017-0165-6

Jeong, W. Y., Jin, J. S., Cho, Y. A., Lee, J. H., Park, S., Jeong, S. W., et al. (2011). Determination of polyphenols in three *Capsicum annuum* L. (bell pepper) varieties using high-performance liquid chromatographytandem mass spectrometry: their contribution to overall antioxidant and anticancer activity. *J. Sep. Sci.* 34, 2967–2974. doi: 10.1002/jssc.201100524

Jimenez-Garcia, S. N., Vazquez-Cruz, M. A., Guevara-Gonzalez, R. G., Torres-Pacheco, I., Cruz-Hernandez, A., and Feregrino-Perez, A. A. (2013). Current approaches for enhanced expression of secondary metabolites as bioactive compounds in plants for agronomic and human health purposes - A review. *Polish J. Food Nutr. Sci.* 63, 67–78. doi: 10.2478/v10222-012-0072-6

Kelebek, H., Sevindik, O., Uzlasir, T., and Selli, S. (2020). LC-DAD/ESI MS/MS characterization of fresh and cooked Capia and Aleppo red peppers (*Capsicum annuum* L.) phenolic profiles. *Eur. Food Res. Technol.* 246, 1971–1980. doi: 10.1007/s00217-020-03548-2

Kim, D. H. (2020). Current understanding of flowering pathways in plants: focusing on the vernalization pathway in *Arabidopsis* and several vegetable crop plants. *Hortic. Environ. Biotechnol.* 61, 209–227. doi: 10.1007/s13580-019-00218-5

Kim, H. H., Goins, G. D., Wheeler, R. M., and Sager, J. C. (2004). Green-light supplementation for enhanced lettuce growth under red-and blue-light-emitting diodes. *HortScience* 39, 1617–1622. doi: 10.21273/hortsci.39.7.1617

Kim, T. J., Hyeon, H., Park, N. I. L., Yi, T. G., Lim, S. H., Park, S. Y., et al. (2020). A high-throughput platform for interpretation of metabolite profile data from pepper (*Capsicum*) fruits of 13 phenotypes associated with different fruit maturity states. *Food Chem.* 331:127286. doi: 10.1016/j.foodchem.2020.127286

Kotilainen, T., Aphalo, P. J., Brelsford, C. C., Böök, H., Devraj, S., Heikkilä, A., et al. (2020). Patterns in the spectral composition of sunlight and biologically

meaningful spectral photon ratios as affected by atmospheric factors. *Agric. For. Meteorol.* 291:108041. doi: 10.1016/j.agrformet.2020.108041

Landi, M., Zivcak, M., Sytar, O., Brestic, M., and Allakhverdiev, S. I. (2020). Plasticity of photosynthetic processes and the accumulation of secondary metabolites in plants in response to monochromatic light environments: a review. *Biochim. Biophys. Acta Bioenerg.* 1861:148131. doi: 10.1016/j.bbabio.2019.148131

Legris, M., Ince, Y. Ç, and Fankhauser, C. (2019). Molecular mechanisms underlying phytochrome-controlled morphogenesis in plants. *Nat. Commun.* 10:5219. doi: 10.1038/s41467-019-13045-0

Lemos, V. C., Reimer, J. J., and Wormit, A. (2019). Color for life: biosynthesis and distribution of phenolic compounds in pepper (*Capsicum annuum*). *Agriculture* 9, 1–29. doi: 10.3390/agriculture9040081

Lin, C. (2000). Photoreceptors and regulation of flowering time. *Plant Physiol.* 123, 39–50. doi: 10.1104/pp.123.1.39

Liu, N., Ji, F., Xu, L., and He, D. (2019). Effects of LED light quality on the growth of pepper seedling in plant factory. *Int. J. Agric. Biol. Eng.* 12, 44–50. doi: 10.25165/j.ijabe.20191205.4847

Liu, Y., Fang, S., Yang, W., Shang, X., and Fu, X. (2018). Light quality affects flavonoid production and related gene expression in *Cyclocarya paliurus*. *J. Photochem. Photobiol. B Biol.* 179, 66–73. doi: 10.1016/j.jphotobiol.2018.01.002

Loi, M., Villani, A., Paciolla, F., Mulè, G., and Paciolla, C. (2021). Challenges and opportunities of light-emitting diode (Led) as key to modulate antioxidant compounds in plants. a review. *Antioxidants* 10, 1–35. doi: 10.3390/antiox10010042

Mara de Menezes Epifanio, N., Rykiel Iglesias Cavalcanti, L., Falcão dos Santos, K., Soares Coutinho Duarte, P., Kachlicki, P., Ożarowski, M., et al. (2020). Chemical characterization and in vivo antioxidant activity of parsley (*Petroselinum crispum*) aqueous extract. *Food Funct.* 11, 5346–5356. doi: 10.1039/D0FO00484G

Marín, A., Ferreres, F., Tomás-Barberán, F. A., and Gil, M. I. (2004). Characterization and quantitation of antioxidant constituents of sweet pepper (*Capsicum annuum* L.). *J. Agric. Food Chem.* 52, 3861–3869. doi: 10.1021/jf0497915

Masabni, J., Sun, Y., Niu, G., and Del Valle, P. (2016). Shade effect on growth and productivity of tomato and chili pepper. *Horttechnology* 26, 344–350. doi: 10.21273/horttech.26.3.344

Monostori, I., Heilmann, M., Kocsy, G., Rakszegi, M., Ahres, M., Altenbach, S., et al. (2018). LED lighting – modification of growth, metabolism, yield and flour composition in wheat by spectral quality and intensity. *Front. Plant Sci.* 9:605. doi: 10.3389/fpls.2018.00605

Morales-Soto, A., Gómez-Caravaca, A. M., García-Salas, P., Segura-Carretero, A., and Fernández-Gutiérrez, A. (2013). High-performance liquid chromatography coupled to diode array and electrospray time-of-flight mass spectrometry detectors for a comprehensive characterization of phenolic and other polar compounds in three pepper (*Capsicum annuum* L.) samples. *Food Res. Int.* 51, 977–984. doi: 10.1016/j.foodres.2013.02.022

Murakami, K., Ido, M., and Masuda, M. (2006). Fruit pungency of "Shishito" pepper as affected by a dark interval in continuous fluorescent illumination with temperature alteration. *Shokubutsu Kankyo Kogaku* 18, 284–289. doi: 10.2525/shita.18.284

Naznin, M. T., Lefsrud, M., Gravel, V., and Azad, M. O. K. (2019). Blue light added with red LEDs enhance growth characteristics, pigments content, and antioxidant capacity in lettuce, Spinach, Kale, Basil, and sweet pepper in a controlled environment. *Plants* 8:93. doi: 10.3390/plants8040093

Nwokem, C. O., Agbaji, E. B., Kagbu, J. A., and Ekanem, E. J. (2010). Determination of capsaicin content and pungency level of five different peppers grown in Nigeria. *N.Y. Sci. J.* 33, 17–21.

Olle, M., and Viršile, A. (2013). The effects of light-emitting diode lighting on greenhouse plant growth and quality. *Agric. Food Sci.* 22, 223–234. doi: 10.23986/afsci.7897

Ombódi, A. O., Pék, Z., Szuvandzsiev, P., Lugasi, A., Ledóné Darázsi, H., and Helyes, L. (2016). Effect of coloured shade nets on some nutritional characteristics of a kapia type pepper grown in plastic tunnel. *Columella J. Agric. Environ. Sci.* 3, 25–33. doi: 10.18380/szie.colum.2016.3.2.25

Oney-Montalvo, J. E., Avilés-Betanzos, K. A., Jesús Ramírez-Rivera, E. D., Ramírez-Sucre, M. O., and Rodríguez-Buenl, I. M. (2020). Polyphenols content in *Capsicum* chinense fruits at different harvest times and their correlation with the antioxidant activity. *Plants* 9, 1–15. doi: 10.3390/plants9101394

Pál, M., Ivanovska, B., Oláh, T., Tajti, J., Hamow, K. Á, Szalai, G., et al. (2019). Role of polyamines in plant growth regulation of Rht wheat mutants. *Plant Physiol. Biochem.* 137, 189–202. doi: 10.1016/j.plaphy.2019.02.013

Pierik, R., and Ballaré, C. L. (2021). Control of plant growth and defense by photoreceptors: from mechanisms to opportunities in agriculture. *Mol. Plant* 14, 61–76. doi: 10.1016/j.molp.2020.11.021

Runkle, E. S., and Heins, R. D. (2001). Specific functions of red, far red, and blue light in flowering and stem extension of long-day plants. *J. Am. Soc. Hortic. Sci.* 126, 275–282. doi: 10.21273/jashs.126.3.275

Sarker, U., Hossain, M. N., Iqbal, M. A., and Oba, S. (2020). Bioactive components and radical scavenging activity in selected advance lines of salt-tolerant vegetable amaranth. *Front. Nutr.* 7:587257. doi: 10.3389/fnut.2020.587257

Sarker, U., Islam, M. T., Rabbani, M. G., and Oba, S. (2018c). Phenotypic divergence in vegetable amaranth for total antioxidant capacity, antioxidant profile, dietary fiber, nutritional and agronomic traits. *Acta Agric. Scand. Sect. B Soil Plant Sci.* 68, 67–76. doi: 10.1080/09064710.2017.1367029

Sarker, U., Islam, M. T., and Oba, S. (2018a). Salinity stress accelerates nutrients, dietary fiber, minerals, phytochemicals and antioxidant activity in *Amaranthus tricolor* leaves. *PLoS One* 13:e0206388. doi: 10.1371/journal.pone.0206388

Sarker, U., Islam, M. T., Rabbani, M. G., and Oba, S. (2018b). Antioxidant leaf pigments and variability. *Genetika* 50, 209–220.

Sarker, U., and Oba, S. (2018d). Drought stress enhances nutritional and bioactive compounds, phenolic acids and antioxidant capacity of Amaranthus leafy vegetable. *BMC Plant Biol.* 18:258. doi: 10.1186/s12870-018-1484-1

Sarker, U., and Oba, S. (2018a). Augmentation of leaf color parameters, pigments, vitamins, phenolic acids, flavonoids and antioxidant activity in selected *Amaranthus tricolor* under salinity stress. *Sci. Rep.* 8, 1–9. doi: 10.1038/s41598-018-30897-6

Sarker, U., and Oba, S. (2018b). Catalase, superoxide dismutase and ascorbate-glutathione cycle enzymes confer drought tolerance of *Amaranthus tricolor*. *Sci. Rep.* 8:16496. doi: 10.1038/s41598-018-34944-0

Sarker, U., and Oba, S. (2018c). Drought stress effects on growth, ros markers, compatible solutes, phenolics, flavonoids, and antioxidant activity in *Amaranthus tricolor*. *Appl. Biochem. Biotechnol.* 186, 999–1016. doi: 10.1007/s12010-018-2784-5

Sarker, U., and Oba, S. (2018e). Response of nutrients, minerals, antioxidant leaf pigments, vitamins, polyphenol, flavonoid and antioxidant activity in selected vegetable amaranth under four soil water content. *Food Chem.* 252, 72–83. doi: 10.1016/j.foodchem.2018.01.097

Sarker, U., and Oba, S. (2019a). Antioxidant constituents of three selected red and green color *Amaranthus leafy* vegetable. *Sci. Rep.* 9:18233. doi: 10.1038/s41598-019-52033-8

Sarker, U., and Oba, S. (2019b). Nutraceuticals, antioxidant pigments, and phytochemicals in the leaves of *Amaranthus spinosus* and *Amaranthus viridis* weedy species. *Sci. Rep.* 9:20413. doi: 10.1038/s41598-019-50977-5

Sarker, U., and Oba, S. (2019c). Salinity stress enhances color parameters, bioactive leaf pigments, vitamins, polyphenols, flavonoids and antioxidant activity in selected *Amaranthus leafy* vegetables. *J. Sci. Food Agric.* 99, 2275–2284. doi: 10.1002/jsfa.9423

Sarker, U., and Oba, S. (2020a). Nutraceuticals, phytochemicals, and radical quenching ability of selected drought-tolerant advance lines of vegetable amaranth. *BMC Plant Biol.* 20:564. doi: 10.1186/s12870-020-02780-y

Sarker, U., and Oba, S. (2020b). Phenolic profiles and antioxidant activities in selected drought-tolerant leafy vegetable amaranth. *Sci. Rep.* 10, 1–11. doi: 10.1038/s41598-020-71727-y

Sarker, U., and Oba, S. (2020c). Polyphenol and flavonoid profiles and radical scavenging activity in leafy vegetable *Amaranthus gangeticus*. *BMC Plant Biol.* 20:499. doi: 10.1186/s12870-020-02700-0

Sarker, U., and Oba, S. (2021). Color attributes, betacyanin, and carotenoid profiles, bioactive components, and radical quenching capacity in selected *Amaranthus gangeticus* leafy vegetables. *Sci. Rep.* 11, 1–14. doi: 10.1038/s41598-021-91157-8

Schuerger, A. C., Brown, C. S., and Stryjewski, E. C. (1997). Anatomical features of pepper plants (*Capsicum annuum* L.) Grown under red light-emitting diodes supplemented with blue or far-red light. *Ann. Bot.* 79, 273–282. doi: 10.1006/anbo.1996.0341

Scoville, W. L. (1912). Note on *Capsicums*. *J. Am. Pharm. Assoc.* 1, 453–454. doi: 10.1002/jps.3080010520

Sellaro, R., Crepy, M., Trupkin, S. A., Karayekov, E., Buchovsky, A. S., Rossi, C., et al. (2010). Cryptochrome as a sensor of the blue/green ratio of natural radiation in *Arabidopsis*. *Plant Physiol.* 154, 401–409. doi: 10.1104/pp.110.160820

Song, J. X., Meng, Q. W., Du, W. F., and He, D. X. (2017). Effects of light quality on growth and development of cucumber seedlings in controlled environment. *Int. J. Agric. Biol. Eng.* 10, 312–318. doi: 10.3965/j.ijabe.20171003.2299

Tang, Z., Yu, J., Xie, J., Lyu, J., Feng, Z., Dawuda, M. M., et al. (2019). Physiological and growth response of pepper (*Capsicum annum* L.) seedlings to supplementary red/blue light revealed through transcriptomic analysis. *Agronomy* 9, 1–15. doi: 10.3390/agronomy9030139

Thoma, F., Somborn-Schulz, A., Schlehuber, D., Keuter, V., and Deerberg, G. (2020). Effects of light on secondary metabolites in selected leafy greens: a review. *Front. Plant Sci.* 11:497. doi: 10.3389/fpls.2020.00497

Tohge, T., Alseekh, S., and Fernie, A. R. (2014). On the regulation and function of secondary metabolism during fruit development and ripening. *J. Exp. Bot.* 65, 4599–4611. doi: 10.1093/jxb/ert443

Vrhovsek, U., Masuero, D., Gasperotti, M., Franceschi, P., Caputi, L., Viola, R., et al. (2012). A versatile targeted metabolomics method for the rapid quantification of multiple classes of phenolics in fruits and beverages. *J. Agric. Food Chem.* 60, 8831–8840. doi: 10.1021/jf2051569

Wahyuni, Y., Ballester, A. R., Sudarmonowati, E., Bino, R. J., and Bovy, A. G. (2011). Metabolite biodiversity in pepper (*Capsicum*) fruits of thirty-two diverse accessions: variation in health-related compounds and implications for breeding. *Phytochemistry* 72, 1358–1370. doi: 10.1016/j.phytochem.2011.03.016

Wahyuni, Y., Ballester, A. R., Sudarmonowati, E., Bino, R. J., and Bovy, A. G. (2013). Secondary metabolites of *Capsicum* species and their importance in the human diet. *J. Nat. Prod.* 76, 783–793. doi: 10.1021/np300898z

Wang, H. (2005). Signaling mechanisms of higher plant photoreceptors: a structure-function perspective. *Curr. Top. Dev. Biol.* 68, 227–261. doi: 10.1016/S0070-2153(05)68008-8

Wang, H., and Deng, X. W. (2004). Phytochrome signaling mechanism. *Arab. B.* 3:e0074.1. doi: 10.1199/tab.0074.1

Yap, E. S. P., Uthairatanakij, A., Laohakunjit, N., Jitareerat, P., Vaswani, A., Magana, A. A., et al. (2021). Plant growth and metabolic changes in 'Super Hot' chili fruit (*Capsicum annuum*) exposed to supplemental LED lights. *Plant Sci.* 305:110826. doi: 10.1016/j.plantsci.2021.110826

Zhiyu, M., Shimizu, H., Moriizumi, S., Miyata, M., Douzono, M., and Tazawa, S. (2007). Effect of light intensity, quality and photoperiod on stem elongation of chrysanthemum cv. *Reagan. Environ. Control Biol.* 45, 19–25. doi: 10.2525/ecb.45.19

Zoratti, L., Karppinen, K., Escobar, A. L., Häggman, H., and Jaakola, L. (2014). Light-controlled flavonoid biosynthesis in fruits. *Front. Plant Sci.* 5:534. doi: 10.3389/fpls.2014.00534

Conflict of Interest: The authors declare that the research was conducted in the absence of any commercial or financial relationships that could be construed as a potential conflict of interest.

Publisher's Note: All claims expressed in this article are solely those of the authors and do not necessarily represent those of their affiliated organizations, or those of the publisher, the editors and the reviewers. Any product that may be evaluated in this article, or claim that may be made by its manufacturer, is not guaranteed or endorsed by the publisher.

frontiers | Frontiers in Plant Science

ORIGINAL RESEARCH
published: 26 April 2022
doi: 10.3389/fpls.2022.857616

The Power of Far-Red Light at Night: Photomorphogenic, Physiological, and Yield Response in Pepper During Dynamic 24 Hour Lighting

*Jason Lanoue, Celeste Little and Xiuming Hao**

Harrow Research and Development Centre, Agriculture and Agri-Food Canada, Harrow, ON, Canada

Supplemental light is needed during the winter months in high latitude regions to achieve the desired daily light integral (DLI) (photoperiod × intensity) for greenhouse pepper (*Capsicum annuum*) production. Peppers tend to have short internodes causing fruit stacking and higher labor time for plant maintenance when grown under supplemental light. Far-red light can increase internode length, and our previous study on tomatoes (*Solanum lycopersicum*) also discovered monochromatic blue light at night during continuous lighting (CL, 24 h) increased stem elongation. Furthermore, the use of low-intensity, long photoperiod lighting can reduce light fixture costs and overall electricity costs due to lower power prices during the night. Therefore, we investigated the use of blue and/or far-red light during the night period of CL to increase stem elongation. Three pepper cultivars with different internode lengths/growing characteristics ('Maureno,' 'Gina,' and 'Eurix') were used to investigate the effects on plant morphology in a short experiment, and one cultivar 'Maureno' was used in a long experiment to assess the impact on fruit yield. The five lighting treatments that were used are as follows: 16 h of white light during the day followed by either 8 h of darkness (16W – control), white light (24W), blue light only (16W + 8B), blue + far-red light (16W + 8BFR), or far-red light only (16W + 8FR). Calculated nighttime phytochrome photostationary state (PSS) was 0.833, 0.566, 0.315, and 0.186 for 24W, 16W + 8B, 16W + 8BFR, and 16W + 8FR respectively. All five treatments had the same DLI in photosynthetically active radiation (PAR) and far-red light. The 16W + 8BFR and 16W + 8FR treatments significantly increased internode length compared to 16W and 24W but neither was more impactful than the other. The 16W + 8B treatment also increased internode length but to a lesser extent than 16W + 8BFR and 16W + 8FR. This indicates that a nighttime PSS of 0.315 is sufficient to maximize stem elongation. Both 16W + 8B and 16W + 8BFR drove photosynthesis during the nighttime supporting a similar yield compared to 16W. Therefore, 16W + 8BFR is the most potential lighting strategy as it can lead to a greater reduction in the light fixture and electrical costs while maintaining yield and enhancing internode length.

Keywords: dynamic 24h lighting, greenhouse pepper, far-red light, continuous light, light spectrum, light intensity, photomorphogenesis, photoinjury

OPEN ACCESS

Edited by:
Ep Heuvelink, Wageningen University & Research, Netherlands

Reviewed by:
Dimitrios Fanourakis, Technological Educational Institute of Crete, Greece
Erik Runkle, Michigan State University, United States
Celine C. S. Nicole, Philips Research, Netherlands

****Correspondence:***
Xiuming Hao
Xiuming.Hao@agr.gc.ca

Specialty section:
This article was submitted to Crop and Product Physiology, a section of the journal Frontiers in Plant Science

Received: *18 January 2022*
Accepted: *24 March 2022*
Published: *26 April 2022*

Citation:
Lanoue J, Little C and Hao X (2022) The Power of Far-Red Light at Night: Photomorphogenic, Physiological, and Yield Response in Pepper During Dynamic 24 Hour Lighting. Front. Plant Sci. 13:857616. doi: 10.3389/fpls.2022.857616

INTRODUCTION

The daily light integral (DLI; light intensity × photoperiod duration) plays a vital role in plant biomass accumulation and yield. While the natural solar DLI is dictated by the time of year, global location, and local weather, the total DLI can be augmented by the application of supplemental lighting. Supplemental lighting can aid in the achievement of a desired/target DLI to increase plant growth and yield, specifically during low-light months (McAvoy et al., 1989). The timely use of lighting during low-cost periods can maximize economical gain for growers (Sørensen et al., 2020). Extended photoperiods (up to 24 h) with supplemental light at a lower light intensity reduce the overall fixture need (i.e., capital cost) and move part of daytime electricity use (or demand) to the nighttime when electricity prices are at their lowest; such is the case in Ontario, Canada (Hao et al., 2018a; IESO, 2022). Furthermore, regardless of fixture type [whether it is high-pressure sodium (HPS) or light-emitting diode (LED)] most of the input electricity in light fixtures is eventually converted into heat because plants only convert a small percentage of light energy into biomass (Kozai and Niu, 2016[1]). The law of conservation of energy states that energy can neither be created nor destroyed – only converted from one form of energy to another – i.e., a system always has the same amount of energy[2] unless there is an exchange with outside. During the night when lighting is not used, heating is usually needed to maintain the proper greenhouse temperatures to prevent any low-temperature damage to plants. By utilizing LED lighting during the subjective night period, the heat generated from the application of lighting can help to meet nighttime heating requirements, reducing the use of fossil fuels for heating and associated carbon dioxide (CO_2) emission (Velez-Ramirez et al., 2012) during the night period. However, exceeding the tolerable limits of photoperiods, which are species-specific, can lead to diminished yield, photoperiod-related leaf injury, and an economic disadvantage for growers (Demers and Gosselin, 2002; Hao et al., 2018a). While lettuce (Ohtake et al., 2018) and cucumber (Lanoue et al., 2021b) are more tolerant to extended photoperiods including 24 h continuous lighting (CL), others such as tomato (Velez-Ramirez et al., 2014; Matsuda et al., 2016) and pepper (Demers and Gosselin, 2002) are susceptible to photoperiod related injury. Photoperiod injury can manifest in many ways including interveinal chlorosis which leads to lower photosynthetic rates and ultimately reductions in yield (Sysoeva et al., 2010; Velez-Ramirez et al., 2011). Unlike tomatoes which develop severe leaf chlorosis, pepper leaves tend to be less affected by CL, developing only mild or no chlorosis and subtle leaf deformities (Demers et al., 1998). However, a reduction in pepper yield is still observed under CL indicating that the plant is unable to utilize the additional photons (Demers et al., 1998). While the exact mechanism controlling photoperiod injury is unknown, research in tomatoes suggests that CL tolerance is conferred by a single gene; *type III light-harvesting chlorophyll a/b binding protein 13* (*CAB-13*; Velez-Ramirez et al., 2014).

FIGURE 1 | Fruit stacking due to short internodes in plants grown under supplemental lighting.

However, it should be noted that there are many circadian clock components that form complex interactions indicating that there are potentially many points of the regulation (Inoue et al., 2018). The potential mismatch between internal diurnal patterns of gene expressions and the lack of external light/dark cycles could also play a role in CL injury.

The increase in light intensity due to supplemental lighting during greenhouse production is known to cause plants to become more compact as additional light represses stem elongation and internode length (Hao and Papadopoulos, 1999; Fan et al., 2013). This plant compaction is further observed in peppers when they are grown under CL (Demers et al., 1998). For peppers, this increased plant compaction, specifically a reduction in internode length, may cause fruit stacking which can negatively affect fruit shape (**Figure 1**) and lead to increased labor cost due to the difficulty in removing suckers during plant maintenance. Short internode has been identified as a limiting factor for winter cultivation (such as from December to February) with bell peppers under supplemental light.

Several studies have reported the usefulness of wavelength-specific LEDs, particularly the use of far-red (FR) light, to

[1]https://en.wikipedia.org/wiki/Photosynthetic_efficiency

[2]https://energyeducation.ca/encyclopedia/Law_of_conservation_of_energy

promote stem elongation and leaf expansion in many species including peppers (Brown et al., 1995; Rajapakse and Li, 2004; Kalaitzoglou et al., 2019). By increasing the amount of FR light, the phytochrome photostationary state (PSS) defined as the ratio of phytochrome in the active state (P_{fr}) to the total phytochrome in the active and inactive state ($P_{fr} + P_r$; Sager et al., 1988) under a given light spectra, can be altered. A low PSS will invoke a shade avoidance response leading to increased stem elongation (Cole et al., 2011).

Alterations in the PSS can lead to changes in biomass partitioning. Similar to the shade avoidance response to stem elongation, the addition of FR light can also result in an increase in biomass partitioning of the stem (Brown et al., 1995; Maliakal et al., 1999; Ji et al., 2019, 2020). Furthermore, the addition of FR light has been shown to increase dry mass partitioning to fruit, thus increasing yield, which in vascular plants can indicate preferential carbon export to the fruit (Lanoue et al., 2018a; Kalaitzoglou et al., 2019; Ji et al., 2020; Jin et al., 2021). It should be noted that while phytochrome is traditionally thought of as a photoreceptor for red and FR, it does absorb other wavelengths which can affect the PSS (Eilfeld and Rüdiger, 1985; Sager et al., 1988; Chun et al., 2001; Sullivan et al., 2016).

The use of short-term (typically 15–60 min) end-of-day FR (EOD-FR) light has also been proposed as an alternative to the use of FR during the day (Kasperbauer et al., 1984; Chia and Kubota, 2010; Islam et al., 2014; Kalaitzoglou et al., 2019). EOD-FR treatments provide low PSS as FR is used during a period absent of photosynthetically active radiation (PAR). An EOD-FR treatment typically uses a low FR light intensity which is viewed as more energy efficient in comparison to daytime FR application, while also can invoke a shade avoidance response (i.e., stem elongation and leaf expansion) (Chia and Kubota, 2010; Kalaitzoglou et al., 2019). However, while EOD-FR has been shown to increase light use efficiency (i.e., dry matter accumulated per cumulative incident light; Zou et al., 2019), its use does not have the same impact on plant height as moderate-intensity (∼50 μmol m^{-2} s^{-1}) FR light when used during the day. Kalaitzoglou et al. (2019) showed that an EOD-FR treatment of 17 μmol m^{-2} s^{-1} increased plant height compared to a control treatment without FR; however, the plants are more compact when compared to the use of continuous daytime FR at 54 μmol m^{-2} s^{-1}. Zou et al. (2019) also showed that in lettuce, the use of 50 μmol m^{-2} s^{-1} of FR during a 16 h photoperiod produced larger plants than the use of a 1-h 50 μmol m^{-2} s^{-1} EOD-FR treatment. In peppers that may have internode lengths as low as 2.9 cm when grown under supplemental lighting (Demers et al., 1998), a subtle increase in stem elongation due to EOD-FR would not be sufficient to increase internode length to prevent fruit stacking. Therefore, we hypothesize that the use of low intensity FR light for a longer duration during the night in a dynamic CL strategy (i.e., changes in light intensity and/or spectrum between day and night periods) would provide the internode stretch needed to avert fruit stacking and reduce additional labor cost for plant maintenance.

Blue light (400–500 nm) is traditionally associated with reduced plant height when added to a lighting treatment (Shimizu et al., 2006; Nanya et al., 2012; Hernández and Kubota, 2016). However, a unique phenomenon occurs when blue light is used as a sole source. In the absence of other wavelengths, monochromatic blue light has been shown to increase stem elongation in cucumber (Hernández and Kubota, 2016), tomato (Lanoue et al., 2019), and *Arabidopsis* (Kong and Zheng, 2020). This phenomenon is presumably the opposite of what one would traditionally expect. In the absence of other light, monochromatic blue light can have a low PSS which is known to cause stem elongation (Cole et al., 2011; Kalaitzoglou et al., 2019; Kong and Zheng, 2020). Furthermore, Kong and Zheng (2020) suggest that phototropin II is involved in stem elongation as the absence of this photoreceptor in *Arabidopsis* produced taller plants than the wild-type when grown under blue light. Therefore, sole irradiation with blue light (such would be the case during the night) can increase stem elongation (Hernández and Kubota, 2016; Lanoue et al., 2019; Kong and Zheng, 2020).

The use of dynamic CL lighting has shown promise in other crops in averting photoperiod related injury (Matsuda et al., 2016; Ohtake et al., 2018) and allowed injury-free production in greenhouse tomatoes (Lanoue et al., 2019, 2021a) but no research has been done on greenhouse peppers yet. Therefore, this study was conducted to investigate the effects of dynamic CL lighting with monochromatic blue, far-red or blue + far-red light during the night on plant growth, morphology, leaf gas exchanges, and fruit yield of pepper plants to identify dynamic CL or 24 h lighting strategies that can reduce leaf injury, increase internode length/stem elongation and maintain high fruit yield and quality. The lighting strategies can generate significant economic benefits if the high yield and quality under lighting can be maintained. This is because low-intensity CL reduces light fixture capital cost due to the lower intensity of light utilized to provide the same DLI as the conventional shorter photoperiods of lighting, the lower electricity price during the off-peak period at night, and the lower peak power demand charge (Hao et al., 2018a; IESO, 2022).

MATERIALS AND METHODS

Plant Material and Experimental Design

Two experiments were conducted in this study. The first experiment was aimed at identifying dynamic CL strategies which could prevent injury while either maintaining or increasing fruit yield and quality. Only one cultivar was used in this experiment because of the large space (large plants) requirement of the experiment. The second experiment expanded to three cultivars with different growth characteristics and investigated the effects of different spectra of light during the night on plant morphology/architecture (especially on internode length) and biomass partitioning in young pepper plants. Taken together, the two experiments provided more complete information on the impact of dynamic CL with different spectra of light during the night on the photomorphogenesis, physiology, and yield of pepper plants.

Experiment One

Forty-one-day-old pepper (*Capsicum annuum*) transplants cv. 'Maureno' were planted onto rockwool slabs on October 5th,

TABLE 1 | Supplemental light intensities provided by Sollum SF04 fixtures of lighting treatments in experiments one and two where the daytime is defined as 6:00-22:00 and nighttime is 22:00-6:00.

Treatment	16W	24W	16W + 8B	16W + 8BFR	16W + 8FR
Experiment 1					
Daytime PAR (μmol m^{-2} s^{-1})	220 ± 4	147 ± 3	181 ± 4	180 ± 5	–
Daytime FR (μmol m^{-2} s^{-1})	24 ± 3	17 ± 2	22 ± 2	18 ± 2	–
Daytime PSS	0.834	0.833	0.832	0.840	–
Nighttime PAR (μmol m^{-2} s^{-1})	–	147 ± 3	73 ± 2	74 ± 3	–
Nighttime FR (μmol m^{-2} s^{-1})	–	17 ± 2	–	16 ± 3	–
Nighttime PSS	–	0.833	0.566	0.315	–
PAR DLI (mol m^{-2} d^{-1})	12.7 ± 0.2	12.7 ± 0.3	12.5 ± 0.3	12.5 ± 0.4	–
FR DLI (mol m^{-2} d^{-1})	1.38 ± 0.17	1.47 ± 0.17	1.27 ± 0.12	1.50 ± 0.21	–
Experiment 2					
Daytime PAR (μmol m^{-2} s^{-1})	180 ± 6	121 ± 3	153 ± 4	152 ± 5	182 ± 5
Daytime FR (μmol m^{-2} s^{-1})	19 ± 2	13 ± 1	18 ± 2	13 ± 2	13 ± 1
Daytime PSS	0.834	0.833	0.832	0.840	0.844
Nighttime PAR (μmol m^{-2} s^{-1})	–	121 ± 3	55 ± 2	56 ± 2	–
Nighttime FR (μmol m^{-2} s^{-1})	–	13 ± 1	–	11 ± 1	10 ± 1
Nighttime PSS	–	0.833	0.566	0.315	0.186
PAR DLI (mol m^{-2} d^{-1})	10.4 ± 0.3	10.4 ± 0.3	10.4 ± 0.3	10.4 ± 0.3	10.5 ± 0.3
FR DLI (mol m^{-2} d^{-1})	1.14 ± 0.12	1.14 ± 0.09	1.04 ± 0.12	1.07 ± 0.14	1.04 ± 0.09

Dashes (–) represent no PAR or FR light during that period. PSS was calculated using Sager et al. (1988) via data obtained from a Li-180 spectroradiometer during the night at the apex of the plant in order to eliminate confounding effects of the sunlight.

2020 in two adjacent double-layer polyethylene greenhouses (50 m^2 of growing area each) at the Harrow Research and Development Centre (Agriculture and Agri-Food Canada, Harrow, ON, Canada; 42.03°N, 82.9°W). Plants were trained in a high wire double-stem fashion at a plant density of 7.05 stems m^{-2}. In total, 72 plants were placed under each of the four light treatments. The plants were drip-irrigated as needed using a complete nutrient solution (Ontario Ministry of Agriculture, Food and Rural Affairs [OMAFRA], 2010) with an electrical conductivity of 2.8 dS m^{-1} and a pH of 5.9. The greenhouse was enriched to 800 μL L^{-1} of CO_2 during both day and night when the greenhouse was not vented (actual concentrations 800–1000 μL L^{-1}). The heating temperature during the day was 20.5°C with a venting temperature of 25°C (actual temperature 20.5–25°C, **Supplementary Figure 1A**). Day humidification set point was 65% with a dehumidification set point of 85% (actual humidity 62–80%, **Supplementary Figure 1B**). The nighttime heating temperature was 18°C and venting was 22°C (actual temperature 18.5–20.5°C). Night humidification set point was 55% with a dehumidification set point of 80% (actual humidity 55–65%).

Each greenhouse was subdivided into four sections by light abatement curtains (Obscura 9950 FR W, Ludvig Svensson, Kinna, Sweden). The light abatement curtains were closed on cloudy days and during the night to prevent treatment contamination. On sunny days, the light abatement curtains were opened to prevent the shading of the high-intensity solar radiation. Guard plants were utilized on the outermost rows of each greenhouse. Beginning on November 12th, 2020, four overhead supplemental light treatments (**Table 1**) were implemented with Sollum SF04 LED lighting fixtures (Sollum Technologies Inc., Montréal, QC, Canada). These fixtures have multiple independently controlled diode channels which allow for changes in spectrum and intensity throughout a 24 h period. The light treatments were as follows: 16 h of white light (3257k) during the day followed by 8 h of darkness (control; 16W), continuous white light for 24 h which represents the largest possible reduction in fixture cost (24W), 16 h white light during the day followed by 8 h of blue light (peak wavelength = 451 nm) at night which allowed us to test the hypothesis that sole blue light can increase stem elongation (16W + 8B), and 16 h of white light during the day followed by 8 h of blue and far-red light (peak wavelength = 734 nm) during the night to observe if there was an additive effect of the two wavelengths on stem elongation (16W + 8BFR; **Figure 2**). All daytime white treatments provided the same percentage of blue (400–499 nm), green (500–599 nm), and red (600–699 nm; 12.1% blue, 30.2% green, and 57.7% red) but at different total intensities (**Table 1**). Daytime was defined as 6:00–22:00 and nighttime was defined as 22:00–6:00. The light in each treatment was measured at four locations within each plot in each greenhouse with a 1-m quantum light sensor (Li-COR 191R; Li-COR Biosciences, Lincoln, NE, United States) just above the apex of the plant. The light intensity was adjusted *via* automatic dimming of the light fixtures as needed throughout the experiment to maintain the appropriate light levels (**Table 1**). Spectral composition readings were taken at the apex of the plant using a Li-COR Li-180 spectroradiometer (**Figure 2**). The daily light integrals (DLI) for photosynthetically active radiation (PAR, 12.6 ± 0.1 mol m^{-2} d^{-1}) and for far-red light (FR, 1.41 ± 0.06 mol m^{-2} d^{-1}) were the same for all four lighting treatments (**Table 1**). Supplemental lighting accounted for 47–81% of total DLI depending on solar radiation fluctuations

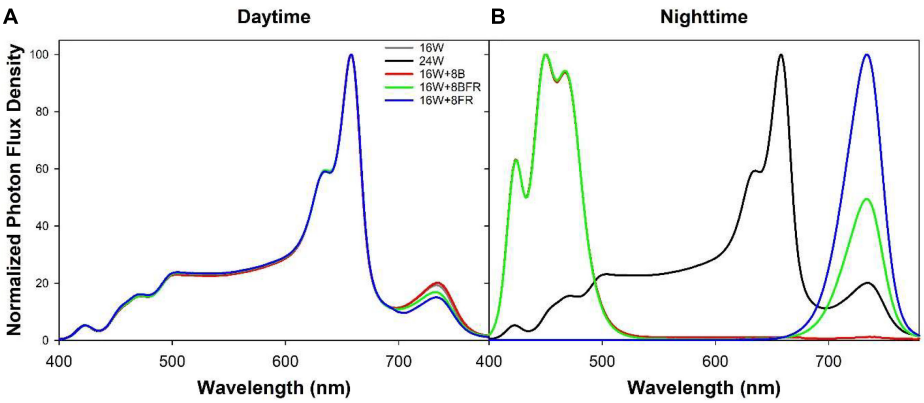

FIGURE 2 | Normalized photon flux density (PFD) of daytime **(A)** and nighttime **(B)** light treatments as determined with a Li-180 spectroradiometer during the night at the head of the plant.

throughout the growing period. The far-red light during the daytime in 16W + 8BFR was reduced accordingly so that same DLI for far-red light could be achieved. PSS values were calculated following the methods of Sager et al. (1988).

All light measurements were performed at night to avoid any contamination from solar radiation. Lights remained on regardless of the natural solar radiation levels to ensure the same DLIs for all lighting treatments. Plants from experiment one were used for all gas exchange measurements, chlorophyll fluorescence measurements, and fruit production evaluation. The experiment was terminated at the end of March because our past research indicates that the effect of supplemental far-red light on greenhouse peppers is negligible after mid-March when there is high intensity of far-red light from sunlight (Hao et al., 2018a).

Experiment Two

Pepper seeds cv. 'Maureno,' 'Gina,' and 'Eurix' were sown into 1 cm × 1 cm rockwool propagation cubes on March 29th, 2021 and placed in a germination chamber with 100% humidity for 8 days. Upon germination, seedlings were transplanted into 2-l pots filled with soil media (BM6, Berger, Saint-Modeste, QC, Canada) and placed in a greenhouse. On April 26th, 2021 40 plants of each cultivar were placed under one of five light treatments (120 plants encompassing all three cultivars under each treatment) in two double-layer polyethylene greenhouses. A fifth treatment was added to better understand the role of sole FR light during the night and its impact on stem elongation (16W + 8FR). The 16W + 8FR treatment represented 16 h of white light followed by 8 h of sole far-red light (**Figure 2** and **Table 1**). The greenhouse roof was covered with light abatement curtains (Obscura 9950 FR W, Ludvig Svensson, Kinna, Sweden) which blocked 90–95% of incoming solar radiation. Measured solar light intensity during solar noon was between 20 and 30 μmol m^{-2} s^{-1} inside the greenhouse. In this way, we could assess the biomass partitioning and growth patterns of peppers without interference from the sun (i.e., in a growth chamber-like setting). Lighting was again provided by Sollum SF04 fixtures. All five lighting treatments had the same PAR DLI (10.4 ± 0.01 mol m^{-2} d^{-1}) and FR DLI (1.09 ± 0.03 mol m^{-2} d^{-1}) measured just above the apex of the plants (**Figure 2** and **Table 1**). Supplemental lighting accounted for between 89 and 96% of the total DLI the plant was exposed to, depending on daily solar radiation. PSS values were calculated following the methods of Sager et al. (1988). The 16W, 24W, 16W + 8B, and 16W + 8BFR treatments were similar to experiment one but had a lower overall DLI. The irrigation management and greenhouse climate parameters were similar to experiment one (**Supplementary Figure 2**). Plants in experiment two were used for plant morphological and biomass partitioning assessment.

Leaf Gas Exchange: Day and Night Measurements

As stated above, all gas exchange data were obtained using plants from experiment 1. Thus the days into the treatment (DIT) are calculated from November 12th, 2020. For day and nighttime measurements, the fifth leaf was placed in the chamber of a Li-COR 6400 (Li-COR Inc., Lincoln, NE, United States) which was fitted with a 2-cm by 3-cm clear top chamber. The leaf temperature was set to 22°C with a relative humidity of 60–70% and a CO_2 level held at 800 μL L^{-1}. Four leaves from separate plants under each treatment were used at 99 DIT for both day and nighttime measurements. Daytime measurements were performed on cloudy days to maximize the effect of supplemental lighting while minimizing the effect of natural sunlight. Nighttime measurements began half an hour after lighting changes (22:30), allowing the leaves to acclimate to the new light environment. Leaves were kept in the chamber until a steady-state photosynthesis rate was obtained, then the average from 2 min was taken.

Leaf Gas Exchange: Light Response Curves

The fifth leaf was placed in the chamber of a Li-COR 6400 photosynthesis system which was fitted with a 2-cm by 3-cm red/blue (88%R/12%B) LED Li-COR standard light source. The leaf temperature was set to 22°C with a relative humidity of 60–70% and a CO_2 level held at 800 μL L^{-1}. Four leaves from

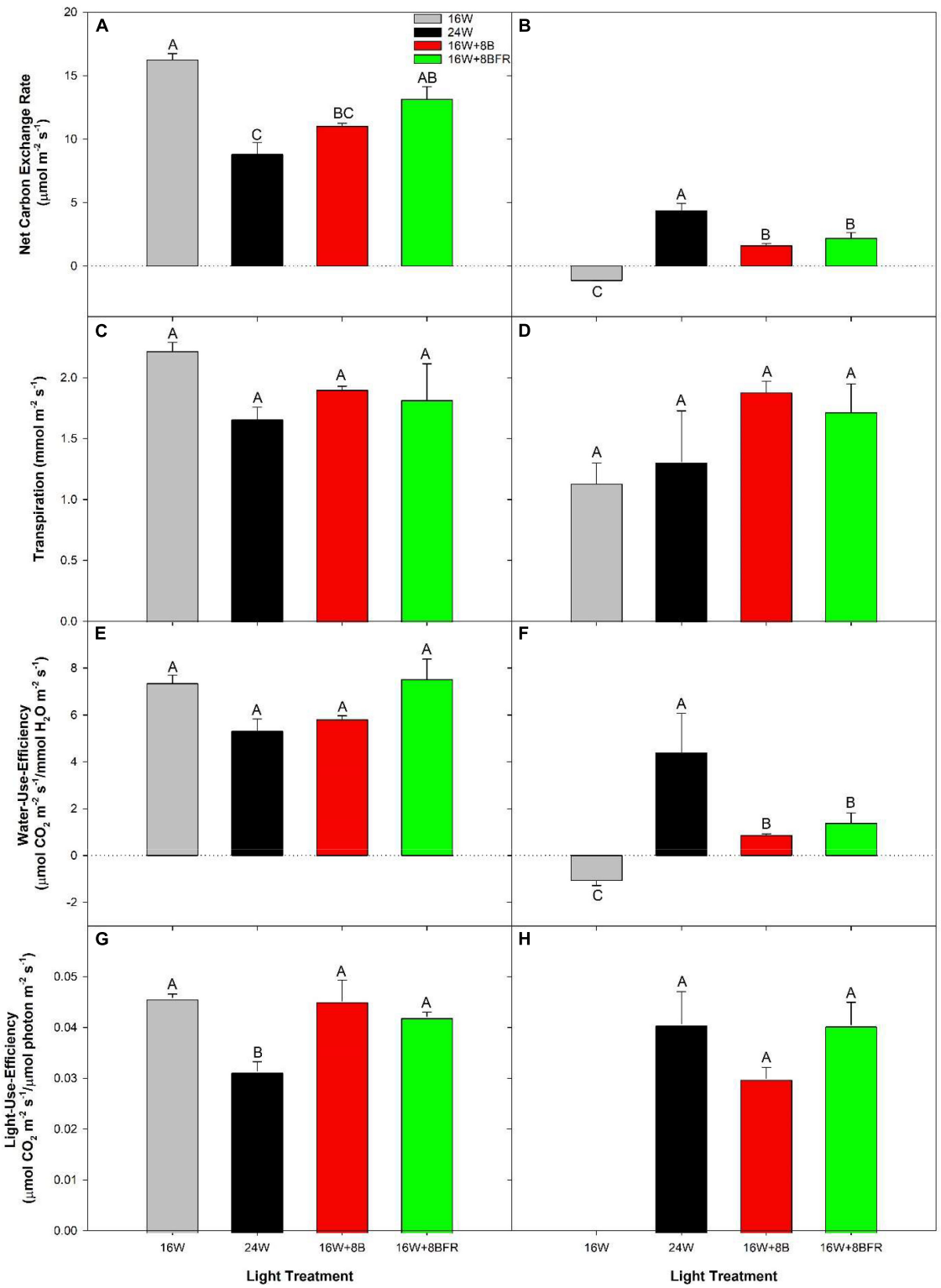

FIGURE 3 | Net carbon exchange rates **(A,B)**, transpiration rates **(C,D)**, water-use-efficiency (WUE; **E,F**), and light-use-efficiency (LUE; **G,H**) of the fifth leaf from pepper plants grown under the lighting treatments at 99 DIT during the daytime **(A,C,E,G)** and nighttime **(B,D,F,H)**. Daytime measurements were performed using a Li-COR 6400 fitted with a clear top chamber on a cloudy day and thus represent the photosynthesis driven mostly by the supplemental lighting. Nighttime measurements were performed after 22:30 (half an hour after night lighting started), allowing leaves to adjust to the new light environmental conditions. Error bars represent the standard errors of the means of $n = 4$. Letter groups (A, B, C) represent a significant difference within a panel between the lighting treatments ($p < 0.05$).

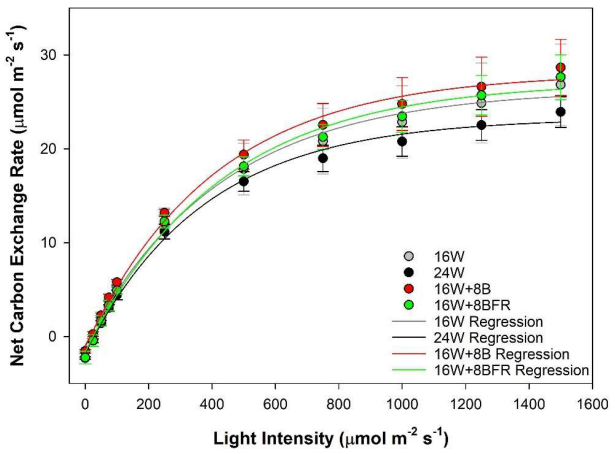

FIGURE 4 | Leaf photosynthetic light response curves of pepper plants grown under the light treatments at 91 DIT as determined using a Li-COR 6400 photosynthesis system with a red/blue standard Li-COR light source. Measurements were made at a CO_2 level of 800 μL L^{-1}, leaf temperature of 22°C, and relative humidity of 60–70%. Regressions lines were fit to $y = y_o + a(1\text{-}e^{(-b^*x)})$ for each lighting treatment.

separate plants under each treatment were used at 91 DIT. Measurements were performed on cloudy days. Leaves were acclimated to high light intensity (1500 μmol m^{-2} s^{-1}) until a steady-state photosynthetic rate was achieved. After the steady-state was achieved, light curves began at a high light intensity and decreased gradually following the procedure from Lanoue et al. (2018b). At each light level, the photosynthetic rate was allowed to reach a steady-state, then measurement was taken for that light level. Photosynthetic rates were plotted against the light intensity and fitted to a regression line following the equation $y = y_o + a(1\text{-}e^{(-b^*x)})$ using SigmaPlot 10.0 to determine the photosynthetic maximum. A linear regression ($y = mx + b$) using the photosynthetic rates between the light levels of 0–100 μmol m^{-2} s^{-1} was used to calculate both the light compensation point (LCP) and quantum yield (QY).

Chlorophyll Fluorescence Imaging

Intact leaves were dark-adapted using aluminum foil for 20 min. After the dark adaptation period, leaflets were detached and immediately used for chlorophyll imaging using a closed FluorCam model FC 800-C with FluorCam v.7.0 software (FluorCam, Photon System Instruments, Brno, Czechia). The minimum fluorescence in a dark-adapted state (F_o) was acquired during a dark period of 5 s, after that, an 800 ms saturating light pulse (3000 μmol m^{-2} s^{-1}) from a blue LED (peak emission of 449 nm) was used to measure the maximum fluorescence in a dark-adapted state (F_m). From F_o and F_m, the variable fluorescence in a dark-adapted state (F_v) was calculated ($F_v = F_m\text{-}F_o$) which was used to determine the maximum photosystem II (PSII) quantum yield (F_v/F_m). In general, the lower the value of F_v/F_m, the more severe the photo-inhibition and thus, the leaf injury (Baker, 2008). By calculating F_v/F_m using chlorophyll fluorescence imaging, we are able to assess not only the prevalence of injury but also the spatial heterogeneity of F_v/F_m from a leaflet. Eight leaflets from the fifth leaf of different plants were used for each light treatment when plants were at 110 DIT.

Yield

Yield analysis was performed on plants from experiment one only. Harvest was performed weekly throughout the experiment beginning on December 31st, 2020 (50 DIT) and finishing on March 24th, 2021 (133 DIT) with peppers being harvested once they reached full size and had gone through a 75% color change.

Biomass Partitioning and Destructive Measurements

Biomass partitioning and destructive harvest measurements were performed on plants from experiment two only. Measurements were done from June 1–3, 2021 (37–39 DIT) and again from June 28–30, 2021 (64–66 DIT) with ten and six plants respectively from each cultivar. During these measurements, plant height, internode length, leaf number, leaf area, and SPAD values of the fifth leaf were determined. Plant height was measured as the distance from the base of the plant in the soil to the top of the tallest stem on that plant. Internode length was the distance from the highest node which contained a leaf longer than 5 cm on the tallest stem to the bifurcation point (i.e., where two stems naturally split). The distance was then divided by the number of nodes between these two points to determine internode length. The leaf area was determined using a Li-COR 3100 (Li-COR Inc.) leaf area meter. SPAD value was determined using a chlorophyll meter taking six measurements on each leaf to determine an average for that leaf (SPAD model 502, Konica Minolta, Osaka, Japan). The leaves and stems were separated from the plant and weighed (fresh weight), then placed in an oven at 65°C for 2 weeks before being weighed for dry weight.

Statistical Analysis

All statistics were performed using SAS Studio 3.5. After the ANOVA, multiple means comparisons between the different treatments were done using a Tukey-Kramer adjustment and a value of $p < 0.05$ to indicate a significant difference. Regression analysis was done using a backward elimination method in SAS Studio 3.5. Final regressions with a $p < 0.05$ were determined to be significant.

RESULTS

Leaf Gas Exchange and Chlorophyll Fluorescence

Clear top photosynthetic measurements were done on cloudy days which allowed for the observation of how each light treatment affected light capture and gas exchange directly (**Figure 3**). Leaves grown under 16W + 8BFR produced similar photosynthetic rates to the control, 16W (**Figure 3A**). Leaves from both 24W and 16W + 8B produced lower photosynthetic rates than the control (16W). There was no significant difference

TABLE 2 | Summary of the major physiological parameters as determined by leaf light response curves (**Figure 4**) from peppers grown under all treatments at 91 DIT.

Treatment	Light compensation point (μmol m^{-2} s^{-1})	Apparent quantum yield (μmol CO_2 m^{-2} s^{-1}/μmol m^{-2} s^{-1})	Pn_{max} (μmol CO_2 m^{-2} s^{-1})
16W	21.42 ± 3.78^{A}	0.069 ± 0.006^{A}	27.34 ± 4.65^{A}
24W	32.19 ± 3.30^{A}	0.068 ± 0.004^{A}	25.14 ± 1.81^{A}
16W + 8B	21.04 ± 3.25^{A}	0.075 ± 0.001^{A}	29.38 ± 3.90^{A}
16W + 8BFR	29.22 ± 8.14^{A}	0.072 ± 0.004^{A}	29.17 ± 2.94^{A}

The light compensation point (LCP) and apparent quantum yield (QY) were calculated from a regression line ($y = mx + b$) fitted to the values between the PAR values of 0–100 μmol m^{-2} s^{-1}. The photosynthetic maximum (Pn_{max}) was calculated from $y = y_o + a(1\text{-}e^{(-b*x)})$. Values ± the standard errors of the means are representative of n = 4. Within each parameter and measurement date, different letters represent a statistical difference as determined by a one-way ANOVA with a Tukey-Kramer adjustment ($p < 0.05$).

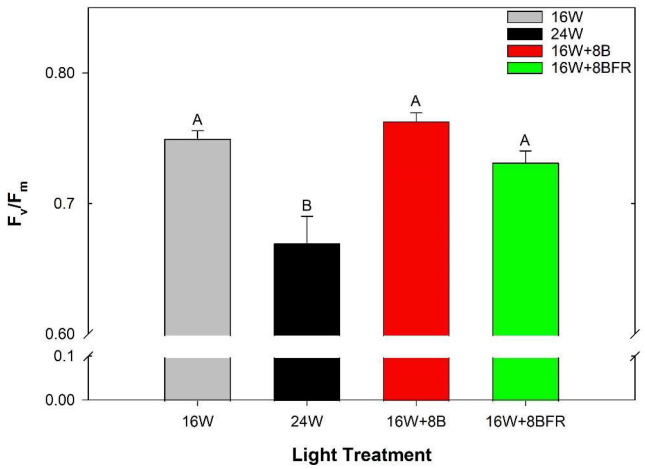

FIGURE 5 | Maximum efficiency of PSII (F_v/F_m) of the fifth leaf from peppers grown under all light treatments at 110 DIT. Error bars represent the standard errors of the means of $n = 8$. Letter groups (A, B) represent a statistical difference as determined by a one-way ANOVA with a Tukey-Kramer adjustment ($p < 0.05$).

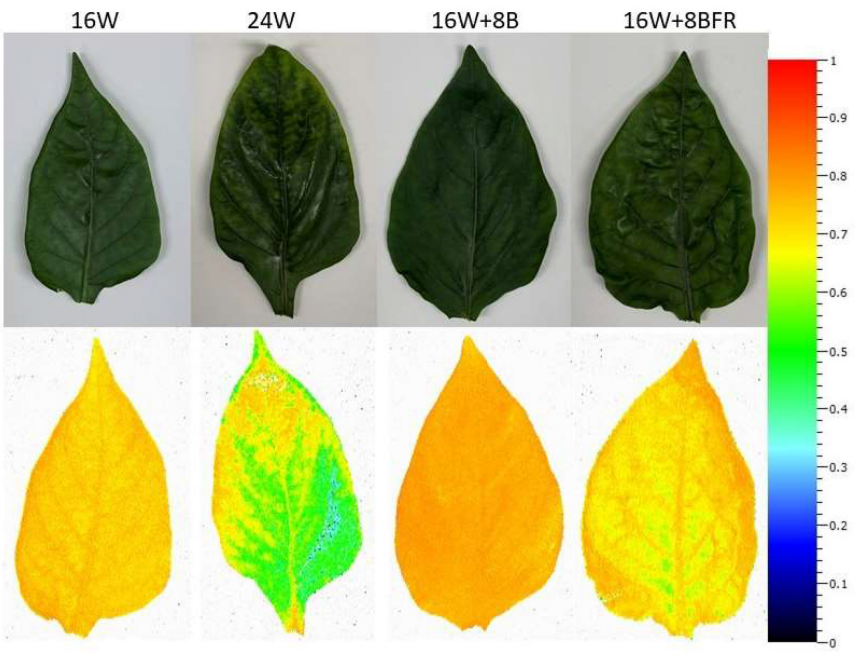

FIGURE 6 | Spatial response of F_v/F_m from the fifth leaf of peppers grown under all light treatments measured at 110 DIT.

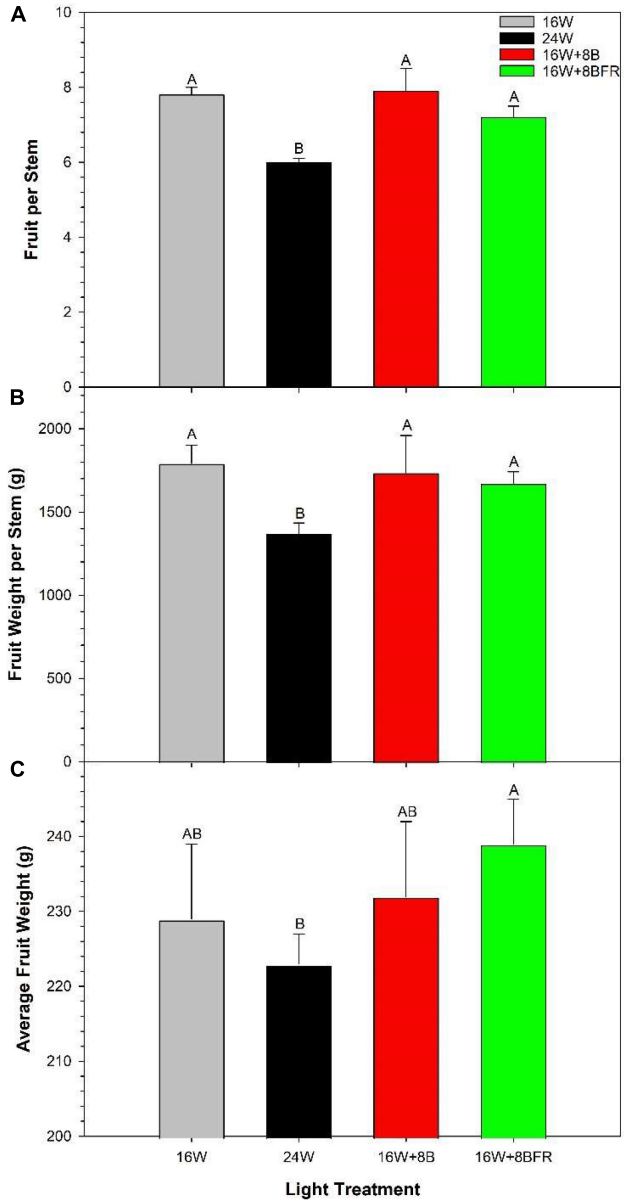

FIGURE 7 | Total yield parameters from peppers grown under all light treatments from October 5th, 2020 to March 24th, 2021. **(A)** Represents the accumulated number of fruit harvested per stem, **(B)** represents the accumulated number of fruit harvested per stem, and **(C)** represents the average weight per fruit (fruit size). Within each panel, letter groups (A, B) represent a statistical difference as determined by a one-way ANOVA with a Tukey-Kramer adjustment ($p < 0.05$).

among all treatments on leaf transpiration rates (**Figure 3C**) and the ratios of CO_2 influx vs. H_2O efflux (water-use-efficiency; WUE) (**Figure 3E**). Calculation of light-use-efficiency (LUE) was also performed which normalized photosynthesis on an incoming photon basis. In this way, we can compare photosynthetic capacity between the light treatments with different intensities. This parameter also allows us to remove any small effects of changing solar radiation intensity, even though these measurements are taken on cloudy days. The 16W, 16W + 8B, and 16W + 8BFR treatments had similar LUE while 24W was lower (**Figure 3G**). This result indicated that 24W was less efficient at turning incident light into assimilated carbon. Also, even though 16W + 8B was observed to have a lower photosynthetic rate than 16W, it was mainly due to a lower light intensity of the treatment during daytime (**Table 1**).

Leaves from 16W produced a negative net carbon exchange rate (NCER) representing respiration during the night period (**Figure 3B**), as expected. However, leaves from 24W, 16W + 8B, and 16W + 8BFR all produced positive NCERs, indicating photosynthesis. These photosynthetic rates during the night period coupled with daytime photosynthetic rates indicate positive carbon assimilation for a continuous 24 h period. It should be noted that 24W had the highest NCER of all treatments during the night which corresponded with the highest light intensity during that period (**Figure 3B**). Transpiration rates during the night period were similar to all light treatments (**Figure 3D**). As the quotient of NCER and transpiration, WUE closely follows the patterns of NCER with 16W producing the lowest WUE and 24W the highest (**Figure 3F**). LUE values for 16W were non-resultant because there was no light during the nighttime (**Figure 3H**). The LUEs for the three treatments with lighting during the night (24W, 16W + 8B, and 16W + 8BFR) were similar (**Figure 3H**), indicating the photosynthetic capacity of the three treatments was the same and the difference in their net carbon exchange rates was due to difference in night light intensity (**Table 1**).

Photosynthetic light response curves (**Figure 4**) allow for the assessment of how plants grown under different light treatments respond to the different light intensities. The light compensation point (LCP) is the light intensity at which the photosynthetic rate and the respiratory rate are equal to each other (i.e., no net CO_2 gain or loss). Under all treatments, the LCP was similar indicating that plants are able to start carbon assimilation at roughly the same light intensity (**Table 2**). Similar to LUE, apparent quantum yield is a metric that determines how much CO_2 is assimilated with each additional photon added. This parameter is calculated during the linear phase (0–100 $\mu mol\ m^{-2}\ s^{-1}$) of light increase. Continuous lighting had no detrimental effect on apparent quantum yield (**Table 2**). The photosynthetic maximum (Pn_{max}) is a measurement of the maximum photosynthetic rate when light is not a limiting factor. In this sense, it is a proxy for what the plant may encounter during periods of intense natural solar radiation. Similar to other metrics of the light response curve, Pn_{max} was comparable among all treatments, indicating that the photosynthetic performance under strong light was not affected by continuous illumination (**Table 2**).

As stated previously, chlorophyll fluorescence measurements are an unbiased determination of the stress status of a leaf in comparison to visual chlorosis ratings. The maximum quantum efficiency of PSII photochemistry (F_v/F_m) is a parameter that is often used to monitor the stress of a leaf through the measurement of photo-inhibition. The higher the value, the less stressed a leaf is (Demmig and Björkman, 1987; Baker, 2008). Leaves grown under 24W have significantly lower F_v/F_m values than all other treatments, indicating a higher level of stress, even

if this was not visually apparent to the human eye (**Figures 5**, **6**). Furthermore, fluorescence imaging allows for the assessment of the spatial impact of stress. In the bottom image of **Figure 6**, a large area of green is apparent in the image of the leaf grown under 24W, indicating a lower F_v/F_m value and more stress. While 16W + 8BFR also displays some green coloration, it was much less severe. There was no significant difference in Fv/Fm values between 16W + 8BFR and W16 or 16W + 8B (**Figure 4**).

Yield

Ultimately, the feasibility of dynamic CL/24 h lighting hinges on the production of equal to or greater yield than a traditional 16h photoperiod (control, 16W). In **Figures 7A,B**, both 16W + 8B and 16W + 8BFR supported similar fruit production (total fruit number and weight per stem) to 16W (control) while 24W significantly reduced fruit production. The fruit size (average weight per fruit), a metric that often affects fruit grade was lower in 24W than in 16W + 8BFR (**Figure 7C**) while there was no difference among other treatments. Therefore, 16W + 8B and 16W + 8BFR were able to achieve the same fruit yield and grade as the control 16W while 24W reduced fruit yield and grade.

Plant Morphology

Experiment two was conducted to get an in-depth assessment of the morphological changes brought about by the various light treatments (**Figure 8**) using three cultivars with different growth architecture (especially internode length). 'Maureno' and 'Gina' in combination with 16W + 8FR and 16W + 8BFR produced the tallest plants while both 16W and 24W produced the shortest at 37-39 DIT (**Figures 8A,C,E**, **9A**). Interestingly, in 'Eurix' 16W + 8FR produced taller plants than 16W + 8BFR. During the 64-66 DIT measurement period, differences in plant height due to light treatments were much more apparent. Again, both 16W + 8BFR and 16W + 8FR produced the tallest plants while 16W and 24W produced the shortest (**Figures 8B,D,F**, **9B**). In fact, plant height increased by 63, 54, and 56% when comparing 16W + 8FR to 16W for 'Maureno,' 'Gina,' and 'Eurix' respectively. Furthermore, during both measurement periods, blue light at night (16W + 8B) increased stem height compared to 16W. Far-red light during the night either used as a sole source (16W + 8FR) or in addition to blue light (16W + 8BFR) resulted in a further increase (**Figures 8**, **9**).

During the measurement period of 37–39 DIT, internode length was similar between 16W, 24W, and 16W + 8B in all cultivars (**Figure 9C**). Treatments 16W + 8BFR and 16W + 8FR produced similar internode lengths which were longer than those observed in plants grown under 16W, 24W, or 16W + 8B. Notably, 16W + 8BFR and 16W + 8FR both implemented FR light during the night either with blue light or as a sole source. At 64–66 DIT, 16W + 8FR again produced the longest internode for all three cultivars, and 16W + 8BFR produced similarly long internodes in 'Gina' and 'Eurix' (**Figure 9D**). Furthermore, plants are grown under 16W + 8B with monochromatic blue light at night also showed longer internode length when compared to 16W in all three cultivars (**Figure 9D**). This indicates that long-term exposure to blue light during the night period can increase internode length in pepper plants. The plants in 16W + 8BFR and 16W + 8FR had similar plant heights and internode lengths during both measurement periods (**Figure 9**) in all three cultivars except for a small difference in 'Maureno,' indicating the response of plant height and internode length between 16W + 8BFR and 16W + 8FR were mostly similar, and there was a minor influence of cultivars on the response.

Leaf area can give an indication of the light capture ability of a plant which can be impacted by the light environment. Between 37 and 39 DIT, the plants are grown under 24W and 16W + 8B produced the largest leaf area while the plants under 16W + 8FR had the lowest leaf area in 'Gina' (**Table 3**). Coincidentally, at 64–66 DIT all cultivars had the highest leaf area when grown under 16W + 8B which had sole blue light during the night treatment (**Table 3**). Both 16W + 8BFR and 16W + 8FR treatments that contained FR light were also observed to have an increased leaf area compared to 16W. At 37–39 DIT and in 'Maureno', the leaf number was similar among the treatments. In 'Gina' and 'Eurix,' 16W plants had the highest leaf number while 16W + 8BFR or both 16W + 8BFR and 16W + 8FR had the lowest numbers of leaves. At 64–66 DIT, 16W resulted in the highest number of leaves almost for all cultivars. In 'Maureno,' 16W + 8B also produced a high number of leaves, and in 'Gina' 24W produced a similar number of leaves as 16W (**Table 3**). For all three cultivars, treatments that contained far-red (solely or in combination with blue) produced the least number of leaves. Interestingly, at 64–66 DIT, 16W produced the most leaves in all cultivars but had the lowest leaf area indicating that the average leaf size was the smallest in the treatment.

At 37–39 DIT, the specific leaf area (SLA) of plants grown under four CL treatments in all three cultivars was higher than that of plants grown under 16W, indicating CL treatments reduced leaf thickness (**Table 3**). In 'Maureno' and 'Gina,' SLA was similar among all four CL treatments. In 'Eurix,' the plants under 16W + 8FR had higher SLA than that of plants under 16W + 8BFR (**Table 3**). At 64–66 DIT, a much clearer trend emerged where 16W + 8FR consistently produced the highest SLA while 16W produced the lowest SLA followed by 24W in all cultivars. At 37–39 DIT, the SPAD value, a metric closely correlated with chlorophyll content, was consistently the lowest in plants grown under 16W + 8FR and the highest in plants grown under 16W in all cultivars (**Table 3**). This trend continued during the 64–66 DIT measurements (**Table 3**). Taking all the information on leaf area, SLA, and SPAD into consideration, it seems that the plants grown in CL treatments adapted to the low light environment by reducing leaf thickness and increasing leaf area to improve light interception, especially for plants grown under 16W + 8FR.

Regression Analysis of Biomass Partitioning and Internode Length to Phytochrome Photostationary State

Regression analysis was conducted using the nighttime PSS values from CL treatments only where PSS was 0.833, 0.566, 0.315, and 0.186 for 24W, 16W + 8B, 16W + 8BFR, and 16W + 8FR, respectively. The 16W treatment was not included in the analysis due to the non-resultant quotient of the equation (i.e.,

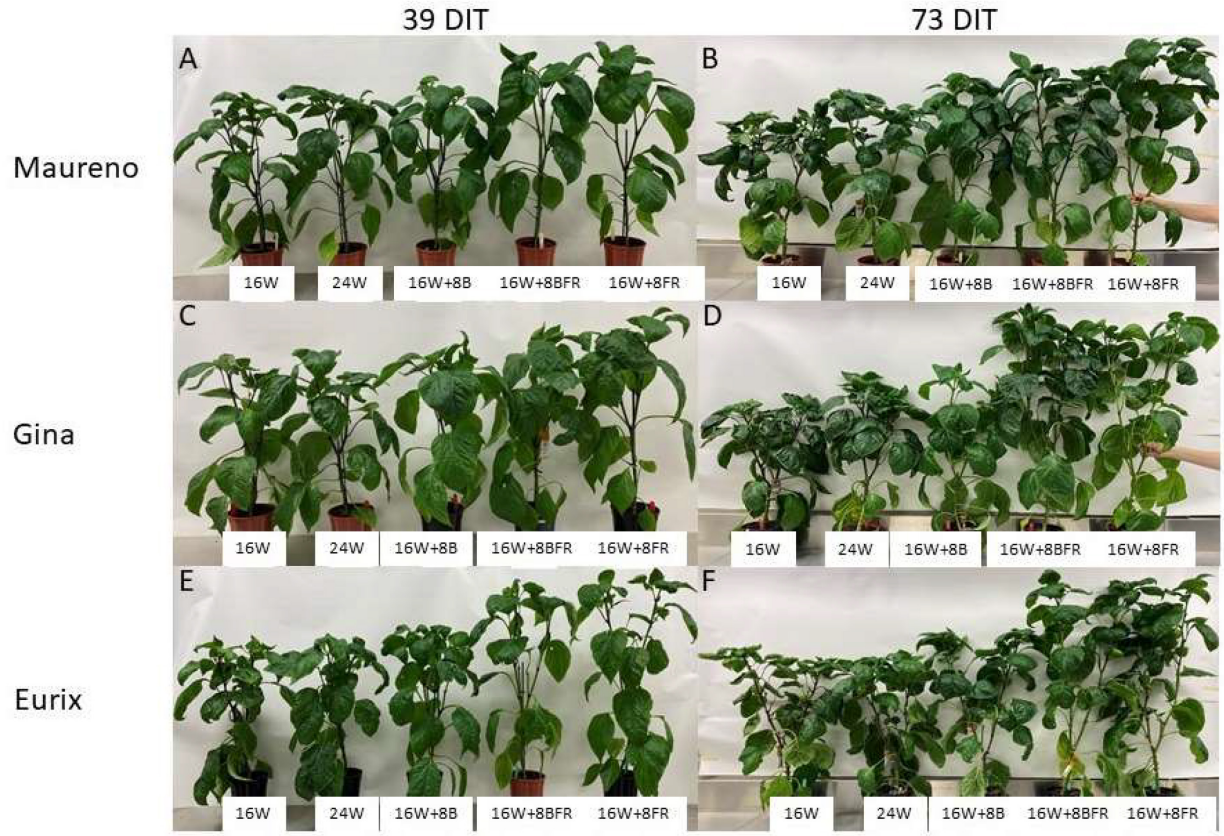

FIGURE 8 | Pepper plants cv. 'Maureno' **(A,B)**, 'Gina' **(C,D)**, and 'Eurix' **(E,F)** grown under five different light treatments at 39 DIT **(A,C,E)** and 73 DIT **(B,D,F)** from experiment two.

because there was no light during the nighttime). A significant relationship between dry matter biomass partitioning to leaves and increasing PSS was only apparent for 'Gina' (**Figure 10A**). Conversely, the biomass partitioning to the stem tended to decrease with increasing PSS and was significant for 'Gina' only (**Figure 10C**). During the 64–66 DIT measurement period, a more obvious trend emerged as the dry biomass partitioning to the leaves increased with increasing PSS and biomass partitioning to the stem decreased with increasing PSS in all cultivars. Both fresh and dry biomass partitioning to leaves increased with increasing nighttime PSS and conversely partitioning to the stem decreased with increasing PSS (**Figures 10B,D**).

A decrease in PSS can enact a shade avoidance response characterized by increased stem elongation and leaf expansion. Here, the alternation of PSS occurred during the nighttime spectral shifts and also showed a shade avoidance response. As PSS decreased, the internode length of all cultivars at both measurement periods increased (**Figure 11**). Notably, below a PSS of 0.315 (16W + 8BFR), a further increase in internode length was not observed with the exception of the cultivar 'Maureno' during the 64-66 DIT measurement period (**Figure 11B**). Although the use of sole FR (16W + 8FR) further decreased the PSS compared to blue + FR (16W + 8BFR), a stronger shade avoidance response (in this case internode length) was not observed. This indicates that a PSS of 0.315 is sufficient to maximize stem elongation and no further increase in stem elongation was observed below this value. Taken together, an increased partitioning to the stem as the PSS decreases can be correlated with the increase in stem elongation under these treatments (**Figures 9–11**).

DISCUSSION

Impact of Dynamic Continuous Lighting on Plant Injury and Yield

The implementation of CL during greenhouse crop production offers an intriguing option for growers. By utilizing light during the night period, the lower light intensity can be used during the daytime while still achieving the desired DLI target (Hao et al., 2018a). This translates to a reduced fixture requirement leading to vast capital cost savings for growers. However, CL means constant photon pressure on the plant which has been shown to cause photoperiod injury in both peppers and tomatoes leading to a reduction in fruit production (Hillman, 1956; Velez-Ramirez et al., 2014; Matsuda et al., 2016; Haque et al., 2017). Therefore, the feasibility of CL strategies hinges on whether the production (yield and quality) is equal to or greater than the

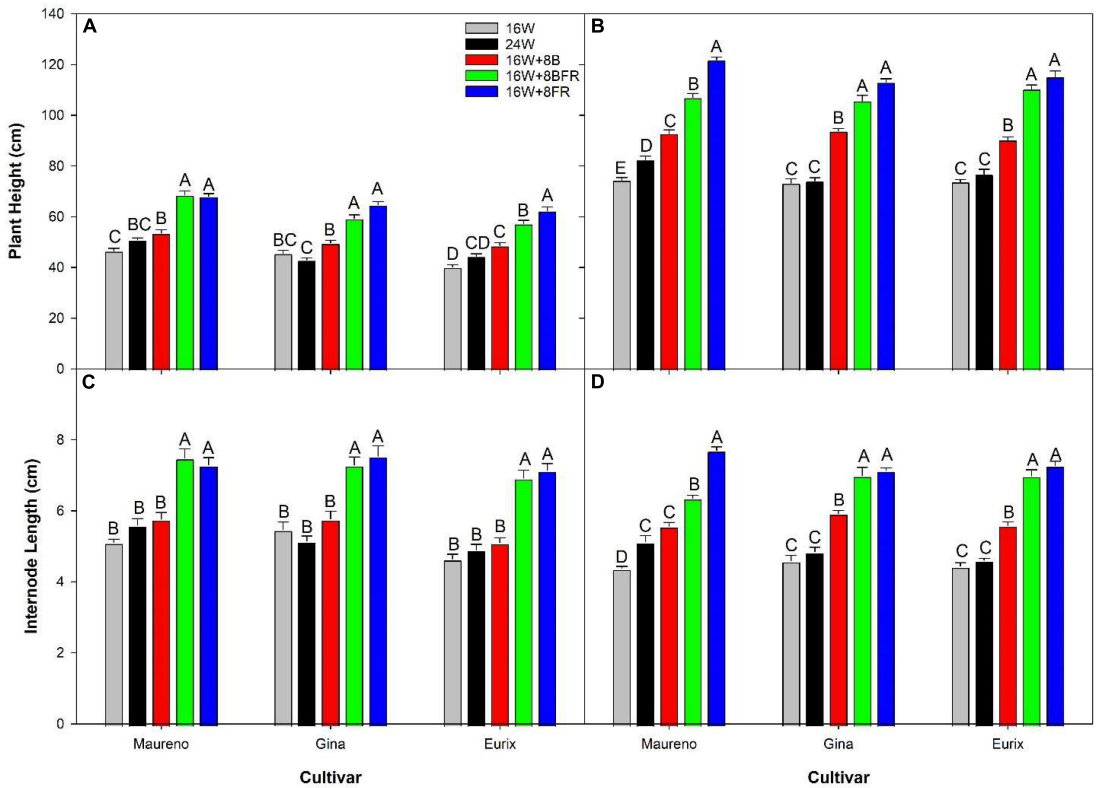

FIGURE 9 | Plant height **(A,B)** and internode length **(C,D)** for cv. 'Maureno,' 'Gina,' and 'Eurix' from experiment two measured at either 37–39 DIT **(A,C)** or 64–66 DIT **(B,D)**. Values and standard errors in **(A,C)** represent ten plants while those in **(B,D)** represent six plants. Within each panel and cultivar, letter groups (A, B, C, D, E) represent a statistical difference as determined by a one-way ANOVA with a Tukey-Kramer adjustment ($p < 0.05$).

conventional 16 h photoperiod lighting (control, 16W in this study). Due to their unique attributes, LEDs allow for the use of a dynamic CL strategy which employs a reduction in light intensity and/or change in spectral composition between day and night periods, which has been shown to eliminate or reduce injury in lettuce (Ohtake et al., 2018), tomato (Matsuda et al., 2016; Lanoue et al., 2019; Pham and Chun, 2020), and cucumber (Lanoue et al., 2021b). In this study with peppers, we showed that plants grown under two dynamic CL strategies (16W + 8B and 16W + 8BFR) were able to avert injury and maintain fruit yield and size (grade) when compared to the 16h control (16W; **Figures 3**, **5**, 7). Both 16W + 8B and 16W + 8BFR employed a daytime PAR reduction of 18.2% while 16W + 8BFR also included a 25% reduction in daytime FR used; a total reduction of 18.9% in the extended PAR (ePAR; 400–780 nm) region (**Table 1**). In addition to the reduction in light fixture costs, electricity costs could also be reduced using the CL strategies because the electricity price is usually higher during the peak daytime than during the off-peak period at night in many regions in the world. Notably, both 16W + 8B and 16W + 8BFR which used dynamic CL performed better than 24W which maintained constant light intensity and spectrum during the 24h period (**Figures 3G**, **5**). This indicates that the dynamic nature of the CL used in this study is essential for removing injury and sustaining fruit production in greenhouse pepper.

In contrast to our current study, the use of monochromatic blue light at 100 μmol m^{-2} s^{-1} (Velez-Ramirez et al., 2017) or 150 μmol m^{-2} s^{-1} (Matsuda et al., 2016) during the night produced a high degree of injury in tomatoes. However, our previous studies on tomato (Lanoue et al., 2019) and cucumber (Lanoue et al., 2021b) differ from this trend and indicate that the use of low intensity monochromatic blue light (50 μmol m^{-2} s^{-1}) during the night was able to avert injury. In this study, nighttime blue light was considerably higher than the light compensation point (**Table 2**), and between that used in Velez-Ramirez et al. (2017) and Lanoue et al. (2019), and drove appreciable amounts of photosynthesis in 16W + 8B and 16W + 8BFR during the night (**Figure 3B**) without causing injury (**Figures 4**, **5**). It should be noted that although 24W used a constant light intensity and spectrum that drove high rates of photosynthesis during the night and injury was observed, it was less than what was reported in other studies with other species (Hillman, 1956; Velez-Ramirez et al., 2014; Matsuda et al., 2016). This indicates that peppers may be less susceptible to long photoperiod injury than other species as previously noted by Demers and Gosselin (1999, 2002).

It is well known that light and temperature interaction has an effect on photosynthesis and yield; in general, an increase in light intensity requires an increase in temperature to maintain an optimum homeostatic balance and drive

TABLE 3 | Leaf area, leaf number, specific leaf area, and SPAD value of 'Maureno,' 'Gina,' and 'Eurix' during the 37–39 DIT and 64–66 DIT measurement periods under different light treatments.

Cultivar	Treatment	Leaf Area (cm^2)	Leaf number	Specific Leaf Area ($m^2\ kg^{-1}$)	SPAD value
37–39 DIT					
Maureno	16W	2448 ± 106^{A}	33.8 ± 1.7^{A}	30.8 ± 0.9^{B}	47.9 ± 1.1^{A}
	24W	2513 ± 121^{A}	32.4 ± 1.1^{A}	40.0 ± 0.9^{A}	46.4 ± 1.0^{AB}
	16W + 8B	2648 ± 63^{A}	32.9 ± 1.5^{A}	38.4 ± 1.8^{A}	43.8 ± 0.9^{BC}
	16W + 8BFR	2361 ± 141^{A}	28.8 ± 1.8^{A}	40.7 ± 0.4^{A}	45.3 ± 0.8^{ABC}
	16W + 8FR	2430 ± 100^{A}	30.7 ± 1.1^{A}	41.6 ± 0.4^{A}	41.8 ± 0.7^{C}
Gina	16W	2567 ± 144^{AB}	35.2 ± 2.5^{A}	32.3 ± 1.0^{B}	47.8 ± 1.5^{A}
	24W	2953 ± 138^{A}	31.8 ± 2.1^{AB}	40.3 ± 1.0^{A}	43.1 ± 0.4^{AB}
	16W + 8B	2852 ± 117^{A}	31.4 ± 1.6^{AB}	41.2 ± 1.9^{A}	41.1 ± 1.7^{B}
	16W + 8BFR	2526 ± 136^{AB}	27.3 ± 0.7^{B}	39.5 ± 0.6^{A}	43.2 ± 0.4^{AB}
	16W + 8FR	2322 ± 88^{B}	27.1 ± 1.2^{B}	41.1 ± 0.8^{A}	42.4 ± 0.7^{B}
Eurix	16W	2568 ± 173^{A}	35.0 ± 2.3^{A}	32.4 ± 0.9^{C}	44.0 ± 0.6^{A}
	24W	2420 ± 132^{A}	32.1 ± 1.1^{AB}	38.3 ± 1.0^{ABC}	44.0 ± 0.7^{A}
	16W + 8B	2709 ± 126^{A}	36.6 ± 2.7^{A}	37.6 ± 2.5^{BC}	41.7 ± 0.7^{AB}
	16W + 8BFR	2451 ± 119^{A}	28.0 ± 1.1^{B}	44.0 ± 0.6^{AB}	41.8 ± 0.8^{AB}
	16W + 8FR	2574 ± 78^{A}	31.7 ± 1.1^{AB}	44.9 ± 1.0^{A}	39.4 ± 0.7^{B}
64–66 DIT					
Maureno	16W	4523 ± 63^{C}	55.3 ± 1.6^{A}	21.1 ± 0.6^{D}	61.4 ± 1.2^{A}
	24W	5535 ± 217^{B}	51.8 ± 1.0^{AB}	25.5 ± 0.7^{C}	57.6 ± 1.4^{AB}
	16W + 8B	6776 ± 254^{A}	55.8 ± 1.6^{A}	30.2 ± 0.8^{AB}	55.4 ± 1.6^{B}
	16W + 8BFR	6003 ± 96^{B}	50.7 ± 1.0^{AB}	28.9 ± 0.3^{B}	59.4 ± 0.9^{AB}
	16W + 8FR	6169 ± 117^{AB}	49.7 ± 0.6^{B}	31.7 ± 0.7^{A}	54.9 ± 0.4^{B}
Gina	16W	5229 ± 113^{D}	52.0 ± 1.3^{A}	23.2 ± 0.4^{D}	61.7 ± 2.5^{A}
	24W	5847 ± 298^{CD}	52.5 ± 2.2^{A}	27.1 ± 0.9^{C}	56.1 ± 0.7^{AB}
	16W + 8B	7399 ± 294^{A}	51.2 ± 2.0^{AB}	33.2 ± 0.8^{AB}	51.1 ± 0.9^{BC}
	16W + 8BFR	7079 ± 147^{AB}	48.3 ± 0.9^{B}	32.2 ± 0.9^{B}	54.7 ± 0.7^{BC}
	16W + 8FR	6433 ± 107^{BC}	48.7 ± 1.0^{B}	36.5 ± 0.4^{A}	49.7 ± 0.7^{C}
Eurix	16W	4908 ± 123^{C}	58.5 ± 2.4^{A}	21.1 ± 0.4^{C}	53.4 ± 1.5^{A}
	24W	5888 ± 196^{B}	51.3 ± 1.8^{AB}	26.5 ± 0.7^{B}	47.9 ± 2.2^{AB}
	16W + 8B	6826 ± 114^{A}	54.8 ± 1.2^{AB}	29.9 ± 0.6^{A}	51.4 ± 1.1^{AB}
	16W + 8BFR	5938 ± 164^{B}	49.7 ± 1.0^{B}	30.8 ± 0.5^{A}	47.7 ± 1.0^{AB}
	16W + 8FR	6888 ± 158^{A}	54.8 ± 1.4^{AB}	31.8 ± 0.3^{A}	46.2 ± 0.7^{B}

Values and standard errors represent 10 plants during the 37–39 DIT measurement period and six plants during the 64–66 DIT measurement period. Within each parameter, cultivar, and measurement period, letter groups (A, B, C, D) represent a statistical difference as determined by a one-way ANOVA with a Tukey-Kramer adjustment ($p < 0.05$).

assimilation (Walters and Lopez, 2021; Song et al., 2022). In our study, nighttime temperatures were not optimized for all four CL treatments, specifically the 24W which had the highest nighttime light intensity. This was because there is a lack of information on optimum temperature management for dynamic CL treatments, and all light treatments were in the same greenhouse and temperature could not be individually adjusted within each treatment. However, the greater SLA in all four CL treatments than 16W (control; **Table 3**) is an indication of the air temperature may be too high for the CL treatments. The plant temperature, especially at the top canopy, might be higher for plants grown under CL because of the continuous exposure to light, when at the same air temperature. Therefore, the optimum air temperature for CL treatments may be lower. Haque et al. (2015, 2017) observed that tomato plants grown under CL with a reduced nighttime temperature (16°C vs. 23°C in the control) had little to no leaf injury under continuous illumination. Hao et al. (2018b, 2020) discovered the response of greenhouse tomatoes, peppers, and cucumbers to long photoperiods of HPS lighting is improved by a temperature drop during the first 3 h after the lighting is off and the temperature control strategy reduced heating energy demand. Leaf injury in tomatoes and peppers is reduced by the temperature drop (Hao et al., 2018b). Therefore, further research is needed to investigate the interaction between temperature control and dynamic CL to determine the optimum air temperature and temperature control strategy for dynamic CL lighting.

The Impact of Nighttime Spectra on Plant Growth

Although the DLI was not controlled for, Demers et al. (1998) observed a significant reduction in plant height, internode length, and leaf area in peppers grown under supplemental HPS light

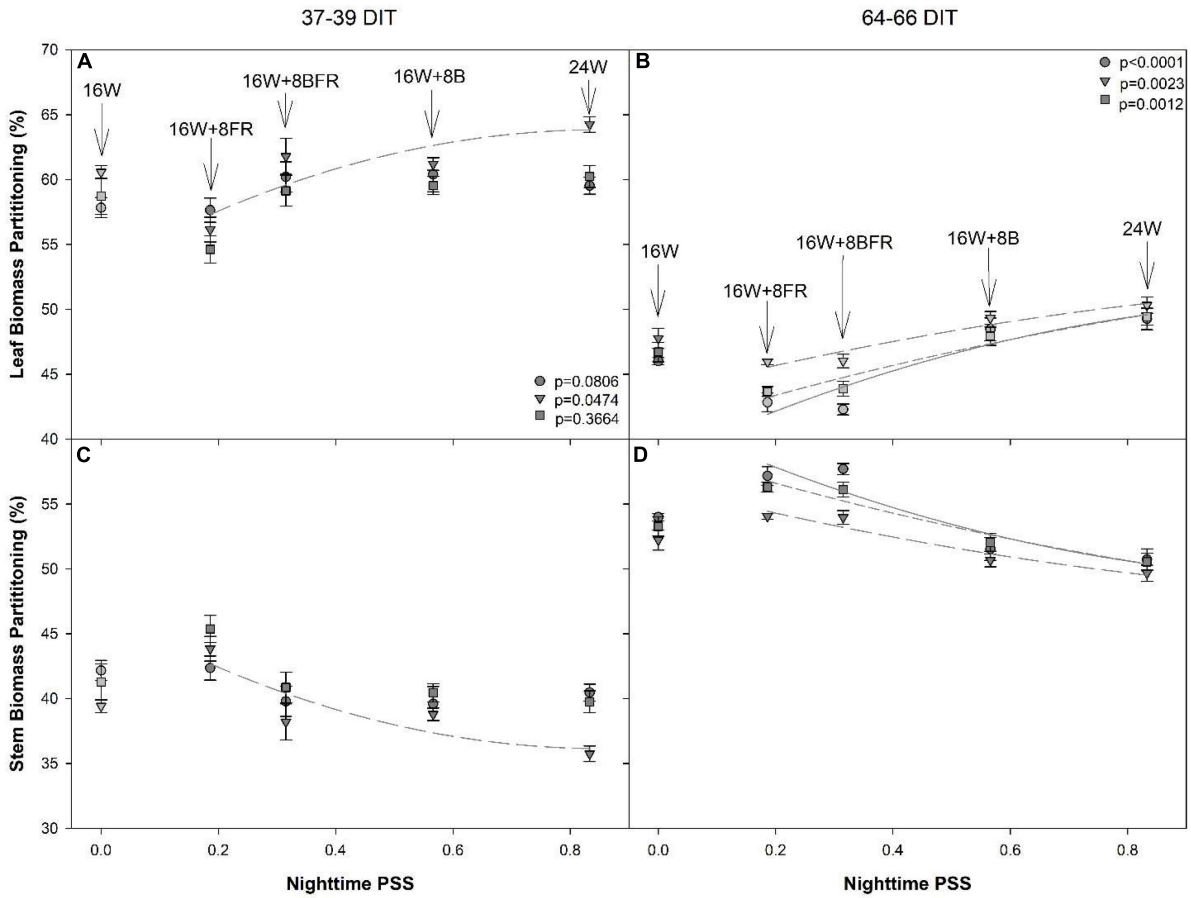

FIGURE 10 | Regression analysis of biomass partition to leaf **(A,B)** and stem **(C,D)** in dry weight from 'Maureno' (circle; solid line), 'Gina' (downward triangle; long dash line), and 'Eurix' (square; short dash line) during the 37–39 DIT measurements **(A,C)** and 64–66 DIT measurements **(B,D)**. Nighttime PSS of 0.833, 0.566,0.315, and 0.186 correspond to treatments 24W, 16W + 8B, 16W + 8BFR, and 16W + 8FR respectively as determined *via* Sager et al. (1988). Regression analysis was done using a backward elimination method. The *p*-values listed are for the final regressions and only regressions which were determined to be significant ($p < 0.05$) are shown. The 16W treatment did not have light at night and thus was non-resultant during the PSS calculation, therefore, it was left out of the regression analysis. The biomass partition values for 16W are plotted in the graph at a PSS value of zero.

for 24 h compared to 14 h. Velez-Ramirez et al. (2014) also noted that even if tomatoes were genetically altered to eliminate the occurrence of CL injury, a reduction in leaf area would hinder plant performance in a practical setting due to reduced light capture. However, the use of sole blue light, such as the application of blue light during the night, has been shown to elicit a response similar to the shade avoidance response of FR (Hernández and Kubota, 2016; Lanoue et al., 2019; Kong and Zheng, 2020). In experiment two, plant height was seen to be greater when plants were grown under 16W + 8B which contained sole blue light during the night period compared to the 16 h control (**Figure 9**). It was also noted that this phenomenon was time-dependent as the difference in plant height increased after the treatments were applied for a longer time (**Figure 9B**). This confirms the studies in tomato and *Arabidopsis* which indicate sole blue light is able to increase plant height (Hernández and Kubota, 2016; Lanoue et al., 2019; Kong and Zheng, 2020). The increase in plant height coupled with an increase in leaf area and specific leaf area indicate that sole illumination with blue light during the night can induce a shade avoidance response (**Table 3**). Not only does this have an impact on plant architecture, but can also allow the plant to better capture light during the daytime period (Hersch et al., 2014).

Far-red light has long been known to elicit a strong photomorphogenic response in plants (Franklin and Whitelam, 2005). Here, we observed that the use of sole FR during the night period resulted in the largest stem elongation of all treatments in peppers (**Figure 9**). Interestingly, it was determined that the movement of just 25% of the total FR DLI from the daytime (16W) to the nighttime (16W + 8BFR and 16W + 8FR) at only 10–11 μmol m^{-2} s^{-1} was able to produce a significantly stronger photomorphogenic response than the use of FR during the daytime only. Indeed, this time-specific use of FR light led to an increase in internode length of 37.6–53.5% during the first destructive measurement and 55.6–75.8% during the second destructive measurement, depending on cultivars. All

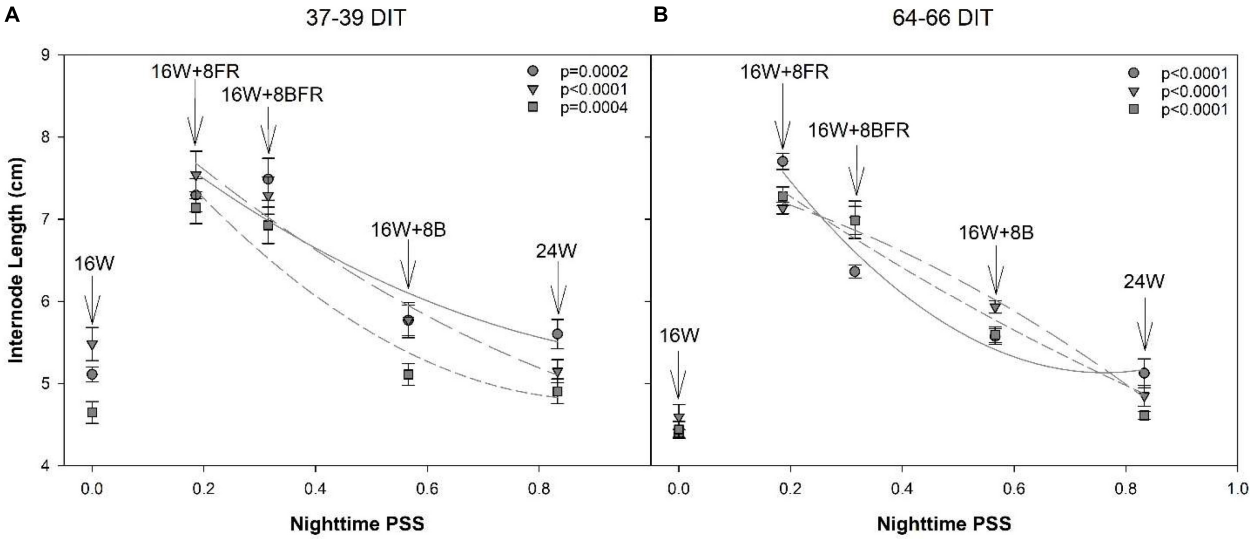

FIGURE 11 | Regression analysis of internode length from 'Maureno' (circle; solid line), 'Gina' (downward triangle; long dash line), and 'Eurix' (square; short dash line) during the 37–39 DIT measurements **(A)** and 64–66 DIT measurements **(B)**. Nighttime PSS of 0.833, 0.566, 0.315, and 0.186 correspond to treatments 24W, 16W + 8B, 16W + 8BFR, and 16W + 8FR respectively as determined *via* Sager et al. (1988). Regression analysis was done using a backward elimination method. The *p*-values listed are for the final regressions and only regressions which were determined to be significant ($p < 0.05$) are shown. The 16W treatment did not have light at the night and thus was non-resultant during the PSS calculation. Therefore, it was left out of the regression analysis. The internode lengths for 16W are plotted in the graph at a PSS value of zero.

treatments within experiment two utilized a similar total FR DLI of approximately 1.09 mol m^{-2} d^{-1} (**Table 1**).

During the initial destructive measurements, dry matter partitioning to the leaves was observed to increase with decreasing PSS only in the 'Gina' cultivar. However, during the subsequent destructive measurements, all plants showed increasing biomass partitioning to the leaves when PSS was decreased. This result is opposite to what was observed in lettuce plants grown with or with sole-source FR (Zou et al., 2021). Species-specific responses to FR could arise due to the differences in plant architecture. Whereas lettuce is a relatively small plant that mainly grows low to the ground and has little internode length, peppers are a vine-type crop grown vertically during production. Therefore, it is likely that FR light is able to penetrate deeper into the pepper crop causing the effect. Further to this, the peppers in our study were under the different treatments for more than 2 months, much longer than the lettuce in Zou et al. (2021) and thus, a time-dependent FR response was also observed which may account for the differences observed.

In this study, there was a significant reduction in PSS during the nighttime from 24W (PSS = 0.833) to 16W + 8FR (PSS = 0.135) allowing for the evaluation of the impact of nighttime FR and PSS on internode length and stem elongation. It was determined that the time-of-use, in this case with or without PAR (daytime or nighttime), can drastically impact the strength of photomorphogenic response as also noted in lettuce (Zou et al., 2021). The use of nighttime FR can have a much larger impact on plant morphology than utilization with broad-spectrum light (i.e., during the daytime) as internode length was seen to increase with decreasing PSS (**Figure 11**). A similar internode lengthening was also observed when PSS was decreased in lisianthus when grown using a 5-h night interruption (Yamada et al., 2011), although the study used fluence rates of only 3 μmol m^{-2} s^{-1}. The plants in our study had a stronger morphological response to the use of nighttime FR than has been previously reported with the use of EOD-FR (Kalaitzoglou et al., 2019). In Kalaitzoglou et al. (2019), the PSS of the EOD-FR was 0.1 which was similar to our lowest nighttime PSS of 0.135 (16W + 8FR) but much higher than the PSS of 0.315 (16W + 8BFR). However, we saw a much more dramatic increase in internode length than previously reported (Kalaitzoglou et al., 2019) and also at a higher PSS (0.315). This indicates that the response to FR light is also dependent on the length of use and not simply a dose-response. It should also be noted that Kalaitzoglou et al. (2019) used tomato as their model whereas our study looked at pepper. This, along with the results from Zou et al. (2019, 2021) indicates that species, and potentially even cultivars within a species, react differently to nighttime FR light. Furthermore, the increase in plant height also corresponded to an increase in biomass partitioning to the stem (**Figures 10C,D**) which is supportive of previous works (Brown et al., 1995; Ji et al., 2019, 2020).

It is also noteworthy that similar to 16W + 8BFR, the 24W treatment included a movement of 25% of FR from the day to the night (**Table 1**). However, an increase in plant height was not observed when compared to 16W with the exception of 'Maureno' during the 64–66 DIT measurements (**Figure 8B**). The 24W and 16W + 8BFR treatments contained the same amount of FR light during the night, however, an increase in stem elongation was only observed in the latter. The notable difference between the two nighttime light treatments is the PAR intensity and

spectrum, as well as PSS. The 24W treatment has approximately doubled the PAR intensity compared to 16W + 8BFR, has a broad-spectrum light as opposed to only blue light, and has a drastically higher PSS value. A lower red:far-red, correlated with a lower PSS, will invoke a shade avoidance response resulting in the greater stem elongation and leaf expansion observed in 16W + 8BFR compared to 24W (Franklin and Whitelam, 2005). Furthermore, the response to FR is dampened even if PSS is controlled for when used in a higher light intensity environment (Kalaitzoglou et al., 2019). These two factors are likely responsible for the different responses to FR during the night between 24W and 16W + 8BFR. However, the lack of further increase in internode length from 16W + 8BFR (PSS = 0.315) to 16W + 8FR (PSS = 0.135) indicates that there may be a threshold (PSS = 0.315) at which a further reduction in PSS does not increase internode length. A PSS value of 0.315 is comparable to the PSS threshold (PSS = 0.23) determined for arugula and mustard microgreens beyond which no further stem elongation was observed (Ying et al., 2020). Therefore, with respect to plant height and internode length, FR during the night had a larger impact on the morphological outcome as plants subjected to 16W + 8BFR tended to have values more closely to 16W + 8FR (**Figure 9**). On the other hand, plants under 16W + 8BFR had a total leaf area closer to that of 16W + 8B plants indicating blue at night supported leaf expansion (**Table 3**). This indicates that the two shade avoidance processes may be controlled by different mechanisms which can be preferentially controlled by blue or FR independently.

Implication on Greenhouse Pepper Production

Short internode lengths during lit pepper production have been well documented and can have negative implications during plant maintenance and fruit harvest. The use of extended (8 h) periods of FR light during the night resulted in an improved canopy architecture with increased internode length, preventing fruit stacking, and could reduce labor costs for plant maintenance (**Figure 11**). The addition of FR in 16W + 8BFR and 16W + 8FR during the night created a more "open" canopy. This allows workers a better view of the plant material allowing for quicker and more precise determination of offshoot and suckers and faster removal of offshoot/sucker by hand, reducing the labor time for routine maintenance. The stem elongation observed with the use of nighttime FR also creates a larger distance between nodes. During fruit growth, this provides more room for the fruit to grow unimpeded. As opposed to the 2.9 cm internodes observed by Demers et al. (1998), the use of FR at night extended internode length close to 8 cm providing ample room for normal pepper fruit growth.

Light pollution from greenhouses has been seen as a nuisance to neighboring municipalities including residents and businesses. Recently, bylaws have been enacted in Ontario, Canada, and Netherlands mandating the use of light abatement curtains to prevent light emissions from the greenhouses during the night (Hanifin, 2019). Light abatement curtains not only block light but also block 50–70% of heat loss from a greenhouse (Svensson, 2020), leading to overheating and high-temperature stress to crops due to the buildup of heat from lighting application, especially in greenhouse fruit vegetable production. For greenhouse tomato, pepper, and cucumber production, conventional lighting strategies usually use about 200–250 μmol m^{-2} s^{-1} light for 16 h (such as 1:00 to 17:00 or 0:00 to 16:00, Hao et al., 2018a). To prevent crop damage caused by high temperature, the curtains need to be partially opened (so-called "gapping") to ventilate out the heat when the outside temperature is not cold enough to bring down the greenhouse temperature. This is not feasible with the bylaw in Netherlands. The bylaw mandates the blocking of 98% of light during the night if the light intensity is > 15,000 lux (about 183 μmol m^{-2} s^{-1} for HPS, Ashdown, 2020). The use of low intensity of lighting in together with LEDs can eliminate this issue, allowing the curtains to be fully closed to prevent light emission from the greenhouse during the night.

It has been demonstrated that dynamic CL (i.e., 16W + 8B and 16W + 8BFR) did not harm the plants and led to a similar yield when compared to the control (16W). Notably, 16W + 8BFR did produce a much more open canopy which has positive labor benefits as mentioned above. While smart LEDs with the capability to control both spectrum and intensity are generally more complex leading to higher initial cost per light fixture than the LED fixture with fixed intensity and spectral composition at present time, dynamic low-intensity CL can help to reduce initial capital costs. In this study, 16W + 8BFR can reduce the intensity or installed capacity of light fixtures by 19% (**Table 1**). A dynamic CL using a smart 24 h LED system can reduce light intensity/fixture capacity by a third and is more cost-effective than a conventional 16 h LED system in mini-cucumber production based on the cost of electricity per unit of produce, in Ontario (Lanoue et al., 2021b). The benefit of the reduction in light intensity/fixture requirement with the dynamic low-intensity CL will not change regardless of the electrical prices during the day/night. Other studies that used fixed light spectral composition and dynamic light intensity control in response to sunlight intensity fluctuations have shown that electricity consumption can be reduced by 10–30% in comparison to a traditional on-off regime (Pinho et al., 2013; van Iersel and Gianino, 2017). The smart LED fixtures used for the implementation of dynamic CL in this study can control both light intensity and spectral compositions. Therefore, there is a good potential in future research and development to combine the sunlight-based intensity control strategy with the dynamic CL strategy for reducing both light fixture cost and electricity consumption.

CONCLUSION

In conclusion, experiment 1 provided data that indicates that pepper plants can be grown under CL lighting without the leaf injury associated with a continuous photoperiod. Moreover, it was determined that in order to have injury-free production, a dynamic CL lighting strategy was needed. The application

of either blue and/or FR light at night reduced PSS which led to a shade avoidance response and increase in internode length, and the response to the application of far-red during the night was much stronger than the application during the daytime. Moreover, when blue and FR were combined at night, the response was not additive but similar to 16W + 8FR. This indicates a potential threshold of PSS (0.315) beyond which no further stem elongation is enabled. In 16W + 8BFR, the use of blue light was able to drive photosynthesis during the night and blue + FR at night was able to evoke positive morphological responses reducing fruit stacking. Taken together, 16W + 8BFR, a treatment that provided white light during the day followed by both blue and FR during the night, is potentially the best CL for pepper production in this study, because it has the largest potential to reduce capital fixture cost, and daytime light intensity and electricity cost. Furthermore, its yield and fruit grade/quality were similar to 16W while also addressing the short internode issue in pepper production with supplemental lighting. While 16W + 8BFR did not improve the yield compared to 16W, it improved the canopy architecture making routine plant maintenance easier and faster, potentially reducing labor costs for producers.

DATA AVAILABILITY STATEMENT

The original contributions presented in the study are included in the article/**Supplementary Material**, further inquiries can be directed to the corresponding author/s.

AUTHOR CONTRIBUTIONS

JL and XH were involved in the conceptualization, methodology development, and writing and editing of the manuscript. JL and CL were involved in data curation and the day-to-day upkeep of the experiment. JL performed the data analysis. XH was responsible for funding acquisition. All authors have read and agreed to the submitted manuscript.

FUNDING

This project is funded by the Grid Innovation Fund of Independent Electricity System Operator (IESO) for Ontario, Canada to XH (J-002725.001.01).

ACKNOWLEDGMENTS

We would like to thank Kassim Tremblay and Sollum Lighting Technologies for providing the lighting fixtures and technical support for this study. Enza Zaden Canada provided the seeds of 'Maureno' and 'Eurix' for the study.

SUPPLEMENTARY MATERIAL

The Supplementary Material for this article can be found online at: https://www.frontiersin.org/articles/10.3389/fpls.2022.857616/full#supplementary-material

REFERENCES

Ashdown, I. (2020). *Greenhouses and Light Pollution*. Available online at: https://www.allthingslighting.org/tag/light-pollution/

Baker, N. R. (2008). Chlorophyll fluorescence: a probe of photosynthesis *in vivo*. *Annu. Rev. Plant Biol.* 59, 89–113. doi: 10.1146/annurev.arplant.59.032607.092759

Brown, C. S., Schuerger, A. C., and Sager, J. C. (1995). Growth and photomorphogenesis of pepper plants under red light-emitting diodes with supplemental blue or far-red lighting. *J. Am. Soc. Hortic. Sci.* 120, 808–813. doi: 10.21273/jashs.120.5.808

Chia, P. L., and Kubota, C. (2010). End-of-day far-red light quality and dose requirements for tomato rootstock hypocotyl elongation. *Hortscience* 45, 1501–1506. doi: 10.21273/hortsci.45.10.1501

Chun, L., Kawakami, A., and Christopher, D. A. (2001). Phytochrome a mediates blue light and UV-A-dependent chloroplast gene transcription in green leaves. *Plant Physiol.* 125, 1957–1966. doi: 10.1104/pp.125.4.1957

Cole, B., Kay, S. A., and Chory, J. (2011). Automated analysis of hypocotyl growth dynamics during shade avoidance in Arabidopsis. *Plant J.* 65, 991–1000. doi: 10.1111/j.1365-313X.2010.04476.x

Demers, D. A., Dorais, M., Wien, C. H., and Gosselin, A. (1998). Effects of supplemental light duration on greenhouse tomato (*Lycopersicon esculentum* Mill.) plants and fruit yields. *Sci. Hortic.* 74, 295–306. doi: 10.1016/S0304-4238(98)00097-1

Demers, D. A., and Gosselin, A. (1999). Supplemental lighting of greenhouse vegetables: Limitations and problems related to long photoperiods. *Acta Hortic.* 481, 469–473. doi: 10.17660/actahortic.1999.481.54

Demers, D. A., and Gosselin, A. (2002). Growing greenhouse tomato and sweet pepper under supplemental lighting: optimal photoperiod, negative effects of long photoperiod and their causes. *Acta Hortic.* 580, 83–88. doi: 10.17660/ActaHortic.2002.580.9

Demmig, B., and Björkman, O. (1987). Comparison of the effect of excessive light on chlorophyll fluorescence (77K) and photon yield of O2 evolution in leaves of higher plants. *Planta* 171, 171–184. doi: 10.1007/BF00391092

Eilfeld, P., and Rüdiger, W. (1985). Absorption spectra of phytochrome intermediates. *Zeitschrift fur Naturforsch. Sect. C J. Biosci.* 40, 109–114. doi: 10.1515/znc-1985-1-221

Fan, X. X., Xu, Z. G., Liu, X. Y., Tang, C. M., Wang, L. W., and Han, X. (2013). Effects of light intensity on the growth and leaf development of young tomato plants grown under a combination of red and blue light. *Sci. Hortic.* 153, 50–55. doi: 10.1016/j.scienta.2013.01.017

Franklin, K. A., and Whitelam, G. C. (2005). Phytochromes and shade-avoidance responses in plants. *Ann. Bot.* 96, 169–175. doi: 10.1093/aob/mci165

Hanifin, R. (2019). *Keeping it lit - Controlling Greenhouse Light Pollution. Greenhouse Canada*. Available online at: https://www.greenhousecanada.com/keeping-it-lit-controlling-greenhouse-light-pollution-33114/

Hao, X., Guo, X., Lanoue, J., Zhang, Y., Cao, R., Zheng, J., et al. (2018a). A review on smart application of supplemental lighting in greenhouse fruiting vegetable production. *Acta Hortic.* 1227, 499–506. doi: 10.17660/ActaHortic.2018.1227.63

Hao, X., Zhang, Y., Guo, X., Little, C., and Zheng, J. (2018b). Dynamic temperature control strategy with a temperature drop improves responses of greenhouse tomatoes and sweet peppers to long photoperiods of supplemental lighting and saves energy. *Acta Hortic.* 1227, 291–298. doi: 10.17660/ActaHortic.2018.1227.35

Hao, X., and Papadopoulos, A. P. (1999). Effects of supplemental lighting and cover materials on growth, photosynthesis, biomass partitioning, early yield and quality of greenhouse cucumber. *Sci. Hortic.* 80, 1–18. doi: 10.1016/S0304-4238(98)00217-9

Hao, X., Zhang, Y., Little, C., and Zheng, J. (2020). Dynamic temperature control strategy with a temperature drop improved responses of greenhouse cucumbers to long photoperiods of supplemental lighting. *Acta Hortic.* 1271, 33–39. doi: 10.17660/ActaHortic.2020.1271.5

Haque, M. S., de Sousa, A., Soares, C., Kjaer, K. H., Fidalgo, F., Rosenqvist, E., et al. (2017). Temperature variation under continuous light restores tomato leaf photosynthesis and maintains the diurnal pattern in stomatal conductance. *Front. Plant Sci.* 8:1602. doi: 10.3389/fpls.2017.01602

Haque, M. S., Kjaer, K. H., Rosenqvist, E., and Ottosen, C. O. (2015). Continuous light increases growth, daily carbon gain, antioxidants, and alters carbohydrate metabolism in a cultivated and a wild tomato species. *Front. Plant Sci.* 6:522. doi: 10.3389/fpls.2015.00522

Hernández, R., and Kubota, C. (2016). Physiological responses of cucumber seedlings under different blue and red photon flux ratios using LEDs. *Environ. Exp. Bot.* 121, 66–74. doi: 10.1016/j.envexpbot.2015.04.001

Hersch, M., Lorrain, S., De Wit, M., Trevisan, M., Ljung, K., Bergmann, S., et al. (2014). Light intensity modulates the regulatory network of the shade avoidance response in Arabidopsis. *Proc. Natl. Acad. Sci. U.S.A.* 111, 6515–6520. doi: 10.1073/pnas.1320355111

Hillman, W. S. (1956). Injury of tomato plants by continuous light and unfavorable photoperiodic cycles. *Am. J. Bot.* 43, 89–96. doi: 10.1002/j.1537-2197.1956.tb10469.x

IESO (2022). *Independent Electricity System Operator – Power Data.* Available online at: https://www.ieso.ca/power-data

Inoue, K., Araki, T., and Endo, M. (2018). Circadian clock during plant development. *J. Plant Res.* 131, 59–66. doi: 10.1007/s10265-017-0991-8

Islam, M. A., Tarkowská, D., Clarke, J. L., Blystad, D. R., Gislerød, H. R., Torre, S., et al. (2014). Impact of end-of-day red and far-red light on plant morphology and hormone physiology of poinsettia. *Sci. Hortic.* 174, 77–86. doi: 10.1016/j.scienta.2014.05.013

Ji, Y., Nuñez Ocaña, D., Choe, D., Larsen, D. H., Marcelis, L. F. M., and Heuvelink, E. (2020). Far-red radiation stimulates dry mass partitioning to fruits by increasing fruit sink strength in tomato. *New Phytol.* 228, 1914–1925. doi: 10.1111/nph.16805

Ji, Y., Ouzounis, T., Courbier, S., Kaiser, E., Nguyen, P. T., Schouten, H. J., et al. (2019). Far-red radiation increases dry mass partitioning to fruits but reduces *Botrytis cinerea* resistance in tomato. *Environ. Exp. Bot.* 168:103889. doi: 10.1016/j.envexpbot.2019.103889

Jin, W., Urbina, J. L., Heuvelink, E., and Marcelis, L. F. M. (2021). Adding far-red to red-blue light-emitting diode light promotes yield of lettuce at different planting densities. *Front. Plant Sci.* 11:609977. doi: 10.3389/fpls.2020.609977

Kalaitzoglou, P., van Ieperen, W., Harbinson, J., van der Meer, M., Martinakos, S., Weerheim, K., et al. (2019). Effects of continuous or end-of-day far-red light on tomato plant growth, morphology, light absorption, and fruit production. *Front. Plant Sci.* 10:322. doi: 10.3389/fpls.2019.00322

Kasperbauer, M. J., Hunt, P. G., and Sojka, R. E. (1984). Photosynthate partititoning and nodule formation in soybean plants that reveived red or far-red light at the end of the photosynthetic period. *Physiol. Plant.* 61, 549–554. doi: 10.1111/j.1399-3054.1984.tb05168.x

Kong, Y., and Zheng, Y. (2020). Phototropin is partly involved in blue-light-mediated stem elongation, flower initiation, and leaf expansion: a comparison of phenotypic responses between wild Arabidopsis and its phototropin mutants. *Environ. Exp. Bot.* 171:103967. doi: 10.1016/j.envexpbot.2019.103967

Kozai, T., and Niu, G. (2016). "Plant factory as a resource-efficient closed plant production system," in *Plant Factory: An Indoor Vertical Farming System for Efficient Quality Production*, eds T. Kozai, G. Niu, and M. Takagaki (Amsterdam: Elsevier Inc), 69–90. doi: 10.1016/B978-0-12-801775-3.00004-4

Lanoue, J., Leonardos, E. D., and Grodzinski, B. (2018a). Effects of light quality and intensity on diurnal patterns and rates of photo-assimilate translocation and transpiration in tomato leaves. *Front. Plant Sci.* 9:756. doi: 10.3389/fpls.2018.00756

Lanoue, J., Leonardos, E. D., Khosla, S., Hao, X., and Grodzinski, B. (2018b). Effect of elevated CO2 and spectral quality on whole plant gas exchange patterns in tomatoes. *PLoS One* 13:205861. doi: 10.1371/journal.pone.0205861

Lanoue, J., Thibodeau, A., Little, C., Zheng, J., Grodzinski, B., and Hao, X. (2021a). Light spectra and root stocks affect response of greenhouse tomatoes to long photoperiod of supplemental lighting. *Plants* 10, 1–23. doi: 10.3390/plants10081674

Lanoue, J., Zheng, J., Little, C., Grodzinski, B., and Hao, X. (2021b). Continuous light does not compromise growth and yield in mini-cucumber greenhouse production with supplemental led light. *Plants* 10, 1–18. doi: 10.3390/plants10020378

Lanoue, J., Zheng, J., Little, C., Thibodeau, A., Grodzinski, B., and Hao, X. (2019). Alternating red and blue light-emitting diodes allows for injury-free tomato production with continuous lighting. *Front. Plant Sci.* 10:1114. doi: 10.3389/fpls.2019.01114

Maliakal, S. K., McDonnell, K., Dudley, S. A., and Schmitt, J. (1999). Effects of red to far-red ratio and plant density on biomass allocation and gas exchange in Impatiens capensis. *Int. J. Plant Sci.* 160, 723–733. doi: 10.1086/314157

Matsuda, R., Yamano, T., Murakami, K., and Fujiwara, K. (2016). Effects of spectral distribution and photosynthetic photon flux density for overnight LED light irradiation on tomato seedling growth and leaf injury. *Sci. Hortic.* 198, 363–369. doi: 10.1016/j.scienta.2015.11.045

McAvoy, R. J., Janes, H. W., Godfriaux, B. L., Secks, M., Duchai, D., and Wittman, W. K. (1989). The effect of total available photosynthetic photon flux on single truss tomato growth and production. *J. Hortic. Sci.* 64, 331–338. doi: 10.1080/14620316.1989.11515961

Nanya, K., Ishigami, Y., Hikosaka, S., and Goto, E. (2012). Effects of blue and red light on stem elongation and flowering of tomato seedlings. *Acta Hortic.* 956, 261–266. doi: 10.17660/ActaHortic.2012.956.29

Ohtake, N., Ishikura, M., Suzuki, H., Yamori, W., and Goto, E. (2018). Continuous irradiation with alternating red and blue light enhances plant growth while keeping nutritional quality in lettuce. *Hortscience* 53, 1804–1809. doi: 10.21273/HORTSCI13469-18

Ontario Ministry of Agriculture, Food and Rural Affairs [OMAFRA] (2010). *Growing Greenhouse Vegetables in Ontario.* Toronto, ON: Queen's Printer.

Pham, D. M., and Chun, C. (2020). Growth and leaf injury in tomato plants under continuous light at different settings of constant and diurnally varied photosynthetic photon flux densities. *Sci. Hortic.* 269:109347. doi: 10.1016/j.scienta.2020.109347

Pinho, P., Hytönen, T., Rantanen, M., Elomaa, P., and Halonen, L. (2013). Dynamic control of supplemental lighting intensity in a greenhouse environment. *Light. Res. Technol.* 45, 295–304. doi: 10.1177/1477153512444064

Rajapakse, N. C., and Li, S. (2004). Exclusion of far red light by photoselective greenhouse films reduces height of vegetable seedlings. *Acta Hortic.* 631, 193–199. doi: 10.17660/ActaHortic.2004.631.25

Sager, J. C., Smith, W. O., Edwards, J. L., and Cyr, K. L. (1988). Photosynthetic efficiency and phytochrome photoequilibria determination using spectral data. *Trans. Am. Soc. Agric. Eng.* 31, 1882–1889. doi: 10.13031/2013.30952

Shimizu, H., Ma, Z., Douzono, M., Tazawa, S., Runkle, E. S., and Heins, R. D. (2006). Blue light inhibits stem elongation of chrysanthemum. *Acta Hortic.* 711, 363–367. doi: 10.17660/actahortic.2006.711.50

Song, J., Chen, Z., Zhang, A., Wang, M., Jahan, M. S., Wen, Y., et al. (2022). The positive effects of increased light intensity on growth and photosynthetic performance of tomato seedlings in relation to night temperature level. *Agronomy* 12:343 doi: 10.3390/agronomy12020343

Sørensen, H. K., Fanourakis, D., Tsaniklidis, G., Bouranis, D., Nejad, A. R., and Ottosen, C. O. (2020). Using artificial lighting based on electricity price without a negative impact on growth, visual quality or stomatal closing response in Passiflora. *Sci. Hortic.* 267:109354. doi: 10.1016/j.scienta.2020.109354

Sullivan, S., Hart, J. E., Rasch, P., Walker, C. H., and Christie, J. M. (2016). Phytochrome a mediates blue-light enhancement of second-positive phototropism in Arabidopsis. *Front. Plant Sci.* 7:290. doi: 10.3389/fpls.2016.00290

Svensson, L. (2020). *Keeping it Lit - Controlling Greenhouse Light Pollution. Ludvig Svensson*. Available online at: https://www.ludvigsvensson.com/en/climate-screens/news/posts/2020/april/2020/may/keeping-it-lit-controlling-greenhouse-light-pollution/.

Sysoeva, M., Markovskaya, E., and Shibaeva, T. (2010). Plants under continuous light: a review. *Plant Stress* 4, 5–17.

van Iersel, M. W., and Gianino, D. (2017). An adaptive control approach for light-emitting diode lights can reduce the energy costs of supplemental lighting in greenhouses. *Hortscience* 52, 72–77. doi: 10.21273/HORTSCI11385-16

Velez-Ramirez, A. I., Dünner-Planella, G., Vreugdenhil, D., Millenaar, F. F., and Van Ieperen, W. (2017). On the induction of injury in tomato under continuous

light: circadian asynchrony as the main triggering factor. *Funct. Plant Biol.* 44, 597–611. doi: 10.1071/FP16285

Velez-Ramirez, A. I., Van Ieperen, W., Vreugdenhil, D., and Millenaar, F. F. (2011). Plants under continuous light. *Trends Plant Sci.* 16, 310–318. doi: 10.1016/j.tplants.2011.02.003

Velez-Ramirez, A. I., Van Ieperen, W., Vreugdenhil, D., Van Poppel, P. M. J. A., Heuvelink, E., and Millenaar, F. F. (2014). A single locus confers tolerance to continuous light and allows substantial yield increase in tomato. *Nat. Commun.* 5, 1–13. doi: 10.1038/ncomms5549

Velez-Ramirez, A. I., Vreugdenhil, D., Heuvelink, E., Van Ieperen, W., and Millenaar, F. F. (2012). Continuous light as a way to increase greenhouse tomato production: expected challenges. *Acta Hortic.* 956, 51–57. doi: 10.17660/ActaHortic.2012.956.3

Walters, K. J., and Lopez, R. G. (2021). Modeling growth and development of hydroponically grown dill, parsley, and watercress in response to photosynthetic daily light integral and mean daily temperature. *PLoS One* 16:248662. doi: 10.1371/journal.pone.0248662

Yamada, A., Tanigawa, T., Suyama, T., Matsuno, T., and Kunitake, T. (2011). Effects of red:Far-red light ratio of night-break treatments on growth and flowering of *Eustoma grandiflorum* (Raf.) shinn. *Acta Hortic.* 907, 313–318. doi: 10.17660/actahortic.2011.907.51

Ying, Q., Kong, Y., and Zheng, Y. (2020). Applying blue light alone, or in combination with far-red light, during nighttime increases elongation without compromising yield and quality of indoor-grown microgreens. *Hortscience* 55, 876–881. doi: 10.21273/HORTSCI14899-20

Zou, J., Fanourakis, D., Tsaniklidis, G., Cheng, R., Yang, Q., and Li, T. (2021). Lettuce growth, morphology and critical leaf trait responses to far-red light during cultivation are low fluence and obey the reciprocity law. *Sci. Hortic.* 289:110455. doi: 10.1016/j.scienta.2021.110455

Zou, J., Zhang, Y., Zhang, Y., Bian, Z., Fanourakis, D., Yang, Q., et al. (2019). Morphological and physiological properties of indoor cultivated lettuce in response to additional far-red light. *Sci. Hortic.* 257:108725. doi: 10.1016/j.scienta.2019.108725.

Conflict of Interest: The authors declare that the research was conducted in the absence of any commercial or financial relationships that could be construed as a potential conflict of interest.

Publisher's Note: All claims expressed in this article are solely those of the authors and do not necessarily represent those of their affiliated organizations, or those of the publisher, the editors and the reviewers. Any product that may be evaluated in this article, or claim that may be made by its manufacturer, is not guaranteed or endorsed by the publisher.

frontiers | Frontiers in Plant Science

TYPE Original Research
PUBLISHED 01 February 2024
DOI 10.3389/fpls.2024.1292753

OPEN ACCESS

EDITED BY
Xiuming Hao,
Agriculture and Agri-Food Canada (AAFC), Canada

REVIEWED BY
Antonio Pompeiano,
Mendel University in Brno, Czechia
Jamal Y Ayad,
The University of Jordan, Jordan

*CORRESPONDENCE
Muhammad Naveed
naveed1735@yahoo.com

RECEIVED 12 September 2023
ACCEPTED 15 January 2024
PUBLISHED 01 February 2024

CITATION
Naveed M, Bansal U and Kaiser BN (2024) Impact of low light intensity on biomass partitioning and genetic diversity in a chickpea mapping population. *Front. Plant Sci.* 15:1292753. doi: 10.3389/fpls.2024.1292753

Impact of low light intensity on biomass partitioning and genetic diversity in a chickpea mapping population

Muhammad Naveed[1,2*], Urmil Bansal[2,3,4] and Brent N. Kaiser[1,2,3]

[1]Centre for Carbon, Water and Food, The University of Sydney, NSW, Australia, [2]School of Life and Environmental Sciences, The University of Sydney, NSW, Australia, [3]Sydney Institute of Agriculture, The University of Sydney, NSW, Australia, [4]Plant Breeding Institute, Cobbitty, The University of Sydney, NSW, Australia

With recent climatic changes, the reduced access to solar radiation has become an emerging threat to chickpeas' drought tolerance capacity under rainfed conditions. This study was conducted to assess, and understand the effects of reduced light intensity and quality on plant morphology, root development, and identifying resistant sources from a Sonali/PBA Slasher mapping population. We evaluated 180 genotypes, including recombinant inbred lines (RILs), parents, and commercial checks, using a split-block design with natural and low light treatments. Low light conditions, created by covering one of the two benches inside two growth chambers with a mosquito net, reduced natural light availability by approximately 70%. Light measurements encompassed photosynthetic photon flux density, as well as red, and far-red light readings taken at various stages of the experiment. The data, collected from plumule emergence to anthesis initiation, encompassed various indices relevant to root, shoot, and carbon gain (biomass). Statistical analysis examined variance, treatment effects, heritability, correlations, and principal components (PCs). Results demonstrated significant reductions in root biomass, shoot biomass, root/shoot ratio, and plant total dry biomass under suboptimal light conditions by 52.8%, 28.2%, 36.3%, and 38.4%, respectively. Plants also exhibited delayed progress, taking 9.2% longer to produce their first floral buds, and 19.2% longer to commence anthesis, accompanied by a 33.4% increase in internodal lengths. A significant genotype-by-environment interaction highlighted differing genotypic responses, particularly in traits with high heritability (> 77.0%), such as days to anthesis, days to first floral bud, plant height, and nodes per plant. These traits showed significant associations with drought tolerance indicators, like root, shoot, and plant total dry biomass. Genetic diversity, as depicted in a genotype-by-trait biplot, revealed contributions to PC1 and PC2 coefficients, allowing discrimination of low-light-tolerant RILs, such as 1_52, 1_73, 1_64, 1_245, 1_103, 1_248, and 1_269, with valuable variations in traits of interest. These RILs could be used to breed desirable chickpea cultivars for sustainable production under water-limited conditions. This study concludes that low light stress disrupts the balance between root and shoot morphology, diverting

photosynthates to vegetative structures at the expense of root development. Our findings contribute to a better understanding of biomass partitioning under limited-light conditions, and inform breeding strategies for improved drought tolerance in chickpeas.

KEYWORDS

abiotic stress, biomass partitioning, chickpea, genetic diversity, low light, mapping population, phenological plasticity

1 Introduction

Chickpea (*Cicer arietinum* L.), a source of vegan protein, is extensively farmed between 20° to 40° latitudes in more than 50 countries, worldwide (Abbo et al., 2003; FAOSTAT, 2021). It is a long day plant, and grows well under certain light conditions, such as 16 h day length with red and blue light wavelengths, ranged 610-700 nm and 425-490 nm, respectively (Soltani et al., 2004; Pettai et al., 2005). However, a slight deviation in their levels may lead to modifications in central processes related to biochemistry, cell division, morphology, phenology, physiology, and so on (Fan et al., 2018; Yang et al., 2018). For example, reduction of photoperiod to 11-12 h delays flowering in chickpea by 120 to 150 days, whereas, variation in light quality and intensity, promotes competition for carbon gain among different plant parts (Woźny and Jerzy, 2007; Poudel et al., 2008; Yu et al., 2017).

Among abiotic stresses, light or solar radiation is the leading factor that regulates plant growth and expansion under any environment (Shafiq et al., 2021). Three components of light i.e. quality, intensity, and photoperiod, largely determine a plants' photosynthetic capacity, establishment, and yielding ability (Khalid et al., 2019). Chickpea, being a rainfed crop, has major cultivation under subtropical and Mediterranean zones (Chen et al., 2017). Drought and heat are the characteristic features of these climates, and have long been considered as major yield constraining factors. Suboptimal light intensity and quality, caused by various climatic events (prolonged cloud cover, foggy weather etc.), and cultural practices, is now becoming an emerging challenge to sustainable chickpea production under these environments (Jha et al., 2014; Naveed, 2022). Because, this triggers unbalanced partitioning between root and shoot morphology due to variation in interception of photosynthetic photon flux density (PPFD), and underlying processes regulating plant growth and expansion (Park and Runkle, 2017). As in the study by Gao et al. (2017) on maize, they observed that plants reallocate a greater proportion of photosynthetic resources to above-ground organs, reducing the root-to-shoot ratio. This shift led to abnormal plant structure and increased lodging. More precisely, the elongation of petioles and stems leads to a decrease in leaf size and thickness, along with an increase in internode length, ultimately resulting in reduced stem thickness, weakened structural integrity, and diminished shoot biomass (Okoli and Wilson, 1986; Su et al., 2014; Liu et al., 2018). Likewise, low light effects on root biomass are also extreme. Lake and Sadras (2014) in an experiment on chickpea, and Sparkes et al. (2008) on wheat, reported more than two fold decrease in root-length density, diameter, absorption area, and root biomass under low light compared to control treatment. This reduced root growth could constrain a plants ability to extract water deeper from the soil layers (Kashiwagi et al., 2015; Gao et al., 2017). We lack information on these aspects in chickpeas, as the available literature predominantly covers soybean and other crops. Total plant biomass, particularly the biomass of roots and shoots, is a crucial adaptive strategy in water-limited conditions. This may be a potential factor contributing to low productivity under suboptimal light in rainfed agricultural systems (Green-Tracewicz et al., 2011; Liu et al., 2018).

Breeding for low light tolerance is the most effective strategy for mitigating these yield losses (Rai et al., 2021). This approach can lead to the development of light-insensitive genotypes capable of maintaining their natural traits even in challenging environments through enhanced light interception, and photosynthetic ability. Mapping populations provide a valuable toolbox that integrates genomics with breeding, and related disciplines to identify desirable recombinants (Aryamanesh et al., 2010; Scott et al., 2020). To exploit all these, we need comprehensive knowledge of chickpea plant responses, traits variability, and underlying genetic mechanisms controlling targeted indices under these environments (Tardieu and Tuberosa, 2010; Choudhary et al., 2018; Ao et al., 2019). Contrastingly, in prior field trials, we observed variations in chickpea yield and the responses of various growth parameters across years, driven by distinct climatic conditions and varying levels of solar radiation (Kaloki, 2017). Higher yields of 46% to 54% were recorded during mostly sunny growing seasons, while overcast conditions resulted in taller plants (7 cm to 10 cm) with an overall lower yield (Naveed, 2022). This behavior could be due to the onset of the shade avoidance mechanism, which has more significant effects on crop root architecture and biomass accumulation of cultivars (Franklin, 2008; Green-Tracewicz et al., 2011). These adjustments might compromise chickpeas' ability to tolerate water-deficit conditions. This study aimed to achieve the stated goals using a Sonali/PBA Slasher mapping population under controlled environmental conditions.

2 Materials and methods

2.1 Plant material and experimental design

This study was conducted in 2020 at the Plant Breeding Institute of the University of Sydney, Narrabri campus, NSW, Australia. The plant material comprised 180 test entries and included 176 RILs, which were developed using two drought tolerant commercial lines, Sonali as a female while PBA Slasher as a male parent (Kaloki, 2017). In addition, two high yielding and disease resistant commercial cultivars, PBA Seamer and PBA Striker, were used as standard checks (Vance et al., 2021). This mapping population has a range of variation for some of the plant traits such as architecture, cropping period, and plant biomass useful for conferring drought tolerance in chickpea (Ramamoorthy et al., 2016; Maqbool et al., 2017; Ramamoorthy et al., 2017). Details of entries along with characteristic features are given in Supplementary Table 1. All these lines were evaluated under two light treatments in a fully replicated trial, being laid out inside two growth chambers of a glasshouse. The experimental pots were placed side-by-side on two parallel benches, facing north and south, and separated by an entryway. Northern bench comprised natural light (NL), while southern consisted of low light (LL) treatment. The design used was split-block with four replications, and included 1440 pots. These were randomized in twenty rows by 36 columns, with each replicate block of 180 genotypes comprising ten rows by 18 columns, using DiGGer package of R software (Coombes, 2009). Two replicates were placed in each growth chamber under each treatment, with every pot assigned a unique identification number. This process was completed with utmost care to avoid any type of error.

For potting purpose, soil (rich in clay) and sand were mixed together in a 3:1 ratio, respectively, to fill the pots with 9×9×20 cm diameter. All the pots were watered until dripping to ensure the soil had enough moisture contents on the day of sowing. Two seeds, 3 cm deep and 5 cm apart, were sown per pot. Seeds, which germinated and cracked through the soil surface first, were retained in each pot while others, once emerged, were pulled out with caution immediately. All the plants in both treatments were fertilized (N 6.1%, P 12%, K 22.5%, S 2.2%, Zn 0.55%) with Cotton Sustain (Incitec Pivot Fertilisers, Australia) 10 days after sowing at a rate of 0.3 g per pot. On the same day, the plants were inoculated with a peat-based inoculant of Rhizobia (Nodule N, New Edge Microbials, Albury, Australia) to establish root symbiosis, and promote root nodulation. This was achieved by diluting 20 g of inoculum in 5 L of water, and distributing it to all 1440 pots uniformly. Further, a dose of liquid fertilizer (Thrive, Yates Australia, Padstow, Australia) enriched with NPK (25:5:8.8) and micronutrients (S 4.6, Mg 0.5, Fe 0.18, B 0.005, Cu 0.005, Zn 0.004, Mo 0.001) was applied 24 days after sowing to overcome any micronutrient deficiencies. All the plants were watered regularly to avoid water stress, and were staked upright when the shoot started bending or falling. Reverse cycle air conditioning was used to maintain daily day/night temperatures of both the growth chambers at 24 ± 2/16 ± 2°C, respectively. Whereas dehumidifiers (Quest series) were used to control humidity, which was set 50% to 70% to avoid mold or any other fungal disease incidence.

2.2 Treatments

Two light treatments i.e. natural light (NL) and reduced/low light (LL), were used to raise plants from seed sowing up to anthesis stage. Plants were harvested once anthesis commenced. The LL treatment was created using a mosquito net (1.2 mm mesh), covering the top and sides of one bench in each growth chamber. Seeds in both the treatments and growth chambers were sown once the benches allocated for LL treatment were covered with mosquito nets. Readings on light parameters were made starting at 11 am, which indicated a reduction of ~70% light in LL compared to NL treatment (Supplementary Table 2).

2.3 Measurement of available light

Readings on photosynthetic photon flux density (PPFD), red (R), and far-red (FR) light received by plants in both glasshouse chambers were done at five different experimental stages, and commenced at 11 am. At each stage, six measurements were performed on the same genotypes, comprising both parents, Sonali and PBA Slasher, two commercial cultivars, PBA Seamer and PBA Striker, and two RILs, 1_17 and 1_50, representing different positions in each replication of a treatment. First measurement was done a day before seed sowing, whereas the second was taken a week after seed sowing, followed by at 3, 4-leaf, and anthesis stages. PPFD measurements were carried out using AP4 Porometer (Delta-T Devices Ltd, Cambridge, UK) by holding the light sensor about 10 cm above the canopy. Whereas R and FR light measurements were performed using LightScout red/far red meter (Spectrum Technologies, Inc., Aurora, IL, USA). Red and far-red light measurements were assessed right after estimating PPFD by placing the sensor at the same spot as the PPFD sensor, and writing down the values, immediately.

2.4 Measurement of photosynthetic rate of parents

Because of the small window, it was not feasible to measure the photosynthesis of 180 genotypes in four replicates and two treatments. Therefore, it was assessed only for parents, Sonali and PBA Slasher. Measurements were done at three-growth stages viz., 3-leaf stage, 4-leaf stage, and at anthesis using a portable CIRAS-3 machine (PP Systems, Amesbury, MA, USA). This photosynthesis system has a leaf cuvette of 4.5 cm^2, and can set light closest to the approximation of sunlight (38% red, 37% green, and 25% blue) using light-emitting diodes. The flow rate set was 400 cc min^{-1}, and the reference CO_2 at 400 µmol mol^{-1}. These measurements were performed between 9:00 am and 4:00 pm by selecting fully developed youngest leaves. At each selected stage, all

photosynthetic measurements were done four times apiece on both the parents at growing PPFD, starting from zero to 1500 µmol m^{-2} s^{-1}. PPFD increased by 100-µmol m^{-2} s^{-1} every time for 16 levels. The actual values of photosynthetic rate were adjusted to the real chickpea leaf area, which was estimated using ImageJ software.

2.5 Phenotyping

Following traits were measured in eight (4 + 4) replicates under NL and LL treatments as per procedure explained in Supplementary Table 2, and used by previous researchers (Ali et al., 2010; Walia et al., 2020; Naveed, 2022).

2.5.1 Days to emergence (DTE)
2.5.2 Days to first floral bud (DFFB)
2.5.3 Days to anthesis (DTA)
2.5.4 Plant height (PH)
2.5.5 Nodes per plant (NPP)
2.5.6 Internodal length (IL)
2.5.7 Branches per plant (BPP)
2.5.8 Shoot dry biomass per plant (SDBPP)
2.5.9 Root dry biomass per plant (RDBPP)
2.5.10 Root to shoot ratio (RSR)
2.5.11 Plant total dry biomass (PTDB)

2.6 Statistical analysis

All statistical analyses such as ANOVA, correlation, and principal component reported herein were performed on traits given in section 2.5 using "Genstat" computer software version 16.0 (Payne et al., 2011). Treatment effects (individual and interactive) were estimated ($P < 0.05$) using function "RML linear mixed model" and comprised genotypes (G), and treatments (T) as fixed-terms, whereas replications within treatments, as random-terms. For the measurements done over time, such as photosynthesis, genotypes (G), treatments (T), and growth stages (GS) were used as fixed-terms, and replications within treatments as random-terms. We preferred Wald test (also known as Wald Chi-Squared test) over others because it is based on parametric statistical measures, and provide information, collectively, on the significance of a set of independent variables in a model. It is simple, quicker, and can add or remove the parameters for certain explanatory variables depending upon their contribution in the model (Arango-Botero et al., 2023). Heritability in broad-sense ($H^2_{B.S.}$) was also worked out for all the traits using formula given by Nyquist and Baker (1991). H^2 was considered as high (> 60%), moderate (30-60%), and low (< 30%), as per Johnson et al. (1955). Correlation coefficients among various indices such as DTE, DTFFB, DTA, PH, IL, NPP, BPP, SDBPP, RDBPP, RSR, and PTDB, in NL and LL conditions were computed following Pearson's technique. Principal component analysis was also done on the same parameters using the multivariate analysis function of Genstat software. Principal components with > 1 eigenvalues were tabulated, and used to construct biplot using the same software. The curves were fitted on photosynthetic rate over time against growing PPFD (detail given in section 2.4) captured at selected three growth stages under NL and LL treatments, using nonlinear polynomial regression function of software GraphPad prism version 7.0 (GraphPad Software incorporation, USA) (Schneider et al., 2012).

3 Results

In the present study, changes in optimum light intensity, critically impacted rate of photosynthesis, and carbon gain of genotypes. This created a competition among different plant organs to intercept maximum light, resulting in, modified shoot and root structures. Specifically, plant biomass was reduced, and this reduction was greater for roots compared to shoots. In addition, shoots become thinner, longer, and prone to breakage. Still, few entries in this mapping population performed better, and exhibited phenotypic plasticity across environments. Greater heritability values for some of the desired traits, PTDB, RDBPP, and SDBPP suggested their potential utilization, and scope of improvement in breeding programs. Detailed results are presented in the following subsections.

3.1 Analysis of variance for recorded traits

The variance analysis revealed significant differences between both light treatments. Low light resulted in 72% reduction in PPFD, implying that only 28% ambient light was available to plants to carry various gas exchange processes. Similarly, the optimum light quality for normal plant growth in the form of red, far-red, and their ratios was deteriorated by 71%, 71% and 2%, respectively (Supplementary Table 3). Two factor ANOVA for G, T and their interaction showed significant ($P < 0.001$) differences for traits like DTE, DTFFB, DTA, PH, IL, NPP, BPP, SDBPP, RDBPP, RSR and PTDB except BPP which was non-significant even at $P > 0.05$ (Supplementary Table 5). Higher estimates of G than G×E suggested larger genotype effects than environments on the traits investigated.

3.2 Impact of light treatments on parental photosynthesis

Effects of light treatments (T) on net photosynthetic rate of parental genotypes (G), assessed at different growth stages (GS), revealed significant differences between T ($P < 0.001$), and G×T interaction ($P < 0.05$), as indicated in Supplementary Table 4. Effects of LL on Pn or carbon gain were greater for PBA Slasher, and reduced its net photosynthetic rate by 38.8% compared to 14.8% of Sonali. Pn for PBA Slasher was greater under NL, and for Sonali under LL treatments (Supplementary Table 4). The fitting of polynomial regression curves revealed 53.5% variation for this trait. Initially, Pn was negative at zero PPFD, while it increased gradually from growing PPFD of 100 umol m^{-2} s^{-1}, and reached highest at 1500 umol m^{-2} s^{-1} under NL and LL treatments (Figure 1).

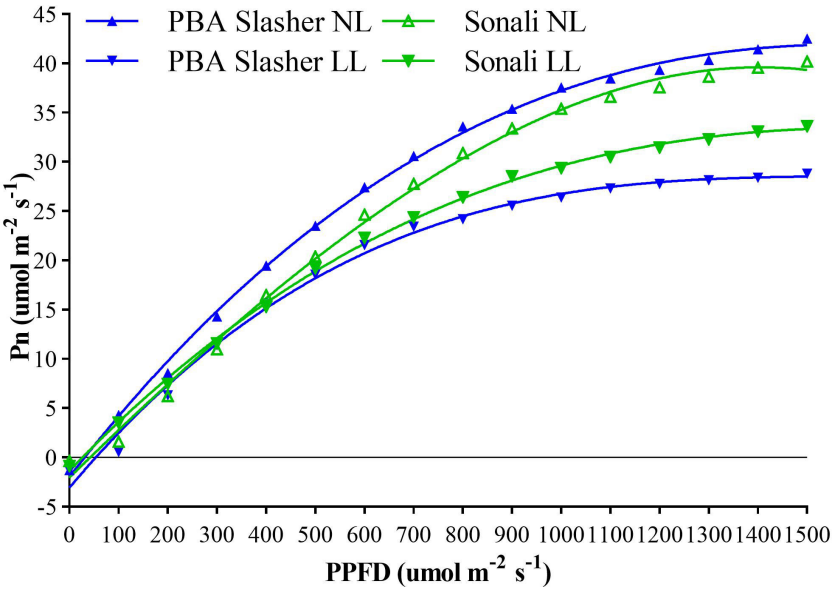

FIGURE 1
Association between photosynthesis (Pn) and photosynthetic photon flux density (PPFD) of Sonali and PBA Slasher recorded over different growth stages under natural light (NL) and low light (LL) treatments.

3.3 Response of RILs and parents to varied light conditions

Alteration in quality and quantity of light had altered the expression of majority of the indices under both light treatments (Table 1). Comparison of trait means of Sonali in NL vs LL revealed a reduction in DTE, DTFFB, SDBPP, RDBPP, RSR and PTDB, and an increase in DTA, PH, IL and NPP, with no effect recorded on BPP under LL. For PBA Slasher, estimates of DTFFB, NPP, BPP, SDBPP, RDBPP, and RSR were reduced, whereas, for DTE, DTA, PH, and IL increased in LL environment. Overall, trait means for DTE, SDBPP, RDBPP, RSR, and PTDB were greater under NL than DTFFB, DTA, PH, IL, NPP, and BPP, which were higher under LL treatment. The range of variation as indicated by CV% was 54.6% to 8.3% in LL, and 56.1% to 6.3% under NL conditions. It was highest for RDBPP (54.6% vs 37.5%), PTDB (32.7% vs 28.9%), and BPP (50.7% vs 56.1%) in LL vs NL environments, respectively, which showed their potential use, and possibility of further improvement.

3.4 Impact of low light on plant traits captured

It was assessed through % increase/decrease using trait means under NL and LL treatments (Table 1). Overall, chickpea seedlings took fewer days to emerge (-3.7%) under LL, but showed greater reduction in RDBPP (-52.8%), PTDB (-38.4%), RSR (-36.3%), and SDBPP (-28.2%) once harvested at anthesis stage. However, these took more days to develop first floral buds (9.2%), and to commence anthesis (19.2%), but with greater PH (39.9%), IL (33.4%), NPP (4.9%), and BPP (1.7%) compared to NL treatment.

3.5 Appraisal of heritability (H^2) values for traits investigated

The use of desirable plant traits in any breeding scheme depends upon their heritability values. The estimates of broad-sense heritability in this study were moderate to high, and ranged from 36.1% to 81.2% (Table 1). For all the traits (DTA, DTFFB, PH, NPP, TBP, SBPP, RBPP, BPP, RSR, and DTE) except IL, these were greater than 50% suggesting that variability in respective traits were due to genetic differences among plant material. For IL, it was lowest with 36.1%, implying greater environmental influence.

3.6 Association among different plant traits

All the parameters recorded under NL and LL treatments revealed positive and significant correlation coefficients with few exceptions (Supplementary Table 6). In NL, DTE was positively and significantly associated with DTFFB (r= 0.63) and DTA (r= 0.76). Likewise, the association of DTA with PTDB (r= 0.88), RSR (r= 0.81), RDBPP (r= 0.90), SDBPP (r= 0.84), BPP (r= 0.60), NPP (r= 0.93), IL (r= 0.17), and PH (r= 0.94) was positive and significant. The association of PTDB with RDBPP (r= 0.99) and SDBPP (r= 0.99) was near to one because it was estimated by adding both shoot and root biomass. The relationship of IL with DTFFB and RDBPP was positive, whereas with NPP and RSR, it was negative, but non-significant. Except these, the other correlation coefficients determined among other traits like DTE, DTFFB, DTA, PH, IL, NPP, BPP, SDBPP, RDBPP, RSR and PTDB were positive and significant. Under LL treatment, except for the association of IL with NPP, which was negative and non-significant, all other correlation coefficients among

TABLE 1 Various statistical measures of genotypes (parents & RILs) on plant traits recorded at anthesis stage, and impact of natural light (NL) and low light (LL) treatments on their expression (% increase/decrease) inside a glasshouse.

Traits	NL					LL					% change	H^2 B.S. %
	Sonali	Slasher	Mean ± SEM	RILs range	CV %	Sonali	Slasher	Mean ± SEM	RILs range	CV %		
DTE	15.3	6.8	6.45 ± 0.13	4.5-15	27.5	8.0	8.0	6.21 ± 0.11	4.3-15.5	23.0	-3.7	61.4
DTFFB	39.5	34.3	33.2 ± 0.47	21.5-56.5	19.1	39.0	32.5	36.3 ± 0.58	21.8-70.8	21.5	9.2	80.6
DTA	48.8	55.0	43.8 ± 0.71	29.5-68	21.9	56.8	56.3	52.2 ± 0.86	29.8-85	22.0	19.2	81.2
PH	39.5	33.0	37.5 ± 0.44	25.3-56.5	15.8	50.5	48.6	52.4 ± 0.61	28.5-74.6	15.5	39.9	77.8
IL	2.1	1.5	1.82 ± 0.01	1.53-2.77	6.3	2.5	2.2	2.43 ± 0.02	2.24-4.8	8.3	33.4	36.1
NPP	20.5	22.8	20.6 ± 0.22	10.5-27.8	14.3	21.0	21.8	21.6 ± 0.22	8.5-27.3	13.7	4.9	77.2
BPP	4.3	10.0	6.12 ± 0.26	1.0-21.3	56.1	4.3	9.3	6.22 ± 0.24	1.0-16.8	50.7	1.7	72.4
SDBPP	1.1	1.2	1.09 ± 0.02	0.62-2.3	23.3	0.8	0.6	0.78 ± 0.01	0.22-1.44	23.2	-28.2	75.6
RDBPP	0.8	1.2	0.78 ± 0.02	0.24-2.01	37.5	0.4	0.2	0.37 ± 0.02	0.1-1.01	54.6	-52.8	75.1
RSR	68.3	97.5	69.7 ± 0.97	31.4-96.7	18.6	53.5	35.8	44.4 ± 1.08	19.3-88.9	32.7	-36.3	67.9
PTDB	1.9	2.4	1.87 ± 0.04	0.97-4.09	28.9	1.2	0.7	1.15 ± 0.03	0.34-2.38	32.7	-38.4	76.8

DTE, Days to emergence (days); DTFFB, Days to first floral bud (days); DTA, Days to anthesis (days); PH, Plant height (cm); IL, Internodal length (cm); NPP, Nodes per plant; BPP, Branches per plant; SDBPP, Shoot dry biomass per plant (g); RDBPP, Root dry biomass per plant (g); RSR, Root/shoot ratio (%); PTDB, Plant total dry biomass (g).

different parameters were positive, significant, and similar to those obtained under NL conditions, therefore, not repeated here. However, values of coefficients for most of the traits in LL treatment were higher than the corresponding ones obtained under NL conditions.

3.7 Principal component analysis (PCA) for plant traits and genotypes

Prior to running PCA, we explored our data through descriptive statistics, and correlation analysis to cognize its characteristics, and address PCA limitations. Firstly, we identified outliers in the residual table, removed them using the masking tool, and run the recalculation to automatically update the output. Secondly, PCA presume that the data is linear, and in case of non-linear, will not detect underlying structure properly. Therefore to ensure equal weight and influence of each of the variable, we standardized it using Z-scores. Thirdly, sample size is very important for reliable, and robust PCA analysis. Mostly, a small input file can lead to misleading pattern/correlation between variables due to sampling error (Shaukat et al., 2016). Whereas, this probability will vanish with increasing sample size (Björklund, 2019). Generally, it is recommended that data set should have at least 150 samples (Sofroniou and Hutcheson, 1999) or larger than five times the number of variables for valid results (Hatcher, 1994). Our data set comprising 1440 cases, completely fulfilled this requirement. Fourthly, to validate results, reliability and robustness is crucial in PCA, and to check it, we permuted one variable at a time, and kept the others as fixed i.e. independently, and sequentially (Linting et al., 2011; Storm, 2012).

Afterwards, the PCA performed across both light treatments, collectively, explained 87.4% (PC1 = 58.9% & PC2 = 28.6%) of the total variation observed in Sonali/PBA Slasher RILs population (Supplementary Table 7). Except IL, all other parameters (NPP, DTFFB, PTDB, SDBPP, RDBPP, BPP, DTA, DTE, RSR, and PH) shared positive scores on PC1, ranging from 35% to 20%, respectively. In contrast, PC2 was largely influenced by IL (52%), and PH (47.3%) with positive, and RSR, RDBPP, PTDB and SDBPP, with negative values (-31.4% to -24.9%). A genotype-by-trait biplot constructed between PC1 and PC2 displayed indices with positive associations (< 90°), independent or no associations (= 90°), and negative associations (> 90°) based on the angle between them (Figure 2). It identified positive correlations among vegetative (BPP, NPP, and PH), phenology (DTE, DTFFB, and DTA), and biomass (SDBPP, PTDB, RDBPP, and RSR) parameters. However, relationship of IL with biomass indices, and that of PH with RSR was found to be negative. Overall, association among biomass parameters seemed stronger than vegetative, and phenological traits. Nevertheless, positively correlated all the traits contributed more towards the LL tolerance of genotypes, so can be selected as markers at anthesis stage in chickpea.

To assess the performance of genotypes, PCA biplot identified entries, #147, #161, #153, #86, and #107 as distant with strong positive association with carbon gain indicators i.e. SDBPP, PTDB, RDBPP, and RSR (Figures 2, 3), on NL quadrant. These entries contributed the highest values for these traits on PC1. Entries, #50, and #17 were recognized as far-off but with negative associations, and minimum scores for biomass parameters. The rest of the genotypes might have low to medium values for these indices. All the vegetative, and phenological traits occupied LL quadrant, where entries #107, #77, #97, #122, #4, and #110 suggested strong positive

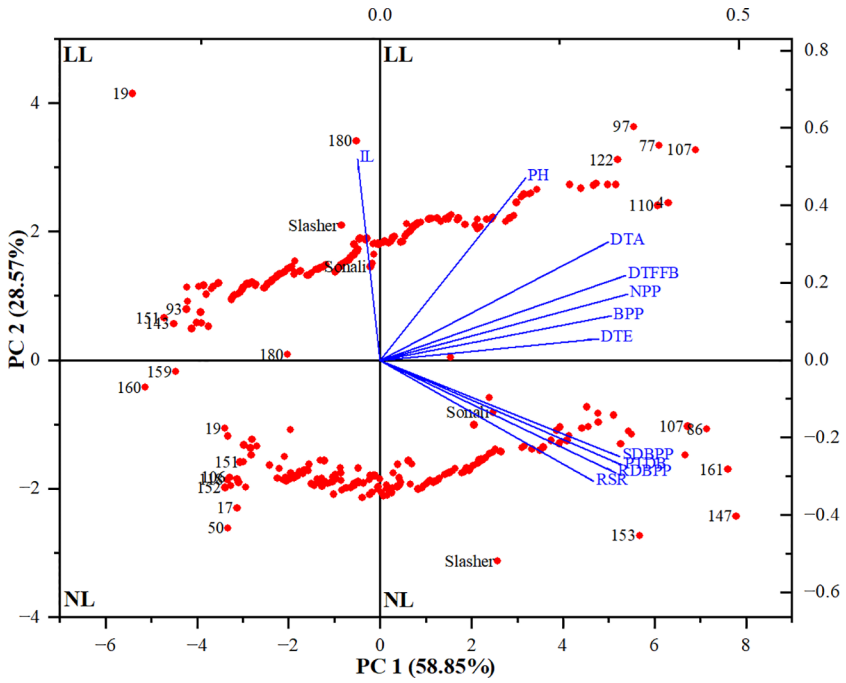

FIGURE 2
Biplot between principal components 1 and 2 (PC1 & PC2) showing the contribution of different traits (blue font) and genotypes (red font) in total variability under natural light (NL) and low light (LL) treatments. DTE, Days to emergence (days); DTFFB, Days to first floral bud (days); DTA, Days to anthesis (days); PH, Plant height (cm); IL, Internodal length (cm); NPP, Nodes per plant; BPP, Branches per plant; SDBPP, Shoot dry biomass per plant (g); RDBPP, Root dry biomass per plant (g); RSR, Root/shoot ratio (%); PTDB, Plant total dry biomass (g).

association, and maximum values for these traits on PC2. This biplot also displayed entries #19, #180, and #151 as away from origin with strong negative correlation, and lowest share for biomass indices under LL. This is also evident from clustering of entries between both light treatments, and distances from centroid in each environment, indicating their share in phenotypic variance (Figure 3). Between parents, PBA Slasher influenced both the environments with greater percentage than Sonali. This share was much higher in NL compared to LL treatment.

3.8 Best versus poor performing genotypes identified in PCA biplot

The superior and underperforming entries, given in section 3.7, were further assessed for biomass and anthesis period, being vital for drought tolerance in chickpea (Table 2). Among those, entries #147, #161, #153, and #107 initiated anthesis, on average, in about 56 to 66 days (DTA) in NL, and accumulated highest PTDB (4.09 to 3.12 g), RDBPP (2.01 to 1.38 g), SDBPP (2.08 to 1.74 g) with greater RSR (96.5 to 79.3%), respectively. In comparison, light-sensitive entries viz., #118, #106, #151, and #159 were early into flowering (~30 to 31 days), and produced less than half PTDB, RDBPP, SDBPP with lowest RSR than best entries under the same environment. Under LL, top entries, #107, #4, #110, and #122, in pursuit to adapt to prevailing conditions, delayed anthesis, on average, by ~10 days compared to best performing genotypes under NL, and by more than double to underperforming entries, #93, #143, #151, and #160, in reduced light treatment. Therefore, values of PTDB (2.38 to 2.01 g vs 0.55 to 0.34 g), RDBPP (1.01 to 0.79 g vs 0.14 to 0.12 g), SDBPP (1.44 to 1.22 vs 0.41 to 0.22 g), and RSR (79.3 to 65.1% vs 56.5 to 34.0%) were bigger for best genotypes than others in this environment, respectively. Estimates of parents for most of these traits were between best and poor performing RILs, implying presence of desirable recombinants.

4 Discussion

The uncertain chickpea production under variable environmental conditions is often attributed to multiple biotic and abiotic stresses (Shah et al., 2020). Breeding for improved cultivars against these factors requires investigation of all possible causes responsible for low and unstable chickpea yields (Maqbool et al., 2017). Effects of shade or LL on different agro-morphological plant traits are least investigated in chickpea. However, to formulate any breeding strategy, assessment of plant responses, and trait variability are one of the preliminary steps, and the major objectives of this study (Chen et al., 2017). It was revealed on reviewing literature that no such study was conducted in chickpea, previously, that specifically investigated effects of LL on morphology, phenology, and physiology at the anthesis stage. Apparently except light availability, this experiment was conducted under favorable temperature, moisture, and nutrients

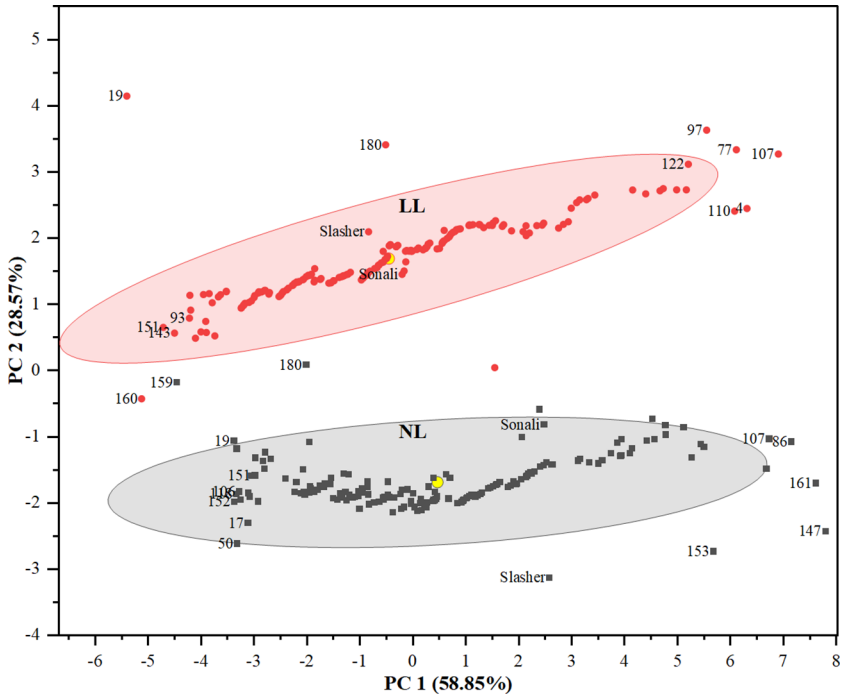

FIGURE 3
Clustering of genotypes in a PCA biplot (PC1 & PC2) showing the position of different genotypes from centroid (yellow circle) under natural light (NL) and low light (LL) treatments.

TABLE 2 Trait means of selected four superior and four poor performing recombinant inbred lines based on accumulated plant total dry biomass (PTDB) across two light treatments.

Entry	Natural light (NL)					Entry	Low light (LL)				
	PTDB	RDBPP	SDBPP	RSR	DTA		PTDB	RDBPP	SDBPP	RSR	DTA
147	4.09	2.01	2.08	96.7	56.3	107	2.38	0.94	1.44	65.6	75.0
161	3.83	1.71	2.12	80.5	56.3	4	2.36	1.01	1.36	74.3	75.0
153	3.82	1.52	2.30	65.8	56.3	110	2.27	1.01	1.27	79.3	74.8
107	3.12	1.38	1.74	79.3	66.3	122	2.01	0.79	1.22	65.1	74.8
Sonali	*1.86*	*0.75*	*1.11*	*68.0*	*48.8*	*Sonali*	*1.23*	*0.42*	*0.81*	*52.0*	*56.8*
Slasher	*2.42*	*1.20*	*1.23*	*97.5*	*55.0*	*Slasher*	*0.74*	*0.20*	*0.55*	*35.8*	*56.3*
118	1.05	0.29	0.76	37.9	30.5	93	0.55	0.14	0.41	34.6	34.3
106	1.04	0.38	0.66	56.8	32.3	143	0.52	0.13	0.39	34.0	33.8
151	1.02	0.37	0.65	56.5	32.0	151	0.50	0.14	0.36	39.1	33.3
159	1.00	0.24	0.76	31.9	31.3	160	0.34	0.12	0.22	56.5	29.8
Mean	*2.33*	*0.99*	*1.34*	*67.1*	*46.5*	*Mean*	*1.29*	*0.49*	*0.80*	*53.8*	*54.4*
SEM	*0.41*	*0.21*	*0.21*	*7.02*	*4.29*	*SEM*	*0.27*	*0.13*	*0.15*	*5.42*	*6.3*
SD	*1.30*	*0.66*	*0.66*	*22.2*	*13.6*	*SD*	*0.87*	*0.40*	*0.48*	*17.1*	*19.9*

PTDB, Plant total dry biomass (g); RDBPP, Root dry biomass per plant (g); Shoot dry biomass per plant (g); RSR, Root/shoot ratio (%); Days to anthesis (days); SEM, Standard error of mean; SD, Standard deviation from mean.
Entries given above parents (Sonali & Slasher) produced highest PTDB, whereas below lowest.

supply, hence, potential effects determined were mostly by light composition.

4.1 Evaluation of methodology executed for inducing low light environment

Differences observed in PPFD, RL, FRL, and RL/FRL ratio between two light treatments were significant, suggesting that the method used to mimic reduced light conditions in this study had successfully simulated the LL environment. Previous studies had also reported significant differences in quality of light, induced using different procedures. Li et al. (2010) in a field study on chickpea used a black commercial shade cloth to create LL environment up to vegetative phase, and found 45% decrease in incident PPFD. In soybean, Yao et al. (2017) generated 50% and 75% shade conditions by covering 2 m above ground level with black nets. They reported 4 and 2.5 fold decrease in photosynthetic photon flux density (PPFD) in 75%, and 50% shade compared to unshaded treatment, respectively. Liu et al. (2018) in a maize-soybean relay intercropping measured different light parameters when soybean seedlings were 16 d older, and informed a reduction of 82.7%, 50.0%, 65.5%, and 52.3% in RL, FRL, their ratios, and PPFD, respectively over normal light. Based on these values, we can say that our method of inducing low light conditions is comparable with previous studies in terms of effectiveness. It can replicate the same level of reduction in light composition due to defined net mesh size, and other controlled conditions, such as temperature and humidity. However, we can improve on consistency and validity of the experimental treatments throughout the study period by employing temperature and reliable light sensors capable of measuring not only light intensity but also related parameters (red/far-red components) alongwith installation of automated systems for irrigation and fertigation purposes.

4.2 Implication of ANOVA genotype-treatment interaction

The significant G×T interaction for the traits investigated (DTE, DTFFB, DTA, PH, IL, NPP, BPP, SDBPP, RDBPP, RSR and PTDB) indicated existence of different genotypic responses to altered light composition. These findings are in agreement with previous studies where significant genotype-by-treatment interaction had influenced PH (Getachew et al., 2015), DTA (Desai et al., 2016), SDBPP (Arif et al., 2021), RDBPP and PTDB (Nayak et al., 2010) in chickpea but under different conditions.

4.3 Effects of LL on photosynthetic response of parents

These were greater for PBA Slasher as indicated by 27.9% reduction in net photosynthetic rate compared to 12.8% of Sonali over NL treatment due to reduced PPFD under LL (Shrestha et al., 2019). LL severely affected this parental line in contrast to Sonali, and modified its true phenotypic expression through substantial increase in plant height (47.3% vs 27.8%), and internodes length (46.7% vs 19.0%), and decrease in branches (7.0% vs 0.0%), nodes (4.4% vs 2.4%), biomass of roots (83.3% vs 50.0%), shoots (50.0% vs 27.3%), root/shoot ratio (63.3% vs 21.7%), and total plant biomass (70.8% vs 36.8%), respectively. It also delayed seedling emergence (-17.6% vs 47.7%), and anthesis (- 2.4% vs 1.3%) in PBA Slasher as opposed to Sonali, wherein, these were induced much earlier in the season. The better response of Sonali to these conditions, especially for vegetative (PH, IL) and biomass (RDBPP, SDBPP, RSR, PTDB) indices, was attributed to superior light harvesting, net photosynthetic rate, and production of photosynthates (Cai, 2011; Shafiq et al., 2021). This is also evident from the performance of PBA Slasher under NL conditions, where it maintained 8.1% more Pn than Sonali, and excelled in crucial indices such as RDBPP, RSR, PTDB, and SDBPP by 33.3%, 29.9%, 20.8%, and 8.3%, and BPP and NPP by 57.0% and 10.1%, respectively. In maize and soybean, previous researchers also reported a significant reduction in photosynthetic capacity, and carbon gain of genotypes under suboptimal PPFD, and other light components (Pausch et al., 1991; Gao et al., 2017). Because, plants grown at different irradiance levels develop photosynthetic apparatus with altered features, so varied carbon fixation potential with overall reduced rate of photosynthesis (Bailey et al., 2001; Sun et al., 2014; Irving, 2015).

4.4 Effects of LL on plant phenology

Differences in days to emergence were observed among genotypes, which indicated varied thermal time requirement between two light treatments. The LL significantly promoted seed germination, resulting in, 3.7% less days to emerge from date of sowing than NL, suggesting minimum or no role of light, and had been reported previously in chickpea (Vignoli, 1936), and some other species (Chanyenga et al., 2012). Seed germination largely depends upon soil temperature, moisture, and seeding depth (Soltani et al., 2006). Since we kept all these requirements close to optimum in both the treatments, this accelerated emergence might be due to comparatively low temperature under shade which allowed seeds to imbibe enough water content to initiate germination earlier than NL (Tewfik, 2003; Ahmed et al., 2014).

The current study found that LL not only impeded first floral buds development but also commencement of anthesis, on average, by 3.1 and 8.4 more days, compared to NL, respectively. This is a consequence of drop in PPFD which substantially impacted photosynthetic process, hence, energy production and access to genotypes (Jiang and Egli, 1993; Cai, 2011). Previous studies on chickpea (Sandhu and Hodges, 1971; Samineni et al., 2020), and alfalfa (Lorenzo et al., 2019) also informed similar findings. Generally, plants employ two flowering strategies to counter shade. They either accelerate reproductive development as reported in *Oryza sative*, *Lotus japonicus*, and *Arabidopsis thaliana* (Cerdán and Chory, 2003; Ueoka-Nakanishi et al., 2011;

Carriedo et al., 2016) or delay it, comparable to this, and previous other studies on sunflower, tomato, and alfalfa, possibly, as an adaptive strategy (Qin et al., 2022). The delayed flowering reported herein, allowed chickpea plants to intercept greater proportion of PAR, thus, more assimilates for sustaining vegetative and reproductive development, and production of biomass (Lake, 2017).

4.5 Effects of LL on shoot architecture

Suboptimal light causes reduction in thickness of leaf and palisade tissues, chlorophyll contents, and leaf area, resultantly, decreased light interception. This impacts the activity of gas exchange processes (stomatal density, conductance), consequently, inadequate CO_2 transport. Further, transfer of electron from photosystem II to I is obstructed, and level of enzymes biosynthesis is modified. Moreover, reactive oxygen species (O_2^-, O_2H, OH, & O) are produced, which interferes with the normal functioning of photosynthetic apparatus. These leads to reduction in rate of CO_2 assimilation, net photosynthesis, and greater biomass partitioning to stems (Gong et al., 2015; Shafiq et al., 2021). We found that variation in RL : FRL ratio had enhanced plant height and internodal length of genotypes, on average, by 14.9 cm and 0.6 cm, respectively. Stem elongation is a well-known adaptive strategy in plants to altered light (Sessa et al., 2018; Wang et al., 2020). Increased plant height, and nodes length is a typical sign of shade avoidance syndrome (SAS), by which, plants elongate their stems in search of light. This resulted in weaker and slender stems, and had been reported by previous researchers in soybean (Green-Tracewicz et al., 2011; Zhang et al., 2011), sunflower, and Arabidopsis (Yang and Li, 2017). Low RL/FRL ratio, initially, promotes shade escape mechanism (Ballaré et al., 1990), and then inactivates phytochrome-interacting factors to produce increased level of auxins, which results in stem elongation (Li et al., 2012). Low PPFD is also responsible for this growth due to increased production level of gibberellin in hypocotyls, leaves, internodes, and shoots (Beall et al., 1996; Kurepin et al., 2007). Stem strength greatly depends upon synthesis of biochemical compounds, such as lignin, starch, pectin, sucrose, semi-fiber, and LL serves as a constraining factor in their production due to reduced enzymatic activities of phenylalanine, dehydrogenase, peroxidase, and ligase (Wu et al., 2017a; Hussain et al., 2019; Shafiq et al., 2021). Hormones, such as auxin and gibberellins, control LL induced plant growth and expansion (Yang and Li, 2017). This study has informed production of more NPP compared to NL conditions, similar to the report of Nico et al. (2015) in soybean. In contrast, Raai et al. (2020) in a study on winged beans found that non-shaded plants produced higher NPP than moderately shaded, and heavily shaded plants. For branches per plant, non-significant treatment effects were recorded. However, genotypic differences were recorded under both light treatments. Raai et al. (2020) in the same study also observed substantial variation in BPP, non-shaded being higher in BPP than shaded plants. This increase in NPP and BPP was due to delayed anthesis, and energy conserved over the extended time period, possibly, to endure challenging environments (Lorenzo et al., 2019).

4.6 Effects of LL on biomass production and partitioning

The ratio of biomass partitioning to above and below-ground plant parts is a way to study biomass allocation. Shoots represent the light-harvesting, energy-producing part, while roots are essential for nutrients, and water uptake from the soil. The larger the root system a plant develops, the higher its biomass and root-to-shoot ratio will be (Poorter and Nagel, 2000; Mašková and Herben, 2018). Among all the traits we investigated, LL effects were highest on biomass indices such as roots, shoots, root/shoot ratio, and plant total dry biomass. On average, it reduced RDBPP and SDBPP by 52.8% (0.4 g) and 28.2% (0.3 g), RSR by 36.3%, and PTDB by 38.4% (0.7 g) over NL treatment. Poor light intensity not only modified the true phenotypes through shifting of greater energy resources to vegetative parts (stem, nodes and branches) but also restricted root development. This resulted in insufficient carbon gain of roots, altering root/shoot ratio, and morphology of genotypes. These results are consistent with the previous studies on chickpea, which also revealed a reduction in these plant parts on reducing light artificially (Verghis et al., 1999; Li et al., 2010; Lake and Sadras, 2014). Similar observations were also reported in other crops like soybean, maize, and is a typical outcome of SAS when plants perceive low RL/FRL signal through phytochromes (Kurepin et al., 2007; Gao et al., 2017; Wu et al., 2017b; Wang et al., 2020). Biosynthesis of some of the phyto-hormones, such as auxin and ethylene increases under these conditions, which severely impacts root growth and development (Růžička et al., 2007). Underdeveloped roots could seriously affect tolerance of plants to water-deficit environments, and genotypes with compromised root system are more susceptible to drought, which is a severe issue in chickpea, particularly during reproductive phase (Pierik and Testerink, 2014; Blessing et al., 2018; Dreccer et al., 2018). Therefore, to mitigate these effects, genotypes as well as target traits are required to be identified for achieving sustainability in chickpea production.

4.7 Relationship among different plant traits

Across both light conditions, genotypes who took higher days to initiate flowering (DTA) produced greater RDBPP, SDBPP, RSR, and PTDB. These also exhibited slower growth rates as they took longer for DTE, and DTFFB development. Over the longer growing period, these genotypes attained higher PH with greater IL, NPP, and BPP. However, late flowering genotypes, as identified in NL and LL treatments (Table 2), performed better due to maximum light-harvesting, radiation use efficiency, and higher energy production (Li et al., 2008; Bai et al., 2016; Shafiq et al., 2021).

4.8 Genetic variation and heritability of plant traits captured

The existence of genetic diversity within or between crop species is indispensable for crop improvement against various stresses (Swarup et al., 2021). This offers plant breeders a chance to select for superior genotypes for use in breeding programs aimed at germplasm development, or release of cultivars for commercial cultivation (Naveed et al., 2020). The genotypic variation observed in this study was also impressive for some of the targeted traits, especially roots (0.10 to 1.01 g), shoots (0.22 to 1.44 g), total plant biomass (0.34 to 2.38 g), and days to anthesis (29.8 to 85.0 d) under LL conditions. For instance, RILs #107 (2.38 g), #4 (2.36 g), #107 (2.27 g), and #122 (2.01 g) outperformed parents, Sonali (1.23 g), PBA Slasher (0.74 g), and other lines (1.29 g) for total plant biomass as indicated by means. Likewise for root dry biomass per plant, RILs #93 (0.14 g), #151 (0.14 g), #143 (0.13 g), and #160 (0.12 g) failed to exceed parents, Sonali (0.42 g), PBA Slasher (0.20 g), and other genotypes (0.49 g). These results revealed presence of genetic diversity, continuous variation, and transgressive recombinants (+ve & -ve) for some of the parameters compared here of Sonali/PBA Slasher mapping population (Polania et al., 2017). Mapping populations are an excellent source of genetic diversity, and have been reported to possess transgressive segregants for salinity (Pushpavalli et al., 2015) and heat (Paul et al., 2018) tolerance in chickpea.

High broad-sense heritability estimates were recorded for indices such as DTE, DTFFB, DTA, PH, NPP, BPP, SDBPP, RDBPP, RSR and PTDB, under NL and LL conditions, except for IL. This suggested the least influence of environments on the expression of these parameters, and the potential of direct selection for further improvement under similar conditions (Hussain et al., 2016; Naveed et al., 2016).

4.9 Discrimination of genotypes for biomass traits

Among multivariate techniques, PCA biplot is the most effective method for assessing performance of genotypes, and interaction of traits. It has been extensively practiced to examine the association among traits in chickpea, and other field crops (Erdemci, 2018; Sharma et al., 2023). Biplots provided a new direction in understanding plant responses, and respective stress-tolerance mechanisms under various environmental conditions (Sivakumar et al., 2020; Rani et al., 2023).

In the present study, PCA biplot indicated strong associations among various plant traits under both the treatments, implying potential breeding strategies to emphasize for further improvement (Kushwah et al., 2022). The positive correlation of days to anthesis with total plant biomass (r= 0.88, 0.95), root biomass (r= 0.90, 0.93), and shoot biomass (r= 0.84, 0.94), as exhibited by biplot and Pearson's correlation coefficients under NL and LL, respectively, suggested that genotypes with late maturity period produced plant parts, above and below ground, with greater biomass. Association of three biomass parameters, PTDB with RDBPP (r= 0.99, 0.99), SDBPP (r= 0.99, 0.98), and RDBPP with SDBPP (r= 0.95, 0.94), revealed correlated response with coefficients near to 1.0, and heritability values greater than 75.0%, indicating least environmental influence, and possibility of simultaneous improvement using different selection strategies (Rana et al., 2019). Direct selection, as early as, from F_2 generation would be rewarding for progressing further in these traits (Sehrawat et al., 2012). Entries such as #147 (1_52), #161 (1_73), #153 (1_64), #86 (1_223), and #107 (1_245) revealed an increase of 43.0 to 25.3%, 50.7 to 28.3%, and 35.6 to 23.0% in total plant biomass, root biomass, and shoot biomass compared to respective trait means under NL conditions. Likewise, entries #107 (1_245), #77 (1_212), #97 (1_233), #122 (1_269), #4 (1_103), and #110 (1_248) surpassed trait means for biomass of roots, shoots, and total plant biomass by 47.9 to 38.0%, 44.4 to 34.4%, and 45.8 to 35.8%, respectively, under LL environment. Detailed analysis of these entries revealed that RILs viz., 1_52, 1_73, 1_64, 1_245, 1_103, 1_248, and 1_269, overall, produced more biomass (PTDB, RDBPP, SDBPP) with greater number of nodes, branches over 17.4 to 29.9% longer phenological period to start anthesis. Entry #107 (1_245) revealed phenotypic plasticity across both NL and LL with good scores for TPDB (3.12 vs 2.01 g), RDBPP (1.38 vs 0.79 g) and SDBPP (1.74 vs 1.22 g), therefore, could be used regardless of the specific environment (Sadras et al., 2016). This biplot also showed negative association of internodal length with all biomass traits, with heritability value of 36.1%, implying greater environmental effects, and delay in selection up to later generations, such as F_5 or F_6 through pedigree method would be rewarding (Khan et al., 2016).

All the promising RILs identified here could be utilized in different breeding schemes for creating new, and desirable recombinants, and developing shade-tolerant chickpea germplasm (Gommers et al., 2013; Naveed et al., 2015; Sulistyowati et al., 2016). Classical methods such as introduction, selection, and hybridization, are the most common breeding approaches used for selecting plant material with targeted features. However, these require greater time-period, and resources when traits of interest (such as root, shoot and total plant biomass etc.) are polygenic and correlated with each other. The selection process becomes even more complicated if there is a greater G×E interaction or trade-off (phenology and yield in chickpea etc.) among traits (Maqbool et al., 2017). To overcome these challenges, molecular techniques such as linkage maps and marker-assisted selection (MAS) could be used, being stable and unaffected by environmental fluctuations, and easily noticeable, regardless of growth stage. However, production of mapping populations is one of the basic requirement for constructing a linkage map and establishing marker-trait association (Collard et al., 2005). For this purpose, the RILs discriminated here could be used for developing segregating populations involving two or multiple parents. This could lead in identifying quantitative trait loci (QTL) associated with drought tolerance indices (root biomass, shoot biomass, and total plant

biomass), and their incorporation through various MAS schemes. Completion of chickpea genome sequencing has further opened up avenues for crop improvement through omics techniques such as genomics, transcriptomics, and phenomics. We can combine QTL mapping with these methods to study the expression of genes, and molecular mechanisms regulating these parameters, and shade tolerance in genetic material so developed using these RILs. This would accelerate incorporation, and selection for shade tolerance traits (Mir et al., 2012; Dutta et al., 2018). Therefore, a multidisciplinary approach integrating genomics with breeding, coupled with precise phenotyping is suggested for conferring this type of stress in chickpea.

5 Conclusion

Modifications in optimum light conditions as revealed by reduced photosynthetic active radiation, red and far-red lights, and their ratios proved that our methodology of using mosquito net, had effectively, simulated low light conditions. The responses of chickpea genotypes to these changes were severe, as most of them altered their morphology with greater investment of available photosynthates on shoot growth at the expense of root development. Specifically, plants were slow in growth, produced greater plant heights, internodal lengths, and nodes per plant, however, with reduced root, shoot, and total plant biomass, and altered root to shoot ratios, possibly as an adaptive strategy, similar to the hypothesis of shade avoidance syndrome. Modifications in some biochemical and molecular processes might also be responsible for all these effects, but, were not part of our research, and would be of great worth in understanding shade effects, and possible mechanisms in future studies. Overall, low light effects were greater on biomass relevant parameters (root, shoot, their ratio, and total plant biomass), which are vital part of drought tolerance strategy in chickpea. Superior RILs identified through PC analysis, viz., 1_52, 1_73, 1_64, 1_245, 1_103, 1_248, and 1_269, produced highest TPDB with greater RDBPP, and SDBPP. These RILs, along with others identified in this study, could be the source material to develop light-insensitive chickpea cultivars through integrated breeding approaches.

Data availability statement

The raw data supporting the conclusions of this article will be made available by the authors, without undue reservation.

Author contributions

MN: Data curation, Investigation, Methodology, Writing – original draft. UB: Supervision, Writing – review & editing. BNK: Funding acquisition, Supervision, Writing – review & editing.

Funding

The author(s) declare financial support was received for the research, authorship, and/or publication of this article. This study was funded by the ARC Industrial Transformation Research Hub - Legumes for Sustainable Agriculture (IH140100013) and the Grains Research and Development Corporation (GRDC), Australia.

Acknowledgments

The authors greatly appreciate the role of Dr. Helen Bramley, Ex-Senior Lecturer, the University of Sydney, Australia in planning, and Laura Turchi, in setting-up this experiment.

Conflict of interest

The authors declare that the research was conducted in the absence of any commercial or financial relationships that could be construed as a potential conflict of interest.

Publisher's note

Supplementary material

The Supplementary Material for this article can be found online at: https://www.frontiersin.org/articles/10.3389/fpls.2024.1292753/full#supplementary-material.

References

Abbo, S., Berger, J., and Turner, N. C. (2003). Evolution of cultivated chickpea: four bottlenecks limit diversity and constrain adaptation. *Funct. Plant Biol.* 30 (10), 1081–1087. doi: 10.1071/FP03084

Ahmed, L. T., Warrag, E. I., and Abdelgadir, A. Y. (2014). Effect of shade on seed germination and early seedling growth of Moringa oleifera Lam. *J. For. Prod. Indust.* 3 (1), 20–26.

Ali, Q., Ahsan, M., and Farooq, J. (2010). Genetic variability and trait association in chickpea (*Cicer arietinum* L.) genotypes at seedling stage. *Electron. J. Plant Breed.* 1 (3), 334–341.

Ao, N., Ma, J., Xu, T., Su, J., Yang, X., Guan, Z., et al. (2019). Genetic variation and QTL mapping for cold tolerance in a *chrysanthemum* F1 population at different growth stages. *Euphytica* 215 (5), 88. doi: 10.1007/s10681-019-2412-7

Arango-Botero, D., Hernández-Barajas, F., and Valencia-Arias, A. (2023). Misspecification in generalized linear mixed models and its impact on the statistical wald test. *Appl. Sci.* 13 (2), 977. doi: 10.3390/app13020977

Arif, A., Parveen, N., Waheed, M. Q., Atif, R. M., Waqar, I., and Shah, T. M. (2021). A comparative study for assessing the drought-tolerance of chickpea under varying natural growth environments. *Front. Plant Sci.* 11, 2228. doi: 10.3389/fpls.2020.607869

Aryamanesh, N., Nelson, M., Yan, G., Clarke, H. J., and Siddique, K. (2010). Mapping a major gene for growth habit and QTLs for ascochyta blight resistance and flowering time in a population between chickpea and *Cicer reticulatum*. *Euphytica* 173 (3), 307–319. doi: 10.1007/s10681-009-0086-2

Bai, Z., Mao, S., Han, Y., Feng, L., Wang, G., Yang, B., et al. (2016). Study on light interception and biomass production of different cotton cultivars. *PloS One* 11 (5), e0156335. doi: 10.1371/journal.pone.0156335

Bailey, S., Walters, R. G., Jansson, S., and Horton, P. (2001). Acclimation of *Arabidopsis thaliana* to the light environment: the existence of separate low light and high light responses. *Planta* 213 (5), 794–801. doi: 10.1007/s004250100556

Ballaré, C. L., Scopel, A. L., and Sanchez, R. A. (1990). Far-red radiation reflected from adjacent leaves: an early signal of competition in plant canopies. *Science* 247 (4940), 329–332. Available at: https://www.science.org/doi/10.1126/science.247.4940.329.

Beall, F. D., Yeung, E. C., and Pharis, R. P. (1996). Far-red light stimulates internode elongation, cell division, cell elongation, and gibberellin levels in bean. *Canad. J. Bot.* 74 (5), 743–752. doi: 10.1139/b96-093

Björklund, M. (2019). Be careful with your principal components. *Evolution* 73 (10), 2151–2158. doi: 10.1111/evo.13835

Blessing, C. H., Mariette, A., Kaloki, P., and Bramley, H. (2018). Profligate and conservative: water use strategies in grain legumes. *J. Exp. Bot.* 69 (3), 349–369. doi: 10.1093/jxb/erx415

Cai, Z. (2011). Shade delayed flowering and decreased photosynthesis, growth and yield of Sacha Inchi (*Plukenetia volubilis*) plants. *Ind. Crops Prod.* 34 (1), 1235–1237. doi: 10.1016/j.indcrop.2011.03.021

Carriedo, L. G., Maloof, J. N., and Brady, S. M. (2016). Molecular control of crop shade avoidance. *Curr. Opin. Plant Biol.* 30, 151–158. doi: 10.1016/j.pbi.2016.03.005

Cerdán, P. D., and Chory, J. (2003). Regulation of flowering time by light quality. *Nature* 423 (6942), 881–885. Available at: https://www.nature.com/articles/nature01636.

Chanyenga, T., Geldenhuys, C., and Sileshi, G. (2012). Germination response and viability of an endangered tropical conifer Widdringtonia whytei seeds to temperature and light. *S. Afr. J. Bot.* 81, 25–28. doi: 10.1016/j.sajb.2012.04.002

Chen, Y., Ghanem, M. E., and Siddique, K. H. (2017). Characterising root trait variability in chickpea (*Cicer arietinum* L.) germplasm. *J. Exp. Bot.* 68 (8), 1987–1999. doi: 10.1093/jxb/erw368

Choudhary, A. K., Sultana, R., Vales, M. I., Saxena, K. B., Kumar, R. R., and Ratnakumar, P. (2018). Integrated physiological and molecular approaches to improvement of abiotic stress tolerance in two pulse crops of the semi-arid tropics. *Crop J.* 6 (2), 99–114. doi: 10.1016/j.cj.2017.11.002

Collard, B. C., Jahufer, M., Brouwer, J., and Pang, E. (2005). An introduction to markers, quantitative trait loci (QTL) mapping and marker-assisted selection for crop improvement: the basic concepts. *Euphytica* 142 (1), 169–196. doi: 10.1007/s10681-005-1681-5

Coombes, N. (2009). *DiGGer design search tool in R*. (New South Wales Department of Primary Industry, Australia).

Desai, K., Tank, C., Gami, R., and Patel, A. (2016). G × E interaction and stability analysis in chickpea (*Cicer arietinum* L.). *Int. J. Agric. Environ. Biotechnol.* 9 (4), 479–484. doi: 10.5958/2230-732X.2016.00063.2

Dreccer, M. F., Fainges, J., Whish, J., Ogbonnaya, F. C., and Sadras, V. O. (2018). Comparison of sensitive stages of wheat, barley, canola, chickpea and field pea to temperature and water stress across Australia. *Agric. For. Meteorol.* 248, 275–294. doi: 10.1016/j.agrformet.2017.10.006

Dutta, S. S., Tyagi, W., Pale, G., Pohlong, J., Aochen, C., Pandey, A., et al. (2018). Marker–trait association for low-light intensity tolerance in rice genotypes from Eastern India. *Mol. Genet. Genomics* 293 (6), 1493–1506. doi: 10.1007/s00438-018-1478-6

Erdemci, I. (2018). Investigation of genotype× environment interaction in chickpea genotypes using AMMI and GGE biplot analysis. *Turkish J. Field Crop* 23 (1), 20–26. doi: 10.17557/tjfc.414846

Fan, Y., Chen, J., Cheng, Y., Raza, M. A., Wu, X., Wang, Z., et al. (2018). Effect of shading and light recovery on the growth, leaf structure, and photosynthetic performance of soybean in a maize-soybean relay-strip intercropping system. *PloS One* 13 (5), e0198159. doi: 10.1371/journal.pone.0198159

FAOSTAT (2021). *The food and agriculture organization of the United Nations* (UNFAO, Rome, Italy).

Franklin, K. A. (2008). Shade avoidance. *New Phytol.* 179 (4), 930–944. doi: 10.1111/j.1469-8137.2008.02507.x

Gao, J., Shi, J., Dong, S., Liu, P., Zhao, B., and Zhang, J. (2017). Grain yield and root characteristics of summer maize (*Zea mays* L.) under shade stress conditions. *J. Agron. Crop Sci.* 203 (6), 562–573. doi: 10.1111/jac.12210

Getachew, T., Firew, M., Asnake, F., and Million, E. (2015). Genotype x environment interaction and stability analysis for yield and yield related traits of Kabuli-type Chickpea (*Cicer arietinum* L.) in Ethiopia. *Afr. J. Biotechnol.* 14 (18), 1564–1575. doi: 10.5897/AJB2014.14320

Gommers, C. M., Visser, E. J., St Onge, K. R., Voesenek, L. A., and Pierik, R. (2013). Shade tolerance: when growing tall is not an option. *Trends Plant Sci.* 18 (2), 65–71. doi: 10.1016/j.tplants.2012.09.008

Gong, W., Jiang, C., Wu, Y., Chen, H., Liu, W., and Yang, W. (2015). Tolerance vs. avoidance: two strategies of soybean (*Glycine max*) seedlings in response to shade in intercropping. *Photosynthetica* 53, 259–268. doi: 10.1007/s11099-015-0103-8

Green-Tracewicz, E., Page, E. R., and Swanton, C. J. (2011). Shade avoidance in soybean reduces branching and increases plant-to-plant variability in biomass and yield per plant. *Weed Sci.* 59 (1), 43–49. doi: 10.1614/WS-D-10-00081.1

Hatcher, L. (1994). Step-by-step approach to using the SAS system for factor analysis and structural equation modeling. Cary, NC *SAS Institute*, 1–41.

Hussain, M. A., Hossain, M. S., Bhuiyan, M. S. R., Zeba, N., and Mohsin, S. M. (2016). Field performance and genetic analysis in some advanced lines of mustard (*Brassica rapa* L.). *Agriculturists* 14 (1), 112–121. doi: 10.3329/agric.v14i1.29109

Hussain, S., Iqbal, N., Rahman, T., Liu, T., Brestic, M., Safdar, M. E., et al. (2019). Shade effect on carbohydrates dynamics and stem strength of soybean genotypes. *Environ. Exp. Bot.* 162, 374–382. doi: 10.1016/j.envexpbot.2019.03.011

Irving, L. J. (2015). Carbon assimilation, biomass partitioning and productivity in grasses. *Agriculture* 5 (4), 1116–1134. doi: 10.3390/agriculture5041116

Jha, U. C., Chaturvedi, S. K., Bohra, A., Basu, P. S., Khan, M. S., Barh, D., et al. (2014). Abiotic stresses, constraints and improvement strategies in chickpea. *Plant Breed.* 133 (2), 163–178. doi: 10.1111/pbr.12150

Jiang, H., and Egli, D. (1993). Shade induced changes in flower and pod number and flower and fruit abscission in soybean. *Agron. J.* 85 (2), 221–225. doi: 10.2134/agronj1993.00021962008500020011x

Johnson, H. W., Robinson, H., and Comstock, R. (1955). Estimates of genetic and environmental variability in soybeans 1. *Agron. J.* 47 (7), 314–318. doi: 10.2134/agronj1955.00021962004700070009x

Kaloki, P. K. (2017). *Breeding for increased water use efficiency in chickpea* (The University of Sydney, Australia). PhD thesis. Available at: https://ses.library.usyd.edu.au/handle/2123/17345.

Kashiwagi, J., Krishnamurthy, L., Purushothaman, R., Upadhyaya, H., Gaur, P., Gowda, C., et al. (2015). Scope for improvement of yield under drought through the root traits in chickpea (*Cicer arietinum* L.). *Field Crops Res.* 170, 47–54. doi: 10.1016/j.fcr.2014.10.003

Khalid, M., Raza, M., Yu, H., Sun, F., Zhang, Y., Lu, F., et al. (2019). Effect of shade treatments on morphology, photosynthetic and chlorophyll fluorescence characteristics of soybeans (*Glycine max* L. Merr.). *Appl. Ecol. Environ. Res.* 17 (2), 1–19. doi: 10.15666/aeer/1702_25512569

Khan, N. H., Ahsan, M., Naveed, M., Sadaqat, H. A., and Javed, I. (2016). Genetics of drought tolerance at seedling and maturity stages in *Zea mays* L. *Span. J. Agric. Res.* 14 (3), 13. doi: 10.5424/sjar/2016143-8505

Kurepin, L. V., Emery, R. N., Pharis, R. P., and Reid, D. M. (2007). Uncoupling light quality from light irradiance effects in *Helianthus annuus* shoots: putative roles for plant hormones in leaf and internode growth. *J. Exp. Bot.* 58 (8), 2145–2157. doi: 10.1093/jxb/erm068

Kushwah, A., Bhatia, D., Singh, G., Singh, I., Vij, S., Bindra, S., et al. (2022). Phenotypic evaluation of agronomic and root related traits for drought tolerance in recombinant inbred line population derived from a chickpea cultivar (*C. arietinum* L.) and its wild relative (C. reticulatum). *Physiol. Mol. Biol. Plants* 28 (7), 1437–1452. Available at: https://link.springer.com/article/10.1007/s12298-022-01218-z

Lake, L. (2017). *Physiology of yield determination in chickpea (Cicer arietinum L.): critical period for yield determination, patterns of environmental stress, competitive ability and stress adaptation* (Australia: University of Adelaide).

Lake, L., and Sadras, V. O. (2014). The critical period for yield determination in chickpea (*Cicer arietinum* L.). *Field Crops Res.* 168, 1–7. doi: 10.1016/j.fcr.2014.08.003

Li, L., Bueckert, R. A., Gan, Y., and Warkentin, T. (2008). Light interception and radiation use efficiency of fern-and unifoliate-leaf chickpea cultivars. *Can. J. Plant Sci.* 88 (6), 1025–1034. doi: 10.4141/CJPS07056

Li, L., Gan, Y., Bueckert, R., and Warkentin, T. (2010). Shading, defoliation and light enrichment effects on chickpea in northern latitudes. *J. Agron. Crop Sci.* 196 (3), 220–230. doi: 10.1111/j.1439-037X.2009.00409.x

Li, L., Ljung, K., Breton, G., Schmitz, R. J., Pruneda-Paz, J., Cowing-Zitron, C., et al. (2012). Linking photoreceptor excitation to changes in plant architecture. *Genes Dev.* 26 (8), 785–790. doi: 10.1101/gad.187849.112

Linting, M., Van Os, B. J., and Meulman, J. J. (2011). Statistical significance of the contribution of variables to the PCA solution: an alternative permutation strategy. *Psychometrika* 76, 440–460. doi: 10.1007/s11336-011-9216-6

Liu, W.-g., REN, M.-l., Ting, L., DU, Y.-l., Tao, Z., LIU, X.-m., et al. (2018). Effect of shade stress on lignin biosynthesis in soybean stems. *J. Integr. Agric.* 17 (7), 1594–1604. doi: 10.1016/S2095-3119(17)61807-0

Lorenzo, C. D., Alonso Iserte, J., Sanchez Lamas, M., Antonietti, M. S., Garcia Gagliardi, P., Hernando, C. E., et al. (2019). Shade delays flowering in Medicago sativa. *Plant J.* 99 (1), 7–22. doi: 10.1111/tpj.14333

Maqbool, M. A., Aslam, M., Ali, H., and Varshney, R. (2017). Breeding for improved drought tolerance in Chickpea (*Cicer arietinum* L.). *Plant Breed.* 136 (3), 300–318. doi: 10.1111/pbr.12477

Mašková, T., and Herben, T. (2018). Root: shoot ratio in developing seedlings: How seedlings change their allocation in response to seed mass and ambient nutrient supply. *Ecol. Evol.* 8 (14), 7143–7150. doi: 10.1002/ece3.4238

Mir, R. R., Zaman-Allah, M., Sreenivasulu, N., Trethowan, R., and Varshney, R. K. (2012). Integrated genomics, physiology and breeding approaches for improving drought tolerance in crops. *Theor. Appl. Genet.* 125 (4), 625–645. doi: 10.1007/s00122-012-1904-9

Naveed, M. (2022). *Improving chickpea against moisture and low light stresses: breeding, genetics, and physiological interventions* (Australia: The University of Sydney).

Naveed, M., Ahsan, M., Akram, H. M., Aslam, M., and Ahmed, N. (2016). Genetic effects conferring heat tolerance in a cross of tolerant× susceptible maize (Zea mays L.) genotypes. *Front. Plant Sci.* 7, 729. doi: 10.3389/fpls.2016.00729

Naveed, M., Shafiq, M., Chaudhry, M. R., and Zahid, M. A. (2015). Genetic diversity in new chickpea accessions for'fusarium'wilt resistance, canopy temperature and yield components under drought milieus. *Aust. J. Crop Sci.* 9 (6), 538.

Naveed, M., Shafiq, M., Nadeem, M., Haq, A.u., and Zahid, M. A. (2020). " Noor-2013" a bold seeded and high yielding chickpea kabuli variety developed indigenously. *J. Anim. Plant Sci.* 30 (4), 885–894.

Nayak, S. N., Zhu, H., Varghese, N., Datta, S., Choi, H.-K., Horres, R., et al. (2010). Integration of novel SSR and gene-based SNP marker loci in the chickpea genetic map and establishment of new anchor points with Medicago truncatula genome. *Theor. Appl. Genet.* 120 (7), 1415–1441. doi: 10.1007/s00122-010-1265-1

Nico, M., Miralles, D. J., and Kantolic, A. G. (2015). Post-flowering photoperiod and radiation interaction in soybean yield determination: Direct and indirect photoperiodic effects. *Field Crops Res*. 146, 45–55.

Nyquist, W. E., and Baker, R. (1991). Estimation of heritability and prediction of selection response in plant populations. *Crit. Rev. Plant Sci.* 10 (3), 235–322. doi: 10.1080/07352689109382313

Okoli, P. S., and Wilson, G. (1986). Response of cassava (*Manihot esculenta* Crantz) to shade under field conditions. *Field Crops Res.* 14, 349–359. doi: 10.1016/0378-4290(86)90069-9

Park, Y., and Runkle, E. S. (2017). Far-red radiation promotes growth of seedlings by increasing leaf expansion and whole-plant net assimilation. *Environ. Exp. Bot.* 136, 41–49. doi: 10.1016/j.envexpbot.2016.12.013

Paul, P. J., Samineni, S., Thudi, M., Sajja, S. B., Rathore, A., Das, R. R., et al. (2018). Molecular mapping of QTLs for heat tolerance in chickpea. *Int. J. Mol. Sci.* 19 (8), 1–20. doi: 10.3390/ijms19082166

Pausch, R., Britz, S., and Mulchi, C. (1991). Growth and photosynthesis of soybean (*Glycine max* (L.) Merr.) in simulated vegetation shade: influence of the ratio of red to far-red radiation. *Plant Cell Environ.* 14 (7), 647–656. doi: 10.1111/j.1365-3040.1991.tb01537.x

Payne, R., Murray, D., Harding, S., Baird, D., and Soutar, D. (2011). An introduction to genStat for windows. *VSN International: Hemel Hempstead UK.*, 1–41

Pettai, H., Oja, V., Freiberg, A., and Laisk, A. (2005). The long-wavelength limit of plant photosynthesis. *FEBS Lett.* 579 (18), 4017–4019. doi: 10.1016/j.febslet.2005.04.088

Pierik, R., and Testerink, C. (2014). The art of being flexible: how to escape from shade, salt, and drought. *Plant Physiol.* 166 (1), 5–22. doi: 10.1104/pp.114.239160

Polania, J., Rao, I. M., Cajiao, C., Grajales, M., Rivera, M., Velasquez, F., et al. (2017). Shoot and root traits contribute to drought resistance in recombinant inbred lines of MD 23–24× SEA 5 of common bean. *Front. Plant Sci.* 8, 296. doi: 10.3389/fpls.2017.00296

Poorter, H., and Nagel, O. (2000). The role of biomass allocation in the growth response of plants to different levels of light, CO2, nutrients and water: a quantitative review. *Funct. Plant Biol.* 27 (12), 1191–1191. doi: 10.1071/PP99173_CO

Poudel, P. R., Kataoka, I., and Mochioka, R. (2008). Effect of red-and blue-light-emitting diodes on growth and morphogenesis of grapes. *Plant Cell Tiss. Org. Cult.* 92 (2), 147–153. doi: 10.1007/s11240-007-9317-1

Pushpavalli, R., Krishnamurthy, L., Thudi, M., Gaur, P. M., Rao, M. V., Siddique, K. H., et al. (2015). Two key genomic regions harbour QTLs for salinity tolerance in ICCV 2× JG 11 derived chickpea (*Cicer arietinum* L.) recombinant inbred lines. *BMC Plant Biol.* 15 (1), 1–15. Available at: https://bmcplantbiol.biomedcentral.com/articles/10.1186/s12870-015-0491-8.

Qin, F., Shen, Y., Li, Z., Qu, H., Feng, J., Kong, L., et al. (2022). Shade delayed flowering phenology and decreased reproductive growth of medicago sativa L. *Front. Plant Sci.* 13, 835380. doi: 10.3389/fpls.2022.835380

Raai, M. N., Zain, N. A. M., Osman, N., Rejab, N. A., Sahruzaini, N. A., and Cheng, A. (2020). Effects of shading on the growth, development and yield of winged bean (*Psophocarpus tetragonolobus*). *Ciec. Rural* 50 (2), 1–7. doi: 10.1590/0103-8478cr20190570

Rai, M., Dutta, S. S., and Tyagi, W. (2021). Molecular breeding strategies for enhancing rice yields under low light intensity. *Mol. Breed. Rice Abiotic Stress Tolerance Nutr. Qual.*, 201–214. doi: 10.1002/9781119633174.ch10

Ramamoorthy, P., Lakshmanan, K., Upadhyaya, H. D., Vadez, V., and Varshney, R. K. (2016). Shoot traits and their relevance in terminal drought tolerance of chickpea (*Cicer arietinum* L.). *Field Crops Res.* 197, 10–27. doi: 10.1016/j.fcr.2016.07.016

Ramamoorthy, P., Lakshmanan, K., Upadhyaya, H. D., Vadez, V., and Varshney, R. K. (2017). Root traits confer grain yield advantages under terminal drought in chickpea (*Cicer arietinum* L.). *Field Crops Res.* 201, 146–161. doi: 10.1016/j.fcr.2016.11.004

Rana, M., Sood, A., Hussain, W., Kaldate, R., Sharma, T. R., Gill, R., et al. (2019). "Gene pyramiding and multiple character breeding," in *Lentils* (London EC2Y 5AS, United Kingdom: Elsevier), 83–124.

Rani, R., Raza, G., Ashfaq, H., Rizwan, M., Shimelis, H., Tung, M. H., et al. (2023). Analysis of genotype× environment interactions for agronomic traits of soybean (*Glycine max* [L.] Merr.) using association mapping. *Front. Genet.* 13, 1090994. doi: 10.3389/fgene.2022.1090994

Růžička, K., Ljung, K., Vanneste, S., Podhorská, R., Beeckman, T., Friml, J.i., et al. (2007). Ethylene regulates root growth through effects on auxin biosynthesis and transport-dependent auxin distribution. *Plant Cell* 19 (7), 2197–2212. doi: 10.1105/tpc.107.052126

Sadras, V. O., Lake, L., Li, Y., Farquharson, E. A., and Sutton, T. (2016). Phenotypic plasticity and its genetic regulation for yield, nitrogen fixation and δ13C in chickpea crops under varying water regimes. *J. Exp. Bot.* 67 (14), 4339–4351. doi: 10.1093/jxb/erw221

Samineni, S., Sen, M., Sajja, S. B., and Gaur, P. M. (2020). Rapid generation advance (RGA) in chickpea to produce up to seven generations per year and enable speed breeding. *Crop J.* 8 (1), 164–169. doi: 10.1016/j.cj.2019.08.003

Sandhu, S., and Hodges, H. (1971). Effects of photoperiod, light intensity, and temperature on vegetative growth, flowering, and seed production in *cicer arietinum* L. 1. *Agron. J.* 63 (6), 913–914. doi: 10.2134/agronj1971.00021962006300060028x

Schneider, C. A., Rasband, W. S., and Eliceiri, K. W. (2012). NIH Image to ImageJ: 25 years of image analysis. *Nat. Methods* 9 (7), 671–675. doi: 10.1038/nmeth.2089

Scott, M. F., Ladejobi, O., Amer, S., Bentley, A. R., Biernaskie, J., Boden, S. A., et al. (2020). Multi-parent populations in crops: A toolbox integrating genomics and genetic mapping with breeding. *Heredity* 125 (6), 396–416. doi: 10.1038/s41437-020-0336-6

Sehrawat, S., Dahiya, D., Singh, S., Rana, G., Sunitha, H., Hunje, R., et al. (2012). Selection criteria for yield improvement in chickpea (*Cicer arietinum* L) breeding. *J. Agric. Sci. Technol.* 37 (3), 379.

Sessa, G., Carabelli, M., Possenti, M., Morelli, G., and Ruberti, I. (2018). Multiple pathways in the control of the shade avoidance response. *Plants* 7 (4), 102. doi: 10.3390/plants7040102

Shafiq, I., Hussain, S., Raza, M. A., Iqbal, N., ASGHAR, M. A., Ali, R., et al. (2021). Crop photosynthetic response to light quality and light intensity. *J. Integr. Agric.* 20 (1), 4–23. doi: 10.1016/S2095-3119(20)63227-0

Shah, T. M., Imran, M., Atta, B. M., Ashraf, M. Y., Hameed, A., Waqar, I., et al. (2020). Selection and screening of drought tolerant high yielding chickpea genotypes based on physio-biochemical indices and multi-environmental yield trials. *BMC Plant Biol.* 20, 1–16. doi: 10.1186/s12870-020-02381-9

Sharma, A., Yadav, R., Sheoran, R., Kaushik, D., Mohanta, T. K., Sharma, K., et al. (2023). Estimation of heterosis and the combining ability effect for yield and its attributes in field pea (*Pisum sativum* L.) using PCA and GGE biplots. *Horticulturae* 9 (2), 256. doi: 10.3390/horticulturae9020256

Shaukat, S. S., Rao, T. A., and Khan, M. A. (2016). Impact of sample size on principal component analysis ordination of an environmental data set: effects on eigenstructure. *Ekológia (bratislava)* 35 (2), 173–190. doi: 10.1515/eko-2016-0014

Shrestha, A., Buckley, T. N., Lockhart, E. L., and Barbour, M. M. (2019). The response of mesophyll conductance to short-and long-term environmental conditions in chickpea genotypes. *AoB Plants* 11 (1), ply073. doi: 10.1093/aobpla/ply073

Sivakumar, J., Prashanth, J. E. P., Rajesh, N., Reddy, S. M., and Pinjari, O. B. (2020). Principal component analysis approach for comprehensive screening of salt stress-tolerant tomato germplasm at the seedling stage. *J. Biosci. (Bangalore)* 45, 1–11. doi: 10.1007/s12038-020-00111-9

Sofroniou, N., and Hutcheson, G. D. (1999). The multivariate social scientist: Introductory statistics using generalized linear models. *Multivariate Soc. Scientist*, 1–288.

Soltani, A., Robertson, M., Torabi, B., Yousefi-Daz, M., and Sarparast, R. (2006). Modelling seedling emergence in chickpea as influenced by temperature and sowing depth. *Agric. For. Meteorol.* 138 (1-4), 156–167. doi: 10.1016/j.agrformet.2006.04.004

Soltani, A., Torabi, B., Zeinali, E., and Sarparast, R. (2004). Response of chickpea to photoperiod as a qualitative long-day plant. *Asian J. Plant Sci.* 3 (6), 705–708. doi: 10.3923/ajps.2004.705.708

Sparkes, D., Berry, P., and King, M. (2008). Effects of shade on root characters associated with lodging in wheat (*Triticum aestivum*). *Ann. Appl. Biol.* 152 (3), 389–395. doi: 10.1111/j.1744-7348.2008.00230.x

Storm, C. (2012). *Permutation procedures for ANOVA, regression and PCA* (Hatfield, Pretoria, 0002, South Africa: University of Pretoria).

Su, B., Song, Y., Song, C., Cui, L., Yong, T., and Yang, W. (2014). Growth and photosynthetic responses of soybean seedlings to maize shading in relay intercropping system in Southwest China. *Photosynthetica* 52 (3), 332–340. doi: 10.1007/s11099-014-0036-7

Sulistyowati, D., Chozin, M., Syukur, M., Melati, M., and Guntoro, D. (2016). Selection of shade-tolerant tomato genotypes. *J. Appl. Hortic.* 18 (2), 154–159. doi: 10.37855/jah.2016.v18i02.27

Sun, J.-l., SUI, X.-l., HUANG, H.-y., WANG, S.-h., WEI, Y.-x., and ZHANG, Z.-x. (2014). Low light stress down-regulated Rubisco gene expression and photosynthetic capacity during cucumber (*Cucumis sativus* L.) leaf development. *J. Integr. Agric.* 13 (5), 997–1007. doi: 10.1016/S2095-3119(13)60670-X

Swarup, S., Cargill, E. J., Crosby, K., Flagel, L., Kniskern, J., and Glenn, K. C. (2021). Genetic diversity is indispensable for plant breeding to improve crops. *Crop Sci.* 61 (2), 839–852. doi: 10.1002/csc2.20377

Tardieu, F., and Tuberosa, R. (2010). Dissection and modelling of abiotic stress tolerance in plants. *Curr. Opin. Plant Biol.* 13 (2), 206–212. doi: 10.1016/j.pbi.2009.12.012

Tewfik, L. (2003). *Effect of shade on seed germination, growth and xylem development of moringa oleifera seedlings* (University of Khartoum, Al-Gammaa Avenue, Khartoum 11111, Sudan: UOFK).

Ueoka-Nakanishi, H., Hori, N., Ishida, K., Ono, N., Yamashino, T., Nakamichi, N., et al. (2011). Characterization of shade avoidance responses in Lotus japonicus. *Biosci. Biotechnol. Biochem.* 75 (11), 2148–2154. doi: 10.1271/bbb.110442

Vance, W., Pradeep, K., Strachan, S. R., Diffey, S., and Bell, R. W. (2021). Novel sources of tolerance to aluminium toxicity in wild cicer (*Cicer reticulatum* and *Cicer echinospermum*) collections. *Front. Plant Sci.* 12, 678211. doi: 10.3389/fpls.2021.678211

Verghis, T. I., McKenzie, B. A., and Hill, G. D. (1999). Phenological development of chickpeas(*Cicer arietinum*) in Canterbury, New Zealand. *N. Z. J. Crop Hortic. Sci.* 27 (3), 249–256. doi: 10.1080/01140671.1999.9514103

Vignoli, L. (1936). Utilization des reserves pendant la germination de Cicer arietinum a la lumiere et a l obscurite. *Bull. Soc Bot. Fr.* 83, 853.

Walia, M. K., Mohammed, Y. A., Franck, W. L., and Chen, C. (2020). Evaluation of early seedling development of Chickpea and its relation to seed yield. *Agrosyst. Geosci. Environ.* 3 (1), e20005. doi: 10.1002/agg2.20005

Wang, X., Gao, X., Liu, Y., Fan, S., and Ma, Q. (2020). Progress of research on the regulatory pathway of the plant shade-avoidance syndrome. *Front. Plant Sci.* 11, 439. doi: 10.3389/fpls.2020.00439

Woźny, A., and Jerzy, M. (2007). Effect of light wavelength on growth and flowering of narcissi forced under short-day and low quantum irradiance conditions. *J. Hortic. Sci. Biotechnol.* 82 (6), 924–928. doi: 10.1080/14620316.2007.11512327

Wu, Y., Gong, W., and Yang, W. (2017b). Shade inhibits leaf size by controlling cell proliferation and enlargement in soybean. *Sci. Rep.* 7 (1), 1–10. doi: 10.1038/s41598-017-10026-5

Wu, L., Zhang, W., Ding, Y., Zhang, J., Cambula, E. D., Weng, F., et al. (2017a). Shading contributes to the reduction of stem mechanical strength by decreasing cell wall synthesis in japonica rice (*Oryza sativa* L.). *Front. Plant Sci.* 8, 881. doi: 10.3389/fpls.2017.00881

Yang, F., Fan, Y., Wu, X., Cheng, Y., Liu, Q., Feng, L., et al. (2018). Auxin-to-gibberellin ratio as a signal for light intensity and quality in regulating soybean growth and matter partitioning. *Front. Plant Sci.* 9, 56. doi: 10.3389/fpls.2018.00056

Yang, C., and Li, L. (2017). Hormonal regulation in shade avoidance. *Front. Plant Sci.* 8, 1527. doi: 10.3389/fpls.2017.01527

Yao, X., Li, C., Li, S., Zhu, Q., Zhang, H., Wang, H., et al. (2017). Effect of shade on leaf photosynthetic capacity, light-intercepting, electron transfer and energy distribution of soybeans. *Plant Growth Regul.* 83 (3), 409–416. doi: 10.1007/s10725-017-0307-y

Yu, W., Liu, Y., Song, L., Jacobs, D. F., Du, X., Ying, Y., et al. (2017). Effect of differential light quality on morphology, photosynthesis, and antioxidant enzyme activity in Camptotheca acuminata seedlings. *J. Plant Growth Regul.* 36 (1), 148–160. doi: 10.1007/s00344-016-9625-y

Zhang, J., Smith, D. L., Liu, W., Chen, X., and Yang, W. (2011). Effects of shade and drought stress on soybean hormones and yield of main-stem and branch. *Afr. J. Biotechnol.* 10 (65), 14392–14398. doi: 10.5897/AJB11.2143

frontiers | Frontiers in Plant Science

TYPE Original Research
PUBLISHED 10 April 2024
DOI 10.3389/fpls.2024.1371435

OPEN ACCESS

EDITED BY
Xiuming Hao,
Agriculture and Agri-Food Canada (AAFC), Canada

REVIEWED BY
Liangyu Liu,
Capital Normal University, China
Sofia D. Carvalho,
Independent Researcher, Laramie, United States
Yuhai Cui,
Agriculture and Agri-Food Canada (AAFC), Canada

*CORRESPONDENCE
Tingquan Wu
tingquanwu@sina.com
Changyuan Zhang
zcy79130@163.com

RECEIVED 16 January 2024
ACCEPTED 25 March 2024
PUBLISHED 10 April 2024

CITATION
Cao H, Wang R, Zhao J, Shi L, Huang Y, Wu T and Zhang C (2024) Genome-wide identification and expression analysis of the cryptochromes reveal the *CsCRY1* role under low-light-stress in cucumber.
Front. Plant Sci. 15:1371435.
doi: 10.3389/fpls.2024.1371435

Genome-wide identification and expression analysis of the cryptochromes reveal the *CsCRY1* role under low-light-stress in cucumber

Haishun Cao[1], Rui Wang[1], Junhong Zhao[1], Liangliang Shi[1], Yuan Huang[2], Tingquan Wu[1]* and Changyuan Zhang[1]*

[1]Institute of Facility Agriculture, Guangdong Academy of Agricultural Sciences, Guangzhou, China, [2]National Key Laboratory for Germplasm Innovation & Utilization of Horticultural Crops, College of Horticulture and Forestry Sciences, Huazhong Agricultural University, Wuhan, China

Introduction: Low-light-stress is a common meteorological disaster that can result in slender seedlings. The photoreceptors play a crucial role in perceiving and regulating plants' tolerance to low-light-stress. However, the low-light-stress tolerance of cucumber has not been effectively evaluated, and the functions of these photoreceptor genes in cucumber, particularly under low-light-stress conditions, are not clear.

Methods: Herein, we evaluated the growth characteristics of cucumber seedlings under various LED light treatment. The low-light-stress tolerant cucumber CR and intolerant cucumber CR were used as plant materials for gene expression analysis, and then the function of *CsCRY1* was analyzed.

Results: The results revealed that light treatment below 40 μmol m^{-2} s^{-1} can quickly and effectively induce low-light-stress response. Then, cucumber CR exhibited remarkable tolerance to low-light-stress was screened. Moreover, a total of 11 photoreceptor genes were identified and evaluated. Among them, the cryptochrome 1 (*CRY1*) had the highest expression level and was only induced in the low-light sensitive cucumber CS. The transcript *CsaV3_3G047490.1* is predicted to encode a previously unknown CsCRY1 protein, which lacks 70 amino acids at its C-terminus due to alternative 5′ splice sites within the final intron of the *CsCRY1* gene.

Discussion: CRY1 is a crucial photoreceptor that plays pivotal roles in regulating plants' tolerance to low-light stress. In this study, we discovered that alternative splicing of *CsCRY1* generates multiple transcripts encoding distinct CsCRY1 protein variants, providing valuable insights for future exploration and utilization of CsCRY1 in cucumber.

KEYWORDS

cryptochromes, cucumber, low-light-stress, photoreceptors, alternative splicing

1 Introduction

Light is one of the most critical environmental factors for living organisms on Earth. Plants can convert light energy into carbohydrates through photosynthesis, as it provides a source of energy for humans (Xu et al., 2015). However, global warming has resulted in an increasing frequency of extreme weather events, particularly for continuously cloudy weather or rainfall (Zhu, 2016). Consequently, low-light-stress has emerged as one of the most significant meteorological disasters worldwide, ultimately impacting photosynthesis, growth, accelerating reproductive development, and leading to lower plant biomass and decreased crop yield and quality (Liu et al., 2014; Sekhar et al., 2019; Casal and Fankhauser, 2023; Li et al., 2023). Over the past few decades, scientists have gradually unraveled crucial molecular mechanisms and signaling pathways by conducting research on photoreceptor genes in Arabidopsis. Nevertheless, there has been limited progress in understanding the mechanism of light signal transduction in cucurbits, particularly cucumbers.

Plants are sessile, so they must constantly adapt to the ever-changing light environment. To achieve this, they employ multiple photoreceptors to respond to wavelengths of light with different intensities ranging from ultraviolet to the far-red regions (Galvão and Fankhauser, 2015). The primary source of low-light-stress is the reduction in sunlight intensity due to continuous cloudy weather, rainfall (Ma et al., 2021), or crowded plant canopies (Casal, 2013). Photoreceptors have the ability to perceive various low-light-stress conditions. In plants, there are four primary types of photoreceptors, including the UVB receptor (280–315 nm UV light), PHYs (600–750 nm red and far-red light), CRYs (350–500 nm blue light), and phototropins (320–500 nm blue light) (De Wit et al., 2016). Among them, PhyB is a critical photoreceptor that can perceive low R: FR of shade light (Casal and Fankhauser, 2023). CRY1 and CRY2 are mainly responsible for sensing the changes in blue light intensity (de Wit et al., 2016; Pedmale et al., 2016). These photoreceptors can regulate gene expression by modulating the activity of transcription factors under low-light-stress, thereby promoting the extension of hypocotyls, stems, and petioles. These responses are collectively referred to as the shade avoidance response (SAR) (Casal, 2013; Pedmale et al., 2016). Currently, the majority of knowledge regarding the activity of photoreceptors was derived from shade-intolerant plants, while their specific roles in low-light-stress tolerant crops remain unexplored.

The cucumber (*Cucumis sativus L.*) is an economically important crop. Low-light-stress will lead to the formation of weak cucumber seedlings with small leaves, long stems, and fewer female flowers (Zhou et al., 2022; Cao et al., 2023; Li et al., 2023). LED supplementary lighting technology has been widely applied to enhance crop growth under low-light-stress, particularly for horticulture crops (Ma et al., 2021; Grishchenko et al., 2022). By utilizing LED supplementary lighting, we can also significantly enhance seedling growth and boost the fruit yield of cucumbers (Song et al., 2019; Gajc-wolska et al., 2021). However, there is limited knowledge about strategies for cucumber response to low-light-stress. In soybean, the cultivars that are sensitive to low-light-stress respond to the decrease in light intensity by significantly increasing the length of their cells. Conversely, in tolerant cultivars, the rate of cell elongation is reduced, yet their photosynthetic efficiency and yield are higher (Lorenzo et al., 2019). Furthermore, it has also been observed that enhancement of *CRY1*-signaling activity can significantly improve yield potential of soybean under low-light-stress conditions (Lyu et al., 2021). The research conducted above has demonstrated that genes in the photoreceptor-signaling pathway play crucial roles in regulating plants' tolerance to low-light-stress. Nevertheless, the low-light tolerance of cucumber has not been effectively evaluated, and the functions of these photoreceptor genes in cucumber, particularly under low-light-stress conditions, are not clear. In our research, we have established a rapid and efficient evaluation system for assessing cucumber tolerance to low-light-stress and obtained one cucumber material with significantly better tolerance. Additionally, the photoreceptor genes of cucumber were also identified, and a comprehensive analysis was conducted on the role of *CsCRY1* under low-light-stress.

2 Materials and methods

2.1 Plant materials and LED light treatments

The cucumber (*Cucumis sativus*) CS and CR were used as materials in this study, which were preserved at Institute of Facility Agriculture, Guangdong Academy of Agricultural Sciences. CS (EA background) was identified from North South China ecotype cucumber varieties, which is commonly used in modern cucumber breeding with high-quality genome and very rich omics data (Huang et al., 2009; Li et al., 2019). CR (EA background) was identified from the South China ecotype cucumber varieties. Plants were grown in plug trays in a plant incubator that maintained a temperature of (25 ± 1) °C and a 14-hour light/10-hour dark cycle. The relative humidity was 60%-80%. To determine the optimal low-light-stress condition, six distinct white LED light intensity treatments (0, 10, 40, 80, 120, 160 μmol m^{-2} s^{-1}) were applied to the CS and CR plants, respectively. The effect of light quality on the growth of cucumber seedlings (CS) was evaluated by four different wavelengths LED light treatment, including 40 μmol m^{-2} s^{-1} white light LED (WL40), 160 μmol m^{-2} s^{-1} white light LED (WL160), 160 μmol m^{-2} s^{-1} LED light composed of blue light (16 μmol m^{-2} s^{-1}) and red light (144 μmol m^{-2} s^{-1}) (RB91), 160 μmol m^{-2} s^{-1} LED light composed of blue light (144 μmol m^{-2} s^{-1}) and red light (16 μmol m^{-2} s^{-1}) (RB19) (Figure 1A). After two weeks, the growth characteristics of cucumber seedlings were measured.

2.2 Identification and characterization of the photoreceptor genes in cucumber

To identify the photoreceptor genes (PHYs, CRYs, UVRs, PHOTs) involved in low-light-stress, the protein sequences of *Arabidopsis thaliana* were retrieved from the The Arabidopsis Information

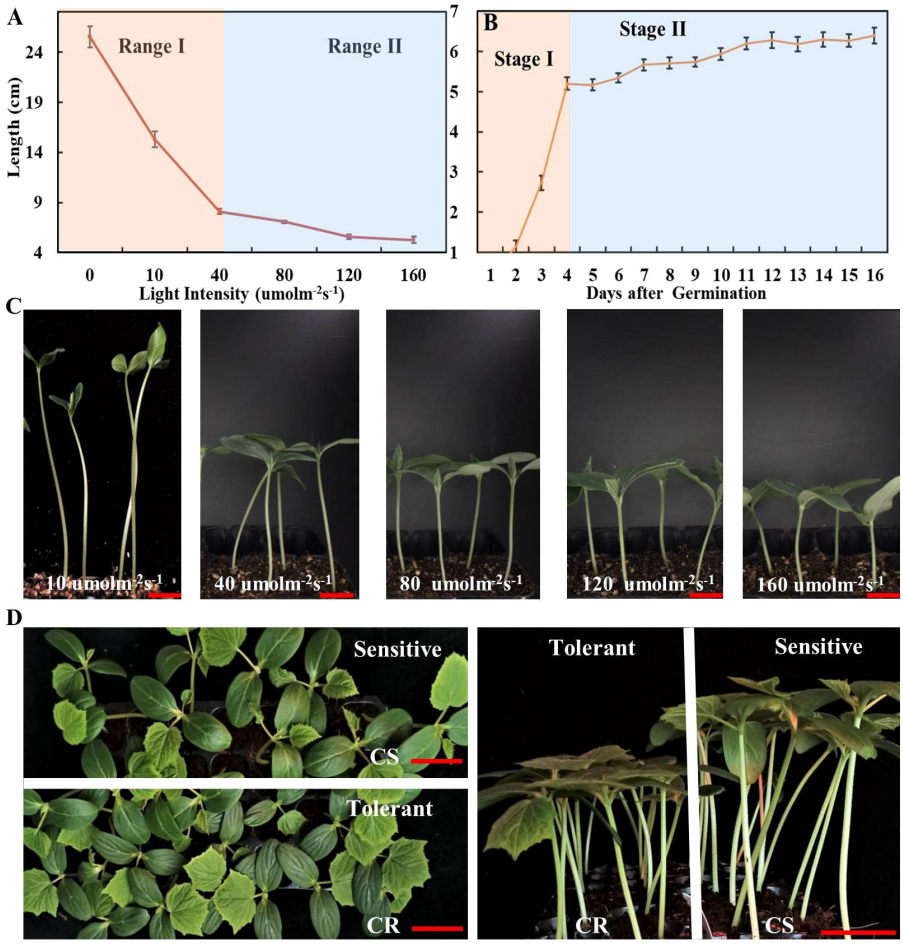

FIGURE 1
The effect of different light intensities on elongation of cucumber hypocotyl. **(A)** The cucumber hypocotyl length of cucumber seedlings (CS) growth under different light intensities of 10, 40, 80, 120, 160 μmol m^{-2} s^{-1} for one week. **(B)** The length of cucumber hypocotyls (CS) from 0 to 16d under white LED light (160 μmol m^{-2} s^{-1}). **(C)** The phenotype of cucumber seedlings (CS) growth under 10, 40, 80, 120, 160 μmol m^{-2} s^{-1} for one week. **(D)** The phenotype of low-light-stress tolerant (CR) and sensitive cucumber (CS) lines under low-light-stress (40 μmol m^{-2} s^{-1}) treatment at seedling stage for two weeks. The red scale bar represents a length of 2cm.

Resource (TAIR) database (https://www.arabidopsis.org/), and these sequences were used as queries to identify the photoreceptors in cucumber by conducting BLASTP searches in the CuGenDBv2 database (http://cucurbitgenomics.org/v2/) (Yu et al., 2023). Then, the Pfam (https://www.ebi.ac.uk/Tools/hmmer/search/phmmer) and MEME suite (http://meme-suite.org/) were utilized to analyze and validate the conserved motifs of these photoreceptor proteins.

2.3 Phylogenetic tree, conserved motifs and gene structure analysis of the CRYs

The CRY protein sequences of *Cucumis sativus*, *Citrullus lanatus*, *Cucumis melo*, *Cucurbita moschata*, *Momordica charantia*, *Lagenaria siceraria*, *Benincasa hispida*, *Sechium edule*, *Luffa cylindrical*, *Trichosanthes anguina*, and *Cucurbita pepo* were obtained from CuGenDB (http://cucurbitgenomics.org/v2/), and those of *Solanum lycopersicum* were from the Sol Genomics Network (https://solgenomics.net/), and those of *Arabidopsis thaliana* were from TAIR (https://www.arabidopsis.org/). The phylogenetic tree was constructed using MEGA 7 software (Institute of Molecular Evolutionary Genetics, USA). The gene structure of *CsCRY1* was predicted using GSDS 2.0 (http://gsds.gao-lab.org/). The protein length, molecular weight (Mw), and theoretical isoelectric point (pI) of CRY1 were analyzed by the ExPASy ProtParam (https://web.expasy.org/protparam/). The subcellular location of CRY1 was predicted by INSP (http://www.csbio.sjtu.edu.cn/bioinf/INSP/).

2.4 Gene expression analysis of *CsCRY1* and the photoreceptor genes from cucurbits

To analyze the gene expression of these photoreceptor genes, we retained the expression data from the Cucurbit Expression Atlas (http://cucurbitgenomics.org/v2/). Among them, tissue expression data of cucumber photoreceptor genes was obtained from the transcriptome atlas of cucumber (PRJNA312872), and tissue

expression data of melon was obtained from gene expression atlas of melon (PRJDB6414) (Yano et al., 2018). Tissue expression data of watermelons was obtained from transcriptome profiling of watermelon fruit development (PRJNA543725) (Guo et al., 2019). Then, the heatmaps were constructed using TBtools (Chen et al., 2020).

2.5 Alternative splicing (AS) analysis of *CsCRY1* gene from cucumber

Total RNA was extracted from different cucumber tissue of CS (Rt: root, Sm: stem, Tl: tendril, Ap: apical point, Yl: young leaves, Ml: young leaves, Ol: young leaves, Pe: petal, St: stigma, Pi: pistil, Ov: ovary), using an OminiPlant RNA Kit (DNAaseI) from CWBIO (www.cwbio.com). The PrimeScriptTM RT reagent kit (TakaRa, Dalian, China) was using to produce reverse transcribed cDNA. The TSINGKE TSE030 T3 Super PCR Mix was used for RT-PCR assays. We selected *CsACTIN* as the reference gene. All the primer pairs in this study were listed in Supplementary Table 1. Three biological replicates were performed. To analyze the expression of *CsCRY1* gene under low-light-stress, RNA-seq of cucumber was conducted using Illumina Novaseq6000 by Gene Denovo Biotechnology Co. (Guangzhou, China). The hypocotyls of CS and CR cucumber were sampled for RNA-seq and RT-PCR after 40 μmol m^{-2} s^{-1} low-light-stress (LL) and 160 μmol m^{-2} s^{-1} normal light (CK) treatments 72h. The software rMATS (version 4.0.1) (http://rnaseq-mats.sourceforge.net/index.html) was used to identify significant AS events with a false discovery rate (FDR) <0.05 (Shen et al., 2014). The *CsCRY1* transcripts structure information was analyzed using IGV-GSAman software (https://gitee.com/CJchen/IGV-sRNA).

2.6 Subcellular localization analysis of CsCRY1.1

The full-length CDS of *CsCRY1.1* from CS was amplified by PCR using 2 × High-Fidelity Master Mix (Tsingke, Inc., Beijing, China), and the PCR fagments were inserted in the *KpnI* and *XbaI* site of the pCambia1301-35s-EGFP vector by using ClonExperess II one Step cloning Kits (Vazyme, Piscataway, NJ, United States). The 35S::*CsCRY1.1*-GFP fusion protein was subsequently generated, controlled by the Cauliflower mosaic virus (CaMV) 35S promoter. The vector and the empty vector were each transformed into Agrobacterium strain GV3101. Subsequently, the positive strains were infiltrated into the leaves of tobacco (Nicotiana benthamiana) using the Agrobacterium-mediated transformation method (Sheludko et al., 2007). Finally, laser scanning confocal microscope (CarlZeiss LSM710) was used to take the GFP fluorescence signal pictures.

2.7 Statistical analysis

Statistical analysis of the experimental data was performed using SAS statistical package. Results were expressed as means ± standard deviation (SD). Differences in data from treatments were analyzed by one-way ANOVA and the analysis results were corrected with Turkey's multiple comparison tests at a significance level of $P<0.05$.

3 Results

3.1 Low-light-stress can induce rapid elongation of cucumber hypocotyls at the early seedling stage of cucumber

The low-light-stress has a significantly negative impact on the quality of seedlings. However, there is a lack of optimal parameters for evaluating low-light-stress, thus resulting in limited understanding of the mechanism underlying low stress tolerance in cucumber. Therefore, we evaluated the growth characteristics of cucumber (CS) under various light intensities, including 0, 10, 40, 80, 120, and 160 μmol m^{-2} s^{-1}, respectively. The hypocotyls elongation was observed to be rapidly promoted, while the leaf size was significantly inhibited by light treatments below 40 μmol m^{-2} s^{-1} (Figures 1A, C; Supplementary Figure 1). Furthermore, the elongation of cucumber hypocotyl (CS) was evaluated at the whole seedling stage under 160 μmol m^{-2} s^{-1}. The results indicated that the elongation process of cucumber hypocotyl can be categorized into two distinct stages: stage I (0-4 days) characterized by rapid elongation of hypocotyl, and stage II characterized by slower elongation of hypocotyl (5-16 days) (Figure 1B). Additionally, we also compared the growth of two cultivars (CS and CR) under different light intensities. Firstly, we found that elongation of both material hypocotyls gradually stop after stage I. Secondly, there was a significant difference in the hypocotyls length of CS and CR under 40 μmol m^{-2} s^{-1}, while the difference gradually became smaller in other light intensities treatments (Figure 1D; Supplementary Figure 1). Therefore, we selected 40μmol m^{-2} s^{-1} white LED light treatment for 7 days as the optimal parameters for evaluating low-light-stress. This approach allowed us to quickly and efficiently identify a low-light tolerant cucumber line (CR) and a low-light-sensitive cucumber line (CS) (Figure 1D). Notably, CR had a significantly shorter hypocotyl, better photosynthesis capacity, and superior resistance to lodging under low-light-stress compared with CS (Figure 1D; Supplementary Figure 2).

3.2 The decrease in blue light intensity is the primary reason of low-light-stress in cucumber

To assess the effect of different light qualities under low-light-stress, we cultivated cucumber seedlings for two weeks under four LED conditions with different intensity of blue and red light: WL40 (40 μmol m^{-2} s^{-1} total light intensity, containing 10 μmol m^{-2} s^{-1} blue light intensity), WL160 (160 μmol m^{-2} s^{-1} total light intensity, containing 40 μmol m^{-2} s^{-1} blue light intensity), RB91 (160 μmol m^{-2} s^{-1} total light intensity, containing 16 μmol m^{-2} s^{-1} blue light intensity) and RB19 (160 μmol m^{-2} s^{-1} total light intensity, containing 144 μmol m^{-2} s^{-1} blue light intensity) (Figure 2A). The results

10.3389/fpls.2024.1371435

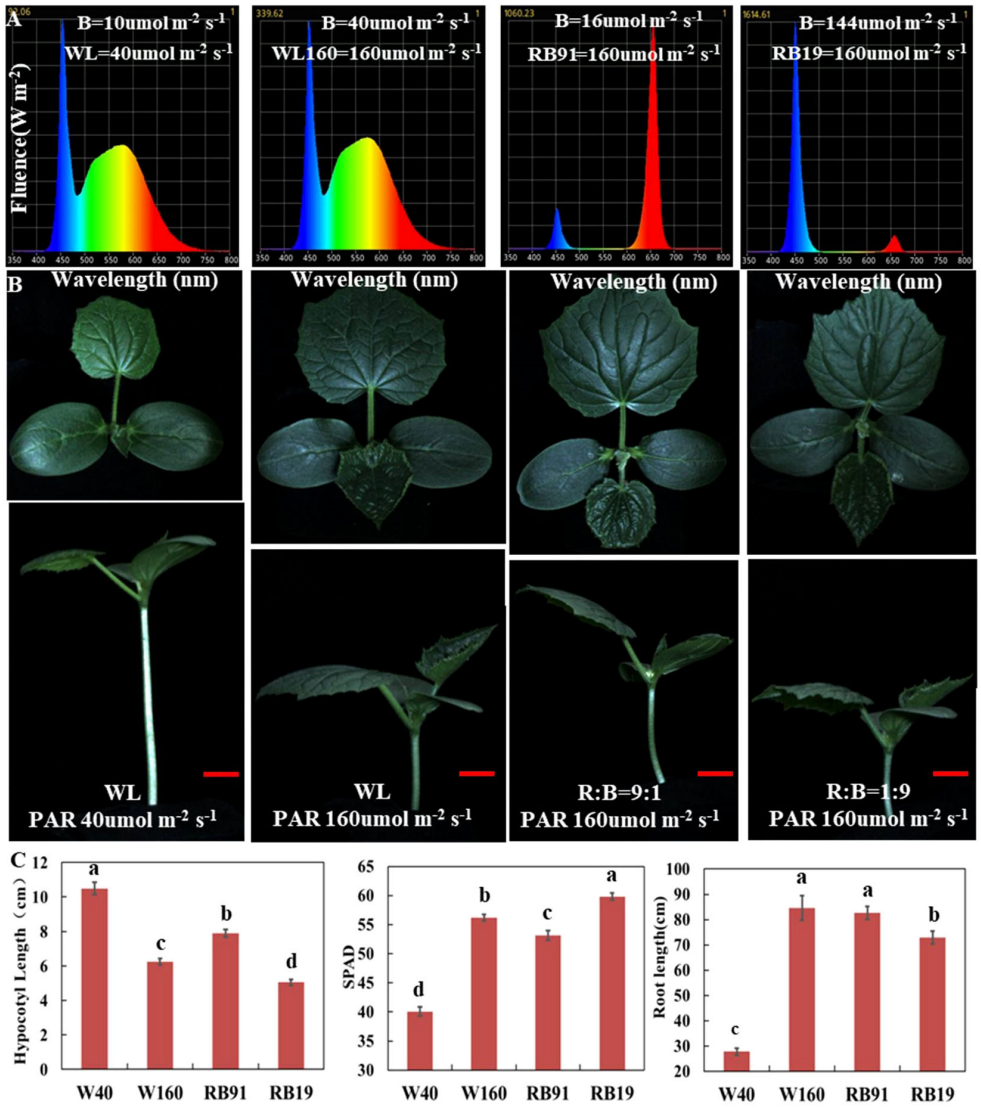

FIGURE 2
The effect of different light qualities on cucumber seedlings. **(A)** The spectra of four different light combinations. **(B)** Cucumber seedling (CS) phenotypes under four different light combinations. **(C)** The values of hypocotyl length, SPAD and total root length of cucumber seedlings grown for two weeks under four light combinations. Here, the low case letters indicate significant differences at $P < 0.05$ by the least significant difference test. The red scale bar represents a length of 2cm.

revealed that under the WL40 condition, the hypocotyl length was the longest, whereas the SPAD value and total root length were the smallest. When the light intensity was the same, the hypocotyl of treatment RB91 was the longest, followed by treatment WL160, and the shortest was treatment RB19. The results indicated that the hypocotyl length was totally negatively correlated with the intensity of blue light (Figures 2B, C). Additionally, our findings revealed that CR exhibited significantly shorter hypocotyls compared to CS when exposed to blue light treatment. However, no significant difference was observed in hypocotyl length between CS and CR under red light treatment (Supplementary Figure 3). Furthermore, the supplementary LED experiment demonstrated that the elongation of CS hypocotyls can also be most effectively inhibited by supplement of blue light, whereas red light exhibited the least effective inhibitory effect (Supplementary Figure 4). The research findings indicated that the reduction in blue light intensity is the primary factor responsible for inducing low-light-stress in cucumber.

3.3 CsaV3_3G047490 is highest expressed photoreceptor genes in cucumber

Photoreceptors play a critical role in regulating low-light-stress tolerance of plants. However, in cucurbit crops, photoreceptor genes have not been clearly explained in detail. Here, we identified the major classes of photoreceptors (*CRYs, UVRs, PHYs, PHOTs*) and analyzed their expression patterns in different cucurbit crops. A total of 11 and 13 photoreceptor genes were identified in cucumber and melon, respectively. The gene ID information of these factors was shown in Supplementary Table 2. Chromosome mapping results revealed that

10.3389/fpls.2024.1371435

the 11 photoreceptor genes in cucumber were each mapped to five distinct chromosomes. In the photoreceptors, the *PHYA* and *PHOT2* genes have an additional copy in almost all cucurbit crops. Furthermore, a segmental duplication gene pair (PHOT2) was identified through syntenic analysis (Figure 3A). It is well-recognized that analyzing the expression of these genes across different tissues is pivotal in deciphering their function. The heatmaps, created using expression data from the Cucurbit Expression Atlas, revealed that *CsaV3_3G047490.1* consistently exhibited a higher expression level than other photoreceptor genes in various cucurbit crops, including cucumber, melon, watermelon, and bitter melon (Figures 3B, C; Supplementary Figure 5). Additionally, CRY1 was also highly expressed in the hypocotyls of cucumber seedlings (Figure 3B).

3.4 *CsaV3_3G047490.1* belongs to the cryptochrome blue light receptors and was named *CsCRY1*

CsaV3_3G047490 was annotated as the cryptochrome blue light receptors in the cucumber genome. To further identify the *CsCRY* genes, we used 3 CRYs (AtCRY1, AtCRY2 and AtCRY3) protein

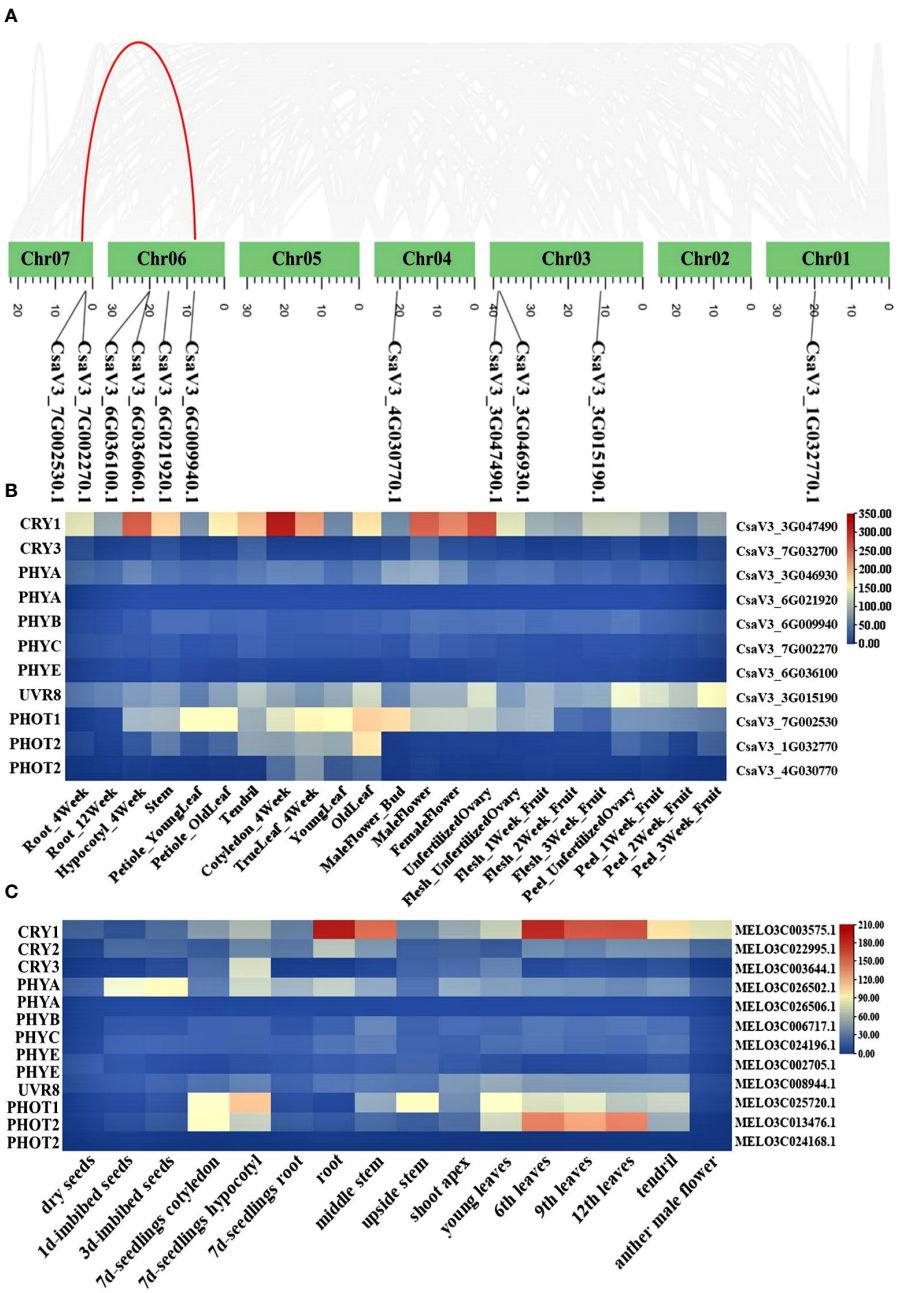

FIGURE 3
Chromosome location of photoreceptor genes in cucumber **(A)**; Heat map of photoreceptor genes in different tissue from cucumber **(B)** and melon **(C)**.

10.3389/fpls.2024.1371435

sequences from Arabidopsis as queries to carry out a Blastp search. As a result, only two *CRYs* genes were identified in the Chinese Long v3 genome of cucumber. To investigate the evolutionary relationships among the CRY proteins in cucurbit crops, a phylogenetic tree was constructed using MEGA 7. All the CRYs proteins in cucurbits crops could be divided into three subfamilies: CRY1, CRY2, and CRY3 according to the classification of CRYs in Arabidopsis. The CRY1 subfamily has the highest number of members, with a total of 17. Conversely, the CRY2 subfamily is the smallest with only 13 members (Figure 4A).

The physical and chemical properties of CsCRY1 and CsCRY3 were shown in Table 1. The amino acid sequence lengths of CsCRY1 and CsaCRY3 are 613 amino acids and 592 amino acids, respectively, while their pI values are 5.46 and 9.4. Both *CRYs* genes are mapped to almost the same region of chromosome 3 (Figure 3A). Interestingly, the *CRY2* gene is absent in the cucumber 9930 genome, but not in other cucurbit crops such as melon, watermelon, pumpkin, and bitter melon (Table 1; Supplementary Table 2). Therefore, we identified the cucumber *CRY2* gene in the remaining four reference cucumber genomes within CuGenDBv2 database. Interestingly, we identified a completely intact *CRY2* gene (636aa) in *Cucumis hystrix var* (2n = 2x = 24), a wild cucumber species that can hybridize with cultivated cucumber varieties (*C. sativus* L., 2n =2x = 14). The *CRY2* is incomplete (229 amino acids) in the genome of wild/semi-wild varieties *Cucumis sativus* var. *hardwickii* cv. *PI 183967*. All cultivated cucumbers (*Cucumis sativus L.* var. *sativus* cv. *Chinese*

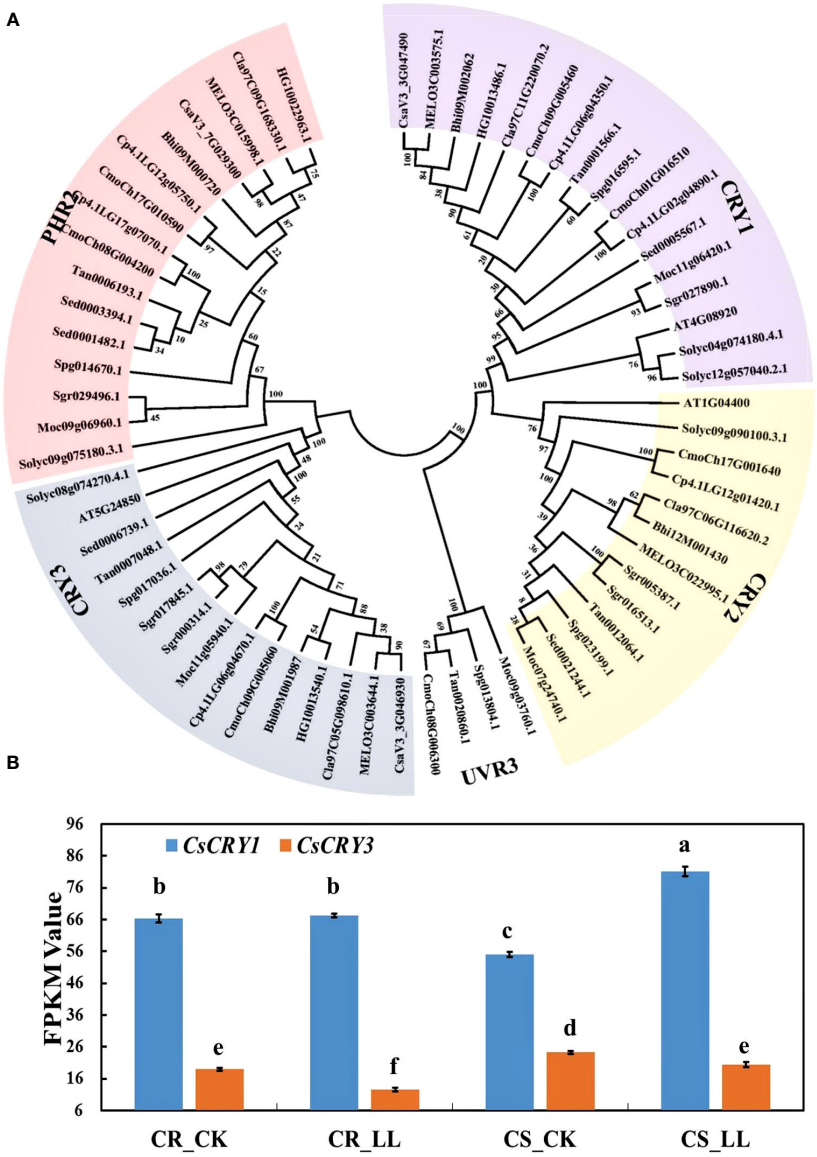

FIGURE 4
The phylogenetic tree and expression analysis of *CsaCRYs* gene in cucumber. **(A)** The phylogenetic tree and subgroup classifications of CRY proteins in cucumber, melon, watermelon, bitter melon, wax gourd, bottle gourd, pumpkin, tomato, and Arabidopsis. **(B)** Expression profiles of *CsCRY1* and *CsCRY3* genes in low-light-stress -tolerant (CR) and light-stress-sensitive (CS) cucumber cultivars under 40μmol m^{-2} s^{-1} low-light-stress treatment (LL) and 160μmol m^{-2} s^{-1} control (CK) treatment. Here, the low case letters indicate significant differences at $P < 0.05$ by the least significant difference test.

TABLE 1 Characteristics of *CsCRYs* genes and their annotated information in *Cucumis sativus L.*

Gene ID	Gene name	Strand	Gene position	CDS/bp	Proten/aa	MW/kD	pI	Subcellar location
CsaV3_3 G047490	*CsCRY1*	+	38763751-38768676	1839	612	69.366	5.46	Nucleus
CsaV3_3 G046930	*CsCRY3*	–	38309641-38315065	1779	592	67.434	9.4	Nucleus

Long, Cucumis sativus L. var. *sativus* cv. *Gy14, and Cucumis sativus L.* var. *sativus cv B10*) lack the *CRY2* gene (Supplementary Table 3). The findings suggest that the *CsCRY2* gene has been explicitly lost over a long evolution from wild to cultivated varieties.

3.5 The expression of *CsCRY1 was* induced by low-light-stress

To investigate the responses of the *CsCRY* genes to low stress, RNA-seq analysis was conducted on tolerant and sensitive cucumber hypocotyls. The hypocotyls were sampled after 72 hours of treatment under 40μmol m^{-2} s^{-1} (LL) and 160μmol m^{-2} s^{-1} (CK) white light LED. During this period, the hypocotyl length of the tolerant cucumber CR was significantly shorter than that of the sensitive cucumber CS under low-light-stress (Supplementary Figure 6). The expression result of *CsCRY1* and *CsCRY3* indicated that the expression level of *CsCRY1* was much higher than *CsCRY3*. Additionally, the expression of *CsCRY3* was significantly depressed by low-light-stress treatment in both tolerant and sensitive cucumber material. However, only in the sensitive cucumber material, the expression of *CsCRY1* was significantly induced by low-light-stress (Figure 4B). Therefore, the above results indicated *CsCRY1* may play a critical role under low-light-stress.

3.6 Cucumber CsCRY1 protein lost the last 70 aa in the C-terminal

To further understand the functions of CsCRY1, we aligned the amino acid of CRY1 protein from various cucurbit species. Our findings indicated that CRY1 is highly conserved, particularly in its N-terminal PHR domain. However, the length of all CRY1 proteins from various crops is almost 681 amino acids, except for cucumber (Supplementary Table 4). The C-terminal of CCT domain in CsCRY1 of cucumber was short 70 aa (Figure 5). Then, we cloned the CsCRY1 gene and verified the presence of CsCRY1 mRNA in the cucumber genome, which is capable of encoding a short CsCRY1 protein. It is well-established that both *CRY1* and *CRY2* regulate low-light-stress, albeit a relatively minor role for *CRY2* compared with that of *CRY1 in* Arabidopsis. However, *CsCRY2* was absent in cucumber. The absence of the *CsCRY2* gene in cultivated cucumber leads to a significant role for CsCRY1 in low-light-stress conditions.

3.7 AS leads to form one special transcript that encoded CsCRY1.1 protein lost 70 aa

To further elucidate the distinct features of cucumber *CsCRY1*, we have successfully obtained 34 transcripts including 15 full-length transcripts of *CsCRY1* through single-molecule long-read sequencing in cucumber CS (Supplementary Figure 7). By utilizing the IGV-GSAman software to align these *CsCRY1* transcripts to the cucumber genome, we discovered that the pre-mRNA of *CsCRY1* undergoes alternative splicing (AS). Additionally, alternative 5′ splice sites (5'SS) in the last intron was the major AS events. Interestingly, there were five kinds of 5'SS events in intron four, one total intron retention event, three partial intron retention events, and one total intron splicing event. We predicted the open reading frames (ORFs) of these *CsCRY1* transcripts. The findings indicated that intron 4 contains a crucial coding sequence, with the stop codon positioned at the midpoint of intron four. Therefore, the five splice variants can be translated into three kinds of splice proteins with different lengths of C-terminal domains (Figure 6A). The transcripts *CsaV3_3G047490.3*, *CsaV3_3G047490.4*, and *CsaV3_3G047490.5* encode the full-length protein of CRY1, designated as CsCRY1.3. The transcripts *CsaV3_3G047490.1* and *CsaV3_3G047490.2* encode two different truncated C-terminal CRY1 proteins, named CsCRY1.1 and CsCRY1.2 (Figure 6B). We analyzed the conserved domains of these spliced proteins by HMMER. All the spliced protein contains an intact DNA photolyase domain and FAD binding domain. However, only *CsaV3_3G047490.1* contained an impaired CCT domain (Figure 6C). Moreover, we did not find the 5'SS of *CRY1* in other species including melon, pumpkin, Arabidopsis, etc. (Supplementary Figure 8). Therefore, we concluded that 55'SS of *CsCRY1* is responsible for the formation of various transcripts with diverse coding capabilities in cucumber. However, the precise role of *CsCRY1* remains elusive.

3.8 Analysis of 5'SS of *CsCRY1* in cucumber different tissues and stress treatment

To further validate the AS of CsCRY1, we conducted a transcriptome analysis of both CR and CS cucumber hypocotyls following 72 hours of exposure to low-light-stress (40 μmol m^{-2} s^{-1}) and normal light (160 μmol m^{-2} s^{-1}) treatment. The results reaffirmed the presence of a 5'SS in the last intron of *CsCRY1* in both CR and CS (Figure 7A; Supplementary Figure 9). To unravel the expression pattern of *CsCRY1* splicing variants in different tissues, we designed a pair of the primer crossing the intron four to perform RT-PCR assay. The results revealed that there were four spliced transcripts identified in almost all the samples. Among them, the expression level of *CsaV3_3G047490.3* was the highest, followed by *CsaV3_3G047490.4* and *CsaV3_3G047490.1*. In contrast, the expression of *CsaV3_3G047490.5* was the lowest, while no expression of *CsaV3_3G047490.2* was detected (Figures 7B, C). Furthermore, all four transcripts were present in

10.3389/fpls.2024.1371435

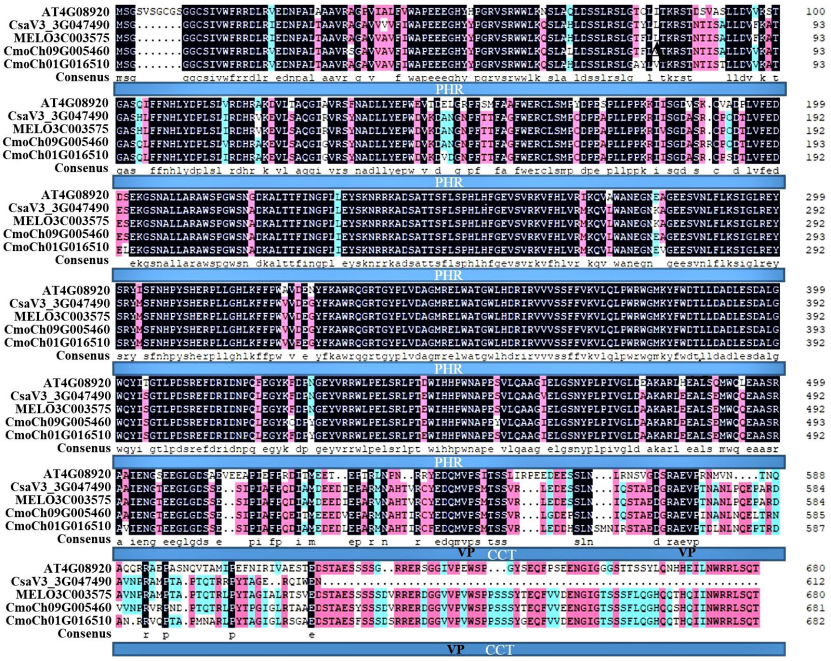

FIGURE 5
Multiple protein sequence alignment of cucumber CsCRY1. CRY1 protein sequences included AT4G08920 from Arabidopsis, CsaV3_3G047490.1 from *Cucumis sativus L.* var. *sativus* cv. *Chinese Long*, MELO3C003575.2.1 from *Cucumis melo* cv. *DHL92*, CmoCh09G005460, and CmoCh01G016510 from *Cucurbita moschata* var. *Rifu*.

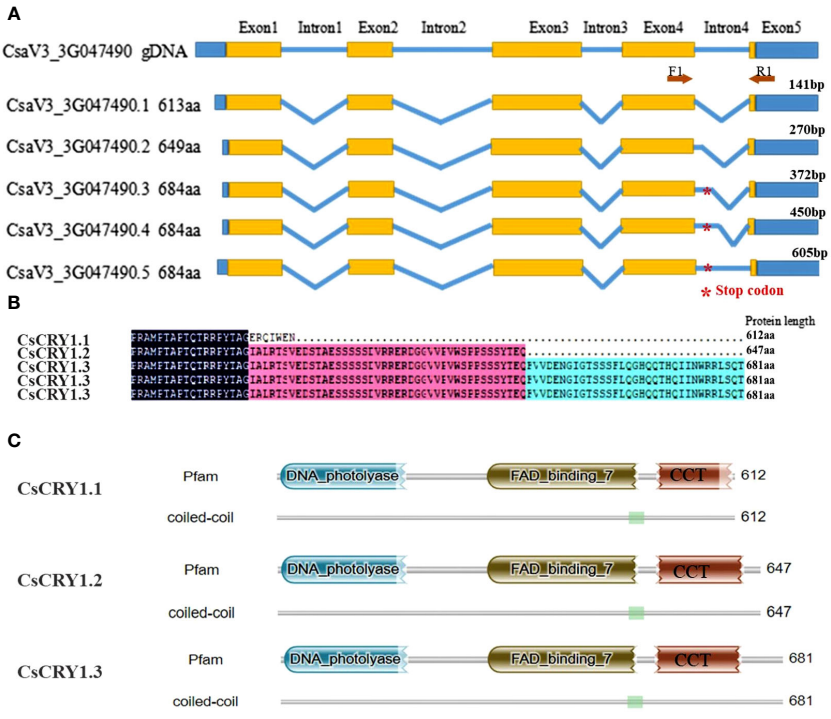

FIGURE 6
The whole-length transcripts structure of cucumber *CsCRY1*. **(A)** five kinds of 5′SS events in intron 4, * represent the stop codon at the middle of intron 4. **(B)** Alignment of the spliced protein encoding by five splicing variants. Here, only the C-terminal protein was shown. **(C)** The conserved motif analysis of the spliced protein using HMM.

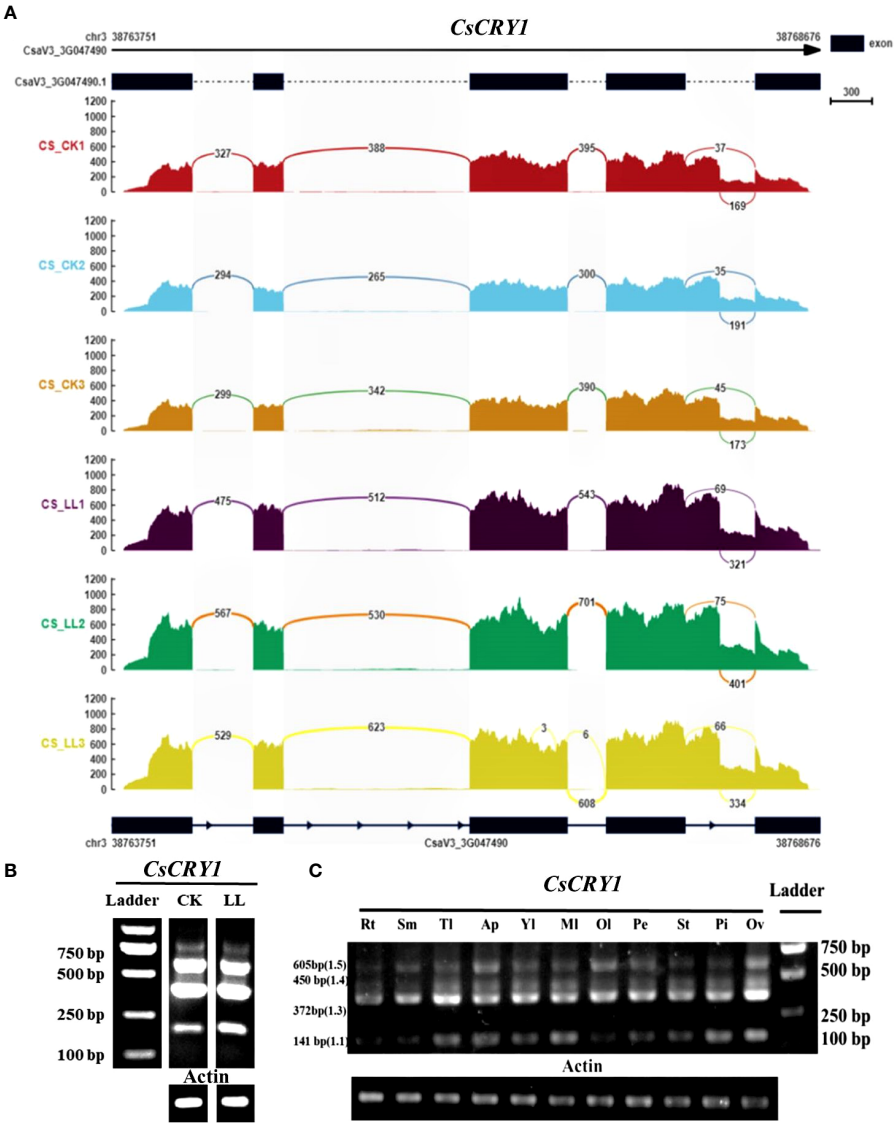

FIGURE 7
The transcripts read mapping **(A)** and RT-PCR results **(B)** of *CsCRY1* under control and low-light-stress condition, RT-PCR results of *CsCRY1* from different tissues **(C)** (Rt, root; Sm, stem; Tl, tendril; Ap, Apical point; Yl, young leaves; Ml, young leaves; Ol, young leaves; Pe, petal; St, stigma; Pi, pistil; Ov, ovary). CS was used as material. The PCR product size of splicing variant *CsaV3_3G047490.1* was 141bp, the PCR product size of splicing variant *CsaV3_3G047490.1* was 270bp, The PCR product size of splicing variant *CsaV3_3G047490.3* was 372bp, The PCR product size of splicing variant *CsaV3_3G047490.4* was 450bp, and The PCR product size of splicing variant *CsaV3_3G047490.5* was 605bp.

hypocotyls under low-light-stress conditions. However, we only found that the expression of *CsaV3_3G047490.1* was induced by low-light-stress, and the RNA-seq analysis confirmed these findings (Figure 7; Supplementary Figure 9).

The CsCRY1.1 protein, a newly identified blue light receptor in plants, was cloned and its subcellular localization was evaluated. Here, we found that the subcellular localization of CsCRY1.1 was same to GFP. The fluorescence signal was widely observed in both the cytoplasm and nucleus (Figure 8). The result indicated that loss of the last valine-proline-containing (VP) motif did not change subcellular localization of CsCRY1.1. But, whether CsCRY1.1 without the last VP motif can interact with the COP1/SPA complex is still unknown.

4 Discussion

Recently, low-light-stress frequently occurs worldwide. It has the potential to induce excessive growth in stems, lead to a decrease in female flowers, and consequently, reduce fruit production (Zhou et al., 2022; Cao et al., 2023; Li et al., 2023). Cucumber is an important crop cultivated in facilities, and also very sensitive to low-light-stress. CS was commonly used in China modern cucumber breeding with high-quality genome and very rich omics data (Huang et al., 2009; Li et al., 2019). Utilizing CS, we established a screening system for low-light-stress tolerance, revealing that blue light and photoreceptor gene *CsCRY1* may play significant roles in this process. The photoreceptor genes play a crucial role in

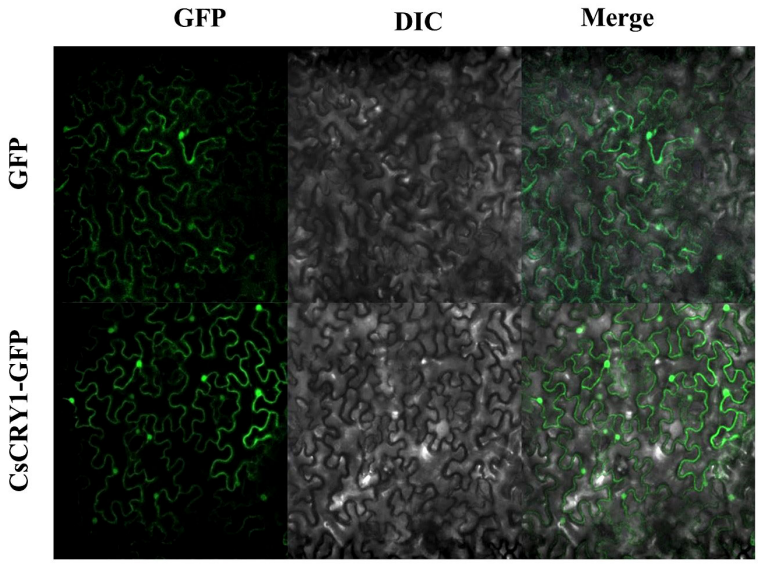

FIGURE 8
Subcellular localization of CsCRY1.1 CsCRY1.1-GFP fusion proteins and GFP were transiently expressed in tobacco leaves under control of the CaMV 35S promoter and observed under a laser scanning confocal microscope, GFP images, DAPI stained images, differential interference contrast images (DIC), and merged images were taken.

regulating flowering, growth, and production under low-light-stress, particularly for CRYs and PHYs (Yu et al., 2010; Casal and Fankhauser, 2023). There are three *CRYs*, but *CRY3* does not regulate hypocotyl elongation under low-light-stress (Yu et al., 2010). *CRY1* and *CRY2* can interact with PIFs to regulate hypocotyl growth in a limited blue light environment (de Wit et al., 2016; Pedmale et al., 2016). The cry1cry2 double mutant, as mentioned, displayed the most remarkable long hypocotyl phenotype compared to the single mutant cry1 or cry2. Additionally, in comparison to *CRY2*, *CRY1* played a more crucial role in inhibiting hypocotyl growth. Overexpression of *AtCRY1* can result in the failure of hypocotyl elongation under low-light-stress. By elevating the CRY1-signaling activity in soybean, its yield can be significantly enhanced under low-light conditions (Lyu et al., 2021). The findings above suggested that *CRYs* genes played a crucial role in regulating plant tolerance to low-light-stress.

Most plants possess two well-characterized cryptochromes, *CRY1* and *CRY2* (Wang et al., 2021). However, we found that the *CRY2* gene has been lost specifically over a long period of evolution from wild to cultivated cucumber varieties. *CRY2* can also regulate photomorphogenesis, albeit playing a relatively minor role compared with that of *CRY1*. *CRY2* primarily mediated blue-light photoperiodic control of floral initiation, and the cry2 mutant exhibits a late-flowering phenotype (Yu et al., 2010; Liu et al., 2018). Arabidopsis is a long-day (LD) flowering plant (Wang et al., 2016). However, Xishuangbanna (XIS) cucumber, a semi-wild cucumber, is strictly short-day plants, while cultivated cucumber is day-neutral plants. The expression of *FLOWERING LOCUS T* (*FT*) gene under LD and SD conditions is responsible for regulating short-day flowering in the XIS cucumber (Song et al., 2023). In Arabidopsis, *CRY2* can promote *FT* gene expression by suppressing the degradation of the CO (CONSTANS) protein and activating CIB1 (CRY2-interacting bHLH1) (Liu et al., 2018). *CRY2* is highly conserved, and it's possible that cucumber CRY2 can also regulate the *FT* gene expression under various photoperiod conditions. Therefore, we can infer that the loss of *CRY2* could be crucial for cultivated cucumbers to become day-neutral plants.

In cucumber, only one *CRY1* gene was identified, and we found that *CRY1* was also the highest-expressed photoreceptor gene. Additionally, the blue light most effectively inhibits the elongation of hypocotyls (Figure 2; Supplementary Figure 1). The findings suggest that *CsCRY1* plays a crucial role in cucumber's response to low-light-stress. The CRY1 protein, a highly conserved blue light receptor, possesses an N-terminal domain (PHR) that has evolved from DNA photolyase and a CCT domain (Yu et al., 2010; Wang et al., 2021). The CCT domain can relay the blue light signals perceived by PHR domain, and subsequently interact with the WD40 domain of constitutive photomorphogenic1 (COP1) and suppressor of phya-105 (SPA) in a blue light-specific manner (Yu et al., 2007). Overexpression of CCT1 or CCT2 fused to β-glucuronidase (GUS) resulted in a constitutive photomorphogenic phenotype (shorted hypocotyls, enhanced anthocyanin production and early flowering phenotype) (Yang et al., 2000). Moreover, the homodimerization of CRY1 is crucial for the function of CCT (Sang et al., 2005). Hence, CCT domain of CRY1 is very important.

The CCT domain of CsCRY1 in cucumber was not intact, lacking the last VP motif. In contrast, AtCRY1 carried 3 VP motifs in its CCT domain, while CRY2 only carried 1 VP motif. COP1-SPAs complex usually interacted with the proteins possessing VP motifs (Holm et al., 2001). In Arabidopsis, it was demonstrated that the VP motif in CRY2 was necessary for the CRY2–COP1 interaction (Zuo et al., 2011; Ponnu et al., 2019). Moreover, GFP-CRY2 fully complemented the elongated hypocotyl phenotype of

cry1 cry2 in blue light. In contrast, The GFP-CRY2-VP with a mutated VP motif failed to complement the cry1 cry2 mutant phenotype (Ponnu et al., 2019). Therefore, the VP motif plays a crucial role in the CRYs' function. Furthermore, it was reported that AtCRY2 is exclusively localized in the nucleus. On the other hand, AtCRY1 is present in both the nucleus and cytoplasm, regardless of light or dark conditions, without experiencing a significant alteration in its relative subcellular concentration (Yu et al., 2010). Additionally, it is the nuclear, rather than cytoplasmic, form of CRY1 that effectively inhibits growth (Wu and Spalding, 2007). Here, we found that the subcellular localization of CsCRY1.1 was same to AtCRY1 and GFP. The fluorescence signal was widely observed in both the cytoplasm and nucleus (Figure 8). The result indicated that loss of the last VP motif did not change subcellular localization of CsCRY1.1. However, it remains unclear whether CsCRY1.1, which lacks the VP motif, can interact with the COP1/SPA complex.

Through AS, one gene locus can be used to produce multiple crucial mRNA splicing variants with different coding sequences by the spliceosome for coping with fluctuating light environments in eukaryotes (Kathare and Huq, 2021). In Arabidopsis, it was reported almost 85% of genes were multiexon, and 70% of them were alternatively spliced (Martín et al., 2021). Among them, several crucial factors in the light signaling pathway, including *PIF3*, *PIF6*, *ELONGATED HYPOCOTYL5* (*HY5*), and *SPA3*, undergo alternative splicing (Kathare and Huq, 2021). In this study, we present a novel alternative splicing (AS) event in cucumber, specifically the 5'SS of CsCRY1. This AS event results in the production of a unique and distinct CsCRY1.1 protein variant that lacks the VP motif found at the protein's C-terminus. This novel CsCRY1.1 protein variant may play a pivotal role in the adaptive response of cucumber, a specialized crop, to low-light-stress.

5 Conclusions

In this study, we establish an efficient system for evaluation of cucumber low-light-stress tolerance. One cucumber material CR was screened out. Furthermore, a total of 11 photoreceptor genes (*CRYs*, *UVRs*, *PHYs*, *PHOTs*) were identified in cucumber, including 2 *CRYs* genes, *CsCRY1* and *CsCRY3*. Transcriptome data revealed that *CsCRY1* had the highest expression level and was induced expression. Additionally, blue light can most effectively inhibit hypocotyl elongation. CsCRY1 was lost 70 aa in CCT domain. Through single-molecule long-read sequencing and transcriptome analysis, we also found that *CsCRY1* suffer 5'SS in the last intron leading to forming five splicing variants. Among them, *CsaV3_3G047490.1* was predicted to encode the CsCRY1 protein in the reference genome. And its expression was also induced by low-light-stress, which was confirmed by RNA-seq and RT-PCR experiment. Taken together, these results provided crucial information for further research and utilization of *CsCRY1* in cucumber.

Data availability statement

The datasets presented in this study can be found in National Genomics Data Center (NGDC) repositories, accession numbers (PRJCA024948 and CRA015726).

Author contributions

HC: Formal analysis, Investigation, Methodology, Writing – original draft. RW: Methodology, Resources, Writing – review & editing. JZ: Investigation, Methodology, Software, Writing – review & editing. LS: Formal analysis, Resources, Supervision, Writing – review & editing. YH: Investigation, Supervision, Writing – review & editing. TW: Data curation, Formal analysis, Methodology, Resources, Supervision, Writing – review & editing. CZ: Data curation, Formal analysis, Funding acquisition, Resources, Writing – review & editing.

Funding

The author(s) declare financial support was received for the research, authorship, and/or publication of this article. This research was supported by the Guangdong Basic and Applied Basic Research Foundation (2021A1515110515) and the Innovation fund of Guangdong Academy of Agricultural Sciences (202208 and 202149).

Conflict of interest

The authors declare that the research was conducted in the absence of any commercial or financial relationships that could be construed as a potential conflict of interest.

Publisher's note

Supplementary material

The Supplementary Material for this article can be found online at: https://www.frontiersin.org/articles/10.3389/fpls.2024.1371435/full#supplementary-material

References

Cao, H., Wu, T., Shi, L., Li, Y., and Zhang, C. (2023). Alternative splicing control of light and temperature stresses responses and its prospects in vegetable crops. *Veg. Res.* 3, 17. doi: 10.48130/VR-2023-0017

Casal, J. J. (2013). Photoreceptor signaling networks in plant responses to shade. *Annu. Rev. Plant Biol.* 64, 403–427. doi: 10.1146/annurev-arplant-050312-120221

Casal, J. J., and Fankhauser, C. (2023). Shade avoidance in the context of climate change. *Plant Physiol.* 191, 1475–1491. doi: 10.1093/plphys/kiad004

Chen, C., Chen, H., Zhang, Y., Thomas, H. R., Frank, M. H., He, Y., et al. (2020). TBtools: an integrative toolkit developed for interactive analyses of big biological data. *Mol. Plant* 13, 1194–1202. doi: 10.1016/j.molp.2020.06.009

De Wit, M., Galvão, V. C., and Fankhauser, C. (2016). Light-mediated hormonal regulation of plant growth and development. *Annu. Rev. Plant Biol.* 67, 513–537. doi: 10.1146/annurev-arplant-043015-112252

de Wit, M., Keuskamp, D. H., Bongers, F. J., Hornitschek, P., Gommers, C. M. M., Reinen, E., et al. (2016). Integration of phytochrome and cryptochrome signals determines plant growth during competition for light. *Curr. Biol.* 26, 3320–3326. doi: 10.1016/j.cub.2016.10.031

Gajc-wolska, J., Kowalczyk, K., Przybysz, A., Mirgos, M., and Orliński, P. (2021). Photosynthetic efficiency and yield of cucumber (Cucumis sativus L.) grown under HPS and LED lighting in autumn–winter cultivation. *Plants* 10 (10), 2042. doi: 10.3390/plants10102042

Galvão, V. C., and Fankhauser, C. (2015). Sensing the light environment in plants: Photoreceptors and early signaling steps. *Curr. Opin. Neurobiol.* 34, 46–53. doi: 10.1016/j.conb.2015.01.013

Grishchenko, O. V., Subbotin, E. P., Gafitskaya, I. V., Vereshchagina, Y. V., Burkovskaya, E. V., Khrolenko, Y. A., et al. (2022). Growth of Micropropagated Solanum tuberosum L. Plantlets under Artificial Solar Spectrum and Different Mono- and Polychromatic LED Lights. *Hortic. Plant J.* 8, 205–214. doi: 10.1016/j.hpj.2021.04.007

Guo, S., Zhao, S., Sun, H., Wang, X., Wu, S., Lin, T., et al. (2019). Resequencing of 414 cultivated and wild watermelon accessions identifies selection for fruit quality traits. *Nat. Genet.* 51, 1616–1623. doi: 10.1038/s41588-019-0518-4

Holm, M., Hardtke, C. S., Gaudet, R., and Deng, X. W. (2001). Identification of a structural motif that confers specific interaction with the WD40 repeat domain of Arabidopsis COP1. *EMBO J.* 20, 118–127. doi: 10.1093/emboj/20.1.118

Huang, S., Li, R., Zhang, Z., Li, L., Gu, X., Fan, W., et al. (2009). The genome of the cucumber, Cucumis sativus L. *Nat. Genet.* 41, 1275–1281. doi: 10.1038/ng.475

Kathare, P. K., and Huq, E. (2021). Light-regulated pre-mRNA splicing in plants. *Curr. Opin. Plant Biol.* 63, 102037. doi: 10.1016/j.pbi.2021.102037

Li, Q., Li, H., Huang, W., Xu, Y., Zhou, Q., Wang, S., et al. (2019). A chromosome-scale genome assembly of cucumber (Cucumis sativus L.). *Gigascience* 8 (6), giz072. doi: 10.1093/gigascience/giz072

Li, D., Yu, F., Zhang, Y., Hu, K., Dai, D., Song, S., et al. (2023). Integrative analysis of different low-light-tolerant cucumber lines in response to low-light stress. *Front. Plant Sci.* 13. doi: 10.3389/fpls.2022.1093859

Liu, Y., Li, X., Ma, D., Chen, Z., Wang, J., and Liu, H. (2018). CIB 1 and CO interact to mediate CRY 2-dependent regulation of flowering. *EMBO Rep.* 22 (1), 35. doi: 10.15252/embr.201845762

Liu, Q.-h., Wu, X., Chen, B.-c., Ma, J.-q., and Gao, J. (2014). Effects of low light on agronomic and physiological characteristics of rice including grain yield and quality. *Rice Sci.* 21, 243–251. doi: 10.1016/S1672-6308(13)60192-4

Lorenzo, C. D., Alonso Iserte, J., Sanchez Lamas, M., Antonietti, M. S., Garcia Gagliardi, P., Hernando, C. E., et al. (2019). Shade delays flowering in Medicago sativa. *Plant J.* 99, 7–22. doi: 10.1111/tpj.14333

Lyu, X., Cheng, Q., Qin, C., Li, Y., Xu, X., Ji, R., et al. (2021). GmCRY1s modulate gibberellin metabolism to regulate soybean shade avoidance in response to reduced blue light. *Mol. Plant* 14, 298–314. doi: 10.1016/j.molp.2020.11.016

Ma, Y., Xu, A., and Cheng, Z. M. (2021). Effects of light emitting diode lights on plant growth, development and traits a meta-analysis. *Hortic. Plant J.* 7, 552–564. doi: 10.1016/j.hpj.2020.05.007. (Max).

Martín, G., Márquez, Y., Mantica, F., Duque, P., and Irimia, M. (2021). Alternative splicing landscapes in Arabidopsis thaliana across tissues and stress conditions highlight major functional differences with animals. *Genome Biol.* 22. doi: 10.1186/s13059-020-02258-y

Pedmale, U. V., Huang, S. S. C., Zander, M., Cole, B. J., Hetzel, J., Ljung, K., et al. (2016). Cryptochromes interact directly with PIFs to control plant growth in limiting blue light. *Cell* 164, 233–245. doi: 10.1016/j.cell.2015.12.018

Ponnu, J., Riedel, T., Penner, E., Schrader, A., and Hoecker, U. (2019). Cryptochrome 2 competes with COP1 substrates to repress COP1 ubiquitin ligase activity during Arabidopsis photomorphogenesis. *Proc. Natl. Acad. Sci. U.S.A.* 116, 27133–27141. doi: 10.1073/pnas.1909181116

Sang, Y., Li, Q. H., Rubio, V., Zhang, Y. C., Mao, J., Deng, X. W., et al. (2005). N-terminal domain-mediated homodimerization is required for photoreceptor activity of Arabidopsis Cryptochrome 1. *Plant Cell* 17, 1569–1584. doi: 10.1105/tpc.104.029645

Sekhar, S., Panda, D., Kumar, J., Mohanty, N., Biswal, M., Baig, M. J., et al. (2019). Comparative transcriptome profiling of low light tolerant and sensitive rice varieties induced by low light stress at active tillering stage. *Sci. Rep.* 9 (1), 5753. doi: 10.1038/s41598-019-42170-5

Sheludko, Y. V., Sindarovska, Y. R., Gerasymenko, I. M., Bannikova, M. A., and Kuchuk, N. V. (2007). Comparison of several Nicotiana species as hosts for high-scale Agrobacterium-mediated transient expression. *Biotechnol. Bioeng.* 96 (3), 608–14. doi: 10.1002/bit.21075

Shen, S., Park, J. W., Lu, Z. X., Lin, L., Henry, M. D., Wu, Y. N., et al. (2014). rMATS: Robust and flexible detection of differential alternative splicing from replicate RNA-Seq data. *Proc. Natl. Acad. Sci. U.S.A.* 111, E5593–E5601. doi: 10.1073/pnas.1419161111

Song, J., Cao, K., Hao, Y., Song, S., Su, W., and Liu, H. (2019). Hypocotyl elongation is regulated by supplemental blue and red light in cucumber seedling. *Gene* 707, 117–125. doi: 10.1016/j.gene.2019.04.070

Song, S., Hao, Q., Su, L., Xia, S., Zhang, R., Liu, Y., et al. (2023). FLOWERING LOCUS T (FT) gene regulates short-day flowering in low latitude Xishuangbanna cucumber (Cucumis sativus var. xishuangbannanesis). *Veg. Res.* 3, 15. doi: 10.48130/VR-2023-0015

Wang, W., Mao, Z., Guo, T., Kou, S., and Yang, H. Q. (2021). The involvement of the N-terminal PHR domain of Arabidopsis cryptochromes in mediating light signaling. *aBIOTECH* 2, 146–155. doi: 10.1007/s42994-021-00044-3

Wang, Q., Zuo, Z., Wang, X., Gu, L., Yoshizumi, T., Yang, Z., et al. (2016). Photoactivation and inactivation of Arabidopsis cryptochrome 2. *Sci. (80-.).* 354, 343–347. doi: 10.1126/science.aaf9030

Wu, G., and Spalding, E. P. (2007). Separate functions for nuclear and cytoplasmic cryptochrome 1 during photomorphogenesis of Arabidopsis seedlings. *Proc. Natl. Acad. Sci. U.S.A.* 104, 18813–18818. doi: 10.1073/pnas.0705082104

Xu, X., Paik, I., Zhu, L., and Huq, E. (2015). Illuminating progress in phytochrome-mediated light signaling pathways. *Trends Plant Sci.* 20, 641–650. doi: 10.1016/j.tplants.2015.06.010

Yang, H. Q., Wu, Y. J., Tang, R. H., Liu, D., Liu, Y., and Cashmore, A. R. (2000). The C termini of Arabidopsis cryptochromes mediate a constitutive light response. *Cell* 103, 815–827. doi: 10.1016/S0092-8674(00)00184-7

Yano, R., Nonaka, S., and Ezura, H. (2018). Melonet-DB, a grand RNA-seq gene expression atlas in melon (Cucumis melo L.). *Plant Cell Physiol.* 59, E4. doi: 10.1093/pcp/pcx193

Yu, X., Liu, H., Klejnot, J., and Lin, C. (2010). The cryptochrome blue light receptors. *Arab. B.* 8, e0135. doi: 10.1199/tab.0135

Yu, X., Shalitin, D., Liu, X., Maymon, M., Klejnot, J., Yang, H., et al. (2007). Derepression of the NC80 motif is critical for the photoactivation of Arabidopsis CRY2. *Proc. Natl. Acad. Sci. U.S.A.* 104, 7289–7294. doi: 10.1073/pnas.0701912104

Yu, J., Wu, S., Sun, H., Wang, X., Tang, X., Guo, S., et al. (2023). CuGenDBv2: an updated database for cucurbit genomics. *Nucleic Acids Res.* 51, D1457–D1464. doi: 10.1093/nar/gkac921

Zhou, X., Tan, Z., Zhou, Y., Guo, S., Sang, T., Wang, Y., et al. (2022). Physiological mechanism of strigolactone enhancing tolerance to low light stress in cucumber seedlings. *BMC Plant Biol.* 22 (1), 30. doi: 10.1186/s12870-021-03414-7

Zhu, J. K. (2016). Abiotic stress signaling and responses in plants. *Cell* 167, 313–324. doi: 10.1016/j.cell.2016.08.029

Zuo, Z., Liu, H., Liu, B., Liu, X., and Lin, C. (2011). Blue light-dependent interaction of CRY2 with SPA1 regulates COP1 activity and floral initiation in arabidopsis. *Curr. Biol.* 21, 841–847. doi: 10.1016/j.cub.2011.03.048

frontiers | Frontiers in Plant Science

TYPE Original Research
PUBLISHED 18 April 2024
DOI 10.3389/fpls.2024.1386950

OPEN ACCESS

EDITED BY
Giulia Conversa,
University of Foggia, Italy

REVIEWED BY
Athanasios Koukounaras,
Aristotle University of Thessaloniki, Greece
Toyoki Kozai,
Japan Plant Factory Association, Japan
Domenico Ronga,
University of Salerno, Italy
Federica Caradonia,
University of Modena and Reggio Emilia, Italy
Francesco Fabiano Montesano,
University of Bari Aldo Moro, Italy

*CORRESPONDENCE
Leo F. M. Marcelis
leo.marcelis@wur.nl

RECEIVED 16 February 2024
ACCEPTED 27 March 2024
PUBLISHED 18 April 2024

CITATION
Karpe M, Marcelis LFM and Heuvelink E (2024) Dynamic plant spacing in tomato results in high yields while mitigating the reduction in fruit quality associated with high planting densities.
Front. Plant Sci. 15:1386950.
doi: 10.3389/fpls.2024.1386950

Dynamic plant spacing in tomato results in high yields while mitigating the reduction in fruit quality associated with high planting densities

Margarethe Karpe, Leo F. M. Marcelis* and Ep Heuvelink

Horticulture and Product Physiology, Department of Plant Sciences, Wageningen University & Research, Wageningen, Netherlands

High planting densities achieve high light interception and harvestable yield per area but at the expense of product quality. This study aimed to maintain high light interception without negative impacts on fruit quality. Dwarf tomato was grown at four densities in a climate-controlled room—at two constant densities (high and low) and two dynamic spacing treatments (maintaining 90% and 75% ground coverage by decreasing planting density in 3–4 steps)—resulting in ~100, 19, 54, and 41 plants/m^2 averaged over 100 days of cultivation, respectively. Constant high density resulted in the highest light use efficiency (LUE; 7.7 g fruit fresh weight per mol photons incident on the canopy) and the highest harvestable fruit yield (11.1 kg/m^2) but the lowest fruit size and quality. Constant low density resulted in the lowest LUE and yield (2.3 g/mol and 3.2 kg/m^2, respectively), but higher fruit size and quality than high density. Compared to low density, maintaining 90% ground coverage increased yield (9.1 kg/m^2) and LUE (6.4 g/mol). Maintaining 75% ground coverage resulted in a 7.2 kg/m^2 yield and 5.1 g/mol LUE. Both dynamic spacing treatments attained the same or slightly reduced fruit quality compared to low density. Total plant weight per m^2 increased with planting density and saturated at a constant high density. Assimilate shortage at the plant level and flower abortion lowered harvestable fruit yield per plant, sweetness, and acidity under constant high density. Harvestable fruit yield per plant was the highest under dynamic spacing and low density. Under constant high density, morphological responses to lower light availability per plant—i.e., higher specific leaf area, internode elongation, and increased slenderness—coincided with the improved whole-plant LUE (g plant dry weight per mol photons). We conclude that a constant high planting density results in the highest harvestable fruit yield per area, but with reduced fruit quality. Dynamic spacing during cultivation produces the same fruit quality as constant low density, but with more than double the harvestable yield per area.

KEYWORDS

light interception, planting density, dry matter partitioning, light use efficiency, dynamic spacing, dwarf tomato

1 Introduction

Agriculture aims to maximize yield and product quality to meet increasing consumer demands for nutritious food (Godfray et al., 2010). Optimizing planting density benefits both productivity per unit of cultivation area and product quality. At the start of cultivation, the total leaf area covering 1 m^2 of cultivation area [leaf area index (LAI)] is low. Most of the incoming light is not intercepted by leaves and therefore lost for growth and yield formation. Consequently, growing small plants at high planting densities is favorable to increasing light capture, which drives subsequent physiological processes. Maximum light interception is usually reached at LAIs of three to four, with hardly any gain—but increasing competition for light—at higher LAIs (Heuvelink et al., 2004; Postma et al., 2021).

The degree of competition between plants continuously changes during growth and results in resource competition between individual plants at higher densities if resource availability is constant (Postma et al., 2021). Competition and resource limitations start once plants receive signals of neighboring plants' proximity (Postma et al., 2021). Proximity (shading) signals from nearby vegetation include reduced light intensity, an increased red-to-far-red ratio (Franklin, 2008), and the touching of leaves (de Wit et al., 2012). Competition responses in dense canopies include limitations in biomass assimilation, changes in assimilate partitioning within the plant, and morphological adaptations to low-light environments (Franklin, 2008; Weiner and Freckleton, 2010; Postma et al., 2021). At high planting densities, plants are expected to have thinner leaves, thinner stems, more leaf senescence, and a lower reproductive effort (i.e., fruiting success; Postma et al., 2021). In tomatoes, high planting density—provided it is not so high that it prevents plants from producing enough assimilates to support generative growth—can hamper fruit set (Heuvelink, 1995; Amundson et al., 2012) and reduces fruit size and thus marketability, but it increases fruit yield per unit cultivation area (Cockshull and Ho, 1995).

In controlled environments where plants are commonly cultivated out of the soil, planting density can be managed through dynamic spacing to improve the efficiency of light and space. Especially in indoor plant production systems with solely artificial lighting (e.g., vertical farms), cultivation areas and electricity for light are expensive. Lighting was reported to constitute up to 80% of a vertical farm's energy costs (Zeidler et al., 2017; Graamans et al., 2018; Kozai et al., 2019; Liu et al., 2023). If initially high planting densities can be reduced in several steps to maintain a constant degree of plant–plant competition while using available light efficiently, high productivity per cultivation area can be achieved, and fruit quality reductions can be avoided. Dynamic spacing during the cultivation of numerous crops, including dwarf tomato, is technically possible and viable with increasing automation. Few papers have been published on dynamic spacing (Leakey, 1971; Cockshull and Ho, 1995; Ioslovich and Gutman, 2000). Their applicability to commercial indoor production with artificial light spectra (which is often without far-red; Poorter et al., 2016) is limited mainly due to the presence of the solar light spectrum. Further limitations to implementing findings of those previous studies on indoor cultivation are 1) the choice of crop (barley in Leakey, 1971; high-wire tomato in Cockshull and Ho, 1995), 2) the applicability of the method to increase planting density during cultivation (resowing in Leakey, 1971; retention of additional high-wire tomato side shoots in Cockshull and Ho, 1995), and 3) the chosen mathematical modeling approach to determine optimal spacing in the absence of experimental validation (Ioslovich and Gutman, 2000).

We aimed to determine the effects of frequently decreasing planting density during cultivation on harvestable tomato fruit yield (per plant and per m^2), light use efficiency (LUE; harvestable fruit yield per incident mol of photons), and consequences for fruit quality. We hypothesized that decreasing planting densities in tomato cultivation while maintaining a high ground coverage of 90% would outperform a constant high planting density due to trade-offs between fruit quality and harvestable yield under a constant high planting density. Constant high planting density was expected to result in morphological adaptations to low-light environments, such as undesired flower abortion and fewer, smaller fruits but also a more elongated, open architecture that benefits light interception throughout the canopy. A constant low planting density was hypothesized to intercept the lowest fraction of incident photons and to have the lowest harvestable yield per cultivation area and thus the lowest LUE. A fruit crop, the commercially available dwarf tomato cultivar "Plum Tomato Red", was chosen as the experimental crop.

2 Materials and methods

2.1 Plant material and experimental setup

Dwarf tomato (*Solanum lycopersicum* "Plum Tomato Red", Vreugdenhil, De Lier, the Netherlands) was grown in 12 compartments (plots; 150 × 100 × 83 cm, L × W × H) in a climate-controlled room at 22°C/19°C air temperature, 16-hour photoperiod, 70% relative humidity, and 800 ppm CO_2. Seeds were sown into stonewool plug trays (Rockwool Grodan, Roermond, the Netherlands), covered with a layer of vermiculite, kept 24 hours in the dark in the climate chamber, and then exposed to an incident photosynthetic photon flux density (PPFD) of 213 ± 2.2 µmol m^{-2} s^{-1} which was provided by red (R; 600-700 nm) and blue (B; 400-500 nm) LEDs (89% R and 11% B; Philips, GPL PM 210 DRBWFR_R L150 3.1 C4; Phytochrome Photostationary State (PSS) 0.89, based on Sager et al., 1988). Initial incident PPFD was measured at stonewool block height with a quantum sensor (LI-COR, LI-250A Lincoln, NE, USA). On day 19 after sowing, seedlings with two true leaves were transplanted into stonewool blocks (10 × 10 × 7 cm, L × W × H). Side shoots were removed twice a week upon appearance. Plants were pruned to three trusses with nine flowers each and supported with wooden sticks on day 28 after transplanting (DAT). Plants were grown for 100 DAT. Ebb-and-flow irrigation with nutrient solution was supplied twice per week from 0 to 50 DAT and daily from 50 to 100 DAT. The nutrient

solution (electrical conductivity 2.1 dS/m, pH 5.5) contained 1.2 mM NH_4^+, 7.2 mM K^+, 4.0 mM Ca^{2+}, 1.8 mM Mg^{2+}, 12.4 mM NO_3^-, 3.3 mM SO_4^{2-}, 1.0 mM PO_4^{2-}, 35 µM Fe^{3+}, 8.0 µM Mn^{2+}, 5.0 µM Zn^{2+}, 20 µM B, 0.5 µM Cu^{2+}, and 0.5 µM MoO_4^{2-}.

2.2 Treatments

Four treatments, with two constant planting densities (high density and low density) and two dynamic spacing treatments (90% ground coverage [GC] and 75% GC), resulted in 100, 19, 54, and 41 plants/m^2 averaged over 100 days from transplant to destructive harvest (detailed information on spacing in Supplementary S1). High planting density was chosen based on the smallest stonewool block size (10 × 10 × 7 cm) available for growing dwarf tomato. Low planting density was chosen based on information provided by the breeder, who reported a final plant distance of 25 cm for "Plum Tomato Red" plants (Petra Molenaar, pers. comm.), which was implemented in a checkerboard pattern (25-cm interplant distance within rows and 21.6-cm distance between rows). On 0 DAT, the dynamic spacing treatments were arranged identically to the high density. Ground coverage was measured twice per week using the smartphone application "Canopy Cover Free" (based on the "Easy Leaf Area" software, Easlon and Bloom, 2014; Supplementary S1). When ground coverage exceeded 90% and 75% for the 90% GC and 75% GC treatments, respectively, plants were manually spaced apart to 90% and 75%, respectively. Spacings, and thus a reduction in ground coverage, took place under 75% GC on 21, 35, 42, and 49 DAT and under 90% GC on 28, 42, and 49 DAT (Figure 1A).

2.3 Plant morphology

Truss and flower pruning to three trusses with nine flowers each allowed for a maximum of 27 fruits per plant. Measurements were performed on each of the 12 replicate plants per plot. Flower and green fruit numbers were recorded weekly. Harvest of fully red-ripe fruits took place twice per week from 70 to 100 DAT. Harvested fruits were recorded for each plant. Fruit number and fresh weight were recorded collectively for each truss position per plot. The 100-day and annual harvestable yields (3.65 times 100-day yield) of 1 m^2 were calculated based on the average planting density and yield per plot (i.e., 12 plants; Figure 2B). At each harvest, up to three fruits from the three truss positions per plot were used to determine individual fruit weight and quality parameters. Fruits were dried in a ventilated oven for 48 hours (4 hours at 70°C and 44 hours at 105°C) to determine dry weight. On 99 DAT, the temperatures of a top leaf and the stem base of each plant were measured using an infrared thermometer (Fluke 63 Infrared Thermometer).

On 100 DAT, all remaining ripe and unripe fruits were harvested. Fruits with blossom-end rot were excluded from the harvestable fruit yield and were not considered in the calculation of dry matter partitioning. Green fruits were considered for calculating dry matter partitioning but were not considered as harvestable yield. Before destructively harvesting plants from their plot, dropped leaves were collected from underneath the canopy and included in the leaf dry weight. Plants were dissected into leaves and stems (including trusses), and the existing leaves and leaf scars were counted. Stem diameter was measured using a caliper at the stem base along the smaller side of the cross-section. Stem length from the stem base to the beginning of the top leaf or truss was measured using a measuring tape. Leaf area was determined using an LI-3100 Area Meter (LI-COR, Lincoln, UK) and used to calculate the final LAI. Stonewool blocks, including roots, were discarded. All above-ground plant material was oven-dried for 48 hours (4 hours at 70°C and 44 hours at 105°C).

2.4 Yield components and light-use efficiency

Treatment effects on fresh fruit weight were analyzed based on the underlying yield components (Figure 2). Total fruit fresh weight refers to green and red-ripe fruit dry weight divided by fruit dry matter content. Total fruit dry weight depends on plant dry weight and assimilate partitioning to fruits. Plant dry weight accumulation is driven by light interception. Plant morphological parameters such as LAI, plant compactness, dry matter allocation, and specific leaf area influence the plants' efficiency in converting light into biomass. Harvested fruit fresh weight per plant is the product of the red-ripe fruit number per plant and their mean individual fruit fresh weight.

Incident and intercepted LUE were calculated as the ratio of harvested fruit fresh weight (g/m^2 over 100 days) to the cumulative incident and intercepted PPFD, respectively. Intercepted light was estimated to be the product of the incident daily light integral (DLI; cumulative PPFD per day) and ground coverage, which was measured twice per week and linearly interpolated to obtain daily values. Incident DLI was calculated based on canopy height and PPFD measurements at different canopy heights. Daily canopy height was calculated based on weekly measured canopy height (from 0 to 42 DAT) and individual plant height measurements on 99 DAT and linear interpolation between measurements (Supplementary S3). Canopy-incident PPFD increased from 213 ± 2.2 µmol m^{-2} s^{-1} (12.5 mol m^{-2} day^{-1}) at the cultivation start to 249 ± 2.8 µmol m^{-2} s^{-1} (14.3 mol m^{-2} day^{-1}) at the final average canopy height (indicated as a gray line in Figure 1C; Supplementary S3C).

2.5 Fruit quality

Fruit quality measurements were performed on red-ripe harvested fruits without blossom-end rot that were not located in the first position of the truss. Individual fruit fresh weight, length, diameter, and hardness were measured. Fruit hardness, expressed as the maximum force (N) needed for penetration of the probe (2.5 mm diameter) into the fruit through the tomato skin, was measured using a Zwick machine (Zwick/Roell 2.5kN zwicki RetroLine, Ulm, Germany). Fruits were held in place by a perforated metal cylinder (outer diameter 19.9 mm, inner diameter 8.3 mm, height 23 mm, and hole depth 18 mm). Then, the juice of individual fruits was squeezed into Eppendorf

10.3389/fpls.2024.1386950

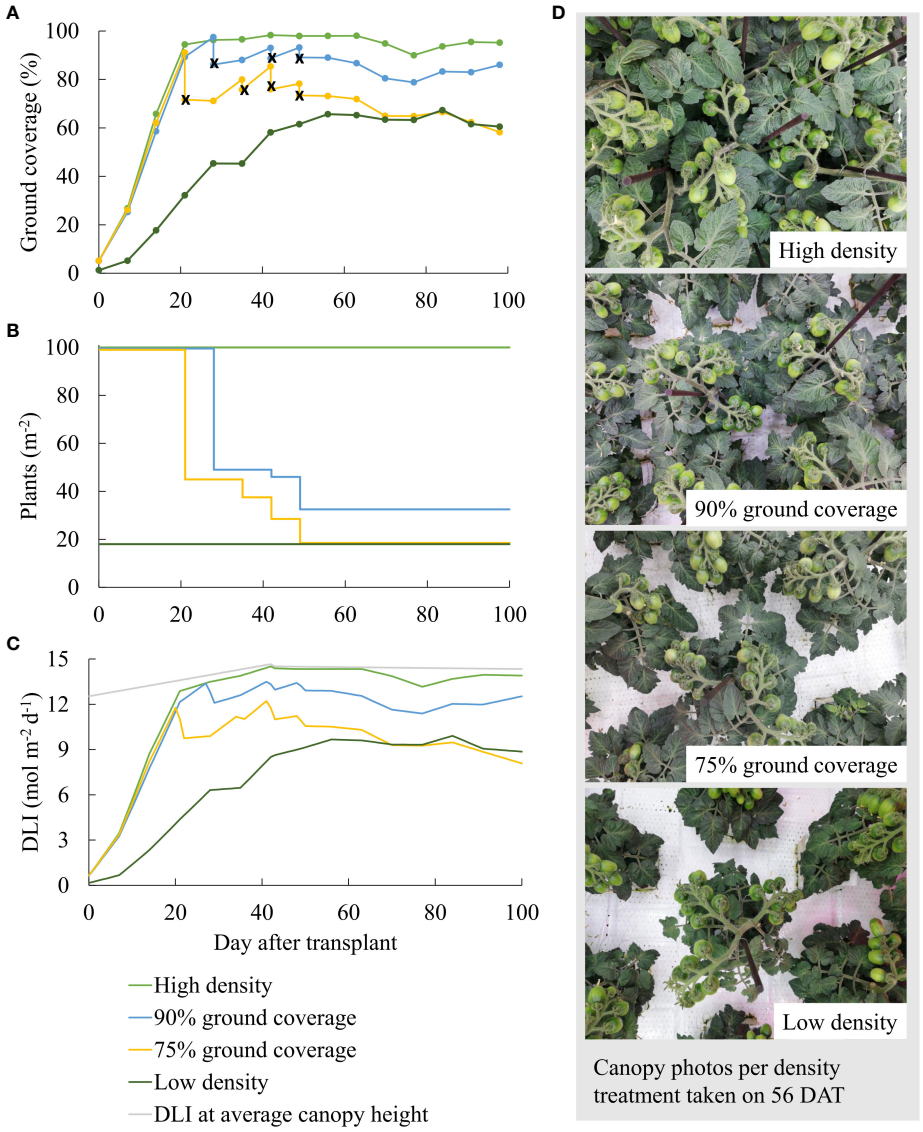

FIGURE 1
(A) Ground coverage, **(B)** resulting planting densities, **(C)** incident (in gray) and intercepted daily light integral (DLI; in colors) per day after transplant, and **(D)** representative canopy photos taken on 56 DAT per density treatment. In **(A)** ground coverage after the spacing of the plants is indicated with an x. In **(C)** the light gray line indicates incident daily light integral (DLI) at average canopy height across all treatments. The density treatments resulted in 100, 54, 41, and 19 plants per m^2 averaged over the whole growth cycle.

tubes, from which one drop was transferred to the Atago Pocket Brix-Acidity Meter (PAL-BX|ACID Fukaya-Shi, Saitama, Japan) to determine the total soluble solid content (°Brix). The tubes were stored at −80°C. After defrosting, fruit juice was diluted 50-fold with pure water to measure the titratable acid content (% citric acid) using the Atago Pocket Brix-Acidity Meter (Fanwoua et al., 2019; Ji et al., 2019; Ji et al. 2020).

2.6 Statistical setup and analysis

The experiment was designed as a randomized complete block design with four treatments and three replications in space, with repetitions in space representing the blocks. Nevertheless, no block effects were found; thus, the data were analyzed using a completely randomized design. Each plot consisted of 12 replicate plants (three rows of four plants), which were surrounded by a row of border plants. The Shapiro–Wilk test was applied to test for the normality of the residuals. Equal variances were assumed due to the low number of replicates. A one-way analysis of variance (ANOVA) was conducted followed by mean separation according to Fisher's protected least significant difference (LSD) test ($p = 0.05$). In one occasion (intercepted DLI per plant in Table 1), the normality of residuals was rejected by the Shapiro–Wilk test; the QQ plot was examined visually, and the data were deemed adequate to perform a subsequent ANOVA.

10.3389/fpls.2024.1386950

TABLE 1 Plant morphological parameters, canopy-incident daily light integral (DLI), and intercepted DLI per plant.

	High density	90% GC	75% GC	Low density	p-Value of F-statistic
Canopy height averaged over 100 days (cm)	20.6 a	19.5 b	18.3 c	18.4 c	0.00***
Incident light intensity averaged over 100 days (mol m^{-2} day^{-1})	14.4 a	14.2 b	14.1 c	14.1 c	0.00***
Intercepted light intensity averaged over 100 days (mol day^{-1} per plant)	0.12 c	0.20 b	0.22 b	0.38 a	0.00***
Internode length (cm)	2.4 a	2.1 ab	2.0 b	1.9 b	0.02*
Basal stem diameter (mm)	6.1 c	8.5 b	9.0 a	9.0 a	0.00***
Slenderness (%; cm/cm)	0.4 a	0.3 b	0.2 c	0.2 c	0.00***
Specific stem length (cm/g)	11.3 a	5.2 b	4.1 bc	3.7 c	0.00***

Letters indicating significant differences [least significant difference (LSD) test] between treatments and the p-value of the F-statistic are provided (*$p < 0.05$ and ***$p < 0.001$). Data are the means over three blocks (n = 3), each with a canopy consisting of 12 replicate plants. The density treatments resulted in 100, 54, 41, and 19 plants per m^2 on average.
GC, ground coverage.

3 Results

3.1 High planting density increased light interception, especially during early cultivation

Higher planting density resulted in higher ground coverage and hence higher light interception, particularly early during cultivation (Figure 1). Incident PPFD at the canopy top slightly increased when the canopy grew in height. Canopy height was slightly larger at high density (Table 1).

Ground coverage was used as a proxy for the fraction of the intercepted PPFD. The initial increase in ground coverage over time was due to the rapid leaf expansion of young plants (0–20 DAT in Figure 1A). From 21 DAT, manual spacing primarily determined ground coverage differences between the density treatments. During fruiting (75–100 DAT), numerous fruits were located on top of the canopy and were (falsely) detected as leaf areas while they were green and as non-leaf areas while they were red.

3.2 Higher light interception resulted in more plant and fruit biomass

Differences in light interception (Figures 1C, 3F) were primarily caused by differences in ground coverage, which decreased by 43% at low density compared to high density. Differences in incident PPFD were less of a consequence of differences in plant height, which varied by a maximum of 11% (75% GC compared to high density in Table 1). In addition to the resulting highest light

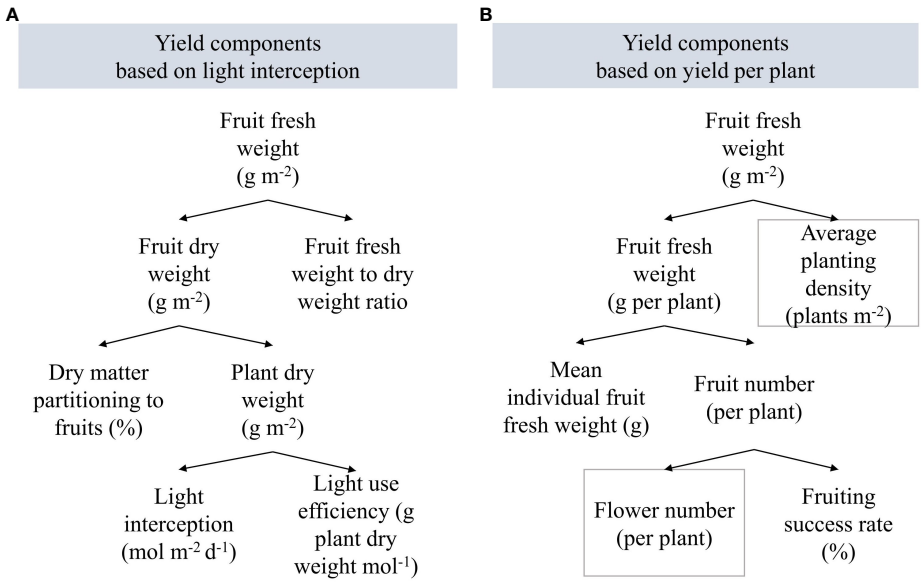

FIGURE 2
Yield components **(A)** based on light interception, dry matter partitioning, and fresh weight to dry weight ratio, and **(B)** based on fruiting success rate, fruit number and size, and average planting density. Gray boxes indicate fixed parameters.

10.3389/fpls.2024.1386950

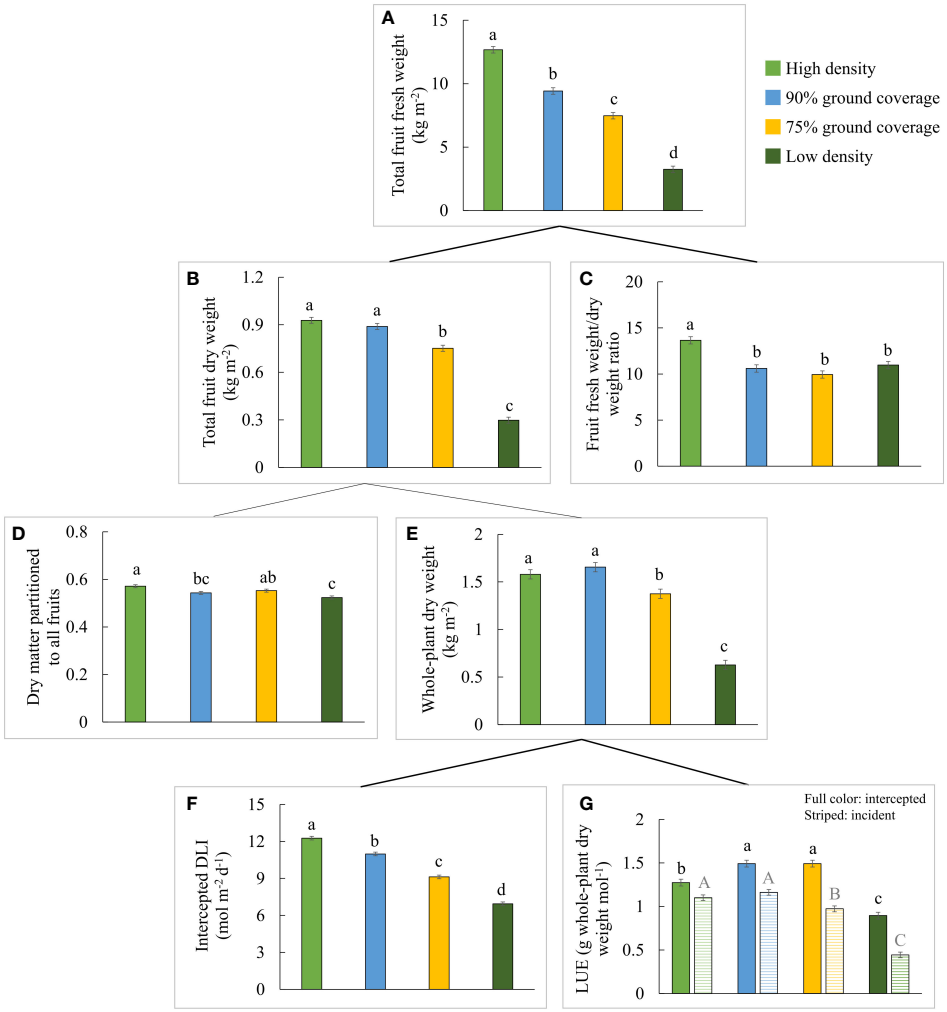

FIGURE 3
Effects of planting density on yield components constituting the total fruit fresh weight of all (red-ripe and green) fruits from a 1-m^2 cultivation area over 100 days: **(A)** total fruit fresh weight, **(B)** total fruit dry weight, **(C)** fruit fresh weight to dry weight ratio, **(D)** dry matter partitioned to fruits, **(E)** cumulative whole-plant dry weight, **(F)** intercepted daily light integral (DLI), and **(G)** intercepted (full color) and incident (striped) whole-plant light use efficiency. The letters indicate significant differences [least significant difference (LSD) test, p = 0.05]. Data are the means over three blocks (n = 3), each with a canopy consisting of 12 replicate plants, surrounded by border plants. Error bars indicate standard errors of means. The density treatments resulted in 100, 54, 41, and 19 plants per m^2 on average.

interception (Figure 3F), a constant high planting density produced the highest total fruit fresh weight per m^2 (Figure 3A), although the total fruit dry weight per m^2 was not significantly different from 90% GC (Figure 3B). Whole-plant dry weight per m^2 was the highest at high density and 90% GC (Figure 3E). The efficiency of a plant to convert light that was intercepted at the top leaves to plant dry weight was highest at 90% and 75% GC, lower at high density, and lowest at low density (Figure 3G). Whole-plant incident LUE was higher at higher planting densities (Figure 3G).

A slightly higher partitioning of dry matter to fruits was observed at high density compared to low density (Figure 3D). Dry matter partitioned to the leaves did not differ significantly between the density treatments, but dry matter partitioned to the stem increased from high to low density (Figure 4). Absolute stem dry weight and absolute leaf dry weight per plant on day 100 were more than doubled under all other densities compared to high densities.

3.3 High planting density resulted in the highest fruit yield per area despite fruit yield reductions per plant

High density resulted in 11.1 kg/m^2 fruit weight of red-ripe harvested fruits over 100 days. Thus, 40.5 kg/m^2 annual harvestable fruit yield can be obtained under continuous high-density cultivation. Compared to high density, the dynamic spacing and low-density treatments resulted in 18%, 36%, and 71% reductions in red-ripe fruit fresh weight per m^2 (Figure 5; Supplementary S4). At the plant level, high density resulted in reduced productivity: it had the lowest fruit fresh weight per plant, individual fruit fresh weight, fruit number per plant, and also the lowest fraction of flowers that turned into harvested ripe fruits (fruiting success rate; i.e., most flower abortion and non-ripened fruits on 100 DAT). High density yielded on average 2.83 unripe fruits per plant on day 100, more than 90% GC (0.94 unripe fruits), 75% GC (0.94 unripe fruits), and

10.3389/fpls.2024.1386950

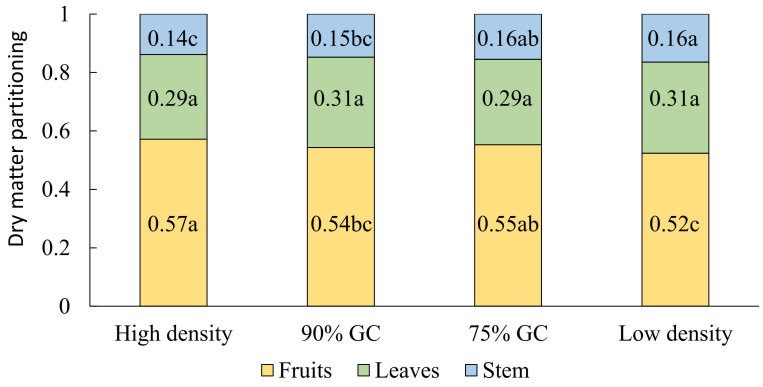

FIGURE 4
Effects of planting density on the fraction of dry matter partitioned among all (red-ripe and green) fruits, stem plus trusses, and leaves. Means followed by different letters indicate significant differences [least significant difference (LSD) test, p = 0.05]. Data are the means over three blocks (n = 3), each with a canopy consisting of 12 replicate plants. The density treatments resulted in 100, 54, 41, and 19 plants per m^2 on average. GC, ground coverage.

low density (0.56 unripe fruits). No significant density-driven temperature differences were observed: on 98 DAT, neither the temperatures of leaves at the top of the canopy nor those of stems close to its base were statistically different between the treatments. There was no noticeable difference between treatments regarding the timing of flowering and fruit ripening (Supplementary S5).

3.4 Plants grown at higher planting densities converted light more efficiently into fruit yield

Higher planting density resulted in a higher efficiency of plants in converting incident and intercepted PPFD into red-ripe fruits (Figure 6). Intercepted DLI per plant was more than tripled (+206%) at low density compared to high density (Table 1), while fresh fruit weight per plant was 55% higher (Figure 5). Internode elongation with increasing density showed that plants were less compact at high density (Table 1). Stem diameter was reduced at high density (Table 1). Thus, plant slenderness (height of plants over diameter of stems) and specific stem length (stem length divided by stem mass) were higher at high density (Table 1). At low density, leaf area per plant was 55% and leaf dry weight 192% higher than at high density, resulting in reductions in specific leaf area (Figure 7). Each plant initiated on average 10.8 leaves, with no significant differences between treatments. High-density plants had dropped on average 4.9 of their lowest leaves until day 100, thus resulting in a higher observed dry matter partitioning to fruits compared to leaves at the final harvest. Leaf dropping occurred less in the other densities (maximum 0.75 leaves per plant under low density). LAI on day 100 (excl. senescent leaves) was highest at high density (6.7), lower at 90% GC (3.9), and lowest at 75% GC and low density (2.1 and 2.2, respectively).

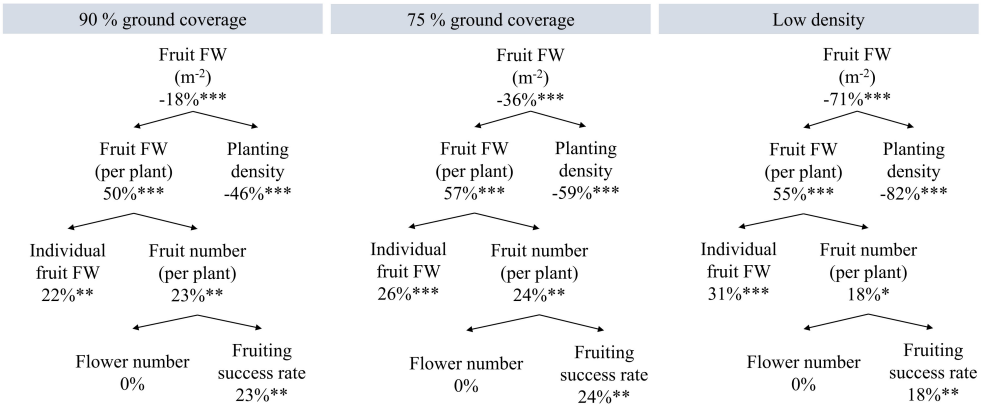

FIGURE 5
Effects of planting density on yield components constituting fruit fresh weight (FW) of red-ripe harvested fruits from a 1-m^2 cultivation area over 100 days. Percentages are the increments compared to high density. High density resulted in 11.1 kg fruit FW m^{-2}, 111 g fruit FW per plant; 100 plants/m^2 average planting density; 19.4 harvested fruits per plant; 5.7 g average FW per fruit; 27 flowers per plant (plants had been pruned to 27 flowers); and a 72% flower fruiting success rate. *p < 0.05, **p < 0.01, and ***p < 0.001. Data are the means over three blocks (n = 3), each with a canopy consisting of 12 replicate plants.

10.3389/fpls.2024.1386950

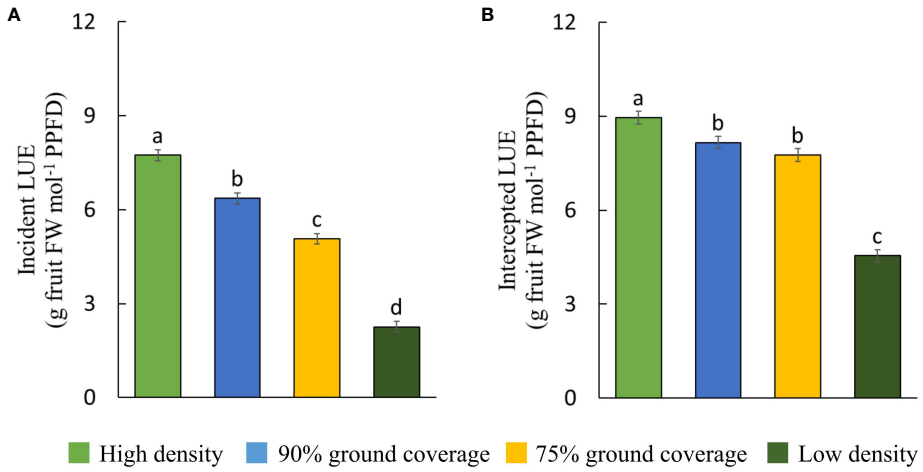

FIGURE 6
Light use efficiency (LUE) of **(A)** incident and **(B)** intercepted photosynthetic photon flux density per density treatment. Fruit fresh weight refers to harvested red-ripe fruits over 100 days. The letters indicate significant differences [least significant difference (LSD) test, p = 0.05]. Data are the means over three blocks (n = 3) each with a canopy consisting of 12 replicate plants. Error bars indicate standard errors of means. The density treatments resulted in 100, 54, 41, and 19 plants per m^2 on average.

3.5 Dynamic spacing mitigated fruit quality-reducing effects of high planting density

Fruit quality was reduced at high density (Table 2). No or marginal fruit quality differences were observed between 90% GC, 75% GC, and low density. Individually measured fresh fruit weight and fruit size were reduced at high density. Individual fruit weight measurements were consistent with the results of the calculated individual fresh fruit weight (total fresh fruit weight divided by fruit number; Figure 5). At high density, fruit hardness, total soluble solid content, and citric acid content were the lowest. The ratio between soluble solids and acidity was not significantly different between treatments. Blossom-end rot in red-ripe fruits hardly occurred; however, more fruits were affected at low density (2.5%) compared to all other densities (0.3%–0.5%). The variability of fruit length and diameter within each plot did not differ significantly between planting densities, but total soluble solid content was less uniform at constant high density compared to all lower densities (Table 2).

4 Discussion

4.1 Maintaining high ground coverage based on canopy photos improves space and light use

Dynamic spacing can be used to maintain high ground coverage to allow for efficient use of incident light while avoiding competition-induced assimilate shortages at the plant level. Much light is lost when plants are young and do not intercept all available light. Light is also lost after seedlings are transplanted to pots or substrate blocks. Providing far-red light (700–750 nm) can accelerate early leaf expansion, canopy closure, and subsequent light interception (Jin et al., 2021; Carotti et al., 2023) until dynamic spacing is adequate to control ground coverage.

In our experiment, growing transplanted seedlings at the maximum possible density resulted in faster canopy closure and higher daily light interception than under low density (Figure 1C). The steep increase in ground coverage under 100 plants/m^2 during early cultivation indicates that dynamic spacing is advantageous

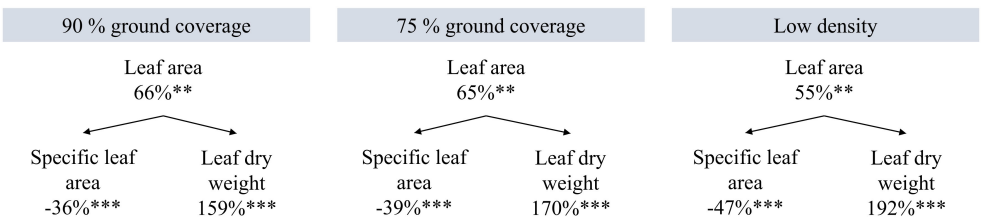

FIGURE 7
Effects of planting density on leaf area, specific leaf area, and leaf dry weight per plant on day 100. Percentages are the increments compared to high density. High density resulted in 733 cm^2 leaf area per plant, 203 cm^2/g specific leaf area, and 3.6 g leaf dry weight per plant. **p < 0.01, and ***p < 0.001. Data are the means over three blocks (n = 3) each with a canopy consisting of 12 replicate plants.

10.3389/fpls.2024.1386950

TABLE 2 Fruit quality parameters of red-ripe fruits based on individual fruit measurements per density treatment between 70 and 100 DAT (total fruit n = 835, with high-density n = 181, 90% GC n = 218, 75% GC n = 226, and low-density n = 210).

	High density	90% GC	75% GC	Low density	p-Value of F-statistic
Fruit weight (g per fruit)	6.0 b *CV 0.15 a*	7.3 a *CV 0.11 b*	7.4 a *CV 0.13 ab*	7.6 a *CV 0.13 ab*	0.00*** *0.11 ns*
Fruit length (mm)	22.7 b *CV 0.06 a*	24.8 a *CV 0.05 a*	25.0 a *CV 0.05 a*	25.0 a *CV 0.05 a*	0.00*** *0.50 ns*
Fruit diameter (mm)	21.1 b *CV 0.07 a*	22.4 a *CV 0.06 a*	22.3 a *CV 0.07 a*	22.8 a *CV 0.07 a*	0.00*** *0.40 ns*
Fruit hardness (N_{max})	5.5 c *CV 0.21 b*	7.2 ab *CV 0.23 b*	7.4 a *CV 0.23 ab*	6.7 b *CV 0.26 a*	0.00*** *0.07 ns*
Total soluble solids (°Brix)	6.6 c *CV 0.11 a*	8.9 b *CV 0.06 b*	9.4 a *CV 0.05 b*	9.4 a *CV 0.04 b*	0.00*** *0.00***
Titratable acids (% citric acid)	0.8 b *CV 0.25 a*	1.0 a *CV 0.27 a*	1.0 a *CV 0.26 a*	1.0 a *CV 0.24 a*	0.00*** *0.81 ns*
Ratio of total soluble solids to titratable acid	9.4 a *CV 0.33 a*	9.6 a *CV 0.34 a*	9.8 a *CV 0.36 a*	9.9 a *CV 0.25 a*	0.58 ns *0.55 ns*
Blossom end rot (% of all red-ripe harvested fruits)	0.5 b	0.3 b	0.5 b	2.5 a	0.07 ns

Letters indicating significant differences [least significant difference (LSD) test] between treatments and the p-value of the F-statistic are provided (***p < 0.001). Data are the means over three blocks (n = 3) each with a canopy consisting of 12 replicate plants. The coefficient of variation (CV) within a plot is shown in italics. The density treatments resulted in 100, 54, 41, and 19 plants per m^2 on average.
GC, ground coverage; ns, non-significant difference.

over growing plants constantly at the spacing treatment's average planting density (e.g., constant 54 plants/m^2 instead of step-wise decreasing density from 100 to 32.5 plants/m^2 at 90% GC; Supplementary Table S1C). Accelerating canopy closure during early cultivation by growing at high planting density allows for higher intercepted DLI (Figure 1) and whole-plant LUE (Figure 3G), which result in more biomass and fruit yield per cultivation area (Figures 3E, A). Nevertheless, planting density must be reduced before plants develop yield-reducing responses to high densities, such as flower abortion (Papadopoulos and Ormrod, 1991). By maintaining 90% ground coverage, a percentage close to 100%, we aimed for a high harvestable fruit yield without reducing quality.

Ground coverage was measured based on bird's-eye view photos of the canopy, which is easily applicable, fast, and non-destructive. Yet, actual light interception occurs at multiple leaf layers, not only at the top leaves. We decided against dynamic spacing based on LAI since LAI determination requires regular destructive measurements and lacks practicability for implementation in commercial vertical farms. Utilizing the app "Canopy Cover Free", ground coverage was determined based on the ratio of green (500–600 nm) to red (600–700 nm) in the photo (Easlon and Bloom, 2014).

4.2 Individual plants experience assimilate shortage at very high planting densities

Light interception depends on the percentage of cultivation area covered by plants. In line with Postma et al. (2021), we showed that planting density affects plant dry weight per cultivation area (Figure 3E) and light interception (Figure 3F). Under constant high planting density, the final whole-plant dry weight per area was not significantly higher than at 90% GC, which indicates a lower assimilate availability per plant. Further, the dropping of lower, shaded leaves at high density caused an underestimation of the total dry weight produced per plant over 100 days. Dropped leaf biomass was collected from underneath the dense canopy prior to the destructive harvest, but in the meantime, leaf dry weight was lost through decomposition. Lost leaf biomass resulted in an underestimation of dry matter partitioning to leaves and an overestimation of dry matter partitioning to fruits and stems (Figures 3D, 4). Under constant high density, dry matter partitioned to fruits was higher compared to lower densities, but the fruit number per plant was lower. Thus, we propose that the sink strength of individual fruits may have increased under constant high density. Distal fruits on a truss were reported to have a lower fruit sink strength than fruits located higher on the truss (Bertin, 1995). At high density, mostly distal flowers were aborted. Consequently, individual fruit sink strength at high densities may have been higher than under lower densities.

4.3 Flower abortion and reduced assimilate availability limit fruit yield per plant at high planting density

Higher planting density resulted in higher plant dry weight, fruit dry weight, and fruit fresh weight per cultivation area (Figures 3E, B, 5). Similarly, harvestable greenhouse tomato yield per area was reported to increase under constantly higher (Heuvelink, 1995) or dynamically increased stem densities (Cockshull and Ho, 1995). Postma et al. (2021) found that total and generative dry weight per area increases with planting density, but only until a density threshold

is exceeded and plant-level resource deficiencies inhibit growth. In our experiment, whole-plant dry weight per cultivation area (Figure 3E) and productivity per plant (Figure 5) showed those density-driven limitations under constant high density. For instance, the lowest flowers per plant (max. 27) developed into red-ripe fruits compared to all other densities due to higher flower abortion, higher breaking-off of green fruits, and possibly slower ripening (Figure 5; Supplementary Figure S5B). The latter indicates that plant development was slowed down by a few days at constant high density; thus, marginally more harvestable fruit yield could be obtained with a longer cultivation cycle for the remaining green fruits to turn fully red, but at the expense of LUE.

Interestingly, we did not find a significant vertical temperature gradient within the canopies. Still, temperature gradients within dense canopies can be expected, especially since controlled environments are generally characterized by lower wind speeds compared to open-field production (Poorter et al., 2016). Postma et al. (2021) mentioned a possible (temperature-driven) 2% increase in days until flowering for a wide range of species when planting density is doubled. Source-sink ratios rarely affect flowering rate (de Koning, 1994). However, possibly, fewer assimilates were available to distal fruits on the truss (Bertin, 1995)—like the ones that remained green until day 100 under the high-density treatment (Figure 5).

Assimilate partitioning to the fruits and, consequently, the harvest index (HI; fruit dry weight over total above-ground plant dry weight) in tomatoes is impacted by crop maintenance. For instance, side-shoot removal and pruning affect plant morphology and biomass allocation in the plant. Langenfeld and Bugbee (2023) reported HI (based on fresh weight) ranges of <8% to 46% for eight dwarf tomato cultivars (note that these fractions would have been lower when expressed on a dry mass basis, as the dry matter content of tomato fruits is lower than that of leaves and stems). Those eight cultivars received no side-shoot removal (Noah Langenfeld, pers. comm.), which certainly resulted in higher assimilate partitioning to vegetative plant organs and reduced HI. In our experiment, dry matter partitioning to fruits was above 50% for all densities.

4.4 Plant acclimation to high planting densities increases light use efficiency

Generally, it is expected that incident LUE increases with higher planting densities (Figure 6A; Jin et al., 2023). Postma et al. (2021) found that yield reductions per cultivation area when doubling planting densities are smaller than reductions in resource use (e.g., space and light); thus, resource use efficiency increases. We observed marginal increases in incident PPFD due to a slight increase in canopy height with increasing planting density and because PPFD was higher closer to the lamps (Table 1). Within a canopy, most incident light is usually intercepted at an LAI of three to four in a wide range of crops, with hardly any gain at higher LAIs (Heuvelink et al., 2004; Postma et al., 2021). At the final harvest, high density resulted in an excessively high LAI despite the prior dropping of leaves, 90% GC in a desirable LAI, and 75% GC and low density in low LAIs.

Maximum reported incident LUE ranges from 1.26 to 1.81 g dry weight per mol photons for canopies that intercept 90%–95% of incident light (e.g., Loomis and Williams, 1963; Zhu et al., 2010; in Jin et al., 2023). Whole-plant incident LUEs for dwarf tomato grown over 100 days under dynamic and constantly high planting densities (1.16 g/mol under 90% GC and 1.10 g/mol at high density) are close to the maximum reported LUE. This may be possible due to the achievement of high instantaneous incident LUEs during early cultivation, which are usually—at constant and lower planting densities—low at transplant and increase with leaf expansion until final harvest (Jin et al., 2023).

In this study, the morphological responses to high planting densities differ from the mentioned references, e.g., from the reviews on shade avoidance (Franklin, 2008) and planting density (Postma et al., 2021), in that there was no solar light—importantly, no far-red light— present in the applied red-blue light spectrum. Also, root zone competition in the stonewool blocks was assumed to be absent and was not assessed. Typical shade avoidance responses of plants grown in soil and under solar light are adaptations to complex interactions of reduced light intensity, reduced red-to-far-red ratio within shaded canopies (e.g., Franklin, 2008), and reduced nutrient availability at the plant level. Here, high-density responses were attributed mainly to differences in PPFD.

4.5 Assimilate shortage reduces fruit quality at high planting density

High planting density results in lower individual fruit weight and size, more fruit size variability, and therefore reduced marketability (Cockshull and Ho, 1995; Heuvelink, 1995). We observed a reduction in fruit size, but—contrary to Cockshull and Ho (1995)—no increase in fruit size variability under constant high density (Table 2), which was likely due to truss pruning. A dynamic high planting density (maintaining 90% ground coverage) did not significantly decrease fruit size.

Under constant high density, the total soluble solid content (i.e., sweetness) and citric acid content of red-ripe harvested fruits were reduced (Table 2), and fruit dry matter content increased (Figure 3C). Nevertheless, the sweetness was shown to decline with decreasing fruit size due to a positive correlation between fruit size and the source–sink ratio (Li et al., 2015). The seed company Vreugdenhil aims for 7°Brix (Jan van Heijst, pers. comm.) in this cultivar, which was not achieved at high density, presumably due to assimilate shortage at the plant level. Red-ripe harvested cherry tomatoes were reported to range from 4.5 to 6.9°Brix and 0.1% to 1.4% citric acid content (Borba et al., 2021; del Carmen Damas-Job et al., 2023; Pattanapo et al., 2023), resulting in a sweetness-to-acidity ratio of 10 to 100, a ratio that is slightly higher than we obtained (9.4 to 9.9; Table 2). Malundo et al. (1995) found that perceived tomato flavor benefits from higher sweetness if citric acid content is ≥0.8%. To enhance sweetness, far-red light can be applied to increase dry matter partitioning in fruits and subsequent sugar accumulation in fruits (Fanwoua et al., 2019; Ji et al., 2019; Ji et al., 2020).

Blossom-end rot was observed rarely, but most often at low density. The absence of a closed canopy resulted in higher light interception, likely leading to higher transpiration rates per plant and higher growth rates, thus causing deficiencies in calcium (Hagassou et al., 2019).

Fruit hardness, besides flesh firmness, constitutes fruit texture. Hardness positively influences shelf-life (Beckles, 2012) and perceived visual tomato quality (i.e., surface smoothness; Batu, 2004). The hardness of red-ripe cherry tomatoes at harvest is ca. 2 N (del Carmen Damas-Job et al., 2023; cf., table grapes range from 6 to 11.7 N; Deng et al., 2005; Rolle et al., 2011; Balic et al., 2022). Thus, the observed hardness under all planting densities (Table 2) is within the reported ranges of comparable fruit crops.

4.6 Implementation and future research

The present experiment is proof of the concept that dynamic spacing results in high harvestable fruit yields while mitigating the fruit quality-reducing effects of high planting densities. For implementation, this concept can be tested on a larger scale, extended to different light spectra and other varieties and crops, and in combination with different pruning techniques. Also, dynamic light management, dynamic climate control, and their interactions should be explored to improve resource use efficiency (i.e., energy and space use efficiency) and thus the environmental and economic performance of highly controlled crop production systems. Finally, the economic cost–benefit ratio of spacing must be determined, where benefits are related to yield, and costs are related to increased labor and/or automation. The cost-effectiveness of manual versus automated spacing depends, among others, on the scale of production and the costs of labor and equipment. Ideally, the capacity for automated spacing is considered during the design phase of a new production unit.

5 Conclusions

Our results demonstrate that high ground coverage and thus high light interception throughout cultivation are key to maximizing both yield per area and LUE: plants grown under constant high planting density utilized light most efficiently for fruit yield formation (11.1 kg/m^2 with an LUE of 7.7 g yield mol^{-1} photons incident on the canopy) due to a rapid canopy closure and then consistently high ground coverage of ~96%. Nevertheless, fruit quality was reduced under constant high density. As hypothesized, constant low planting density resulted in the lowest light interception, which resulted in the lowest yield per cultivation area (3.2 kg/m^2) and the lowest LUE (2.3 g yield mol^{-1}). Dynamic spacing—i.e., growing plants initially at a high planting density but then spacing them apart to maintain constant ground coverages of 75% and 90%—resulted in the same fruit quality, but more than double the yield compared to low density. Thus, dynamic spacing mitigates density-induced trade-offs between fruit yield and quality in dwarf tomato.

Data availability statement

The original contributions presented in the study are included in the article/Supplementary Material. Further inquiries can be directed to the corresponding author.

Author contributions

MK: Conceptualization, Data curation, Formal analysis, Investigation, Visualization, Writing – original draft, Writing – review & editing. LM: Conceptualization, Funding acquisition, Methodology, Writing – review & editing. EH: Conceptualization, Funding acquisition, Methodology, Writing – review & editing.

Funding

The author(s) declare financial support was received for the research, authorship, and/or publication of this article. This project was funded by the MERIAN Fund, NWO, the Netherlands.

Acknowledgments

We would like to thank Gerrit Stunnenberg, Dieke Smit, Nik Woning, Sam Loontjes, and Qianxixi Min for their technical assistance and their help with crop maintenance and measurements and Elias Kaiser for helpful advice throughout the project.

Conflict of interest

The authors declare that the research was conducted in the absence of any commercial or financial relationships that could be construed as a potential conflict of interest.

The author(s) declared that they were an editorial board member of Frontiers, at the time of submission. This had no impact on the peer review process and the final decision.

Publisher's note

Supplementary material

The Supplementary Material for this article can be found online at: https://www.frontiersin.org/articles/10.3389/fpls.2024.1386950/full#supplementary-material

References

Amundson, S., Deyton, D. E., Kopsell, D. A., Hitch, W., Moore, A., and Sams, C. E. (2012). Optimizing plant density and production systems to maximize yield of greenhouse-grown 'Trust' Tomatoes. *HortTechnology* 22, pp.44–pp.48. doi: 10.21273/HORTTECH.22.1.44

Balic, I., Olmedo, P., Zepeda, B., Rojas, B., Ejsmentewicz, T., Barros, M., et al. (2022). Metabolomic and biochemical analysis of mesocarp tissues from table grape berries with contrasting firmness reveals cell wall modifications associated to harvest and cold storage. *Food Chem.* 389, 133052. doi: 10.1016/j.foodchem.2022.133052

Batu, A. (2004). Determination of acceptable firmness and colour values of tomatoes. *J. Food Eng.* 61, 471–475. doi: 10.1016/S0260-8774(03)00141-9

Beckles, D. M. (2012). Factors affecting the postharvest soluble solids and sugar content of tomato (Solanum lycopersicum L.) fruit. *Postharvest Biol. Technol.* 63, 129–140. doi: 10.1016/j.postharvbio.2011.05.016

Bertin, N. (1995). Competition for assimilates and fruit position affect fruit set in indeterminate greenhouse tomato. *Ann. Bot.* 75, 55–65. doi: 10.1016/S0305-7364(05)80009-5

Borba, K. R., Aykas, D. P., Milani, M. I., Colnago, L. A., Ferreira, M. D., and Rodriguez-Saona, L. E. (2021). Portable near infrared spectroscopy as a tool for fresh tomato quality control analysis in the field. *Appl. Sci.* 11, 3209. doi: 10.3390/app11073209

Carotti, L., Pistillo, A., Zauli, I., Meneghello, D., Martin, M., Pennisi, G., et al. (2023). Improving water use efficiency in vertical farming: Effects of growing systems, far-red radiation and planting density on lettuce cultivation. *Agric. Water Manage.* 285, 108365. doi: 10.1016/j.agwat.2023.108365

Cockshull, K. E., and Ho, L. C. (1995). Regulation of tomato fruit size by plant density and truss thinning. *J. Hortic. Sci.* 70, 395–407. doi: 10.1080/14620316.1995.11515309

de Koning, A. N. (1994). *Development and dry matter distribution in glasshouse tomato: a quantitative approach* (Wageningen, Netherlands: Wageningen University and Research).

del Carmen Damas-Job, M., Soriano-Melgar, L. D. A. A., Rodríguez-Herrera, R., Peralta-Rodríguez, R. D., Rivera-Cabrera, F., and Martínez-Vazquez, D. G. (2023). Effect of broccoli fresh residues-based extracts on the postharvest quality of cherry tomato (Solanum lycopersicum L.) fruits. *Scientia Hortic.* 317, 112076. doi: 10.1016/j.scienta.2023.112076

Deng, Y., Wu, Y., and Li, Y. (2005). Effects of high O_2 levels on post-harvest quality and shelf life of table grapes during long-term storage. *Eur. Food Res. Technol.* 221, 392–397. doi: 10.1007/s00217-005-1186-4

de Wit, M., Kegge, W., Evers, J. B., Vergeer-van Eijk, M. H., Gankema, P., Voesenek, L. A., et al. (2012). Plant neighbor detection through touching leaf tips precedes phytochrome signals. *Proc. Natl. Acad. Sci.* 109, 14705–14710. doi: 10.1073/pnas.1205437109

Easlon, H. M., and Bloom, A. J. (2014). Easy Leaf Area: Automated digital image analysis for rapid and accurate measurement of leaf area. *Appl. Plant Sci.* 2, 1400033. doi: 10.3732/apps.1400033

Fanwoua, J., Vercambre, G., Buck-Sorlin, G., Dieleman, J. A., de Visser, P., and Génard, M. (2019). Supplemental LED lighting affects the dynamics of tomato fruit growth and composition. *Scientia Hortic.* 256, 108571. doi: 10.1016/j.scienta.2019.108571

Franklin, K. A. (2008). Shade avoidance. *New Phytol.* 179, 930–944. doi: 10.1111/j.1469-8137.2008.02507.x

Godfray, H. C. J., Beddington, J. R., Crute, I. R., Haddad, L., Lawrence, D., Muir, J. F., et al. (2010). Food security: the challenge of feeding 9 billion people. *science* 327, 812–818. doi: 10.1126/science.1185383

Graamans, L., Baeza, E., Van Den Dobbelsteen, A., Tsafaras, I., and Stanghellini, C. (2018). Plant factories versus greenhouses: Comparison of resource use efficiency. *Agric. Syst.* 160, 31–43. doi: 10.1016/j.agsy.2017.11.003

Hagassou, D., Francia, E., Ronga, D., and Buti, M. (2019). Blossom end-rot in tomato (Solanum lycopersicum L.): A multi-disciplinary overview of inducing factors and control strategies. *Scientia Hortic.* 249, 49–58. doi: 10.1016/j.scienta.2019.01.042

Heuvelink, E. (1995). Effect of plant density on biomass allocation to the fruits in tomato (Lycopersicon esculentum Mill.). *Scientia Hortic.* 64, 193–201. doi: 10.1016/0304-4238(95)00839-X

Heuvelink, E., Bakker, M. J., Elings, A., Kaarsemaker, R. C., and Marcelis, L. F. M. (September 2004). Effect of leaf area on tomato yield. *Acta Hortic.* 691, 43–50. doi: 10.17660/ActaHortic.2005.691.2

Ioslovich, I., and Gutman, P. O. (2000). Optimal control of crop spacing in a plant factory. *Automatica* 36, 1665–1668. doi: 10.1016/S0005-1098(00)00086-8

Ji, Y., Nunez Ocana, D., Choe, D., Larsen, D. H., Marcelis, L. F. M., and Heuvelink, E. (2020). Far-red radiation stimulates dry mass partitioning to fruits by increasing fruit sink strength in tomato. *New Phytol.* 228, 1914–1925. doi: 10.1111/nph.16805

Ji, Y., Ouzounis, T., Courbier, S., Kaiser, E., Nguyen, P. T., Schouten, H. J., et al. (2019). Far-red radiation increases dry mass partitioning to fruits but reduces Botrytis cinerea resistance in tomato. *Environ. Exp. Bot.* 168, 103889. doi: 10.1016/j.envexpbot.2019.103889

Jin, W., Formiga Lopez, D., Heuvelink, E., and Marcelis, L. F. M. (2023). Light use efficiency of lettuce cultivation in vertical farms compared with greenhouse and field. *Food Energy Secur.* 12, e391. doi: 10.1002/fes3.391

Jin, W., Urbina, J. L., Heuvelink, E., and Marcelis, L. F. M. (2021). Adding far-red to red-blue light-emitting diode light promotes yield of lettuce at different planting densities. *Front. Plant Sci.* 11. doi: 10.3389/fpls.2020.609977

Kozai, T., Amagai, Y., and Hayashi, E. (2019). "Towards sustainable plant factories with artificial lighting (PFALs): From greenhouses to vertical farms," in *Achieving sustainable greenhouse cultivation* (Cambridge, UK: Burleigh Dodds Science Publishing), 177–202.

Langenfeld, N., and Bugbee, B. (2023). Evaluation of micro-dwarf tomato cultivars for controlled environment research. *Crop Psychol. Lab.*, 1.

Leakey, R. R. B. (1971). The effect of changing plant density on floral initiation and development of barley (cv. Sultan). *J. Agric. Sci.* 77, 135–139. doi: 10.1017/S0021859600023571

Li, T., Heuvelink, E. P., and Marcelis, L. F. M. (2015). Quantifying the source–sink balance and carbohydrate content in three tomato cultivars. *Front. Plant Sci.* 6. doi: 10.3389/fpls.2015.00416

Liu, Y., Kusuma, P., and Marcelis, L. F. M. (2023). "Research and technology in plant factories with artificial lighting: past, present and future," in *Advances in plant factories: New technologies in indoor vertical farming* (Cambridge, UK: Burleigh Dodds Science Publishing), 39–72.

Loomis, R. S., and Williams, W. A. (1963). Maximum crop productivity: An estimate. *Crop Sci.* 3, 67–72. doi: 10.2135/cropsci1963.0011183X000300010021x

Malundo, T. M. M., Shewfelt, R. L., and Scott, J. W. (1995). Flavor quality of fresh tomato (Lycopersicon esculentum Mill.) as affected by sugar and acid levels. *Postharvest Biol. Technol.* 6, 103–110. doi: 10.1016/0925-5214(94)00052-T

Papadopoulos, A. P., and Ormrod, D. P. (1991). Plant spacing effects on growth and development of the greenhouse tomato. *Can. J. Plant Sci.* 71, 297–304. doi: 10.4141/cjps91-040

Pattanapo, W., Wanchai, K., and Chanasut, U. (2023). Effects of electrolyzed reducing water on pesticides reduction and postharvest qualities in cherry tomato. *Natural Life Sci. Commun.* 22, e2023056. doi: 10.12982/NLSC.2023.056

Poorter, H., Fiorani, F., Pieruschka, R., Wojciechowski, T., van der Putten, W. H., Kleyer, M., et al. (2016). Pampered inside, pestered outside? Differences and similarities between plants growing in controlled conditions and in the field. *New Phytol.* 212, 838–855. doi: 10.1111/nph.14243

Postma, J. A., Hecht, V. L., Hikosaka, K., Nord, E. A., Pons, T. L., and Poorter, H. (2021). Dividing the pie: A quantitative review on plant density responses. *Plant Cell Environ.* 44, 1072–1094. doi: 10.1111/pce.13968

Rolle, L., Giacosa, S., Gerbi, V., and Novello, V. (2011). Comparative study of texture properties, color characteristics, and chemical composition of ten white table-grape varieties. *Am. J. Enology Viticulture* 62, 49–56. doi: 10.5344/ajev.2010.10029

Sager, J. C., Smith, W. O., Edwards, J. L., and Cyr, K. L. (1988). Photosynthetic efficiency and phytochrome photoequilibria determination using spectral data. *Trans. ASAE* 31, 1882–1889. doi: 10.13031/2013.30952

Weiner, J., and Freckleton, R. P. (2010). Constant final yield. *Annu. Rev. Ecology Evolution Systematics* 41, 173–192. doi: 10.1146/annurev-ecolsys-102209-144642

Zeidler, C., Schubert, D., and Vrakking, V. (2017). *Vertical farm 2.0: Designing an economically feasible vertical farm-A combined European endeavor for sustainable urban agriculture* (Munich, Germany: Association for Vertical Farming). Available at: https://elib.dlr.de/116034/. Doctoral dissertation.

Zhu, X. G., Long, S. P., and Ort, D. R. (2010). Improving photosynthetic efficiency for greater yield. *Annu. Rev. Plant Biol.* 61, 235–261. doi: 10.1146/annurev-arplant-042809-112206

frontiers | Frontiers in Plant Science

TYPE Original Research
PUBLISHED 30 April 2024
DOI 10.3389/fpls.2024.1383100

OPEN ACCESS

EDITED BY
Antonio Pannico,
University of Naples Federico II, Italy

REVIEWED BY
Antonio Ferrante,
University of Milan, Italy
Giuseppe Carlo Modarelli,
University of Naples Federico II, Italy
Jung Eek Son,
Seoul National University, Republic of Korea
Obyedul Kalam Azad,
Boise State University, United States

*CORRESPONDENCE
Leo F. M. Marcelis
leo.marcelis@wur.nl

†These authors share first authorship

RECEIVED 06 February 2024
ACCEPTED 15 April 2024
PUBLISHED 30 April 2024

CITATION
Van Brenk JB, Courbier S, Kleijweg CL, Verdonk JC and Marcelis LFM (2024) Paradise by the far-red light: Far-red and red:blue ratios independently affect yield, pigments, and carbohydrate production in lettuce, *Lactuca sativa*.
Front. Plant Sci. 15:1383100.
doi: 10.3389/fpls.2024.1383100

Paradise by the far-red light: Far-red and red:blue ratios independently affect yield, pigments, and carbohydrate production in lettuce, *Lactuca sativa*

Jordan B. Van Brenk[1†], Sarah Courbier[1,2,3†], Celestin L. Kleijweg[1], Julian C. Verdonk[1] and Leo F. M. Marcelis[1*]

[1]Horticulture and Product Physiology, Plant Sciences Group, Wageningen University and Research, Wageningen, Netherlands, [2]Faculty of Biology II, University of Freiburg, Freiburg, Germany, [3]Centre for Integrative Biological Signalling Studies (CIBSS), University of Freiburg, Freiburg, Germany

In controlled environment agriculture, customized light treatments using light-emitting diodes are crucial to improving crop yield and quality. Red (R; 600-700 nm) and blue light (B; 400-500 nm) are two major parts of photosynthetically active radiation (PAR), often preferred in crop production. Far-red radiation (FR; 700-800 nm), although not part of PAR, can also affect photosynthesis and can have profound effects on a range of morphological and physiological processes. However, interactions between different red and blue light ratios (R:B) and FR on promoting yield and nutritionally relevant compounds in crops remain unknown. Here, lettuce was grown at 200 µmol m^{-2} s^{-1} PAR under three different R:B ratios: R:$B_{87.5:12.5}$ (12.5% blue), R:$B_{75:25}$ (25% blue), and R:$B_{60:40}$ (40% blue) without FR. Each treatment was also performed with supplementary FR (50 µmol m^{-2} s^{-1}; R:$B_{87.5:12.5}$+FR, R:$B_{75:25}$+FR, and R:$B_{60:40}$+FR). White light with and without FR (W and W+FR) were used as control treatments comprising of 72.5% red, 19% green, and 8.5% blue light. Decreasing the R:B ratio from R:$B_{87.5:12.5}$ to R:$B_{60:40}$, there was a decrease in fresh weight (20%) and carbohydrate concentration (48% reduction in both sugars and starch), whereas pigment concentrations (anthocyanins, chlorophyll, and carotenoids), phenolic compounds, and various minerals all increased. These results contrasted the effects of FR supplementation in the growth spectra; when supplementing FR to different R:B backgrounds, we found a significant increase in plant fresh weight, dry weight, total soluble sugars, and starch. Additionally, FR decreased concentrations of anthocyanins, phenolic compounds, and various minerals. Although blue light and FR effects appear to directly contrast, blue and FR light did not have interactive effects together when considering plant growth, morphology, and nutritional content. Therefore, the

individual benefits of increased blue light fraction and supplementary FR radiation can be combined and used cooperatively to produce crops of desired quality: adding FR increases growth and carbohydrate concentration while increasing the blue fraction increases nutritional value.

KEYWORDS

controlled environment agriculture, light quality, far-red light, red:blue ratio, nutritional quality, metabolic compounds, product physiology

1 Introduction

Vertical farming (VF) is a method of controlled environmental agriculture (CEA) wherein plant production occurs in stacked layers in an enclosed growth area, without impact from the external environment (Kozai et al., 2020). In CEA, among the most controlled conditions are air temperature, nutrient solution composition, carbon dioxide concentration, and light quality (*i.e.*, spectra/wavelength of light) and quantity (*i.e.* intensity/amount of light) (SharathKumar et al., 2020; van Delden et al., 2021). As the predominant contributor to CEA start-up and production costs, light is consistent target of growers to design growth recipes minimizing production costs while maintaining or increasing yield and quality. This is now more accessible by transitioning to LEDs (light-emitting diodes) from other lighting methods (*e.g.*, high-pressure sodium lamps, fluorescent lights). The adoption of LEDs in CEA is attributed to their efficiency, reduced heat output, and production of different light wavelengths including blue light (B; 400-500 nm), red light (R; 600-700 nm), and far-red light (FR; 700-800 nm). In CEA systems with programmable and customizable LED modules (Neo et al., 2022), a plethora of custom growth recipes with specific light wavelengths, intensities, day lengths, and combinations thereof can be designed, creating an unprecedented capacity for controlling crop cultivation.

As the most effectively absorbed wavelengths by photosynthetic machinery, R and B are commonly used in VF systems. Red light is highly efficient in driving photosynthesis (McCree, 1971) and is responded to by phytochromes, photoreceptors that influence plant morphology through photomorphogenesis (Sharrock, 2008). Although R light is more cost- and energy-efficient to produce than B light, B is often needed. The B photoreceptors cryptochrome and phototropin steer plant growth by suppressing leaf expansion and stem elongation, regulating photomorphogenesis, and inducing pigment formation (Lin et al., 1998; Inoue et al., 2008; Wollaeger and Runkle, 2015). Far-red light positively increases tissue expansion and elongation, which contribute to shade avoidance (SA) mechanisms in nature (Smith and Whitelam, 1997; Keller et al., 2011). Far-red light converts phytochrome from its active FR-absorbing form (Pfr) to an inactive R-absorbing (Pr) form (Ballaré, 1999; Sharrock, 2008). Greater FR leads to a lower red:far-red ratio (R:FR), which boosts stem length, petiole length, and biomass (de Wit et al., 2016; Jin et al., 2021). In lettuce, leaf area often increases with decreasing R:FR, promoting light capture and consequent biomass (Liu and van Iersel, 2022).

Other than yield, nutritional compound concentrations also change in response to different light conditions. For example, high B exposure can increase anthocyanin concentration in some plants (Samuolienė et al., 2012; Liu et al., 2022). Anthocyanins are red- or purple-colored pigments with antioxidant activity (Khoo et al., 2017). Anthocyanins are a subclass of flavonoids (Falcone Ferreyra et al., 2012), which themselves are a subclass of phenolic compounds (Cheynier et al., 2013). Because of their antioxidant properties, phenolic compounds, flavonoids, and anthocyanins are highly sought-after health compounds in consumer foods (Sarkar and Shetty, 2014; Panche et al., 2016). In plants, they scavenge free radicals (Gould, 2004; Khoo et al., 2017), protect from ultraviolet light (UV; Woodall and Stewart, 1998), and defend from abiotic stressors (Kovinich et al., 2014, Kovinich et al., 2015; Naing and Kim, 2021).

A different class of pigments, the carotenoids, also increase with high B exposure in some plant genotypes (Samuolienė et al., 2017). Carotenoids are a group of lipid-soluble yellow/orange pigments that harvest and subsequently transfer light energy to chlorophyll for photosynthesis, also protecting chlorophyll by absorbing reactive oxygen species (ROS) (Maoka, 2020; Zulfiqar et al., 2021). In animals, carotenoids are not synthesized *de novo*, but dietary carotenoids are provitamins converted to vitamin A in the intestinal tract (Zia-Ul-Haq et al., 2021). Carbohydrates are another nutritional and energy source for plants and humans (Apriyanto et al., 2022). They can also be enriched by increasing supplemental FR in an R:B background (Van De Velde et al., 2023) or with high light intensity at the end of production (Min et al., 2021). They also affect consumer perception by increasing lettuce shelf life, sweetness, and crispness (Witkowska and Woltering, 2010; Lin et al., 2013; Min et al., 2021).

Elevating yield and enriching nutritional content via improved cultivation methods can improve antioxidant and nutrient intake of human diets (Mou, 2009). However, the solution is not simply to have high fractions of certain wavelengths; in fact, each described wavelength also has negative repercussions. High amounts of blue light (>25% B) causes dwarfed plants with reduced weight (Lin et al., 2013; Pennisi et al., 2019a; Kong and Nemali, 2021).

Physiologically, FR decreases leaf thickness (Smith and Whitelam, 1997; Meng and Runkle, 2019) and FR-induced stem extension can be undesirable in crops such as lettuce as it limits leafy growth (Kong and Nemali, 2021). Metabolically, FR irradiance has been shown to decrease phenolic, anthocyanin, carotenoid, and chlorophyll content (Li and Kubota, 2009; Meng and Runkle, 2019). Finally, crops exposed solely to R exhibit a "red light syndrome", characterized by hampered photosynthesis, biomass accumulation, and morphology (Hogewoning et al., 2010; Trouwborst et al., 2016). This response is mitigated by adding small B fractions, restoring normal photosynthetic and growth functionality (Hoenecke et al., 1992; Hogewoning et al., 2010). Furthermore, the interactions between R/B/FR wavelengths on plant physiology and nutrition are less clear than when focused on individual wavelengths. Blue-sensing cryptochromes and R/FR-sensing phytochromes have complex interactions in light response; in some conditions working cooperatively (Su et al., 2017), in others antagonistically (Mockler et al., 1999), and still other instances acting independently (Hirose et al., 2012; Casal, 2013).

The mixed bag of plant responses to different treatments of R, B, and FR light exemplifies the need to fine-tune crop production through custom LED light recipes focused on growth and desired compound biosynthesis. However, to our knowledge, the growth and nutritional effects of R:B ratios interacting with a constant intensity of supplemental FR has yet to be described. Previous studies comparing lettuce growth and pigments under different R:B and FR conditions have either primarily focused on very young lettuce plants (Meng and Runkle, 2019) or have compared R:B:FR conditions with different total R and B content depending on the inclusion or exclusion of FR (Kong and Nemali, 2021). Because the application of FR with R:B has not thus far been performed consistently, it is unclear if a constant intensity of supplemental FR combined with different R:B ratios may interact cooperatively, negatively, or independently. Therefore, we sought to fill this knowledge gap by applying a constant intensity of supplemental FR with a range of R:B ratios, focusing on growth and nutritional content of lettuce at a harvestable and nutritionally-relevant developmental stage.

In this study, we were interested in the effect of R:B and FR on economically attractive traits, with focus on identifying "balanced" conditions where nutritional value could be promoted whilst maintaining suitable plant growth. Our objective was to quantify the yield and nutritional value of red lettuce grown under LEDs at different R:B ratios with or without FR, additionally determining if the R:B ratios had interactions with FR. To perform this, we applied four treatments with increasing B content in the R:B spectrum, then included or excluded supplemental FR light. Three of these spectra used only R and B light to create the treatment R:B spectra. The fourth treatment spectra was a white light treatment with a high R:B ratio, which was used as a reference spectra with a known high R and low B content, as performed in previous studies (Pennisi et al., 2019b; Ji et al., 2021). Here, pigments (anthocyanins, chlorophyll, and carotenoids), phenolic compounds, carbohydrates, and mineral concentration were quantified as markers for lettuce nutritional value. We hypothesized that FR addition to R:B growth spectra would improve biomass accumulation, albeit with reductions in nutritional value corresponding to decreased foliage pigmentation and phenolic content. The opposite was hypothesized for increasing B fractions, which were conversely expected to decrease biomass accumulation while improving nutritional content. Additionally, we intended to determine if physiological and nutritional phenotypes were results of cooperative, antagonistic, or discrete light responses to B and FR.

2 Materials and methods

2.1 Plant material and germination

Lactuca sativa cv. Barlach (Rijk Zwaan; De Lier, The Netherlands), a red butterhead lettuce, was grown from pelleted seeds sown individually on rockwool plugs (3.5 × 3.5 × 5.9 cm L × W × H; Grodan, Roermond, The Netherlands), covered with a layer of vermiculite. The plugs were imbibed with tap water and kept in a germination tray covered with clear plastic to maintain humidity. The germination trays were placed in darkness for two days at 4°C for stratification, then were moved to a climate room equipped with a CO_2 supplier (800 ppm CO_2) and an air-conditioning system for controlling room temperature (21°C /19°C day/night) and relative humidity (75%). Plants were germinated under white light (GreenPower LED production module deep red/white 150, 2nd generation; Philips, Eindhoven, The Netherlands) for five days at 200 µmol m^{-2} s^{-1} PAR, 18 h light/6h dark. The total incident light intensity (µmol m^{-2} s^{-1} PAR) was measured at plant height using a PAR meter (LI-250A; Li-Cor Biosciences, Lincoln, NE, USA). The spectral photon composition was 8.5% blue (400-500 nm), 19% green-yellow (500-600 nm), 72.5% red (600-700 nm), and 0% FR (700-800 nm) during germination. Spectral composition was measured with a spectrometer (SS-110; Apogee Instruments, Logan, UT, USA).

2.2 Growth conditions

Seven days after sowing, rockwool plugs with morphologically-similar seedlings and two unfurled cotyledons were transplanted to water-soaked rockwool blocks (7.5 × 7.5 × 6.5 cm, L × W × H; Grodan, Roermond, The Netherlands). Eight groups of 22 plants were arranged in individual growth compartments (0.82 m^2, 27 plants m^{-2}) with different light treatments (Section 3.3), and plant positions were randomized weekly within a compartment. All plants continued to be grown at 21°C /19°C (day/night), 75% relative humidity, and 800 ppm CO_2. Every three days, plants received a nutrient solution (as used in Jin et al., 2021) containing 12.92 mM NO_3^-, 8.82 mM K^+, 4.22 mM Ca^{2+}, 1.53 mM Cl^-, 1.53 mM SO_4^{2-}, 1.53 mM $H_2PO_4^-$, 1.15 mM Mg^{2+}, 0.38 mM NH_4^+, 0.38 mM SiO_3^{2-}, 0.12 mM HCO_3^-, 38.33 µM B, 30.67 µM Fe_3^+, 3.83 µM Mn_2^+, 3.83 µM Zn^{2+}, 0.77 µM Cu^{2+}, and 0.38 µM Mo, at an EC of 2.3 dS m^{-1} and pH 6-6.5. As this solution has a greater osmotic pressure than water, seedlings were adapted to it by diluting the nutrient solution with water to EC values of 0.5, 1.0, 1.5, and 2.0 at 0, 2, 4, and 6 days after transplanting, respectively. Nutrient solution EC was verified using an EC meter (Elmeco EC handmeter V2.0, Tasseron, Nootdorp, The Netherlands).

2.3 Light treatments

Plants were grown at 200 μmol m^{-2} s^{-1} PAR (18 h light/6h dark) under either white light (W) or one of three R:B ratios: 87.5:12.5 (R:$B_{87.5:12.5}$, 12.5% B), 75:25 (R:$B_{75:25}$, 25% B), or 60:40 (R:$B_{60:40}$, 40% B), either with or without far-red addition (+FR; 50 μmol m^{-2} s^{-1}; separate from, but equivalent to 25% PAR) (Table 1; Supplementary Figure 1). PAR was provided by combinations of Greenpower LEDs (GreenPower LED production module deep red/white 150, GP LED production DR/B 150 LB, GP LED production B 120 LO, 1st and 2nd generation; Philips, Eindhoven, The Netherlands); FR was provided by GreenPower LED production module far red 150cm (Philips, Eindhoven, The Netherlands). PAR was maintained at 200 μmol m^{-2} s^{-1} by adjusting the height of the LED modules suspended above the plant canopy. For brevity, when presenting and discussing results, the treatments (R:$B_{87.5:12.5}$, R:$B_{75:25}$, R:$B_{60:40}$) and the resulting data are referred to by the blue content in the R:B spectrum; importantly, this means in this context that increased B content also corresponds to reduced R content. This is not exactly the same for W treatments, which also involve green-yellow wavelengths. However, W treatments were analyzed as a good comparison treatment to consider the effect of a lower content of B and R with the presence of green-yellow. Therefore, W treatments here were used as a reference treatment, an approach performed in other previous light studies (Pennisi et al., 2019b; Ji et al., 2021).

2.4 Morphological measurement

Non-destructive morphological measurements were performed 7, 14, and 21 days after transplant (DAT) for five growth cycles. These measurements consisted of projected leaf area (PLA; the area of leaves exposed to light in cm^2 $plant^{-1}$) and number of leaves (L_N; # $plant^{-1}$). For PLA measurements (and morphological characteristics), overhead photos of individual plants were taken using a stand-mounted digital camera (EOS 1100D, Canon, Tokyo, Japan). Photos were captured with a black background and size reference, with which PLA was calculated using ImageJ (U. S. National Institutes of Health, Bethesda, MD, USA). Leaf number was determined by counting all leaves >0.5 cm^2.

For further morphological and metabolic data collection, plants from three growth cycles were harvested 21 DAT. Of the 22 plants per treatment per growth cycle, ten plants were randomly selected for morphological measurements: leaf area (cm^2 $plant^{-1}$), shoot fresh weight (g $plant^{-1}$), and shoot dry weight (g $plant^{-1}$). Shoot fresh weight and leaf area was determined by separating leaves and measuring with a leaf area meter (LI-3100, Li-Cor Biosciences, Lincoln, NE, USA). These same leaves and stems were used for shoot dry weight determination after being dehydrated in a forced-air oven at 105°C for 48 hours (Elbanton Special Products by Hettich Benelux, Geldermalsen, The Netherlands). With these data, specific leaf area (SLA; cm^2 g^{-1}) and dry matter content (%) were calculated. From the remaining twelve plants per treatment and growth cycle, eight plants were used for anthocyanin determination and four were used for other metabolite analysis (Section 3.5).

2.5 Metabolic compound measurements

From light-exposed regions of leaves, four leaf disks (~1cm diameter) from each plant were collected and weighed in Eppendorf tubes containing ceramic grinding balls, then flash frozen in liquid nitrogen and stored at -80°C. Two tubes were created per treatment, one for anthocyanin analysis and one for other metabolite analysis. After freezing, leaf disks were subsequently freeze-dried (Alpha 1-4 LSCbasic, Martin Christ, Osterode am Harz, Germany) for a minimum of 36 hours, then ground into a fine powder with the preloaded balls using a mixer mill (MM 200, Retsch, Dale i Sunnfjord, Norway). The leaf disk fresh weights were measured prior to freezing, therefore the resulting data for metabolite concentrations are expressed per gram of fresh weight.

TABLE 1 Spectral compositions, light intensity, and phytochrome photostationary state of eight different light treatments.

Treatment	Spectral composition of PAR (%)			Intensity (μmol m^{-2} s^{-1})		R:B	R:FR	PSS value
	Blue 400-500 nm	Green-Yellow 500-600 nm	Red 600-700 nm	PAR 400-700 nm	Far-red 700-800 nm			
Germination	8.5	19.0	72.5	200	0	8.53	N/A	0.88
W	8.5	19.0	72.5	200	0	8.53	N/A	0.88
R:$B_{87.5:12.5}$	12.5	0.0	87.5	200	0	7.00	N/A	0.88
R:$B_{75:25}$	25.0	0.0	75.0	200	0	3.00	N/A	0.88
R:$B_{60:40}$	40.0	0.0	60.0	200	0	1.50	N/A	0.87
W+FR	8.5	19.0	72.5	200	50	8.53	1.45	0.81
R:$B_{87.5:12.5}$+FR	12.5	0.0	87.5	200	50	7.00	1.75	0.82
R:$B_{75:25}$+FR	25.0	0.0	75.0	200	50	3.00	1.50	0.81
R:$B_{60:40}$+FR	40.0	0.0	60.0	200	50	1.50	1.20	0.78

W, white light; R:$B_{87.5:12.5}$, R:$B_{75:25}$, R:$B_{60:40}$, R:B ratios used in this study; FR, supplemental far-red light; PAR, photosynthetically active radiation; R:FR, red:far-red ratio; PSS, phytochrome photostationary state, calculated using the different spectral treatments at 200 μmol m^{-2} s^{-1} PAR.
N/A, not applicable.

Anthocyanins were measured following previous descriptions, with some modifications (Lange et al., 1971; Wu et al., 2014). Anthocyanins were extracted from ~10 mg of freeze-dried and ground leaf material using 1 mL of extraction buffer (18% [v/v] 1-propanol, 1% [v/v] HCl and 81% [v/v] MilliQ water). Samples and blanks (no plant tissue, only buffer) were boiled for three minutes at 100°C and incubated for two hours in the dark at room temperature, then centrifuged. Sample absorbances at 535 nm (A_{535}) and 650 nm (A_{650}) were determined using a spectrometer (SpectraMax iD5, San Jose, CA, USA) and corrected with blank values. Anthocyanin content was measured as (A_{535}-2.2·A_{650})/mg FW.

Chlorophyll a (Chl_a), chlorophyll b (Chl_b), total chlorophyll (Chl_{a+b}), malondialdehyde (MDA), total phenolic compounds, total flavonoids, sugars, and starch concentrations were measured according to López-Hidalgo et al. (2021), using ~10 mg of freeze-dried tissue.

2.6 Mineral concentration measurement

For mineral composition analysis, plants from two growth cycles were harvested 21 days after transplantation. To achieve the necessary 200 grams of cumulative fresh shoot biomass for mineral analysis, multiple plants were collected for each treatment, noting the number and fresh weight of individual plants required to satisfy 200 grams of tissue (10 to 26 plants, depending on the plant fresh weight from different treatments). Mineral composition was determined by a certified nutrient testing company (Eurofins Agro NL, Wageningen, The Netherlands), determining macro- and micro-element concentrations for plants in each treatment.

2.7 Radiation- and energy-use efficiency calculations

Radiation-use efficiency and energy-use efficiency were calculated based on typical performance values of photon efficacy for LED packages (B = 2.8 μmol J^{-1}, R = 4.1 μmol J^{-1}, FR = 3.6 μmol J^{-1}, white = 2.8 μmol J^{-1}) (Kusuma et al., 2022). These were calculated considering plant fresh weight by treatment, plant density (27 plants m^{-2}), treatment duration (21 days), and total radiation received within the 400-800 nm range.

2.8 Experimental design and statistical analyses

The experiment was conducted five times in a row, resulting in five growth cycles. Three growth cycles were used for morphological and metabolic data collection, therefore for these measurements there were three statistical replicates (n = 3). Two growth cycles were used for mineral data collection, therefore for these measurements there were two statistical replicates (n = 2). The growth cycles were treated as blocks in the statistical analysis; each light treatment was randomly allocated to a growth compartment, but due to technical restrictions, the same randomization was used in each growth cycle. For each growth cycle, from the 22 plants grown under each treatment, ten plants were used for collecting morphological data, eight plants for anthocyanin analysis, and four plants for metabolite determination as in López-Hidalgo et al. (2021). For both mineral content growth cycles, one measurement per aggregate set of plants from each light treatment was made. For every variate, a two-way analysis of variance (ANOVA) was conducted (factors FR and background light spectrum, each with two levels), taking account for the blocks was conducted. This was followed by mean separation according to Fisher's unprotected least significant difference (LSD) test. Furthermore, a two-way ANOVA in blocks was conducted using FR presence as a qualitative factor and B% in the spectrum (excluding the white light treatments) as a quantitative factor with polynomial contrasts. All tests were conducted at $\alpha = 0.05$ and Genstat software (21st edition, VSN International LTD, Hemel Hempstead, UK) was used for all statistical tests.

3 Results

3.1 Supplemental FR improves plant growth in R:B backgrounds

As important parameters for crop production, the morphological traits of lettuce grown under different R:B and FR treatments were measured. Considering the different R:B ratios, shoot fresh weight decreased by 20% from R:$B_{87.5:12.5}$ to R:$B_{60:40}$ treatments, at similar magnitudes with or without FR (Figure 1A). With the addition of 50 μmol m^{-2} s^{-1} FR radiation, shoot fresh weight increased by 100% on average for each R:B ratio. There was no statistical interaction found between FR addition and B content on shoot fresh weight. There was also no effect on dry matter content for both B content and FR addition, resulting in similar trends observed between shoot fresh and dry weight (Table 2; Supplementary Figure 2A). Adding FR to R:B treatments resulted in a 106% increase of total leaf area over treatments without FR (Figure 1B). There did appear to be a trend of decreased leaf area with increased B content, but this was not found to be significant (Figure 1B). Specific leaf area increased linearly with higher blue light percentage (Table 2); as SLA is inversely proportional to leaf thickness, leaves were thinner as B content increased, made slightly thinner when FR was added (Table 2). Canopy openness (total projected leaf area divided by leaf area) slightly decreased with supplemental FR but was unaffected by B content (Table 2). The number of leaves per plant increased with supplemental FR and did not appear to be affected by B content, except for the R:$B_{75:25}$+FR treatment, which had a lower number of leaves compared to R:$B_{87.5:12.5}$+FR and R:$B_{60:40}$+FR (Table 2).

10.3389/fpls.2024.1383100

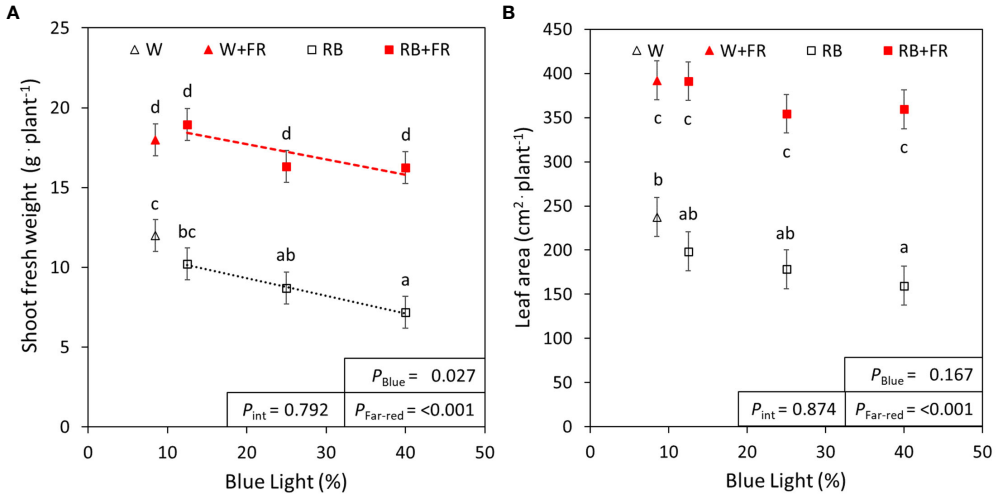

FIGURE 1
Lettuce fresh weight and leaf area under red:blue ratios with and without far-red. **(A)** Shoot fresh weight and **(B)** leaf area of lettuce grown under three different red:blue ratios presented by blue light % in the R:B spectrum (R:$B_{87.5:12.5}$ = 12.5% blue; R:$B_{75:25}$ = 25% blue; and R:$B_{60:40}$ = 40% blue), with additional far-red light (RB+FR) or no far-red (RB). White light (~8.5% blue) is used as a comparison, with far-red (W+FR) or without (W). Trendlines were drawn to indicate the probability of a linear relationship with blue light (P_{Blue}, α = 0.05). Different letters indicate significantly different values for each combination of R:B ratio and FR light treatments, according to an unprotected Fisher LSD Test (α = 0.05). Datapoints represent treatment means with error bars representing standard error means of three growth cycles (n = 3), each consisting of ten replicate plants. $P_{Far\text{-}red}$ = probability of an effect from far-red, P_{int} = probability of an interactive effect between blue content and far-red addition.

3.2 Leaf pigments increase with increased B, but not FR, in an R:B background

To ascertain the differences in lettuce pigmentation between treatments, photosynthetic and photoprotective pigment contents were quantified. Generally, leaf pigments increased with increased B content in an R:B spectrum (Figure 2). From R:$B_{87.5:12.5}$ to R:$B_{60:40}$, there was linear increase of chlorophyll (24%) and carotenoid (21%) concentration; these pigments were not significantly affected by adding FR (Figures 2A, B). However, there was an interaction when adding FR to an R:B background for carotenoid concentration. The Chl_a:Chl_b ratio decreased slightly from R:$B_{87.5:12.5}$ to R:$B_{60:40}$, further decreased with addition of FR (Supplementary Table 1). Anthocyanins increased by 40% from R:$B_{87.5:12.5}$ to R:$B_{60:40}$ independently of FR, which decreased anthocyanin content for all R:B treatments by 13% (Figure 2C). The effects of FR and B content on anthocyanins can also be visualized in Figure 3, as the red color of red lettuce can be a proxy for relative anthocyanin content.

TABLE 2 Morphological characteristics of lettuce grown under different light spectra.

	Unit	FR	W	R:$B_{87.5:12.5}$	R:$B_{75:25}$	R:$B_{60:40}$	SEM[‡]	P_{Blue}[#]	$P_{Far\text{-}red}$[##]
DMC	%	No FR	4.95^{a}	5.09^{a}	5.22^{a}	5.12^{a}	± 0.153	0.649	0.081
		+FR	4.98^{a}	4.88^{a}	5.00^{a}	4.97^{a}			
PLA	$cm^2\ plant^{-1}$	No FR	50.63^{a}	56.26^{a}	61.55^{ab}	73.84^{b}	± 5.13	0.220	<0.001*
		+FR	116.49^{c}	112.84^{c}	108.41^{c}	106.03^{c}			
$\frac{PLA}{LA}$		No FR	0.350^{ab}	0.356^{ab}	0.349^{ab}	0.365^{b}	± 0.011	0.942	0.030*
		+FR	0.336^{ab}	0.336^{ab}	0.339^{ab}	0.325^{a}			
SLA	$cm^2\ g^{-1}$	No FR	404.0^{abc}	386.0^{a}	401.2^{ab}	444.4^{bc}	± 16.36	0.010*	0.022*
		+FR	444.9^{bc}	427.2^{abc}	439.5^{bc}	451.0^{c}			
No. of leaves	# $plant^{-1}$	No FR	15.89^{a}	15.39^{a}	14.46^{a}	15.19^{a}	± 0.587	0.895	<0.001*
		+FR	19.80^{bc}	20.10^{bc}	18.39^{b}	20.15^{c}			

DMC, shoot dry matter content; PLA, projected leaf area; PLA/LA, leaf canopy closure; SLA, specific leaf area; W, white light; R:$B_{87.5:12.5}$, R:$B_{75:25}$, R:$B_{60:40}$, R:B ratios used in this study; FR, supplemental far-red light.
[‡]SEM, standard error means of three growth cycles (n = 3), each consisting of ten replicate plants for all eight light treatments. Different letters indicate significantly different values for each combination of R:B ratio and FR light treatments, using an unprotected Fisher LSD Test (α = 0.05).
[#]P-value for blue content effects among the three levels of blue light according to a two-way ANOVA.
[##]P-value for far-red light effects among the three levels of blue light according to a two-way ANOVA.
*Denotes a significant effect of either P^{Blue} or $P^{Far\text{-}red}$ (α = 0.05).

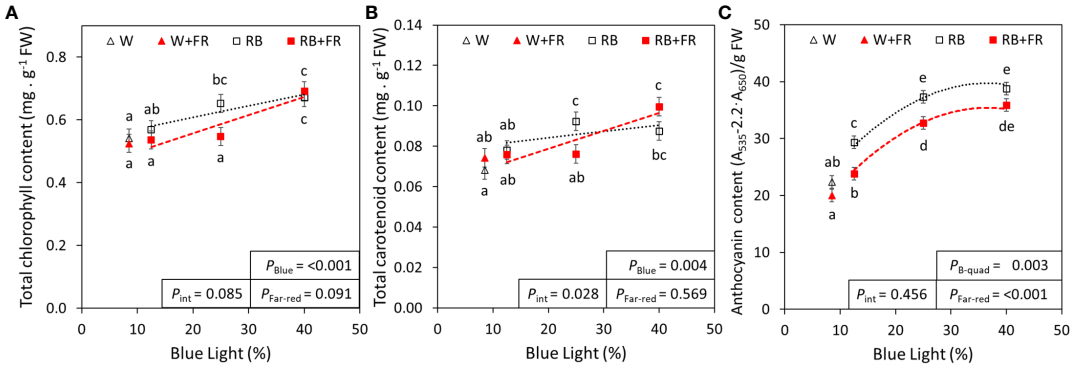

FIGURE 2
Pigment concentrations of lettuce grown under red:blue treatments with and without far-red. Total chlorophyll **(A)**, carotenoid **(B)**, and anthocyanin **(C)** concentrations of lettuce grown under different red:blue ratios presented by blue light % in the R:B spectrum (R:$B_{87.5:12.5}$ = 12.5% blue; R:$B_{75:25}$ = 25% blue; and R:$B_{60:40}$ = 40% blue), with additional far-red light (RB+FR) or no far-red (RB). White light (~8.5% blue) is used as a comparison, with far-red (W +FR) or without (W). Trendlines were drawn to indicate the probability of a linear (P_{Blue}) or quadratic ($P_{B\text{-}quad}$) relationship with blue light, α = 0.05. Different letters indicate significantly different values for each combination of R:B ratio and FR light treatments, according to an unprotected Fisher LSD Test (α = 0.05). Datapoints represent treatment means with error bars representing standard error means of three growth cycles (n = 3), each consisting of four or eight replicate plants. $P_{Far\text{-}red}$ = probability of an effect from far-red, P_{int} = probability of an interactive effect between blue content and far-red addition.

3.3 Specialized metabolites, carbohydrates, and minerals are differentially affected by R:B ratios and FR supplementation

To quantify additional indicators of nutritional value, the concentrations of flavonoids, phenolic compounds, carbohydrates, and minerals were assessed. The concentrations of total flavonoids and phenolic compounds increased linearly from R:$B_{87.5:12.5}$ to R:$B_{60:40}$ by 35% and 20%, respectively; however, neither were significantly affected with supplemental FR (Figure 4A; Supplementary Figure 2B). There appeared to be no effect of FR or B content on MDA concentration (Supplementary Figure 2C). For carbohydrates, total soluble sugars and starch showed strong linear decreases from R:$B_{87.5:12.5}$ to R:$B_{60:40}$ (both 47%, Figures 4B, C). On average, with supplemental FR, soluble sugars increased by 65% and starch increased by 54% over treatments without FR. For each of flavonoids, phenolic compounds, MDA, sugars, and starch, no interaction was found between blue light percentage and FR.

Of the analyzed macro- and micro-elements, four are showcased in Figure 5 due to their use in fertilizers (nitrogen, phosphorus, and potassium) or involvement in lettuce tipburn studies (calcium) (Frantz et al., 2004). The remainder of the analyzed elements are summarized in Table 3. Most macro- and micro-elements increased linearly with increased B content, except for magnesium, chloride,

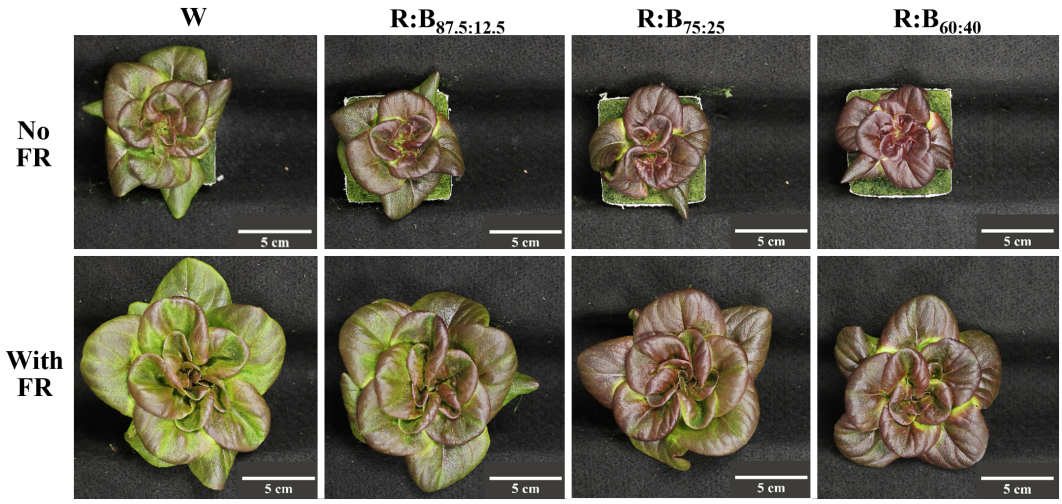

FIGURE 3
Morphology of "Barlach" lettuce grown under different light conditions. Left to right: Representative photographs of lettuce grown under white light (W) or three R:B light ratios (R:$B_{87.5:12.5}$, R:$B_{75:25}$, and R:$B_{60:40}$). The percentage of blue in PAR for each treatment was 8.5%, 12.5%, 25%, and 40%, respectively. Plants were grown without far-red (top row, No FR) and with 50 µmol m^{-2} s^{-1} supplementary far-red (bottom row, With FR).

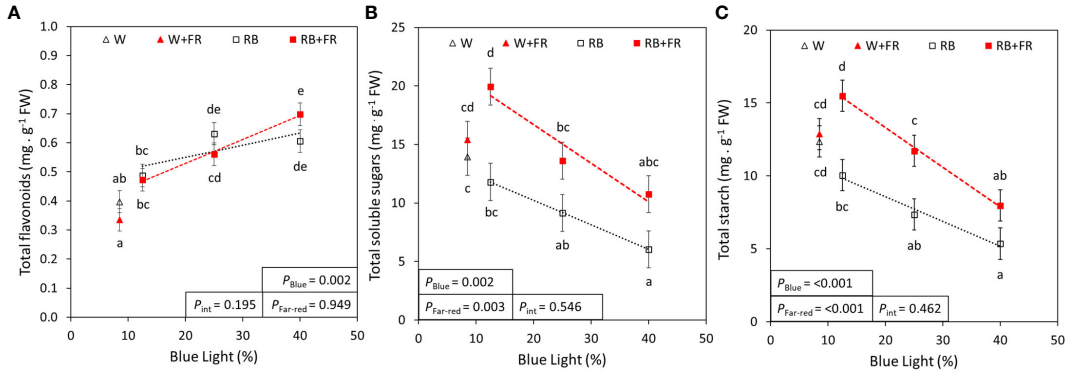

FIGURE 4
Blue content and far-red effects on total flavonoids, soluble sugars, and starch. Total flavonoid **(A)**, soluble sugar **(B)**, and starch **(C)** concentrations of lettuce grown under grown under different red:blue ratios presented by blue light % in the R:B spectrum (R:$B_{87.5:12.5}$ = 12.5% blue; R:$B_{75:25}$ = 25% blue; and R:$B_{60:40}$ = 40% blue), with additional far-red light (RB+FR) or no far-red (RB). White light (~8.5% blue) is used as a comparison, with far-red (W+FR) or without (W). Trendlines were drawn to indicate the probability of a linear relationship with blue light (P_{Blue}, α = 0.05). Different letters indicate significantly different values for each combination of R:B ratio and FR light treatments, according to an unprotected Fisher LSD Test (α = 0.05). Datapoints represent treatment means with error bars representing standard error means of three growth cycles (n = 3), each consisting of four replicate plants. $P_{Far-red}$ = probability of an effect from far-red, P_{int} = probability of an interactive effect between blue content and far-red addition.

iron, and boron. With added FR, there were significant decreases in the mineral concentrations of calcium, magnesium, manganese, and phosphorus. Generally, the increase in mineral concentration due to increased B content was often greater than the decrease in mineral concentration due to FR addition. Finally, when considering the whole plant nutrient content (which was calculated from the measured concentrations in Table 3), there was a significant effect of FR for each mineral (Supplementary Table 2).

3.4 White light treatments were not significantly different from blue light trends in R:B spectra

Overall, for most analyzed parameters, the effects of white light (W and W+FR) were not significantly different from the closest B light content R:B ratio (R:$B_{87.5:12.5}$ and R:$B_{87.5:12.5}$+FR), except for anthocyanin (Figure 2C) and flavonoid (Figure 4A) concentration. Anthocyanin content was lower in W compared to R:$B_{87.5:12.5}$ and W+FR was lower than R:$B_{87.5:12.5}$+FR. For flavonoids, only W+FR was significantly lower than R:$B_{87.5:12.5}$+FR. For all other parameters, W followed R:B considering its B light content (~8.5%) and W+FR followed R:B+FR.

3.5 Energy-use efficiency of R:B ratios with and without additional FR

As B light content increased in the treatments without FR, there was a significant decrease in radiation-use efficiency (21%) and energy-use efficiency (26%) (Figure 6). These decreases due to B content were not significant in treatments with additional FR (Figure 6). Additional FR increased both radiation-use efficiency from 17% to 59% (depending on B content) and energy-use efficiency from 20% to 87% (depending on B content) (Figure 6).

4 Discussion

4.1 FR and increased B content have contrasting roles in morphology

Overall, an increased B fraction in R:B decreased lettuce shoot fresh weight, dry weight, and leaf area, while adding FR to each R:B ratio consistently increased each of these parameters (Figure 1; Supplementary Figure 2A). Smaller plants due to increased B light content has been previously described (Wollaeger and Runkle, 2015; Pennisi et al., 2019b; Kong and Nemali, 2021), suggested by Snowden et al. (2016) to be due to reduced radiation capture from smaller leaves. Conversely, FR characteristically extends stems, internodes, petioles, and expands leaves, causing greater light interception, resulting in increased overall growth (Devlin et al., 1998; Keller et al., 2011; de Wit et al., 2016; Jin et al., 2021). The red-leafed lettuce in this study showed leaf expansion due to FR content, which has been shown to occur in many cultivars of lettuce and tomato, but not all (Ji et al., 2021; Liu and van Iersel, 2022). Increased leaf area (Figure 1B) without changing dry matter content (Table 2) can increase light interception, enhancing growth with FR addition (Supplementary Figure 3). Increased B content corresponded with decreased leaf thickness (higher SLA), contrary to commonly observed thicker leaves in many plant species (Wollaeger and Runkle, 2015; Shengxin et al., 2016; Zheng and Van Labeke, 2017). However, decreased leaf thickness with increased B has been found more often in lettuce (Clavijo-Herrera et al., 2018; Pennisi et al., 2019b; Kong and Nemali, 2021). Plants with supplemental FR also had slightly thinner—but larger—leaves (Table 2), which has been seen to occur with FR presence (Smith and Whitelam, 1997; Keller et al., 2011; Meng and Runkle, 2019). Interestingly, FR also increased leaf number, although literature shows that FR inclusion often decreases or does not affect leaf number, which can be species- or genotype-specific (Ji et al., 2020; Jin et al., 2021; Kong and Nemali, 2021). The combined

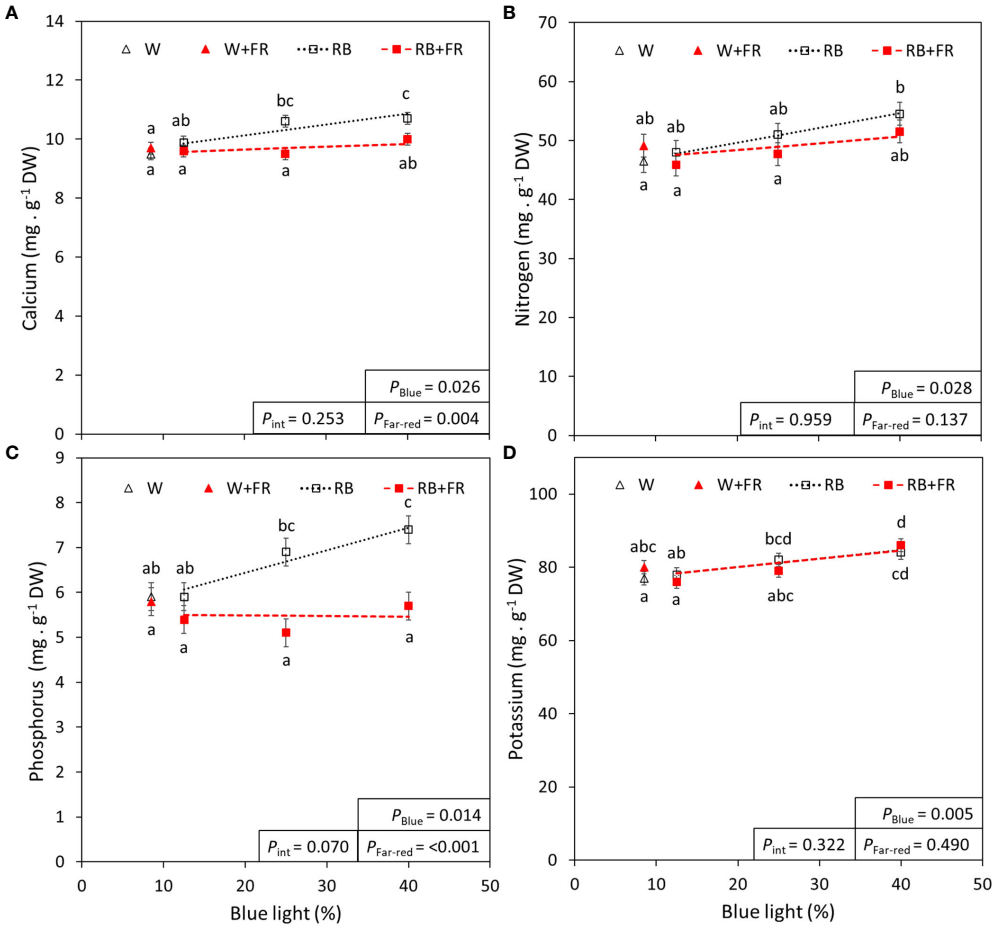

FIGURE 5
Blue light and far-red light effects on calcium, nitrogen, phosphorus, and potassium. The concentration of calcium **(A)**, nitrogen **(B)**, phosphorus **(C)**, and potassium **(D)** in lettuce grown under different red:blue ratios presented by blue light % in the R:B spectrum (R:$B_{87.5:12.5}$ = 12.5% blue; R:$B_{75:25}$ = 25% blue; and R:$B_{60:40}$ = 40% blue), with additional far-red light (RB+FR) or no far-red (RB). White light (~8.5% blue) is used as a comparison, with far-red (W+FR) or without (W). Trendlines were drawn to indicate the probability of a linear relationship with blue light (P_{Blue}, α = 0.05). Different letters indicate significantly different values for each combination of R:B ratio and FR light treatments, according to an unprotected Fisher LSD Test (α = 0.05). Datapoints represent treatment means with error bars representing standard error means of two growth cycles (n = 2) with measurements corresponding to an aggregate set of plants from each treatment. $P_{Far\text{-}red}$ = probability of an effect from far-red, P_{int} = probability of an interactive effect between blue content and far-red addition.

positive effects of FR with a low R:B ratio on yield, leaf area, and morphology exceeded the negative impact of increased B in an R:B background. Therefore, FR addition can positively impact tissue production, plant size, and shoot fresh and dry weight under decreasing R:B ratios (which would otherwise negatively impact these parameters), allowing for growers to improve factors such as nutritional value with different R:B conditions.

4.2 Antioxidants are induced with greater B content, but differentially affected by FR addition

Apart from leaf size, the most prominent lettuce phenotype observed was a progressively deeper, redder, pigmentation with increased B content, especially in treatments without FR (Figure 3). The deeper red is linked to the production of anthocyanins, associated with human health because of their antioxidant capacity (Sarkar and Shetty, 2014; Panche et al., 2016; Khoo et al., 2017). In our analysis, anthocyanins increased as B content increased, which has been found to occur via upregulation from the activated cryptochrome photoreceptor CRY1 (Bouly et al., 2007). This upregulation aligns with anthocyanin function, protecting plants from reduced photosynthesis from photoinhibition, often caused by stressors such as a greater incidence of higher-intensity blue light (Smillie and Hetherington, 1999). Increased anthocyanin content with greater blue light fraction has also been found in a variety of species and organs including pepper fruit (Liu et al., 2022) strawberry fruit (Zhang et al., 2018), and tea leaves (Zheng et al., 2019). Here, anthocyanin content decreased with added FR, which has been previously described in lettuce (Kong and Nemali, 2021). However, the decrease in anthocyanin content with added FR is noticeably lower than the increase in fresh weight of FR-grown lettuce; therefore, larger plants grown under FR can still gain deeper pigmentation and nutritional benefits from low R:B ratios.

TABLE 3 Macro- and micro-elements in lettuce grown under different light spectra.

Element	FR	W	R:B 87.5:12.5	R:B 75:25	R:B 60:40	SEM[‡]	P_{Blue}[#]	$P_{Far\text{-}red}$[##]	P_{int}[###]
Boron (μg g^{-1} DW)	No FR	23.2^{a}	23.1^{a}	23.2^{a}	23.9^{a}	± 0.64	0.076	1.000	0.683
	+FR	23.3^{a}	22.4^{a}	23.4^{a}	24.2^{a}				
Chloride (mg g^{-1} DW)	No FR	7.0^{a}	7.3^{a}	7.4^{a}	7.2^{a}	± 0.19	0.471	1.000	0.840
	+FR	7.3^{a}	7.3^{a}	7.5^{a}	7.2^{a}				
Copper (μg g^{-1} DW)	No FR	7.5^{a}	7.6^{a}	9.1^{c}	9.6^{c}	± 0.36	0.005*	0.060	0.608
	+FR	7.6^{a}	7.1^{a}	7.8^{ab}	9.0^{bc}				
Iron (μg g^{-1} DW)	No FR	160^{a}	145^{a}	260^{b}	195^{ab}	± 29.4	0.392	0.475	0.374
	+FR	135^{a}	165^{ab}	185^{ab}	190^{ab}				
Magnesium (mg g^{-1} DW)	No FR	2.3^{a}	2.5^{ab}	2.7^{b}	2.8^{b}	± 0.09	0.143	0.011*	0.606
	+FR	2.4^{a}	2.4^{a}	2.4^{a}	2.5^{a}				
Manganese (μg g^{-1} DW)	No FR	36^{ab}	34^{ab}	40^{bc}	42^{c}	± 2.0	0.021*	0.003*	0.223
	+FR	32^{a}	30^{a}	30^{a}	32^{a}				
Molybdenum (μg g^{-1} DW)	No FR	0.8^{a}	0.8^{a}	0.9^{a}	1.0^{ab}	± 0.09	0.025*	0.518	0.218
	+FR	0.9^{a}	0.8^{a}	0.8^{a}	1.2^{b}				
Nitrate (mg g^{-1} DW)	No FR	30.6^{a}	30.8^{a}	34.7^{ab}	41.5^{ab}	± 3.73	0.027*	0.821	0.737
	+FR	37.7^{ab}	32.2^{a}	32.0^{a}	44.9^{b}				
Sodium (mg g^{-1} DW)	No FR	0.7^{a}	0.7^{a}	0.9^{ab}	1.0^{b}	± 0.05	0.013*	0.465	0.572
	+FR	0.8^{a}	0.7^{a}	0.9^{ab}	0.9^{ab}				
Sulfur (mg g^{-1} DW)	No FR	2.7^{a}	2.8^{ab}	3.0^{bc}	3.2^{c}	± 0.06	<0.001*	0.156	0.508
	+FR	2.9^{ab}	2.8^{ab}	2.9^{ab}	3.2^{c}				
Zinc (μg g^{-1} DW)	No FR	24^{ab}	22^{a}	26^{abc}	28^{bc}	± 1.5	0.013*	0.578	0.542
	+FR	24^{ab}	24^{ab}	25^{ab}	30^{c}				

W, white light; $R:B_{87.5:12.5}$, $R:B_{75:25}$, $R:B_{60:40}$, R:B ratios used in this study; FR, supplemental far-red light; DW, dry weight.
[‡]SEM, standard error means of two growth cycles (n = 2), consisting of multiple plants (10 to 26, depending on treatment) for all eight light treatments. Different letters indicate significantly different values for each combination of R:B ratio and FR light treatments, using an unprotected Fisher LSD Test (α = 0.05).
[#]P-value for blue content effects among the three levels of blue light according to a two-way ANOVA.
[##]P-value for far-red light effects among the three levels of blue light according to a two-way ANOVA.
[###]P-value for interactive effects between far-red and blue light according to a two-way ANOVA.
*Denotes a significant effect of either P_{Blue} or $P_{Far\text{-}red}$ (α = 0.05).

As they are also antioxidants associated with health-promoting activity (Sarkar and Shetty, 2014; Panche et al., 2016), flavonoid and phenolic compound concentrations were explored. In this study, total flavonoids and phenolic compounds were both found to increase with elevated B in an R:B background. Interestingly, although anthocyanins had a quadratic response to increased B light (Figure 2C), total flavonoid and phenolic compound concentrations had linear responses (Figure 4A; Supplementary Figure 2B), suggesting a point of diminishing returns for anthocyanin production serving for light protection. Although the photoprotective anthocyanins expectedly increased as high-energy B increases in R:B, at a certain point, anthocyanin content appeared to plateau, whereas flavonoids and phenolic compounds steadily increased with higher B. This may indicate that past the point of anthocyanin production plateau, the metabolism of other antioxidants and phenolic compounds may become of primary focus, to tackle existing ROS created by oxidative stress (Cheynier et al., 2013; Dumanović et al., 2021), in this case caused by the high-energy B light incidence. As MDA normally accumulates as a breakdown product of ROS-induced lipid peroxidation of hydroperoxides (Esterbauer et al., 1991), it can indicate ROS-related plant stress and lipid injury (Davey et al., 2005). In the present research, MDA was unaffected by any R:B or FR combination (Supplementary Figure 2C), indicating that the ROS-scavenging abilities of these antioxidant compounds were sufficient to maintain lasting ROS-related damage to consistent and manageable levels. Finally, in this study, phenolic compound concentration (Supplementary Figure 2B) was lower than total flavonoid concentration (Figure 4A), an anomaly that is likely inaccurate as flavonoids are a subclass of phenolic compounds. This inaccuracy is prospectively due to different extraction methods and quantification with different standards; therefore, total phenolic compound concentrations should be considered relative and only be compared to each other for trends based on B content and FR presence.

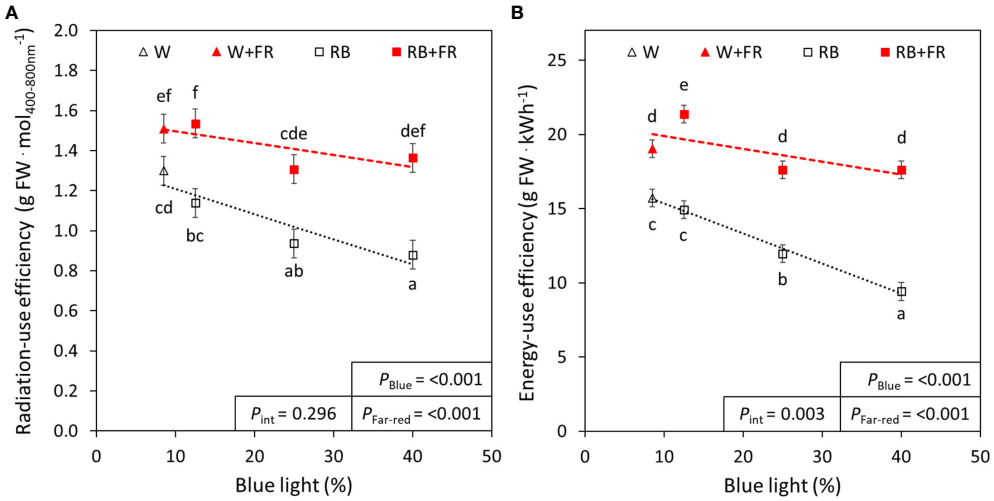

FIGURE 6
Radiation-use efficiency and energy-use efficiency of red:blue and far-red treatments. The radiation-use efficiency **(A)** and energy-use efficiency **(B)** of different red:blue ratios presented by blue light % in the R:B spectrum (R:$B_{87.5:12.5}$ = 12.5% blue; R:$B_{75:25}$ = 25% blue; and R:$B_{60:40}$ = 40% blue), with additional far-red light (RB+FR) or no far-red (RB). White light (~8.5% blue) is used as a comparison, with far-red (W+FR) or without (W). Trendlines were drawn to indicate the probability of a linear relationship with blue light (P_{Blue}, α = 0.05). Different letters indicate significantly different values for each combination of R:B ratio and FR light treatments, according to an unprotected Fisher LSD Test (α = 0.05). Datapoints represent treatment means with error bars representing standard error means of three growth cycles (n = 3), each consisting of ten replicate plants. $P_{Far\text{-}red}$ = probability of an effect from far-red, P_{int} = probability of an interactive effect between blue content and far-red addition.

Other pigments, chlorophyll and carotenoids, also increased as R:B decreased (Figure 2). Carotenoids have photoprotective mechanisms, controlling the energy flux to chlorophylls and managing oxidative stress. In lettuce, the two most common carotenoids are lutein and β-carotene, other group members include zeaxanthin, violaxanthin, astaxanthin, and lactucaxanthin (Phillip and Young, 1995; Mou, 2009; Kim et al., 2016; Yang et al., 2022). Although this study did not explore individual carotenoids, it would be prudent to further explore these individual carotenoids. This would determine if all carotenoid production is induced under high blue irradiation, or if specific carotenoids are induced. Additionally, some carotenoids convert to other carotenoids as a stress response to changes in light intensity (Sajilata et al., 2008). Therefore, it is probable that oxidative stress from higher-energy blue light may induce similar types of carotenoid conversion. There have been reports of increased B content resulting in increased carotenoids in several plant species and microalgae (Samuolienė et al., 2017; Zhang et al., 2022), but B content-induced carotenoid interconversion has yet to be explored in detail. This can further be expanded by including FR, as we found a novel interactive effect between FR and B on carotenoid concentration, where B light caused greater carotenoid content with added FR (Figure 2B).

4.3 Carbohydrates increase from FR addition, decrease with increased B content

We analyzed carbohydrates because they are nutritional and energy sources for plants and humans (Apriyanto et al., 2022). Here, carbohydrate concentration decreased with B content but increased with FR addition, but the two spectra had no interaction. This pattern was similar to the measurements of shoot fresh weight and leaf area, likely because carbohydrate pools are tightly associated with plant growth. Plant carbohydrates are classified as structural or non-structural, either contributing to cell wall and plant stem structural components (Martínez-Vilalta et al., 2016; Tarasov et al., 2018), or steering plant metabolism as sources of energy resulting from photosynthesis (Bolton, 2009; Rosa et al., 2009; Apriyanto et al., 2022). This energy primarily is in the form of soluble sugars or starch, a storage carbohydrate that can be metabolized to provide plant organs with carbon and energy (Zeeman et al., 2010; Apriyanto et al., 2022). Soluble sugars are the accessible form of this energy, but starch contributes to plant growth, protection, improving tolerance to drought, temperature, and salinity stress (Rosa et al., 2009; Krasavina et al., 2014). The reduction of carbohydrates under low R:B is possibly a result of a shift in prioritizing energy resources towards specialized metabolite synthesis, as was seen in this study with increased antioxidant compound accumulation. Such a transition to focus on specialized metabolism over growth may occur in plants experiencing environmental stressors including light stresses, drought, and temperature stress (Dixon and Paiva, 1995; Seigler, 1998; Qaderi et al., 2023). Intriguingly, we found that FR restores the decrease in carbohydrates due to low R:B, also improving or equaling the highest carbohydrate concentration of plants grown without FR. Elevated carbohydrate content with FR confirms previous research (Yang et al., 2016; Courbier et al., 2020) and may improve consumer perceptions by increasing lettuce shelf life, sweetness, and crispness (Witkowska and Woltering, 2010; Lin et al., 2013; Min et al., 2021). Hence, growers will find it attractive to use FR to simultaneously improve carbohydrate content and crop growth.

4.4 Macronutrients and micronutrients

Finally, we analyzed mineral content because humans require a balanced intake of minerals for their health and metabolism. While blue light has been shown to increase the concentration of common nutritional minerals in crops such as broccoli and lettuce, effects differ depending on the mineral of interest (Kopsell et al., 2014; Lee et al., 2019). Most of the analyzed macro- and micronutrient concentrations in the present study were unaffected by FR addition, with FR only significantly decreasing the concentration of calcium (reduced with FR addition from high R:B to low R:B by 3-9%), phosphorus (9-27%), magnesium (5-15%), and manganese (13-25%) (Figure 5, Table 3). There was no interaction between FR and B content found to affect any mineral concentrations, but a higher percentage of blue light in an R:B spectrum did increase the mineral concentrations for most elements (ranging from 7-26%), with the exception of boron, chloride, iron, and magnesium (Figure 5, Table 3). While intriguing that increases with B content occurred for most nutrients, these changes in mineral concentrations should be put into perspective with biologically relevant changes in mineral concentration. Although there were significantly different changes in mineral concentration, each was within range of commonly found lettuce nutrient concentrations (Hartz et al., 2007). This being said, we also saw that when considering the macro- and micronutrient content in terms of micro- or milligrams per plant (Supplementary Table 2), there was a significant effect of FR for each nutrient. This is logical, as the plants grown under FR light had a much larger size, resulting in more total nutrients per plant, while still having a reduced concentration per gram of fresh weight. However, we propose that the nutrient concentration per gram is more valuable as a nutritional aspect for equal portions of food, as concentration is more of a determinant of the leaf tissue nutritional potency. The effect of R:B and FR on mineral and nutritional content requires further investigation, as some nutrients seem to be enhanced by altering R:B ratio, while others by FR, and others don't appear to be affected by either. Finally, as nitrates are an important factor for human health considerations, it is prudent to mention that the nitrate concentration of lettuce in this study (~1250 – 2250 mg/kg fresh weight) was well below the 5000 mg/kg maximal limitation set in place by the EU (Commission Regulation (EU) No. 1258/2011).

4.5 The effects of blue light and FR radiation in an R:B spectrum were additive

In a previous study, Meng and Runkle (2019) found that additional FR radiation antagonized blue radiation effects on growth in an R:B background. In the present study, many effects of FR were equally affected with each corresponding increase in B content, meaning individual effects were more or less additive. The discrepancy here may be because young lettuce seedlings were the focus in Meng and Runkle (2019), whereas the present study analyzed lettuce grown to a harvestable and nutritionally relevant stage. Therefore, early growth stages may have interactive effects from R:B and FR, however over the course of development, these effects transition to be additive. This may also indicate that the light response pathways and triggered regulatory genes for growth and nutritional compounds in lettuce have more specific regulatory patterns.

Very high fractions of blue light may change the Pr/Pfr ratio (Hogewoning et al., 2010). However, the values of PSS, which can be considered as an estimate for this ratio (Sager et al., 1988), did not vary a lot among the R:B treatments applied in this research, while the PSS values by the additional FR were reduced from 0.87-0.88 to 0.78-0.82 (Table 1). This, combined with the determination that there were individual responses to R:B and FR treatments, we postulate that the plant responses to FR act via phytochromes independently from the response to R:B acting via B light photoreceptors. This may be further supported considering the results of the reference white light treatments. White light (with and without FR) had very similar PSS values to the closest corresponding R:B ratio ($R:B_{87.5:12.5}$, with or without FR), and nearly every measured parameter under white light was not significantly different from those of the nearest corresponding R:B ratio. Therefore, morphology, metabolites, and minerals were more greatly affected by the B content, FR addition, or both together, rather than the presence of green-yellow light or small changes to PSS value.

Because of the additive effects of FR and R:B ratios, their individual benefits can be harnessed by utilizing combined spectra applications to cooperatively benefit both growth and nutrition. By designing growth recipes considering both yield and nutritional quality, growers can improve produce for end consumers by producing more nutritional crops in greater size or number. Growers do not directly benefit from plants' nutritional contents – consumers consume the crops. However, nutritional quality is largely recognized by consumers, boosting or reducing sales of growers' crop. Conversely, consumers, often unaware of their purchased vegetables' growth cycles, are nonetheless affected by food shortages due to long cultivation periods. This duality of recognizing the primary desires of both parties, should also be considered by both parties. Ultimately, it falls to growers to address each aspect during cultivation; both yield and nutritional quality should be considered and valued throughout the lifetime of a crop, from sowing to consumption.

4.6 Increased B content decreases energy-use efficiency, whereas FR increases efficiency

Although LEDs are overall more efficient than other lighting technologies like fluorescent or high-pressure sodium lights (Pennisi et al., 2019b; Neo et al., 2022), there are differences in efficacy of LEDs producing different wavelengths (Kusuma et al., 2022). Of the studied wavelengths, at present, B LEDs have the lowest efficacy, followed by FR, then R, which has the highest efficacy of LED-produced wavelengths (Kusuma et al., 2022). Simply, high B content in a growth recipe often results in a lower efficiency than a growth recipe with lower B, which has previously

been described in the growth of tomato plants (Kusuma et al., 2023). Consequently, a balance is required while improving plant growth or nutritional content, considering radiation- or energy-use efficiency. Here, the addition of FR had a significant increase in radiation- and energy-use efficiency for all spectra (Figure 6), confirming previous studies in lettuce (Jin et al., 2021). That is, although the total light and resulting electricity usage were increased, plants were able to utilize light energy more efficiently, ultimately producing greater biomass per photon or kilowatt of energy. Furthermore, we found that the negative effect of increased B content was ameliorated when FR was added to the spectra (Figure 6). Therefore, the enhanced production of metabolites under high B can also be harnessed using this improved efficiency with FR inclusion. Importantly, we recognize that the presented values of radiation- and energy-use efficiency were overall relatively low, which is due to the low planting density of this study; high planting densities have previously been found to dramatically increase both radiation- and energy-use efficiencies (Jin et al., 2021). The efficiency values reported here can easily be increased by growing plants in more dense arrangements, as the plants in this study had ample room for growth.

4.7 Considerations and future directions

Some considerations for this study are important to note. First, although FR addition on average reduced metabolite and nutrient concentrations, these values were calculated on the basis of per gram of fresh lettuce tissue (or per gram dried lettuce tissue as for the analyzed macro- and micro-elements). Far-red application resulted in larger plants, therefore the total amount of nutrients per plant (instead of per unit fresh or dry weight) could be even greater with added FR, however with less potency than the R:B counterparts. Secondly, as previously mentioned, this work correlates the analyzed parameters with the content of B light in an R:B spectrum, so with an increase of B, there is a corresponding decrease of R. Therefore, responses may be due to increased B content, decreased R content, or both. This may require further analysis, potentially by replacing R or B with another wavelength (e.g. green light) to determine monochromatic ratio effects. Finally, the estimated phytochrome photostationary state (PSS) value is slightly different for the R:B +FR treatments in this study, due to their different spectral compositions (Table 1). PSS is the ratio of Pfr (i.e. the active form of phytochrome) to the total phytochrome and represents the amount of phytochrome that can perform physiological responses (Kreslavski et al., 2018). This may indicate that the results analyzed when considering FR may be due to the general supplementation of FR, the changed R:FR, or PSS value.

This study's methodology used light treatments of FR with R:B ratios throughout cultivation to present the advantages of spectral growth conditions primarily in two directions. One direction (FR addition) improves carbohydrates and yield, while the other direction (high B in an R:B background) holds more potency in improved nutritional quality. Consequently, CEA can utilize light treatments that capitalize on the benefits of multiple wavelengths. By performing customized recipes there may be an approach to have the best of both worlds, maximizing yield and nutritional quality.

5 Conclusions

In this study, we described that far-red and red:blue ratios affect plant growth and nutritional quality in an additive manner. Higher amounts of blue light in a red:blue background improved the concentrations of antioxidant metabolites and certain nutrients in lettuce, compounds which are associated with elevated nutritional value. When supplemental far-red was added to any red:blue background, lettuce consistently had improved growth and carbohydrate concentration compared to the red:blue backgrounds without far-red. Specifically, a low red:blue ratio, when combined with supplemental far-red, was most successful at maintaining growth (or limiting the negative growth effects of a low red:blue ratio without far-red). Importantly, lettuce growth under low red:blue ratios with supplemental far-red light also accumulated greater concentrations of (non-)photosynthetic pigments, sugars, starch, and certain key nutrients. Lastly, this study was designed using treatments that can feasibly be implemented into a controlled environment agriculture system with little modulation necessary, adjustable based on desired growth or nutritional preferences. Future studies should further analyze red:blue and far-red interactions on the production of these, and other, nutritional compounds via -omics studies to further improve the growing repertoire of knowledge on plant production in controlled environment agriculture.

Data availability statement

The original contributions presented in the study are included in the article/Supplementary Material. Further inquiries can be directed to the corresponding author.

Author contributions

JB: Data curation, Formal analysis, Investigation, Methodology, Validation, Visualization, Writing – original draft, Writing – review & editing. SC: Conceptualization, Investigation, Methodology, Supervision, Writing – review & editing, Data curation, Formal analysis, Validation, Visualization. CK: Data curation, Formal analysis, Investigation, Methodology, Writing – original draft, Visualization. JV: Supervision, Writing – review & editing. LM: Funding acquisition, Project administration, Supervision, Writing – review & editing.

Funding

The author(s) declare financial support was received for the research, authorship, and/or publication of this article. This research is part of the TTW Perspectief program "Sky High",

which is supported by AMS Institute, Bayer, Bosman van Zaal, Certhon, Fresh Forward, Grodan, Growy, Own Greens/Vitroplus, Priva, Philips by Signify, Solynta, Unilever, van Bergen Kolpa Architects, and the Dutch Research Council (NWO).

Acknowledgments

We would like to thank the Unifarm Klima staff, namely Gerrit Stunnenberg and Chris van Asselt. Additionally, we would like to thank Ep Heuvelink for his assistance with statistical analysis. SC was also supported by the Deutsche Forschungsgemeinschaft (DFG, German Research Foundation) under Germany's Excellence Strategy (CIBSS-EXC-2189-Project ID 390939984) during writing and editing of the manuscript.

Conflict of interest

The authors declare that the research was conducted in the absence of any commercial or financial relationships that could be construed as a potential conflict of interest.

The reviewer AF declared a past collaboration with the author JV to the handling editor.

The author(s) declared that they were an editorial board member of Frontiers, at the time of submission. This had no impact on the peer review process and the final decision.

Publisher's note

Supplementary material

The Supplementary Material for this article can be found online at: https://www.frontiersin.org/articles/10.3389/fpls.2024.1383100/full#supplementary-material

References

Apriyanto, A., Compart, J., and Fettke, J. (2022). A review of starch, a unique biopolymer – Structure, metabolism and in planta modifications. *Plant Sci.* 318, 111223. doi: 10.1016/j.plantsci.2022.111223

Ballaré, C. L. (1999). Keeping up with the neighbours: Phytochrome sensing and other signalling mechanisms. *Trends Plant Sci.* 4, 97–102. doi: 10.1016/S1360-1385(99)01383-7

Bolton, M. D. (2009). Primary metabolism and plant defense—Fuel for the fire. *Mol. Plant-Microbe Interactions®* 22, 487–497. doi: 10.1094/MPMI-22-5-0487

Bouly, J.-P., Schleicher, E., Dionisio-Sese, M., Vandenbussche, F., van der Straeten, D., Bakrim, N., et al. (2007). Cryptochrome blue light photoreceptors are activated through interconversion of flavin redox states. *J. Biol. Chem.* 282, 9383–9391. doi: 10.1074/jbc.M609842200

Casal, J. J. (2013). Photoreceptor signaling networks in plant responses to shade. *Annu. Rev. Plant Biol.* 64, 403–427. doi: 10.1146/annurev-arplant-050312-120221

Cheynier, V., Comte, G., Davies, K. M., Lattanzio, V., and Martens, S. (2013). Plant phenolics: Recent advances on their biosynthesis, genetics, and ecophysiology. *Plant Physiol. Biochem.* 72, 1–20. doi: 10.1016/j.plaphy.2013.05.009

Clavijo-Herrera, J., van Santen, E., and Gómez, C. (2018). Growth, water-use efficiency, stomatal conductance, and nitrogen uptake of two lettuce cultivars grown under different percentages of blue and red light. *Horticulturae* 4, 16. doi: 10.3390/horticulturae4030016

Courbier, S., Grevink, S., Sluijs, E., Bonhomme, P.-O., Kajala, K., Van Wees, S. C. M., et al. (2020). Far-red light promotes *Botrytis cinerea* disease development in tomato leaves via jasmonate-dependent modulation of soluble sugars. *Plant Cell Environ.* 43, 2769–2781. doi: 10.1111/pce.13870

Davey, M. W., Stals, E., Panis, B., Keulemans, J., and Swennen, R. L. (2005). High-throughput determination of malondialdehyde in plant tissues. *Analytical Biochem.* 347, 201–207. doi: 10.1016/j.ab.2005.09.041

Devlin, P. F., Patel, S. R., and Whitelam, G. C. (1998). Phytochrome E influences internode elongation and flowering time in Arabidopsis. *Plant Cell* 10, 1479–1487. doi: 10.1105/tpc.10.9.1479

de Wit, M., Keuskamp, D. H., Bongers, F. J., Hornitschek, P., Gommers, C. M. M., Reinen, E., et al. (2016). Integration of phytochrome and cryptochrome signals determines plant growth during competition for light. *Curr. Biol.* 26, 3320–3326. doi: 10.1016/j.cub.2016.10.031

Dixon, R. A., and Paiva, N. L. (1995). Stress-induced phenylpropanoid metabolism. *Plant Cell* 7, 1085–1097. doi: 10.2307/3870059

Dumanović, J., Nepovimova, E., Natić, M., Kuča, K., and Jaćević, V. (2021). The significance of reactive oxygen species and antioxidant defense system in plants: A concise overview. *Front. Plant Sci.* 11. doi: 10.3389/fpls.2020.552969

Esterbauer, H., Schaur, R. J., and Zollner, H. (1991). Chemistry and biochemistry of 4-hydroxynonenal, malonaldehyde and related aldehydes. *Free Radical Biol. Med.* 11, 81–128. doi: 10.1016/0891-5849(91)90192-6

Falcone Ferreyra, M. L., Rius, S. P., and Casati, P. (2012). Flavonoids: Biosynthesis, biological functions, and biotechnological applications. *Front. Plant Sci.* 3. doi: 10.3389/fpls.2012.00222

Frantz, J. M., Ritchie, G., Cometti, N. N., Robinson, J., and Bugbee, B. (2004). Exploring the limits of crop productivity: Beyond the limits of tipburn in lettuce. *J. Am. Soc. Hortic. Sci.* 129, 331–338. doi: 10.21273/JASHS.129.3.0331

Gould, K. S. (2004). Nature's Swiss army knife: The diverse protective roles of anthocyanins in leaves. *J. Biomedicine Biotechnol.* 2004, 314–320. doi: 10.1155/S1110724304406147

Hartz, T. K., Johnstone, P. R., Williams, E., and Smith, R. F. (2007). Establishing lettuce leaf nutrient optimum ranges through DRIS analysis. *HortScience* 42, 143–146. doi: 10.21273/HORTSCI.42.1.143

Hirose, F., Inagaki, N., Hanada, A., Yamaguchi, S., Kamiya, Y., Miyao, A., et al. (2012). Cryptochrome and phytochrome cooperatively but independently reduce active gibberellin content in rice seedlings under light irradiation. *Plant Cell Physiol.* 53, 1570–1582. doi: 10.1093/pcp/pcs097

Hoenecke, M. E., Bula, R. J., and Tibbitts, T. W. (1992). Importance of "blue" photon levels for lettuce seedlings grown under red-light-emitting diodes. *HortScience: A Publ. Am. Soc. Hortic. Sci.* 27, 427–430. doi: 10.21273/HORTSCI.27.5.427

Hogewoning, S. W., Trouwborst, G., Maljaars, H., Poorter, H., van Ieperen, W., and Harbinson, J. (2010). Blue light dose-responses of leaf photosynthesis, morphology, and chemical composition of Cucumis sativus grown under different combinations of red and blue light. *J. Exp. Bot.* 61, 3107–3117. doi: 10.1093/jxb/erq132

Inoue, S., Kinoshita, T., Matsumoto, M., Nakayama, K. I., Doi, M., and Shimazaki, K. (2008). Blue light-induced autophosphorylation of phototropin is a primary step for signaling. *Proc. Natl. Acad. Sci.* 105, 5626–5631. doi: 10.1073/pnas.0709189105

Ji, Y., Nuñez Ocaña, D., Choe, D., Larsen, D. H., Marcelis, L. F. M., and Heuvelink, E. (2020). Far-red radiation stimulates dry mass partitioning to fruits by increasing fruit sink strength in tomato. *New Phytol.* 228, 1914–1925. doi: 10.1111/nph.16805

Ji, Y., Ouzounis, T., Schouten, H. J., Visser, R. G. F., Marcelis, L. F. M., and Heuvelink, E. (2021). Dissecting the genotypic variation of growth responses to far-red radiation in tomato. *Front. Plant Sci.* 11. doi: 10.3389/fpls.2020.614714

Jin, W., Urbina, J. L., Heuvelink, E., and Marcelis, L. F. M. (2021). Adding far-red to red-blue light-emitting diode light promotes yield of lettuce at different planting densities. *Front. Plant Sci.* 11. doi: 10.3389/fpls.2020.609977

Keller, M. M., Jaillais, Y., Pedmale, U. V., Moreno, J. E., Chory, J., and Ballaré, C. L. (2011). Cryptochrome 1 and phytochrome B control shade-avoidance responses in

Arabidopsis via partially independent hormonal cascades. *Plant J.* 67, 195–207. doi: 10.1111/j.1365-313X.2011.04598.x

Khoo, H. E., Azlan, A., Tang, S. T., and Lim, S. M. (2017). Anthocyanidins and anthocyanins: Colored pigments as food, pharmaceutical ingredients, and the potential health benefits. *Food Nutr. Res.* 61, 1361779. doi: 10.1080/16546628.2017.1361779

Kim, M. J., Moon, Y., Tou, J. C., Mou, B., and Waterland, N. L. (2016). Nutritional value, bioactive compounds and health benefits of lettuce (*Lactuca sativa* L.). *J. Food Composition Anal.* 49, 19–34. doi: 10.1016/j.jfca.2016.03.004

Kong, Y., and Nemali, K. (2021). Blue and far-red light affect area and number of individual leaves to influence vegetative growth and pigment synthesis in Lettuce. *Front. Plant Sci.* 12. doi: 10.3389/fpls.2021.667407

Kopsell, D. A., Sams, C. E., Barickman, T. C., and Morrow, R. C. (2014). Sprouting broccoli accumulate higher concentrations of nutritionally important metabolites under narrow-band light-emitting diode lighting. *J. Am. Soc. Hortic. Sci.* 139, 469–477. doi: 10.21273/JASHS.139.4.469

Kovinich, N., Kayanja, G., Chanoca, A., Otegui, M. S., and Grotewold, E. (2015). Abiotic stresses induce different localizations of anthocyanins in *Arabidopsis*. *Plant Signaling Behav.* 10, e1027850. doi: 10.1080/15592324.2015.1027850

Kovinich, N., Kayanja, G., Chanoca, A., Riedl, K., Otegui, M. S., and Grotewold, E. (2014). Not all anthocyanins are born equal: distinct patterns induced by stress in *Arabidopsis*. *Planta* 240, 931–940. doi: 10.1007/s00425-014-2079-1

Kozai, T., Niu, G., and Takagaki, M. (2020). *Plant Factory. 2nd Edition*. Eds. T. Kozai, G. Niu and M. Takagaki (London, United Kingdom; San Diego, CA, United States; Cambridge, MA, United States; Kidlington, Oxford, United Kingdom: Elsevier - Academic press). doi: 10.1016/C2018-0-00969-X

Krasavina, M. S., Burmistrova, N. A., and Raldugina, G. N. (2014). The role of carbohydrates in plant resistance to abiotic stresses. *Emerging Technol. Manage. Crop Stress Tolerance: Biol. Techniques* 1, 229–270. doi: 10.1016/B978-0-12-800876-8.00011-4

Kreslavski, V. D., Los, D. A., Schmitt, F.-J., Zharmukhamedov, S. K., Kuznetsov, V. V., and Allakhverdiev, S. I. (2018). The impact of the phytochromes on photosynthetic processes. *Biochim. Biophys. Acta (BBA) - Bioenergetics* 1859, 400–408. doi: 10.1016/j.bbabio.2018.03.003

Kusuma, P., Ouzounis, T., Hawley, D., Kerstens, T., Marcelis, L. F. M., and Heuvelink, E. (2023). On the pros and cons of red photons for greenhouse tomato production: Increasing the percentage of red photons improves LED efficacy but plant responses are cultivar-specific. *J. Hortic. Sci. Biotechnol.* 98, 443–453. doi: 10.1080/14620316.2022.2147101

Kusuma, P., Pattison, P. M., and Bugbee, B. (2022). "Photon efficacy in horticulture," in *Plant Factory Basics, Applications and Advances* (London, United Kingdom; San Diego, CA, United States; Cambridge, MA, United States; Kidlington, Oxford, United Kingdom: Elsevier - Academic Press), 115–128. doi: 10.1016/B978-0-323-85152-7.00006-9

Lange, H., Shropshire, W., and Mohr, H. (1971). An analysis of phytochrome-mediated anthocyanin synthesis. *Plant Physiol.* 47, 649–655. doi: 10.1104/pp.47.5.649

Lee, M., Xu, J., Wang, W., and Rajashekar, C. B. (2019). The effect of supplemental blue, red and far-red light on the growth and the nutritional quality of red and green leaf lettuce. *Am. J. Plant Sci.* 10, 2219–2235. doi: 10.4236/ajps.2019.1012157

Li, Q., and Kubota, C. (2009). Effects of supplemental light quality on growth and phytochemicals of baby leaf lettuce. *Environ. Exp. Bot.* 67, 59–64. doi: 10.1016/j.envexpbot.2009.06.011

Lin, K.-H., Huang, M.-Y., Huang, W.-D., Hsu, M.-H., Yang, Z.-W., and Yang, C.-M. (2013). The effects of red, blue, and white light-emitting diodes on the growth, development, and edible quality of hydroponically grown lettuce (*Lactuca sativa* L. var. *capitata*). *Scientia Hortic.* 150, 86–91. doi: 10.1016/j.scienta.2012.10.002

Lin, C., Yang, H., Guo, H., Mockler, T., Chen, J., and Cashmore, A. R. (1998). Enhancement of blue-light sensitivity of *Arabidopsis* seedlings by a blue light receptor cryptochrome 2. *Proc. Natl. Acad. Sci.* 95, 2686–2690. doi: 10.1073/pnas.95.5.2686

Liu, Y., Schouten, R. E., Tikunov, Y., Liu, X., Visser, R. G. F., Tan, F., et al. (2022). Blue light increases anthocyanin content and delays fruit ripening in purple pepper fruit. *Postharvest Biol. Technol.* 192, 112024. doi: 10.1016/j.postharvbio.2022.112024

Liu, J., and van Iersel, M. W. (2022). Far-red light effects on lettuce growth and morphology in indoor production are cultivar specific. *Plants* 11, 2714. doi: 10.3390/plants11202714

López-Hidalgo, C., Meijón, M., Lamelas, L., and Valledor, L. (2021). The rainbow protocol: A sequential method for quantifying pigments, sugars, free amino acids, phenolics, flavonoids and MDA from a small amount of sample. *Plant Cell Environ.*, 44 (6), 1977–1986. doi: 10.1111/pce.14007

Maoka, T. (2020). Carotenoids as natural functional pigments. *J. Natural Medicines* 74, 1–16. doi: 10.1007/s11418-019-01364-x

Martínez-Vilalta, J., Sala, A., Asensio, D., Galiano, L., Hoch, G., Palacio, S., et al. (2016). Dynamics of non-structural carbohydrates in terrestrial plants: A global synthesis. *Ecol. Monogr.* 86, 495–516. doi: 10.1002/ecm.1231

McCree, K. J. (1971). The action spectrum, absorptance and quantum yield of photosynthesis in crop plants. *Agric. Meteorology* 9, 191–216. doi: 10.1016/0002-1571(71)90022-7

Meng, Q., and Runkle, E. S. (2019). Far-red radiation interacts with relative and absolute blue and red photon flux densities to regulate growth, morphology, and pigmentation of lettuce and basil seedlings. *Scientia Hortic.* 255, 269–280. doi: 10.1016/j.scienta.2019.05.030

Min, Q., Marcelis, L. F. M., Nicole, C. C. S., and Woltering, E. J. (2021). High light intensity applied shortly before harvest improves lettuce nutritional quality and extends the shelf life. *Front. Plant Sci.* 12. doi: 10.3389/fpls.2021.615355

Mockler, T. C., Guo, H., Yang, H., Duong, H., and Lin, C. (1999). Antagonistic actions of *Arabidopsis* cryptochromes and phytochrome B in the regulation of floral induction. *Development* 126, 2073–2082. doi: 10.1242/dev.126.10.2073

Mou, B. (2009). Nutrient content of lettuce and its improvement. *Curr. Nutr. Food Sci.* 5, 242–248. doi: 10.2174/157340109790218030

Naing, A. H., and Kim, C. K. (2021). Abiotic stress-induced anthocyanins in plants: Their role in tolerance to abiotic stresses. *Physiologia Plantarum* 172, 1711–1723. doi: 10.1111/ppl.13373

Neo, D. C. J., Ong, M. M. X., Lee, Y. Y., Teo, E. J., Ong, Q., Tanoto, H., et al. (2022). Shaping and tuning lighting conditions in controlled environment agriculture: A review. *ACS Agric. Sci. Technol.* 2, 3–16. doi: 10.1021/acsagscitech.1c00241

Panche, A. N., Diwan, A. D., and Chandra, S. R. (2016). Flavonoids: an overview. *J. Nutr. Sci.* 5, e47–e62. doi: 10.1017/jns.2016.41

Pennisi, G., Blasioli, S., Cellini, A., Maia, L., Crepaldi, A., Braschi, I., et al. (2019a). Unraveling the role of red:blue LED lights on resource use efficiency and nutritional properties of indoor grown sweet basil. *Front. Plant Sci.* 10. doi: 10.3389/fpls.2019.00305

Pennisi, G., Orsini, F., Blasioli, S., Cellini, A., Crepaldi, A., Braschi, I., et al. (2019b). Resource use efficiency of indoor lettuce (*Lactuca sativa* L.) cultivation as affected by red:blue ratio provided by LED lighting. *Sci. Rep.* 9, 14127. doi: 10.1038/s41598-019-50783-z

Phillip, D., and Young, A. J. (1995). Occurrence of the carotenoid lactucaxanthin in higher plant LHC II. *Photosynthesis Res.* 43, 273–282. doi: 10.1007/BF00029940

Qaderi, M. M., Martel, A. B., and Strugnell, C. A. (2023). Environmental factors regulate plant secondary metabolites. *Plants* 12, 447. doi: 10.3390/plants12030447

Rosa, M., Prado, C., Podazza, G., Interdonato, R., González, J. A., Hilal, M., et al. (2009). Soluble sugars—Metabolism, sensing and abiotic stress. *Plant Signaling Behav.* 4, 388–393. doi: 10.4161/psb.4.5.8294

Sager, J. C., Smith, W. O., Edwards, J. L., and Cyr, K. L. (1988). Photosynthetic efficiency and phytochrome photoequilibria determination using spectral data. *Trans. ASAE* 31, 1882–1889. doi: 10.13031/2013.30952

Sajilata, M. G., Singhal, R. S., and Kamat, M. Y. (2008). The carotenoid pigment zeaxanthin—A review. *Compr. Rev. Food Sci. Food Saf.* 7, 29–49. doi: 10.1111/j.1541-4337.2007.00028.x

Samuolienė, G., Sirtautas, R., Brazaitytė, A., and Duchovskis, P. (2012). LED lighting and seasonality effects antioxidant properties of baby leaf lettuce. *Food Chem.* 134, 1494–1499. doi: 10.1016/j.foodchem.2012.03.061

Samuolienė, G., Viršilė, A., Brazaitytė, A., Jankauskienė, J., Sakalauskienė, S., Vaštakaitė, V., et al. (2017). Blue light dosage affects carotenoids and tocopherols in microgreens. *Food Chem.* 228, 50–56. doi: 10.1016/j.foodchem.2017.01.144

Sarkar, D., and Shetty, K. (2014). Metabolic stimulation of plant phenolics for food preservation and health. *Annu. Rev. Food Sci. Technol.* 5, 395–413. doi: 10.1146/annurev-food-030713-092418

Seigler, D. S. (1998). *Plant Secondary Metabolism* (Springer US). doi: 10.1007/978-1-4615-4913-0

SharathKumar, M., Heuvelink, E., and Marcelis, L. F. M. (2020). Vertical Farming: Moving from genetic to environmental modification. *Trends Plant Sci.* 25, 724–727. doi: 10.1016/j.tplants.2020.05.012

Sharrock, R. A. (2008). The phytochrome red/far-red photoreceptor superfamily. *Genome Biol.* 9, 230. doi: 10.1186/gb-2008-9-8-230

Shengxin, C., Chunxia, L., Xuyang, Y., Song, C., Xuelei, J., Xiaoying, L., et al. (2016). Morphological, photosynthetic, and physiological responses of rapeseed leaf to different combinations of red and blue lights at the rosette stage. *Front. Plant Sci.* 7. doi: 10.3389/fpls.2016.01144

Smillie, R. M., and Hetherington, S. E. (1999). Photoabatement by anthocyanin shields photosynthetic systems from light stress. *Photosynthetica* 36, 451–463. doi: 10.1023/A:1007084321859

Smith, H., and Whitelam, G. C. (1997). The shade avoidance syndrome: multiple responses mediated by multiple phytochromes. *Plant Cell Atid Environ.* 20, 840–844. doi: 10.1046/j.1365-3040.1997.d01-104.x

Snowden, M. C., Cope, K. R., and Bugbee, B. (2016). Sensitivity of seven diverse species to blue and green light: Interactions with photon flux. *PloS One* 11, e0163121. doi: 10.1371/journal.pone.0163121

Su, J., Liu, B., Liao, J., Yang, Z., Lin, C., and Oka, Y. (2017). Coordination of cryptochrome and phytochrome signals in the regulation of plant light responses. *Agronomy* 7, 25. doi: 10.3390/agronomy7010025

Tarasov, D., Leitch, M., and Fatehi, P. (2018). Lignin–carbohydrate complexes: Properties, applications, analyses, and methods of extraction: A review. *Biotechnol. Biofuels* 11, 269. doi: 10.1186/s13068-018-1262-1

Trouwborst, G., Hogewoning, S. W., van Kooten, O., Harbinson, J., and van Ieperen, W. (2016). Plasticity of photosynthesis after the "red light syndrome" in cucumber. *Environ. Exp. Bot.* 121, 75–82. doi: 10.1016/j.envexpbot.2015.05.002

van Delden, S. H., SharathKumar, M., Butturini, M., Graamans, L. J. A., Heuvelink, E., Kacira, M., et al. (2021). Current status and future challenges in implementing and upscaling vertical farming systems. *Nat. Food* 2, 944–956. doi: 10.1038/s43016-021-00402-w

Van De Velde, E., Steppe, K., Labeke, M.-C. V., Gauthier, P. P. G., Cammarisano, L., Qian, Y., et al. (2023). Leaf morphology, optical characteristics and phytochemical traits of butterhead lettuce affected by increasing the far-red photon flux. *Front. Plant Sci.* 14. doi: 10.3389/fpls.2023.1129335

Witkowska, I., and Woltering, E. J. (2010). Pre-harvest light intensity affects shelf-life of fresh-cut lettuce. *Acta Hortic.* 877, 223–227. doi: 10.17660/ActaHortic.2010.877.23

Wollaeger, H. M., and Runkle, E. S. (2015). Growth and acclimation of impatiens, salvia, petunia, and tomato seedlings to blue and red light. *HortScience* 50, 522–529. doi: 10.21273/HORTSCI.50.4.522

Woodall, G. S., and Stewart, G. R. (1998). Do anthocyanins play a role in UV protection of the red juvenile leaves of Syzygium? *J. Exp. Bot.* 49 (325), 1447–1450. doi: 10.1093/jxb/49.325.1447

Wu, H.-Y., Liu, K.-H., Wang, Y.-C., Wu, J.-F., Chiu, W.-L., Chen, C.-Y., et al. (2014). AGROBEST: An efficient *Agrobacterium*-mediated transient expression method for versatile gene function analyses in *Arabidopsis* seedlings. *Plant Methods* 10, 19. doi: 10.1186/1746-4811-10-19

Yang, X., Gil, M. I., Yang, Q., and Tomás-Barberán, F. A. (2022). Bioactive compounds in lettuce: Highlighting the benefits to human health and impacts of preharvest and postharvest practices. *Compr. Rev. Food Sci. Food Saf.* 21, 4–45. doi: 10.1111/1541-4337.12877

Yang, D., Seaton, D. D., Krahmer, J., and Halliday, K. J. (2016). Photoreceptor effects on plant biomass, resource allocation, and metabolic state. *Proc. Natl. Acad. Sci. United States America* 113, 7667–7672. doi: 10.1073/pnas.1601309113

Zeeman, S. C., Kossmann, J., and Smith, A. M. (2010). Starch: Its metabolism, evolution, and biotechnological modification in plants. *Annu. Rev. Plant Biol.* 61, 209–234. doi: 10.1146/annurev-arplant-042809-112301

Zhang, Z., Han, T., Sui, J., and Wang, H. (2022). Cryptochrome-mediated blue-light signal contributes to carotenoids biosynthesis in microalgae. *Front. Microbiol.* 13. doi: 10.3389/fmicb.2022.1083387

Zhang, Y., Jiang, L., Li, Y., Chen, Q., Ye, Y., Zhang, Y., et al. (2018). Effect of red and blue light on anthocyanin accumulation and differential gene expression in strawberry (*Fragaria* × *ananassa*). *Molecules* 23, 820. doi: 10.3390/molecules23040820

Zheng, C., Ma, J.-Q., Ma, C.-L., Shen, S.-Y., Liu, Y.-F., and Chen, L. (2019). Regulation of growth and flavonoid formation of tea plants (*Camellia sinensis*) by blue and green light. *J. Agric. Food Chem.* 67, 2408–2419. doi: 10.1021/acs.jafc.8b07050

Zheng, L., and Van Labeke, M.-C. (2017). Long-term effects of red- and blue-light emitting diodes on leaf anatomy and photosynthetic efficiency of three ornamental pot plants. *Front. Plant Sci.* 8. doi: 10.3389/fpls.2017.00917

Zia-Ul-Haq, M., Dewanjee, S., and Riaz, M. (2021). "Carotenoids: Structure and function in the human body," in *Carotenoids: Structure and Function in the Human Body* (Cham, Switzerland: Springer International Publishing). doi: 10.1007/978-3-030-46459-2

Zulfiqar, S., Sharif, S., Saeed, M., and Tahir, A. (2021). "Role of carotenoids in photosynthesis," in *Carotenoids: Structure and Function in the Human Body* (Cham, Switzerland: Springer International Publishing), 147–187. doi: 10.1007/978-3-030-46459-2_5

frontiers | Frontiers in Plant Science

TYPE Original Research
PUBLISHED 22 May 2024
DOI 10.3389/fpls.2024.1384518

OPEN ACCESS

EDITED BY
Leo Marcelis,
Wageningen University and Research, Netherlands

REVIEWED BY
Sofia D. Carvalho,
Independent Researcher, Laramie, United States
Roland Valcke,
University of Hasselt, Belgium
Sachchidanand Tripathi,
University of Delhi, India

*CORRESPONDENCE
Telesphore R. J. G. Marie
mariet@uoguelph.ca

RECEIVED 09 February 2024
ACCEPTED 01 May 2024
PUBLISHED 22 May 2024

CITATION
Marie TRJG, Leonardos ED, Rana N and Grodzinski B (2024) Tomato and mini-cucumber tolerance to photoperiodic injury involves photorespiration and the engagement of nighttime cyclic electron flow from dynamic LEDs.
Front. Plant Sci. 15:1384518.
doi: 10.3389/fpls.2024.1384518

Tomato and mini-cucumber tolerance to photoperiodic injury involves photorespiration and the engagement of nighttime cyclic electron flow from dynamic LEDs

Telesphore R. J. G. Marie*, Evangelos Demos Leonardos, Naheed Rana and Bernard Grodzinski

Department of Plant Agriculture, University of Guelph, Guelph, ON, Canada

Controlled environment agriculture (CEA) is critical for achieving year-round food security in many regions of the world. CEA is a resource-intensive endeavor, with lighting consuming a large fraction of the energy. To lessen the burden on the grid and save costs, an extended photoperiod strategy can take advantage of off-peak time-of-day options from utility suppliers. However, extending the photoperiod limits crop production morphologically and physiologically if pushed too long. Here, we present a continuous-light dynamic light-emitting diode (LED) strategy (involving changes in spectra, intensity, and timing), that overcomes these limitations. We focused on tomato, a well described photoperiodic injury–sensitive species, and mini-cucumber, a photoperiodic injury-tolerant species to first assess morphological responses under control (16-h photoperiod, unchanging spectrum), constant (24-h photoperiod, unchanging spectrum), and two variations of a dynamic LED strategy, dynamic 1 (16-h "day", 3-h "peak", 8-h "night" spectra) and dynamic 2 (20-h "day", 5-h "peak", 4-h "night" spectra). Next, we tested the hypothesis of photorespiration's involvement in photoperiodic injury by using a leaf gas exchange coupled with chlorophyll fluorescence protocol. We further explored Adenosine triphosphate (ATP): Nicotinamide adenine dinucleotide phosphate (NADPH) ratio supply/demand responses by probing photosynthetic electron flow and proton flow with the MultispeQ instrument. We found canopy architecture can be tuned by minor variations of the same dynamic LED strategy, and we highlight dynamic 1 as the optimal choice for both tomato and mini-cucumber as it improved biomass/architecture and first-yield, respectively. A central discovery was that dynamic 1 had a significantly higher level of photorespiration than control, for both species. Unexpectedly, photorespiration was comparable between species under the same treatments, except under constant. However, preliminary data on a fully tolerant tomato genotype grown under constant treatment upregulated photorespiration similar to mini-cucumber. These results suggest that photoperiodic injury tolerance involves a sustained higher level of photorespiration under extended photoperiods. Interestingly, diurnal MultispeQ measurements point to the importance of cyclic electron flow at subjective nighttime that may also partially explain why dynamic LED strategies

mitigate photoperiodic injury. We propose an ontology of photoperiodic injury involving photorespiration, triose phosphate utilization, peroxisomal H_2O_2-catalase balance, and a circadian external coincidence model of sensitivity that initiates programmed cell death.

KEYWORDS

photoperiodic injury, photorespiration, dynamic LEDs, cyclic electron flow, tomato, cucumber, continuous light, circadian rhythm

1 Introduction

Controlled environment agriculture (CEA), which includes indoor and greenhouse production systems, is becoming increasingly valuable for supplementing the nutritional needs of people across the world such as in northern regions with cold low-light winters, arid landscapes with drought-limiting field agriculture, tropical islands with high import expenses and hurricane susceptibility, and any metropolis with a dense urban population that creates food desert zones. However, CEA comes at a high energy cost. One of the largest consumers of energy in a CEA operation is lighting, with sole-source lighting in indoor facilities consuming much more than supplemental lighting in greenhouses that varies depending on geographical location and season (Harbick and Albright, 2016; Graamans et al., 2018; Weidner et al., 2021).

To tackle this obstacle, there have been recent advances in using an extended photoperiod strategy that takes advantage of off-peak time-of-day options provided by many utility suppliers to better manage the grid and costs (Tewolde et al., 2016; Hao et al., 2018). In fact, Ontario, Canada, can be one of the cheapest electricity sources in the world for large-scale operations if they follow the Industrial Conservation Initiative peak-shaving incentive (IESO, 2022; Ontario Energy Board, 2023; Hao, personal communications). Not only that, but the reason why peak costs are so high for utility providers is because the grid must be supplemented with fossil fuel generators during those times. During off-peak hours, the grid can be sustained by clean energy sources like hydro, wind, solar, and nuclear, which would, otherwise, be wasted if not used. Therefore, CEA would benefit, economically and environmentally, if it adheres to similar conservative energy-use policies.

Theoretically, if the supplemental light can be used for 24-h photoperiods, then the supplemental light intensity can be reduced by one-third while maintaining the same daily light integral (DLI) (Hao et al., 2018). However, a major limitation to the extended photoperiod strategy is the poor response that many species have to continuous light (e.g., eggplant, peanut, geranium, tomato, potato, lichen, and moss) (Velez-Ramirez et al., 2011). In the context of CEA-relevant species such as tomato, at worst, it causes photoperiodic injury, where yield is decreased and chlorotic leaves manifest (Garner and Allard, 1927; Dorais, 2003). At best, it is tolerated, as is the case for greenhouse cucumber (Hao et al., 2020; Lanoue et al., 2021). In many cases, it causes an overly compact plant architecture (Warner et al., 2023). For example, although continuous-light–tolerant tomato genotypes have been identified, continuous light decreases leaf area and height of these young transplants (Hao et al., 2018). Photoperiodic injury–tolerant tomato transplants must acclimate over 7 weeks by incrementally increasing the photoperiod from 16 h to 24 h, to effectively retain vegetative-generative balance (van Ieperen, 2016; Hao et al., 2018). Regardless of genotype, developmental stage, and species, the application of continuous light is not physiologically beneficial even though it is driving photosynthesis day and night.

If successful acclimation strategies can be identified for tomato (*Solanum lycopersicum* L. 'Money Maker'), as a model photoperiodic injury–sensitive species and model tomato cultivar, then they would likely be useful for other species as well. Accordingly, we include a comparative study on mini-cucumber (*Cucumis sativus* L. 'Beesan') as a photoperiodic injury–tolerant species. We also report preliminary data on a completely photoperiodic injury–tolerant tomato genotype 'UofGPIT.'

Both species were subjected to identical LED treatments that are modified versions of an alternating red-daytime dim-blue nighttime LED strategy that grew greenhouse tomato without injury (Lanoue et al., 2019). Photoperiodic injury in tomato is related to an arrhythmic circadian rhythm (Highkin and Hanson, 1954; Hillman, 1956; Velez-Ramirez et al., 2017a), and it is our perspective that efforts directed toward entraining the circadian rhythm will improve acclimation to extended photoperiod/continuous light (Marie et al., 2022). Furthermore, understanding circadian rhythm entrainment can help with guiding/compensating for the daily shifts in peak electrical pricing when growers would need daily fidelity in shifting supplemental lighting intensity without unbalancing the crop.

While constrained by the central motive of circadian entrainment, we can modify the alternating LED strategy to steer toward a better canopy architecture and measure the induced photosynthetic effects to gain insights that may further improve our understanding of photoperiodic injury tolerance. It would be helpful to identify specific photosynthetic traits that are diagnostic of successful acclimation to photoperiod extension. Or better yet, can we identify mechanisms that optimize photosynthesis under photoperiod extension and postulate future modifications that

would engage them? Knowledge about these mechanisms would also aid in CEA-specific breeding efforts.

One proposition that can be largely agreed on is photoperiod extension imposing a state of excess energy. Depending on the source-sink balance and environmental factors, when there exists a state of excess incoming energy, different types of dissipative/protective mechanisms can be engaged in the short term. Long-term acclimation to excess excitation involves downregulation of source capacity and upregulation of sink capacity (Huner et al., 2003). The opposite response is induced under limited light availability. Collectively, these balancing responses are termed photostasis (Huner et al., 2003). In this context, we hypothesize photorespiration and its associated effects on metabolism/light reactions as a major mechanism involved with acclimating to extended photoperiods.

Photorespiration refers to a complex pathway that is initiated by oxygen (O_2) competing against carbon dioxide (CO_2) as a substrate with ribulose bisphosphate (RuBP) catalyzed by RuBP carboxylase/oxygenase (RuBisCO), creating an alternative pathway at the first step of the Calvin cycle (Ogren, 1984). Oxygenation of RuBP results in the production of phosphoglycolate and one phosphoglycerate, instead of two phosphoglycerates from RuBP carboxylation. In C3 plants, phosphoglycolate is eventually converted into phosphoglycerate to contribute to the Calvin cycle after several steps progressing through the chloroplast, peroxisomes, mitochondria, and back. A detailed description of these steps is not the focus of this manuscript, but some of them are highlighted as having significant implications for photoperiod extension.

Photorespiration has been reported to be an important energetic sink mechanism being used under drought stress (Valentini et al., 1995; Guan and Gu, 2009), salt stress (Hannachi et al., 2022), and combined high temperature/light stress (Osei-Bonsu et al., 2021). However, Smith et al. (2023) found that photorespiration is not a short-term energy dissipative pathway that directly alleviates photosystem II (PSII) damage. Rather, photorespiration has a role in sustaining the Calvin cycle that allows for the timely synthesis of D1 protein slotted for PSII repair (Takahashi et al., 2007). It sustains the Calvin cycle by ensuring sufficient inorganic phosphate (P_i) substrate for ATP turnover. The relationship between photorespiration and Calvin cycle turnover can be best observed as triose phosphate utilization (TPU) limitation (Sharkey, 1985; McClain and Sharkey, 2019). Photorespiratory-mediated P_i release, which has a positive effect under TPU-limited conditions, also has an impact on ATP: NADPH stoichiometry. It has been established that increased relative levels of photorespiration increases relative ATP demand, changing the ATP: NADPH demand stoichiometry, which needs to be balanced by increasing the ATP: NADPH ratio supply via upregulating ATP-generating (cyclic) or NADPH-consuming/alternative electron sink (pseudo-cyclic) mechanisms (Kramer and Evans, 2011).

In addition to a hypothesized increase in photorespiration under successful acclimation to extended photoperiods, we also hypothesize an associated increase in cyclic/pseudo-cyclic mechanism to sustain it. Our objectives were to 1) measure basic morphological and biomass partitioning in tomato and mini-cucumber under dynamic LEDs, 2) employ a combined gas exchange and fluorescence protocol to quantify photorespiration, 3) probe ATP balancing mechanisms during the short-term diurnal phases of the dynamic LED treatments and the long-term acclimated steady state, and 4) assess the similarities and differences between photoperiodic injury–sensitive tomato 'Money Maker' and photoperiodic injury–tolerant mini-cucumber 'Beesan' (along with supplemental comparisons to a tolerant tomato genotype).

2 Methods

2.1 Plant material and growth conditions

At the University of Guelph, Ontario, Canada, tomato 'Money Maker' was sown and placed in a growth chamber (Conviron, Winnipeg, Canada) for 2 weeks, under humidity domes with environmental conditions set to 25°C (day/night) and fluorescent lighting (5,000-K white, single pin T12 tubes, Sylvania Inc., Wilmington, MA, USA) set to 150 μmol m^{-2} s^{-1} photosynthetic photon flux density (PPFD) for 16-h light/8-h dark photoperiod. Mini-cucumber 'Beesan' was sown under identical conditions but for 1 week. The most vigorous plants were then transplanted into 15-cm-wide plastic square pots filled with standard potting mix (Sungro professional growing mix #1, Soba Beach, AB, Canada) and transferred into a "nursery" growth chamber (GC-20 Bigfoot series, Biochamber, Winnipeg, Canada) equipped with LEDs (see below lighting treatment) for 7 days set to 21°C (day/night), 65% relative humidity, 300 μmol m^{-2} s^{-1} PPFD, and 16-h light/8-h dark photoperiod. Afterward, plants were transferred to treatment chambers (GC-20 Bigfoot series, Biochamber, Winnipeg, Canada), all under identical environmental conditions (previously calibrated with external sensors) except for the lighting treatments described below. Fertigation was supplied as needed with 20–8-20 fertilizer (Plant Products Inc., Leamington, ON, Canada) mixed in regular tap water (Guelph, Ontario tap water is relatively high in carbonates, pH approximately 7, electrical conductivity (EC) approximately 0.85 mS/cm) and adjusted to a pH of 5.6 with phosphoric acid to a final EC of 1.75 mS/cm. Leaf gas exchange and fluorescence measurements were done 42 days after sowing (DAS) for tomato and 35 DAS for mini-cucumber, targeting the third true leaf. After photosynthetic measurements, an additional 4 days were given until destructive analysis (all on the same day of the given week). At this relatively large transplant age, 'Money Maker' only had small primordial floral development, but mini-cucumber 'Beesan' had several fruits of harvestable size. To assess this early yield, no thinning was performed prior to destructive harvest and only fruits that were >5-cm long were included in the weight (in some cases, there were a dozen or more<2-cm fruits that were not included in weight measurements).

2.2 Lighting treatments

Biochambers had four independently controllable light banks that were each equipped with T5-type ballast compatible replacement LEDs tubes (red LEDs, SKU F54T5HO-LED36R, Growlights Canada Inc., Beamsville, ON, CAN; blue LEDs, SKU F54T5HO-LED36B, Growlights Canada Inc., Beamsville, ON, CAN; 3,500-K white, LED25WT5HO/46/835-G8DR, Lumenco Inc., Trois-Rivières, QC, CAN; and 5,000-K white, LED25WT5HO/46/850-G8DR, Lumenco Inc., Trois-Rivières, QC, CAN). Depending on the treatment, different designated light banks were use to supply the needed spectrum that had either control (steady unchanging spectrum for 16-h photoperiod), constant (steady unchanging spectrum for 24-h photoperiod), dynamic 1 (changing spectrum and intensity depending on time of day), or dynamic 2 (changing spectrum and intensity depending on time of day) (Figure 1). The spectrum was changed by using biochamber control software for timing different light banks with the addition of separate far-red LED fixtures on a timer (FGI Far Red, FARREDLB, Forever Green Indoors Inc., Seattle, WA, USA). Total DLI and far-red DLI were the same across all treatments; however, blue DLI was only the same between control and constant or dynamic 1 and dynamic 2 (Supplementary Material 1).

2.3 Leaf gas exchange and chlorophyll fluorescence

Simultaneous gas exchange and chlorophyll fluorescence were performed using two LiCor 6400 (LI-COR Biosciences, NE, USA) instruments side by side, each with the 6400–40 leaf chamber fluorometer head. All measurements were done with the LiCor 6400 heads fixed inside a growth chamber to maintain ambient lighting and temperature around the whole plant while protocols were being done on the individual leaf.

A quick transition between 21% and 2% O_2 (Supplementary Material 2) was done to follow the photorespiration protocol explained by Bellasio et al. (2014). The protocol provides the necessary variables to derive RuBisCO activities (Equation 1). Photorespiration is calculated as the ratio between RuBisCO oxygenase activities (V_O) and RuBisCO carboxylation activities (V_C), V_O/V_C. The equation requires gross assimilation (GA under 21% O_2 and GA under low O_2) as inputs, and, in our case, we used dark respiration (rather than day respiration estimation techniques) to calculate it from net assimilation (and net assimilation under low O_2) as it was simply more convenient in our protocol. In support of this decision, variations in day respiration estimates only sway the results by approximately 4% according to the sensitivity analysis done by Bellasio et al. (2014). The equation also requires PSII photochemical quantum yield (YII) under ambient O_2 and low O_2.

$$\frac{V_O}{V_C} = \frac{2\mathrm{GA}_{\mathrm{Low\,O2}} \frac{Y(II)}{Y(II)_{Low\ O2}} - 2\mathrm{GA}}{\mathrm{GA}_{\mathrm{Low\,O2}} \frac{Y(II)}{Y(II)_{Low\ O2}} + 2\mathrm{GA}} \quad (1)$$

2.4 MultispeQ measurements

The MultispeQ (PhotosynQ Inc., MI, USA) is a leaf spectrophotometer/fluorometer designed for open-source research (Kuhlgert et al., 2016). The programmability and customizations available make it a very useful tool. The "Photosynthesis RIDES 2.0" protocol was selected as it has very high throughput and provides over 14 photosynthetic response variables in approximately 1 min. An overview of the equations used in the protocol can be found on PhotosynQ's webpage "documentation" under the subsection "references and parameters" (Kramer et al., 2023). The protocol

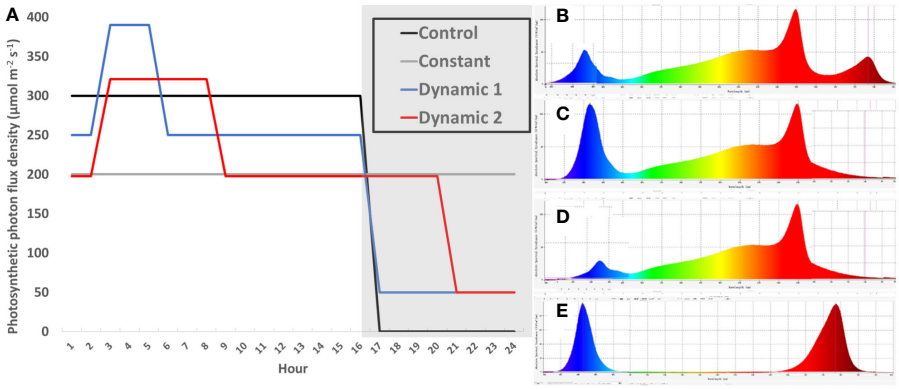

FIGURE 1
Schedule of light treatments. A single diurnal cycle is represented by non-shaded (day) and shaded bars (night) (hour 1 = 8 am) **(A)**. Light intensity is plotted across time-of-day for each light treatment, which are sum to equivalent DLIs (17.28 mol m^{-2} d^{-1}) **(A)**. Control (solid line) and constant (double thin line) both had the same relative spectra for their entire photoperiod **(B)**, consisting of cool-white supplemented with red and far-red spectra (CW + R + FR). Dynamic 1 and dynamic 2 had a "day" spectrum of warm-white plus red (WW + R) for the first 2 h after subjective dawn **(D)**. They then received a "peak" spectrum **(C)** that supplemented 140 PPFD of pure blue on top of day spectrum (WW + R + Bl) for 3 h and 5 h, respectively. After the peak phase was finished, they returned to "day" spectrum until the end of their 16-h and 20-h photoperiods, respectively. During subjective night, they each received dim-blue and far-red (Bl + FR) **(E)**, although the intensity of far-red was higher in dynamic 2 to ensure all treatments received the same dose of FR (Supplementary Material 1).

and associated macro were used in their original form, without modifications. The protocol also offers the measurement of broadband electrochromic shift (ECS) under dark-interval relaxation kinetic (DIRK) assays that can be used in combination with fluorescence techniques, described by Baker et al. (2007). Together, using the "Photosynthesis RIDES 2.0" protocol, it is possible to probe both electron flow and proton flow under steady-state light-adapted conditions. Two parameters were calculated separately in excel that combine fluorescence and absorption parameters provided by the MultispeQ according to Baker et al. (2007). Proton motive force from linear electron flow (LEF) only (pmf_{LEF}) was calculated by dividing the fluorescence-based parameter LEF by the ECS DIRK absorption–based parameter that estimates ATP synthase conductivity/activity (gH^+). Proton pumping by cyclic electron flow (CEF) ($v_{H+}LEF^{-1}$) was calculated by dividing the ECS DIRK absorption–based relative proton flux (v_{H+}) by fluorescence-based LEF and multiplying it by 1,000 (Avenson et al., 2005; Baker et al., 2007). Apparent conductance of cytochrome b_6f was calculated by dividing LEF by the portion of closed PSII reaction centers, where open reaction centers follow the lake model (qL), giving a parameter notation [LEF $(1 - qL)^{-1}$] (Johnson et al., 2021).

Depending on the experimental design, either the plants were transferred to a growth chamber for measurements under identical environmental conditions (PPFD, RH%, and temperature) (for 3-week acclimated representative steady state) or the measurements were taken under the actual conditions for the designated treatments (with different PPFD/spectrum) (for short-term time-course experiment).

Note that, throughout the time course, the plants acclimated to changes in light intensity and quality, but our measurements were done under a common light quality (red, 660 nm) that only responds to ambient light intensity sensed on the top of the MultispeQ. This is simply the programming of the Photosynthesis RIDES 2.0 protocol. Future studies could customize light quality differences, but these results serve as a good indication of photosynthetic mechanisms using an unaltered protocol that is widely available and repeatable.

2.5 Whole-plant biomass and partitioning

Plants were harvested destructively for total above-ground biomass, biomass partitioning (between leaves, petioles, and stems), and plant architecture (stem height, leaf surface area, specific leaf area, etc.). Partitioned plant materials were dried in an oven to get the measurement of dried weights. Leaf area was measured by using a personal smartphone, with the Easy Leaf Area app (Easlon and Bloom, 2014), rigged to a retort stand to maintain consistent lighting and distance from a black cloth background with a 4-cm^2 red cardboard square for automatic scaling in the app. Once the best green/blue/red scales were adjusted to ensure uniform leaf and red square highlighting, the same settings were used for all future pictures through the app.

2.6 Statistics

Statistical analyses were done using Proc Glimmix in SAS Studio 3.81. One-way analysis of variance (ANOVA) was performed on the destructive whole-plant datasets according to a completely randomized block design, with light treatment as fixed factor and random factor blocked by week of sowing. Tomato had 10–12 samples over 5 successive weeks of sowing. Week of sowing was blocked as it contained a high amount of variability due to slight age differences between cohorts of sowing and other unknown random factors. When ANOVAs were significant ($p< 0.05$), means comparisons were performed using Tukey–Kramer adjustment, testing the significant difference ($p< 0.05$).

3 Results

3.1 Tomato canopy architecture, biomass, and partitioning

Over a 3-week course of treatment, constant light accumulated the least biomass resulting in a significant difference in total biomass compared to all other treatments (Table 1). Specific leaf area was the highest under constant light compared to all other light treatments, and, inversely, the leaf mass per area was significantly lower under constant light. Biomass partitioning analysis found that constant light allocated more dry weight to stem mass fraction at the expense of leaf mass fraction, both significantly different from control. Leaf area under constant light was not significantly different from control or dynamic 2, but it was significantly lower than dynamic 1. The same was true for height.

Dynamic 1 had a significantly higher total biomass than control and constant but not significantly different from dynamic 2. Dynamic 1 was the tallest of all light treatments (Figure 2). Biomass partitioning trends for dynamic 1 showed a higher stem mass fraction than control at the expense of petiole mass fraction, with no significant difference in leaf mass fraction. Specific leaf area and leaf mass per area were not significantly different from control; however, they were both different from constant.

Dynamic 2 accumulated more total biomass than constant but was not significantly different from control or dynamic 1. Leaf mass per area was higher in dynamic 2 compared to all other treatments, but specific leaf area did not reflect this difference. Dynamic 2 height, leaf area, and stem mass fraction were not significantly different from control or constant. Dynamic 2 petiole mass fraction was lower than control and constant but the same as dynamic 1. Leaf mass fraction was higher than constant and dynamic 1 but not significantly different from control.

On a qualitative visual level of leaves, dynamic 1 did not have any observable chlorosis (nor did control), whereas constant had a severe chlorosis that was variable in degree across replicates. Dynamic 2 had a very minor form of chlorosis that was almost imperceptible, and it was not noticed in some replicates.

10.3389/fpls.2024.1384518

TABLE 1 Biomass and partitioning traits measured from destructive analysis comparing tomato 'Money Maker' grown under different photoperiod extension strategies in growth chambers.

Light treatment		Control	Constant	Dynamic 1	Dynamic 2
Total Biomass	*(g)*	10.63 ± 1.16 B	7.86 ± 1.16 C	12.90 ± 1.14 A	11.73 ± 1.14 AB
Height	*(cm)*	28.0 ± 2.1 B	30.3 ± 2.1 B	40.1 ± 2.0 A	29.9 ± 2.0 B
Leaf area	*(m^2)*	0.206 ± 0.018 AB	0.183 ± 0.018 B	0.230 ± 0.018 A	0.186 ± 0.018 B
Specific leaf area (m^2 kg^{-1})		29.0 ± 1.9 B	37.6 ± 1.9 A	27.5 ± 1.8 B	24.0 ± 1.8 B
Leaf mass per area	*(g m^{-2})*	35.6 ± 1.9 B	27.7 ± 1.9 C	37.1 ± 1.8 B	43.0 ± 1.8 A
Stem mass fraction	*(g g^{-1})*	0.16 ± 0.007 C	0.19 ± 0.007 AB	0.20 ± 0.007 A	0.17 ± 0.007 BC
Petiole mass fraction	*(g g^{-1})*	0.16 ± 0.003 A	0.17 ± 0.003 A	0.14 ± 0.003 B	0.15 ± 0.003 B
Leaf mass fraction	*(g g^{-1})*	0.67 ± 0.008 AB	0.64 ± 0.008 C	0.66 ± 0.008 BC	0.68 ± 0.008 A

Mass fractions (in dry weight) were calculated by dividing the organ of interest by total above-ground biomass. Means and standard error (n = 10–12) are presented with letters to denote if a significant difference was found using least square means with Tukey–Kramer adjustment ($p < 0.05$), same letters are not significantly different from each other.

FIGURE 2
Representative size and architecture of **(A)** tomato 'Money Maker' and **(B)** mini-cucumber 'Beesan' after being exposed to indicated light treatments for 3 weeks. Both species are represented by spliced images, with the same control plant that was not moved from its position in each cropped section.

3.2 Mini-cucumber canopy architecture, biomass, and partitioning

Overall, dynamic 1 had higher total biomass and greater height than constant and dynamic 2 treatments, but neither variable was significantly different from control (Table 2). Interestingly, leaf morphology looked different between dynamic 1 and control; however, it was not quantified (Figure 2).

Dynamic 1 had the highest yield compared to all other treatments. Furthermore, the fruit in both dynamic treatments looked much greener and of higher quality than control and constant (Figure 3). Biomass partitioning showed that dynamic 1 allocated more dry matter to petiole mass fraction than any other treatment and allocated less to leaf mass fraction than the others. Dynamic 1 had the highest harvest index; however, it was not significantly different from control unless the alpha value is relaxed to 0.10 ($p = 0.0921$), which would help interpretation considering the higher yield and significantly less allocation to leaf mass fraction while maintaining similar total biomass.

Constant-light treatment had the lowest total biomass compared to all other treatments. Yield was significantly less under constant light than the other treatments, except for dynamic 2. Height and leaf area showed the same trend, with constant light being less than control and dynamic 1, but not

TABLE 2 Biomass and partitioning traits measured from destructive analysis comparing mini-cucumber 'Beesan' grown under different photoperiod extension strategies in growth chambers.

Light treatment		Control	Constant	Dynamic 1	Dynamic 2
Total biomass	*(g)*	17.05 ± 1.09 AB	11.05 ± 1.09 C	18.17 ± 1.09 A	15.43 ± 1.07 B
Yield	*(g)*	70.42 ± 13.36 B	31.17 ± 13.36 C	93.77 ± 13.35 A	52.42 ± 13.20 BC
Height	*(cm)*	81.09 ± 4.12 A	54.72 ± 4.12 B	70.44 ± 4.12 A	52.08 ± 3.98 B
Leaf area	*(m^2)*	0.290 ± 0.018 A	0.225 ± 0.018 B	0.283 ± 0.018 A	0.228 ± 0.017 B
Specific leaf area (m^2 kg^{-1})		30.22 ± 1.40 A	32.59 ± 1.40 A	31.58 ± 1.40 A	23.88 ± 1.32 B
Leaf mass per area	*(g m^{-2})*	33.90 ± 1.47 B	31.06 ± 1.47 B	31.98 ± 1.47 B	42.07 ± 1.1.40 A
Stem mass fraction	*(g g^{-1})*	0.18 ± 0.01 A	0.18 ± 0.01 A	0.17 ± 0.01 A	0.14 ± 0.01 B
Petiole mass fraction	*(g g^{-1})*	0.058 ± 0.003 C	0.054 ± 0.003 C	0.078 ± 0.003 A	0.068 ± 0.003 B
Leaf mass fraction	*(g g^{-1})*	0.57 ± 0.03 B	0.64 ± 0.03 A	0.50 ± 0.03 C	0.62 ± 0.03 AB
Harvest index	*(g g^{-1})*	0.19 ± 0.03 AB*	0.12 ± 0.03 C	0.25 ± 0.03 A*	0.17 ± 0.03 BC

Mass fractions (in dry weight) were calculated by dividing the organ of interest by total above-ground biomass. Yield was the first harvest from unpruned 6- to 7-week-old plants (fresh weight). Means and standard error (n = 8–9) are presented with letters to denote if a significant difference was found using least square means with Tukey–Kramer adjustment ($p < 0.05$), same letters are not significantly different from each other.
*Harvest index difference between control and dynamic 1 ($p = 0.0921$).

significantly different from dynamic 2. Biomass partitioning shows constant light induced more dry matter to be allocated to leaf mass fraction than harvest index compared to control.

Dynamic 2 had a total biomass that was significantly higher than constant. However, height and leaf area were both comparable to constant. The extra biomass was observed to come from an increase in leaf mass per area, which was significantly higher than all other treatments. Dynamic 2 diverted the most partitioning away from stem mass fraction compared to all treatments. Interestingly, it had an intermediate level of partitioning to petiole mass fraction that was significantly greater than control, but significantly less than dynamic 1. It also retained more partitioning to leaf mass fraction than dynamic 1, being comparable to both constant and control. Finally, dynamic 2 yield and harvest index were significantly lower than dynamic 1 and not significantly different from either control or constant.

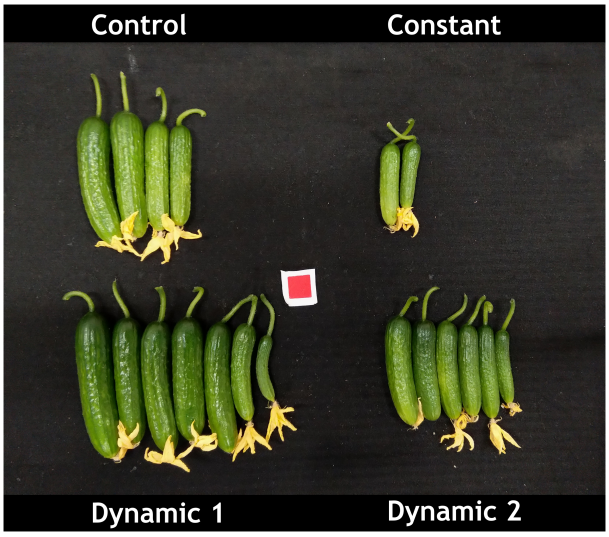

FIGURE 3
Representative image of mini-cucumber 'Beesan' first harvest (from two plants) after approximately 3 weeks of growth under the indicated light treatments. Dynamic 1 had the highest yield as depicted in the image, and it was statistically significant. Note that both dynamic LED treatments induced a greener fruit, which was not quantified in the present study.

3.3 Photosynthesis and photorespiration of tomato and mini-cucumber under ambient conditions after 3-week acclimation

The initial survey measurements described in Methods section "Leaf gas exchange and chlorophyll fluorescence" were designed to follow a high throughput screening method for determining rates of photorespiration (Bellasio et al., 2014). The intention was to quantify photorespiration at ambient conditions for each lighting treatment.

Upon a standard gas exchange analysis of dark respiration, net assimilation (ambient O_2), and net assimilation (low O_2), the only apparent significant difference across treatments is the severe decline found under constant light for tomato (Figure 4). Constant-light treatment for cucumber, however, maintained all parameters similar to control with the exception of having significantly greater respiration in the dark. Although net assimilation under low O_2 seems higher under constant for cucumber, the variability between samples masks any significant differences. Net assimilation under ambient O_2 was significantly lower under dynamic 2 than control for cucumber but was not different under low O_2.

The same differences across treatments, relative to constant-light treatment depending on species, were found from a standard chlorophyll fluorescence analysis of maximum quantum yield (Fv/Fm) of PSII and PSII photochemical quantum yield (YII), where only constant-light treatment for tomato was significantly lower

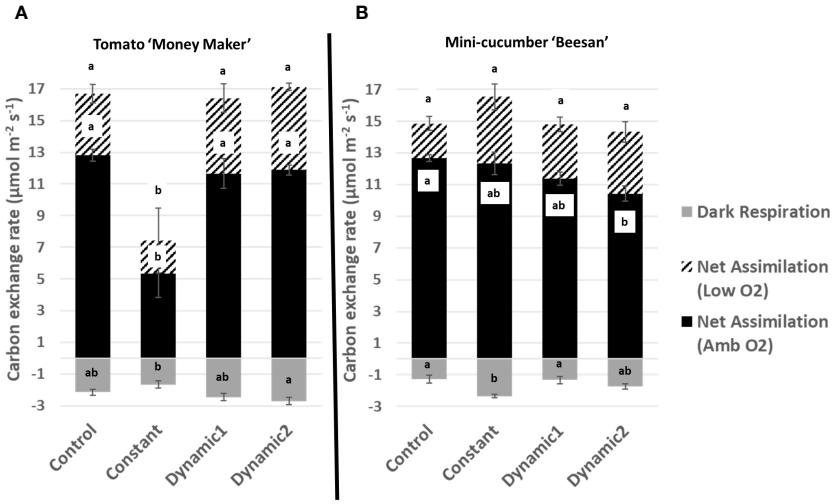

FIGURE 4
Carbon exchange rates measured under ambient conditions from tomato 'Money Maker' **(A)** and mini-cucumber 'Beesan' **(B)** leaves acclimated to different lighting treatments. For tomato, all treatments, except constant, are not significantly different from each other. For mini-cucumber, constant seems to have a higher net assimilation (low O_2), but it is not significant. However, constant has a larger dark respiration than all other treatments. Dynamic 2 has a lower net assimilation (ambient O_2) than control, but it is not significantly different from constant and dynamic 1. Means and standard error (n = 4) are presented with letters to denote if a significant difference was found using least square means with Tukey–Kramer adjustment ($p< 0.05$), same letters mean they are not significantly different from each other.

(Figure 5). These results on their own are commonly reported in the literature and used to assess the effectiveness of treatments.

All treatments, except constant light, had comparable RuBisCO carboxylation activities (V_C) and RuBisCO oxygenase activities (V_O) for tomato (Figure 6), whereas cucumber V_C was significantly lower in dynamic 2 than control and V_O was significantly higher in constant than control. For tomato, the RuBisCO oxygenase to carboxylation activity ratio (V_O/V_C) shows a significant increase in dynamic 1 compared to control, whereas V_O/V_C in constant-light treatment balanced out to be equivalent to the other treatments, which makes sense considering it was equally depressed in both V_C and V_O. For cucumber, V_O/V_C was significantly higher in all photoperiod extension treatments than control.

3.4 Long-term MultispeQ-derived photosynthetic variables of tomato

After 3 weeks of acclimation to respective lighting treatments, tomato plants were transferred (at approximately 2 pm) to a common growth chamber so that they all may be measured under similar conditions. In terms of fluorescence-based parameters provided by the MultispeQ instrument (Table 3), all analyzed light treatments had comparable LEF. PSII maximum efficiency (Fv'/Fm') and non-photochemical quenching (NPQt) were significantly lower and higher, respectively, in dynamic 2 compared to control and dynamic 1. Although NPQt was reported, the protocol does not distinguish between quenching mechanisms possible through time-dependent quenching assays for q_E, q_T, and q_I. Dynamic 1 had a significantly lower fraction of open PSII reaction centers (qL) than control, but dynamic 2 was not significantly different from either. Dynamic 1 also had a significantly lower apparent conductance of cytochrome b_6f (Cyt b_6f) [LEF $(1 - qL)^{-1}$], a parameter derived from Johnson et al. (2021).

Quantum yield of PSII (ϕ_{PSII}) is significantly lower in both dynamic treatments than control. However, the fraction of dissipated energy as regulated NPQ (ϕ_{NPQ}) is higher in dynamic 2 than control and dynamic 1, whereas non-regulated dissipation (ϕ_{NO}) is higher in dynamic 1 than control, but not different from dynamic 2.

Absorption-based parameters give further information on thylakoid dynamics. Dynamic 1 had a significantly higher steady-state proton efflux/conductivity through ATP synthase (gH+) compared to both control and dynamic 2. Also, the total (light to dark) proton motive force across the thylakoid membrane (ECSt) was significantly lower in dynamic 1 than control and somewhat lower than dynamic 2 but not significantly. Relative proton flux (v_{H+}) was not significantly different between any treatments, although dynamic 2 seemed lower.

Combining fluorescence and absorption-based parameters gives some more relationships to explore. The proton motive force from LEF only (pmf_{LEF}) was lower in dynamic 1 than both control and dynamic 2. However, proton pumping by CEF (v_{H+} LEF^{-1}) was not significantly different between any treatment. In addition, ECSt maintained the same relative relationship with the lowered pmf_{LEF}, again indicating that CEF did not significantly increase. However, there is one limitation to the comparisons found through the relationship between pmf_{LEF} and v_{H+} being different in dynamic 1

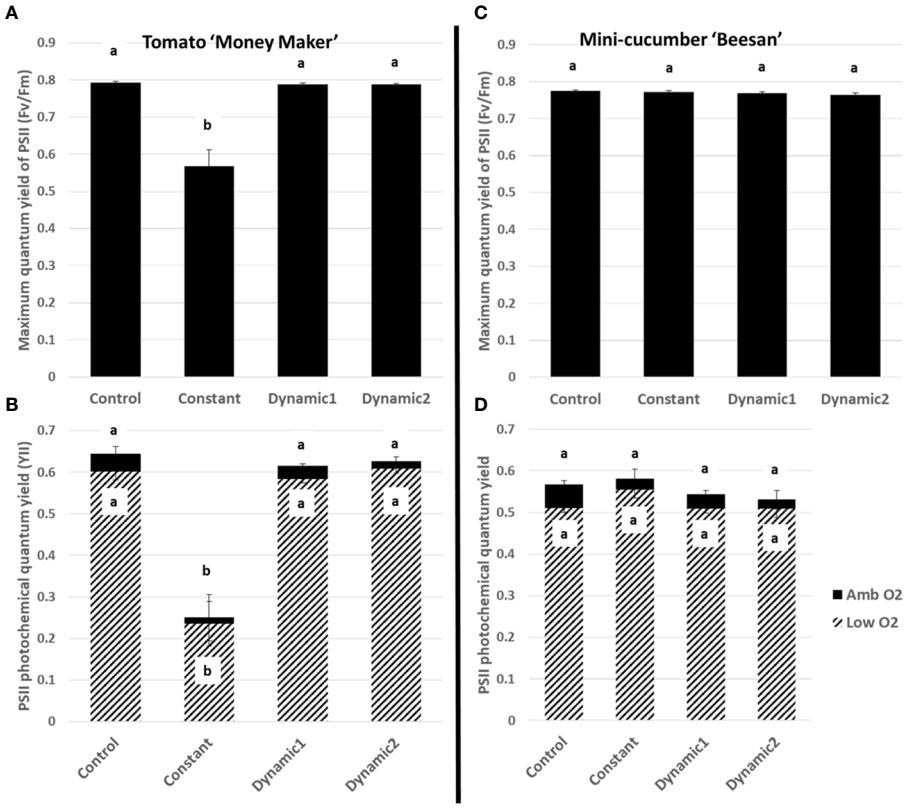

FIGURE 5
Fluorescence parameters measured under ambient conditions from tomato leaves acclimated to different lighting treatments. Maximum quantum yield of PSII (Fv/Fm) **(A, C)** and PSII photochemical quantum yield (YII) **(B, D)**. For tomato, all treatments, except constant, are not significantly different from each other. For cucumber, constant retained PSII function similar to all other light treatments. Means and standard error (n = 4) are presented with letters to denote if a significant difference was found using least square means with Tukey–Kramer adjustment ($p < 0.05$), same letters are not significantly different from each other.

compared to both control and dynamic 2. This can either indicate a pigment composition change or differing ECS response. Considering dynamic 2 has a differing pigment composition (SPAD), it may be difficult to draw conclusions for it. It is also important to reiterate that dynamic 2 had some very mild injury, but it did provide information on imbalances compared to control and dynamic 1.

Finally, the analysis of the electron transport chain can be completed by observing the oxidation state of PSI centers using the absorption-based methods programmed into the RIDES 2.0 protocol of the MultispeQ. Both dynamic 1 and dynamic 2 had significantly higher fraction of over reduced PSI centers than control. However, dynamic 1 PSI oxidized centers and PSI open centers were not significantly different than control, whereas dynamic 2 was. Nonetheless, dynamic 1 seemed to be under slightly less pressure than dynamic 2. Dynamic 2 also had higher active PSI centers than control, and dynamic 1 was between the two showing no significant difference either way. Combined with the fact that qL was significantly lower in dynamic 1 than control (and dynamic 2 was lower but not significantly than control) and the differing gH+/NPQt responses, we can interpret that both dynamic 1 and dynamic 2 had more reduced electron transport chains than control, and they each engaged different mechanisms to deal with it.

3.5 Short-term diurnal MultispeQ patterns under different lighting treatments in tomato

Upon the first day of tomato plants being transferred to their respective treatments (from a shared growth chamber), a time-course series of MultispeQ measurements were taken under *in situ* conditions (Figures 7, 8). "Post-Dawn Hour 1 Day 1" was taken 1 h to 2 h after transfer/start of the photoperiod. "Mid-Day Hours 4–6" was taken between 4 h and 6 h into the photoperiod, with the range implying that dynamic 1 and dynamic 2 were measured near the end of their respective high blue light phase to capture the full effect of duration (control and constant were measured between them). "Hour 8" and "Hour 12" did not have any measurements, rather they are shown to ensure the x-axis time points are evenly spaced. "Pre-Dusk Hour 16" was measured just prior to the end of the control photoperiod (<16 h), whereas "Pre-Dusk Hour 20" represents the end of the photoperiod for dynamic 2 treatment (<20 h). "Pre-Dawn Hour 23" was measured prior to the start of the next photoperiod (<24 h). "Post-Dawn Hour 1 Day 2" was measured 1 h to 2 h after the start of the next photoperiod, 24 h after post-dawn (day 1).

10.3389/fpls.2024.1384518

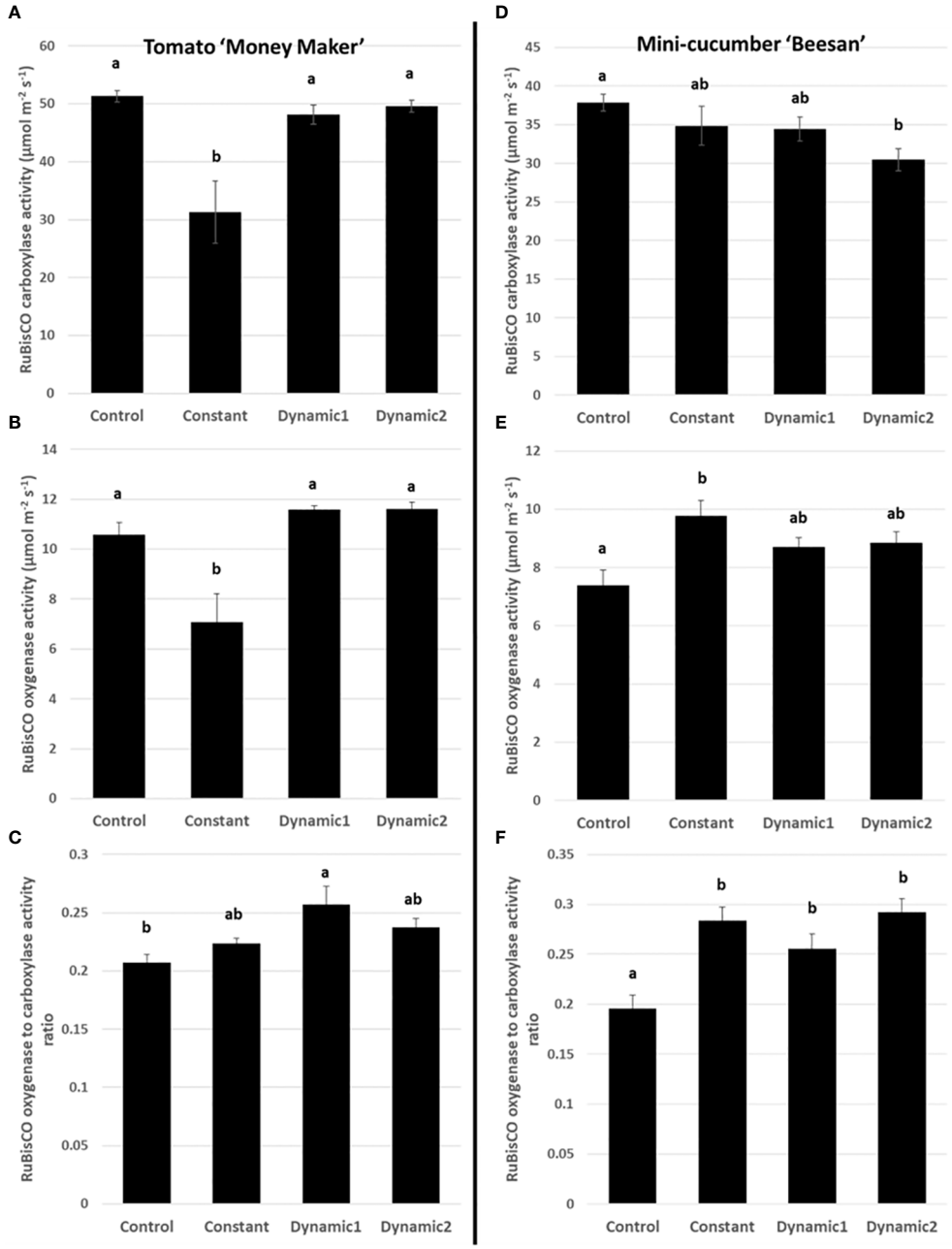

FIGURE 6
RuBisCO carboxylase **(A, D)** and oxygenase **(B, E)** activities under ambient conditions (V_C and V_O) and photorespiration estimated by their ratio (V_O/V_C) **(C, F)**. Constant-light treatment for tomato had a significantly lower V_C and V_O than control. Dynamic 1 and dynamic 2 were similar to control in V_C and V_O, and both were significantly higher than constant. V_O/V_C was significant different between control and dynamic 1. Cucumber, however, maintains higher V_O/V_C under constant (and both dynamic LED treatments) than control. Means and standard error (n = 4) are presented with letters to denote if a significant difference was found using least square means with Tukey–Kramer adjustment ($p < 0.05$), same letters are not significantly different from each other.

Generally, for all treatments, PSII maximum efficiency (Fv'/Fm') (A) tends to decrease to its lowest values by the end of the acclimated photoperiod (Pre-Dusk Hour 16) with absolute values largely dependent on light intensity. The impact is seen in a likewise decline of PSII operating efficiency (Φ_{PSII}) (B) over the photoperiod, largely explained by increases in regulated dissipation of excitons through NPQ (Φ_{NPQ}) (C) and NPQt (H). However, non-regulated dissipation (Φ_{NO}) adds an independent source of diurnal variation to Φ_{PSII} through changes in the fraction of PSII open reaction centers (qL), which is indicative of basal/dark quenching. At mid-day, under unchanging light of control and constant, there is an increase in Φ_{NO} (decrease in qL) that is mitigated by acclimation to an increase of blue light intensity in both dynamic treatments (this is not intuitive as qL generally

10.3389/fpls.2024.1384518

TABLE 3 A comparison of photosynthetic variables from tomato leaves grown under different photoperiod extension strategies in growth chambers acquired with MultispeQ using the protocol "Photosynthesis RIDES 2.0".

Light treatment		Control	Dynamic 1	Dynamic 2
Linear electron flow	*LEF*	64.38 ± 1.192 A	61.40 ± 0.766 A	61.64 ± 0.801 A
PSII maximum efficiency	*Fv'/Fm'*	0.783 ± 0.002 A	0.781 ± 0.001 A	**0.772 ± 0.002 B**
Non-photochemical quenching	*NPQt*	0.352 ± 0.018 B	0.366 ± 0.010 B	**0.443 ± 0.020 A**
Fraction of PSII centers in open state	*qL*	0.623 ± 0.015 A	**0.551 ± 0.010 B**	0.569 ± 0.018 AB
Apparent conductance of Cyt b_6f to linear electron flow	*LEF $(1 - qL)^{-1}$*	173.6 ± 10.70 A	**138.2 ± 4.069 B**	146.9 ± 8.121 AB
Quantum yield of PSII (fraction of excitons driving LEF)	ϕ_{PSII}	0.691 ± 0.006 A	**0.662 ± 0.004 B**	**0.657 ± 0.008 B**
Fraction of excitons dissipated through regulated non-photochemical quenching	ϕ_{NPQ}	0.080 ± 0.004 B	0.090 ± 0.002 B	**0.105 ± 0.005 A**
Fraction of excitons dissipated through non-regulated mechanisms	ϕ_{NO}	0.228 ± 0.004 B	**0.247 ± 0.003 A**	0.238 ± 0.005 AB
Steady-state relative thylakoid proton efflux (ATP synthase conductivity/activity)	g_{H+}	143.9 ± 9.789 B	**186.9 ± 8.300 A**	133.8 ± 8.272 B
Relative proton flux (H^+/ATP ratio multiplied by ATP synthesis rate)	v_{H+}	0.084 ± 0.003 A	0.082 ± 0.002 A	0.076 ± 0.003 A
Proton pumping by cyclic electron flow (×1,000)	v_{H+} LEF^{-1}	1.300 ± 0.045 A	1.344 ± 0.049 A	1.241 ± 0.054 A
Proton motive force from linear electron flow only	pmf_{LEF}	0.484 ± 0.033 A	**0.344 ± 0.016 B**	0.482 ± 0.035 A
Total light-dark Δ pmf (×1,000)	*ECSt*	0.627 ± 0.055 A	**0.453 ± 0.020 B**	0.603 ± 0.066 AB
Lifetime of steady-state ATP synthase proton efflux (×1,000)	*ECS*	7.476 ± 0.536 A	**5.543 ± 0.220 B**	7.682 ± 0.538 A
Oxidized PSI centers, where acceptors lack electrons	PSI_{ox}	0.237 ± 0.027 A	0.166 ± 0.053 AB	**0.114 ± 0.029 B**
Over reduced PSI centers, where acceptors are saturated with electrons	PSI_{or}	0.276 ± 0.084 B	**0.551 ± 0.050 A**	**0.557 ± 0.033 A**
Open PSI centers that are ready to accept electrons	PSI_o	0.669 ± 0.093 A	0.382 ± 0.067 AB	**0.313 ± 0.047 B**
Active PSI centers that are "operational" to receive/pass electrons	PSI_A	1.390 ± 0.088 B	1.597 ± 0.074 B	**1.959 ± 0.078 A**
Relative chlorophyll content	*SPAD*	50.44 ± 1.969 B	54.23 ± 0.810 B	**58.48 ± 0.955 A**

Note that the dataset originally contained the constant-light treatment, but it was excluded for this analysis. The data were highly variable, and the leaves were visibly unhealthy/chlorotic. It was determined that 3 weeks of constant treatment causes damage so extensive that the MultispeQ data do not provide information on the imbalances that caused the injury (particularly electrochromic shift and photosystem 1 absorption-based methods). Means and standard error (n = 8) are presented with letters to denote if a significant difference was found using least square means with Tukey–Kramer adjustment ($p < 0.05$), same letters are not significantly different from each other.

All plants, which have been acclimating to their respective lighting treatments for 3 weeks, were transferred to the same growth chamber during mid-day to measure at steady state under similar conditions.

Values that are significantly different are bolded (in addition to ascribed letters that denote significance) to make it easier to see.

decreases with increases in light intensity). As the photoperiod is extended beyond Hour 16 for constant, it seems there is a slight rhythm in Φ_{PSII} and Φ_{NO}/qL, whereas Φ_{NPQ}, but more so NPQt, plateaus at Pre-Dusk Hour 16, only slightly declining over the rest of the night into the next day. For both dynamic treatments, Fv'/Fm' (with NPQt) does not recover for the first 4 h of the low-light portion of their respective nighttime spectral treatments and, in both cases, recovers most prominently upon re-introduction to "day spectrum" from Pre-Dawn Hour 23 to Post-Dawn Day 2 Hour 1. The total light-dark proton motive force (ECSt) (G) agrees well with NPQt for control and constant during the acclimated photoperiod, indicating that luminal pH was driving NPQt as expected (although we cannot officially differentiate quenching components with this protocol). However, during Pre-Dusk Hour 20 and Pre-Dawn Hour 23 and just Pre-Dawn Hour 23, when dynamic 1 and dynamic 2 were in their subjective nights, respectively, ECSt was no longer associated with NPQt. NPQt remained high, whereas ECSt dropped, showing a persistent form of photoinhibition rather than a quick reversible quenching. ECSt must have dramatically dropped thanks to a large drop in light intensity that decreased relative proton flux (v_{H+}) (J) along with an increase in ATP synthase activity (gH+) (I). There was also a profound three- to five-fold increase in proton pumping mediated by CEF (v_{H+} LEF^{-1}) (L) that aligns closely with the increased gH+. A drop in proton motive force driven by LEF (pmf_{LEF}) (K) and a five-fold drop in apparent conductance of cytochrome b_6f to LEF [LEF $(1 - qL)^{-1}$] (F) confirm a transition from LEF to CEF once low-light nighttime treatment started regardless of timing. Overlaid on this light-dependent recovery mechanism was a time-dependent mechanism. Dynamic 1 had an advantage, much more than dynamic 2, between Pre-Dusk (Hour 16) and Pre-Dusk (Hour 20) that shows there was a conditional and different kind of recovery through Φ_{NO}/qL when transferred into low light. Dynamic 2 seems to have missed this Φ_{NO}/qL window and instead displays the complete opposite response when it is transferred into low light. Both dynamic LED responses, considered together but in shifted phases, indicate a nighttime recovery from a non-regulated quenching mechanism (and a susceptibility to it) that seems to be gated, creating a coincidence between circadian rhythm and metabolism fluctuation. The background circadian signal can be seen in the slight Φ_{NO}/qL rhythm in constant at the same phases and the dramatic increase

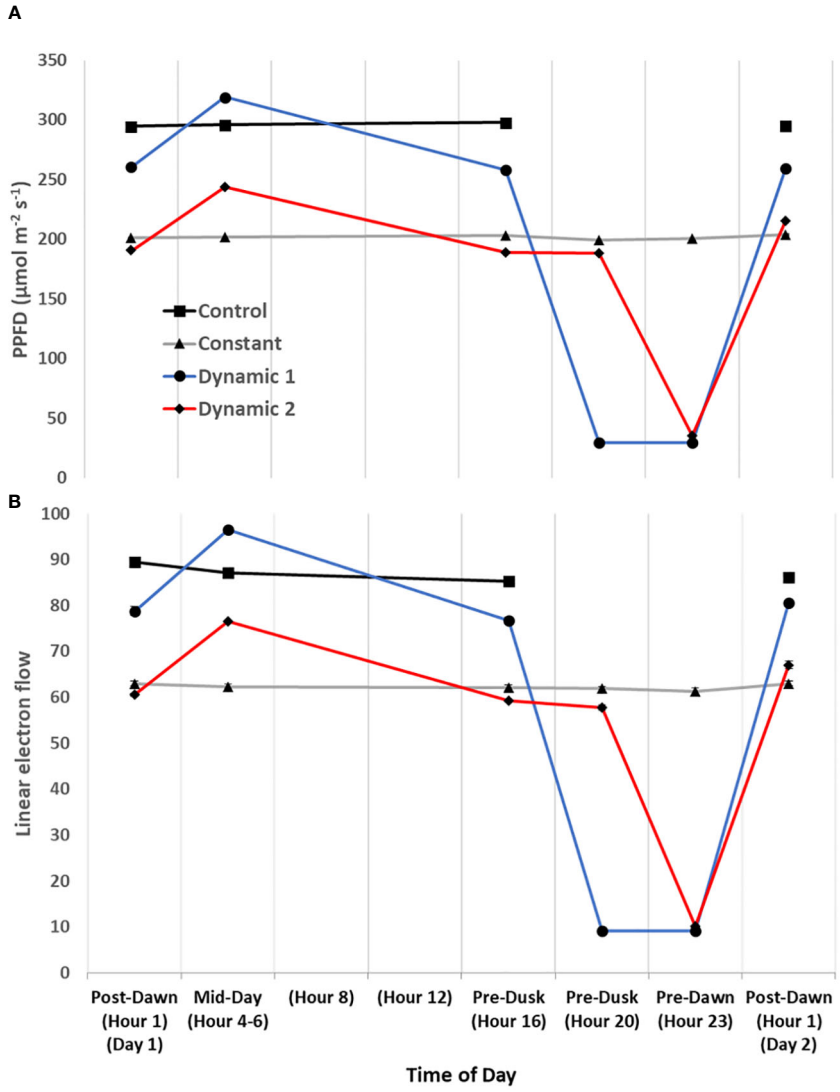

FIGURE 7
Diurnal light intensity and linear electron flow. The diurnal time-course of tomato measured under their respective treatment conditions for the first day. Actinic light intensity used in fluorescence- and absorption-based protocols is plotted as ambient light intensity **(A)**. Overall, linear electron flow (LEF) **(B)** responds as expected to light intensity, but there does seem to be a subtle decrease of LEF over time of day that is most noticeable in control. Each measurement was an average of three technical replicates for each biological replicate in a repeated measures design. Mean and standard error from n = 4.

of Φ_{NO}/qL in dynamic 1 at the Pre-Dusk Hour 20 phase. This is a significant finding, as the same light treatment effect (shifting to low nighttime light intensity) would be expected to give a similar metabolic response regardless of phase, but, here, we see that they amplify a background circadian rhythm instead. Aside from these large happenings at subjective night, during mid-day, both dynamic LED treatments drop v_{H+} LEF^{-1} during their blue light additions, again likely responding to light intensity. However, the dynamic treatments differ from each other in pmf_{LEF}, with dynamic 1 having a large increase. There was also a small increase in gH+ and v_{H+} in dynamic 2 but not in dynamic 1. It could be that dynamic 2 was suffering from proton leakage (Avenson et al., 2005). This can be interpreted as optimal duration of high blue light that has an observable beneficial effect at<3 h but could be detrimental after<5 h. Interestingly, v_{H+} LEF^{-1} appears to increase toward the end of the photoperiod in constant and control but reaches a maximum pre-dusk (Hour 16) and slightly drops as the photoperiod extends.

One of the most notable results that is relevant to photorespiration and daily ATP budgeting is the large relative increase of cyclic electron transport during low light at subjective nighttime for both dynamic treatments.

3.6 Short-term diurnal MultispeQ patterns under constant light comparing tomato and mini-cucumber

Initial fluorescence-based parameters show nearly identical response patterns during the first constant day between tomato

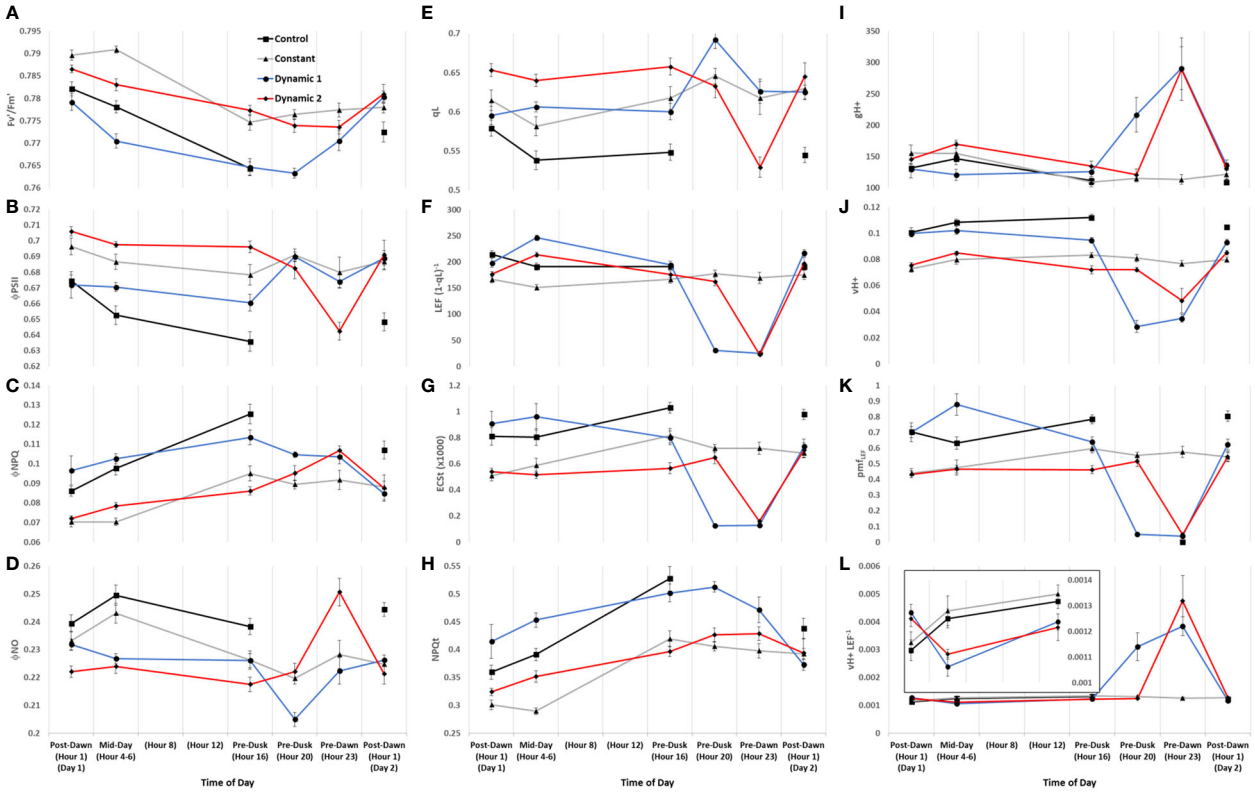

FIGURE 8
Diurnal MultispeQ fluorescence- and absorption-based parameters during the first day of tomato plants exposed to light treatments. Estimated parameters across all light treatments show strong diurnal patterns with notable treatment effects. PSII maximum efficiency (Fv'/Fm') **(A)**, PSII operating efficiency (Φ_{PSII}) **(B)**, quantum yield of non-photochemical quenching (Φ_{NPQ}) **(C)**, quantum yield of non-regulated dissipation (Φ_{NO}) **(D)**, fraction of PSII open reaction centers (qL) **(E)**, apparent conductance of cytochrome b_6f to linear electron flow [LEF $(1 - qL)^{-1}$] **(F)** (Johnson et al., 2021), total light-dark proton motive force (ECSt) **(G)**, light adapted non-photochemical quenching NPQt **(H)** (Tietz et al., 2017), ATP synthase activity (gH+) **(I)**, relative proton flux (v_{H+}) **(J)**, proton motive force driven by linear electron flow (pmf_{LEF}) **(K)**, and cyclic electron flow (v_{H+} LEF^{-1}) **(L)**. Overall, we can summarize that upstream NPQt regulatory processes act distinctly from qL/Φ_{NO}-related quenching processes, the former being dependent on the duration of the photoperiod and light intensity shifts, whereas the latter showing an interesting circadian gating phenomenon. We can also highlight that nighttime under dim-light promotes high levels of cyclic electron flow regardless of feedback inhibitions reflected in qL or degree of NPQt. Plants were analyzed using a repeated measures design showing mean and standard error from n = 4.

'Money Maker' and mini-cucumber 'Beesan' (Figure 9). The most remarkable difference between tomato and cucumber can be seen in ECSt patterns (G). Firstly, ECSt, which can be associated with luminal pH, is closely linked with NPQt (H) in tomato, whereas it is not associated in cucumber. This shows that tomato is engaging a fast-relaxing quenching responses over the acclimated photoperiod, whereas cucumber is accumulating slow-relaxing photoinhibition. In fact, cucumber has a constitutively higher Φ_{NPQ} (C)/NPQt to begin with, showing that this species has an inherently higher photoinhibition that tomato in our system. The separation of NPQt response from ECSt may be attributed to cucumber's ability in maintaining ATP synthase activity (gH+) (I) longer than tomato. It is not until the photoperiod is extended past its acclimated amount (Pre-Dusk Hour 20) when gH+ begins to drop causing ECSt along with NPQt to rise in cucumber. Interestingly, CEF (v_{H+} LEF^{-1}) (L) has a peak at Pre-Dawn Hour 23 in cucumber, whereas tomato seems to have upregulated CEF earlier and then downregulates it at that time. Cucumber uniquely seems to build up pmf Pre-Dawn through increases in CEF and other LEF mechanisms without a matched ATP synthase activity for proton efflux until the subsequent Post-Dawn when the issue resolves. In both species, there is an ephemeral increase in Φ_{NO} (D) at Mid-Day Hours 4–6, a dip at Pre-Dusk Hour 20, and a return to base-level at Pre-Dawn Hour 23. The opposite pattern is reflected in open PSII reaction centers (qL) (E) and cytochrome b_6f conductance to LEF [LEF $(1 - qL)^{-1}$] (F). These last patterns are indicative of an endogenous circadian rhythm of non-regulated quenching, which is remarkably similar in both unrelated species.

4 Discussion

4.1 Using dynamic LEDs to guide canopy architecture and biomass partitioning

Dynamic LEDs, which can change spectra and timing, offer a flexible system that can be tailored to the plant growth objectives needed. Our objectives were to extend the photoperiod without

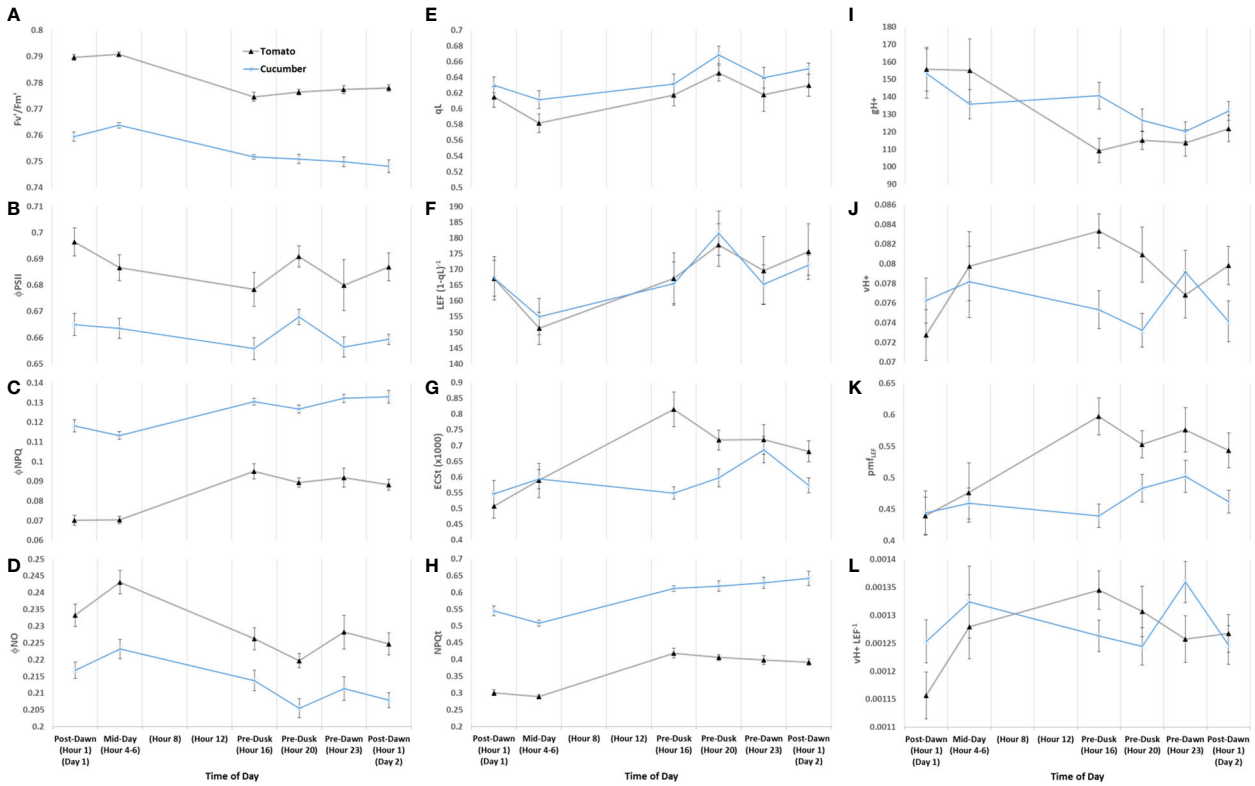

FIGURE 9
Diurnal combined absorption- and fluorescence-based parameters of tomato and mini-cucumber under the first day of constant light. PSII maximum efficiency (Fv'/Fm') **(A)**, PSII operating efficiency (Φ_{PSII}) **(B)**, quantum yield of non-photochemical quenching (Φ_{NPQ}) **(C)**, quantum yield of non-regulated dissipation (Φ_{NO}) **(D)**, fraction of PSII open reaction centers (qL) **(E)**, apparent conductance of cytochrome b_6f to linear electron flow [LEF $(1 - qL)^{-1}$] **(F)** (Johnson et al., 2021), total light-dark proton motive force (ECSt) **(G)**, light adapted non-photochemical quenching NPQt **(H)** (Tietz et al., 2017), ATP synthase activity (gH+) **(I)**, relative proton flux (v_{H+}) **(J)**, proton motive force driven by linear electron flow (pmf_{LEF}) **(K)**, and cyclic electron flow (v_{H+} LEF^{-1}) **(L)**. These patterns are indicative of an endogenous circadian rhythm of non-regulated quenching, which is remarkably similar in both unrelated species. Plants were analyzed using a repeated measures design showing mean and standard error from n = 4.

compromising canopy architecture and inducing photoperiodic injury. Dynamic LEDs enabled a successful photoperiod extension strategy by starting with a base circadian entrainment program that includes a timed "peak spectrum" overlayed on a "day spectrum" and then a transition into a "night spectrum." The strategy allows for flexibility in dosing the "peak spectrum" and "night spectrum" cues independently to adjust canopy architecture.

The "peak spectrum" consisted of a short duration (3 h to 5 h) high blue light enrichment during late morning/afternoon. The discrete signal was intended to mimic the natural increase in high light/blue light of the solar spectrum at mid-day, when the circadian rhythm would have an anticipated sensitivity to it. Rather than a homogenous increase in light intensity from the LED fixture, which is costly, we attempted to mimic a strong high light response by focusing all the energy into blue light. Blue light is known to induce the signal for short- and long-term acclimation responses (Hogewoning et al., 2010; Hoffmann et al., 2015; Huché-Thélier et al., 2016: Kang et al., 2021). Blue light also stimulates stomatal opening, which is important for balancing solar radiation energy input with transpiration driven energy output (Geelen et al., 2019; Marie et al., [In press]). Also, blue LEDs are efficacious, contributing to a higher total LED fixture efficacy if the fixture has a relatively higher proportion of blue LEDs than white LEDs (Kusuma et al., 2020).

However, there are drawbacks to how much blue light should be added in a growth spectrum, as excessive blue light from artificial lighting sources can cause photoinhibition and leaf damage, likely from the combination of photosensitizers in the electron transport chain/chlorophyll that produce damaging singlet oxygen and the over-excitation of PSII water-splitting manganese complex that releases manganese ions in the lumen acting as inhibitors in other PSII reaction centers (Zavafer and Mancilla, 2021). However, more likely at the levels that we are proposing, too much relative (and absolute) blue light can create an overly compact plant architecture that reduces canopy radiation capture (Snowden et al., 2016; Kaiser et al., 2019; Kalaitzoglou et al., 2021). Extending the photoperiod also aggravates the compactness problem (Warner et al., 2023). Therefore, compensating for these two impacts on canopy architecture is a basic requirement for a successful dynamic LED strategy to be integrated with practical management practices.

Far-red light has the opposite effect by inducing stem elongation and leaf expansion to varying degrees in most species, collectively termed the shade-avoidance response (Demotes-Mainard et al., 2016). Adding far-red to a blue-rich spectrum during the

photoperiod also results in an interesting interplay of counteracting morphological and photosynthetic responses (Meng and Runkle, 2019; Kong and Nemali, 2021). If far-red is applied during the photoperiod, then the effects on canopy morphology are dependent on total light intensity, but it is not a general rule across all species (Kusuma and Bugbee, 2023). Far-red can also induce morphological effects whether supplied during the photoperiod or at end of day (EOD) (Kalaitzoglou et al., 2019). Concentrating the full dose of far-red at EOD drives a stronger response than if spread throughout the photoperiod, and the effect is even stronger if given after the photoperiod (Zou et al., 2021).

Far-red supplied during the photoperiod, from a photosynthetic point of view, not only is beneficial when combined with other spectra for driving assimilation (Zhen and Bugbee, 2020) but also has photoprotective effects under fluctuating high light conditions (Kono et al., 2017). However, far-red applied throughout the photoperiod decreases expression of morning circadian genes and increases expression of evening genes, resulting in suppressed amplitude of transcript rhythms (Wenden et al., 2011). In addition, while far-red induces useful generative behavior in greenhouse tomato, it also increases susceptibility to disease if supplied throughout the photoperiod (Ji et al., 2019; Kim et al., 2019; Meijer et al., 2023).

Therefore, there is an upper limit on how much far-red can be added in a photoperiod, necessitating the reliance on EOD far-red to counteract most of the blue light plus extended photoperiod induced morphological responses. An example of this was found in greenhouse pepper, which becomes overly compact under continuous light but was completely alleviated if far-red was added to the nighttime phase of the alternating LED spectrum (Lanoue et al., 2022). These considerations informed the implementation of far-red in addition to dim-blue during the nighttime spectra.

The effects from dynamic LED treatments were uncertain because there is not an extensive database for greenhouse crops under dynamic changing spectra. Differences in biomass partitioning, particularly, were under question as the far-red induced shade avoidance response was needed for plant height gains but is commonly at the expense of leaf mass per area (LMA) (Casal, 2012; Chitwood et al., 2015). Additionally, dim-blue light at nighttime engages an additional shade-avoidance response through phototropins (Kong and Zheng, 2020). Interestingly, the short 3-h pulse of blue light at early to mid-day in dynamic 1 treatment on tomato was sufficient to counteract the leaf-level LMA shade-avoidance response, all while not impacting the stem-level aspect of the response in tomato (Figure 2; Table 1). The segregation of LMA and leaf area from plant height in dynamic 1 proved to be valuable for total biomass gains and an ideal canopy architecture. Mini-cucumber under dynamic 1, however, did not differ from control morphologically except with an increased partitioning to petioles, which may have improved canopy architecture.

Dynamic 2 in tomato had a significantly higher LMA and no difference in plant height compared to control. The increased partitioning of dry weight to leaves, increased LMA, decreased leaf area, decreased plant height, and decreased partitioning to stem in dynamic 2 clearly follows the trend of increased daytime blue light fraction found in another study using similar aged tomato transplants and treatment duration (Kalaitzoglou et al., 2021). Compared to dynamic 1, the increase in LMA was most likely associated with the longer 5-h pulse of blue light. However, dynamic 1 and dynamic 2 had equal blue and far-red DLI doses, demonstrating that timing played a major role in the differing responses. Mini-cucumber seemed much more sensitive to the blue light timing, showing decreases in plant height and leaf area along with an increase in LMA. Clearly biomass partitioning was diverted away from stem fraction and put into leaf fraction, but oddly also in petiole fraction. This suggests that nighttime far-red timing plays a stronger role on petiole morphology than stem morphology, whereas blue light timing mid-day has a stronger impact on stem morphology in mini-cucumber 'Beesan.'

The optimal dynamic LED recipe for mini-cucumber still needs to be devised as the presented experimental design did not thoroughly explore all timing and dosing options. In addition, these differing responses across greenhouse crops highlight the importance of the need for flexibility in supplemental lighting strategies. In this work, we presented a small case study where the same dynamic LED formula induced profound canopy differences by tuning minor blue and far-red timing variations. These variations can certainly be optimized on a crop-by-crop basis (and even adjusted on a weekly basis as needed by the grower in tandem with existing dynamic temperature control strategies).

4.2 Dynamic 1 exhibits potential for increased yield in mini-cucumber

Unexpectedly, mini-cucumber yield (from unpruned plants) was significantly higher in dynamic 1 (93.77 g ± 13.35 g) than control (70.42 g ± 13.36 g), and far greater than constant (31.17 g ± 13.36 g) (Table 2). However, total biomass, leaf area, and height were not significantly different than control (Table 2), which is a stark contrast to the responses seen in tomato. Although, there was a subtle morphological difference that is discernable in visual appearance of the plants (Figure 2), which may be partially explained by a greater biomass partitioning to petioles in dynamic 1 (Table 2). Interestingly, not only yield was greater in dynamic 1, but it also had a much greener fruit, contributing to a higher shelf appeal in terms of fruit quality (dynamic 2 shared this response) (Figure 3). These results were not expected as the similar red/dim-blue alternating LED strategy in a greenhouse experiment demonstrated no net-positive effects on mini-cucumber yield compared to constant or control (Lanoue et al., 2021). Our differing results are most likely due to the differences between greenhouses and growth chambers. However, it would be worth trying nighttime far-red in the greenhouse (as an optimization of the existing alternating red/dim-blue strategy), as that was never done before and shows promise for increasing mini-cucumber yield from our growth chamber study. Also, the addition of short-duration mid-day blue in greenhouse production may be beneficial for enhancing fruit quality (greenness), especially in winter when several consecutive cloudy days limit blue light from natural sunlight.

4.3 Successful acclimation to extended photoperiods depends on sustained photorespiration

At present, there are no explanatory stress markers for photoperiodic injury other than reductions in Fv/Fm, which represents a general photoinhibition. First, we assessed fast screening methodologies to see if we could define possible mechanisms easily. Fortunately, after 3 weeks of treatment, we were able to see a very mild injury developing in dynamic 2, which served as a much better comparison to healthy control and dynamic 1 than the excessively injured constant treatment. Indeed, the constant-light treatment had a much lower Fv/Fm, which we interpret as the late stages of photoinhibition, but dynamic 2 did not exhibit any measurable photoinhibition.

A quick comparison between net assimilation rates, respiration in the dark, Fv/Fm, and quantum yield of PSII (YII) under ambient growth conditions shows no significant differences between control, dynamic 1, and dynamic 2 for tomato (Figures 4, 5). Also, identical treatment comparisons were made for mini-cucumber 'Beesan' (Figures 4, 5) and a photoperiodic injury–tolerant tomato genotype 'UofGPIT' grown under constant (Supplementary Materials 3–6). To dig deeper, we implemented a high-throughput screening method for photorespiration rate (V_O/V_C) (Bellasio et al., 2014) under ambient conditions (air temperature 21°C, PPFD 300 µmol m^{-2} s^{-1}, C_a 440 µmol mol^{-1}). Increases in V_O/V_C were hypothesized to ameliorate stress induced by extended photoperiods in both dynamic treatments. For photoperiodic injury–sensitive tomato 'Money Maker,' we seen a significant increase of V_O/V_C in dynamic 1 (0.257 ± 0.016) compared to control (0.207 ± 0.007). Dynamic 2, on the other hand, did not have a significant increase of V_O/V_C (0.237 ± 0.007) compared to control (although its value was in between control and dynamic 1) (Figure 6). The original intention of dynamic 2 was to improve the electrical cost efficiency of the alternating 12-h/12-h red/dim-blue introduced by Lanoue et al. (2019) by extending the "daytime" photoperiod to 20-h/4-h. However, the presented configuration of dynamic 2 pushed the limits, and we can use this opportunity to find out why.

Interestingly, V_O/V_C was significantly greater than control in dynamic 1, dynamic 2, and constant for the photoperiodic injury–tolerant species mini-cucumber 'Beesan.' Furthermore, a photoperiodic injury–tolerant tomato genotype 'UofGPIT' grown under constant light also displayed a higher V_O/V_C (Supplementary Material 6). Unexpectedly, the photoperiodic injury–tolerant tomato cultivar 'UofGPIT' and mini-cucumber 'Beesan' had nearly the same photorespiration level under constant light (0.295 ± 0.003 and 0.284 ± 0.014, respectively). Also, under the dynamic 1 LED treatment, photorespiration was nearly the same between photoperiodic injury–sensitive tomato 'Money Maker' (0.257 ± 0.016) and tolerant mini-cucumber 'Beesan' (0.256 ± 0.014). The comparisons may be justified by the fact that control had similar levels between tomato 'Money Maker' (0.207 ± 0.007) and mini-cucumber 'Beesan' (0.196 ± 0.014). These results are highly suggestive that photoperiodic injury tolerance derived from both adaptation (across unrelated species/tolerant genotypes within species) and acclimation (using dynamic LEDs) involves the upregulation of photorespiration.

The fact that tomato 'Money Maker' was displaying a very mild form of photoperiodic injury under dynamic 2 and was found to not upregulate photorespiration to the degree that mini-cucumber did under dynamic 2 (unlike their similarity under dynamic 1) can point toward a downstream limitation. The MultispeQ was used to further explore this limitation in 3-week acclimated tomato (Table 3). The light-dark difference in total proton motive force (ECSt) (also related to luminal pH) and conductance of protons through ATP synthase (gH+) together indicate dynamic 1 had either a more sensitive ATP synthase activity (possibly a higher P_i substrate availability) and/or more abundant ATP synthase content in the thylakoids than control and dynamic 2 (Avenson et al., 2005). The notion of a higher ATP synthase content/activity in dynamic 1 is supported by the lack of additional NPQt above control, meaning the proton efflux through ATP activity/content was able to maintain luminal pH within a healthy non-dissipative inducing range that was useful for ATP: NADPH balancing (type I response) (Kramer and Evans, 2011). Whereas dynamic 2 did not maintain a healthy ATP synthase activity/content that did not enable appropriate proton efflux, observed as a lower gH+ and higher ECSt, which caused a significant induction of NPQt (type II response) (Kramer and Evans, 2011).

Dynamic 1 also had a lower fraction of proton motive force from LEF (pmf_{LEF}), but it was not due to an increase in CEF (v_{H+} LEF^{-1}), rather it was due to the ease of proton efflux through ATP synthase, which did not need as much pmf (Takizawa et al., 2008). Therefore, the difference in ATP synthase activity could be due to P_i substrate availability, being limiting in dynamic 2 but not limited in dynamic 1, causing the buildup of protons in dynamic 2. This is supported by the finding that photorespiratory P_i substrate–alleviating qualities are deficient in dynamic 2, implying a cause and effect.

The upstream question remains, for tomato 'Money Maker' dynamic 2, what caused a failure to fully upregulate photorespiration yet maintain a high carboxylation capacity? Many photorespiratory genes/enzymes are regulated by light and metabolic feedback signals (Aroca et al., 2023). One interesting negative feedback regulator of photorespiration is an increase in serine pools, which has been shown to selectively inhibit transcription of photorespiratory genes (Timm et al., 2013). In addition, glycine decarboxylase in the mitochondria, responsible for the conversion of glycine to serine, is regarded as the central modulator of photorespiratory flux, which can exert immediate control via post-translational modifications (Timm and Hagemann, 2020). The serine-to-glycine ratio downregulates photorespiration if high and upregulates it if low (Timm et al., 2016). Serine has been described to interconnect S, N, and C1 metabolism and be involved with stress acclimation (Aroca et al., 2023). In addition, although photorespiration accounts for most of the serine production in plants, two other glycolysis-branch serine pathways are engaged during stress, act in non-photosynthetic tissues, and are allosterically inhibited by serine, and many mutations in these pathways are embryo lethal that implicates glycine to serine ratio as having a crucial role in primary metabolism (Igamberdiev and

Kleczkowski, 2018). Future research could measure photoperiod dependent accumulation and export of glycine/serine pools that are possibly associated with selective suppression of photorespiration (i.e., without affecting RuBP carboxylation) and the hypothesized differences in export over the nighttime spectra of dynamic LED recipes (along with simple photoperiod extension).

Importantly, selectively inhibiting photorespiration does not relax associated ATP-compensating mechanisms that were originally engaged with it (Smith et al., 2023). For example, exposure to low O_2 increased lumen acidification, which was attributed to a decrease in apparent ATP synthase activity caused by an ATP surplus (i.e., suddenly reducing photorespiration will drop ATP consumption and lead to another form of TPU/P_i limitation) (Smith et al., 2023). Regarding dynamic 2, it could be that excessive serine was suppressing photorespiration, which caused a build up of unused ATP that subsequently led to a P_i limitation/ATP synthase activity bottleneck.

4.4 Short-term acclimation mechanisms under dynamic LEDs

TPU limitation was reported to occur upon the first day of photoperiod extension in rice grown in a controlled environment (Fabre et al., 2019). Once TPU is reached, there is an immediate imbalance in P_i availability, causing dynamic changes in redox states (McClain et al., 2023). We observed that early stages of acclimation to extended photoperiod (and dynamic treatments) involve a time-of-day regulated redox and P_i balancing act, with CEF playing a huge role in driving ATP synthase during the nighttime low-light (and far-red rich) phases of dynamic LED treatments (Figures 7, 8). The relative increase in ATP supply at nighttime in both dynamic treatments could be satisfying (or almost satisfying, respectively) a total daily ATP budget. Tied to ATP/proton management is the differing degree of relaxation of NPQt responses across treatments. Constant light was constitutively unrelaxed, dynamic 2 had approximately 50% recovery, whereas dynamic 1 fully recovered. Mini-cucumber seemed to have a more delayed onset of NPQt under constant light than tomato, likely due to the maintenance of ATP synthase activity for a longer duration (Figure 9).

Independent from the CEF and NPQt responses, a major difference between dynamic 1 and dynamic 2 redox balance can be observed during their nighttime phases. They have totally opposite responses of opening/closing PSII reaction centers (qL) due to basal/dark quenching regulation (ϕ_{NO}). ϕ_{NO} represents excitation dissipation through thermal and fluorescence emission independent of NPQ, likely from closed PSII reaction centers quenching/dissipating the energy (Kramer et al., 2004; Klughammer and Schreiber, 2008). Constant-light treatment also displayed a subtle phase response, qL opening and subsequent closing 4 h later, which may point toward a circadian regulation mechanism. Interestingly, tomato and mini-cucumber share a nearly identical circadian pattern of qL and ϕ_{NO} under constant-light treatment too, showing this circadian phenomena may be conserved across unrelated species. It just so happens that dynamic 1 shifts to low light when reaction centers are opening (between Post-Dusk Hour 16 and Hour 20), emphasizing a potential peak circadian phase. Dynamic 2 shifts to low light while the reaction centers are closing (between Post-Dusk Hour 20 and Pre-dawn Hour 23), emphasizing a potential trough circadian phase. If it were purely an electron transport chain over-reduced signal, then we would expect the same qL response but differing amplitude, between dynamic LED treatments, which was not the case. This circadian gating effect inspires future experiments that could explore the link between P_i regulation of ATP synthase activity and CEF with the potential circadian phasing of basal/dark feedback inhibition and opening/closing of PSII reaction centers.

Short-term TPU limitation could be alleviated by an initial increase of photorespiration (McClain et al., 2023). However, TPU limitation quickly disappears after 30 h of acclimation and is balanced by downregulation of other processes (McClain et al., 2023). For example, RuBisCO is deactivated and q_E is engaged until long-term acclimation strategies take over (McClain et al., 2023). In a preliminary experiment, after 4 nights of continuous light, the photoperiodic injury–sensitive tomato cultivar 'Basket Vee' maintained higher photorespiration than control (data not shown), confirming the early onset of photorespiration and that it persists for several days, and up to/longer than 3-weeks if it can be sustained as was shown for photoperiodic injury–tolerant mini-cucumber 'Beesan' and tomato 'UofGPIT.'

4.5 Photorespiration, peroxisomal catalase, and the circadian external coincidence model as a hypothesis for photoperiodic injury

The physiological causes and effects during photoperiodic injury are an on-going area of research. Velez-Ramirez et al. (2017b) reasoned that an ATP: NADPH imbalance resulted from the accumulation of carbohydrates and the associated decrease in Calvin cycle enzyme transcription. They found a strong correlation between carbohydrate accumulation and decreases in Fv/Fm. This supports it as a driver that induces early senescence, possibly through reactive oxygen species (ROS) derived from an over-reduced electron transport chain (Velez-Ramirez et al., 2011; 2017b). However, although carbohydrate accumulation has received a lot of attention as a cause of photoperiodic injury, it is not the full story, as other photoperiodic injury studies have not found correlations between carbohydrates accumulation and photoperiodic injury (Pham and Chun, 2020; Shibaeva et al., 2023).

We suggest it is not necessarily the accumulation of carbohydrates that causes the damage directly, rather it is initiated by TPU limitation effect on P_i availability. Then, the need for photorespiratory-related freeing of P_i substrate, as well as the consequences of photorespiration, becomes an important piece to the photoperiodic injury puzzle. The many roles photorespiration plays in balancing metabolic flux between mitochondria, peroxisome, and chloroplast are complex and offer many modes of action to investigate. However, peroxisomal H_2O_2 production, a by-product from glycolate oxidase's reaction with

glycolate producing glyoxylate, may be a prime candidate for ROS signaling. Furthermore, photoinhibition was found to not be directly related to photoperiodic injury (Dorais et al., 1995; Velez-Ramirez et al., 2017a). We observed over-reduced electron transport chains in both dynamic LED treatments after 3 weeks of acclimation, but dynamic 1 had no signs of injury, whereas dynamic 2 did, leading us to speculate photorespiratory H_2O_2 as having a more direct role.

In Arabidopsis, a photorespiration-derived H_2O_2 redox signal was found to be governed by a peroxisome localized *CATALASE2* (*CAT2*) in a photoperiod dependent manner, independent of light intensity and oxidative stress duration (Queval et al., 2007; 2012; Yang et al., 2019). Short-day acclimated plants show a pronounced increase in sensitivity and upregulation of oxidative marker genes in the photorespiratory *cat2* mutant (high H_2O_2 signal), supporting a protective glutathione antioxidant pathway and a salicylic acid–dependent antioxidant signaling pathway among others. However, long-day acclimated plants do not show this sensitivity and are unable to scavenge the excess H_2O_2, which then initiates programmed cell death, presumed to be a circadian rhythm mismatch (Queval et al., 2007; 2012; Yang et al., 2019). *CAT2* transcription itself is regulated by the circadian rhythm, with a peak at subjective dawn, which is dependent on the morning complex CIRCADIAN CLOCK-ASSOCIATED 1 (*CCA1*) (McClung, 1997; Lai et al., 2012). Indeed, when a *cca1* mutant was exposed to photoperiod extension stress, catalase activity was significantly lowered, and the plant became injured (Nitschke et al., 2016; Abuelsoud et al., 2020). The initiation of injury was also associated with an apoplastic increase in peroxidases, reminiscent of the oxidative burst response from pathogen infections (Nitschke et al., 2016; Abuelsoud et al., 2020). This may then have led to programmed cell death.

These studies are also relevant to tomato. Peroxisomal catalase in tomato (*SLCAT2*) expression has been shown to be upregulated during the circadian morning complex-related phase under a normal photoperiod, which shows *CAT2* in Arabidopsis and *SLCAT2* in tomato share a conserved circadian regulation pattern (Kabir and Wang, 2011). When exposed to continuous light, a tomato 'Money Maker' cross exhibited a constitutively lower expression of the circadian morning complex (and high expression of evening complex) (Müller et al., 2016), which could infer lower *SLCAT2* expression. For example, photorespiration and whole-leaf catalase activity were found to be higher than control when tomato plants were exposed to continuous light with the addition of temperature differentials, resulting in photoperiodic injury tolerance (Haque et al., 2017). The authors noted that there was a possible connection between peroxisomal-localized photorespiratory H_2O_2 release and increased catalase activity, but they were unsure of the sub-cellular localization of catalase activity. Glutathione activity was also found to be increased in this treatment, which is reminiscent of the healthy short-day response of Arabidopsis.

This leads us to hypothesize that photoperiodic injury may not be caused by absolute indiscriminate amounts of ROS, rather it could be a critical threshold of ROS during a vulnerable circadian phase. The hypothesis follows the external coincidence model of photoperiodism that has been extensively studied for flower induction (Song et al., 2015). For photoperiodic injury, the external coincidence model posits that photorespiration would be producing H_2O_2 in the light above a certain threshold during a circadian clock time when expression of the morning complex (with peroxisomal catalase) is low, thus initiating a programmed cell death response (akin to pathogen infection). The hypothesis is certainly testable by manipulations of the coincidence between internal circadian phase and external light signaling cue. For example, *cca1* mutant would have a constitutively lower morning complex expression and be more prone to photoperiodic injury, whereas a *toc1*-overexpressing mutant would display a similar response, both providing evidence for the circadian phase component. If a variety of photoperiodic injury–tolerant genotypes/species with these mutations showed injury, then that would be supportive evidence of its canonical nature. Non–24-h lighting (i.e., 6-h light/6-h dark and 24-h light/24-h dark) treatments have been shown to induce photoperiodic injury (Velez-Ramirez et al., 2017a), which makes sense if it follows an external coincidence model, as both treatments supply light during a sensitive phase. However, a phase-response curve of photoperiodic injury would provide definitive evidence in building the photoperiodic injury external coincidence model. We suggested that peroxisomal catalase is involved, so its activity phase response curve should be opposite to that of photoperiodic injury. Similar phase response curves of injury could be had for discrete modulations of photorespiration (elevated/lowered CO_2) and applications of exogenous H_2O_2/selective catalase inhibitors.

5 Conclusion

Two variations of dynamic LED strategies induced differing canopy responses, opening the potential to adjust canopy architecture through counterbalances in the peak spectrum (blue) and night spectrum (far-red). Both tomato and cucumber responded well to the dynamic 1 strategy by avoiding the overly compact morphology induced by extended photoperiods. Future research will explore more variations and work on modeling the counterbalancing act for predictive programs to be applied in CEA facilities. Next, we wanted to explore a physiological foundation for successfully growing plants under continuous light. Photorespiration was hypothesized to provide a photoperiod dependent photorespiratory-P_i stoichiometric compensation, which would be beneficial in maintaining triose-phosphate utilization. Photoperiodic injury–tolerant mini-cucumber 'Beesan,' photoperiodic injury–tolerant tomato 'UofGPIT,' and the successful acclimation to photoperiod extension in photoperiodic injury–sensitive tomato 'Money Maker' (by dynamic 1 LED strategy) all displayed higher photorespiration, supporting our hypothesis. We also found that the night spectrum of dynamic LEDs promotes relatively higher engagement of CEF and ATP synthase activities that would be beneficial for the higher ATP demands of photorespiration, potentially balancing a diurnal ATP:

NADPH stoichiometry. Future research could perform more in-depth modeling by using light curves and CO_2 curves to confirm and quantify these early findings. If true, then a conceptual framework explored the possible ontology of photoperiodic injury and its relationship with photorespiration. The proposed ontology describes a photorespiratory-antioxidant balance is de-stabilized due to a circadian rhythm external coincidence model. Specifically, light-dependent photorespiratory-H_2O_2 is not neutralized by proper circadian regulation of peroxisomal catalase and is in a sensitive phase leading to programmed cell death/pathogen defense type response. From this multiple pathway perspective, we can explain the various types of photoperiodic injury tolerance reported in the literature. Tolerance can be achieved by proper circadian rhythm entrainment given by light cues like those found by dynamic/alternating LEDs (Lanoue et al., 2019, and the presented study), circadian entrainment by temperature cues (Ikkonen et al., 2015; Hao et al., 2017b; Haque et al., 2017), a more persistent rhythmicity of the circadian rhythm like that found in photoperiodic injury–tolerant tomato species adapted to equatorial regions (Müller et al., 2016; 2018), improved energy dissipation ability/connectivity in the LHCII like that found by restoring wildtype *CAB-13* transcription (Velez-Ramirez et al., 2014), or higher constitutive catalase activity as found in photoperiodic injury–tolerant greenhouse peppers (Murage and Masuda, 1997; Demers and Gosselin, 2002). Each species may lean more heavily on one pathway or another, but we propose the overall basal need for P_i substrate by pushing photorespiration is the driving factor that a particular acclimation strategy or a unique genotype adaptation must account for to deal with photoperiodic injury.

Data availability statement

The original contributions presented in the study are included in the article/Supplementary Material. Further inquiries can be directed to the corresponding author.

Author contributions

TM: Conceptualization, Data curation, Formal analysis, Investigation, Methodology, Visualization, Writing – original draft, Writing – review & editing. EL: Data curation, Methodology, Writing – review & editing. NR: Methodology, Writing – review & editing. BG: Funding acquisition, Supervision, Writing – review & editing.

Funding

The author(s) declare that financial support was received for the research, authorship, and/or publication of this article. Ontario Ministry of Agriculture, Food and Rural Affairs (OMAFRA) (UG-T1-21-100933), Ontario Greenhouse Vegetable Growers (OGVG) (UG-TA-055596), BASF Vegetable Seeds/Nunhems (UG-TA-055590), and Genoptic LED Inc (UG-TC-005631).

Acknowledgments

We thank Elizabeth Gordon from LI-COR Biosciences Inc. for helping us navigate the LI-COR 6400 pump and user constant settings when switching between 21% and 2% oxygen. TM thanks the University of Guelph scholarship committee and sponsors of the Mrs. Fred Ball Scholarship.

Conflict of interest

The authors declare that the research was conducted in the absence of any commercial or financial relationships that could be construed as a potential conflict of interest.

The authors declare that this study received funding from Genoptic LED Inc and BASF Vegetable Seeds/Nunhems. The funders were not involved in the study design, collection, analysis, interpretation of data, the writing of this article, or the decision to submit it for publication.

Publisher's note

Supplementary material

The Supplementary Material for this article can be found online at: https://www.frontiersin.org/articles/10.3389/fpls.2024.1384518/full#supplementary-material

References

Abuelsoud, W., Cortleven, A., and Schmülling, T. (2020). Photoperiod stress induces an oxidative burst-like response and is associated with increased apoplastic peroxidase and decreased catalase activities. *J. Plant Physiol.* 253, 153252. doi: 10.1016/j.jplph.2020.153252

Aroca, A., García-Díaz, I., García-Calderón, M., Gotor, C., Márquez, A. J., and Betti, M. (2023). Photorespiration: regulation and new insights on the potential role of persulfidation. *J. Exp. Bot.* 74, 6023–6039. doi: 10.1093/jxb/erad291

Avenson, T. J., Cruz, J. A., Kanazawa, A., and Kramer, D. M. (2005). Regulating the proton budget of higher plant photosynthesis. *Proc. Natl. Acad. Sci.* 102, 9709–9713. doi: 10.1073/pnas.0503952102

Baker, N. R., Harbinson, J., and Kramer, D. M. (2007). Determining the limitations and regulation of photosynthetic energy transduction in leaves. *Plant Cell Environ.* 30, 1107–1125. doi: 10.1111/j.1365-3040.2007.01680.x

Bellasio, C., Burgess, S. J., Griffiths, H., and Hibberd, J. M. (2014). A high throughput gas exchange screen for determining rates of photorespiration or regulation of C4 activity. *J. Exp. Bot.* 65, 3769–3779. doi: 10.1093/jxb/eru238

Casal, J. J. (2012). Shade avoidance. *Arabidopsis Book* 10, e0157. doi: 10.1199/tab.0157

Chitwood, D. H., Kumar, R., Ranjan, A., Pelletier, J. M., Townsley, B. T., Ichihashi, Y., et al. (2015). Light-induced indeterminacy alters shade-avoiding tomato leaf morphology. *Plant Physiol.* 169, 2030–2047. doi: 10.1104/pp.15.01229

Demers, D. A., and Gosselin, A. (2002). Growing greenhouse tomato and sweet pepper under supplemental lighting: Optimal photoperiod, negative effects of long photoperiod and their causes. *Acta Hortic.* 580, 83–88. doi: 10.17660/ActaHortic.2002.580.9

Demotes-Mainard, S., Péron, T., Corot, A., Bertheloot, J., Le Gourrierec, J., Pelleschi-Travier, S., et al. (2016). Plant responses to red and far-red lights, applications in horticulture. *Environ. Exp. Bot.* 121, 4–21. doi: 10.1016/j.envexpbot.2015.05.010

Dorais, M. (2003). "The use of supplemental lighting for vegetable crop production: light intensity, crop response, nutrition, crop management, cultural practices," in *Canadian greenhouse conference 2003* (Toronto, ON, Canada), 1–8. doi: 10.1080/15592324.2017.1342026

Dorais, M., Carpentier, R., Yelle, S., and Gosselin, A. (1995). Adaptability of tomato and pepper leaves to changes in photoperiod: effects on the composition and function of the thylakoid membrane. *Physiologia Plantarum* 94, 692–700. doi: 10.1111/j.1399-3054.1995.tb00986.x

Easlon, H. M., and Bloom, A. J. (2014). Easy leaf area: automated digital image analysis for rapid and accurate measurement of leaf area. *Appl. Plant Sci.* 2 (7), 1400033. doi: 10.3732/apps.1400033

Fabre, D., Yin, X., Dingkuhn, M., Clément-Vidal, A., Roques, S., Rouan, L., et al. (2019). Is triose phosphate utilization involved in the feedback inhibition of photosynthesis in rice under conditions of sink limitation? *J. Exp. Bot.* 70, 5773–5785. doi: 10.1093/jxb/erz318

Garner, W. W., and Allard, H. A. (1927). Effect of short alternating periods of light and darkness on plant growth. *Sci. (American Assoc. Advancement Science)* 66, 40–42. doi: 10.1126/science.66.1697.40

Geelen, P. A. M., van Weel, P. A., and Voogt, J. O. (2019). *Plant empowerment : the basic principles : how an integrated approach based on physics and plant physiology leads to balanced growing method for protected crops resulting in healthy resilient plants, high yield and quality, low energy costs and economic greenhouse concepts* (Vlaardingen, The Netherlands: Letsgrow.com).

Graamans, L., Baeza, E., Van Den Dobbelsteen, A., Tsafaras, I., and Stanghellini, C. (2018). Plant factories versus greenhouses: Comparison of resource use efficiency. *Agric. Syst.* 160, 31–43. doi: 10.1016/j.agsy.2017.11.003

Guan, X., and Gu, S. (2009). Photorespiration and photoprotection of grapevine (*Vitis vinifera* L. cv. Cabernet Sauvignon) under water stress. *Photosynthetica* 47, 437–444. doi: 10.1007/s11099-009-0067-7

Hannachi, S., Steppe, K., Eloudi, M., Mechi, L., Bahrini, I., and Van Labeke, M. C. (2022). Salt stress induced changes in photosynthesis and metabolic profiles of one tolerant ('Bonica') and one sensitive ('Black beauty') eggplant cultivars (*Solanum melongena* L.). *Plants* 11, 590. doi: 10.3390/plants11050590

Hao, X., Guo, X., Lanoue, J., Zhang, Y., Cao, R., Zheng, J., et al. (2018). A review on smart application of supplemental lighting in greenhouse fruiting vegetable production. *Acta Hortic.* 1227, 499–506. doi: 10.17660/ActaHortic.2018.1227.63

Hao, X., Lanoue, J., and Zheng, J. (2020). Continuous LED lighting can significantly reduce light fixture costs without compromising fruit yield and quality in greenhouse cucumber production. *HortScience* 55, S363.

Hao, X., Zhang, Y., Guo, X., Little, C., Zheng, J. M., and Khosla, S. (2017). Temperature drop improved responses of greenhouse fruit vegetables to long photoperiod of supplemental lighting. *Acta Hortic.* 1182, 185–192. doi: 10.17660/ActaHortic.2017.1182.22

Haque, S. M., de Sousa, A., Soares, C., Kjaer, H. K., Fidalgo, F., Rosenqvist, E., et al. (2017). Temperature variation under continuous light restores tomato leaf photosynthesis and maintains the diurnal pattern in stomatal conductance. *Front. Plant Sci.* 8. doi: 10.3389/fpls.2017.01602

Harbick, K., and Albright, L. D. (2016). Comparison of energy consumption: greenhouses and plant factories. Acta Hortic. 1134. 285–292. doi: 10.17660/ActaHortic.2016.1134.38

Highkin, H. R., and Hanson, J. B. (1954). Possible interaction between light-dark cycles and endogenous daily rhythms on the growth of tomato plants. *Plant Physiol.* 29, 301–302. doi: 10.1104/pp.29.3.301

Hillman, S. W. (1956). Injury of tomato plants by continuous light and unfavorable photoperiodic cycles. *Am. J. Bot.* 43, 89–96. doi: 10.1002/j.1537-2197.1956.tb10469.x

Hoffmann, A. M., Noga, G., and Hunsche, M. (2015). High blue light improves acclimation and photosynthetic recovery of pepper plants exposed to UV stress. *Environ. Exp. Bot.* 109, 254–263. doi: 10.1016/j.envexpbot.2014.06.017

Hogewoning, S. W., Trouwborst, G., Maljaars, H., Poorter, H., van Ieperen, W., and Harbinson, J. (2010). Blue light dose–responses of leaf photosynthesis, morphology, and chemical composition of *Cucumis sativus* grown under different combinations of red and blue light. *J. Exp. Bot.* 61, 3107–3117. doi: 10.1093/jxb/erq132

Huché-Thélier, L., Crespel, L., Le Gourrierec, J., Morel, P., Sakr, S., and Leduc, N. (2016). Light signaling and plant responses to blue and UV radiations—Perspectives for applications in horticulture. *Environ. Exp. Bot.* 121, 22–38. doi: 10.1016/j.envexpbot.2015.06.009

Huner, N. P. A., Öquist, G., and Melis, A. (2016). "Photostasis in plants, green algae and cyanobacteria: the role of light harvesting antenna complexes," in *Light-Harvesting Antennas in Photosynthesis. Advances in Photosynthesis and Respiration*, vol 3, eds. B. R. Green and W. W. Parson (Dordrecht: Springer). doi: 10.1007/978-94-017-2087-8_14

Igamberdiev, A. U., and Kleczkowski, L. A. (2018). The glycerate and phosphorylated pathways of serine synthesis in plants: the branches of plant glycolysis linking carbon and nitrogen metabolism. *Front. Plant Sci.* 9, 318. doi: 10.3389/fpls.2018.00318

Ikkonen, E. N., Shibaeva, T. G., Rosenqvist, E., and Ottosen, C.-O. (2015). Daily temperature drop prevents inhibition of photosynthesis in tomato plants under continuous light. *Photosynthetica* 53, 389–394. doi: 10.1007/s11099-015-0115-4

Independent Electricity System Operator. (2022). Available at: https://www.ieso.ca/-/media/Files/IESO/Document-Library/global-adjustment/ICI-Backgrounder.ashx (Accessed January 2024).

Ji, Y., Ouzounis, T., Courbier, S., Kaiser, E., Nguyen, P. T., Schouten, H. J., et al. (2019). Far-red radiation increases dry mass partitioning to fruits but reduces Botrytis cinerea resistance in tomato. *Environ. Exp. Bot.* 168, 103889. doi: 10.1016/j.envexpbot.2019.103889

Johnson, J. E., Field, C. B., and Berry, J. A. (2021). The limiting factors and regulatory processes that control the environmental responses of C 3, C 3–C 4 intermediate, and C 4 photosynthesis. *Oecologia* 197, 1–26. doi: 10.1007/s00442-021-05062-y

Kabir, M. H., and Wang, M. H. (2011). Functional studies on two catalase genes from tomato (*Solanum lycopersicum* L.). *J. Hortic. Sci. Biotechnol.* 86, 84–90. doi: 10.1080/14620316.2011.11512730

Kaiser, E., Ouzounis, T., Giday, H., Schipper, R., Heuvelink, E., and Marcelis, L. F. M. (2019). Adding blue to red supplemental light increases biomass and yield of greenhouse-grown tomatoes, but only to an optimum. *Front. Plant Sci.* 9, 2002. doi: 10.3389/fpls.2018.02002

Kalaitzoglou, P., Taylor, C., Calders, K., Hogervorst, M., van Ieperen, W., Harbinson, J., et al. (2021). Unraveling the effects of blue light in an artificial solar background light on growth of tomato plants. *Environ. Exp. Bot.* 184, 104377. doi: 10.1016/j.envexpbot.2021.104377

Kalaitzoglou, P., van Ieperen, W., Harbinson, J., van der Meer, M., Martinakos, S., Weerheim, K., et al. (2019). Effects of continuous or end-of-day far-red light on tomato plant growth, morphology, light absorption, and fruit production. *Front. Plant Sci.* 10, 1–11. doi: 10.3389/fpls.2019.00322

Kang, C., Zhang, Y., Cheng, R., Kaiser, E., Yang, Q., and Li, T. (2021). Acclimating cucumber plants to blue supplemental light promotes growth in full sunlight. *Front. Plant Sci.* 12, 782465. doi: 10.3389/fpls.2021.782465

Kim, H. J., Lin, M. Y., and Mitchell, C. A. (2019). Light spectral and thermal properties govern biomass allocation in tomato through morphological and physiological changes. *Environ. Exp. Bot.* 157, 228–240. doi: 10.1016/j.envexpbot.2018.10.019

Klughammer, C., and Schreiber, U. (2008). Complementary PS II quantum yields calculated from simple fluorescence parameters measured by PAM fluorometry and the Saturation Pulse method. *PAM Appl. Notes* 1, 201–247.

Kong, Y., and Nemali, K. (2021). Blue and far-red light affect area and number of individual leaves to influence vegetative growth and pigment synthesis in lettuce. *Front. Plant Sci.* 12, 667407. doi: 10.3389/fpls.2021.667407

Kong, Y., and Zheng, Y. (2020). Phototropin is partly involved in blue-light-mediated stem elongation, flower initiation, and leaf expansion: A comparison of phenotypic responses between wild Arabidopsis and its phototropin mutants. *Environ. Exp. Bot.* 171, 103967. doi: 10.1016/j.envexpbot.2019.103967

Kono, M., Yamori, W., Suzuki, Y., and Terashima, I. (2017). Photoprotection of PSI by far-red light against the fluctuating light-induced photoinhibition in Arabidopsis thaliana and field-grown plants. *Plant Cell Physiol.* 58, 35–45. doi: 10.1093/pcp/pcw215

Kramer, D. M., Avenson, T. J., and Edwards, G. E. (2004). Dynamic flexibility in the light reactions of photosynthesis governed by both electron and proton transfer reactions. *Trends Plant Sci.* 9, 349–357. doi: 10.1016/j.tplants.2004.05.001

Kramer, D. M., and Evans, J. R. (2011). The importance of energy balance in improving photosynthetic productivity. *Plant Physiol.* 155, 70–78. doi: 10.1104/pp.110.166652

Kramer, D. M., Weebadde, P., Kuhlgert, S., Cruz, J., Swanson, R., and Sooriyapathirana, S. (2023). *References & parameters* (East Lansing, MI, United States: PhotosynQ Documentation). Available at: https://help.photosynq.com/view-and-analyze-data/references-and-parameters.html#reviews-articles.

Kuhlgert, S., Austic, G., Zegarac, R., Osei-Bonsu, I., Hoh, D., Chilvers, M. I., et al. (2016). MultispeQ Beta: a tool for large-scale plant phenotyping connected to the open PhotosynQ network. *R. Soc. Open Sci.* 3, 160592. doi: 10.1098/rsos.160592

Kusuma, P., and Bugbee, B. (2023). On the contrasting morphological response to far-red at high and low photon fluxes. *Front. Plant Sci.* 14, 1185622. doi: 10.3389/fpls.2023.1185622

Kusuma, P., Pattison, P. M., and Bugbee, B. (2020). From physics to fixtures to food: Current and potential LED efficacy. *Horticulture Res.* 7, 56. doi: 10.1038/s41438-020-0283-7

Lai, A. G., Doherty, C. J., Mueller-Roeber, B., Kay, S. A., Schippers, J. H., and Dijkwel, P. P. (2012). CIRCADIAN CLOCK-ASSOCIATED 1 regulates ROS homeostasis and

oxidative stress responses. *Proc. Natl. Acad. Sci.* 109, 17129–17134. doi: 10.1073/pnas.1209148109

Lanoue, J., Little, C., and Hao, X. (2022). The power of far-red light at night: photomorphogenic, physiological, and yield response in pepper during dynamic 24 hour lighting. *Front. Plant Sci.* 13. doi: 10.3389/fpls.2022.857616

Lanoue, J., Zheng, J., Little, C., Grodzinski, B., and Hao, X. (2021). Continuous light does not compromise growth and yield in mini-cucumber greenhouse production with supplemental LED light. *Plants* 10, 1–18. doi: 10.3390/plants10020378

Lanoue, J., Zheng, J., Little, C., Thibodeau, A., Grodzinski, B., and Hao, X. (2019). Alternating red and blue light-emitting diodes allows for injury-free tomato production with continuous lighting. *Front. Plant Sci.* 10. doi: 10.3389/fpls.2019.01114

Marie, T. R. J. G., Leonardos, E. D., and Grodzinski, B. "Using whole-plant diurnal transpiration and remotely sensed thermal indices to phenotype circadian rhythm traits," in *Handbook of Photosynthesis, 4th ed*. Ed. M. Pessarakli (CRC Press). [In Press]. doi: 10.1201/9781003295013-34.

Marie, T. R. J. G., Leonardos, E. D., Lanoue, J., Hao, X., Micallef, B. J., and Grodzinski, B. (2022). A perspective emphasizing circadian rhythm entrainment to ensure sustainable crop production in controlled environment agriculture: dynamic use of LED cues. *Front. Sustain. Food Syst.* 6. doi: 10.3389/fsufs.2022.856162

McClain, A. M., Cruz, J. A., Kramer, D. M., and Sharkey, T. D. (2023). The time course of acclimation to the stress of triose phosphate use limitation. *Plant Cell Environ.* 46, 64–75. doi: 10.1111/pce.14476

McClung, C. R. (1997). Regulation of catalases in arabidopsis. *Free Radical Biol. Med.* 23, 489–496. doi: 10.1016/S0891-5849(97)00109-3

Meijer, D., van Doesburg, F., Jungerling, L., Weldegergis, B. T., Kappers, I. F., Van Oystaeyen, A., et al. (2023). Supplemental far-red light influences flowering traits and interactions with a pollinator in tomato crops. *Environ. Exp. Bot.* 213, 105438. doi: 10.1016/j.envexpbot.2023.105438

Meng, Q., and Runkle, E. S. (2019). Far-red radiation interacts with relative and absolute blue and red photon flux densities to regulate growth, morphology, and pigmentation of lettuce and basil seedlings. *Scientia Hortic.* 255, 269–280. doi: 10.1016/j.scienta.2019.05.030

Müller, N. A., Wijnen, C. L., Srinivasan, A., Ryngajllo, M., Ofner, I., Lin, T., et al. (2016). Domestication selected for deceleration of the circadian clock in cultivated tomato. *Nat. Genet.* 48, 89–93. doi: 10.1038/ng.3447

Müller, N. A., Zhang, L., Koornneef, M., and Jiménez-Gómeza, J. M. (2018). Mutations in EID1 and LNK2 caused light-conditional clock deceleration during tomato domestication. *PNAS* 115, 7135–7140. doi: 10.1073/pnas.1801862115

Murage, E. N., and Masuda, M. (1997). Response of pepper and eggplant to continuous light in relation to leaf chlorosis and activities of antioxidative enzymes. *Scientia Hortic.* 70, 269–279. doi: 10.1016/S0304-4238(97)00078-2

Nitschke, S., Cortleven, A., Iven, T., Feussner, I., Havaux, M., Riefler, M., et al. (2016). Circadian stress regimes affect the circadian clock and cause jasmonic acid-dependent cell death in cytokinin-deficient Arabidopsis plants. *Plant Cell* 28, 1616–1639. doi: 10.1105/tpc.16.00016

Ogren, W. L. (1984). Photorespiration: pathways, regulation, and modification. *Annu. Rev. Plant Physiol.* 35, 415–442. doi: 10.1146/annurev.pp.35.060184.002215

Ontario energy board (2023) Managing costs with time-of-use rates. Available online at: https://www.oeb.ca/consumer-information-and-protection/electricity-rates/managing-costs-time-use-rates (Accessed January 2024).

Osei-Bonsu, I., McClain, A. M., Walker, B. J., Sharkey, T. D., and Kramer, D. M. (2021). The roles of photorespiration and alternative electron acceptors in the responses of photosynthesis to elevated temperatures in cowpea. *Plant Cell Environ.* 44, 2290–2307. doi: 10.1111/pce.14026

Pham, D. M., and Chun, C. (2020). Growth and leaf injury in tomato plants under continuous light at different settings of constant and diurnally varied photosynthetic photon flux densities. *Scientia Hortic.* 269, 109347. doi: 10.1016/j.scienta.2020.109347

Queval, G., Issakidis-Bourguet, E., Hoeberichts, F. A., Vandorpe, M., Gakière, B., Vanacker, H., et al. (2007). Conditional oxidative stress responses in the Arabidopsis photorespiratory mutant cat2 demonstrate that redox state is a key modulator of daylength-dependent gene expression, and define photoperiod as a crucial factor in the regulation of H2O2-induced cell death. *Plant J.* 52, 640–657. doi: 10.1111/j.1365-313X.2007.03263.x

Queval, G., Neukermans, J., Vanderauwera, S., Van Breusegem, F., and Noctor, G. (2012). Day length is a key regulator of transcriptomic responses to both CO2 and H2O2 in Arabidopsis. *Plant Cell Environ.* 35, 374–387. doi: 10.1111/j.1365-3040.2011.02368.x

Sharkey, T. D. (1985). O2-insensitive photosynthesis in C3 plants: its occurrence and a possible explanation. *Plant Physiol.* 78, 71–75. doi: 10.1104/pp.78.1.71

Sharkey, T. D. (2019). Is triose phosphate utilization important for understanding photosynthesis? *J. Exp. Bot.* 70, 5521–5525. doi: 10.1093/jxb/erz393

Shibaeva, T. G., Mamaev, A. V., and Titov, A. F. (2023). Possible physiological mechanisms of leaf photodamage in plants grown under continuous lighting. *Russian J. Plant Physiol.* 70, 1–11. doi: 10.1134/S1021443722602646

Smith, K., Strand, D. D., Kramer, D. M., and Walker, B. J. (2023). The role of photorespiration in preventing feedback regulation via ATP synthase in *Nicotiana tabacum*. *Plant Cell Environ.* 47, 1–13. doi: 10.1111/pce.14759

Snowden, M. C., Cope, K. R., and Bugbee, B. (2016). Sensitivity of seven diverse species to blue and green light: Interactions with photon flux. *PloS One* 11, e0163121. doi: 10.1371/journal.pone.0163121

Song, Y. H., Shim, J. S., Kinmonth-Schultz, H. A., and Imaizumi, T. (2015). Photoperiodic flowering: time measurement mechanisms in leaves. *Annu. Rev. Plant Biol.* 66, 441–464. doi: 10.1146/annurev-arplant-043014-115555

Takahashi, S., Bauwe, H., and Badger, M. (2007). Impairment of the photorespiratory pathway accelerates Photoinhibition of Photosystem II by suppression of repair but not acceleration of damage processes in *Arabidopsis*. *Plant Physiol.* 144, 487–494. doi: 10.1104/pp.107.097253

Takizawa, K., Kanazawa, A., and Kramer, D. M. (2008). Depletion of stromal Pi induces high 'energy-dependent'antenna exciton quenching (qE) by decreasing proton conductivity at CFO-CF1 ATP synthase. *Plant Cell Environ.* 31, 235–243. doi: 10.1111/j.1365-3040.2007.01753.x

Tewolde, F. T., Lu, N., Shiina, K., Maruo, T., Takagaki, M., Kozai, T., et al. (2016). Nighttime supplemental LED inter-lighting improves growth and yield of single-truss tomatoes by enhancing photosynthesis in both winter and summer. *Front. Plant Sci.* 7, 188100. doi: 10.3389/fpls.2016.00448

Tietz, S., Hall, C. C., Cruz, J. A., and Kramer, D. M. (2017). NPQ (T): a chlorophyll fluorescence parameter for rapid estimation and imaging of non-photochemical quenching of excitons in photosystem-II-associated antenna complexes. *Plant Cell Environ.* 40, 1243–1255. doi: 10.1111/pce.12924

Timm, S., Florian, A., Fernie, A. R., and Bauwe, H. (2016). The regulatory interplay between photorespiration and photosynthesis. *J. Exp. Bot.* 67, 2923–2929. doi: 10.1093/jxb/erw083

Timm, S., Florian, A., Wittmiß, M., Jahnke, K., Hagemann, M., Fernie, A. R., et al. (2013). Serine acts as a metabolic signal for the transcriptional control of photorespiration-related genes in Arabidopsis. *Plant Physiol.* 162, 379–389. doi: 10.1104/pp.113.215970

Timm, S., and Hagemann, M. (2020). Photorespiration—how is it regulated and how does it regulate overall plant metabolism? *J. Exp. Bot.* 71, 3955–3965. doi: 10.1093/jxb/eraa183

Valentini, R., Epron, D., De Angelis, P., Matteucci, G., and Dreyer, E. (1995). *In situ* estimation of net CO2 assimilation, photosynthetic electron flow and photorespiration in Turkey oak (Q. cerris L.) leaves: diurnal cycles under different levels of water supply. *Plant Cell Environ.* 18, 631–640. doi: 10.1111/j.1365-3040.1995.tb00564.x

van Ieperen, W. (2016). Plant growth control by light spectrum: fact or fiction? *Acta Hortic.* 1134, 19–24. doi: 10.17660/ActaHortic.2016.1134.3

Velez-Ramirez, A. I., Carreño-Quintero, N., Vreugdenhil, D., Millenaar, F. F., and van Ieperen, W. (2017b). Sucrose and starch content negatively correlates with PSII maximum quantum efficiency in tomato (*Solanum lycopersicum*) exposed to abnormal light/dark cycles and continuous light. *Plant Cell Physiol.* 58, 1339–1349. doi: 10.1093/pcp/pcx068

Velez-Ramirez, A. I., Dünner-Planella, G., Vreugdenhil, D., Millenaar, F. F., and van Ieperen, W. (2017a). On the induction of injury in tomato under continuous light: circadian asynchrony as the main triggering factor. *Funct. Plant Biol.* 44, 597–611. doi: 10.1071/FP16285

Velez-Ramirez, A. I., van Ieperen, W., Vreugdenhil, D., and Millenaar, F. F. (2011). Plants under continuous light. *Trends Plant Sci.* 16, 310–318. doi: 10.1016/j.tplants.2011.02.003

Velez-Ramirez, A. I., van Ieperen, W., Vreugdenhil, D., van Poppel, P. M. J. A., Heuvelink, E., and Millenaar, F. F. (2014). A single locus confers tolerance to continuous light and allows substantial yield increase in tomato. *Nat. Commun.* 5, 1–13. doi: 10.1038/ncomms5549

Warner, R., Wu, B. S., MacPherson, S., and Lefsrud, M. (2023). How the distribution of photon delivery impacts crops in indoor plant environments: a review. *Sustainability* 15, 4645. doi: 10.3390/su15054645

Weidner, T., Yang, A., and Hamm, M. W. (2021). Energy optimisation of plant factories and greenhouses for different climatic conditions. *Energy Conversion Manage.* 243, 114336. doi: 10.1016/j.enconman.2021.114336

Wenden, B., Kozma-Bognár, L., Edwards, K. D., Hall, A. J., Locke, J. C., and Millar, A. J. (2011). Light inputs shape the Arabidopsis circadian system. *Plant J.* 66, 480–491. doi: 10.1111/j.1365-313X.2011.04505.x

Yang, Z., Mhamdi, A., and Noctor, G. (2019). Analysis of catalase mutants underscores the essential role of CATALASE2 for plant growth and day length-dependent oxidative signaling. *Plant Cell Environ.* 42, 688–700. doi: 10.1111/pce.13453

Zavafer, A., and Mancilla, C. (2021). Concepts of photochemical damage of Photosystem II and the role of excessive excitation. *J. Photochem. Photobiol. C: Photochem. Rev.* 47, 100421. doi: 10.1016/j.jphotochemrev.2021.100421

Zhen, S., and Bugbee, B. (2020). Far-red photons have equivalent efficiency to traditional photosynthetic photons: Implications for redefining photosynthetically active radiation. *Plant Cell Environ.* 43, 1259–1272. doi: 10.1111/pce.13730

Zou, J., Fanourakis, D., Tsaniklidis, G., Cheng, R., Yang, Q., and Li, T. (2021). Lettuce growth, morphology and critical leaf trait responses to far-red light during cultivation are low fluence and obey the reciprocity law. *Scientia Hortic.* 289, 110455. doi: 10.1016/j.scienta.2021.110455

frontiers | Frontiers in Plant Science

TYPE Original Research
PUBLISHED 31 May 2024
DOI 10.3389/fpls.2024.1372886

OPEN ACCESS

EDITED BY
Ep Heuvelink,
Wageningen University and Research, Netherlands

REVIEWED BY
Roberta Paradiso,
University of Naples Federico II, Italy
Ricardo Hernandez,
North Carolina State University, United States

*CORRESPONDENCE
Xiuming Hao
xiuming.hao@agr.gc.ca

RECEIVED 18 January 2024
ACCEPTED 29 April 2024
PUBLISHED 31 May 2024

CITATION
Lanoue J, St. Louis S, Little C and Hao X (2024) Photosynthetic adaptation strategies in peppers under continuous lighting: insights into photosystem protection.
Front. Plant Sci. 15:1372886.
doi: 10.3389/fpls.2024.1372886

Photosynthetic adaptation strategies in peppers under continuous lighting: insights into photosystem protection

Jason Lanoue, Sarah St. Louis, Celeste Little and Xiuming Hao*

Harrow Research and Development Centre, Agriculture & Agri-Food Canada, Harrow, ON, Canada

Energy efficient lighting strategies have received increased interest from controlled environment producers. Long photoperiods (up to 24 h - continuous lighting (CL)) of lower light intensities could be used to achieve the desired daily light integral (DLI) with lower installed light capacity/capital costs and low electricity costs in regions with low night electricity prices. However, plants grown under CL tend to have higher carbohydrate and reactive oxygen species (ROS) levels which may lead to leaf chlorosis and down-regulation of photosynthesis. We hypothesize that the use of dynamic CL using a spectral change and/or light intensity change between day and night can negate CL-injury. In this experiment we set out to assess the impact of CL on pepper plants by subjecting them to white light during the day and up to 150 µmol m^{-2} s^{-1} of monochromatic blue light at night while controlling the DLI at the same level. Plants grown under all CL treatments had similar cumulative fruit number and weight compared to the 16h control indicating no reduction in production. Plants grown under CL had higher carbohydrate levels and ROS-scavenging capacity than plants grown under the 16h control. Conversely, the amount of photosynthetic pigment decreased with increasing nighttime blue light intensity. The maximum quantum yield of photosystem II (F_v/F_m), a metric often used to measure stress, was unaffected by light treatments. However, when light-adapted, the operating efficiency of photosystem II (ΦPSII) decreased and non-photochemical quenching (NPQ) increased with increasing nighttime blue light intensity. This suggests that both acclimated and instantaneous photochemistry during CL can be altered and is dependent on the nighttime light intensity. Furthermore, light-adapted chlorophyll fluorescence measurements may be more adept at detecting altered photochemical states than the conventional stress metric using dark-adapted measurements.

KEYWORDS

continuous lighting, chlorophyll fluorescence, carbohydrates, reactive oxygen species, circadian rhythm, dynamic 24h lighting

1 Introduction

Light is the driving force for carbon assimilation in plants, however there is a species-specific desired/optimum daily light integral (DLI – photoperiod x light intensity) – an excessive or deficient amount can impact plants negatively. Too much light can be harmful to plants as it significantly reduces the efficiency of photosynthesis which can lead to photoinhibition causing damage to photosystem II (PSII) (Barber and Andersson, 1992). Long photoperiods can also be harmful to plants. While the photoperiodic threshold is different for each plant species, generally, photoperiods longer than 17h can cause leaf damage observed as interveinal chlorosis and decreased maximum quantum efficiency of PSII (F_v/F_m); an indicator of stress (Baker, 2008; Sysoeva et al., 2010; Velez-Ramirez et al., 2011).

Theoretically, the implementation of CL strategies can increase yield if photoperiod-related injury is averted (Velez-Ramirez et al., 2012). While some crops are tolerant to CL (Ohtake et al., 2018; Lanoue et al., 2021b), others, such as pepper, are observed to have altered leaf shape, chlorosis, and reductions in yield when compared to peppers grown under shorter photoperiods (Demers et al., 1998b; Demers and Gosselin, 1999). Lengthening the photoperiod can also lead to reduced stem elongation in peppers (Demers et al., 1998a) resulting in fruit being too close together and misshapen which negatively impacts fruit quality (Lanoue et al., 2022b). It is therefore important to identify long photoperiod (including CL) strategies which can overcome reductions in stem elongation and maintain adequate fruit quality.

The underlying mechanism of CL-injury is unknown. Current hypotheses include a mismatch between the endogenous circadian rhythm and exogenous environmental cues (Velez-Ramirez et al., 2017b; Marie et al., 2022), improper gene expression (Velez-Ramirez et al., 2014; Inoue et al., 2018), and over-accumulation of photosynthetic products leading to feedback inhibition (Velez-Ramirez et al., 2017a; Pham et al., 2019). Exposure to CL means plants are under constant photon pressure which will continuously drive photosynthesis if the light level is above the light compensation point. With constant photosynthesis comes continuous production of photosynthetic products such as soluble sugars and starch (Globig et al., 1997; Matsuda et al., 2014; Pham et al., 2019). This accumulation of carbohydrates is linked to chloroplast membrane damage, inevitably causing a downregulation of photosynthesis via feedback loops caused by over-reduction of the electron transport chain components (Foyer et al., 2012; Zhu et al., 2020). Consequently, many believe that the buildup of photosynthetic products during CL will impact gene expression and ultimately reduce photosynthesis leading to a reduction in light-use-efficiency (Pammenter et al., 1993; Van Gestel et al., 2005; Smith and Stitt, 2007; Stitt et al., 2010). Our recent research has shown that tomatoes grown under CL with 50 μmol m^{-2} s^{-1} of blue light during the night had similar carbohydrate patterns and levels as those grown under a 16 h control with 8 h darkness (Lanoue et al., 2019). However this light intensity was around the light compensation point and did not drive high rates of photosynthesis which could cause feedback inhibition. Conversely, tomatoes grown under CL with a constant 147 μmol m^{-2} s^{-1} of white light for 24 h showed elevated fructose, sucrose, and starch levels at the end of the subjective night compared to a 16 h control treatment (Haque et al., 2015). The elevated carbohydrate status corresponded with a reduction in F_v/F_m values indicating CL-injury. This suggests that a higher nighttime light intensity without a change in spectrum can raise the carbohydrate levels in plants that are associated with CL-injury.

In addition, the use of CL can significantly increase the amount of photo-oxidative stress a plant is subjected to. Reactive oxygen species (ROS) are a normal by-product of photosynthesis, but when produced in higher quantities during periods of high or prolonged light (such as CL) they can become harmful to the plant. An excess accumulation of ROS can cause severe and irreversible DNA damage resulting in cell death (Huang et al., 2019). In mutated *Arabidopsis* which had reduced antioxidant content (2-Cys peroxiredoxin), plants showed decreased photosynthetic rates during CL compared to wild-type plants (Pulido et al., 2010). Coincidentally, mutated plants also had higher levels of carbonyl groups and hydrogen peroxide in the leaves indicating that a reduction in antioxidant capacity increased ROS concentrations and led to diminished photosynthetic rates (Pulido et al., 2010). ROS can also be used as a signaling molecule to alert the plant to stressful conditions such as high or prolonged light. In this way, a healthy balance between ROS production and scavenging can maintain homeostasis since ROS accumulation can initiate gene expression of detoxifying enzymes (Huang et al., 2019). It has been shown that plants with naturally higher levels of antioxidants and ROS-detoxifying enzymes have less injury when exposed to prolonged photoperiods, even CL (Murage and Masuda, 1997). It is therefore speculated that the ability to scavenge ROS may also play a role in averting CL-injury based on their role in photo-oxidative stress (Kim et al., 2008).

In this study, we set out to identify the impact of different nighttime blue light intensities during CL on the morphology, physiology, and yield of pepper plants. Specifically, we wanted to identify how plant performance (i.e., photosynthesis and chlorophyll fluorescence parameters) would adapt under higher (up to 150 μmol m^{-2} s^{-1}) nighttime blue light intensities. Blue light was chosen due to its ability to cause stem elongation when provided as a monochromatic light source (Hernández and Kubota, 2016; Lanoue et al., 2019; Kong and Zheng, 2020). We also chose to measure the carbohydrate metabolism and oxidative stress levels in leaves, since literature suggesting that both carbohydrate accumulation and ROS scavenging ability can play a role in CL-injury. It is hypothesized that underlying biochemicals processes may play an important role in mitigating CL-injury in peppers when exposed to dynamic 24h lighting. Additionally, the traditional stress metric, F_v/F_m, may not be the most appropriate measurement to determine plant health/stress or ability to utilize incoming radiation.

2 Materials and methods

2.1 Plant material and experimental design

Five-week-old pepper (*Capsicum annuum*) cv. 'Gina' transplants were planted onto rockwool slabs in a 200m^2 glass

greenhouse at the Harrow Research and Development Centre (Agriculture and Agri-Food Canada, Harrow, Ontario, Canada; 42.03°N, 82.9°W) on September 15th, 2021. Plants were trained in a high wire "V" system with 2 stems from each plant at a plant density of 6.0 stems m^{-2}. The plants were drip-irrigated as needed using a complete nutrient solution with an electrical conductivity of 2.8 dS m^{-1} and a pH of 5.9. The greenhouse was enriched to 800 µmol mol^{-1} of CO_2 during both day and night when the greenhouse was not vented. Heating temperature during the day was 21°C with a venting temperature of 25°C. Day humidification set point was 75% with a dehumidification set point of 85%. Nighttime heating temperature was 18°C and venting was 22°C. Night humidification set point was 70% with a dehumidification set point of 85%.

The pepper plants were grown on 6 raised gutters/rows. The rows of plants were separated using light abatement curtains (Obscura 9950 FR W, Ludvig Svensson, Kinna Sweden) which allowed for moisture, air, and heat exchange through the fabric but blocked light transmission. The width of each row is 1.5m. The light abatement curtains were closed during cloudy days and during the night to prevent light treatment contamination. On sunny days, the light abatement curtains were opened to prevent shading of the high intensity solar radiation. Rows on the perimeter served as guard rows throughout the experiment and were not subjected to any lighting treatment. The 4 middle rows were used for lighting treatments. The rows ran in a north-south orientation so that each row can receive same amount of sunlight. Each row was divided into 2 independent experimental plots/units. The length of each plot was 2m (or 2.2m including canopy extension). There were 10 plants or 20 stems per plot. Only the middle 8 plants/16 stems were used for data collection. One plant in each of the 2 ends of the plot was used as guard plant. The 2 stems of each plant was trained into a "V" system, one to the west side and the other to the east side, so that the plants in each plot received sunlight from both west and east side. There was a 1.82m gap between the 2 plots in the same row and light reflection boards were applied to the light fixtures in both ends of each plot to prevent any light contaminations between the 2 plots in each row. The application of 4 lighting treatments to the 4 south plots (first replication/block) and the 4 north plots (second replication/block) was randomized. The lighting treatments in the 2 plots within the same row was different. Therefore, the greenhouse experiment was a randomized complete block design with 2 replications.

The 4 supplemental overhead lighting treatments (0B, 50B, 100B, and 150B, Table 1) began on November 3rd, 2021. Daytime supplemental lighting was provided by 6 Sollum SF04 multi-channel LED lighting fixtures (Sollum Technologies Inc. Montréal, Québec, Canada) in each plot. Nighttime supplemental lighting was provided by the 6 SF04 smart LEDs or SF04 smart LEDS and RAY66 blue LEDs (for the 150B treatment) from Fluence (Fluence Bioengineering, Austin, Texas, USA) depending on the blue light intensity requirements. Spectral composition readings were taken at the apex of the plant using a Li-COR Li-180 (Li-COR Biosciences, Lincoln, NE, USA) spectroradiometer (Figure 1). The daytime white light treatment was applied from 6:00–22:00 (Figure 1A) while nighttime blue light treatments, if applicable, were applied from 22:00–6:00 (Figure 1B). The light in each treatment was measured at four locations within each plot with a one meter quantum light sensor (Li-COR 191R; Li-COR Biosciences, Lincoln, Nebraska, USA) just above the apex of the plant (Table 1). Lights were adjusted as needed to maintain the target light intensity at the apex of the plant throughout the experiment. The total supplemental daily light integral (DLI) was kept similar among all treatments (11.6 ± 0.06 mol m^{-2} d^{-1}). All light measurements were performed at night to avoid any contamination from daytime solar radiation. Lights remained on regardless of the natural solar radiation levels to ensure the same total DLIs (sunlight + supplemental light) for all lighting treatments.

TABLE 1 Daytime and nighttime light intensities as measured at four locations within each plot with a one meter quantum light sensor (Li-COR 191R; Li-COR Biosciences, Lincoln, NE, USA) just above the apex of the plant.

Treatment	Daytime (6:00–20:00) Light Intensity (µmol m^{-2} s^{-1})	Nighttime (22:00–6:00) Blue Light Intensity (µmol m^{-2} s^{-1})
0B	200 ± 2	0
50B	175 ± 3	50 ± 1
100B	150 ± 2	100 ± 1
150B	125 ± 2	150 ± 3

Treatment 0B indicates that no light was utilized during the night and that plants in all light treatments were exposed white light spectrum (Figure 1A) for 16h from 6:00–22:00. Values represent the average +/- the standard error of light measurements.

2.2 Morphological measurements

On January 24th, 2022, morphological measurements were performed on eight plants from each treatment. The internode length was determined by measuring the distance between the top of the plant and the tenth node. This distance was then divided by ten to get the average internode length. Leaf length and width of the 5th leaf were measured using a ruler. Stem diameter at the 5th node was measured using a digital caliper. The specific leaf weight (SLW) of the 5th leaf was determined by removing it from the plant, weighing it, and then measuring its leaf area (Li-COR 3100, Li-COR Biosciences Inc. Lincoln, NE, USA). The leaf was then dried in an oven at 70°C. Once dry, the leaf was reweighed. The dry weight was divided by the leaf area to obtain the SLW. Dry matter content was calculated by dividing the dry weight by the fresh weight then multiplying by 100.

2.3 Leaf gas exchange

On January 25th, 2022, one leaf located at the fifth node on four separate plants (2 plants from each plot) under each treatment were placed in a 2 x 3 cm chamber of a Li-COR 6400 (Li-COR Biosciences Inc. Lincoln, NE, USA). The leaf temperature was set to 23°C with a relative humidity of 60–70% and a CO_2 level held at 800 µmol mol^{-1}. Measurements were performed on cloudy days to

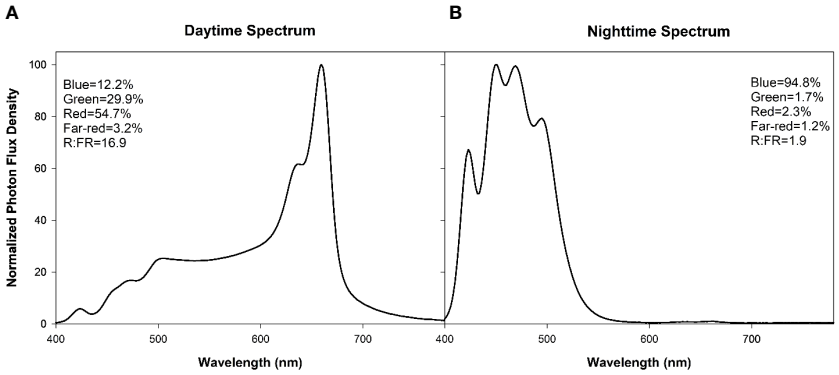

FIGURE 1
Normalized photon flux density (PFD) of daytime (6:00–20:00, **(A)**) and nighttime (20:00–6:00, **(B)**) light treatments as determined with a Li-180 (Li-COR Biosciences, Lincoln, NE, USA) spectroradiometer during the night at the head of the plant. For each spectrum, the percentages of PFD of blue (400–499nm), green (500–599nm), red (600–699nm), far-red (700–780nm), and the red:far-red (R:FR) are included in the Figure.

maximize the effect of supplemental lighting while minimizing the effect of natural sunlight. Leaves were kept in the chamber until a steady-state photosynthetic rate was obtained, then the readings taken over a two-minute period were averaged.

2.4 Chlorophyll fluorescence

On January 27th, 2022, pepper leaves were selected based on location and exposure to supplemental lighting and dark-adapted for 20 minutes using aluminum foil. They were then placed in 6 cm^2 chamber of the Li-COR 6800 fitted with the fluorometer head. The minimum fluorescence in a dark-adapted stated (F_o) was collected once fluorescence stabilized after which an 800ms saturating light pulse (8000 μmol m^{-2} s^{-1}) of red light was emitted to obtain the maximum fluorescence (F_m). From F_o and F_m, the variable fluorescence in a dark-adapted state (F_v) was calculated (F_v=F_m-F_o) to then determine the maximum efficiency of photosystem II (PSII; F_v/F_m). Next, leaves were acclimated to an actinic light level of 400 μmol m^{-2} s^{-1} (360 μmol m^{-2} s^{-1} of red light and 40 μmol m^{-2} s^{-1} of blue light; approximately the light level during a cloudy day) until the fluorescence levels (F_t) stabilized. Once static, leaves were subjected to another saturating light pulse (F'_m) followed by a dark pulse (F'_o; 25 μmol m^{-2} s^{-1} of far-red light). These measurements were used to calculate the efficiency of PSII photochemistry (ΦPSII=(F'_m-F_t)/F'_m), photochemical quenching (qP=(F'_m-F_t)/(F'_m-F'_o)), non-photochemical quenching (NPQ=(F_m-F'_m)/F'_m), and the linear electron transport rate (ETR=ΦPSII*PPFD*0.5 where PPFD is the absorbed light and 0.5 is a factor that accounts for partitioning of energy between the two photosystems).

2.5 Photosynthetic pigment analysis

On January 24th, three circular samples of approximately 1cm in diameter were taken from a selected leaf. Leaves were chosen based on positioning and exposure to supplemental lighting. Ten samples in total were collected for each light treatment, each from a separate leaf. The samples were immediately weighed and flash frozen in liquid nitrogen, and placed in a -80°C freezer until analysis. Samples were extracted in 1mL of 95% ethanol in a warm (50°C) water bath for three hours. The ethanolic fraction was removed and placed into a new tube. The sample was further extracted once more and both aliquots were combined for a total extract volume of 2 mL. After the extractions, the sample was devoid of green color, indicating that the photosynthetic pigment had been completely extracted. Samples were then analyzed at 664 nm, 649 nm, and 470 nm in a UV/Vis spectrophotometer (UV-1600PC. VWR. Mississauga, Ontario, Canada). Concentrations of chlorophyll *a*, *b*, and carotenoids were determined using the equations from (Lichtenthaler, 1987).

2.6 Carbohydrate analysis

Three circular discs of approximately 1 cm in diameter samples were taken from the fifth leaf on six separate plants under each lighting treatment. Leaves were chosen based on positioning and exposure to supplemental lighting. The samples were taken at 21:30 on January 27th, 2022 (PM measurement) and again at 5:30 on January 28th, 2022 (AM measurement). These time points represent the carbohydrate accumulation at the end of the day (PM measurements) and at the end of the night (AM measurements). Samples were immediately weighed and then flash frozen in liquid nitrogen and kept in an -80°C freezer until analysis.

Leaf samples were extracted with 1mL of 80% ethanol in a warm (50°C) water bath for one hour. The supernatant was removed, ensuring no tissue was disturbed, and placed in a clean vial. The procedure was repeated for a total of 3 times until the tissue was devoid of green pigment (Tetlow and Farrar, 1993). The 3mL of ethanolic fraction was then dried using a vacuum concentrator and the paled leaf tissue was kept for further starch analysis. The remains were reconstituted in deionized water and soluble sugars

were assayed using a sucrose/fructose/glucose kit (Megazyme. Wicklow, Ireland). To analyze sucrose, the samples were added to PMMA cuvettes and mixed with β-fructosidase and incubated at room temperature for 5 minutes. Deionized water, a buffer solution, and $NADP^+$/ATP were then added to the cuvette and incubated for an additional 3 minutes at room temperature before analysis at 340 nm ($A1_{suc}$). Hexokinase plus glucose-6-phosphate dehydrogenase was then added and incubated at room temperature for 5 minutes and a second reading was recorded at 340 nm ($A2_{suc}$). The same procedure was repeated without the addition of tissue sample to obtain a blank ($A1_{sblank}$ and $A2_{sblank}$). For glucose and fructose assays, the sample was mixed in a PMMA cuvette with deionized water, a buffer solution, and $NADP^+$/ATP and left to incubate for 3 minutes before analysis at 340 nm ($A1_{g+f}$). Hexokinase plus glucose-6-phosphate dehydrogenase was then added to the sample, mixed, and was left to incubate at room temperature for 5 minutes before a second reading was taken at 340 nm ($A2_{g+f}$). Lastly, phosphoglucose isomerase was added to the cuvette and incubated for 10 minutes at room temperature before a final analysis at 340nm ($A3_{g+f}$). The same procedure was completed without any analyte to obtain blank values ($A1_{g+fblank}$, $A2_{g+fsblank}$, and $A3_{g+fblank}$). Absorbance values were determined using the following equations:

$$A_{glucose} = (A2_{g+f} - A1_{g+f}) - (A2_{g+fblank} - A1_{g+fblank})$$

$$A_{sucrose} = ((A2_{suc} - A1_{suc}) - (A2_{sblank} - A1_{sblank})) - A_{glucose}$$

$$A_{fructose} = A3_{g+f} - A2_{g+f}$$

The content (C; mg g^{-1} of fresh weight (FW)) of each soluble carbohydrate was then calculated with the following:

$$C(mg\ \ g^{-1}FW) = \left(\frac{(\frac{V*MW}{\epsilon*d*v})*A}{c}\right)$$

Where V is the final volume of the solution, MW is the molecular weight of the carbohydrate being analyzed (i.e., glucose, fructose, or sucrose), ϵ is the extinction coefficient of NADPH at 340 nm, d is the light path (cm), v is the sample volume, A is the absorbance of the carbohydrate being analyzed (i.e., $A_{glucose}$, $A_{fructose}$, or $A_{sucrose}$), and c is the concentration of the ethanolic extract (g mL^{-1}).

To assay starch, paled tissue after ethanolic extraction was lyophilized overnight and ground in a homogenizer before suspension in sodium acetate (100 mM). Thermostable α-amylase was then added to the sample. The sample was vortexed then placed in a boiling water bath for 15 minutes and was periodically vortexed throughout. The sample was then placed in a 50°C water bath for 5 minutes to equilibrate the temperature. Amyloglucosidase was then added to the sample, vortexed, and incubated in a warm (50°C) water bath for 30 minutes. The sample was removed from the warm water bath and left to cool at room temperature for 10 minutes. The sample was then centrifuged at 13,000 rpm for 5 minutes. A subsample of the supernatant was mixed with sodium acetate buffer and vortexed to create a stock solution. The stock solution was mixed with GOPOD reagent, incubated at 50°C for 20 minutes then analyzed in a spectrophotometer at 510 nm (A_s) in PS cuvettes. A blank was obtained using the same procedure without the tissue sample (A_b). Starch content was calculated using the following equation:

$$Starch\ \ (g\ \ 100mL^{-1}) = \ (A_s - A_b)*F*\frac{DV}{SV}*0.9$$

Where F is the absorbance value of glucose, DV is the diluted sample volume, and SV is the sample volume taken for analysis. The starch content was then converted to mg g^{-1} FW using the weight of the sample taken before the tissue was frozen.

2.7 Antioxidant analysis

The antiradical activity in pepper leaves was determined based on a modified version of a previously reported method (Alrifai et al., 2020). Three leaf samples from six separate leaves under each lighting treatment were taken on February 11th, 2022, weighed, and then flash frozen in liquid nitrogen and placed in a -80°C freezer. Before performing the analysis, the tissue was lyophilized overnight. Freeze-dried tissue was ground in a homogenizer and a subsample was transferred into a new microcentrifuge tube. The subsamples were homogenized further and 1 mL of 100% methanol was added to each microfuge tube. The samples were then left on a nutator overnight at room temperature. The next morning, the samples were centrifuged at 13,000 rpm for five minutes. The supernatant was collected in a clean tube before suspending the pellet in 1mL of fresh 100% methanol. Again, the sample was placed on a nutator for three hours before being centrifuged and having the supernatant removed. Both supernatant fractions were mixed together in a single tube and placed in a -20°C freezer until analysis. Fresh 2,2-diphenyl-1-picrylhydrazly (DDPH; 350 µM) was prepared immediately before analysis. In a cuvette, 1 mL of DPPH was mixed with 125 µL of methanolic sample extract and placed in the dark to incubate for 30 minutes before the absorbance was measured at 517 nm. The procedure was completed in duplicate. A standard curve was prepared in quadruplicate using the same assay technique but replacing the methanolic sample extract with ascorbic acid (AA; 0.025 mM-1 mM concentrations). All samples were expressed as µg AA mg^{-1} FW.

The ferric reducing antioxidant power (FRAP) assay of pepper leaves was determined using a modified version of a previously reported method (Alrifai et al., 2020). FRAP reagent was prepared fresh and consisted of 300 mM acetate buffer (pH 3.6), 20 mM $FeCl_3$, and 10 mM 2, 4, 6-Tris (2-pyridyl)-s-triazine (TPTZ) in 40 mM HCl. 100 µL of methanolic sample extract was mixed with 900 µL of FRAP reagent and incubated on a heat block at 37°C for 1 h before reading the absorbance at 593 nm. A standard curve was completed using the same assay technique but ascorbic acid (AA; 0.025 mM-0.25 mM concentrations) was used instead of the tissue sample. All samples were expressed as µg AA mg^{-1} FW.

2.8 Yield

Pepper harvest began on November 23rd, 2021 and continued weekly until April 5th, 2022. Peppers were harvested once they had reached full maturity and had gone through a 75% color change.

2.9 Statistical analysis

All statistics were performed using SAS Studio 3.5. After the analysis of variance (ANOVA), multiple means comparisons between the different treatments were done using a Tukey-Kramer adjustment and a value of $p<0.05$ to indicate a significant difference. The greenhouse experiment was a randomized complete block design with 2 replications. Regression analysis was done using a backward elimination method. Final regressions with a $p<0.05$ were determined to be significant.

3 Results

Plants grown under the 100B treatment had significantly longer internodes than the control (0B) treatment (20.9% increase, Table 2). Plants grown under 150B did not have a increase in internode length and were similar to plants under 0B. The length and width of the 5th leaf as well as the stem diameter measured at the 5th internode were statistically similar. The percent leaf dry matter ($p=0.096$) and specific leaf weight (SLW; $p=0.057$) were also similar under all light treatments (Table 2).

Daytime photosynthetic rates from the 50B treatment were similar to the control (0B) treatment, but both 100B and 150B treatments had reduced photosynthetic rates when compared to both 0B and 50B (Figure 2A). Since the intrinsic supplemental lighting intensity was different between all four treatments, the photosynthetic rate was normalized on the incoming light intensity (both supplemental and natural) that each leaf was subjected to (i.e., light-use-efficiency). After normalization, leaves under the 50B light treatment still fixed similar amounts of CO_2 per photon as leaves under the 0B treatment. Again, leaves under both 100B and 150B treatments produced lower light-use-efficiencies than leaves under the control (Figure 2B). In all treatments, the amount of water loss due to transpiration was similar (Figure 2C). Accordingly, in leaves under the 150B treatment water-use-efficiency was lowest.

T1he maximum efficiency of photosystem II (PSII) in the dark-adapted state (F_v/F_m) is typically used to identify stress in the plant caused by the light treatment (Kitajima and Butler, 1975; Baker, 2008). In this study, leaves under all light treatments had the same F_v/F_m indicating that no photoperiod-related injury occurred even under the highest nighttime blue light intensity (Figure 3A). In contrast to the results from the dark-adapted measurements, PSII operating efficiency in the light-adapted state (ΦPSII) was observed to significantly decrease with increasing nighttime light intensity after exposure to a 400 μmol m^{-2} s^{-1} actinic light (Figure 3B). This was most-likely an attempt at photoprotection by means of inactivation of PSII reaction centers. The inactivation of PSII subsequently led to a decrease in linear electron transport rate (ETR); a phenomenon that was also observed as the nighttime light intensity increased (Figure 3C). As the inactivation of PSII increases with nighttime light intensity, a growing amount of incoming radiation must be dissipated in order to protect the leaf. One way that excess light energy is dispelled is through non-photochemical quenching (NPQ) which is achieved through thermal dissipation. Therefore, as PSII inactivation occurs, NPQ increases with increasing nighttime light intensity (Figure 3D). Subsequently, as NPQ increases and ΦPSII decreases, photochemical quenching (qP) as well as the fraction of open PSII reaction centers (qL) also decreased (Figures 3E, F). Although dark-adapted measurements showed no photoperiod related injury, when we consider all the above information, it is clear that as the nighttime light intensity increased, the biochemical use of the incoming radiation shifted from usage in the light reactions to energy dissipation via NPQ in an effort to protect the photosynthetic machinery.

Both chlorophyll *a* and *b*, and to a lesser extent carotenoids, are important pigments which funnel light into the photosynthetic pathway. Generally speaking, the higher the photosynthetic pigment concentration, the more light the plant will be able to capture and utilize. In our study, we observed a decreasing linear relationship between all three photosynthetic pigments with increasing nighttime blue light intensity (Figures 4A, B, D). In contrast, the ratio of chlorophyll *a* to *b* was unaffected by the light treatments (Figure 4C).

Analysis of leaf carbohydrates provides insight in to the leaf's ability to produce and export the end product of photosynthesis. Here, we observed that as the nighttime light intensity increased, so

TABLE 2 Internode length, length and width of the 5th leaf, stem diameter, dry matter percentage of the fifth leaf and specific leaf weight (SLW) of pepper cv. 'Gina' measured on January 24th, 2022 under four different lighting treatments.

Treatment	Internode Length (cm)	5th Leaf Length (cm)	5th Leaf Width (cm)	Stem Diameter (mm)	% Leaf Dry Matter	SLW (g m^{-2})
0B	4.39 ± 0.20^{B}	17.8 ± 0.7^{A}	9.9 ± 0.5^{A}	8.44 ± 0.32^{A}	13.4 ± 0.3^{A}	20.1 ± 0.7^{A}
50B	4.51 ± 0.34^{AB}	17.9 ± 1.0^{A}	10.6 ± 0.5^{A}	8.53 ± 0.32^{A}	14.7 ± 0.5^{A}	17.8 ± 1.2^{A}
100B	5.31 ± 0.18^{A}	18.8 ± 0.9^{A}	11.4 ± 0.4^{A}	9.03 ± 0.31^{A}	14.7 ± 0.5^{A}	19.5 ± 1.2^{A}
150B	4.69 ± 0.17^{AB}	16.0 ± 0.5^{A}	10.0 ± 0.2^{A}	8.55 ± 0.30^{A}	14.6 ± 0.3^{A}	16.8 ± 0.6^{A}

Mean values +/- standard error are representative of n=8. Within each parameter, different letters indicate significant differences as determined by a one-way ANOVA with a Tukey-Kramer adjustment ($p<0.05$).

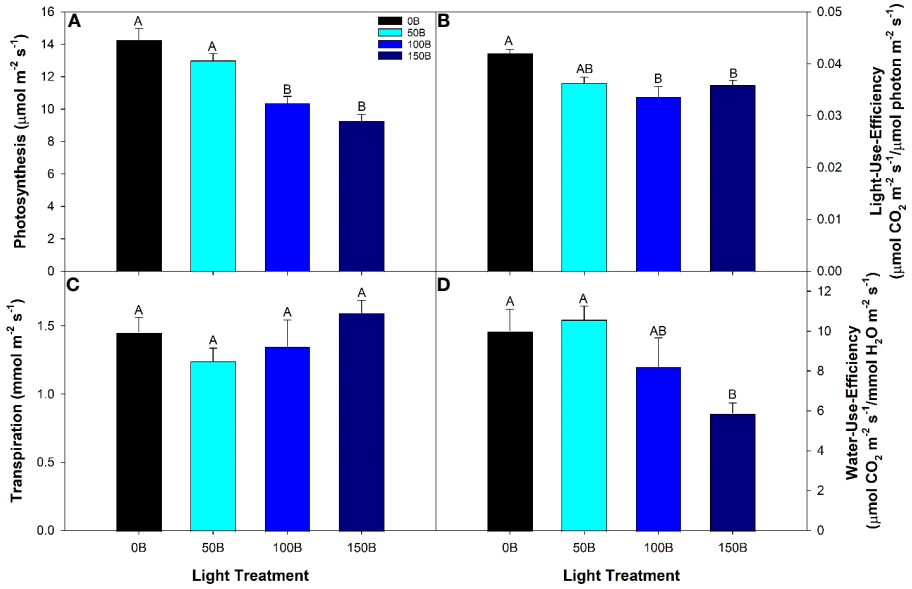

FIGURE 2
Photosynthesis **(A)**, light-use-efficiency **(B)**, transpiration **(C)**, and water-use-efficiency **(D)** of the 5th leaf of pepper cv. 'Gina' grown under the different lighting treatments. Measurements were performed with a Li-COR 6400 fitted with a 2 x 3 cm clear top chamber on a cloudy day and thus represent the parameters mostly driven by the supplemental lighting. Mean values +/- standard error are representative of n=4. Within each parameter, different letters indicate significant differences as determined by a one-way ANOVA with a Tukey-Kramer adjustment (p<0.05).

too did the concentration of soluble carbohydrates (i.e., glucose, fructose, and sucrose; Figures 5A–C) as determined during the AM sampling period. Starch, which is mainly thought of as a storage molecule, typically degrades during the night period to support the carbon needs of the plant. However, as the nighttime light intensity increased, starch levels in the leaf remained high; an indication that starch was not being converted at the same rate as in plants that had an 8h dark period (0B; Figure 5D). In fact, the starch level in plants grown under 150B was almost four times higher than observed in 0B plants.

PM sampling measurements represent the accumulation of carbohydrates during the day period. Both glucose and fructose showed no significant differences among light treatments (Figures 5A, B). Leaves grown under 0B had drastically increased glucose and fructose concentrations compared to the AM sampling, as would be expected. Interestingly, as the nighttime light intensity increased, a difference between the concentrations of glucose and fructose during the PM sampling and AM sampling was nearly non-existent. In all CL treatments (50B, 100B, and 150B), the daytime light intensity was reduced proportionally to keep the DLI similar to the control (0B). Therefore, it would be expected that lower amounts of carbohydrates would be synthesized compared to plants grown under the 0B treatment during the daytime. However, the similar soluble sugar concentrations during the AM and PM sampling indicate a lack of movement of these carbohydrates during the night period revealing a potential bottleneck in carbon metabolism. Lastly, concentrations of both sucrose and starch were observed to increase as the nighttime light intensity increased in the PM sampling (Figures 5C, D).

Antioxidants are produced to inhibit oxidation and the production of free radicals; both of which can damage the cell. DPPH radical-scavenging activity was observed to increase as the nighttime light intensity increased (Figure 6A). Similarly, the ferric reducing antioxidant power (FRAP) was also observed to increase with increasing nighttime light intensity (Figure 6B). This indicates that plants under higher nighttime light intensities were under more oxidative stress than those which had lower or no nighttime lighting (Figure 6).

Cumulative fruit number (Figure 7A) and cumulative fruit weight (Figure 7B) followed very similar trends throughout the 20-week harvest period and were unaffected by the light treatments indicating that CL treatments (50B, 100B and 150B) can sustain crop yield similar to the 16 h control (0B). During the initial harvest period, the average fruit weight was high in all light treatments (Figure 7C). Throughout the remainder of the experiment, while average fruit weight tended to oscillate, the general trend was that fruit size decreased in all treatments.

4 Discussion

4.1 Dynamic CL with monochromatic blue light sustains plant growth in peppers

With sustainability driving many innovations in the agricultural space, the implementation of low intensity, long photoperiod lighting strategies (including CL) has received much interest as a way to shift electricity usage to the off-peak, nighttime hours (Velez-Ramirez et al., 2012; Haque et al., 2015; Hao et al., 2018; Lanoue et al., 2019; Lanoue et al., 2021a, b). During photoperiod lengthening or CL, the circadian rhythm of the plant is often disrupted due to the lack of synchronization between the

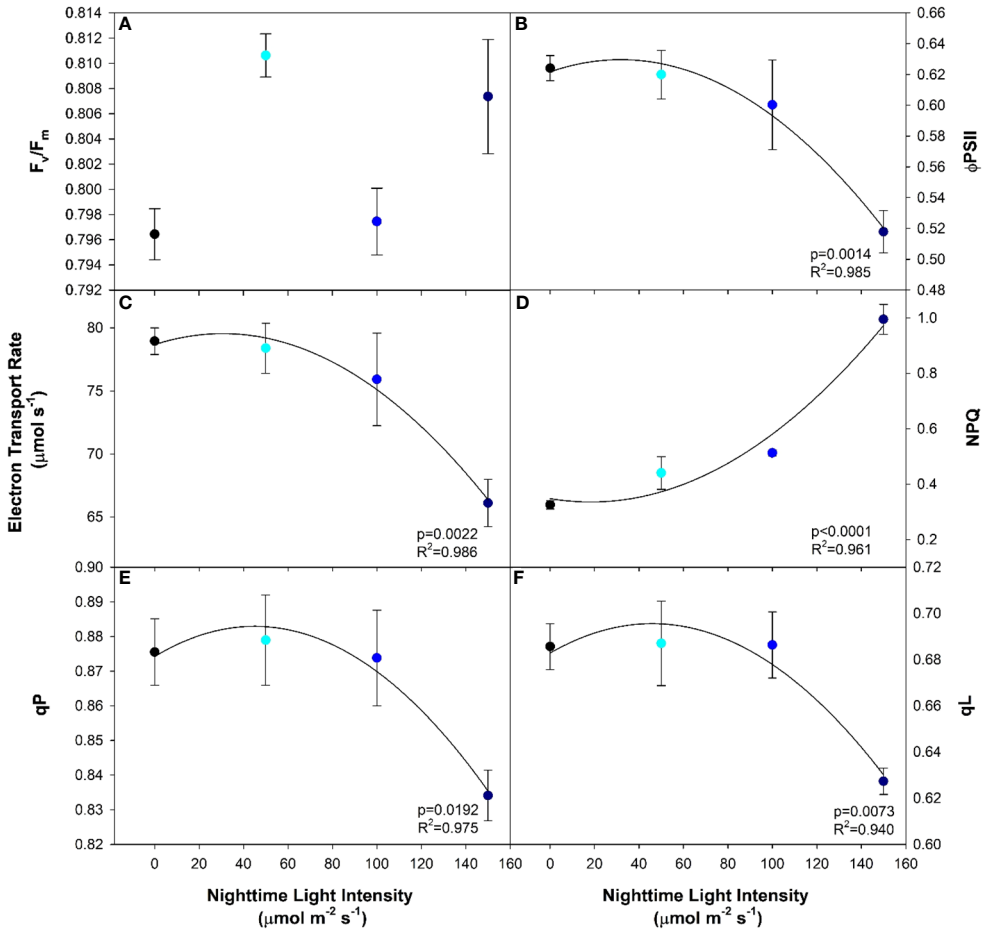

FIGURE 3
Chlorophyll fluorescence parameters including maximum efficiency of photosystem II in the dark-adapted state (F_v/F_m; **(A)**), the efficiency of photosystem II chemistry in the light-adapted state (ΦPSII; **(B)**), the electron transport rate (ETR; **(C)**), the non-photochemical quenching (NPQ; **(D)**), photochemical quenching (qP; **(E)**), and fraction of PSII reaction centers which are open (qL; **(F)**) from pepper leaves cv. 'Gina' grown under all light treatments. Regression analysis was completed using the backwards elimination method. Each data point represents the mean +/- the standard error of n=4. Only significant ($p<0.05$) regression analyses are represented in the graphs with p-values found in the bottom right corner of each respective graph.

endogenous periodicity and exogenous environmental stimuli (Velez-Ramirez et al., 2017b). This asynchrony leads to a down regulation of photosynthesis accompanied by leaf chlorosis and a reduction in yield. However, CL could increase plant biomass and yield if injury were to be prevented (Velez-Ramirez et al., 2012; Lanoue et al., 2019).

The results presented in this paper indicate that pepper plants were able to grow under supplemental CL with a nighttime light intensity of up to 150 μmol m^{-2} s^{-1} of blue light without obvious visual injury. While most morphological parameters were unchanged by growth under CL, it is notable that plants grown under 100B had increased internode length when compared to the 16 h control (20.9% increase, Table 2). Conversely, Demers et al., 1998b showed that broad spectrum CL from HPS lamps caused shorter pepper plants. However, in our study, monochromatic blue light was used during the night period and when used as a sole source, blue light can increase stem elongation (Hernández and Kubota, 2016; Lanoue et al., 2019; Kong and Zheng, 2020). The increased stem elongation can aid in reducing fruit stacking brought about by short internodes with supplemental lighting which may cause misshapen fruit, impacting quality (Lanoue et al., 2022b). A further increase in internode length was not observed when the nighttime light intensity was raised to 150 μmol m^{-2} s^{-1}. Under a low level of monochromatic blue light, phototropin is activated and this can promote stem elongation (Kong and Zheng, 2020). However, as the blue light intensity increases, a shift to higher activation rates of cryptochrome occurs, inhibiting stem elongation (Kong and Zheng, 2020). Although the light intensity at which this change in blue light photoreceptor activation occurs is unknown, it is clear that levels above 100 μmol m^{-2} s^{-1} of sole blue light did not further increase stem elongation. It should be noted that other methods to increase internode length thereby averting fruit stacking does exist. The increase in the difference between the day and night temperature (typically facilitated by the increase of the daytime temperature) has been observed to have a positive impact on stem elongation (Carvalho et al., 2002). Additionally, the introduction of far-red

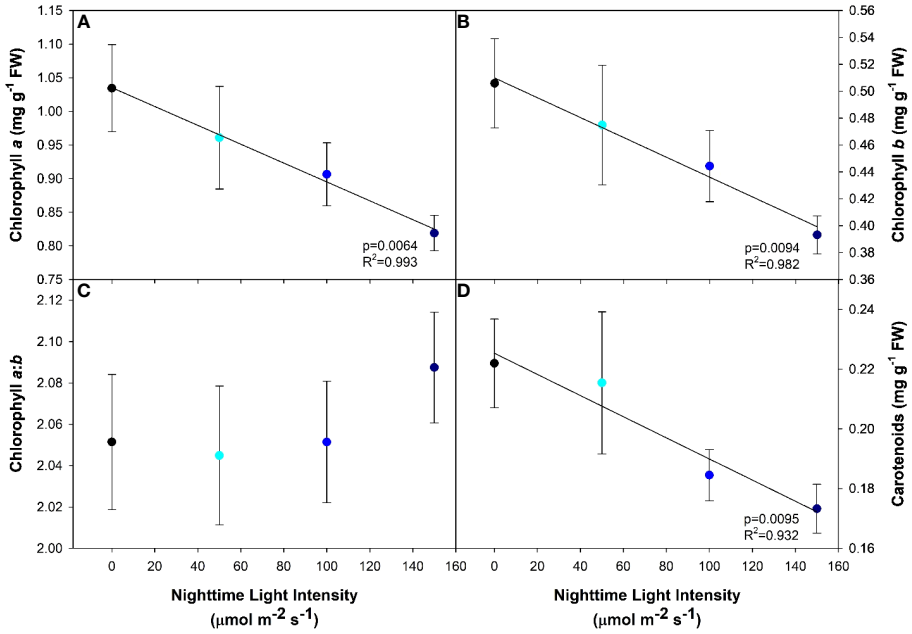

FIGURE 4
Photosynthetic pigment concentrations of pepper cv. 'Gina' leaves grown under all light treatments. Chlorophyll *a* **(A)**, chlorophyll *b* **(B)**, chlorophyll *a:b* **(C)** and carotenoids **(D)** from leaf samples. Regression analysis was completed using the backwards elimination method. The data points represent the mean +/- standard error of n=10. Only significant ($p<0.05$) regression analyses are represented in the graphs with p-values found in the bottom right corner of each respective graph.

lighting into a supplemental lighting strategy can also increase stem elongation. Additional far-red light will shift the phytochrome photo-stationary state in favor of phytochrome being in the inactive form which in turn stimulates stem and internode elongation (Demotes-Mainard et al., 2016). Both of these strategies would also elicit an increase in internode length similar to that observed in the 100B treatment. However, the blue light played a dual role in meeting the DLI requirement for photo-assimilate and biomass production and promoting proper morphological change.

Throughout the experiment, the yield and fruit size were similar regardless of which light treatment the pepper plants were grown under (Figure 7). Notably, fruit quality as measured by Brix analysis was unaffected by CL treatments (data not shown) which indicates that elevated carbohydrate levels in the leaves of plants grown under CL did not translate to increased sugar levels in the fruit. Previous research has shown that the utilization of a drastically lower nighttime light intensity compared to the daytime can reduce the chlorotic damage caused by CL (Matsuda et al., 2016; Velez-Ramirez et al., 2017b; Lanoue et al., 2019; Pham and Chun, 2020; Lanoue et al., 2021b). In contrast, our previous study utilized a similar nighttime light intensity (147 ± 3 µmol m^{-2} s^{-1}) but with broad spectrum white light and observed chlorosis and yield reduction in peppers (Lanoue et al., 2022b). Since both studies used pepper plants and the nighttime light intensities were almost identical, the conflicting results can be explained by the light spectra used. However, it should be noted that the pepper cultivar used in these two studies were different and therefore a genotype-dependent response could also be possible. These studies indicate that to avoid CL-injury, a reduction in nighttime light intensity or a change in spectral spectrum is needed. If CL is to be successful in averting injury and maintaining yield, a dynamic strategy with changes in light intensity, or light spectrum or both between daytime and nighttime must be employed.

The circadian rhythm of the plant is altered by the use of CL which can cause changes in the expression of proteins and enzymes. Notably, *type III light harvesting chlorophyll a/b binding protein 13* (*CAB-13*) has been identified as a key player in CL-injury in tomato (Velez-Ramirez et al., 2014). However, the circadian rhythm complexes are intricate, allowing for many possible points of regulation (Inoue et al., 2018). Utilizing a dynamic spectral shift during CL (i.e., a change in the light spectra between the day and night) has shown promise in reducing CL-injury and increasing yield in several crops (Matsuda et al., 2016; Ohtake et al., 2018; Lanoue et al., 2019). Implementing dynamic CL as opposed to maintaining a continuous intensity of broad spectrum light, has the potential to partially restore the plant's natural circadian rhythm, aiding in injury prevention. In fact, Velez-Ramirez et al., 2017b found that dim blue light (10 µmol m^{-2} s^{-1}) during the night following a white light spectrum also reduced CL-injury in tomato. Furthermore, our previous research on peppers and tomatoes has shown that up to 75 µmol m^{-2} s^{-1} of blue light during the night did not cause CL-injury (Lanoue et al., 2019; Lanoue et al., 2021b). Therefore, the switch from white light during the day to blue light at night may be able to maintain circadian synchrony allowing for proper gene expression of *CAB-13*.

The current understanding related to blue light averting or preventing injury is poorly understood. Regarding spectral quality,

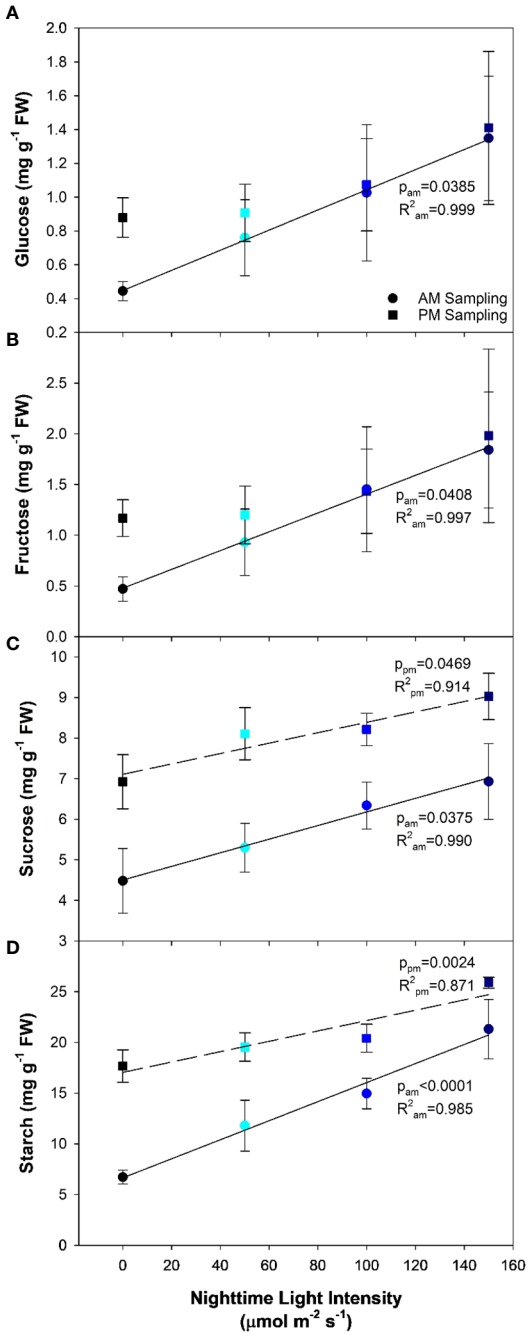

FIGURE 5
Glucose **(A)**, fructose **(B)**, sucrose **(C)**, and starch **(D)** concentrations from the analysis of the 5th leaf of pepper cv. 'Gina' plants representing each of the 4 lighting treatments. The leaves were sampled twice, once in the AM (5:30) and once in the PM (21:30). The AM sampling represents what happens to the carbohydrate profile during the night period while the PM sampling represents what happens during the daytime. Regression analysis was completed using the backwards elimination method. Mean values +/- the standard error are representative of n=6. Only significant ($p<0.05$) regression analyses are represented in the graphs with the coloring of the regression line and p-value corresponding to the sampling time.

photoreceptors become a natural area of interest to understand the interaction with circadian entrainment (Marie et al., 2022); in the case of blue light, specifically cryptochrome. While not entraining the circadian rhythm itself, cryptochrome can interact with other protein regulators which have known to impact on the core circadian clock (Shor et al., 2017). Under continuous blue light, the circadian rhythm of leaf movement is naturally entrained to a 24h period, whereas exposure to continuous darkness, green light, red light, or far-red light resulted in a phase shift away from a 24h period (Halaban, 1969). The incidence of blue light can stabilize cryptochrome which can determine the phase of the circadian rhythm (He et al., 2022). In the case of the current research and previous literature (Halaban, 1969; Lanoue et al., 2019; Lanoue et al., 2022a), blue light was able to entrain the circadian rhythm to 24h, simulating a natural 24h period involving light and dark periods (such as 16h light, 8h darkness). The interaction between blue light and cryptochrome has also been postulated to regulate circadian clock associated 1 (CCA1) expression. It was found that in plants deficient in cryptochrome 1 and 2, an arrhythmic circadian rhythm was observed, again indicating that cryptochrome plays an important role in entrainment (Mo et al., 2022). Mo et al. (2022) postulated that a possible mechanism for circadian entrainment was the blue light input loop, in which blue light activated a down stream effect, mediated through cryptochrome. However, the exact mechanism has yet to be determined and therefore requires further research.

4.2 Continuous lighting, photosynthetic feedback, and photochemistry

The constant photosynthetic pressure from CL led to increased carbohydrate levels compared to plants grown under the 16 h photoperiod (0B), regardless of nighttime light intensity (Figure 5). Demers et al., 1998b observed higher levels of starch in pepper leaves grown under CL compared to a 14 h photoperiod, whereas soluble sugars were unaffected. Due to this high carbohydrate accumulation, an inevitable increase in ROS production also occurred, which can be attributed to the over-reduction of electron acceptors under constant light pressure (Velez-Ramirez et al., 2011; Zha et al., 2019; Kumar et al., 2022). Similar to other studies (Haque et al., 2015; Zha et al., 2019; Wen et al., 2021; Kumar et al., 2022) the antioxidant capacity increased under CL and displayed a significant linear relationship with increasing nighttime light intensity (Figure 6). This increase in DPPH and FRAP activity suggests an increased need from the plant for ROS-scavenging in order to prevent further oxidative stress to the photosynthetic machinery as well as DNA damage (Huang et al., 2019). In fact, the increase in ROS-scavenging ability may be partially responsible for the lack of chlorosis observed in peppers as similar responses have been observed in lettuce, a species which is CL-tolerant (Wen et al., 2021). Similar increases in ROS-scavenging were observed by Haque et al., 2017 when a variable temperature strategy was used during CL to mitigate injury. Consequently, we hypothesize that high nighttime blue light intensities (150 µmol m^{-2} s^{-1}) are causing a hermetic/adaptive effect, which may be absent when the light spectrum remains constant (Jalal et al., 2021). This allows for the plant to manage the elevated ROS levels through increased ROS-scavenging abilities thus limiting photosynthetic reduction (Huang et al., 2019).

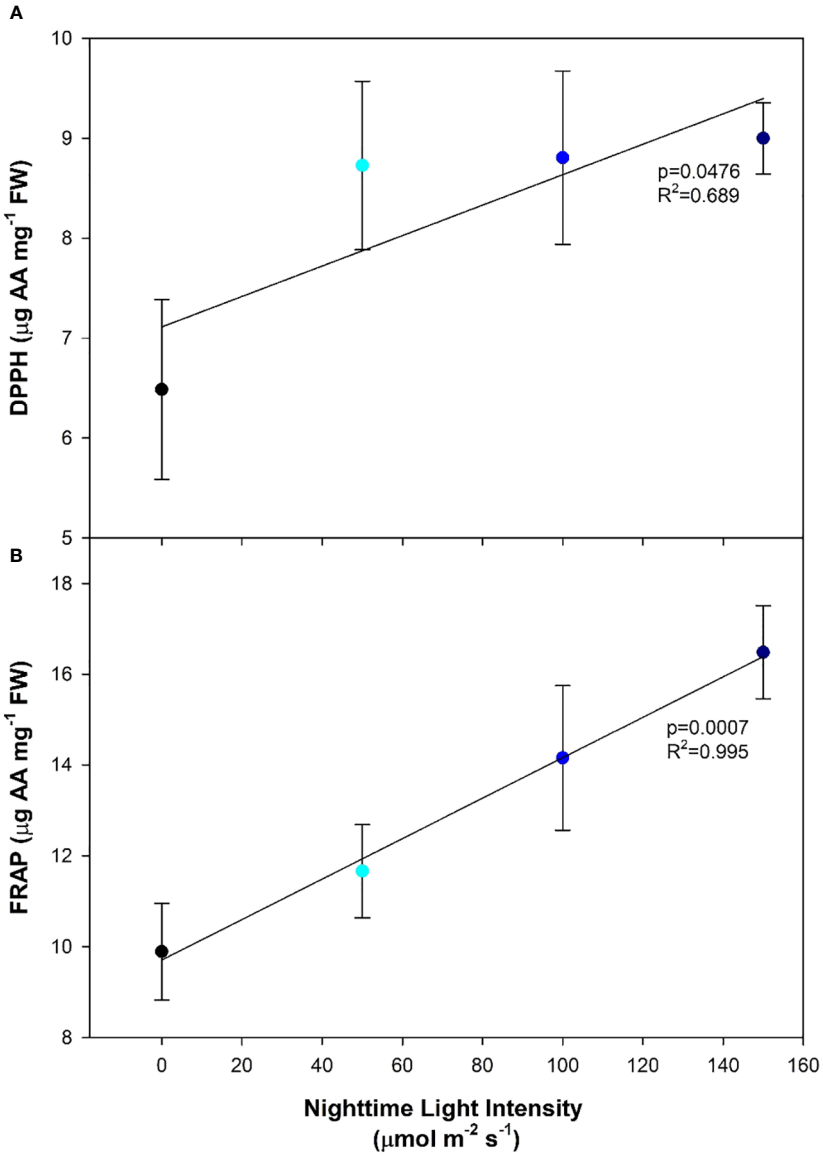

FIGURE 6
Antioxidant activity levels of pepper cv. 'Gina' leaves measured by 2,2-diphenyl-1-picrylhydrazyl (DPPH; **(A)**) and ferric reducing antioxidant power (FRAP; **(B)**) grown under various light treatments. DPPH is expressed as µg of ascorbic acid (AA) mg^{-1} of fresh weight. Regression analysis was completed using the backwards elimination method. Mean values +/- the standard error are representative of n=6.

Together with the increase in antioxidant capacity, a subsequent reduction in photosynthetic pigments was also observed. As the nighttime light intensity increased, chlorophyll *a*, chlorophyll *b*, and carotenoid content decreased (Figure 4). In peppers, the literature is inconclusive regarding the relationship between photosynthetic pigments and CL. Some literature suggests that chlorophyll content in peppers was negatively correlated with the lengthening of the photoperiod (Dorais, 1992), while others found that chlorophyll was unaffected by CL (Murage and Masuda, 1997). Conversely, our DLI was 34% higher than that used by Murage and Masuda, 1997 which could account for the disparities seen between the two studies.

When plants are exposed to excess light or an environment with a fluctuating light intensity, they must be able to cope with the abiotic stress while maintaining efficient light harvesting processes to avoid photodamage (Kaiser et al., 2015). In the case of CL, radiation pressure is constant and can elicit plant stress responses. Similar to an increase in antioxidants, a decrease in photosynthetic pigments, such as chlorophyll, can aid in the reduction of photo-oxidative stress caused by excess light when carbohydrate levels are increased. By reducing the amount of chlorophyll pigment, and coincidentally the antenna size/efficiency (Jin et al., 2016), less light energy would be transferred to the primary electron acceptor. Collectively, the reduction in chlorophyll content and the production of ROS-scavenging enzymes represent acclimation responses to the constant photon pressure of CL to mitigate further oxidative stress of PSII.

Without question, growth under CL can cause plants to undergo a stress response. However, the extent to which the abiotic factor

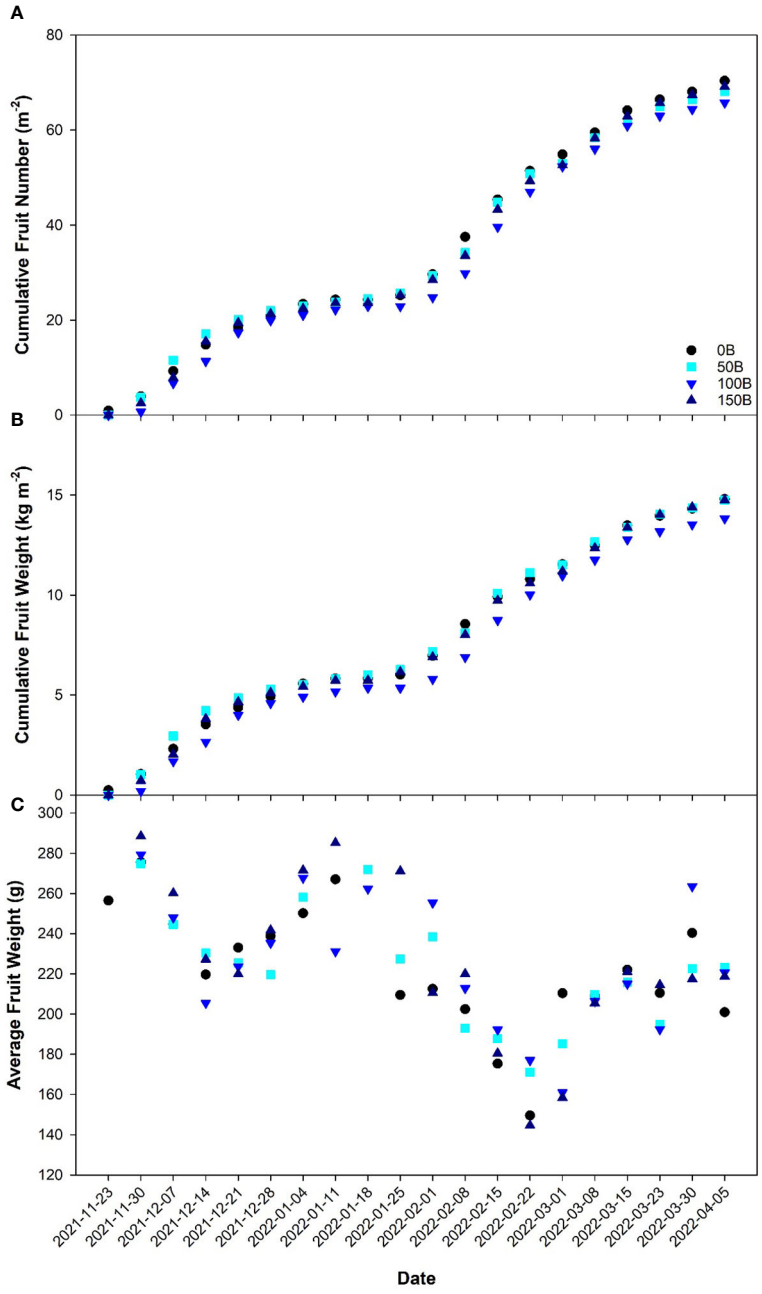

FIGURE 7
Cumulative fruit number **(A)**, cumulative fruit weight **(B)**, and average fruit weight **(C)** of pepper cv. 'Gina' grown under all light treatments as recorded weekly from November 23rd, 2021 to April 5th, 2022.

causing the stress response becomes harmful to the plant as opposed to beneficial is difficult to quantify. A common metric used to measure plant stress is assessing the maximum efficiency of PSII using F_v/F_m (Bilger et al., 1995; Baker, 2008; Janka et al., 2015; Guidi et al., 2019). F_v/F_m is quantified using a dark-adapted leaf, and therefore measures the reaction center of PSII in the open state (i.e., when the primary acceptor quinine is fully oxidized). In this way, we believe this measurement places the plant in an artificial state which is not representative of normal growth conditions. Our study shows that even under CL with high nighttime light intensity of 150 µmol m^{-2} s^{-1}, F_v/F_m was unaffected when compared to plants grown under 0B; a traditional 16 h photoperiod. In a light-adapted state, PSII operating efficiency at the actinic light intensity (ΦPSII) and quenching coefficients (NPQ and qP) as well as ETR can be determined. A contrasting narrative unfolded when employing light adapted metrics. Although the actinic light level was identical during measurements of all treatments (400 µmol m^{-2} s^{-1}), ΦPSII, ETR, qP, and qL are observed to decrease with increasing light intensity while NPQ is seen to increase (Figure 3). This suggests that when measured in a dark-adapted state, leaves appear to be without injury, while during light-adapted measurements, PSII was unable to perform optimally as the nighttime light intensity increased. Since NPQ is used as a

photoprotective mechanism to preserve PSII (Ruban et al., 2007; Ruban and Murchie, 2012), it then stands to reason that as the nighttime light intensity increased, plants exhibit reduced capability to utilize incoming light in the photosynthetic process and are protecting themselves from the light they are exposed to. In an effort to alleviate photodamage of PSII, it is possible that there was an uptick in cyclic electron flow around PSI (Yamori and Shikanai, 2016). In this instance, an imbalance would be created between ATP and NADPH formation, creating a large proton gradient needed for NPQ, and have downstream implications on carbon metabolism (Joliot and Johnson, 2011). In contrast to a decrease in photosynthetic pigment and increase in antioxidant capacity, PSII photochemistry is an instantaneous response to current conditions (Muller et al., 2001). With the underlying acclimation response, light-adapted chlorophyll fluorescence measurements were able to elucidate the real-time response of leaves to incoming radiation. Together, a reduction in photosynthetic pigments, increase in ROS-scavenging, and increase in NPQ aimed to mitigate the harmful effects of excessive radiation, in this case, CL, during plant growth. While the photosynthetic rate and LUE were reduced as nighttime light intensity increased (Figure 2), reductions in LUE were minimized due to their coping mechanisms thus yield in peppers was unaffected.

One suggested mechanism for the observed impact of nighttime intensity on light-adapted measurements, while dark-adapted measurements remain unaffected, is the rate of ribulose 1,5-biphosphate (RuBP) regeneration (Baker, 2008). In *Phaseolus vulgaris* L. leaves which had artificially elevated carbohydrate levels due to sucrose treatment, RuBP regeneration was observed to be the limiting factor in photosynthetic performance (Araya et al., 2006). In the present study, the carbohydrate levels when plants were grown under all CL treatments were observed to be higher than in plants grown under treatment 0B which involved an 8h dark period (Figure 5). The presence of increased carbohydrate under CL coincided with reduced photosynthesis and LUE (Figures 2A, B). Furthermore, it was observed that carbohydrate levels remained unaltered (glucose and fructose) or only marginally decreased (sucrose and starch) after the nighttime period (AM sampling) in plants grown under CL compared to the PM sampling (Figure 5). The lack of carbohydrate loss during the night period was similar to that found in tomatoes grown under CL (Demers and Gosselin, 2002; Haque et al., 2015). This shows a disconnect between the light intensity, photosynthetic rate, carbon export, and carbohydrate status of the leaf. Typically, carbon export, the process by which soluble carbohydrates are moved out of the leaf, increases with light intensity (Jiao and Grodzinski, 1996) and daytime export is always higher than nighttime export due to the presence of light (Lanoue et al., 2018). Here, we observed elevated leaf carbohydrate levels even when the nighttime light level was 150 μmol m^{-2} s^{-1} suggesting an imbalance between source and sink tissue activity. Since light is present, but export seemed to be lacking, enzymes related to the export pathway may be under circadian control (Chincinska et al., 2013) similar to those in the sucrose biosynthetic pathway (Jones and Ort, 1997). With a build-up of carbohydrates in the leaves, but yield being sustained in the current CL treatments, examination of the link between carbon export and CL is of interest in potentially realizing yield gain under such a lighting strategy.

5 Conclusion

Although increased carbohydrate content and ROS-scavenging capability as well as decreased photosynthetic pigment content signal a potential adverse response to CL, it was not observed to impair the yield of pepper plants in this study. Furthermore, based on the commonly used stress metric F_v/F_m, measured in a dark adapted state, all plants grown under CL treatments displayed low levels of stress, similar to the 0B treatment. Interestingly, although dark-adapted chlorophyll fluorescence measurements were unaffected by light treatment, light-adapted chlorophyll fluorescence measurements seemed to be impacted. The data implies that ΦPSII and ETR decreased while NPQ increased with increasing nighttime light intensity. In dark-adapted chlorophyll fluorescence measurements, the saturating light pulse is meant to occur fast enough that photosynthesis will not be initiated. While dark-adapted measurements do not drive photosynthesis, light-adapted measurements incorporate feedback about the downstream photosynthetic products. Light adapted measurements integrate the feedback that carbohydrate levels are elevated and respond with a reduction in ΦPSII, ETR, and qP and an increase in NPQ. Therefore, we suggest the use of light-adapted chlorophyll fluorescence measurements may be a more appropriate method in identifying stress in CL tolerant crop-types.

Data availability statement

The original contributions presented in the study are included in the article/Supplementary Material. Further inquiries can be directed to the corresponding author.

Author contributions

JL: Conceptualization, Data curation, Formal Analysis, Investigation, Methodology, Writing – original draft, Writing – review & editing. SS: Data curation, Investigation, Writing – review & editing. CL: Data curation, Investigation, Writing – review & editing. XH: Conceptualization, Funding acquisition, Investigation, Methodology, Project administration, Supervision, Writing – review & editing.

Funding

The author(s) declare that financial support was received for the research, authorship, and/or publication of this article. The project is funded by the Grid Innovation Fund of Independent Electricity System Operator (IESO) for Ontario, Canada to X. Hao (J-002725.001.02).

Acknowledgments

Sollum (Sollum Technologies Inc. Montréal, Québec, Canada) provided the LED light fixtures for the lighting treatments and helped with light treatment setup.

Conflict of interest

The authors declare that the research was conducted in the absence of any commercial or financial relationships that could be construed as a potential conflict of interest.

Publisher's note

Supplementary material

The Supplementary Material for this article can be found online at: https://www.frontiersin.org/articles/10.3389/fpls.2024.1372886/full#supplementary-material

References

Alrifai, O., Hao, X., Liu, R., Lu, Z., Marcone, M. F., and Tsao, R. (2020). Amber, red and blue LEDs modulate phenolic contents and antioxidant activities in eight Cruciferous microgreens. *J. Food Bioactives* 11, 95–109. doi: 10.31665/JFB.2020.11241

Araya, T., Noguchi, K., and Terashima, I. (2006). Effects of carbohydrate accumulation on photosynthesis differ between sink and source leaves of Phaseolus vulgaris L. *Plant Cell Physiol.* 47, 644–652. doi: 10.1093/pcp/pcj033

Baker, N. R. (2008). Chlorophyll fluorescence: a probe of photosynthesis *in vivo*. *Annu. Rev. Plant Biol.* 59, 89–113. doi: 10.1146/annurev.arplant.59.032607.092759

Barber, J., and Andersson, B. (1992). Too much of a good thing: light can be bad for photosynthesis. *Trends Biochem. Sci.* 17, 61–66. doi: 10.1016/0968-0004(92)90503-2

Bilger, W., Schreiber, U., and Bock, M. (1995). Determination of the quantum efficiency of photosystem II and of non-photochemical quenching of chlorophyll fluorescence in the field. *Oecologia* 102, 425–432. doi: 10.1007/BF00341354

Carvalho, S. M. P., Heuvelink, E., Cascais, R., and Van Kooten, O. (2002). Effect of day and night temperature on internode and stem length in Chrysanthemum: Is everything explained by DIF? *Ann. Bot.* 90, 111–118. doi: 10.1093/aob/mcf154

Chincinska, I., Gier, K., Krugel, U., Liesche, J., He, H., Grimm, B., et al. (2013). Photoperiodic regulation of the sucrose transporter StSUT4 affects the expression of circadian-regulated genes and ethylene production. *Front. Plant Sci.* 4, 26. doi: 10.3389/fpls.2013.00026

Demers, D. A., Dorais, M., Wien, C. H., and Gosselin, A. (1998a). Effects of supplemental light duration on greenhouse tomato (Lycopersicon esculentum Mill.) plants and fruit yields. *Scientia Hortic.* 74, 295–306. doi: 10.1016/S0304-4238(98)00097-1

Demers, D. A., and Gosselin, A. (1999). Supplemental lighting of greenhouse vegetables: Limitations and problems related to long photoperiods. *Acta Hortic.* 481, 469–473. doi: 10.17660/ActaHortic.1999.481.54

Demers, D. A., and Gosselin, A. (2002). Growing greenhouse tomato and sweet pepper under supplemental lighting: Optimal photoperiod, negative effects of long photoperiod and their causes. *Acta Hortic.* 580, 83–88. doi: 10.17660/ActaHortic.2002.580.9

Demers, D. A., Gosselin, A., and Wien, C. H. (1998b). Effects of supplemental light duration on greenhouse sweet pepper plants and fruit yields. *J. Amer. Soc Hortic. Sci.* 123, 202–207. doi: 10.21273/JASHS.123.2.202

Demotes-Mainard, S., Péron, T., Corot, A., Bertheloot, J., Le Gourrierec, J., Pelleschi-Travier, S., et al. (2016). Plant responses to red and far-red lights, applications in horticulture. *Environ. Exp. Bot.* 121, 4–21. doi: 10.1016/j.envexpbot.2015.05.010

Dorais, M. (1992). *Aspects culturaux et physiologiques de la tomate et du poivron de serre soumis a un eclairage d'appoint*. Doctoral dissertaion. (University of Laval).

Foyer, C. H., Neukermans, J., Queval, G., Noctor, G., and Harbinson, J. (2012). Photosynthetic control of electron transport and the regulation of gene expression. *J. Exp. Bot.* 63, 1637–1661. doi: 10.1093/jxb/ers013

Globig, S., Rosen, I., and Janes, H. W. (1997). Continuous light effects on photosynthesis and carbon metabolism in tomato. *Acta Hortic.* 418, 141–151. doi: 10.17660/ActaHortic.1997.418.19

Guidi, L., Lo Piccolo, E., and Landi, M. (2019). Chlorophyll fluorescence, photoinhibition and abiotic stress: does it make any difference the fact to be a C3 or C4 species? *Front. Plant Sci.* 10, 174. doi: 10.3389/fpls.2019.00174

Halaban, R. (1969). Effects of light quality on the circadian rhythm of leaf movement of a short-day-plant. *Plant Physiol.* 44, 973–977. doi: 10.1104/pp.44.7.973

Hao, X., Guo, X., Lanoue, J., Zhang, Y., Cao, R., Zheng, J., et al. (2018). A review on smart application of supplemental lighting in greenhouse fruiting vegetable production. *Acta Hortic.*, 499–506. doi: 10.17660/ActaHortic.2018.1227.63

Haque, M. S., Kjaer, K. H., Rosenqvist, E., and Ottosen, C. O. (2015). Continuous light increases growth, daily carbon gain, antioxidants, and alters carbohydrate metabolism in a cultivated and a wild tomato species. *Front. Plant Sci.* 6, 522. doi: 10.3389/fpls.2015.00522

Haque, M. S., de Sousa, A., Soares, C., Kjaer, K. H., Fidalgo, F., Rosenqvist, E., et al. (2017). Temperature variation under continuous light restores tomato leaf photosynthesis and maintains the diurnal pattern in stomatal conductance. *Front. Plant Sci* 8, 1602. doi: 10.3389/fpls.2017.01602

He, Y., Yu, Y., Wang, X., Qin, Y., Su, C., and Wang, L. (2022). Aschoff's rule on circadian rhythms orchestrated by blue light sensor CRY2 and clock component PRR9. *Nat. Commun.* 13, 5869. doi: 10.1038/s41467-022-33568-3

Hernández, R., and Kubota, C. (2016). Physiological responses of cucumber seedlings under different blue and red photon flux ratios using LEDs. *Environ. Exp. Bot.* 121, 66–74. doi: 10.1016/j.envexpbot.2015.04.001

Huang, H., Ullah, F., Zhou, D. X., Yi, M., and Zhao, Y. (2019). Mechanisms of ROS regulation of plant development and stress responses. *Front. Plant Sci.* 10, 800. doi: 10.3389/fpls.2019.00800

Inoue, K., Araki, T., and Endo, M. (2018). Circadian clock during plant development. *J. Plant Res.* 131, 59–66. doi: 10.1007/s10265-017-0991-8

Jalal, A., De Oliveira Junior, J. C., Ribeiro, J. S., Fernandes, G. C., Mariano, G. G., Trindade, V. D. R., et al. (2021). Hormesis in plants: physiological and biochemical responses. *Ecotoxicology Enviornment Saf.* 207. doi: 10.1016/j.ecoenv.2020.111225

Janka, E., Korner, O., Rosenqvist, E., and Ottosen, C. O. (2015). Using the quantum yields of photosystem II and the rate of net photosynthesis to monitor high irradiance and temperature stress in chrysanthemum (Dendranthema grandiflora). *Plant Physiol. Biochem.* 90, 14–22. doi: 10.1016/j.plaphy.2015.02.019

Jiao, J., and Grodzinski, B. (1996). The effect of leaf temperature and photorespiratory conditions on export of sugars during steady-state photosynthesis in Salvia splendens. *Plant Physiol.* 111, 169–178. doi: 10.1104/pp.111.1.169

Jin, H., Li, M., Duan, S., Fu, M., Dong, X., Liu, B., et al. (2016). Optimization of light-harvesting pigment improves photosynthetic efficiency. *Plant Physiol.* 172, 1720–1731. doi: 10.1104/pp.16.00698

Joliot, P., and Johnson, G. N. (2011). Regulation of cyclic and linear electron flow in higher plants. *PNAS* 108. doi: 10.1073/pnas.1110189108

Jones, T. L., and Ort, D. R. (1997). Circadian regulation of sucrose phosphate synthase activity in tomato by protein phosphatase activity. *Plant Physiol.* 113, 1167–1175. doi: 10.1104/pp.113.4.1167

Kaiser, E., Morales, A., Harbinson, J., Kromdijk, J., Heuvelink, E., and Marcelis, L. F. (2015). Dynamic photosynthesis in different environmental conditions. *J. Exp. Bot.* 66, 2415–2426. doi: 10.1093/jxb/eru406

Kim, C., Meskauskiene, R., Apel, K., and Laloi, C. (2008). No single way to understand singlet oxygen signalling in plants. *EMBO Rep.* 9, 435–439. doi: 10.1038/embor.2008.57

Kitajima, M., and Butler, W. L. (1975). Quenching of chlorophyll fluorescence and primary photochemistry in chloroplasts by dibromothymoquinone. *Biochemica Biophys. Acta* 376, 105–115. doi: 10.1016/0005-2728(75)90209-1

Kong, Y., and Zheng, Y. (2020). Phototropin is partly involved in blue-light-mediated stem elongation, flower initiation, and leaf expansion: A comparison of phenotypic responses between wild Arabidopsis and its phototropin mutants. *Environ. Exp. Bot.* 171. doi: 10.1016/j.envexpbot.2019.103967

Kumar, D., Singh, H., Bhatt, U., and Soni, V. (2022). Effect of continuous light on antioxidant activity, lipid peroxidation, proline and chlorophyll content in Vigna radiata L. *Funct. Plant Biol.* 49, 145–154. doi: 10.1071/FP21226

Lanoue, J., Leonardos, E. D., and Grodzinski, B. (2018). Effects of light quality and intensity on diurnal patterns and rates of photo-assimilate translocation and transpiration in tomato leaves. *Front. Plant Sci.* 9, 756. doi: 10.3389/fpls.2018.00756

Lanoue, J., Li, Y., Little, C., Zheng, J., St. Louis, S., Wang, A., et al. (2022a). Do plants need sleep? Dynamic 24h lighting for greenhouse production of tomato, pepper, and cucumber. *Acta Hortic.* 1377, 383–390. doi: 10.17660/ActaHortic.2023.1377.46

Lanoue, J., Little, C., and Hao, X. (2022b). The power of far-red light at night: photomorphogenic, physiological, and yield response in pepper during dynamic 24 hour lighting. *Front. Plant Sci.* 13, 857616. doi: 10.3389/fpls.2022.857616

Lanoue, J., Thibodeau, A., Little, C., Zheng, J., Grodzinski, B., and Hao, X. (2021a). Light spectra and root stocks affect response of greenhouse tomatoes to long photoperiod of supplemental lighting. *Plants (Basel)* 10. doi: 10.3390/plants10081674

Lanoue, J., Zheng, J., Little, C., Grodzinski, B., and Hao, X. (2021b). Continuous light does not compromise growth and yield in mini-cucumber greenhouse production with supplemental LED light. *Plants (Basel)* 10. doi: 10.3390/plants10020378

Lanoue, J., Zheng, J., Little, C., Thibodeau, A., Grodzinski, B., and Hao, X. (2019). Alternating red and blue light-emitting diodes allows for injury-free tomato production with continuous lighting. *Front. Plant Sci.* 10, 1114. doi: 10.3389/fpls.2019.01114

Lichtenthaler, H. K. (1987). Chlorophylls and carotenoids: Pigments of photosynthetic biomembranes. *Methods Enzymology* 148, 350–382. doi: 10.1016/0076-6879(87)48036-1

Marie, T. R. J. G., Leonardos, E. D., Lanoue, J., Hao, X., Micallef, B. J., and Grodzinski, B. (2022). A perspective emphasizing circadian rhythm entrainment to ensure sustainable crop production in controlled environment agriculture: dynamic use of LED cues. *Front. Sustain. Food Syst.* 6. doi: 10.3389/fsufs.2022.856162

Matsuda, R., Ozawa, N., and Fujiwara, K. (2014). Leaf photosynthesis, plant growth, and carbohydrate accumulation of tomato under different photoperiods and diurnal temperature differences. *Scientia Hortic.* 170, 150–158. doi: 10.1016/j.scienta.2014.03.014

Matsuda, R., Yamano, T., Murakami, K., and Fujiwara, K. (2016). Effects of spectral distribution and photosynthetic photon flux density for overnight LED light irradiation on tomato seedling growth and leaf injury. *Scientia Hortic.* 198, 363–369. doi: 10.1016/j.scienta.2015.11.045

Mo, W., Zhang, J., Zhang, L., Yang, Z., Yang, L., Yao, N., et al. (2022). Arabidopsis cryptochrome 2 forms photobodies with TCP22 under blue light and regulates the circadian clock. *Nat. Commun.* 13. doi: 10.1038/s41467-022-30231-9

Muller, P., Li, X.-P., and Niyogi, K. K. (2001). Non-photochemical quenching. A response to excess light energy. *Plant Physiol.* 125, 1558–1566. doi: 10.1104/pp.125.4.1558

Murage, E. N., and Masuda, M. (1997). Response of pepper and eggplant to continuous light in relation to leaf chlorosis and activites of antioxidative enzymes. *Scientia Hortic.* 70, 269–279. doi: 10.1016/S0304-4238(97)00078-2

Ohtake, N., Ishikura, M., Suzuki, H., Yamori, W., and Goto, E. (2018). Continuous irradiation with alternating red and blue light enhances plant growth while keeping nutritional quality in lettuce. *HortScience* 53, 1804–1809. doi: 10.21273/HORTSCI13469-18

Pammenter, N. W., Loreto, F., and Sharkey, T. D. (1993). End product feedback effects on photosynthetic electron transport. *Photosynthesis Res.* 35, 5–14. doi: 10.1007/BF02185407

Pham, D. M., and Chun, C. (2020). Growth and leaf injury in tomato plants under continuous light at different settings of constant and diurnally varied photosynthetic photon flux densities. *Scientia Hortic.* 269. doi: 10.1016/j.scienta.2020.109347

Pham, M. D., Hwang, H., Park, S. W., Cui, M., Lee, H., and Chun, C. (2019). Leaf chlorosis, epinasty, carbohydrate contents and growth of tomato show different responses to the red/blue wavelength ratio under continuous light. *Plant Physiol. Biochem.* 141, 477–486. doi: 10.1016/j.plaphy.2019.06.004

Pulido, P., Spinola, M. C., Kirchsteiger, K., Guinea, M., Pascual, M. B., Sahrawy, M., et al. (2010). Functional analysis of the pathways for 2-Cys peroxiredoxin reduction in Arabidopsis thaliana chloroplasts. *J. Exp. Bot.* 61, 4043–4054. doi: 10.1093/jxb/erq218

Ruban, A. V., Berera, R., Ilioaia, C., Van Stokkum, I. H., Kennis, J. T., Pascal, A. A., et al. (2007). Identification of a mechanism of photoprotective energy dissipation in higher plants. *Nature* 450, 575–578. doi: 10.1038/nature06262

Ruban, A. V., and Murchie, E. H. (2012). Assessing the photoprotective effectiveness of non-photochemical chlorophyll fluorescence quenching: a new approach. *Biochim. Biophys. Acta* 1817, 977–982. doi: 10.1016/j.bbabio.2012.03.026

Shor, E., Paik, I., Kangisser, S., Green, R., and Huq, E. (2017). PHYTOCHROME INTERACTING FACTORS mediate metabolic control of the circadian system in Arabidopsis. *New Phytol.* 215, 217–228. doi: 10.1111/nph.14579

Smith, A. M., and Stitt, M. (2007). Coordination of carbon supply and plant growth. *Plant Cell Environ.* 30, 1126–1149. doi: 10.1111/j.1365-3040.2007.01708.x

Stitt, M., Lunn, J., and Usadel, B. (2010). Arabidopsis and primary photosynthetic metabolism - more than the icing on the cake. *Plant J.* 61, 1067–1091. doi: 10.1111/j.1365-313X.2010.04142.x

Sysoeva, M. I., Markovskaya, E. F., and Shibaeva, T. G. (2010). Plants under continuous light: A review. *Plant Stress* 4, 5–17.

Tetlow, I. J., and Farrar, J. F. (1993). Apoplastic sugar concentration and pH in barley leaves infected with brown rust. *J. Exp. Bot.* 44, 929–936. doi: 10.1093/jxb/44.5.929

Van Gestel, N. C., Nesbit, A. D., Gordon, E. P., Green, C., Pare, P. W., Thompson, L., et al. (2005). Continuous light may induce photosynthetic downregulation in onion - consequences for growth and biomass partitioning. *Physiologia Plantarum* 125, 235–246. doi: 10.1111/j.1399-3054.2005.00560.x

Velez-Ramirez, A. I., Carreno-Quintero, N., Vreugdenhil, D., Millenaar, F. F., and Van Ieperen, W. (2017a). Sucrose and starch content negatively correlates with PSII maximum quantum efficiency in tomato (Solanum lycopersicum) exposed to abnormal light/dark cycles and continuous light. *Plant Cell Physiol.* 58, 1339–1349. doi: 10.1093/pcp/pcx068

Velez-Ramirez, A. I., Dunner-Planella, G., Vreugdenhil, D., Millenaar, F. F., and Van Ieperen, W. (2017b). On the induction of injury in tomato under continuous light: circadian asynchrony as the main triggering factor. *Funct. Plant Biol.* 44, 597–611. doi: 10.1071/FP16285

Velez-Ramirez, A. I., Heuvelink, E., Van Ieperen, W., Vreugdenhil, D., and Millenaar, F. F. (2012). Continuous light as a way to increase greenhouse tomato production: Expected challenges. *Acta Hortic.*, 51–58. doi: 10.17660/ActaHortic.2012.956.3

Velez-Ramirez, A. I., Van Ieperen, W., Vreugdenhil, D., and Millenaar, F. F. (2011). Plants under continuous light. *Trends Plant Sci.* 16, 310–318. doi: 10.1016/j.tplants.2011.02.003

Velez-Ramirez, A. I., Van Ieperen, W., Vreugdenhil, D., Van Poppel, P. M., Heuvelink, E., and Millenaar, F. F. (2014). A single locus confers tolerance to continuous light and allows substantial yield increase in tomato. *Nat. Commun.* 5, 4549. doi: 10.1038/ncomms5549

Wen, Y., Zha, L., and Liu, W. (2021). Dynamic Responses of Ascorbate Pool and Metabolism in Lettuce to Light Intensity at Night Time under Continuous Light Provided by Red and Blue LEDs. *Plants (Basel)* 10. doi: 10.3390/plants10020214

Yamori, W., and Shikanai, T. (2016). Physiological functions of cyclic electron transport around photosystem I in sustaining photosynthesis and plant growth. *Annu. Rev. Plant Biol.* 67, 81–106. doi: 10.1146/annurev-arplant-043015-112002

Zha, L., Liu, W., Zhang, Y., Zhou, C., and Shao, M. (2019). Morphological and physiological stress responses of lettuce to different intensities of continuous light. *Front. Plant Sci.* 10, 1440. doi: 10.3389/fpls.2019.01440

Zhu, M.-D., Chen, X.-L., Zhu, X.-Y., Xing, Y.-D., Du, D., Zhang, Y.-Y., et al. (2020). Identification and gene mapping of the starch accumulation and premature leaf senescence mutant ossac4 in rice. *J. Integr. Agric.* 19, 2150–2164. doi: 10.1016/S2095-3119(19)62814-5

frontiers | Frontiers in Plant Science

TYPE Original Research
PUBLISHED 07 June 2024
DOI 10.3389/fpls.2024.1371702

OPEN ACCESS

EDITED BY
Leo Marcelis,
Wageningen University and Research, Netherlands

REVIEWED BY
Aušra Brazaitytė,
Lithuanian Research Centre for Agriculture and Forestry, Lithuania
Hannah M. Rivedal,
Agricultural Research Service (USDA), United States
Anna Kołton,
University of Agriculture in Krakow, Poland

*CORRESPONDENCE
Ricardo Hernández
rhernan4@ncsu.edu

RECEIVED 16 January 2024
ACCEPTED 06 May 2024
PUBLISHED 07 June 2024

CITATION
Collado CE, Hwang SJ and Hernández R (2024) Supplemental greenhouse lighting increased the water use efficiency, crop growth, and cutting production in *Cannabis sativa*.
Front. Plant Sci. 15:1371702.
doi: 10.3389/fpls.2024.1371702

Supplemental greenhouse lighting increased the water use efficiency, crop growth, and cutting production in *Cannabis sativa*

Cristian E. Collado[1], Seung Jae Hwang[2] and Ricardo Hernández[1]*

[1]Department of Horticultural Science, North Carolina State University, Raleigh, NC, United States, [2]Division of Horticultural Sciences, Institute of Agriculture & Life Sciences, Research Institute of Life Sciences, Division of Crop Sciences, Gyeongsang National University, Jinju, Republic of Korea

The expanding cannabis production sector faces economic challenges, intensified by freshwater scarcity in the main US production areas. Greenhouse cultivation harnesses sunlight to reduce production costs, yet the impact of greenhouse light levels on crucial production components, such as plant growth, branching, and water use efficiency (WUE), remains poorly understood. This study aimed to assess the effects of combined sunlight and supplemental lighting on the crop's main production components and leaf gas exchange of *Cannabis sativa* 'Suver Haze' in the vegetative stage. Within a greenhouse, LED lighting provided at intensities of ~150, 300, 500, and 700 μmol m^{-2} s^{-1} (18-hour photoperiod), combined with solar radiation, resulted in average daily light integrals of 17.9, 29.8, 39.5, and 51.8 mol m^{-2} d^{-1}. Increasing light levels linearly increased biomass, leaf area, and the number of branches per plant and square meter, with respective rates of 0.26 g, 32.5 cm^2, and 0.41 branches per mole of additional light. As anticipated, crop evapotranspiration increased by 1.8-fold with the increase in light intensity yet crop WUE improved by 1.6-fold when comparing the lowest and highest light treatments. Moreover, water requirements per unit of plant biomass decreased from 0.37 to 0.24 liters per gram when lighting increased from ~18 to 52 mol m^{-2} d^{-1}, marking a 35% reduction in evapotranspiration. These results were supported by increments in leaf photosynthesis and WUE with light enhancement. Furthermore, our findings indicate that even 52 mol m^{-2} d^{-1} of supplemental lighting did not saturate any of the crop responses to light and can be economically viable for cannabis nurseries. In conclusion, light supplementation strongly enhanced photosynthesis and plant growth while increasing WUE. Additionally, a comprehensive discussion highlights the shared physiological mechanisms governing WUE in diverse plant species and their potential for water conservation under enhanced lighting conditions.

KEYWORDS

HEMP, stock plant, propagation, water management, water reduction, crop yield, PPFD, DLI

Introduction

The expansion of both medicinal and recreational cannabis sectors within the United States is witnessing persistent growth, attributable to the ongoing legalization efforts across various states (DeCarcer et al., 2021). The cultivation of high-value cannabis crops is predominantly conducted within controlled environments, encompassing indoor sole-source-LED light facilities and greenhouses. While greenhouse cultivation harnesses solar energy to enhance cost-efficiency in production (Vezdos and Martinez, 2021), it confronts the challenge of potentially insufficient natural sunlight levels required to attain targeted crop quality and yield. Furthermore, the escalating demand for water resources poses a pressing concern, as approximately 37% of the freshwater supply in the United States is allocated to irrigation (Dieter et al., 2018). This issue is exacerbated by other factors, including population growth, agricultural demands, complexities in water infrastructure, and recurring drought conditions (GAO, 2014). Furthermore, California, a state deeply affected by water shortages, accounted for 58% of medical and recreational cannabis licenses issued in 2021 (Conway, 2023). Therefore, it is imperative to optimize cannabis production and other crops through the strategic application of supplemental lighting and water-saving approaches. Addressing these multifaceted challenges requires a comprehensive understanding of crop light and water utilization.

Research pertaining to *Cannabis sativa* cultivated under sole-source LED lighting reported a correlation between the daily light integral (DLI) and crop productivity. For instance, cannabis flower yield exhibited a linear increase in response to increasing DLI levels, up to 78 mol m^{-2} d^{-1}, which represented the highest DLI investigated under short-day conditions, 12 h (Rodriguez-Morrison et al., 2021). Moreover, when subjected to long day durations, 16 h, the shoot biomass demonstrated a similar positive trend and increased even with 82 mol m^{-2} d^{-1} (Moher et al., 2021). However, it is essential to acknowledge that the dynamics of light within the context of greenhouse production can deviate substantially from those observed in sole-source LED facilities, and those changes may strongly affect plant physiological and crop efficiencies. Greenhouse environments are characterized by diurnal fluctuations in light intensity, a balanced spectrum encompassing blue, green, red, and far-red wavelengths, as well as the introduction of additional radiation from 800 to 2500 nm. The resultant but dynamic spectral combination between sunlight and electrical lighting further confounds the light environment within greenhouses. These dynamic light conditions can influence diverse facets of plant biology, including growth patterns, morphological attributes, and key physiological processes such as photosynthesis, stomatal conductance, transpiration, and energy balance (Pieruschka et al., 2010; Nelson and Bugbee, 2015; Zhen and Bugbee, 2020). Consequently, it is imperative to emphasize the need for comprehensive characterizations of the lighting environment in greenhouse supplemental lighting studies. Moreover, this research enhances the limited body of knowledge concerning the impact of supplemental lighting on cannabis greenhouse production (David Potter, 2009).

Radiation influences water usage in non-stressed plants, primarily by increasing transpiration rates (Whitehead, 1998; Pieruschka et al., 2010; Pokorny, 2019). While it is known that increased radiation levels correspondingly lead to increased water consumption, a more comprehensive approach for assessing water utilization leads to calculating water-use efficiency (WUE). WUE captures the interaction between plant growth parameters, such as yield and biomass, with transpiration or evapotranspiration and can be quantified at the leaf, plant, and crop levels (Jackson et al., 2016; Hatfield and Dold, 2019).

One of the principal strategies employed to enhance crop WUE is the deliberate reduction of water availability within the soil or substrate, a practice that significantly decreases the transpiration rate. Nonetheless, this approach most often reduces plant productivity, given the associated decrease in photosynthetic rates (Hubick and Farquhar, 1989; Lawson and Blatt, 2014; Xing et al., 2022). Remarkably, research has demonstrated that trees originating from diverse botanical families and adapted to varying geographical regions exhibit reduced leaf transpiration when subjected to elevated radiation levels in comparison to conspecifics grown under lower irradiance conditions, even while concurrently displaying heightened rates of photosynthesis (Idris et al., 2019). This suggested that leaves adapted to highlight environments may possess superior WUE compared to their shade-adapted counterparts when both leaf types are subjected to identical radiation regimes. Therefore, one of the main focuses of this investigation was to quantify leaf and crop water-use efficiencies in the context of cannabis cultivation under increased supplemental light conditions.

Cannabis nurseries and flower producers employ extended photoperiods to increase branch proliferation and plant size. This enhances cutting production in nurseries and conditions plants for higher flower yields. Therefore, enhancing biomass and branch count and minimizing cultivation time is vital for cannabis nurseries, ensuring a seamless supply of plants to cannabis flower producers. Prior investigations have yet to elucidate the impact of lighting on branch development (potential cuttings) and the associated morphological and physiological parameters of cannabis vegetative plants in greenhouses.

The primary objective of this research was to investigate the impacts of greenhouse light levels, encompassing solar radiation in conjunction with various supplemental LED light intensities (~150, 300, 500, and 700 μmol m^{-2} s^{-1}), on growth parameters, the number of branches, water utilization (WU), and water-use efficiency (WUE) in a vegetative crop of *Cannabis sativa* L. Additionally, we aimed to assess the effects of these prolonged light treatments on key leaf physiological attributes, specifically photosynthesis (A), stomatal conductance (g_{sw}), and transpiration (E), which are pivotal determinants of both growth and water consumption.

The study involved the examination of two hypotheses. 1) Increments in the cumulative light dosage would elicit an increase in plant growth and in the number of branches. 2) Leaves of cannabis plants cultivated under an elevated DLI would display higher WUE due to increased photosynthetic rates than their counterparts exposed to a lower DLI when leaves were evaluated under high PPFDs.

Materials and methods

Starting plant material and location

Rooted cuttings of *Cannabis sativa* cv Suver Haze (© Oregon CBD) served as the initial material. The cuttings underwent rooting in a greenhouse for 24 days and a photoperiod of 18 hours. The propagation was conducted by a commercial nursery in Broadway, NC, US (Ryes Greenhouses LLC). On October 9, 2020, 240 plug plants (rooted cuttings) were selected to be planted, as well as five additional and representative samples for destructive measurements. The most uniform plants were selected based on morphological similarities (mean ± SD of five representative samples: number of leaves: 3.6 ± 0.9, shoot fresh and dry mass: 1.4 ± 0.4 g and 0.26 ± 0.08 g, root dry mass: 18.1 ± 7.2 mg, and leaf area: 37.5 ± 10.5 cm^2). The plants were evenly distributed among 12 research plots within a glass greenhouse at the NC State Horticulture Field Lab in Raleigh, NC, USA. Further details can be found in Supplementary Figure S1 of the Supplementary Material section.

Plot sensing and controlling capabilities

Each production-research plot was equipped with two LED dimmable lighting fixtures to establish and maintain specific light levels, as illustrated in Supplementary Figure S1. Additionally, two soil moisture sensors, two load cells, and a solenoid valve were employed to quantify water evapotranspiration and sustain optimal substrate moisture and nutrition due to the crop requirements at each plot. Furthermore, a fine-wire thermocouple and quantum sensor were utilized to address greenhouse air temperature and solar variations. In total, 72 sensors and 12 solenoids were connected to a datalogger and controller through four sensor multiplexers and a relay driver, with data logged at 5-minute intervals. Hardware specifications are detailed in the Supplementary Material section.

The treatments

The day after planting, the supplemental lighting was increased from ~90 µmol m^{-2} s^{-1} to ~ 150, 300, 500, and 700 µmol m^{-2} s^{-1} (Table 1) and maintained for 20 days until harvest. Each light level represents the average of three plots or production areas (Supplementary Figure S1). However, the treatments consisted of a combination of supplemental LED and solar radiation. Details are presented in Table 1, and the light spectra of average sunlight, as well as the lowest and highest light treatments, are presented in Table 2 and Supplementary Figure S2. The calibration and control of the lights are described in the Supplementary Material under the title *Supplemental Light Calibration and Control*.

Greenhouse conditions

The greenhouse air conditions were regulated with forced hot air, a cooling wet pad, two exhaust fans, and a Priva Maximizer control system (De Lier, Netherlands). The average temperature and humidity were 25.4 ± 1.7°C and 73.3 ± 10.4% (mean ± SD) at the center of the greenhouse at canopy height and measured in an aspirated box. The air temperature at the top of the 12 canopies was similar, yielding a mean ± standard deviation between plots of 25.4 ± 0.3°C. The daytime carbon dioxide was around 410 µmol mol^{-1} and monitored right next to the canopy.

Control of the substrate moisture and fertilization

Control of substrate moisture and fertilization was managed through independent irrigation control at each of the 12 plots, utilizing readings from two soil volumetric water content (VWC) sensors per plot. The plot's solenoid valve was activated for 25 minutes based on the lowest substrate moisture reading from two

TABLE 1 Summary of light sources and levels: supplemental PPFD, cumulative supplemental plus solar treatments (∑PPFD), average daily light integral (DLI), average PPFD, and light source.

Supplemental PPFD[z]	∑PPFD[y]	DLI[x]	Average PPFD[w]	Light source:[v]		∑ePAR (400-750 nm)	eDLI (400-750 nm)	PPFD / ePAR
µmol m^{-2} s^{-1}	mol m^{-2}	mol m^{-2} d^{-1}	µmol m^{-2} s^{-1}	**Sun**	**LED**	mol m^{-2}	mol m^{-2} d^{-1}	%
151 ± 0	376 ± 49	17.9	277	48%	52%	408	19.5	92%
300 ± 2	625 ± 8-	29.8	459	38%	62%	669	31.8	94%
501 ± 2	829 ± 59	39.5	610	22%	78%	862	41.1	96%
703 ± 3	1088 ± 55	51.8	800	17%	83%	1121	53.4	97%

∑ePAR and eDLI are cumulative photons based on an extended PAR range 400 to 750 nm (Zhen et al., 2021). Means and standard deviations were calculated from the three greenhouse plots per light level. The photoperiod was maintained at 18 hours.
[z]Photosynthetic photon flux density from 400 to 700 nm) measured with a line quantum sensor (mean ± standard deviation).
[y]Measured continuously for 21 days with quantum sensors (mean ± SD). Twenty-one days include one day of LED (~90 µmol m^{-2} s^{-1}) + solar radiation and 20 days of LED treatments + solar radiation.
[x]DLI = ∑PPFD/21 days.
[w]DLI/Photoperiod * time and mol conversion factors.
[v]Proportions between supplemental (LED) and solar radiation (Sun).

TABLE 2 Solar and LED spectrum measurements and calculations for light quality comparison.

Plant light parameter	wavelength range (nm)	Units	Greenhouse sunlight (Sun)	LED (151 PPFD)	LED (703 PPFD)	Sun + LED (144 + 151 PPFD)	Sun + LED (144 + 703 PPFD)
PPFD	400-700	μmol m^{-2} s^{-1}	144	151	703	295	847
ePAR*	400-750		170	152	707	321	877
UV	300-400		5.0	0.1	0.4	5.1	5.4
Blue	400-500		34.2	27.5	121.6	61.8	155.8
Green	500-600		53.3	0.4	1.5	53.6	54.7
Red	600-700		56.5	123.1	580.4	179.6	636.9
Far Red	700-800		49.3	0.9	4.0	50.2	53.3
Blue/PPFD		%	23.8	18.2	17.3	20.9	18.4
Green/PPFD			37.0	0.2	0.2	18.2	6.5
Red/PPFD			39.3	81.5	82.5	60.9	75.2
Red/Blue			1.65	4.48	4.77	2.91	4.09
Red/Far Red			1.15	132.0	143.7	3.6	11.9
Pfr/Ptotal**			0.73	0.88	0.88	0.83	0.86

The greenhouse sunlight measurements were adjusted to match the average photosynthetic photon flux density of 144 μmol m^{-2} s^{-1}. The calculated solar mean is based on an 18-h photoperiod and an average DLI of 9.3 mol m^{-2} d^{-1} from the solar radiation measurements among the 12 plots. The LED and Sun + LED columns show the lowest and highest lighting treatments. The LED columns represent the greenhouse lighting conditions without solar radiation, while the Sun + LED columns represent average lighting conditions in the 18-h lighting period. This table analysis is based on ~20 and 21 days for the LED conditions and the average greenhouse solar radiation, respectively; thereby, they may differ from values in Table 1.
*ePAR represents an extended PAR or PPFD range (Zhen et al., 2021).
**Phytochrome photoequilibrium (Sager et al., 1988).

plants in each treatment area. Irrigation was initiated when the VWC reached or fell below 0.345 ± 0.014 m^3 m^{-3} (80% of container capacity).

Two irrigation emitters with a combined flow of 5.4 L h^{-1} per pot were employed to ensure uniform moisture and prevent nutrient-salt accumulation. Detailed analysis of nutrient solution composition, pour-thru procedure samples (Table S1), substrate conditions, and moisture calibration can be found in the Supplementary Material section.

Plants for measurements and growing area

the total growing area per plot was made of 20 plants, using a density of 10.8 plants m^{-2}. However, only plants from the center of the plots (6 plants) were used for plant measurements to avoid edge effects.

Vegetative growth measurements

Plant height (measured from the growing tip to substrate level) was assessed every two to four days. Plant biomass and leaf parameters were determined through destructive measurements on day 21. Plant fresh mass was immediately recorded after cutting the plant at ground level. Leaf area, and leaf and stem dry mass were quantified using Li-3100C units (Li-Cor, Lincoln, NE, USA) and drying ovens set at 69°C, respectively. The number of primary and secondary branches (length ≥ 5 cm) was counted on the main stem and the primary branches, respectively.

Evapotranspiration

Evapotranspiration (ET) and evaporation were quantified by measuring changes in the load cell readings (including the weight of water, substrate, pot, and plant for ET, or the weight of water, substrate, and pot for evaporation) after and immediately before the irrigation events occurred (Supplementary Figure S3A). ET was quantified in all plots, while evaporation was measured using a pot without a plant. Refer to the Supplementary Material section for more details.

WUE (Water Use Efficiency): Shoot water use efficiency was calculated as the ratio between the dry mass of leaves and stems and the litters of evapotranspiration in a 21-day period. Similarly, the ratios between primary, secondary, and total branches and evapotranspiration requirements were calculated. Leaf WUE was calculated as the ratio between photosynthesis (A) and transpiration (E).

Metabolite and gas exchange measurements

These measurements were performed on fully expanded, light-exposed top leaves to compare leaves developed under different

light levels. Crops were subjected to light treatments for 18 days before the readings. Chlorophyll, anthocyanin, and flavonol indexes were measured on the adaxial surfaces using a Dualex Scientific handheld leaf-clip meter (Force-A, Orsay, France). On similar leaves, net CO_2 assimilation (A), stomatal conductance to water vapor (g_{sw}), transpiration (E), internal leaf CO_2 concentration (C_i), and leaf temperature measurements were taken using a Li-6800 with a 2-cm² aperture 6800-01A chamber (Li-Cor, Lincoln, NE, USA). Readings were recorded at the center of the leaflets and after the CO_2 assimilation plateaued for at least two minutes. The chamber maintained 18% blue light, 82% red light, 70% relative humidity (RH), 27°C temperature, and 404 ppm of CO_2. The settings were chosen based on greenhouse conditions and instrument capability.

Statistics

For crop parameters and leaf pigments, linear regression and ANOVA were conducted using the mean of one or more subsamples per plot. Subsamples or observational units (OU) consisted of 6 plants for plant height, 3 plants for biomass, leaf area, and branches, 1-2 load cells for evapotranspiration, and 18 leaves for metabolites. The total sample size was defined as N, and in the same way, the number of true replications in one group or light level was n. Because the plot acted as the experimental unit, N and the number of plots were equivalent to 12 (Lazic et al., 2018).

For leaf gas exchange analysis from 150 to 2000 µmol of light m^{-2} s^{-1} (PPFD), only top leaves grown under DLIs of ~18 and 52 mol m^{-2} d^{-1} were analyzed (N=6, n=3, OU=1 leaf per plot). Split-plot models were used on A, E, g_{sw}, and WUE to evaluate responses based on the effects of DLI, PPFD, and DLI*PPFD. Light intensity (150, 300, 500, 700, 1000, 1300, 1600, and 2000 µmol m^{-2} s^{-1}) effects were evaluated at the split-plot level. Consequently, the effects of long light exposure or DLI were assessed at the main plot level. In addition, DLI effects were analyzed using t-tests. T-tests were used to compare specific groups and validate this study's second hypothesis. More specifically, one-tailed t-tests were used to evaluate the effect of DLI on leaf photosynthesis and WUE under elevated PPFDs (≥ 700 µmol m^{-2} s^{-1}), while leaves under lower PPFDs were evaluated under two-tailed t-tests. All analyses and graphs were performed using JMP Pro 16.0 and 17.0 from SAS (Cary, NC, USA).

Results

The results were analyzed using the cumulative light per square meter exposure in 21 days (ΣPPFD), given that plant responses to light are influenced by the spatial and temporal aspects of light capture (Rosati and Dejong, 2003). Nevertheless, considering that the standard practice in research and production often involves quantifying cumulative light on a daily basis rather than over the entire growth period, Daily Light Integral (DLI) was also used for the interpretation of results and discussion. A comprehensive dataset, including specific and general crop responses to light, was provided in Table 3 to facilitate discussion. Additional results, such as leaf temperatures, leaf internal CO_2, and economic feasibility of cutting production, are presented in the Supplementary Material File.

Crop growth, development, and branch production

Plant and crop growth, development, and morphological parameters were evaluated under different greenhouse lighting conditions (Table 1) to characterize the overall plant quality, aiming to produce plants for flower induction and plants for the production of cuttings (stock plants).

Greenhouse lighting from ~18 to 52 mol m^{-2} d^{-1} led to linear increments in fresh mass, dry mass, number of nodes, internode length reduction, stem diameter, leaf area index (LAI), and branches (Table 3, Figures 1–4). In addition, increases in light intensity led to quadratic increments in specific leaf weight (SLW). Notably, under solar and supplemental light intensities between ~700 and 2000 µmol m^{-2} s^{-1} (Supplementary Figure S3B), along with an LAI expansion from 0.04 (initial leaf area) to 4.4 m^2 m^{-2} (Table 3), the vegetative growth of 'Suver Haze' did not exhibit a growth saturation or light efficiency reduction (g mol^{-1}) even when exposed to an average DLI of 52 mol m^{-2} d^{-1}. More specifically, the crop's dry mass linearly increased at a rate of 0.26 g mol^{-1} from 102 to 376 g m^{-2} (Figure 2A). In a similar way, the LAI linearly increased from 2.1 to 4.4 m^2 m^{-2} (Figure 2B; Table 3). Furthermore, higher DLIs and LAIs were generally accompanied by increased SLW (specific leaf weight) and top-leaf metabolite concentrations per area (Table 3).

Despite differences in light quantity and quality (Tables 1, 2), the internode length and plant height exhibited marginal or non-significant responses to the light treatments (Table 3; Figure 3). On the other hand, the numbers of primary, secondary, and total branches linearly increased with more light. However, branching rates displayed a significant contrast; primary branches registered a rate of 0.04 branch mol^{-1} m^{-2}, while secondary branches exhibited a substantially higher rate of 0.36 branch mol^{-1} m^{-2} (Figure 4) with the increase in light intensity. This difference highlighted the branching dynamics in response to light, with secondary branches surpassing primary branches by nine times.

In conclusion, all the results and their statistical analyses support our hypothesis that increments in the cumulative light dosage would elicit an increase in plant growth and the number of branches. In addition, there was no evidence of light saturation.

Crop water use and efficiency

The water usage (evapotranspiration in 21 days) and water use efficiencies (WUE) to produce shoots and branches were quantified from ~18 to 52 mol m^{-2} d^{-1} (DLI). Light supplementation linearly increased the cumulative crop evapotranspiration from 39.8 to 70.6

10.3389/fpls.2024.1371702

TABLE 3 Mean ± standard deviation for whole canopy and ratios of *Cannabis sativa* 'Suver Haze' at four cumulative solar and LED lighting levels in 21 days (∑PPFD).

∑PPFD (mol m^{-2})	Shoot fresh mass (g m^{-2})	Shoot dry mass (g m^{-2})	Water per dry mass (g g^{-1})	Stems (%)	Leaves (%)	
376 ± 49	602 ± 73	102 ± 14	4.9 ± 0.1	37 ± 2	63 ± 2	
625 ± 08	956 ± 87	161 ± 19	5.0 ± 0.2	38 ± 2	62 ± 2	
829 ± 59	1281 ± 114	223 ± 20	4.8 ± 0.0	39 ± 1	61 ± 1	
1088 ± 55	1610 ± 273	284 ± 56	4.7 ± 0.1	40 ± 1	60 ± 1	
	L	L	L	L	L	
∑PPFD (mol m^{-2})	Main stem height (cm)	N° of nodes on the main stem	Internode length (cm)	Main stem diameter (mm)	LAI (m^2 m^{-2})	SLW (g m^{-2})
376 ± 49	52.0 ± 3.8	17 ± 1	3.11 ± 0.06	7.4 ± 0.2	2.1 ± 0.2	31.3 ± 0.7
625 ± 08	55.3 ± 0.9	18 ± 0	3.08 ± 0.10	8.9 ± 0.1	2.8 ± 0.3	35.1 ± 1.1
829 ± 59	57.9 ± 2.9	19 ± 1	3.08 ± 0.20	10.3 ± 0.5	3.6 ± 0.3	37.7 ± 1.2
1088 ± 55	55.9 ± 1.4	20 ± 1	2.85 ± 0.14	11.1 ± 0.9	4.4 ± 0.7	38.6 ± 0.7
	NS	L	L	L	L	Q
∑PPFD (mol m^{-2})	Total branches m^{-2}	1° branches m^{-2}	2° branches m^{-2}	Chlorophyll index	Flavonol index	Anthocyanin index
376 ± 49	218 ± 70	136 ± 9	81 ± 61	32.2 ± 1.1	1.11 ± 0.03	0.122 ± 0.004
625 ± 08	287 ± 29	142 ± 9	145 ± 26	33.7 ± 1.0	1.26 ± 0.02	0.128 ± 0.002
829 ± 59	390 ± 34	160 ± 2	230 ± 32	36.1 ± 1.2	1.39 ± 0.03	0.138 ± 0.002
1088 ± 55	508 ± 37	164 ± 11	344 ± 34	35.9 ± 1.0	1.43 ± 0.07	0.144 ± 0.006
	L	L	L	L	Q	L
∑PPFD (mol m^{-2})	Water use (L m^{-2})	WUE_{Shoot} (g L^{-1})	$WUE_{Total\ branches}$ (Branch L^{-1})	$WUE_{1°\ branches}$ (Branch L^{-1})	$WUE_{2°\ branches}$ (Branch L^{-1})	
376 ± 49	39.8 ± 3.4	2.6 ± 0.3	5.5 ± 1.7	3.4 ± 0.3	2.2 ± 1.2	
625 ± 08	51.1 ± 9.5	3.2 ± 0.5	5.8 ± 1.4	2.9 ± 0.7	2.9 ± 0.8	
829 ± 59	58.7 ± 3.8	3.8 ± 0.5	6.7 ± 0.9	2.7 ± 0.2	3.9 ± 0.7	
1088 ± 55	70.6 ± 10.3	4.1 ± 0.9	7.3 ± 1.4	2.4 ± 0.5	5.0 ± 0.9	
	L	L	NS (p=0.06)	L	L	

Results in square meter (m^2) can be expressed in plant basis by dividing them by density (10.8 plant m^{-2}). Shoot = leaf and stem biomass. LAI, leaf area index; SLW, specific leaf weight; 1° and 2°: primary and secondary; WUE, water use efficiency. % are on shoot biomass basis.
L and Q ($p<0.05$) for linear (L) and quadratic (Q) terms in linear regression analysis; NS ($p\geq0.05$). In all cases, N=12, n=3, and the number of observational units varied, as described in Material and Methods.

liters (L) per square meter (m^{-2}) (Figure 5A). Simultaneously, the pot evaporation was measured at 20.9 L m^{-2}, representing transpiration rates between ~48 to 70% of the evapotranspiration. Despite higher water losses under more light, the shoot WUE increased linearly from 2.7 to 4.2 g L^{-1} by increasing the supplemental lighting (Figure 5B).

At the branch level, the WUE varied based on the type of branches (Figure 5C) and the branch response to the light (Figure 4). For instance, the WUE of primary branches was reduced with light augmentation (Figure 5C) because of the lower degree of light-level dependency of primary branches (Figure 4). However, the increase of light substantially enhanced the WUE of secondary branch production, elevating it from 2 to 5 branches per liter (Figure 5C). This improvement can be attributed to the more pronounced impact of light on secondary branches compared to its influence on primary branches. Consequently, the combined results of WUE for total branches, primary plus secondary branches, suggest a reduced but still considerable effect by the light augmentation, with WUEs from 5.5 to 7.3 for total branches per liter of water (p=0.06, Figure 5C; Table 3). Nevertheless, the water needs for cutting production can exhibit significant variability, ranging from approximately 14 to 19 liters of water for every 100

FIGURE 1
Plot or zone representative *Cannabis sativa* 'Suver Haze' plants grown in a greenhouse after 20 days of four supplemental LED light levels (151, 300, 501, and 703 µmol m^{-2} s^{-1}). Numbers represent the cumulative PPFD and [average DLI] from the LED treatment and sunlight in 21 days at the top of the canopy.

cuttings for highly efficient growers who utilize all available branches to approximately 20 to 50 liters of water for every 100 cuttings for those who selectively employ smaller or larger caliper cuttings (Figure 5D).

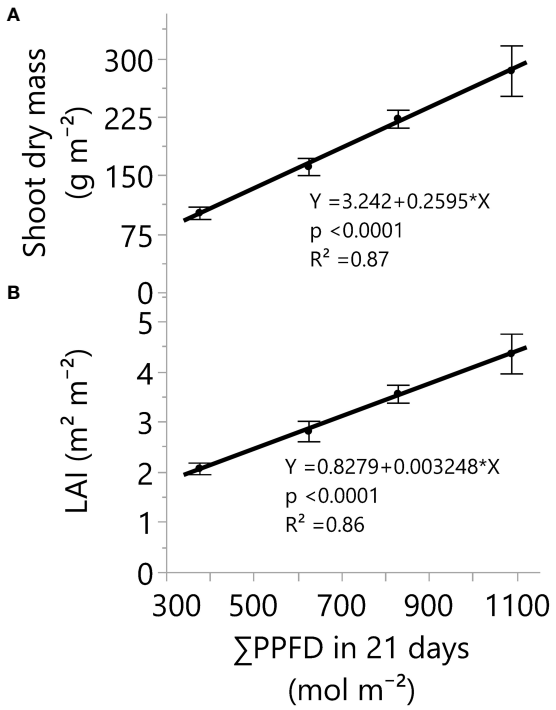

FIGURE 2
Shoot dry mass **(A)** and leaf area index **(B)** responses under four greenhouse cumulative light levels (sunlight plus supplemental LED light). PPFD represents photosynthetic photon flux density. p-values of the slopes (0.26 g m^{-2} and 0.003 m^2 m^{-2}) from linear regression analyses. Dots and error bars represent the mean and standard errors for each light treatment group, respectively. In all cases, N=12, n=3, and OU=3 plants per plot.

Leaf photosynthesis, pigments, stomata, transpiration, and WUE

Top leaves of plants grown under ~18 and 52 mol m^{-2} d^{-1} (DLI) were subjected to a range of short-term light intensities from 150 to 2000 µmol m^{-2} s^{-1} (PPFD) to analyze the impact of long-term greenhouse lighting (DLI) on net photosynthesis, transpiration, stomatal conductance, and leaf WUE. Additionally, chlorophyll, flavonol, and anthocyanin indexes (light pigments) were quantified.

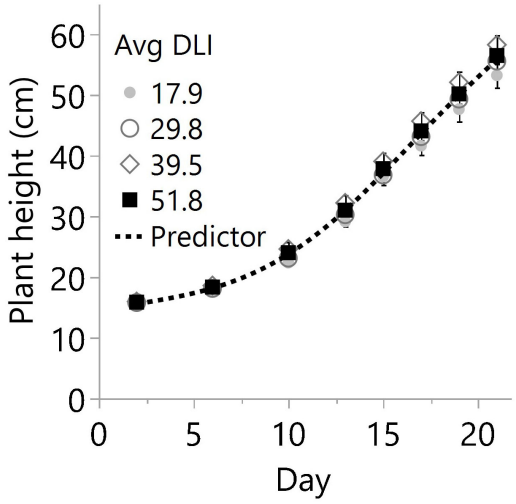

FIGURE 3
Plant heights on different days after planting in the greenhouse for four average daily light integrals (DLI) expressed in mol m^{-2} d^{-1}. Every mark represents the average of 18 plants per date, and bars are the standard error from 3 plots (N=12, n=3, OU=6 plants per plot and date). For each date, linear regression and ANOVA indicated no differences in height from additional lighting ($p \geq 0.075$) or between specific light levels ($p \geq 0.139$), respectively. Therefore, the overall predictor model based only on days after planting is $14.08+((69.20-14.08)/(1+e^{-0.25*(Day-69.20)}))$ with R^2 0.983.

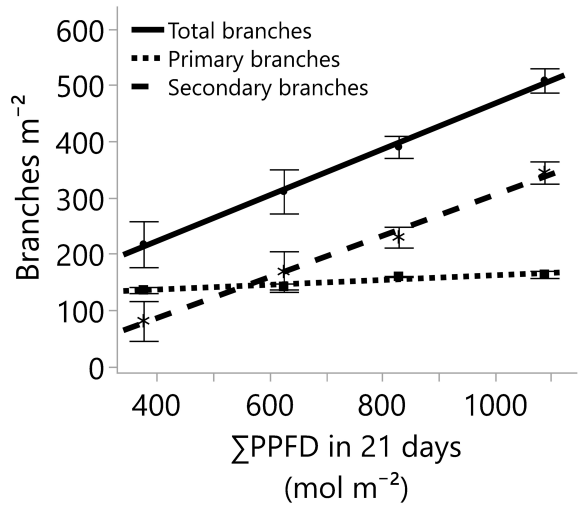

FIGURE 4
The number of branches developed on the main stem (primary branches) and on the primary branches (secondary branches), and the total number of branches (primary and secondary branches) for four greenhouse cumulative light levels (sunlight plus supplemental LED lighting). PPFD represents photosynthetic photon flux density, and the lines represent the regression equations for the primary (Y=119.7 + 0.04235*X; R^2 0.67), secondary (Y=-59.94 + 0.3647*X; R^2 0.84), and total branches per square meter (Y=59.72 + 0.407*X; R^2 0.85). In all cases, the p-values of the linear regression slopes were statistically significant (≤0.001). Dots, stars, and squares represent the means, and error bars represent standard errors for each light treatment group. In all cases, N=12, n=3, and OU=3 plants per plot.

The leaf photosynthetic rates (A) of plants grown under 18- and 52-DLI treatments increased even under 2000 µmol m^{-2} s^{-1}, but the increments in A with more PPFD were dimmed and only 6.2 ± 1.9% (mean ± SD) higher in 2000 than in 1600 µmol m^{-2} s^{-1} for both DLI treatments ($p<0.001$). As a reference, the average proportional increments in A (and PPFD) based on 2000 µmol m^{-2} s^{-1} were 14% (150), 30% (300), 51% (500), 66% (700), 79% (1000), 87% (1300), 94% (1600), and 100% (2000). Furthermore, small photosynthetic differences between DLI treatments were observed under low and high PPFDs; for instance, 52-DLI leaves exhibited higher photosynthetic rates when exposed to short-term PPFDs exceeding 1300 µmol m^{-2} s^{-1}, but photosynthesis was higher under 18-DLI leaves when PPFDs dropped below 500 µmol m^{-2} s^{-1} (Figure 6A). Additionally, leaves grown under 52 mol m^{-2} d^{-1} presented higher concentrations of photosynthetic (chlorophylls) and non-photosynthetic pigments (flavonols and anthocyanins) compared to 18 mol m^{-2} d^{-1} (Table 3).

Unlike photosynthesis, leaf transpiration (E) and stomatal conductance (g_{sw}) increased linearly with PPFD (Figures 6B, C). However, increments in stomatal and transpiration rates were not proportional to the light levels. For example, the transpiration rate per photon of light under 2000 µmol m^{-2} s^{-1} was 7.3 times lower than at 150 µmol m^{-2} s^{-1} or 2.9 vs 21.3 µmol H_2O µmol $photon^{-1}$, respectively. Furthermore, despite the raised g_{sw} and E with short-term increments in PPFD, there were no statistical differences by long-term light levels, 18 vs. 52 mol m^{-2} d^{-1} ($p \geq .29$; Figures 6B, C).

In concordance with the crop WUE, the leaf WUE of upper leaves, or A/E, increased up to a PPFD of 700 µmol m^{-2} s^{-1} ($p<0.001$); differences in WUE were not statistically significant from 700 to 2000 µmol m^{-2} s^{-1} ($\alpha=0.05$). Moreover, the main DLI effect (~18 vs. 52 mol m^{-2} s^{-1}) on leaf WUE or the interaction DLI*PPFD was not statistically significant ($\alpha=0.05$). Therefore, there was no evidence to support this study's second hypothesis: Leaves of cannabis plants cultivated under an elevated DLI would display higher WUE due to increased photosynthetic rates than their counterparts exposed to a lower DLI when leaves were evaluated under high PPFDs.

Discussion

Crop growth and development under greenhouse lighting and its effects on water use efficiency

Light effects and DLI recommendations on plant growth and production

The effects of light on plant growth can exhibit substantial variation across plant species, cultivars, developmental stages, and environmental factors, including plant nutrition, water availability, light intensity, and spectra. This variance stems from the diverse photosynthetic capacities inherent to different species, as well as the intricate interplay of multiple environmental factors (Boyer, 1970; Penning de Vries et al., 1989; Rosati and Dejong, 2003; Zhao et al., 2003; Weaver and Van Iersel, 2020). For instance, cultivating crops under identical DLI values but with lower light levels and extended photoperiods can lead to equivalent or even heightened daily growth. This is attributed to the enhanced efficiency of photosynthesis at both the leaf level (Weaver and Van Iersel, 2020) and the crop level (Hui et al., 2001). Furthermore, light wavelengths outside the Photosynthetically Active Radiation (PAR) range, 400 – 700 nm, can significantly influence growth and development. Far-red light (700 to 800 nm), for instance, promotes leaf expansion and photosynthesis in the 700-750 nm range (Zhen et al., 2021). In light of these findings, an extended PAR range (ePAR) from 400 to 750 nm has been proposed to account for photosynthesis enhancements (Zhen et al., 2021). Therefore, due to the complex interplay of these factors, comparing and adopting light levels across different situations is challenging and should ideally be confined to the specific conditions under evaluation. Nevertheless, for general reference, we provide a comparison with other cannabis studies, crops, and indoor systems employing the conventional DLI range (DLI 400-700nm) while offering the extended range values as a reference (Table 1).

Within the realm of cannabis cultivation, this study, as well as prior investigations employing exclusive LED lighting sources (Moher et al., 2021; Rodriguez-Morrison et al., 2021), provides compelling evidence to classify cannabis among the most elevated lighting requiring crops. For comparison, optimal lettuce production is associated with a maximum of 17 mol m^{-2} d^{-1} for marketable leaf growth, with higher light levels potentially leading to increased biomass but also an elevated risk of leaf tip burn

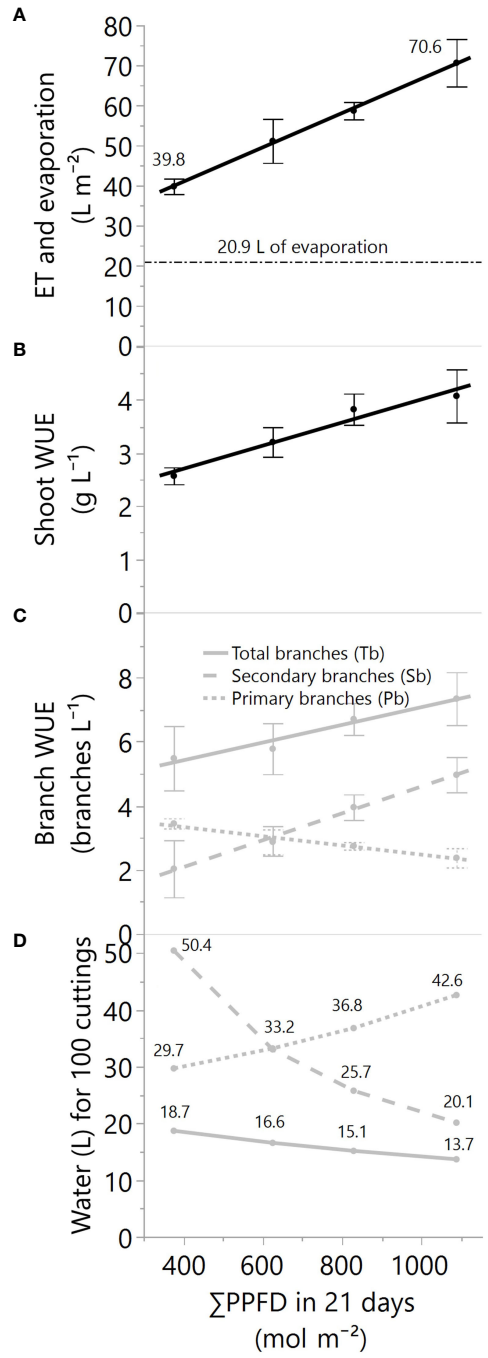

FIGURE 5
(A) The total evapotranspiration or ET (black solid line) and evaporation (black dashed line) in liters per square meter, **(B)** the plant-crop water use efficiency in grams of dry mass per liter of evapotranspired water, **(C)** the WUE for primary, secondary, and all branches, and **(D)** the water needs for 100 cuttings while increasing the greenhouse supplemental light levels. All values are for 21 days of greenhouse production, and PPFD represents photosynthetic photon flux density. For data in panels **(A–C)**, the linear regression fitting equations, R^2, and p-values of the equation slopes are **(A)** ET=23.79 + 0.0429*X, 0.77, p<.01, **(B)** plant WUE=1.83 + 0.0022*X, 0.58, p<.01, and **(C)** Tb-WUE=4.31 + 0.0028*X, 0.29, p=.06, Pb-WUE=3.91 -0.0014*X, 0.49, p=.01, Sb-WUE=0.41 + 0.0042*X, 0.62, p<.01. Dots and error bars represent the mean and standard errors for each light treatment group, respectively. In all cases, N=12, n=3, and OU=1-2 load-cell readings per plot for evapotranspiration and 3 plants per plot for biomass and branches.

(Both, 2002). High-light greenhouse crops like tomatoes and cucumbers require at least 30 mol m^{-2} d^{-1} for optimal yields and fruit quality (Dorais et al., 2017), although significant research into higher light levels may not have been pursued due to economic feasibility constraints for production (van Iersel and Gianino, 2017). In corn breeding, supplemental greenhouse lighting is recommended to reach up to 750 µmol m^{-2} s^{-1} or ≥38 mol m^{-2} d^{-1}, depending on the photoperiod, while corn research in chamber conditions employs as much as 1000 µmol m^{-2} s^{-1} or 58 mol m^{-2} d^{-1} (Eddy and Hahn, 2010). Remarkably, indoor farming studies have shown that cannabis crops can utilize 82 mol m^{-2} d^{-1} for shoot growth (Moher et al., 2021) and 78 mol m^{-2} d^{-1} for flower production (Rodriguez-Morrison et al., 2021).

Despite growth increments in the vegetative stage of cannabis under high light, the light-to-biomass conversions in Moher et al. (2021) were lower than in our study. For instance, the biomass yield in the Moher et al. (2021) study was 246 g m^{-2} with 52 mol m^{-2} d^{-1}, and it increased to 271 g m^{-2} with 82 mol m^{-2} d^{-1}. In contrast, our study yielded an average of 285 g m^{-2} with 52 mol m^{-2} d^{-1} (eDLI: 53; Table 1) and showed no indications of light saturation (Figure 2A); importantly, both studies shared a consistent 21-day timeframe, facilitating a valid DLI-based comparison. It is plausible that the improved greenhouse study result in our research could be attributed to differences in plant genetics (Vanhove et al., 2012; Suchoff et al., 2021), light spectra (Lalge et al., 2017; Zhen et al., 2021), temperature conditions (Chandra et al., 2008, 2011), and/or the effects of water and fertilizer supply. Nevertheless, it is evident that further research into cannabis cultivation and production conditions is necessary to gain a deeper understanding and achieve consistent maximum yields and product quality.

Light effects on LAI

In this investigation, plants were uniformly spaced at intervals of 30.5 cm, resulting in a plant density of 10.8 plants per square meter. In crop production, manipulating plant densities is a strategy to optimize yields and cost-efficiency by capitalizing on resource utilization and enhancing the efficacy of lighting, cooling, and heating per unit area. For instance, elevating plant density leads to an early expanded leaf canopy and improved light interception capacity. Moreover, an optimal leaf area is key to increasing crop photosynthesis and water use efficiency (Hui et al., 2001). However, an excessive plant density does not necessarily translate to increased yields, as seen in cannabis cultivation (Vanhove et al., 2012). The Leaf Area Index (LAI) assesses light interception and quantifies the total leaf area relative to the ground area (m^2 m^{-2}). Previous research across multiple plant species has consistently reported that an LAI in the range of 3 to 4 intercepts approximately 95% of the incident light, whereas an LAI of 2 captures roughly 80% (Shibles and Weber, 1965; De Visser et al., 2007; Brodrick et al., 2013; Tabarzad et al., 2016). Given that an LAI of 3 to 4 represents an optimal threshold for light capture, and values exceeding four may not confer any significant advantages in terms of light interception (De Visser et al., 2007; Brodrick et al., 2013; Tabarzad et al., 2016) and growth

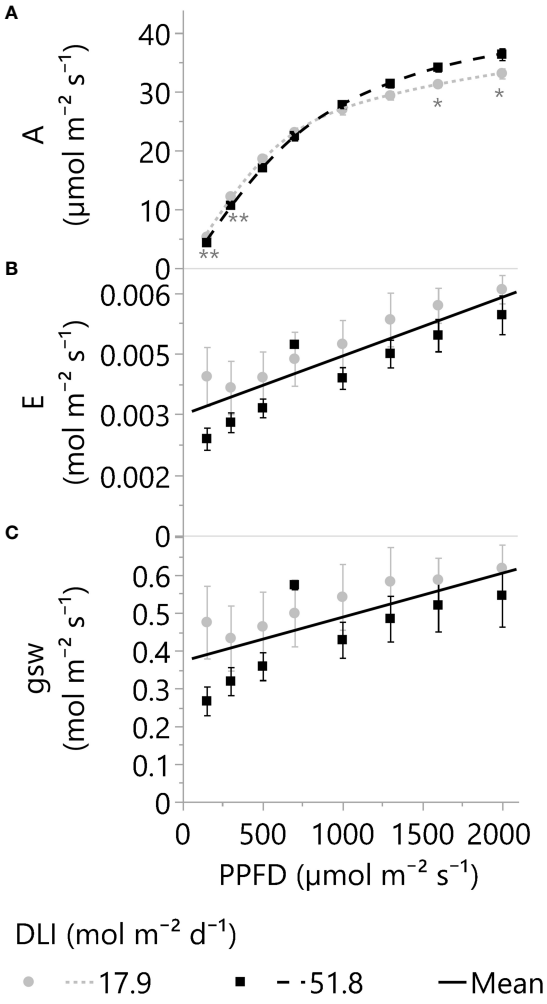

FIGURE 6
(A) Net photosynthetic rates or A, **(B)** transpiration rate or E, and **(C)** stomatal conductance or g_{sw} of leaves adapted to greenhouse DLI levels of ~18 or 52 mol m^{-2} d^{-1}. Young, fully expanded, and light-exposed leaves from both DLI treatments were evaluated at PPFDs of 150, 300, 500, 700, 1000, 1300, 1600, and 2000 µmol m^{-2} s^{-1} (Blue 18% and Red 82%) using a Li-6800 + 6800-01A. Asterisks indicate differences between the two DLI treatments at each PPFD level by one (*) or two (**) tailed T-tests (α 0.05). Split-plot analysis for E and g_{sw} (factors: DLI, PPFD, Time of the day, and DLI*PPFD) indicates differences only because of the PPFD ($p < 0.001$). The E and g_{sw} linear equations (solid lines) are $2.984e^{-3} + 1.45e^{-6}$*PPFD and $0.3715 + 1.16e^{-4}$*PPFD, respectively. Dots and squares represent the mean, and error bars represent the standard errors for each DLI-PPFD combination. In all cases, N=6, n=3, and OU=1 leaf per plot.

(Shibles and Weber, 1965), growers are likely to enhance production efficiency by adjusting plant spacing when the LAI surpasses four. Consequently, for a duration exceeding 21 days and high-light conditions like those presented in this study (leading to an LAI of 4.4), plant density could be reduced or branches trimmed while still maintaining a critical light interception of around 95%. Conversely, for crops subjected to lower light levels (Figures 1, 2B), pruning for harvesting cuttings or conducting formative pruning for flower production may have a negative impact on the LAI and plant growth.

Light effects on plant height and internode elongation

Responses of plant height in conjunction with internode extension are key to understanding whether the plant stretches mainly because of growth or to compete for more light, triggering shade avoidance syndrome or SAS (Kump, 2020).

In this study, the combination of light quantity and quality (Tables 1, 2), did not lead to significant changes in plant height across various light treatments (Figures 1, 3). Still, the light level and spectrum affect SAS responses (Kump, 2020), and perhaps they limited the observed differences in plant height in this study. For example, the lower light condition treatments may have contributed to some stem and internode extensions and vice versa. Furthermore, lower red to far-red ratios have increased stem length in several plant species (Demotes-Mainard et al., 2016). For example, in cucumber and lettuce, stem elongation was only significant when far-red light exceeded 9% at a DLI of 11.5 mol m^{-2} d^{-1}, while the effects were marginal under 29 mol m^{-2} d^{-1} (Kusuma and Bugbee, 2023). In the present cannabis study, the daily average far-red ranged from 8% to 3% across DLIs of 18 to 52 mol m^{-2} d^{-1}. Therefore, significant light spectrum effects would not be expected.

The overall findings and data suggest that the specific light conditions implemented (as outlined in Tables 1 and 2) had only a minor influence on plant height and internode length. These characteristics would be more substantially influenced by plant genetics and developmental factors than light intensity for cannabis.

Light effects on branching and development

Cannabis branches are fundamental in enhancing cutting production and supporting flowers. To assess the impact of light quantity on branch development, the total number of branches was measured and categorized into two groups: primary branches, which develop directly on the main stem, and secondary branches, which sprout from primary branches. The formation, dormancy, and outgrowth of buds that will give place to new stems, leaves, flowers, and branches are regulated by external and internal factors such as genetics, apical dominance, photoperiod, temperature, nutrition, and the amount and quality of the light, among others (Lortie and Aarssen, 1997; Cooke et al., 2012; Leduc et al., 2014). Among those factors, increasing the quantity of light plays a crucial role in reducing SAS responses like internode extension and axillary bud dormancy, while promoting bud outgrowth and overall growth in various species (Gommers et al., 2013; Leduc et al., 2014). Furthermore, the striking similarities in the main stem heights (Figure 3) and differences in primary and secondary branches (Figure 4) suggest that photochemical resources were strongly prioritized and influenced by the main apical meristem. The impact of this effect can be so pronounced that, in certain species or under specific growth conditions, the strong control of branching by the shoot apex may only cease upon removal (Lortie and Aarssen, 1997). Notably, in our study, cannabis branching proliferation was effectively achieved from ~18 to 52 mol m^{-2} d^{-1} (Figure 4) while maintaining a water and nutrient supply upon plant demand.

Light effects on crop water use and efficiency

The effects of increased supplemental lighting on water use and water use efficiency (WUE) were investigated to understand how water is used at a whole plant and production unit (cutting) in a 21-day production cycle. The primary increases in crop WUE observed in the present study are likely attributed to the pronounced benefits of enhanced photosynthesis at both leaf and crop levels, outweighing the potential drawbacks of increased transpiration under increasing lighting conditions. The increment in WUE at the crop level correlated with higher WUE at the leaf level, which is discussed later in this study. The findings of this study are corroborated by prior research conducted on greenhouse-grown sunflowers, wherein continuous measurements of crop photosynthesis and water use were undertaken under greenhouse solar conditions. In this previous study, it was observed that crop WUE throughout the day aligned closely with solar radiation levels, with peak values coinciding with the highest levels of solar radiation and photosynthesis (Hui et al., 2001).

Despite the correlations observed between branches and WUE (Figure 5C), it is imperative to note that the improvement in water efficiency is likely primarily attributable to impacts on photosynthesis and transpiration rather than the specific type of branches.

Crop water use and efficiency in cutting and flower production

Currently, there exists no standardized protocol for growers and researchers to systematically select the most optimal branch for propagating cuttings. Instead, cutting selection predominantly relies on individual preferences. In order to address the various potential scenarios, Figure 5D elucidates the relationship between branch selection and water usage under different light conditions. Based on these findings, on average, a nursery crop operating under conditions similar to those in this study is anticipated to require between 20 and 33 liters of water for every 100 cuttings, assuming that primary branches are mainly used to produce cuttings from secondary branches. Moreover, it's noteworthy that the water demand per cutting is projected to be higher under lower greenhouse lighting levels (<18 mol m^{-2} d^{-1}).

For flower producers, the shoot WUE results imply that to grow the same shoot biomass in 21 days, growers need 0.37 L g^{-1} under 18 mol m^{-2} d^{-1} of light and only 0.24 L g^{-1} under 52 mol m^{-2} d^{-1}, a 35% water reduction in evapotranspiration. Similar effects were found in a greenhouse hydroponic lettuce crop that transpired about 0.5 L g^{-1} under 8 mol m^{-2} d^{-1} and 0.27 L g^{-1} under 22 mol m^{-2} d^{-1}, a 46% water reduction in transpiration (Both, 2002).

Influence of greenhouse supplemental lighting on photosynthesis, stomatal conductance, transpiration in leaves, and their interconnection with Water Use Efficiency

Anatomical and physiological leaf characteristics change based on the prevailing light environment (Chabot and Chabot, 1977; Feng et al., 2019). Leaf photosynthesis (A), stomatal conductance to water vapor (g_{sw}), and transpiration (E) are integral to understanding growth and water usage and efficiency at the leaf level while helping elucidate the broader responses at the crop level.

Photosynthetic responses and significance

This study's results align with similar findings reported for cannabis cultivation under sole-source LED lighting, which exhibited stronger photosynthetic responses and DLI variations (Rodriguez-Morrison et al., 2021). Furthermore, higher leaf maximum-A capacities, as seen in this study and Rodriguez-Morrison et al. (2021), are expected under light augmentation due to increments in leaf weight per area (Penning de Vries et al., 1989). Thicker or denser leaves can produce more RuBisCO (Penning de Vries et al., 1989) and chlorophyll in the same area (Table 3), potentially increasing photosynthesis (Emerson, 1930). On the other hand, higher respiration rates, driven by the elevated biomass and metabolite levels per area (Table 3), may provide an explanation for the lower net photosynthetic rate observed in thicker leaves in cannabis research. In summary, our leaf photosynthetic rates results support the remarkable crop yield increments even at maximum greenhouse radiances of ~2000 µmol m^{-2} s^{-1} (Supplementary Figure S3B).

Stomatal and transpiration responses and regulation

In this study, the observed rise in E with increased light intensity was attributed to the increased stomatal conductance (g_{sw}). Typically, a higher g_{sw} is linked to either a reduction in leaf internal CO_2 concentration (Ci) or an enhancement in photosynthesis (A) through light supplementation (McAusland et al., 2016; Driesen et al., 2020). However, despite the linear increase in g_{sw} with light intensity, the responses of A and Ci did not parallel the stomatal conductance trend observed in our study (Figures 6C, A; Supplementary S4A).

The linear response in g_{sw} compared to the plateau response of A could be explained by additional mechanisms affected by light other than C_i reduction or photosynthesis enhancement. For instance, blue and red radiation is mentioned as direct influencers on guard-cell water status (Driesen et al., 2020), while shortwave radiation, encompassing most or all solar wavelengths, demonstrated an impact on leaf water status (Lawson et al., 2010; Pieruschka et al., 2010). Pieruschka et al. (2010) proposed a regulatory mechanism where the balance between radiation-driven water vapor production and transpiration rate governs stomatal conductance. Moreover, their observations found no specific wavelength effects, establishing only a linear correlation between stomatal conductance and absorbed radiation energy. Another factor affected by radiation is leaf temperature, a pivotal influence in stomatal conductance. Feller (2007) and Urban et al. (2017) demonstrated significant increments in stomatal aperture across temperatures ranging from ~20°C to over 40°C. Moreover, these increments persisted despite reductions in A and water potential and an increase in C_i (Urban et al., 2017). In the present cannabis study, results showed marginal leaf temperature differences (26.1 ± 0.17 to 26.9 ± 0.35°C) when elevating the PPFD from 150 to 2000 µmol m^{-2} s^{-1}

(Supplementary Figure S4B). In conclusion, light can affect photosynthesis and transpiration differently and may act on the stomatal aperture via various mechanisms.

High stomatal conductance and water loss at low radiation levels

Our study found considerably higher E and g_{sw} values per photon of light at lower PPFDs than at higher light intensities, as previously shown in the result section. Moreover, leaf transpiration at 150 µmol m^{-2} s^{-1} constituted a noteworthy 57% of the total water loss found under 2000 µmol m^{-2} s^{-1} (Figure 6B). This can be explained by reports across diverse species (Hui et al., 2001; de Dios et al., 2015; Dayer and Gambetta, 2021; Dayer et al., 2021) that suggest rapid and excessive increments in stomatal opening at low light or in the absence of light, which can increase water losses. Furthermore, data from different species, spanning ferns, gymnosperms, and angiosperms, also revealed that at very low light levels (50 µmol m^{-2} s^{-1}), stomatal conductance constituted between ~16% to 64% of the aperture at 1000 µmol m^{-2} s^{-1} (Deans et al., 2019). These results also align with increments above typical nighttime transpiration rates of 5% to 15% (Caird et al., 2007). Moreover, the observed rapid and predawn stomatal aperture increments have been associated with specific wavelengths (Lawson et al., 2010) and circadian regulation (de Dios et al., 2015; Dayer et al., 2021), while stomatal conductance did not correlate with photosynthesis at low light (Deans et al., 2019).

The benefits of enhancing supplemental lighting on leaf transpiration

In addition to increasing photosynthesis, enhancing supplemental lighting strongly reduced the water use per photon of light. These findings align with the broader context of light effects on stomatal conductance observed across various species (Deans et al., 2019), as previously discussed. Additionally, similar trends in crop transpiration have been documented in beans and cotton subjected to maximum PPFDs of 500 and 1500 µmol m^{-2} s^{-1}. Notably, nocturnal water losses constituted 23% and 12% of daytime requirements under lower and higher PPFDs, respectively (de Dios et al., 2015). These results suggest that optimizing lighting conditions can significantly mitigate the impact of both night-time and day-time water losses.

Stomatal slow response implications

Stomatal conductance and transpiration exhibited linear increases by increasing PPFD, as detailed earlier. However, the absence of statistical evidence for DLI effects between 18 and 52 mol m^{-2} d^{-1} was unexpected. It is plausible that the lack of statistical differences is linked to the substantial variability in transpiration and stomatal conductance due to the interaction of our procedure's sampling speed and stomatal acclimation periods (Lawson and Blatt, 2014; McAusland et al., 2016). Nevertheless, the information and results reviewed emphasize the complex interplay between direct and indirect light effects on guard cells, transpiration, and physiological dynamics, contributing to notable increases in gas exchange within the context of our research. Additionally, it is noteworthy that cannabis leaf temperatures remained similar to or below an air temperature of 27°C. This observation suggests that transpiration rates were sufficient to maintain optimal metabolic functions without the risk of overheating (Feller, 2007; Nelson and Bugbee, 2015). Our investigation revealed no physiological constraints on stomatal conductance and transpiration, even under the more demanding conditions of ~2000 µmol m^{-2} s^{-1} of actual greenhouse LED lighting and solar radiation (unshown data). This and previous research stress the robustness of optimal cannabis growth under high-light environments.

The impacts of short and long-term lighting exposure on leaf water use efficiency

The leaf WUE of upper cannabis leaves remarkably increased as a consequence of the curvilinear and linear responses observed for photosynthesis and transpiration (Figures 6A, B, and 7). Consistent with our findings, Deans et al. (2019) reported a substantial increase in intrinsic WUE (A/g_{sw}) under elevated lighting conditions across species, which was driven by a more pronounced increase in photosynthesis than stomatal conductance. In our study, there was weaker evidence indicating that the leaf WUE of the 52-DLI treatment might surpass that of the 18-DLI WUE under light levels of 1000 µmol m^{-2} s^{-1} or higher (p-values >0.05 to 0.09); however, at α 0.05, the statistical support was not robust enough to substantiate our hypothesis that leaves developed under the 52-DLI treatment exhibit higher WUE than leaves under the 18-DLI treatment.

In conclusion, the observed increase in crop WUE with higher lighting, consistent with other species, lighting conditions (Hui et al., 2001; Both, 2002; de Dios et al., 2015), and supported by increments in leaf WUE across various cannabis cultivars (unpublished data) and fifteen different species (Deans et al., 2019), suggests a potential for elevated WUE and yield in unstressed crops exposed to increased lighting conditions.

Spectral differences between treatments

In the current study, variations in light intensity among treatments were achieved through incremental adjustments in blue and red LED lighting, while similar solar radiation was maintained across treatments (Table 1). Consequently, this led to an augmentation in the proportion of blue and red wavelengths relative to other spectrums within the greenhouse solar spectrum. It is noteworthy that differences in the spectral composition of electrical lighting can significantly impact plant physiology, morphology, and growth in growth chambers (Spalholz et al., 2020) and under conditions of low sunlight, 3-5 mol m^{-2} d^{-1} (Hernández and Kubota, 2014; Collado and Hernández, 2022).

While prior research has demonstrated substantial effects of supplemental light spectrum variations under very low sunlight conditions, the impact diminished under higher solar DLIs, ~12-16 mol m^{-2} d^{-1}, in tomatoes and cucumbers (Hernández and Kubota, 2014; Kaiser et al., 2019). Furthermore, the influence of changing light quantity from 11.5 to 29 mol m^{-2} d^{-1} was more pronounced on the biomass of seven primary agricultural crops in growth chambers than alterations in light spectrum (blue, green, and red wavelength

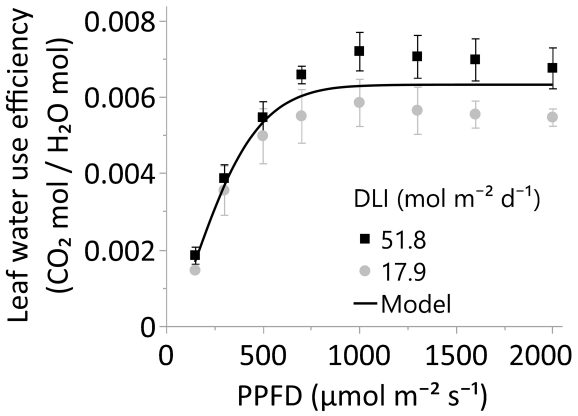

FIGURE 7
The leaf water use efficiency, or A/E, of leaves grown under greenhouse DLI levels of ~18 or 52 mol m^{-2} d^{-1}. Young, fully expanded, and light-exposed leaves from both DLI treatments were evaluated at PPFDs of 150, 300, 500, 700, 1000, 1300, 1600, and 2000 µmol m^{-2} s^{-1} (Blue 18% and Red 82%) using a Li-6800 + 6800-01A. Comparison between DLI treatments at each PPFD level was performed by T-test. Differences between the two DLI levels were not statistically significant (α 0.05). The solid line represents the three-parameter model =0.0063*(1-$e^{-(PPFD/330.76)}$ ^1.49). Equation decay parameters were not different from zero using the JMP Pro 17.0 four-parameter models. In all cases, N=6, n=3, and OU=1 leaf per plot.

ranges: 10.8-27.5%, 1.7-48.0%, and 24.5-86.3%, respectively; a phytochrome photo-equilibrium (PPE) range: 0.83-0.89; Snowden et al., 2016). Similarly, the impact of increasing DLI from 8.7 to 19.7 mol m^{-2} d^{-1} outweighed the effects of modifying the blue and red light ratios in cucumbers (Hernández and Kubota, 2014). In our cannabis research, light exposure ranged from 17.9 to 51.8 mol m^{-2} d^{-1}, while spectrum and PPE ranges (Table 2) were similar to those discussed.

In summary, this experiment does not provide evidence to suggest that spectral differences between treatments significantly influenced plant responses under greenhouse supplemental lighting conditions. Instead, the variations in plant responses can be primarily attributed to the differences in total Photosynthetic Photon Flux Density (∑PPFD). Overall, these findings imply that the effects of light spectrum variations may be relatively smaller, especially in the presence of a complete light spectrum, such as solar radiation.

Conclusions

Enhancing supplemental lighting promoted increased photosynthesis and played a pivotal role in shaping the water use dynamics in cannabis leaves and crops. Most importantly, it could potentially enhance the WUE of most crops while promoting growth. Our findings emphasize the capacity of lighting management to optimize water use efficiency while presenting valuable implications for both research and practical applications in agriculture.

For instance, stakeholders in cannabis nurseries, flower production, and research settings can substantially improve plant growth, yield, and water use efficiency by incorporating supplemental lighting. Specifically, our study indicates a linear growth response within the range of ~18 to 52 mol m^{-2} d^{-1}, suggesting that DLIs exceeding 52 mol m^{-2} d^{-1} could further enhance cuttings and plant growth and surpass existing literature expectations. It is crucial to highlight that these results and expectations are based on meticulous control of water, nutrients, and other growth factors and genetics. In this study, *Cannabis sativa* cv Suver Haze was employed and represents an average-performing cultivar (Suchoff et al., 2021), suggesting that genetic variability may increase or decrease the number of branches and overall plant growth per mole of light.

This study demonstrated notable increases in leaf and crop WUE with elevated light levels while enhancing CO_2 assimilation. Historically, improving WUE without compromising production has been challenging, particularly considering the dependence of photosynthesis on stomata (Lawson and Blatt, 2014; Xing et al., 2022). Furthermore, studies on CO_2 enrichment (Hui et al., 2001) and elevated atmospheric CO_2 (Guerrieri et al., 2019) have also reported improvements in WUE; in alignment with the findings on light supplementation, the enhanced photosynthesis was found to be the main contributing factor. Ultimately, there is evidence showing that the combination of light and CO_2 enrichment can lead to even greater enhancements in water use efficiencies (Hui et al., 2001).

Data availability statement

The raw data supporting the conclusions of this article will be made available by the authors, without undue reservation.

Author contributions

CC: Conceptualization, Data curation, Formal analysis, Investigation, Methodology, Resources, Validation, Visualization, Writing – original draft, Writing – review & editing. SH: Investigation, Methodology, Writing – review & editing. RH: Conceptualization, Data curation, Funding acquisition, Methodology, Project administration, Resources, Supervision, Validation, Visualization, Writing – review & editing.

Funding

The author(s) declare financial support was received for the research, authorship, and/or publication of this article. This research was funded by the Foundation for Food and Agricultural Research (FFAR) grant number [NexGenHemp0000000016]. Gyengsang National University Fund for Professors on Sabbatical Leave, 2020.

Acknowledgments

The authors would like to thank the company CURRENT Horticultural Lighting (Greenville, SC, US) for providing partial funding and LED fixtures. The company was not involved in the study design, collection, analysis, interpretation of data, the writing of

this article, or the decision to submit it for publication. The Authors would like to thank Ryan Patterson from Ryes Greenhouses LLC (Broadway, NC) for providing initial rooted-plug material. The authors would like to thank Bartlett-Golden A., Huber B., Hwang S.J., McLamb S., Shi X., Stanek C., Thompson S.P., and Watson M. for their support during the study. ChatGPT 3.5 was used for language editing.

Conflict of interest

The authors declare that the research was conducted in the absence of any commercial or financial relationships that could be construed as a potential conflict of interest.

Publisher's note

Supplementary material

The Supplementary Material for this article can be found online at: https://www.frontiersin.org/articles/10.3389/fpls.2024.1371702/full#supplementary-material

References

Both, A. J. (2002) *Ten years of hydroponic lettuce research*. Available online at: www.researchgate.net/publication/266453402_ten_years_of_hydroponic_lettuce_research (Accessed January 7, 2024).

Boyer, J. S. (1970). Differing sensitivity of photosynthesis to low leaf water potentials in corn and soybean. *Plant Physiol.* 46, 236–239. doi: 10.1104/pp.46.2.236

Brodrick, R., Bange, M. P., Milroy, S. P., and Hammer, G. L. (2013). Physiological determinants of high yielding ultra-narrow row cotton: Canopy development and radiation use efficiency. *Field Crops Res.* 148, 86–94. doi: 10.1016/j.fcr.2012.05.008

Caird, M. A., Richards, J. H., and Donovan, L. A. (2007). Nighttime stomatal conductance and transpiration in C3 and C4 plants. *Plant Physiol.* 143, 4–10. doi: 10.1104/pp.106.092940

Chabot, B. F., and Chabot, J. F. (1977). Effects of light and temperature on leaf anatomy and photosynthesis in Fragaria vesca. *Oecologia* 26, 363–377. doi: 10.1007/BF00345535

Chandra, S., Lata, H., Khan, I. A., and Elsohly, M. A. (2008). Photosynthetic response of *Cannabis sativa* L. @ to variations in photosynthetic photon flux densities, temperature and CO2 conditions. *Physiol. Mol. Biol. Plants* 14, 299–306. doi: 10.1007/s12298-008-0027-x

Chandra, S., Lata, H., Khan, I. A., and Elsohly, M. A. (2011). Temperature response of photosynthesis in different drug and fiber varieties of *Cannabis sativa* L. *Physiol. Mol. Biol. Plants* 17, 297–303. doi: 10.1007/s12298-011-0068-4

Collado, C. E., and Hernández, R. (2022). Effects of light intensity, spectral composition, and paclobutrazol on the morphology, physiology, and growth of petunia, geranium, pansy, and dianthus ornamental transplants. *J. Plant Growth Regul.* 41, 461–478. doi: 10.1007/s00344-021-10306-5

Conway, J. (2023) *Number of cannabis cultivation licenses in the United States in 2022, by state* (Statista). Available online at: https://www.statista.com/statistics/1108194/cannabis-cultivation-licenses-by-state-us/ (Accessed January 7, 2024).

Cooke, J. E. K., Eriksson, M. E., and Junttila, O. (2012). Dynamic nature of bud dormancy in trees: environmental control and molecular mechanisms. *Plant Cell Environ.* 35, 1707–1728. doi: 10.1111/j.1365-3040.2012.02552.x

David Potter, J. P. (2009) (London, UK: King's College). Available online at: https://archive.org/details/cannabissativaasaphytopharmaceutical (Accessed January 7, 2024).

Dayer, S., and Gambetta, G. A. (2021). Nighttime transpiration: does it contribute to water stress in grape?: Sourced from the research article "Nighttime transpiration represents a negligible part of water loss and does not increase the risk of water stress in grapevine". *Plant Cell Environ.* doi: 10.1111/pce.13923

Dayer, S., Herrera, J. C., Dai, Z., Burlett, R., Lamarque, L. J., Delzon, S., et al. (2021). Nighttime transpiration represents a negligible part of water loss and does not increase the risk of water stress in grapevine. *Plant Cell Environ.* 44, 387–398. doi: 10.1111/pce.13923

Deans, R. M., Brodribb, T. J., Busch, F. A., and Farquhar, G. D. (2019). Plant water-use strategy mediates stomatal effects on the light induction of photosynthesis. *New Phytol.* 222, 382–395. doi: 10.1111/nph.15572

DeCarcer, G. A., Kagia, J., Morrissey, K., McCann, M., Tomares, N., Alvarado, I., et al. (2021) *The global cannabis report growth & Trends through 2025* (New Frontier Data). Available online at: https://newfrontierdata.com/product/the-global-cannabis-report-2021/ (Accessed January 7, 2024).

de Dios, V. R., Roy, J., Ferrio, J. P., Alday, J. G., Landais, D., Milcu, A., et al. (2015). Processes driving nocturnal transpiration and implications for estimating land evapotranspiration. *Sci. Rep.* 5, 10975. doi: 10.1038/srep10975

Demotes-Mainard, S., Péron, T., Corot, A., Bertheloot, J., Le Gourrierec, J., Pelleschi-Travier, S., et al. (2016). Plant responses to red and far-red lights, applications in horticulture. *Environ. Exp. Bot.* 121, 4–21. doi: 10.1016/j.envexpbot.2015.05.010

De Visser, P., van der Heijden, G., and Heuvelink, E. (2007) *3D Modelling of growth and ornamental quality of chrysanthemum at different plant densities*. Available online at: https://www.researchgate.net/publication/40101200_3D_Modelling_of_growth_and_ornamental_quality_of_chrysanthemum_at_different_plant_densities (Accessed January 7, 2024).

Dieter, C. A., Maupin, M. A., Caldwell, R. R., Harris, M. A., Ivahnenko, T. I., Lovelace, J. K., et al. (2018). Estimated use of water in the United States in 2015. *U.S. Geological Survey* 6–8. doi: 10.3133/cir1441

Dorais, M., Mitchell, C. A., and Kubota, C. (2017). ""Lighting greenhouse fruiting vegetables,"," in *Light management in controlled environments*. Eds. R. Lopez and E. S. Runkle (Meister Media Worldwide, Willoughby, OH: Meister Media: Willoughby), 159–169, ISBN: .

Driesen, E., Van Den Ende, W., De Proft, M., and Saeys, W. (2020). Influence of environmental factors light, CO2, temperature, and relative humidity on stomatal opening and development: A review. *Agronomy* 10, 1975. doi: 10.3390/agronomy10121975

Eddy, R., and Hahn, D. T. (2010). Optimizing greenhouse corn production: what is the best lighting and plant density? *Purdue Methods Corn Growth* 13.

Emerson, R. (1930). The chlorophyll factor in photosynthesis. *Am. Nat.* 64, 252–260. doi: 10.1086/280314

Feller, U. (2007). Stomatal opening at elevated temperature: an underestimated regulatory mechanism? *Gen. Appl. Plant Physiol.* 32, 19–31. doi: 10.7892/boris.53995

Feng, L., Raza, M. A., Li, Z., Chen, Y., Khalid, M. H. B., Du, J., et al. (2019). The influence of light intensity and leaf movement on photosynthesis characteristics and carbon balance of soybean. *Front. Plant Sci.* 9. doi: 10.3389/fpls.2018.01952

GAO (2014) *Freshwater: supply concerns continue, and uncertainties complicate planning* (US Government Accountability Office). Available online at: https://www.gao.gov/assets/gao-14-430.pdf (Accessed January 7, 2024).

Gommers, C. M. M., Visser, E. J. W., Onge, K. R. S., Voesenek, L. A. C. J., and Pierik, R. (2013). Shade tolerance: when growing tall is not an option. *Trends Plant Sci.* 18, 65–71. doi: 10.1016/j.tplants.2012.09.008

Guerrieri, R., Belmecheri, S., Ollinger, S. V., Asbjornsen, H., Jennings, K., Xiao, J., et al. (2019). Disentangling the role of photosynthesis and stomatal conductance on rising forest water-use efficiency. *Proc. Natl. Acad. Sci. U.S.A.* 116, 16909–16914. doi: 10.1073/pnas.1905912116

Hatfield, J. L., and Dold, C. (2019). Water-use efficiency: advances and challenges in a changing climate. *Front. Plant Sci.* 10. doi: 10.3389/fpls.2019.00103

Hernández, R., and Kubota, C. (2014). Growth and morphological response of cucumber seedlings to supplemental red and blue photon flux ratios under varied solar daily light integrals. *Scientia Hortic.* 173, 92–99. doi: 10.1016/j.scienta.2014.04.035

Hubick, K., and Farquhar, G. (1989). Carbon isotope discrimination and the ratio of carbon gained to water lost in barley cultivars. *Plant Cell Environ.* 12, 795–804. doi: 10.1111/j.1365-3040.1989.tb01641.x

Hui, D., Luo, Y., Cheng, W., Coleman, J. S., Johnson, D. W., and Sims, D. A. (2001). Canopy radiation- and water-use efficiencies as affected by elevated [CO2]: Canopy Radiation- And Water-Use Efficiencies. *Global Change Biol.* 7, 75–91. doi: 10.1046/j.1365-2486.2001.00391.x

Idris, A., Linatoc, A. C., and Bakar, M. F. B. A. (2019). Effect of light intensity on the photosynthesis and stomatal density of selected plant species of gunung ledang, johor. Malays. *Appl. Biol.* 48, 133–140.

Jackson, P., Basnayake, J., Inman-Bamber, G., Lakshmanan, P., Natarajan, S., and Stokes, C. (2016). Genetic variation in transpiration efficiency and relationships between whole plant and leaf gas exchange measurements in *Saccharum* spp. and related germplasm. *EXBOTJ* 67, 861–871. doi: 10.1093/jxb/erv505

Kaiser, E., Ouzounis, T., Giday, H., Schipper, R., Heuvelink, E., and Marcelis, L. F. M. (2019). Adding blue to red supplemental light increases biomass and yield of greenhouse-grown tomatoes, but only to an optimum. *Front. Plant Sci.* 9. doi: 10.3389/fpls.2018.02002

Kump, B. (2020). The role of far-red light (FR) in photomorphogenesis and its use in greenhouse plant production. *Acta Agric. Slovenica* 116, 93–105. doi: 10.14720/aas.2020.116.1.1652

Kusuma, P., and Bugbee, B. (2023). On the contrasting morphological response to far-red at high and low photon fluxes. *Front. Plant Sci.* 14. doi: 10.3389/fpls.2023.1185622

Lalge, A., Cerny, P., Trojan, V., and Vyhnanek, T. (2017). The effects of red, blue and white light on the growth and development of *Cannabis sativa* L. *MendelNet* 24, 646–651.

Lawson, T., and Blatt, M. R. (2014). Stomatal size, speed, and responsiveness impact on photosynthesis and water use efficiency. *Plant Physiol.* 164, 1556–1570. doi: 10.1104/pp.114.237107

Lawson, T., Von Caemmerer, S., and Baroli, I. (2010). ""Photosynthesis and stomatal behaviour,"," in *Progress in botany*, vol. 72 . Eds. U. E. Lüttge, W. Beyschlag, B. Büdel and D. Francis (Springer Berlin Heidelberg, Berlin, Heidelberg), 265–304. doi: 10.1007/978-3-642-13145-5_11

Lazic, S. E., Clarke-Williams, C. J., and Munafò, M. R. (2018). What exactly is 'N' in cell culture and animal experiments? *PloS Biol.* 16, e2005282. doi: 10.1371/journal.pbio.2005282

Leduc, N., Roman, H., Barbier, F., Péron, T., Huché-Thélier, L., Lothier, J., et al. (2014). Light signaling in bud outgrowth and branching in plants. *Plants* 3, 223–250. doi: 10.3390/plants3020223

Lortie, C. J., and Aarssen, L. W. (1997). Apical dominance as an adaptation in Verbascum thapsus: effects of water and nutrients on branching. *Int. J. Plant Sci.* 158, 461–464. doi: 10.1086/297456

McAusland, L., Vialet-Chabrand, S., Davey, P., Baker, N. R., Brendel, O., and Lawson, T. (2016). Effects of kinetics of light-induced stomatal responses on photosynthesis and water-use efficiency. *New Phytol.* 211, 1209–1220. doi: 10.1111/nph.14000

Moher, M., Llewellyn, D., Jones, M., and Zheng, Y. (2021). High light intensities can be used to grow healthy and robust cannabis plants during the vegetative stage of indoor production. 1–12. doi: 10.20944/preprints202104.0417.v1

Nelson, J. A., and Bugbee, B. (2015). Analysis of environmental effects on leaf temperature under sunlight, high pressure sodium and light emitting diodes. *PloS One* 10, e0138930. doi: 10.1371/journal.pone.0138930

Penning de Vries, F. W. T., Jansen, D. M., ten Berge, H. F. M., and Bakema, A. (1989) *Simulation of ecophysiological processes of growth in several annual crops* (Pudoc: Wageningen). Available online at: https://edepot.wur.nl/108856 (Accessed January 7, 2024).

Pieruschka, R., Huber, G., and Berry, J. A. (2010). Control of transpiration by radiation. *Proc. Natl. Acad. Sci. U.S.A.* 107, 13372–13377. doi: 10.1073/pnas.0913177107

Pokorny, J. (2019). ""Evapotranspiration,"," in *Encyclopedia of ecology* (Elsevier), 292–303. doi: 10.1016/B978-0-12-409548-9.11182-0

Rodriguez-Morrison, V., Llewellyn, D., and Zheng, Y. (2021). Cannabis yield, potency, and leaf photosynthesis respond differently to increasing light levels in an indoor environment. *Front. Plant Sci.* 12. doi: 10.3389/fpls.2021.646020

Rosati, A., and Dejong, T. M. (2003). Estimating photosynthetic radiation use efficiency using incident light and photosynthesis of individual leaves. *Annals of Botany* 91, 7, 869–877. doi: 10.1093/aob/mcg094

Sager, J. C., Smith, W. O., Edwards, J. L., and Cyr, K. L. (1988). Photosynthetic efficiency and phytochrome photoequilibria determination using spectral data. *Trans. ASAE* 31, 1882–1889. doi: 10.13031/2013.30952

Shibles, R. M., and Weber, C. R. (1965). Leaf area, solar radiation interception and dry matter production by soybeans. *Crop Sci.* 5, 575–577. doi: 10.2135/cropsci1965.0011183X000500060027x

Snowden, M. C., Cope, K. R., and Bugbee, B. (2016). Sensitivity of seven diverse species to blue and green light: interactions with photon flux. *PloS One* 11, e0163121. doi: 10.1371/journal.pone.0163121

Spalholz, H., Perkins-Veazie, P., and Hernández, R. (2020). Impact of sun-simulated white light and varied blue:red spectrums on the growth, morphology, development, and phytochemical content of green- and red-leaf lettuce at different growth stages. *Scientia Hortic.* 264, 109195. doi: 10.1016/j.scienta.2020.109195

Suchoff, D., Bloomquist, M., Davis, J., Henriquez Inoa, S., and Learn, K. (2021) *NC state floral hemp variety trial* (North Carolina Extension). Available online at: https://hemp.ces.ncsu.edu/wp-content/uploads/2021/11/2021-NC-State-Variety-Trial-Report.pdf?fwd=no (Accessed January 7, 2024).

Tabarzad, A., Ghaemi, A. A., and Zand-Parsa, S. (2016). Extinction coefficients and radiation use efficiency of barley under different irrigation regimes and sowing dates. *Agric. Water Manage.* 178, 126–136. doi: 10.1016/j.agwat.2016.09.020

Urban, J., Ingwers, M. W., McGuire, M. A., and Teskey, R. O. (2017). Increase in leaf temperature opens stomata and decouples net photosynthesis from stomatal conductance in Pinus taeda and Populus deltoides x nigra. *J. Exp. Bot.* 68, 1757–1767. doi: 10.1093/jxb/erx052

Vanhove, W., Surmont, T., Van Damme, P., and De Ruyver, B. (2012). Yield and turnover of illicit indoor cannabis (Cannabis spp.) plantations in Belgium. *Forensic Sci. Int.* 220, 265–270. doi: 10.1016/j.forsciint.2012.03.013

van Iersel, M. W., and Gianino, D. (2017). An adaptive control approach for light-emitting diode lights can reduce the energy costs of supplemental lighting in greenhouses. *HortScience* 52, 72–77. doi: 10.21273/HORTSCI11385-16

Vezdos, T., and Martinez, R. (2021) *2021 state of the cannabis cultivation industry report* (Cannabis Business Times). Available online at: https://www.cannabisbusinesstimes.com/article/special-report-2021-state-of-the-cannabis-cultivation-industry-report/ (Accessed January 7, 2024).

Weaver, G., and Van Iersel, M. W. (2020). Longer photoperiods with adaptive lighting control can improve growth of greenhouse-grown 'Little gem' Lettuce (Lactuca sativa). *HortsScience* 55, 573–580. doi: 10.21273/HORTSCI14721-19

Whitehead, D. (1998). Regulation of stomatal conductance and transpiration in forest canopies. *Tree Physiol.* 18, 633–644. doi: 10.1093/treephys/18.8-9.633

Xing, D., Mao, R., Li, Z., Wu, Y., Qin, X., and Fu, W. (2022). Leaf intracellular water transport rate based on physiological impedance: A possible role of leaf internal retained water in photosynthesis and growth of tomatoes. *Front. Plant Sci.* 13. doi: 10.3389/fpls.2022.845628

Zhao, D., Raja Reddy, K., Kakani, V. G., Read, J. J., and Carter, G. A. (2003). Corn (Zea mays L.) growth, leaf pigment concentration, photosynthesis and leaf hyperspectral reflectance properties as affected by nitrogen supply. *Plant Soil* 257, 205–218. doi: 10.1023/A:1026233732507

Zhen, S., and Bugbee, B. (2020). Steady-state stomatal responses of C_3 AND C_4 species to blue light fraction: Interactions with CO_2 concentration. *Plant Cell Environ.* 43, 3020–3032. doi: 10.1111/pce.13888

Zhen, S., Van Iersel, M., and Bugbee, B. (2021). Why far-red photons should be included in the definition of photosynthetic photons and the measurement of horticultural fixture efficacy. *Front. Plant Sci.* 12. doi: 10.3389/fpls.2021.693445

frontiers | Frontiers in Plant Science

TYPE Original Research
PUBLISHED 18 June 2024
DOI 10.3389/fpls.2024.1393803

OPEN ACCESS

EDITED BY
Lorenzo Barbanti,
University of Bologna, Italy

REVIEWED BY
Bruce Bugbee,
Utah State University, United States
Sasan Aliniaeifard,
University of Tehran, Iran

*CORRESPONDENCE
Mexximiliaan M. S. F. Holweg
mexx.holweg@wur.nl
Leo F. M. Marcelis
leo.marcelis@wur.nl

RECEIVED 29 February 2024
ACCEPTED 20 May 2024
PUBLISHED 18 June 2024

CITATION
Holweg MMSF, Kaiser E, Kappers IF, Heuvelink E and Marcelis LFM (2024) The role of red and white light in optimizing growth and accumulation of plant specialized metabolites at two light intensities in medical cannabis (*Cannabis sativa* L.).
Front. Plant Sci. 15:1393803.
doi: 10.3389/fpls.2024.1393803

The role of red and white light in optimizing growth and accumulation of plant specialized metabolites at two light intensities in medical cannabis (*Cannabis sativa* L.)

Mexximiliaan M. S. F. Holweg[1]*, Elias Kaiser[1], Iris F. Kappers[2], Ep Heuvelink[1] and Leo F. M. Marcelis[1]*

[1]Horticulture and Product Physiology, Wageningen University, Wageningen, Netherlands, [2]Laboratory of Plant Physiology, Wageningen University, Wageningen, Netherlands

The cultivation of medical cannabis (*Cannabis sativa* L.) is expanding in controlled environments, driven by evolving governmental regulations for healthcare supply. Increasing inflorescence weight and plant specialized metabolite (PSM) concentrations is critical, alongside maintaining product consistency. Medical cannabis is grown under different spectra and photosynthetic photon flux densities (PPFD), the interaction between spectrum and PPFD on inflorescence weight and PSM attracts attention by both industrialists and scientists. Plants were grown in climate-controlled rooms without solar light, where four spectra were applied: two low-white spectra (7B-20G-73R/Narrow and 6B-19G-75R/2Peaks), and two high-white (15B-42G-43R/Narrow and 17B-40G-43R/Broad) spectra. The low-white spectra differed in red wavelength peaks (100% 660 nm, versus 50:50% of 640:660 nm), the high-white spectra differed in spectrum broadness. All four spectra were applied at 600 and 1200 µmol m^{-2} s^{-1}. Irrespective of PPFD, white light with a dual red peak of 640 and 660 nm (6B-19G-75R/2Peaks) increased inflorescence weight, compared to white light with a single red peak of 660 nm (7B-20G-73R/Narrow) (tested at P = 0.1); this was associated with higher total plant dry matter production and a more open plant architecture, which likely enhanced light capture. At high PPFD, increasing white fraction and spectrum broadness (17B-40G-43R/Broad) produced similar inflorescence weights compared to white light with a dual red peak of 640 and 660 nm (6B-19G-75R/2Peaks). This was caused by an increase of both plant dry matter production and dry matter partitioning to the inflorescences. No spectrum or PPFD effects on cannabinoid concentrations were observed, although at high PPFD white light with a dual red peak of 640 and 660 nm (6B-19G-75R/2Peaks) increased terpenoid concentrations compared to the other spectra. At low PPFD, the combination of white light with 640 and 660 nm increased photosynthetic efficiency compared with white light with a single red peak of 660nm, indicating potential benefits in light use efficiency and

promoting plant dry matter production. These results indicate that the interaction between spectrum and PPFD influences plant dry matter production. Dividing the light energy in the red waveband over both 640 and 660 nm equally shows potential in enhancing photosynthesis and plant dry matter production.

KEYWORDS

medical cannabis, *Cannabis sativa* L., light spectrum, light intensity, photosynthetic photon flux density, plant specialized metabolites, morphology, photosynthesis

Introduction

Medical cannabis (*Cannabis sativa* L.) has gained prominence in both the horticultural and pharmaceutical industries due to its pharmacologically active compounds, notably cannabinoids and terpenoids (Karst et al., 2003; Andre et al., 2016; McPartland, 2018). These plant specialized metabolites (PSM) are primarily localized in the glandular trichomes on female inflorescences (Livingston et al., 2020). Medical cannabis is predominantly prescription-based and is endorsed for a variety of medical conditions including chronic neuropathic pain, nausea, vomiting, spasticity associated with multiple sclerosis, anorexia in cancer or HIV/AIDS patients, and symptoms of Tourette's syndrome (De Hoop et al., 2018). While terpenoids possess medicinal attributes, they are primarily noted for their contributions to the aroma and flavor profiles of medical cannabis (Booth and Bohlmann, 2019; Sommano et al., 2020). The cannabinoids serve as the basis for classifying medical cannabis varieties into five distinct chemotypes, determined by the ratio of their dominant cannabinoids, Delta-9-Tetrahydrocannabinol (THC) to Cannabidiol (CBD) (Aizpurua-Olaizola et al., 2016).

Controlled conditions are essential for maintaining consistent production in medical cannabis, in terms of inflorescence yield and PSM concentrations. Considering that unprocessed inflorescences are directly administered to patients, it is of critical importance to achieve uniform PSM concentrations and consistent pharmacological effects (Hazekamp et al., 2006; Kowal et al., 2016). Cultivation in controlled environment conditions without solar light demands substantial energy inputs, particularly for lighting (Zobayed et al., 2005; Mehboob et al., 2020). The expansion of medical cannabis industries globally underscores the necessity for energy-efficient lighting systems (Hall et al., 2019). A transition is occurring from conventional lighting systems, such as fluorescent and high-intensity discharge lamps, to more energy-efficient light-emitting diode (LED) technology (Mitchell et al., 2015; Pattison et al., 2018; Kusuma et al., 2020). LED technology offers benefits such as enhanced energy efficacy, lifespan, and spectrum customization, while maintaining high photosynthetic photon flux densities (PPFD) with reduced heat emission, thus enabling effective manipulation of light to influence plant dry matter production and development (Morrow, 2008; Burgie et al., 2014; Galvão and Fankhauser, 2015; Ouzounis et al., 2015; Krahmer et al., 2018).

Light spectrum affects plant dry matter production and metabolic processes, through photoreceptors including phytochromes, cryptochromes, phototropins, and UVR8 (Folta & Carvalho, 2015; Ouzounis et al., 2015; Pocock, 2015; Thoma et al., 2020), as well as through its effects on net photosynthesis rate (*A*; e.g. McCree, 1971; Hogewoning et al., 2012). Most studies focused on evaluating the individual effects of either spectrum or PPFD on inflorescence weight and PSM concentrations (Magagnini et al., 2018; Eaves et al., 2020; Llewellyn et al., 2021; Rodriguez-Morrison et al., 2021; Danziger and Bernstein, 2021a; Islam et al., 2022). However, there is a growing recognition, observed in other plant species, that spectrum and PPFD interactively influence plant dry matter production and PSM concentrations (Cope & Bugbee, 2013; Ouzounis et al., 2015; Snowden et al., 2016; Eichhorn Bilodeau et al., 2019). LED lighting systems were primarily characterized by peak wavelengths around 660 nm, as these were the first LEDs with adequate output for plant dry matter production (Bula et al., 1991; Morrow, 2008). The peak wavelength of 660 nm closely corresponds with the maximum absorption wavelength of Chlorophyll *a* (Chl *a*; 663 nm), and as Chl *a* is the predominant pigment in the reaction centers of both photosystem II (PSII) and photosystem I (PSI), this alignment has justified the mass production and adoption of 660 nm LEDs in horticulture since 1991 (Tamulaitis et al., 2005; Caffarri et al., 2011; Zhao et al., 2017; Pan et al., 2018; Bula et al., 1991). Exploiting the local absorption peak of Chlorophyll *b* (Chl *b*; 642 nm) could enhance light use efficiency and light absorption further, as Chl *b* is essential in preventing photoinhibition and improving energy transfer between the light-harvesting- and photosystem core complexes (Voitsekhovskaja and Tyutereva, 2015). This is particularly relevant as the highest luminous efficiency in the red region occurs at 640 nm, and aligns with the region of the highest photosynthetic quantum yield, which spans from 600 to 660 nm (McCree, 1971; Inada, 1976; Evans, 1987; Tamulaitis et al., 2005; Hogewoning et al., 2012). Wollaeger and Runkle (2013) investigated the effects of combinations of two wavelengths within the red waveband (634 and 664 nm), with the addition of 10% blue (446

nm) and 10% green (516 nm), on various crops grown at PPFD of 125 and 250 µmol m^{-2} s^{-1}. Their findings indicated limited morphological differences under these conditions. However, it is important to note that medical cannabis, which is often cultivated at significantly higher PPFD, may respond differently.

The spectrum of LED, particularly the red-to-blue ratio, varies in horticultural applications and is crucial for plant dry matter production and development (Kim et al., 2004; Piovene et al., 2015). Red photons are generally more efficient in driving *A*, as they are less strongly absorbed by non-photosynthetic pigments compared to blue and green photons (Emerson and Lewis, 1943; McCree, 1971; Inada, 1976; Farquhar et al., 1980; Evans, 1987). Also, exposure to high PPFD can lead to overexcitation of the photosystems, potentially causing photoinhibition (Miao et al., 2016; Oguchi et al., 2021). Furthermore, overexcitation of pigments, notably under low-white spectra, has been suggested to be associated with the appearance of bleached inflorescences—a loss of pigmentation in the apical inflorescence that adversely impacts marketability (Hawley, 2023). Incorporating a higher white fraction, resulting in a more balanced red-to-blue ratio and increased green fraction, may reduce the risk of photoinhibition within the palisade layer due to increased light penetration within the leaf, and thus foster higher quantum yields at higher PPFD (Terashima et al., 2009; Oguchi et al., 2011, 2021). Such a strategy facilitates a more balanced distribution of light absorption across photosynthetic and non-photosynthetic pigments, thereby decreasing the risk of photoinhibition (Tracewell et al., 2001; Terashima et al., 2009; Hogewoning et al., 2012). Furthermore, LED fixtures exhibit variability in their spectra, ranging from narrow to broad bandwidths. Broadband spectra, offering a more even distribution of light across a wider range of wavelengths, may be more effective in providing balanced light exposure for *A* and plant dry matter production (Hogewoning et al., 2012). Variations in plant responses due to spectra, coupled with their interplay with PPFD, highlight the necessity of selecting an appropriate lighting system tailored to the specific requirements of medical cannabis.

The influence of spectrum on PSM concentrations in medical cannabis has been explored in various studies (Eichhorn Bilodeau et al., 2019; Westmoreland et al., 2021; Islam et al., 2022). While exposure to blue light was correlated with increased cannabinoid concentrations (Hawley et al., 2018; Namdar et al., 2019; Danziger and Bernstein, 2021a), opposite effects were found as well (Wei et al., 2021; Westmoreland et al., 2021). These discrepancies may arise from the use of varying PPFD across studies. In other plant species, both red and blue light have been shown to affect terpenoid concentrations, and this might provide insights for terpenoid production in medical cannabis (Kessler and Kalske, 2018; Ghaffari et al., 2019). Further, while instantaneous responses of *A* in medical cannabis to PPFD, temperature, and [CO_2] are well-documented (Chandra et al., 2008, 2011a, 2011b, 2015), the effects of photosynthetic acclimation to different spectra remain unexplored (Liu and Van Iersel, 2021).

Despite a broad array of spectra and PPFD applied by horticulturists, a significant knowledge gap exists on the effects of these factors in medical cannabis. Previous studies have explored the impact of a single spectrum, leaving room for further investigation into the effects of spectra (Eaves et al., 2020; Llewellyn et al., 2021; Rodriguez-Morrison et al., 2021). Some efforts to clarify this relationship encountered complexities, notably the difficulty in maintaining consistent PPFD across different spectral treatments (Magagnini et al., 2018; Danziger and Bernstein, 2021a; Morello et al., 2022). This study aims to investigate the effects of different red wavelengths (640 and 660 nm), white fraction, and spectrum broadness on plant dry matter production and partitioning, and specialized metabolite accumulation in medical cannabis. It focuses on comprehensively analyzing plant morphology and photosynthetic responses at both low (600 µmol m^{-2} s^{-1}) and high (1200 µmol m^{-2} s^{-1}) PPFD, to clarify the underlying mechanisms of spectrum-PPFD interactions.

Material and methods

Plant material and propagation growth conditions

Cannabis sativa plants (var. King Harmony (Chemotype II, 1:1.5 THC : CBD); Perfect Plants, Honselersdijk, the Netherlands) were cultivated in two sequential growth cycles in climate-controlled chambers (Figure 1). These chambers were each divided into eight sections utilizing white plastic sheets. Genetically identical mother plants, derived from tissue culture and younger than four months, provided 228 unrooted apical cuttings, measuring 10 cm in length and possessing one fully expanded leaf with excised axillary nodes. These cuttings were propagated according to a standard propagation protocol (Text S1).

Growth conditions during vegetative and generative phase

At day 21 of the propagation phase, a uniform selection of 128 plants was transplanted into 15 x 15 x 15 cm stone wool blocks (Hugo Blocks; Grodan) and grown at a planting density of 16 plants m^{-2} for 14 days under long days (18 h photoperiod); plants achieved a height of 30 cm. Subsequently, plants were grown for 56 days at a planting density of 9 plants m^{-2} during the short-day phase (12 h photoperiod), to induce flower development.

Twenty-four hours prior to transplanting, stone wool plugs and blocks were pre-soaked in a nutrient solution (Supplementary Table S1) with electrical conductivity (EC) of 1.5 and 2.2 dS m^{-1}, respectively. The pH of the nutrient solution was ~5.8. Stone wool plugs were irrigated on day 14 of the propagation phase by ebb- and flow. A drip irrigation system administered the nutrient solution six and four times daily for the long-day and short-day phase, respectively at a rate of 60 mL min^{-1} and a duration between two and four minutes, per stone wool block, depending on the irrigation demand for healthy plant growth. EC values of these nutrient solutions were 2.2 and 2.5 dS m^{-1} for the long-day and short-day phase, respectively (Supplementary Table S1).

At day 7 of the long-day phase, four secondary branches per plant were retained, to improve crop uniformity and reduce apical

10.3389/fpls.2024.1393803

FIGURE 1
Photographs of Cannabis sativa under the treatment spectra, 42 days after start of the short-day phase, 56 days after transplanting. Spectra are displayed from left to right as follows: 6B-19G-75R/2Peaks, 7B-20G-73R/Narrow, 15B-42G-43R/Narrow, and 17B-40G-43R/Broad.

dominance, by removing the apical meristem at the seventh node and removing the two lowest secondary branches. At day 10 of the short-day phase, plants were pruned to promote airflow and reduce a high relative humidity in the canopy's microclimate by removing the bottom 20 cm of leaves and tertiary branches (Figure 2); pruned plant material was collected for inclusion in total plant dry matter production. RH was 75% and decreased to 70% on day 7 of the long-day phase to promote transpiration. For the short-day phase, relative humidity was set to 65% and subsequently decreased by 5% weekly until it reached 55% to promote transpiration and thus water uptake, and to prevent infections and infestations such as Botrytis (*Botrytis cinerea*) and powdery mildew (*Golovinomyces ambrosiae* and *Podosphaera macularis*). Air temperature was set to 28/24°C, 27/22°C, 26/22°C, and 25/22°C during the long-day phase, and on days 0-28, 29-42, and day 49-56 of the short-day phase, respectively. This temperature regime aimed to facilitate generative growth. [CO_2] was set to 800/400 and 1000/400 ppm (day/night) during the long-day and short-day phase, respectively.

FIGURE 2
Representative image of Cannabis sativa after pruning 10 days after start of the short-day phase, 24 days after transplanting.

Light treatments

The PPFD at canopy height was 600 and 1200 µmol m^{-2} s^{-1} (26 and 52 mol m^{-2} d^{-1}, respectively), provided by LEDs (ams OSRAM, Munich, Germany) mounted in VYPR fixtures (Fluence, Texas, Austin, USA). Four spectra were applied at both PPFD: two low-white (7B-20G-73R/Narrow and 6B-19G-75R/2Peaks) and two high-white (15B-42G-43R/Narrow and 17B-40G-43R/Broad) spectra (Figure 3). The blue-green-red ratios of the two low-white spectra were approximately equivalent, as well as the ratios of the two high-white spectra (Table 1). The low-white spectra either contained a single peak wavelength at 660 nm (7B-20G-73R/Narrow) or dual peak wavelengths at 640 and 660 nm (6B-19G-75R/2Peaks). The high-white spectra differed in broadness of the white spectrum: narrowband spectrum (42G-43R/Narrow), featuring peak wavelengths at 450 nm and 660 nm, and broadband spectrum (17B-40G-43R/Broad), which displayed a more uniform light distribution across a wide range of wavelengths, approximately spanning 400-750 nm.

10.3389/fpls.2024.1393803

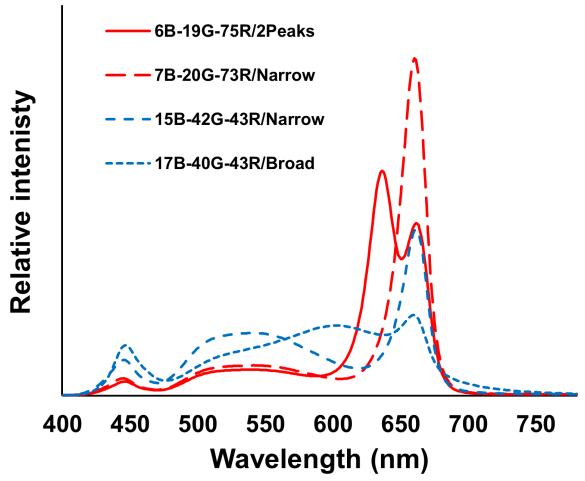

FIGURE 3
Spectral distribution of the four studied spectra with their quantitative parameters shown in Table 1.

During the long-day phase, the PPFD was initially set at 400 µmol m^{-2} s^{-1} and gradually increased to 600 µmol m^{-2} s^{-1} by day 12. In the short-day phase, the PPFD was further increased to 1200 µmol m^{-2} s^{-1} on day 7 for half of the plots. Weekly quantum sensor measurements (MQ-610, Apogee Instruments Inc., Logan, CA, USA) were conducted across nine points per plot to ensure uniform PPFD at canopy height.

Destructive measurements

Per treatment, seven plants per plot were destructively measured at the transition from the long-day to the short-day phase (14 days after transplanting), and nine plants were measured at the end of the experiment (70 days after transplanting). Dry weights of inflorescences, leaves that had been trimmed from the inflorescences, regular leaves, and stems were quantified. Inflorescence weights were determined after trimming inflorescence leaves with an industrial trimmer (MT Tumbler 200; Master Products, Girona, Spain). Leaf area of regular leaves was determined using a LI-3100C area meter (LI-COR Inc., Lincoln, Nebraska, USA). Dry weight was determined using a ventilated oven (24h at 70°C, followed by 48h at 105°C). Inflorescence weight at 10% moisture content was calculated from the oven dry weight of the inflorescence by multiplication with 1.10. Inflorescence length and width were measured on each of the four branches per plant to calculate inflorescence volume (assuming a cylinder shape) by $inflorescence\ volume = inflorescence\ length * \pi * (\frac{inflorescence\ width}{2})^2$. The inflorescence is identified as the complete inflorescence structure on a single branch (Spitzer-Rimon et al., 2019). Inflorescence density was calculated by dividing inflorescence dry weight by inflorescence volume. Light use efficiency (LUE) was determined by dividing inflorescence or total plant dry weight by the cumulative incident photosynthetically active radiation (PAR) at canopy height, across both the long-day and short-day phases (total light integral; TLI).

Leaf light absorptance, transmittance, and reflectance

Leaf light absorptance was measured in accordance to (Taylor et al., 2019), which involved the use of a dark enclosure equipped with two integrating spheres to determine leaf light transmission and reflection. Per treatment, leaf samples were collected from six randomly selected plants, with one leaf per plant, to quantify leaf light absorptance. Selected leaves were fully expanded, containing five or more leaflets, and positioned within 20 cm from the apex, ensuring full exposure to the light. The calculation of absorbed PAR (PAR_{abs}) involved multiplying incident PAR by leaf light absorptance.

Leaf photosynthesis measurements

Leaf photosynthesis was measured using a LI-6800 photosynthesis system (LI-COR) on six randomly selected plants per treatment (6 replicate plants per plot). Gas-exchange measurements were conducted on leaves that were selected on similar criteria as for leaf light absorptance. Data were collected during the fourth and seventh week of the short-day phase. Measurements of leaf photosynthesis light-response curves and operational photosynthesis were conducted within a seven-hour window per measurement day, starting one hour after the lights turned on. Measurements were alternated between treatments to reduce possible time-of-day effects. The infrared gas analyzers were matched between measurements on different plants. Conditions within the fluorometer cuvette were set to 27°C, 60% RH, a fan

TABLE 1 Spectral distribution and Photosynthetic Photon Efficacy (PPE) of the four spectra studied: 6B-19G-75R/2Peaks, 7B-20G-73R/Narrow, 15B-42G-43R/Narrow, and 17B-40G-43R/Broad and ratios of red to blue (R:B), red to green (R:G), blue to green (B:G), and red to far-red (R:FR).

Spectrum	% of total PPFD (400-700 nm)			% of PFD (380-780 nm)		Ratio				PPE (µmol/J)
	Blue	Green	Red	Ultraviolet	Far Red	R:B	R:G	B:G	R:FR	
6B-19G-75R/2Peaks	6	19	75	0.1	1	12	0.2	0.3	69	3.31
7B-20G-73R/Narrow	7	20	73	0.1	1	10.2	0.3	0.4	56.2	3.44
15B-42G-43R/Narrow	15	42	43	0.1	1	2.8	1	0.4	31.8	2.91
17B-40G-43R/Broad	17	40	43	0.1	3	2.6	0.9	0.4	12.7	3.06

speed of 10000 rpm, a flow rate of 400 µmol s^{-1}, 2000 ppm [CO_2], and spectrum of 20B:80R. Following a 15-minute light acclimation period to 3000 µmol m^{-2} s^{-1}, *A* was stabilized and recorded for 120-180 s, depending on the stabilization of *A*. Sequential PPFD were set to: 3000, 2500, 2000, 1500, 1000, 800, 600, 400, 200, 100, and 0 µmol m^{-2} s^{-1}. A non-rectangular hyperbola was fitted to the light response curve data (Thornley, 1977), and the parameters maximum net assimilation rate at saturating light (A_{max}), quantum yield (α_{LRC}), light compensation point (LCP), and dark respiration rate (R_d) were obtained.

Measurements of operational photosynthesis (A_{op}) were obtained using a transparent leaf cuvette at the incident PAR at canopy height. Environmental conditions within the leaf cuvette were set equal to the climate room environment. Quantum yield of photosynthesis (α_{op}) was calculated as $\alpha_{op} = \frac{(A_{op} + R_d)}{PAR_{abs}s}$, where R_d is the average respiration rate per plot, estimated from the light-response curve.

Gas chromatography-mass spectrometry analysis

Cannabinoid and terpenoid concentrations were quantified in inflorescences located at the apical inflorescence above the canopy, within 5 cm from the apical inflorescence. Per treatment, three pooled samples were collected, each three samples at four different times, 0, 5, 10, and 15 days before harvest (DBH). Each pooled sample consisted of three inflorescence clusters, each harvested from a randomly selected plant of a given treatment, totaling approximately 1 g per pooled sample. Bleached inflorescences, which were exclusively found at the tip of the apical inflorescences in the 6B-19G-75R/2Peaks treatment at 1200 µmol m^{-2} s^{-1}, were individually harvested and analyzed, with each sample weighing approximately 0.4 g. Inflorescence samples were stored at -80°C until further processing. Per sample, 0.2 ± 0.01 g were measured into a glass tube, into which 2 mL of *n*-Hexane with 1 mg L^{-1} squalene (Thermo Fisher Scientific, Waltham, Massachusetts, USA) as an internal standard was added. Extraction of PSM was performed for 10 minutes, using an ultrasonic bath without elevated temperatures (Branson 2800; Branson Ultrasonics Corporation, Danbury, CT, USA). The resulting extract was then passed through a filtration column, containing of a Pasteur's pipet filled with glass-wool and anhydrous sodium sulphate (Biosolve B.V., Valkenswaard, the Netherlands), and collected in a 2 ml glass vial for Gas Chromatography-Mass Spectrometry (GC-MS) analysis.

The PSM analysis was conducted using an Agilent Gas Chromatography (GC) Model 7890 (Agilent Technologies, Inc., Santa Clara, CA, USA) system fitted with a 30 x 0.25 mm i.d., 0.25-µm film thickness Zebron 5MS Column (Phenomenex Inc., Torrance, CA, USA), and a Model 5972A Mass Selective (MS) Detector (Hewlett-Packard, Palo Alto, CA, USA). The GC was programmed at an initial temperature of 60°C for two minutes, increased by 5°C min^{-1} until reaching 250°C, accelerated at 10°C min^{-1} to 280°C, and kept at this temperature for 5 min. The temperatures of the injection port, interface, and MS source were set to 250°C, 290°C, and 180°C, respectively. Helium inlet pressure was electronically controlled to sustain a constant column flow rate of 1.0 ml min^{-1}. Ionization was conducted at a potential of 70 eV, and mass scanning ranged from 45 to 400 amu with a scan rate of 5 scans min^{-1}. Samples were diluted 5-fold (i.e. 0.2 ml extract combined with 0.8 ml n-hexane) and one µL of each sample was injected and analyzed in split less mode.

Identification of terpenoid and cannabinoid compounds was based on their respective GC-MS retention times, and spectral comparisons against the NIST11 Mass Spectral Library (National Institute of Standards and Technology, Gaithersburg, MD, USA), the Adams essential oil library (Sparkman, 2005) and a comprehensive *in-house* spectral library generated with authentic standards. For semi-quantification of compounds, areas under the curve (AUC) were computed relative to the AUC of the internal standard (Squalene) and normalized for dilution and sample weight. For each treatment, data are presented as the mean ± SEM derived from three replicates. Concentrations of THC and CBD were determined using calibration curves from authentic standards, while additional cannabinoids and terpenoids were quantified in units relative to the internal standard. Initial quantifications were based on fresh weight, which were then normalized to a 10% moisture content, which reflects the market-standard weight for saleable inflorescences, by accounting for dry matter in the inflorescences. The THC and CBD yields were determined by multiplying their respective cannabinoid concentrations by the dry weight of the inflorescence.

Statistical analysis

The experiment was set up and analyzed as a split-plot design in two blocks (repetition over time) with PPFD (600 and 1200 µmol m^{-2} s^{-1}) as main factor and spectrum (6B-19G-75R/2Peaks, 7B-20G-73R/Narrow, 15B-42G-43R/Narrow, and 17B-40G-43R/Broad) as subfactor. Each plot consisted of 16 plants, of which seven were harvested at an intermediate harvest, and nine at the final harvest. Individual plant responses were averaged per plot and an average was used as a statistical replicate. Due to the limited number of blocks, homogeneity of variances had to be assumed and statistical significance was assessed at $P = 0.1$, which is consistent with standard practices in such conditions (Ott and Longnecker, 2015; Kaiser et al., 2019). No outliers were identified per plot, using Z-score criteria, with thresholds set at -3 and +3 standard deviations. A Shapiro-Wilk test ascertained that the assumptions of normality were met. Analysis of variance (ANOVA) was conducted to evaluate main and interaction effects of spectrum and PPFD on plant morphological traits, physiological traits, and PSM. Fisher's unprotected LSD test was used for means separation. The variance in treatment effects on morphological parameters between the two repetitions could be attributed to an infection of Hop Latent Viroid in the first repetition. This infection, confirmed by Naktuinbouw in Roelofarendsveen, the Netherlands, likely diminished the observed treatment effects. Plants infected with Hop Latent Viroid exhibit symptoms including stunted growth and reduced inflorescence yield (Adkar-Purushothama et al., 2023). The variations observed may also be partly attributed to an earlier harvest by two weeks in the first repetition, necessitated by a

malfunction of the irrigation system. To ensure comparability between the two experimental repetitions, PSM concentrations are presented only for 15 DBH for both repetitions. For a similar reason, photosynthesis data are primarily discussed for the fourth week of the short-day phase, as for the seventh week of the short-day phase only data from one repetition was available. Instances where data from only one repetition are presented are explicitly indicated. Statistical analysis was conducted by using SPSS (Version 26.0; IBM Corp., Armonk, NY, USA).

Results

Plant dry matter production and development

White light with a dual red peak of 640 and 660 nm (6B-19G-75R/2Peaks) increased inflorescence weight compared to white light with a single red peak at 660 nm (7B-20G-73R/Narrow), irrespective of PPFD (Figure 4A). This increase in inflorescence weight was related to an increase in total plant weight, while dry matter partitioning to inflorescences remained unaffected (Figure 4E). Neither increasing the white fraction (15B-42G-43R/Narrow compared to 7B-20G-73R/Narrow) nor increasing spectrum broadness (17B-40G-43R/Broad compared to 15B-42G-43R/Narrow) affected inflorescence weight at either PPFD. Dry matter partitioning to the inflorescences increased when the white fraction increased, irrespective of PPFD (Figure 4E). There was no effect of red wavelength or spectrum broadness on dry matter partitioning to the inflorescences. Dry matter partitioning to the trim and leaves was not affected by spectrum or PPFD. Increasing the white fraction reduced dry matter partitioning towards the stem, irrespective of PPFD. This coincided with a decrease in plant height (Figure 4D), resulting in a more compact plant architecture (Figure 5). Leaf area was not affected by spectrum, and decreased with increasing PPFD (Supplementary Figure S2C). Specific leaf area decreased with increasing spectrum broadness at higher PPFD, and generally decreased with increasing PPFD (Supplementary Figure S2D). There were no effects of spectrum on plant height, specific leaf area, leaf area, and total plant weight and biomass partitioning at intermediate harvest (Supplementary Figure S1). Inflorescence and plant LUE increased under white light with a dual red peak of 640 and 660 nm compared to white light with a single red peak at 660 nm, and decreased with increasing PPFD for this treatment (Figure 4C and Supplementary Figure S2B). Neither increasing the white fraction nor spectrum broadness affected inflorescence and plant LUE, and interestingly, both LUE were also unaffected by PPFD. Furthermore, inflorescence density increased with increasing PPFD, but was unaffected by spectrum (Figure 4B).

Plant specialized metabolites

Spectrum or PPFD did not affect total cannabinoid concentration, nor that of any specific cannabinoid (Figure 6B and Supplementary Table S2). White light with a dual red peak of 640 and 660 nm compared to white light with a single red peak at 660 nm increased total terpenoid concentrations at high PPFD (Figure 6A). Neither increasing the white fraction nor spectrum broadness, irrespective of PPFD, affected total terpenoid concentrations. Total terpenoid concentration was manifested predominantely by β-Myrcene, α-Pinene, β-Pinene, Limonene, and Germacrene D (Supplementary Table S2), and was highest 5 days before harvest (DBH) (Supplementary Figure S3B). Bleached inflorescences were exclusively found at the tip of apical inflorescences in white light with a dual red peak of 640 and 660 nm at 1200 µmol m^{-2} s^{-1}, and not in the other treatments. Bleached inflorescences exhibited increased total cannabinoid concentrations compared to green inflorescences, primarily attributed to CBD as THC was not affected (Figure 6E). The type of inflorescence did not influence total terpenoid concentrations.

Photosynthesis

When measuring light-response curves (LRC) of *A* during the fourth week of flowering, it was remarkable that *A* did not saturate, even at the highest PPFD of 3000 µmol m^{-2} s^{-1}, in any of the treatments (Figure 7A). Also, the increase in *A* at PPFD<1000 µmol m^{-2} s^{-1} was less pronounced in week seven compared to week four of the short-day phase (Supplementary Figure S4E). During week four of the short-day phase, A_{max} increased with increasing PPFD in plants grown under 7B-20G-73R/Narrow and 15B-42G-43R/Narrow (Figure 7B). During week seven of the short-day phase, A_{max} decreased compared to week four, with no effect from spectrum or PPFD (Supplementary Figure S4F). Photosynthetic quantum yield as derived from the light-response curves (α_{LRC}) increased under white light with a dual red peak of 640 and 660 nm compared to white light with a single red peak at 660 nm, and when spectrum broadness increased (Figure 7C) at low PPFD. Conversely, at high PPFD, increasing spectrum broadness reduced α_{LRC}. During the seventh week of the short-day phase, there was a noticeable decrease in α_{LRC} as PPFD increased, without any effect of spectrum (Supplementary Figure S5A).

Dark respiration (R_d) and the light compensation point (LCP) were not influenced by spectrum, but increased with PPFD (Supplementary Figure S4A, C). In the seventh week of the short-day phase, neither spectrum nor PPFD affected R_d and LCP (Supplementary Figure S4B, D). In week seven of the short-day phase at low PPFD, R_d,LCP, and A_{max} remained relatively stable (Supplementary Figure S4B, D, F). However, at high PPFD, these parameters approximately halved compared to week four, suggesting a decline in photosynthetic capacity as leaves aged at high PPFD.

Leaf absorptance within the 400-750 nm range averaged 83% and was unaffected by treatments (Supplementary Table S4). The quantum yield of operational photosynthesis under treatment conditions (α_{op}) increased at low PPFD under white light with a dual red peak of 640 and 660 nm compared to white light with a single red peak at 660 nm, and when increasing the white fraction (Figure 7D). There was no effect of spectrum on α_{op} at high PPFD. In the seventh week of the short-day phase, increasing the PPFD decreased α_{op}, with no effect of spectrum (Supplementary Figure S5B).

10.3389/fpls.2024.1393803

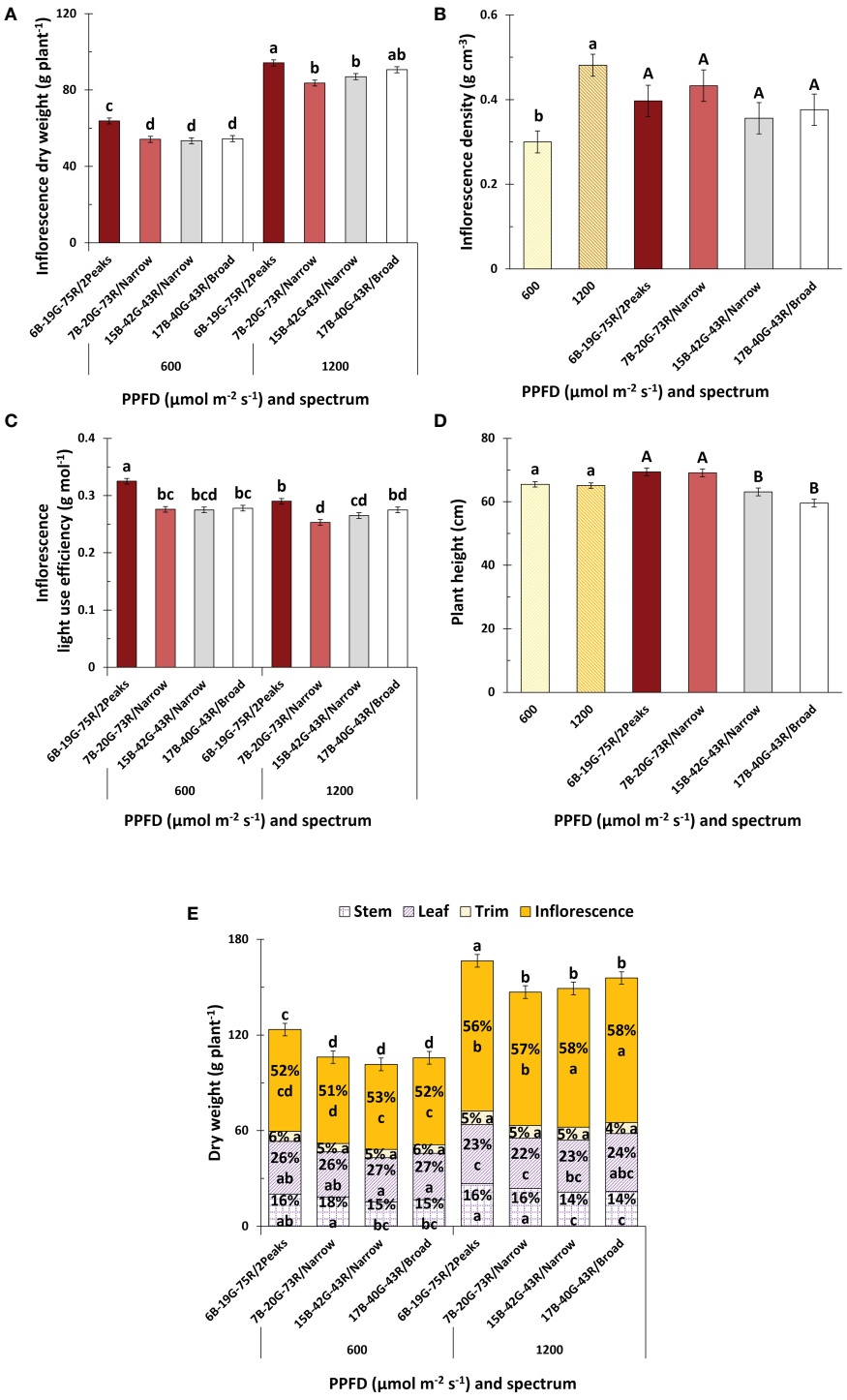

FIGURE 4
Effects of spectrum and PPFD on yield and light use efficiency of *Cannabis sativa*. **(A)** inflorescence dry weight; **(B)** inflorescence density; **(C)** inflorescence light use efficiency; **(D)** plant height; **(E)** and plant dry weight and partitioning. Bars indicate means of two blocks (n = 2) each consisting of 9 replicate plants. Main effects are shown when no interaction is found. Error bars represent standard error of means (SEM). Different letters (within lowercase and uppercase) indicate significant differences between treatments (Fisher's unprotected LSD test, $P = 0.10$).

Discussion

The aim of this study was to investigate the effects of different wavelengths of red (640 and 660 nm), white fraction, and spectrum broadness on the growth and PSM accumulation in *Cannabis sativa*. An in-depth analysis of plant morphology and photosynthetic responses was conducted to elucidate the underlying mechanisms responsible for observed treatment effects.

FIGURE 5
Representative images of Cannabis sativa 20 days after start of the short-day phase, 34 days after transplanting.

White light with dual red peaks at 640 and 660 nm increases inflorescence weight through increased plant dry matter production compared to white light with single red peak At 660 nm

White light with a dual red peak of 640 and 660 nm (6B-19G-75R/2Peaks) increased inflorescence weight (Figure 4A) and light use efficiency (LUE; Figure 4C and Supplementary Figure S2B), compared to white light with a single red peak at 660 nm (7B-20G-73R/Narrow). Similar results were obtained by (Wollaeger and Runkle, 2013) in various ornamental crops. In their study, crops were grown at 125 and 250 µmol m^{-2} s^{-1} PPFD with various combinations of 634 and 664 nm, making up 80% of the spectrum, with 10% blue (446 nm) and 10% green (516 nm). They observed that shoot fresh weight was higher when grown at 40% 634 and 40% 664 nm in comparison to other spectrum combinations, with leaf chlorophyll concentrations being higher under this treatment at low PPFD. Although the light treatment in our study with dual red peak (640 and 660 nm), and single red peak (660 nm) had an equivalent red fraction, the inclusion of two maximum absorption peaks at 640 and 660 nm appeared to drive photosynthesis (α_{LRC} and α_{op}) and plant dry matter production more effectively than a single maximum absorption peak at 660 nm (Figure 7C, D). This effect may be attributed to the fact that, within the red waveband, Chl *b* and Chl *a* have their maximum absorption peaks around 642 nm and 663 nm, respectively (Zhu et al., 2008; Chazaux et al., 2022). Chl *b* is specifically bound to light-harvesting complexes while Chl *a* is bound to both photosystem core- and light-harvesting complexes (Caffarri et al., 2011; Zhao et al., 2017; Pan et al., 2018). Chl *b* is critical in regulating the size of the light-harvesting complexes, absorbing light energy that would otherwise cause photoinhibition when directly absorbed by the photosystem core complexes (Voitsekhovskaja and Tyutereva, 2015). Distributing the light energy over both Chl *b* and Chl *a* likely allowed for more efficient light energy absorption and conversion to chemical energy, preventing photoinhibition due to excessive light energy. However, Chl *a* and Chl *b* coexist alongside both photosynthetic and non-photosynthetic pigments. This assortment of pigments influences the efficacy of various light wavelengths in driving photosynthesis (Walla et al., 2014; Smith et al., 2017).

The use of 660 nm light may trigger phytochrome activation, inhibiting flowering in short-day plants like strawberries (Takeda and Newell, 2006). This phenomenon could explain the reduced inflorescence weights observed under white light with a single red peak at 660 nm compared to white light with a dual red peak of 640 and 660 nm, likely resulting from a prolonged flower induction phase. Park and Runkle (2018) observed a similar response, where inflorescence buds appeared earlier in begonia (*Begonia* spp.), geranium (*Pelargonium* spp.), petunia (*Petunia* spp.), and snapdragon (*Antirrhinum majus*) under 100% white, or 75% white with 25% red light, compared to a combination of 15% blue and 85% red. Although we did not measure the phytochrome stationary state or the precise moment of flower induction, these factors merit consideration in future research exploring the effects of 640 and 660 nm wavelengths on inflorescence development of medical cannabis.

10.3389/fpls.2024.1393803

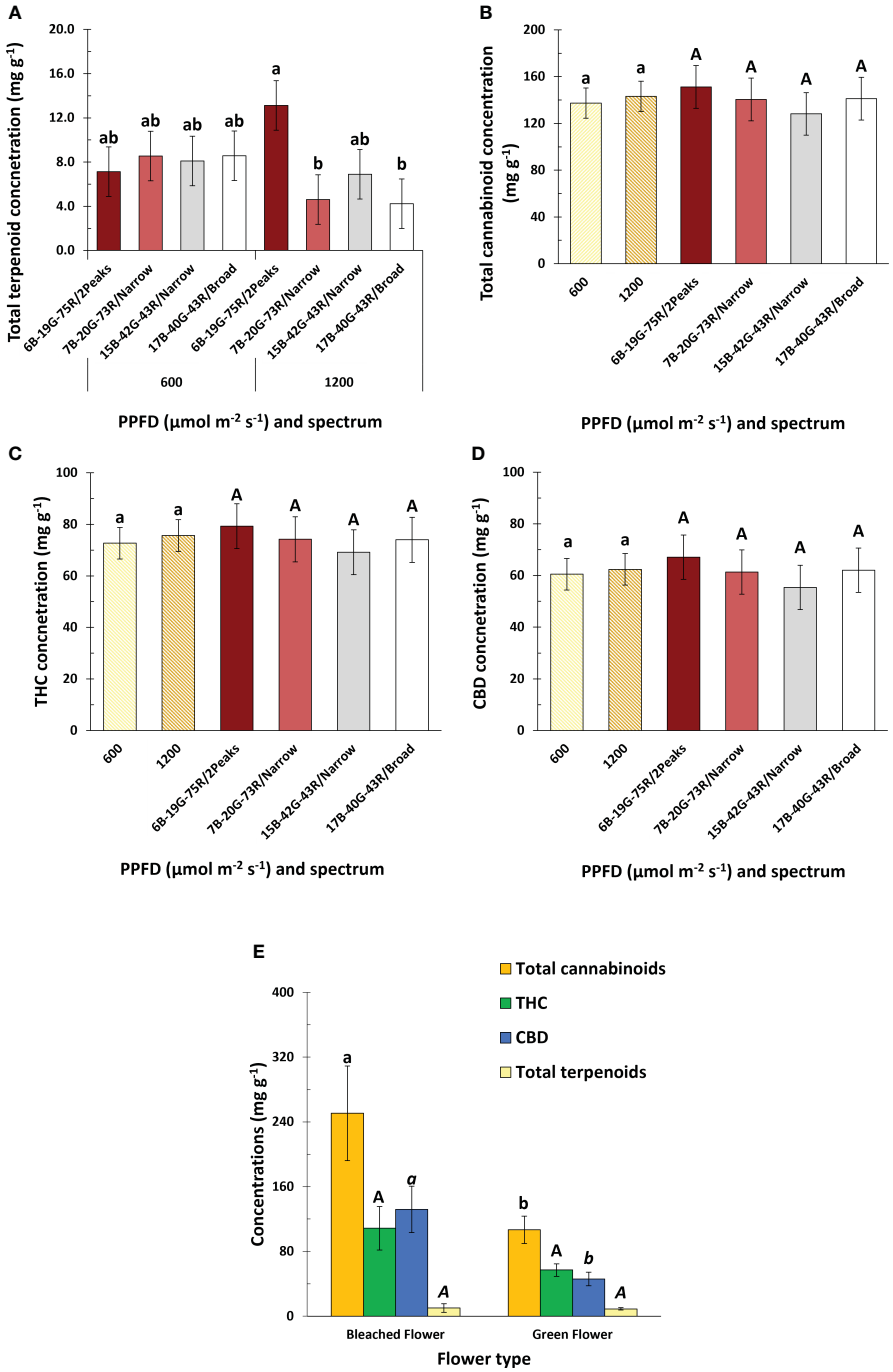

FIGURE 6
Effects of spectrum and PPFD on specialized metabolite concentration of *Cannabis sativa*. **(A)** total terpenoid concentration; **(B)** total cannabinoid concentration; **(C)** THC concentration; **(D)** CBD concentration. **(E)** effect of inflorescence type on total cannabinoid, THC, CBD, and total terpenoid concentration. Bars indicate means of two blocks (n = 2) each consisting of 9 replicate plants, with the exception of panel **(E)** which only consisted of one block. Main effects are shown when no interaction is found. Error bars represent standard error of means (SEM). Different letters (within lowercase and uppercase) indicate significant differences between treatments (Fisher's unprotected LSD test, P = 0.10).

Larger fraction of white light improves dry matter partitioning to the inflorescences, but did not increase plant dry matter production

White fraction did not affect inflorescence weight. Increasing the white fraction in our study caused increases in both blue and green fractions and decrease in red fraction. All these changes in fraction blue, green, and red or their mutual ratios could have contributed to the observed treatment effects. Our study, along with similar research in the field, was conducted at low to average PPFD compared to conventional medical cannabis cultivation (Lumigrow, 2017; Fluence, 2020). We found that leaf-level A still increased at PPFD >1200 µmol m^{-2} s^{-1}, suggesting the potential for further

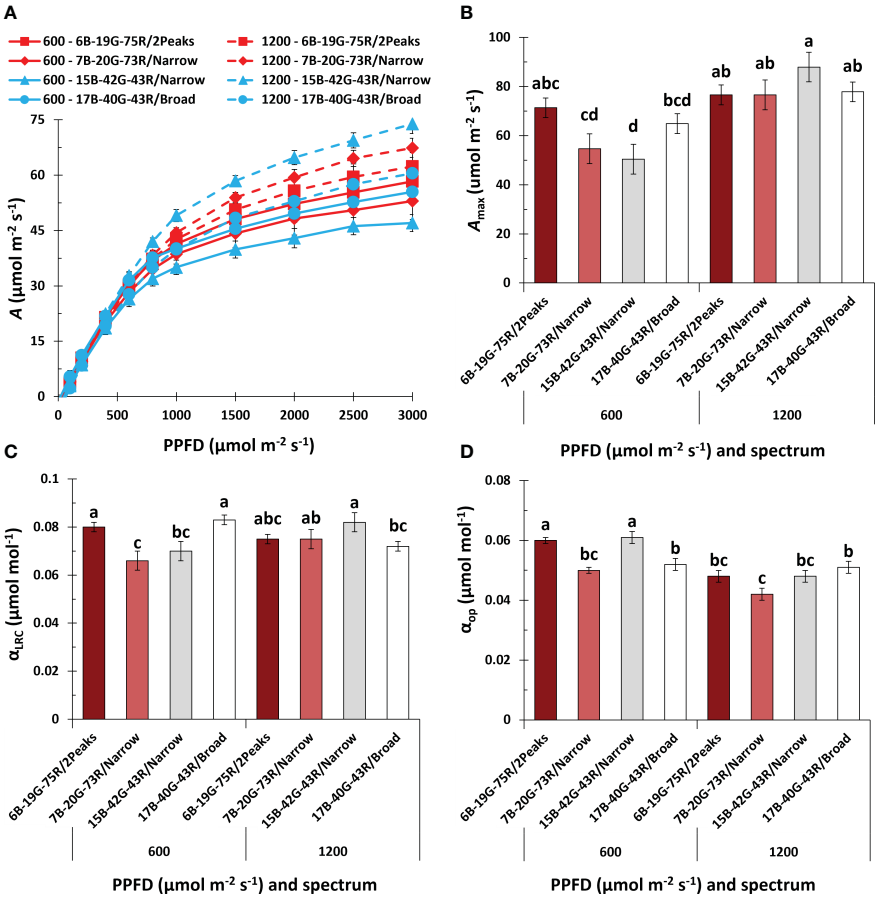

FIGURE 7
Effects of spectrum and PPFD on leaf net photosynthesis rate (*A*) in the fourth week of the short-day phase of *Cannabis sativa*. **(A)** light response curve of *A*; **(B)** maximum *A* at saturating PPFD (A_{max}); **(C)** quantum yield of *A* based on the light response curve (α_{LRC}); **(D)** quantum yield of operational *A* under the treatment conditions (α_{op}). Data was averaged from six plants within each plot, resulting in a single value for each plot. Bars or symbols indicate means of two blocks (n = 2), with the exception of 7B-20G-73R/Narrow and 17B-40G-43R/Broad in panel **(B, C)** which only consisted of one block. Error bars represent standard error of means (SEM). Different letters indicate significant differences between treatments (Fisher's unprotected LSD test, $P = 0.10$) Conditions within the fluorometer cuvette were set to 27°C, 60% RH, a fan speed of 10000 rpm, a flow rate of 400 µmol s^{-1}, 2000 (LRC) and 1000 (OP) ppm [CO_2], and spectrum of 20B:80R (LRC).

exploration at higher PPFD. While high PPFD can overexcite the photosystems and induce stress responses that give rise to destructive reactive-oxygen-species (ROS) (Demmig-Adams and Adams, 1992; Asada, 2006), increasing the white fraction at high PPFD may alleviate this stress due to a larger green fraction, which penetrates deeper in the leaf and thus distributes light more evenly among the chloroplasts, referred to as the 'detour' effect (Terashima et al., 2009; Brodersen and Vogelmann, 2010; Slattery et al., 2016; Smith et al., 2017). In support of this, Liu & Van Iersel (2021) observed higher quantum yields in lettuce under low-white light at 200 µmol m^{-2} s^{-1}, and under a combination of red and green light at 1000 µmol m^{-2} s^{-1}. Similarly, substituting up to 24% of red+blue LED light with green light increased both shoot fresh and dry weight, which was attributed to green light penetrating deeper within folded lettuce leaves (Kim et al., 2004; Bian et al., 2016).

When PPFD increases, light energy is rarely a limiting factor for plant dry matter production. Nevertheless, overexcitation of pigments can lead to the formation of ROS, potentially causing photooxidative damage to the photosystems and ultimately photoinhibition (Bassi and Dall'Osto, 2021). Up to 90% of red and blue light can be absorbed by the chloroplasts located within the upper 20% of the leaf's profile (Nishio et al., 1993). Supplementing saturating white halogen light with monochromatic green light enhanced *A* in *Helianthus annuus* more efficiently than monochromatic red light (Terashima et al., 2009). As such, increasing the green fraction is especially relevant in crops which form dense canopies, and in crops that can be grown at very high PPFD, such as medical cannabis (Smith et al., 2017).

Decreasing the white fraction led to an increase in plant height, which is associated with an increased inflorescence weight. Increased plant height results in a more open plant structure. Such open structures have been associated with increased yields and the production of plant specialized metabolites in several plant species (Bugbee, 2016; Danziger and Bernstein, 2021b). The increase in plant height, which led to a more open plant structure, likely increased light distribution in the canopy and photon capture, thereby increasing both whole-crop photosynthesis and plant dry matter production (Takenaka, 1994; Sarlikioti et al., 2011). This factor is particularly vital

for medical cannabis, a crop with a dense canopy. A larger white fraction increased dry matter allocation to the inflorescences. This finding is consistent with Magagnini et al. (2018), who reported a lower harvest index with increased red fraction. The effect was ascribed to increased dry matter partitioning to the stems, correlating with an increased plant height. This response aligns with findings by Danziger and Bernstein (2021a), who noted a similar response in plants grown under a high red fraction.

Total cannabinoid concentrations were unaffected by spectrum and PPFD. These observations contradict with those of Islam et al. (2022), who reported increased cannabinoid concentrations under spectra with an increased blue-to-red ratio at a PPFD of 300 µmol m^{-2} s^{-1}. Furthermore, in *Mentha* spp., Sabzalian et al. (2014) reported that a combination of red and blue light led to increased essential oil concentrations compared to white light. Studies by Hawley et al. (2018) and Namdar et al. (2018) associated higher blue fractions with increased cannabinoid concentrations. Nevertheless, due to differing experimental conditions, including lower PPFD and shorter durations of the short-day phase, a direct comparison with our findings warrants caution. Westmoreland et al. (2021) and Wei et al. (2021) observed no significant impact of blue fraction on cannabinoid concentrations, and suggested that photoreceptor saturation at high PPFD might underlie these observations. Magagnini et al. (2018) demonstrated that the influence of spectrum on concentrations of THC, CBD, and CBG is cultivar dependent. For instance, Danziger and Bernstein (2021a) observed varying effects on the naturally occurring forms of cannabinoids—Cannabigerolic Acid (CBG), Cannabidiolic Acid (CBD), and Tetrahydrocannabinolic Acid (THC)—across three cultivars when comparing various LED spectra with high-pressure sodium (HPS) lights.

We hypothesize that low-white spectra at high PPFD could overexcite the photosystems, potentially leading to bleached inflorescences, which have been compared to photoinhibition of the leaves, potentially caused by production of reactive oxygen species. A somewhat similar response was observed by (Massa et al., 2008), where white tissue development was observed in peppers grown under 85% red and 15% blue light, specifically on inflorescence sepals. The precise mechanism behind this phenomenon is still uncertain and warrants further investigation. In our research, bleached inflorescences had higher total cannabinoid concentrations, primarily due to more CBD. This could be due to cannabinoids being proposed as potent antioxidants (Mukhopadhyay et al., 2011; Raja et al., 2020), possibly accumulating in greater amounts in tissues with higher concentrations of ROS, to maintain a balance in light-harvesting and energy utilization (Islam et al., 2022).

No clear effect of spectrum broadness on plant dry matter production and photosynthetic efficiency

Despite a scarcity of studies on the effects of broadband versus narrowband wavelengths, some studies report that plant dry matter production tends to increase under broadband light compared to red and blue light combinations alone (Kim et al., 2004; Massa et al., 2008; Hogewoning et al., 2010; Lu et al., 2019). Spectrum in the PPFD waveband is typically categorized by blue (400-500 nm), green (500-600 nm), and red (600-700 nm) wavelengths. For a comprehensive comparison in peer-reviewed studies, a more detailed classification of broadband wavelengths would be useful, as this could aid in accurately evaluating and contrasting the effects of different spectra on plant dry matter production.

Kim et al. (2004) studied the effects of different spectra, particularly of green fraction, on lettuce growth. They observed that a spectrum with 15% blue, 24% green, and 61% red light led to the highest plant dry matter production compared to cool-white fluorescent light. However, their PPFD of 150 µmol m^{-2} s^{-1} may not have fully demonstrated broadband spectrum potential. Green photons could exhibit a quantum yield similar to red photons, and higher than blue photons, as blue is also absorbed by non-photosynthetic flavonoids and carotenoids (McCree, 1971; Hogewoning et al., 2012). At higher PPFD, a greater green fraction may be more advantageous, as it can enhance light penetration within leaves and through the canopy, which has been hypothesized to improve whole-crop photosynthesis. Johkan et al. (2012) supported this, noting that while low PPFD (100 µmol m^{-2} s^{-1}) green light did not significantly impact lettuce growth, higher PPFD (300 µmol m^{-2} s^{-1}) green light enhanced growth compared to white fluorescent light. However, contradicting results on the effect of green fraction on plant dry matter production have also been reported (Wang and Folta, 2013; Snowden et al., 2016), which among other factors, could have been attributed to the reversal of blue-light induced stomatal opening (Frechilla et al., 2000; Talbott et al., 2002). The variability in the effects of green fraction on plant dry matter production warrants further investigation. Although green LEDs exhibit inefficiencies in the conversion of electricity to photons—referred to as the 'green gap' (Pleasants, 2013)—employing white LEDs or a combination of red and blue LEDs could offer a more effective solution for generating a broad light spectrum.

It is important to note that the broad-white spectrum used in our study included 3% far-red light, while the narrow-white spectrum did not (Supplementary Table S1). This is relevant considering that increasing the far-red fraction has been shown lead to an increased growth (Demotes-Mainard et al., 2016). The photosynthetic efficiency of far-red depends on the exact wavelengths used, but can be comparable to PPFD when used in combination with shorter wavelengths (Zhen and Bugbee, 2020a; Zhen and Bugbee, 2020b; Jin et al., 2021). Further research is needed to clarify how the crop responds to different fractions of blue, green, red and far-red light at varying PPFD. Additionally, it is crucial to investigate whether the crop's light requirements change during different stages of development.

Conclusions

Our study revealed an interaction between spectrum and PPFD on plant dry matter production and inflorescence yield of medical cannabis. White light with a dual red peak at 640 and 660 nm,

compared to white light with a single red peak at 660 nm, increased inflorescence yield and light use efficiency, regardless of PPFD. This increase was primarily due to increased total plant dry matter production and a more open plant architecture, which may have improved photon capture. White fraction and spectrum broadness had no effect on inflorescence yield, irrespective of PPFD. There was no treatment effect on total cannabinoid concentrations, which indicates a promising potential for maintaining consistent quality in terms of PSM. However, at higher PPFD, white light with a dual red peak of 640 and 660 nm compared to white light with a single red peak at 660 nm increased terpenoid concentrations. At low PPFD, photosynthetic parameters like maximum photosynthetic rate and quantum yield were increased when grown under white light with a dual red peak of 640 and 660 nm compared to white light with a single red peak at 660 nm, while spectrum had no effect at higher PPFD. The addition of 640 nm alongside 660 nm shows potential in improving light use efficiency and promoting plant dry matter production.

Data availability statement

The original contributions presented in the study are included in the article/Supplementary Material. Further inquiries can be directed to the corresponding authors.

Author contributions

MH: Conceptualization, Data curation, Formal analysis, Investigation, Methodology, Visualization, Writing – original draft, Writing – review & editing, Software, Validation. EK: Methodology, Writing – review & editing, Supervision. IK: Methodology, Writing – review & editing, Supervision. EH: Supervision, Writing – review & editing, Methodology. LM: Conceptualization, Funding acquisition, Supervision, Writing – review & editing, Methodology.

Funding

The author(s) declare financial support was received for the research, authorship, and/or publication of this article. This study was supported by ams OSRAM (Munich, Germany). The funding from ams OSRAM has provided both financial and technical resources crucial for the advancement of this research.

Acknowledgments

We would like to thank the students Luc Rademakers and Beertje Douven for their data collection efforts. We also would like to thank the followings staff members of Wageningen University and Research for their technical support; Gerrit Stunnenberg, David Brink, Jannick Verstegen, Dieke Smit, Chris van Asselt, Sean Geurts, Martijn Verweij, and Jonathan Hovenkamp. We also thank Francel Verstappen for his assistance with the GC-MS analysis. Additionally, we acknowledge the technical support on the lighting system provided by the ams OSRAM System Solution Engineering (SSE) team: Horst Varga, Marcus Hofmann, Chew Wui Chai, Mardiana Bt. Khalid.

Conflict of interest

The authors declare that the research was conducted without any commercial or financial relationships that could be construed as a potential conflict of interest.

The author(s) declared that they were an editorial board member of Frontiers, at the time of submission. This had no impact on the peer review process and the final decision.

Publisher's note

Supplementary material

The Supplementary Material for this article can be found online at: https://www.frontiersin.org/articles/10.3389/fpls.2024.1393803/full#supplementary-material

References

Adkar-Purushothama, C. R., Sano, T., and Perreault, J.-P. (2023). Hop latent viroid: A hidden threat to the cannabis industry. *Viruses* 15, 681. doi: 10.3390/v15030681

Aizpurua-Olaizola, O., Soydaner, U., Öztürk, E., Schibano, D., Simsir, Y., Navarro, P., et al. (2016). Evolution of the Cannabinoid and Terpene Content during the Growth of Cannabis sativa Plants from Different Chemotypes. *J. Nat. Prod* 79, 324–331. doi: 10.1021/acs.jnatprod.5b00949

Andre, C. M., Hausman, J. F., and Guerriero, G. (2016). Cannabis sativa: The plant of the thousand and one molecules. *Front. Plant Sci.* 7. doi: 10.3389/fpls.2016.00019

Asada, K. (2006). Production and scavenging of reactive oxygen species in chloroplasts and their functions. *Plant Physiol.* 141, 391–396. doi: 10.1104/pp.106.082040

Bassi, R., and Dall'Osto, L. (2021). Dissipation of light energy absorbed in excess: the molecular mechanisms. *Annu. Rev. Plant Biol.* 72, 47–76. doi: 10.1146/annurev-arplant-071720-015522

Bian, Z.-H., Cheng, R.-F., Yang, Q.-C., Wang, J., and Lu, C. (2016). Continuous light from red, blue, and green light-emitting diodes reduces nitrate content and enhances

phytochemical concentrations and antioxidant capacity in lettuce. *J. Am. Soc. Hortic. Sci.* 141, 186–195. doi: 10.21273/JASHS.141.2.186

Booth, J. K., and Bohlmann, J. (2019). Terpenes in Cannabis sativa – From plant genome to humans. *Plant Sci.* 284, 67–72. doi: 10.1016/j.plantsci.2019.03.022

Brodersen, C. R., and Vogelmann, T. C. (2010). Do changes in light direction affect absorption profiles in leaves? *Funct. Plant Biol.* 37, 403–412. doi: 10.1071/FP09262

Bugbee, B. (2016). Toward an optimal spectral quality for plant growth and development: the importance of radiation capture. *Acta Hortic.* 1134, 1–12. doi: 10.17660/ActaHortic.2016.1134.1

Bula, R. J., Morrow, R. C., Tibbitts, T. W., Barta, D. J., Ignatius, R. W., and Martin, T. S. (1991). Light-emitting diodes as a radiation source for plants. *HortScience* 26, 203–205. doi: 10.21273/HORTSCI.26.2.203

Burgie, E. S., Bussell, A. N., Walker, J. M., Dubiel, K., and Vierstra, R. D. (2014). Crystal structure of the photosensing module from a red/far-red light-absorbing plant phytochrome. *Proc. Natl. Acad. Sci.* 111, 10179–10184. doi: 10.1073/pnas.1403096111

Caffarri, S., Broess, K., Croce, R., and van Amerongen, H. (2011). Excitation energy transfer and trapping in higher plant photosystem II complexes with different antenna sizes. *Biophys. J.* 100, 2094–2103. doi: 10.1016/j.bpj.2011.03.049

Chandra, S., Lata, H., Khan, I. A., and Elsohly, M. A. (2008). Photosynthetic response of Cannabis sativa L. @ to variations in photosynthetic photon flux densities, temperature and CO2 conditions. *Physiol. Mol. Biol. Plants* 14, 299–306. doi: 10.1007/s12298-008-0027-x

Chandra, S., Lata, H., Khan, I. A., and ElSohly, M. A. (2011a). Photosynthetic response of Cannabis sativa L., an important medicinal plant, to elevated levels of CO2. *Physiol. Mol. Biol. Plants* 17, 291–295. doi: 10.1007/s12298-011-0066-6

Chandra, S., Lata, H., Khan, I. A., and ElSohly, M. A. (2011b). Temperature response of photosynthesis in different drug and fiber varieties of Cannabis sativa L. *Physiol. Mol. Biol. Plants* 17, 297–303. doi: 10.1007/s12298-011-0068-4

Chandra, S., Lata, H., Mehmedic, Z., Khan, I. A., and ElSohly, M. A. (2015). Light dependence of photosynthesis and water vapor exchange characteristics in different high Δ9-THC yielding varieties of Cannabis sativa L. *J. Appl. Res. Med. Aromat Plants* 2, 39–47. doi: 10.1016/j.jarmap.2015.03.002

Chazaux, M., Schiphorst, C., Lazzari, G., and Caffarri, S. (2022). Precise estimation of chlorophyll *a*, *b* and carotenoid content by deconvolution of the absorption spectrum and new simultaneous equations for Chl determination. *Plant J.* 109, 1630–1648. doi: 10.1111/tpj.15643

Cope, K. R., and Bugbee, B. (2013). Spectral effects of three types of white light-emitting diodes on plant growth and development: Absolute versus relative amounts of blue light. *HortScience* 48, 504–509. doi: 10.21273/HORTSCI.48.4.504

Danziger, N., and Bernstein, N. (2021a). Light matters: Effect of light spectra on cannabinoid profile and plant development of medical cannabis (Cannabis sativa L.). *Ind. Crops Prod* 164, 113351. doi: 10.1016/j.indcrop.2021.113351

Danziger, N., and Bernstein, N. (2021b). Shape matters: Plant architecture affects chemical uniformity in large-size medical cannabis plants. *Plants* 10, 1834. doi: 10.3390/plants10091834

De Hoop, B., Heerdink, E. R., and Hazekamp, A. (2018). Medicinal cannabis on prescription in the Netherlands: statistics for 2003-2016. *Cannabis Cannabinoid Res.* 3, 54–55. doi: 10.1089/can.2017.0059

Demmig-Adams, B., and Adams, W. W. (1992). Photoprotection and other responses of plants to high light stress. *Annu. Rev. Plant Biol.* 43, 599–626. doi: 10.1146/annurev.pp.43.060192.003123

Demotes-Mainard, S., Péron, T., Corot, A., Bertheloot, J., Le Gourrierec, J., Pelleschi-Travier, S., et al. (2016). Plant responses to red and far-red lights, applications in horticulture. *Environ. Exp. Bot.* 121, 4–21. doi: 10.1016/j.envexpbot.2015.05.010

Eaves, J., Eaves, S., Morphy, C., and Murray, C. (2020). The relationship between light intensity, cannabis yields, and profitability. *Agron. J.* 112, 1466–1470. doi: 10.1002/agj2.20008

Eichhorn Bilodeau, S., Wu, B., Rufyikiri, A. S., MacPherson, S., and Lefsrud, M. (2019). An update on plant photobiology and implications for cannabis production. *Front. Plant Sci.* 10. doi: 10.3389/fpls.2019.00296

Emerson, R., and Lewis, C. M. (1943). The dependence of the quantum yield of chlorella photosynthesis on wave lenghth of light. *Am. J. Bot.* 30, 165. doi: 10.2307/2437236

Evans, J. (1987). The dependence of quantum yield on wavelength and growth irradiance. *Funct. Plant Biol.* 14, 69. doi: 10.1071/PP9870069

Farquhar, G. D., von Caemmerer, S., and Berry, J. A. (1980). A biochemical model of photosynthetic CO2 assimilation in leaves of C3 species. *Planta* 149, 78–90. doi: 10.1007/BF00386231

Fluence (2020). *Cannabis cultivation guide*. (Texas, Austin, USA).

Folta, K. M., and Carvalho, S. D. (2015). Photoreceptors and control of horticultural plant traits. *HortScience* 50, 1274–1280. doi: 10.21273/HORTSCI.50.9.1274

Frechilla, S., Talbott, L. D., Bogomolni, R. A., and Zeiger, E. (2000). Reversal of blue light-stimulated stomatal opening by green light. *Plant Cell Physiol.* 41, 171–176. doi: 10.1093/pcp/41.2.171

Galvão, V. C., and Fankhauser, C. (2015). Sensing the light environment in plants: photoreceptors and early signaling steps. *Curr. Opin. Neurobiol.* 34, 46–53. doi: 10.1016/j.conb.2015.01.013

Ghaffari, Z., Rahimmalek, M., and Sabzalian, M. R. (2019). Variation in the primary and secondary metabolites derived from the isoprenoid pathway in the Perovskia species in response to different wavelengths generated by light emitting diodes (LEDs). *Ind. Crops Prod* 140, 111592. doi: 10.1016/j.indcrop.2019.111592

Hall, W., Stjepanović, D., Caulkins, J., Lynskey, M., Leung, J., Campbell, G., et al. (2019). Public health implications of legalising the production and sale of cannabis for medicinal and recreational use. *Lancet* 394, 1580–1590. doi: 10.1016/S0140-6736(19)31789-1

Hawley, D. (2023). *Understanding photobleaching in cannabis*. (Texas, Austin, USA: Fluence).

Hawley, D., Graham, T., Stasiak, M., and Dixon, M. (2018). Improving Cannabis bud quality and yield with subcanopy lighting. *HortScience* 53, 1593–1599. doi: 10.21273/HORTSCI13173-18

Hazekamp, A., Sijrier, P., and Verpoorte, M. (2006). An evaluation of the quality of medicinal grade cannabis in the Netherlands. *Cannabinoids* 1, 1–9.

Hogewoning, S. W., Trouwborst, G., Maljaars, H., Poorter, H., van Ieperen, W., and Harbinson, J. (2010). Blue light dose-responses of leaf photosynthesis, morphology, and chemical composition of Cucumis sativus grown under different combinations of red and blue light. *J. Exp. Bot.* 61, 3107–3117. doi: 10.1093/jxb/erq132

Hogewoning, S. W., Trouwborst, G., Meinen, E., and Van Ieperen, W. (2012). Finding the optimal growth-light spectrum for greenhouse crops. *Acta Hortic.* 956, 357–363. doi: 10.17660/ActaHortic.2012.956.41

Inada, K. (1976). Action spectra for photosynthesis in higher plants. *Plant Cell Physiol.* 17 (2), 355-365. doi: 10.1093/oxfordjournals.pcp.a075288

Islam, M. J., Ryu, B. R., Rahman, M. H., Rana, M. S., Cheong, E. J., Wang, M.-H., et al. (2022). Cannabinoid accumulation in hemp depends on ROS generation and interlinked with morpho-physiological acclimation and plasticity under indoor LED environment. *Front. Plant Sci.* 13. doi: 10.3389/fpls.2022.984410

Jin, W., Urbina, J. L., Heuvelink, E., and Marcelis, L. F. M. (2021). Adding far-red to red-blue light-emitting diode light promotes yield of lettuce at different planting densities. *Front. Plant Sci.* 11. doi: 10.3389/fpls.2020.609977

Johkan, M., Shoji, K., Goto, F., Hahida, S., and Yoshihara, T. (2012). Effect of green light wavelength and intensity on photomorphogenesis and photosynthesis in Lactuca sativa. *Environ. Exp. Bot.* 75, 128–133. doi: 10.1016/j.envexpbot.2011.08.010

Kaiser, E., Ouzounis, T., Giday, H., Schipper, R., Heuvelink, E., and Marcelis, L. F. M. (2019). Adding blue to red supplemental light increases biomass and yield of greenhouse-grown tomatoes, but only to an optimum. *Front. Plant Sci.* 9. doi: 10.3389/fpls.2018.02002

Karst, M., Salim, K., Burstein, S., Conrad, I., Hoy, L., and Schneider, U. (2003). Analgesic effect of the synthetic cannabinoid CT-3 on chronic neuropathic pain. *JAMA* 290, 1757. doi: 10.1001/jama.290.13.1757

Kessler, A., and Kalske, A. (2018). Plant secondary metabolite diversity and species interactions. *Annu. Rev. Ecol. Evol. Syst.* 49, 115–138. doi: 10.1146/annurev-ecolsys-110617-062406

Kim, H. H., Goins, G. D., Wheeler, R. M., and Sager, J. C. (2004). Green-light supplementation for enhanced lettuce growth under red-and blue-light-emitting diodes. *HortScience* 39, 1617–1622. doi: 10.21273/HORTSCI.39.7.1617

Kowal, M. A., Hazekamp, A., and Grotenhermen, F. (2016). Review on clinical studies with cannabis and cannabinoids 2010-2014. *Multiple sclerosis* 6, 1515.

Krahmer, J., Ganpudi, A., Abbas, A., Romanowski, A., and Halliday, K. J. (2018). Phytochrome, carbon sensing, metabolism, and plant growth plasticity. *Plant Physiol.* 176, 1039–1048. doi: 10.1104/pp.17.01437

Kusuma, P., Pattison, P. M., and Bugbee, B. (2020). From physics to fixtures to food: current and potential LED efficacy. *Hortic. Res.* 7, 56. doi: 10.1038/s41438-020-0283-7

Liu, J., and Van Iersel, M. W. (2021). Photosynthetic physiology of blue, green, and red light: light intensity effects and underlying mechanisms. *Light intensity effects and underlying mechanisms. Front. Plant Sci.* 12. doi: 10.3389/fpls.2021.619987

Livingston, S. J., Quilichini, T. D., Booth, J. K., Wong, D. C. J., Rensing, K. H., Laflamme-Yonkman, J., et al. (2020). Cannabis glandular trichomes alter morphology and metabolite content during flower maturation. *Plant J.* 101, 37–56. doi: 10.1111/tpj.14516

Llewellyn, D., Golem, S., Foley, E., Dinka, S., Jones, A. M. P., and Zheng, Y. (2021). Cannabis yield increased proportionally with light intensity, but additional ultraviolet radiation did not affect yield or cannabinoid content. *Preprints (Basel)*, 1–19. doi: 10.20944/preprints202103.0327.v1

Lu, N., Saengtharatip, S., Takagaki, M., Maruyama, A., and Kikuchi, M. (2019). How do white LEDs' Spectra affect the fresh weight of lettuce grown under artificial lighting in a plant factory?—A statistical approach. *Agric. Sci.* 10, 957–974. doi: 10.4236/as.2019.107073

Lumigrow (2017). *LED grower's guide for cannabis*. (California, Emeryville, USA: Lumigrow).

Magagnini, G., Grassi, G., and Kotiranta, S. (2018). The effect of light spectrum on the morphology and cannabinoid content of cannabis sativa L. *Med. Cannabis Cannabinoids* 1, 19–27. doi: 10.1159/000489030

Massa, G. D., Kim, H.-H., Wheeler, R. M., and Mitchell, C. A. (2008). Plant productivity in response to LED lighting. *HortScience* 43, 1951–1956. doi: 10.21273/HORTSCI.43.7.1951

McCree, K. J. (1971). The action spectrum, absorptance and quantum yield of photosynthesis in crop plants. *Agric. Meteorology* 9, 191–216. doi: 10.1016/0002-1571(71)90022-7

McPartland, J. M. (2018). Cannabis systematics at the levels of family, genus, and species. *Cannabis Cannabinoid Res.* 3, 203–212. doi: 10.1089/can.2018.0039

Mehboob, N., Farag, H. E. Z., and Sawas, A. M. (2020). Energy consumption model for indoor cannabis cultivation facility. *IEEE Open Access J. Power Energy* 7, 222–233. doi: 10.1109/OJPES

Miao, Y., Wang, X., Gao, L., Chen, Q., and Qu, M. (2016). Blue light is more essential than red light for maintaining the activities of photosystem II and I and photosynthetic electron transport capacity in cucumber leaves. *J. Integr. Agric.* 15, 87–100. doi: 10.1016/S2095-3119(15)61202-3

Mitchell, C. A., Dzakovich, M. P., Gomez, C., Lopez, R., Burr, J. F., Hernández, R., et al. (2015). "Light-emitting diodes in horticulture," in *Horticultural reviews: volume 43* (Wiley) 43, 1–88. doi: 10.1002/9781119107781.ch01

Morello, V., Brousseau, V. D., Wu, N., Wu, B.-S., MacPherson, S., and Lefsrud, M. (2022). Light quality impacts vertical growth rate, phytochemical yield and cannabinoid production efficiency in cannabis sativa. *Plants* 11, 2982. doi: 10.3390/plants11212982

Morrow, R. C. (2008). LED lighting in horticulture. *HortScience* 43, 1947–1950. doi: 10.21273/HORTSCI.43.7.1947

Mukhopadhyay, P., Rajesh, M., Horváth, B., Bátkai, S., Park, O., Tanchian, G., et al. (2011). Cannabidiol protects against hepatic ischemia/reperfusion injury by attenuating inflammatory signaling and response, oxidative/nitrative stress, and cell death. *Free Radic. Biol. Med.* 50, 1368–1381. doi: 10.1016/j.freeradbiomed.2011.02.021

Namdar, D., Charuvi, D., Ajjampura, V., Mazuz, M., Ion, A., Kamara, I., et al. (2019). LED lighting affects the composition and biological activity of Cannabis sativa secondary metabolites. *Ind. Crops Prod* 132, 177–185. doi: 10.1016/j.indcrop.2019.02.016

Namdar, D., Mazuz, M., Ion, A., and Koltai, H. (2018). Variation in the compositions of cannabinoid and terpenoids in Cannabis sativa derived from inflorescence position along the stem and extraction methods. *Ind. Crops Prod* 113, 376–382. doi: 10.1016/j.indcrop.2018.01.060

Nishio, J. N., Sun, J., and Vogelmann, T. C. (1993). Carbon fixation gradients across spinach leaves do not follow internal light gradients. *Plant Cell* 5 (8), 953–961. doi: 10.1105/tpc.5.8.953

Oguchi, R., Douwstra, P., Fujita, T., Chow, W. S., and Terashima, I. (2011). Intra-leaf gradients of photoinhibition induced by different color lights: implications for the dual mechanisms of photoinhibition and for the application of conventional chlorophyll fluorometers. *New Phytol.* 191, 146–159. doi: 10.1111/j.1469-8137.2011.03669.x

Oguchi, R., Terashima, I., and Chow, W. S. (2021). The effect of different spectral light quality on the photoinhibition of Photosystem I in intact leaves. *Photosynth Res.* 149, 83–92. doi: 10.1007/s11120-020-00805-z

Ott, R. L., and Longnecker, M. T. (2015). *An introduction to statistical methods and data analysis* (Cengage Learning).

Ouzounis, T., Rosenqvist, E., and Ottosen, C. O. (2015). Spectral effects of artificial light on plant physiology and secondary metabolism: A review. *HortScience* 50, 1128–1135. doi: 10.21273/HORTSCI.50.8.1128

Pan, X., Ma, J., Su, X., Cao, P., Chang, W., Liu, Z., et al. (2018). Structure of the maize photosystem I supercomplex with light-harvesting complexes I and II. *Sci. (1979)* 360, 1109–1113. doi: 10.1126/science.aat1156

Park, Y., and Runkle, E. S. (2018). Far-red radiation and photosynthetic photon flux density independently regulate seedling growth but interactively regulate flowering. *Environ. Exp. Bot.* 155, 206–216. doi: 10.1016/j.envexpbot.2018.06.033

Pattison, P. M., Tsao, J. Y., Brainard, G. C., and Bugbee, B. (2018). LEDs for photons, physiology and food. *Nature* 563, 493–500. doi: 10.1038/s41586-018-0706-x

Piovene, C., Orsini, F., Bosi, S., Sanoubar, R., Bregola, V., Dinelli, G., et al. (2015). Optimal red:blue ratio in led lighting for nutraceutical indoor horticulture. *Sci. Hortic.* 193, 202–208. doi: 10.1016/j.scienta.2015.07.015

Pleasants, S. (2013). Overcoming the "green gap. *Nat. Photonics* 7, 585–585. doi: 10.1038/nphoton.2013.202

Pocock, T. (2015). Light-emitting diodes and the modulation of specialty crops: Light sensing and signaling networks in plants. *HortScience* 50, 1281–1284. doi: 10.21273/HORTSCI.50.9.1281

Raja, A., Ahmadi, S., de Costa, F., Li, N., and Kerman, K. (2020). Attenuation of oxidative stress by cannabinoids and cannabis extracts in differentiated neuronal cells. *Pharmaceuticals* 13, 328. doi: 10.3390/ph13110328

Rodriguez-Morrison, V., Llewellyn, D., and Zheng, Y. (2021). Cannabis yield, potency, and leaf photosynthesis respond differently to increasing light levels in an indoor environment. *Front. Plant Sci.* 12. doi: 10.3389/fpls.2021.646020

Sabzalian, M. R., Heydarizadeh, P., Zahedi, M., Boroomand, A., Agharokh, M., Sahba, M. R., et al. (2014). High performance of vegetables, flowers, and medicinal plants in a red-blue LED incubator for indoor plant production. *Agron. Sustain Dev.* 34, 879–886. doi: 10.1007/s13593-014-0209-6

Sarlikioti, V., de Visser, P. H. B., Buck-Sorlin, G. H., and Marcelis, L. F. M. (2011). How plant architecture affects light absorption and photosynthesis in tomato: towards an ideotype for plant architecture using a functional–structural plant model. *Ann. Bot.* 108, 1065–1073. doi: 10.1093/aob/mcr221

Slattery, R. A., Grennan, A. K., Sivaguru, M., Sozzani, R., and Ort, D. R. (2016). Light sheet microscopy reveals more gradual light attenuation in light-green versus dark-green soybean leaves. *J. Exp. Bot.* 67, 4697–4709. doi: 10.1093/jxb/erw246

Smith, H. L., McAusland, L., and Murchie, E. H. (2017). Don't ignore the green light: exploring diverse roles in plant processes. *J. Exp. Bot.* 68, 2099–2110. doi: 10.1093/jxb/erx098

Snowden, M. C., Cope, K. R., and Bugbee, B. (2016). Sensitivity of seven diverse species to blue and green light: Interactions with photon flux. *PloS One* 11, e0163121. doi: 10.1371/journal.pone.0163121

Sommano, S. R., Chittasupho, C., Ruksiriwanich, W., and Jantrawut, P. (2020). The cannabis terpenes. *Molecules* 25 (24), 5792. doi: 10.3390/molecules25245792

Sparkman, O. D. (2005). Identification of essential oil components by gas chromatography/quadrupole mass spectroscopy Robert P. Adams. *J. Am. Soc. Mass Spectrom* 16, 1902–1903. doi: 10.1016/j.jasms.2005.07.008

Spitzer-Rimon, B., Duchin, S., Bernstein, N., and Kamenetsky, R. (2019). Architecture and florogenesis in female cannabis sativa plants. *Front. Plant Sci.* 10. doi: 10.3389/fpls.2019.00350

Takeda, F., and Newell, M. (2006). A method for increasing fall flowering in short-day `Carmine' Strawberry. *HortScience* 41, 480–481. doi: 10.21273/HORTSCI.41.2.480

Takenaka, A. (1994). Effects of leaf blade narrowness and petiole length on the light capture efficiency of a shoot. *Ecol. Res.* 9, 109–114. doi: 10.1007/BF02347485

Talbott, L. D., Nikolova, G., Ortiz, A., Shmayevich, I., and Zeiger, E. (2002). Green light reversal of blue-light-stimulated stomatal opening is found in a diversity of plant species. *Am. J. Bot.* 89, 366–368. doi: 10.3732/ajb.89.2.366

Tamulaitis, G., Duchovskis, P., Bliznikas, Z., Breive, K., Ulinskaite, R., Brazaityte, A., et al. (2005). High-power light-emitting diode based facility for plant cultivation. *J. Phys. D Appl. Phys.* 38, 3182–3187. doi: 10.1088/0022-3727/38/17/S20

Taylor, C. R., van Ieperen, W., and Harbinson, J. (2019). Demonstration of a relationship between state transitions and photosynthetic efficiency in a higher plant. *Biochem. J.* 476, 3295–3312. doi: 10.1042/BCJ20190576

Terashima, I., Fujita, T., Inoue, T., Chow, W. S., and Oguchi, R. (2009). Green light drives leaf photosynthesis more efficiently than red light in strong white light: revisiting the enigmatic question of why leaves are green. *Plant Cell Physiol.* 50, 684–697. doi: 10.1093/pcp/pcp034

Thoma, F., Somborn-Schulz, A., Schlehuber, D., Keuter, V., and Deerberg, G. (2020). Effects of light on secondary metabolites in selected leafy greens: A review. *Front. Plant Sci.* 11. doi: 10.3389/fpls.2020.00497

Thornley, J. H. M. (1977). Mathematical models in plant physiology. By J. H. M. Thornley. London: academic press, (1976), PP. 331, £9.80. *Exp. Agric.* 13, 112–112. doi: 10.1017/S0014479700007675

Tracewell, C. A., Vrettos, J. S., Bautista, J. A., Frank, H. A., and Brudvig, G. W. (2001). Carotenoid photooxidation in photosystem II. *Arch. Biochem. Biophys.* 385, 61–69. doi: 10.1006/abbi.2000.2150

Voitsekhovskaja, O. V., and Tyutereva, E. V. (2015). Chlorophyll b in angiosperms: Functions in photosynthesis, signaling and ontogenetic regulation. *J. Plant Physiol.* 189, 51–64. doi: 10.1016/j.jplph.2015.09.013

Walla, P. J., Holleboom, C.-P., and Fleming, G. R. (2014). *Electronic carotenoid-chlorophyll interactions regulating photosynthetic light harvesting of higher plants and green algae.* (Dordrecht: Springer Netherlands) 229–243. doi: 10.1007/978-94-017-9032-1_9

Wang, Y., and Folta, K. M. (2013). Contributions of green light to plant growth and development. *Am. J. Bot.* 100, 70–78. doi: 10.3732/ajb.1200354

Wei, X., Zhao, X., Long, S., Xiao, Q., Guo, Y., Qiu, C., et al. (2021). Wavelengths of LED light affect the growth and cannabidiol content in Cannabis sativa L. *Ind. Crops Prod* 165, 113433. doi: 10.1016/j.indcrop.2021.113433

Westmoreland, M., Kusuma, P., and Bugbee, B. (2021). Cannabis lighting: Decreasing blue photon fraction increases yield but efficacy is more important for cost effective production of cannabinoids. *PloS One* 16, e0248988. doi: 10.1371/journal.pone.0248988

Wollaeger, H. M., and Runkle, E. S. (2013). Growth responses of ornamental annual seedlings under different wavelengths of red light provided by light-emitting diodes. *HortScience* 48, 1478–1483. doi: 10.21273/HORTSCI.48.12.1478

Zhao, L.-S., Li, K., Wang, Q.-M., Song, X.-Y., Su, H.-N., Xie, B.-B., et al. (2017). Nitrogen starvation impacts the photosynthetic performance of porphyridium cruentum as revealed by chlorophyll a fluorescence. *Sci. Rep.* 7, 8542. doi: 10.1038/s41598-017-08428-6

Zhen, S., and Bugbee, B. (2020a). Substituting far-red for traditionally defined photosynthetic photons results in equal canopy quantum yield for CO2 fixation and increased photon capture during long-term studies: implications for re-defining PAR. *Front. Plant Sci.* 11. doi: 10.3389/fpls.2020.581156

Zhen, S., and Bugbee, B. (2020b). Far-red photons have equivalent efficiency to traditional photosynthetic photons: Implications for redefining photosynthetically active radiation. *Plant Cell Environ.* 43, 1259–1272. doi: 10.1111/pce.13730

Zhu, X.-G., Long, S. P., and Ort, D. R. (2008). What is the maximum efficiency with which photosynthesis can convert solar energy into biomass? *Curr. Opin. Biotechnol.* 19, 153–159. doi: 10.1016/j.copbio.2008.02.004

Zobayed, S. M. A., Afreen, F., and Kozai, T. (2005). Necessity and production of medicinal plants under controlled environments. *Environ. Control Biol.* 43, 243–252. doi: 10.2525/ecb.43.243

Frontiers in Plant Science

Cultivates the science of plant biology and its applications

The most cited plant science journal, which advances our understanding of plant biology for sustainable food security, functional ecosystems and human health.

Discover the latest Research Topics

See more →

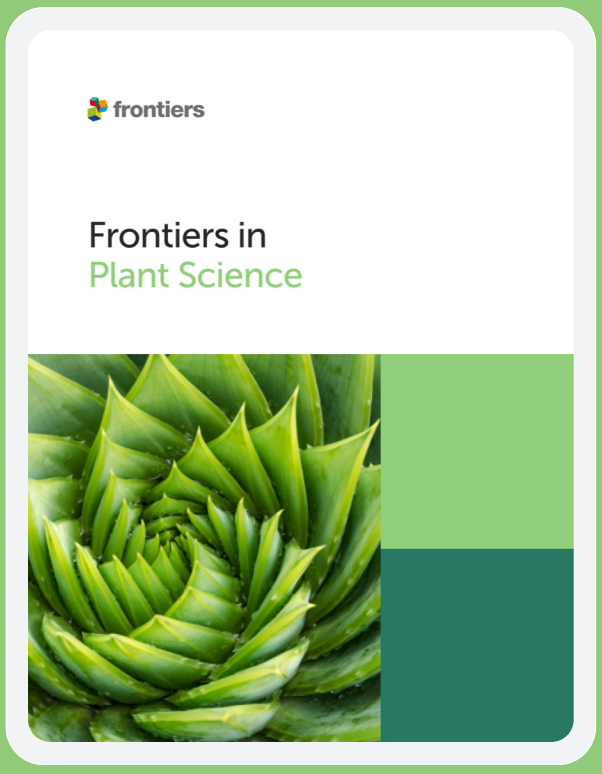

Frontiers

Avenue du Tribunal-Fédéral 34
1005 Lausanne, Switzerland
frontiersin.org

Contact us

+41 (0)21 510 17 00
frontiersin.org/about/contact